Expression and Regulation of Neuron-Specific Enolase

RICHARD MARTIN TWYMAN (B.Sc. Hons.)

Thesis submitted for the degree of
Doctor of Philosophy

MRC Animal Molecular Genetics Group
Department of Biological Sciences
University of Warwick
Coventry
CV4 7AL

November 1995

Table of Contents
(in Brief)

Table of Chapter Contents (in Full)

List of Tables and Figures

Acknowledgements

I wish to thank all members of the department, both past and present who, by generously volunteering their time, advice, practical assistance and laptop computers, have helped me to complete this thesis. Particularly, I would like to thank Liz Jones for experimental guidance, lively discussions, and a seemingly limitless supply of encouragement and enthusiasm through good times and bad.

I acknowledge Sonja Forss-Petter and Patria Danielson for their magnanimous gifts of plasmids pNSElacZ and pcD169, without which this project would not have been possible. Thanks also to David Stott for supplying materials and technical expertise and for munificently generating transgenic mice at very short notice. The financial support of the BBSRC (formerly SERC) and Glaxo is gratefully acknowledged.

This thesis is dedicated to my parents, Peter Richard Twyman and Irene Rose Twyman, whose love and support over the years has taken many forms but has never wavered. It is also dedicated to my wife and best friend, Vicki Twyman, a constant source of motivation and inspiration. Finally, it is dedicated to my baby daughter, Emily Anne Twyman, who is, without doubt, my best result yet.....

Declaration

I hereby declare that the work contained within this thesis was carried out exclusively by myself, with the notable exception that transgenic mice were generated by Dr David Stott. All information sources are acknowledged. None of the data contained herein have been submitted in full or in part for any other degree. However, where indicated, some sections have been published or submitted for publication.

Summary

Neuron-specific enolase (NSE) is an isoform of the glycolytic enzyme enolase which is expressed specifically in neurons and neuroendocrine cells in the mammalian nervous system. Its onset of expression coincides with neuronal differentiation and it has therefore become established as a marker of mature, postmitotic neurons (Zomzely-Neurath, 1983). The molecular basis of neuron-specific gene expression is still poorly understood (Twyman and Jones, 1995b) and the panneuronal *NSE* gene thus represents an excellent model for the investigation of mechanisms responsible for neuronal gene regulation. Recently, the proximal 1.8 kbp of 5' flanking sequence from the rat *NSE* gene was shown to confer neuron-specific and panneuronal expression upon a heterologous gene in transgenic mice (Forss-Petter *et al.*, 1990). This suggested that the sequence probably contained neuron-specific *cis*-acting elements which could be investigated using a deletion-reporter strategy in cultured cells and transgenic mice. The 1.8 kbp flanking sequence has also been shown to respond to NGF and retinoic acid in parallel with the endogenous gene (Alouani *et al.*, 1993).

In this project, the 1.8 kbp 5' flanking sequence was dissected, and various truncated derivatives were compared to the full length construct in cultured cells of neuronal and nonneuronal origin. It was shown that 255 bp of 5' flanking sequence was capable of conferring full cell type-specific regulation upon a heterologous gene, indicating the presence of neuronal *cis*-acting elements within 255 bp of the transcriptional start site. Further transfection experiments, concentrating on this short proximal fragment, showed that elements responsible for neuron-specific gene expression were present in this region and *in vitro* analysis identified at least one specific DNA-protein interaction. Preliminary analysis of *NSE* gene regulation was also carried out in transgenic mice. These experiments, taken together with previous studies, showed that the level of transgene expression was variable and subject to both position and gene dosage effects. It was concluded that further analysis should be carried out in transgenic lines, preferably utilising flanking boundary elements which would protect the *NSE* transgenes from the position effects (to which they were highly susceptible). The impact of the transfection and transgenic experiments was discussed with respect to the published literature and ideas for future experiments were suggested.

Abbreviations

The abbreviations used in this thesis are listed below in alphabetical order. Generally, where an unestablished abbreviation first occurs in the text, it is supported by the unabbreviated term in parentheses. Several classes of abbreviation have been omitted from the list below for the sake of brevity. These include: a) SI units; b) chemical formulae; c) names of cell lines, strains of animals, plants and bacteria; d) accepted gene or phenotype designations, names of plasmids and transgenes, and names of transcription factors; e) abbreviations relating to products, manufacturers and their addresses and f) restriction endonucleases. Where necessary, the abbreviations listed below may be supported by some explanatory text.

A - adenine (base) or adenosine (nucleoside)
AADC - aromatic amino acid decarboxylase
ACA - Actual CAT Activity (see section 5.5)
ACh - Acetylcholine
b, bp - base, base pair
BBS - BES-buffered saline
BDNF - brain-derived neurotrophic factor
BES - *N,N-bis*-[2-hydroxyethyl]-2-aminoethanesulphonic acid
BETA - brain enriched transcriptional activator
bHLH - basic helix-loop-helix motif
BSA - bovine serum albumin
BSF - brain-specific factor
bZIP - basic leucine zipper motif
C - cytosine (base) or cytidine (nucleoside)
cAMP - cyclic AMP (adenosine 5'-monophosphate)
CAT - chloramphenicol acetyltransferase
cDNA - complementary DNA
ch - chicken
CIAP - calf intestinal alkaline phosphatase
CNS - central nervous system
CoA - coenzyme A
CRE - cAMP response element
CTF - CAAT-binding transcription factor
dATP - 2'-deoxyadenosine 5'-triphosphate

dbcAMP - dibutyryl cyclic adenosine 5'-monophosphate
DBH - dopamine β-hydroxylase
dCTP - 2'-deoxycytidine 5'-triphosphate
DEAE-dextran - diethylaminoethyl dextran
DEPC - diethylpyrocarbonate
dGTP - 2'-deoxyguanidine triphosphate
DIG - digoxigenin
DMEM - Dulbecco's modified Eagle's medium
DMSO - dimethylsulphoxide
DNA - 2'-deoxyribonucelic acid
DNase - 2'-deoxyribonuclease
dNTP - Any 2'-deoxynucleoside 5'-triphosphate
DOTAP - *N*-[1-(2,3-dioleyloxy)propyl]-*N*,*N*,*N*-trimethylammonium chloride
DTT - dithiothreitol
dTTP - 2'-deoxythymidine 5'-triphosphate
E (followed by number) - embryonic day
EC - embryonal carcinoma
EDTA - ethylenediaminetetraacetic acid
EGF - epidermal growth factor
ES cells - embryonic stem cells
et al. - *et alia*, and others
FBS - Foetal bovine serum
FCS - Foetal calf serum
FITC - fluorescein isothiocyanate
G - guanine (base) or guanidine (nucleoside)
GABA - γ-aminobutyric acid
GAL - unit β-galactosidase activity (see section 5.5)
GAP - growth associated protein
GCG - Genetics Computer Group
GRE - glucocorticosteroid response element
h - human
HIF - hypoxia-inducible factor
HIV - human immunodeficiency virus
HLH - helix-loop-helix
HMG - high mobility group
hrs - hours
HS - horse serum
HSV - herpes simplex virus

ID - identifier (neuronal identifier element)
IEG - immediate early gene
kb, kbp - kilobase, kilobase pair
kDa - kiloDaltons
Krox - Kruppel-like box
LB - Luria broth
m - mouse
MASH - mammalian *achaete-scute* homologue
MEC - molar equivalence constant (see section 5.5)
MEM - minimal essential medium
min - minimal
mins - minutes
mRNA - messenger RNA
MSE - muscle-specific enolase
MTF - metal-responsive transcription factor
NAA - nonessential amino acids
NF - nuclear factor
NF-H heavy neurofillament
NF-L light neurofillament
NF-M mid-range neurofillament
NGF - nerve growth factor β
NNE - nonneuronal enolase
NRS(B)F - neural restrictive silencer (binding) factor
NRSE - neural restrictive silencer element
NS - neuron-specific
NSE - neuron-specific enolase
NTET - a washing solution containing salt (i.e. NaCl), Tris, EDTA and Tween 20
Oct - octamer
OD - optical density
OMP - olfactory marker protein
ONPG - *o*-nitrophenyl-β-D-galactopyranoside
p - phosphate (denotes single phosphate group, hence CpG, Gppp etc.)
P (followed by number) - postnatal day
PAGE - polyacrylamide gel electrophoresis
PBS - phosphate buffered saline
PBST - PBS containing Tween 20
PCR - polymerase chain reaction

PEP - phospho*enol*pyruvate

2-PGA - 2-phosphoglycerate

PMSF - phenylmethylsulphonylfluoride

PNMT - phenylethanolamine *N*-methyltransferase

PNS - peripheral nervous system

POU - conserved DNA-binding domain originally found in Pit-1, Oct-1 and Oct-2, and Unc-86 transcription factors

PPT - preprotachykinin

R - any puRine

r - rat

RACE - rapid amplification of cDNA ends

RARE - retinoic acid response element

RCA - Relative CAT Activity (see section 5.5)

RNA - ribonucleic acid

RNase - ribonuclease

RSV - Rous sarcoma virus

S - G or C (three bondS)

SCIP - suppressed cAMP inducible POU

scRNA - small cellular RNA

SDS - sodium dodecylsulphate (also known as sodium lauryl sulphate)

secs - seconds

sem - standard error of the mean

SNN - SNN motif (neuronal motif found in synapsin, neurofilament and NGF receptor gene 5' flanking regions)

Sox - Sry-like box*

SSC - Standard saline citrate buffer

STE - a solution containing salt (i.e. NaCl), Tris and EDTA used during plasmid preparations

SV40 - simian virus 40

T - thymine (base) or thymidine (nucleoside)

T3, T4, T7 - tailed phages

TAR - *Trans*-activator region (of the HIV genome)

TAT - *Trans*-activator gene

---

* Nomenclature for *Sox* genes and their products: In this thesis, both chicken and mouse *Sox* genes are discussed. The accepted nomenclature for the mouse genes is *Sox-2, Sox-3* etc., and for their products, Sox-2, Sox-3 etc., whilst for the chicken genes the nomenclature is *cSox2, cSox3* etc., and for the products cSox2, cSox3 etc. Where the *Sox* genes or their products are discussed in a generic sense, the mouse nomenclature is used.

TBE - an electrophoresis buffer containing Tris, borate and EDTA
TBS - Tris-buffered saline
TE - a general purpose buffer containing Tris and EDTA
TELT - a solution containing Tris, EDTA, LiCl and Triton X-100, used for small scale plasmid preparations
TF - transcription factor
TH - tyrosine hydroxylase
TLC - thin layer chromatography
Tris - tris(hydroxymethyl)methylamine
tRNA - transfer RNA
Tween 20 - polyoxyethylenesorbitan monolaurate
U - unit (e.g. of enzyme activity)
U - uracil (base) or uridine (nuceloside)
UPE - upstream promoter element
UTP - uridine 5'-triphosphate
UTR - untranslated region
UV - ultraviolet
v/v - volume per unit volume
w/v - weight per unit volume
X-gal - 5-bomo-4-chloro-3-indolyl-β-D-galactopyranoside
X-phosphate - 5-bomo-4-chloro-3-indolyl phosphate (also called BCIP)
Y - any pYrimidine
zif - zinc finger

Section I - Introduction

Chapter 1 - The Molecular Biology of Enolase in Mammals and Birds

A project involving neuron-specific enolase would be incomplete without an introduction placing the study in the context of enolase research as a whole. The aim of this first introductory chapter is to provide a review of enolase molecular biology in mammals and birds, two branches of the phylogenetic tree where the existence of neuron-specific enolase is undisputed, and as such, this chapter has been submitted in modified form for publication (Twyman and Jones, 1995a).

1.1 There is more than one gene encoding enolase in mammals and birds

The dimeric metalloenzyme enolase is a critical component of glucose metabolism, catalysing the reversible dehydration of 2-phosphoglycerate (2-PGA) to phosphoenolpyruvate (PEP). As an intrinsic part of this ubiquitous metabolic pathway, enolase is probably found in all living cells and it has certainly been isolated from a wide variety of natural sources (Wold, 1971; Brewer, 1981). In eukaryotes, enolase is often found as multiple, distinct isoforms, a property it shares with many other enzymes. Such isozymic heterogeneity reflects the existence of a small, conserved family of enolase genes, the members of which are regulated independently in many species (Twyman and Jones, 1995c). In mammals and birds, there are (at least) three enolase genes whose products combine as homodimers and heterodimers to generate five isoenzymes. The levels of the three subunits vary according to tissue and developmental stage, indicating that the genes encoding them are spatially and temporally regulated. Experiments using various cell lines have also shown that certain agents and growth conditions can modulate the levels of the enolase subunits in cultured cells. Although the specificity, ontogeny and inducibility of enolase gene expression have been studied intensely for over twenty years, it is only recently, with the advent of modern molecular biology techniques, that the mechanisms of gene regulation have been investigated at the molecular level.

1.2 Early studies of the mammalian enolases

Enolase isoenzymes were first studied specifically in mammals as a continuation of investigations into the general heterogeneity of mammalian glycolytic enzymes (Rider and Taylor, 1974). Earlier studies had shown that several other such enzymes were represented by distinct and tissue-specific isoforms (Penhoet *et al.*, 1966; Criss, 1971;

Sato *et al.*, 1972), and it was proposed that such diversity had evolved to allow glycolysis to subserve different functions in different tissues as has been demonstrated for certain plants (Miernyk and Dennis, 1982). In comparative studies carried out in the early 1970s, enolases were isolated from a variety of sources in nature and found to be biochemically and kinetically similar (Cardenas and Wold, 1971; Ruth *et al.*, 1970), however, samples taken from mammals and other animals were all derived from muscle, thus the tissue-specificity of enolase isoenzymes *within* each species was not investigated. Electrophoretic evidence for the existence of enolase isoenzymes in human skin (Halprin and Fukui, 1968) and erythrocytes (Bartels and Vogel, 1971) had been presented. Enolase had also been isolated from bovine brain (Wood, 1964), human erythrocytes (Witt and Witz, 1970), and porcine kidney (Oh and Brewer, 1973) without comparative studies being carried out.

Mammalian enolase isoenzyme diversity was first comprehensively investigated in the rat (Rider and Taylor, 1974; 1975a). These studies showed that three biochemically distinct enolase isoenzymes could be resolved, which, although kinetically indistinguishable, differed in their ontogeny, distribution and immunological properties. Isoenzyme 1 was found in extracts of all of the tissues examined except adult skeletal muscle, and was also the only form of enolase found in the embryo. Conversely, isoenzyme 3 was absent from the embryo and was the only form of enolase found in adult skeletal muscle. Reciprocal immunological cross-reaction between isoenzymes 1 and 3 did not occur, suggesting they contained distinct polypeptides. Heart extracts contained both isoenzymes 1 and 3 along with a third form, isoenzyme 2, which demonstrated biochemical properties intermediate between the other enolases. Isoenzyme 2 was also present (together with isoenzyme 1) in developing skeletal muscle but isoenzyme 3 completely replaced these embryonic forms by postnatal day 30. Although isoenzymes 1 and 3 were shown to be immunologically distinct, antisera raised against each of them cross-reacted to isoenzyme 2, suggesting that this intermediate isoform shared antigenic determinants with both of them. From these initial results, the authors concluded that two discrete enolase polypeptides were encoded by the rat genome, one of which (α-enolase, now called nonneuronal enolase, NNE) was expressed nearly ubiquitously, the other (β-enolase, now called muscle-specific enolase, MSE) was restricted to skeletal muscle and heart. In most tissues, the native enolase dimer was composed of two α or NNE subunits (isoenzyme 1, αα-enolase) whilst in adult muscle, the dimer was composed of two β or MSE subunits (isoenzyme 3, ββ-enolase). The authors further suggested that, during muscle development, a rapid switch from NNE to MSE synthesis occurred resulting in transient expression of the heterodimer (isoenzyme 2, αβ-

enolase) whilst conversely, NNE and MSE subunits were coexpressed in the heart, resulting in the constitutive presence of all three isoenzymes (Rider and Taylor, 1974).

Evidence of enolase heterogeneity in mammalian brain tissue (Kamel and Schwartzfischer, 1975; Pearce *et al.*, 1976; Chen and Giblett, 1976) prompted a careful re-examination of the enolase isoenzyme profile in rat brain (Rider and Taylor, 1975b; Fletcher *et al.*, 1976). A component representing 30% of total enolase activity was discovered which remained uninhibited by antisera raised against either the NNE or MSE subunits. Careful electrophoretic and chromatographic separation of brain extracts identified three peaks of enolase activity, one of which corresponded to isoenzyme 1, the others being novel and brain-specific. One of the new enolases, isoenzyme 5, was almost totally resistant to inactivation by antisera raised against NNE and MSE subunits and the authors concluded that this isoenzyme represented a homodimer of novel subunits, which they termed γ-enolase (now known as neuron-specific enolase, NSE). Because isoenzyme 5 eluted at a characteristic acidic pH, it was also called *acidic brain enolase* in the early literature. The remaining form of enolase, isoenzyme 4, was inhibited by antisera raised against the NNE and NSE subunits and demonstrated biochemical properties intermediate between isoenzymes 1 and 5. It was therefore concluded that this *hybrid brain enolase* was a heterodimer composed of NNE and NSE subunits. At about the same time as the NSE subunit of enolase was discovered, E. Bock and J. Dissing showed that a bovine neuronal antigen known as 14-3-2 protein, which had been isolated some years before (Moore and McGregor, 1965; Moore and Perez, 1966), possessed enolase activity (Bock and Dissing, 1975). Studies of homologous molecules in other mammals soon showed that rat 14-3-2 protein was identical to rat enolase isoenzyme 5 (γγ-enolase) (Marangos *et al.*, 1976; 1977; Bock *et al.*, 1978). The conclusion from these early studies was that the rat genome encoded three distinct enolase subunits which could combine as homodimers and heterodimers to form the observed isoenzymes. A guide to enolase nomenclature is provided in Table 1.1.

1.3 Expression and ontogeny of α-enolase (nonneuronal enolase)

In mammals, α-enolase is known as nonneuronal enolase (NNE) because early studies of its expression in the nervous system indicated (falsely, as it turned out) that it was excluded from the neuronal cell lineage (Schmechel *et al.*, 1978). It is clear that there is a full switchover from NNE to MSE expression in developing skeletal muscle

Locus	Alternative locus names	Gene Product (Subunit name)	Dimer	IUPAC number	Other names
ENO2	*NSE, γENO*	γ-enolase, neuron-specific enolase (NSE)	γγ-enolase	enolase 5	neuron-specific enolase, (NSE), acidic brain enolase [neuron-specific protein, 14-3-2 protein]
			αγ-enolase	enolase 4	hybrid brain enolase
ENO1	*NNE, αENO, αENO/τCRY*	α-enolase, embryonic enolase, nonneuronal enolase (NNE)	αα-enolase	enolase 1	nonneuronal enolase (NNE), embryonic enolase, liver enolase
			αβ-enolase	enolase 2	
ENO3	*MSE, βENO*	β-enolase, muscle specific enolase (MSE)	ββ-enolase	enolase 3	muscle-specific enolase (MSE)
			βγ-enolase	enolase 6	

Table 1.1: Nomenclature of the mammalian and avian enolases. The cytogenetic nomenclature for all enolase gene loci is being brought into line with the human system (used in column 1 of the table), hence the rodent loci are named *Eno1, Eno2* and *Eno3* and the chick loci are named *ENO1, ENO2* and *ENO3* according to species convention. The duck *ENO1* locus is also termed *αENO/τCRY* because the gene encodes a bifunctional protein (see text). Use of the conventional cytogenetic and biochemical nomenclature leads to confusion because the gene products (enolases 1-3) and the various dimers they form (enolases 1-6) do not always correspond. Most authors thus avoid convention in favour of a simpler nomenclature based on the acronyms for nonneuronal enolase, muscle-specific enolase and neuron-specific enolase. These can be used to refer to the genes and their products and the same name is routinely used to describe both the enolase subunit and the homodimer it forms. If it is necessary to specify dimeric structure, the αβγ system shown in column 4 can be used. For NSE, the alternative names shown in square brackets were those used before its enolase activity had been determined. βγ-enolase is not found *in vivo* because the corresponding subunits are never coexpressed. However, such an isoenzyme can be prepared *in vitro*, using a method described in Shimizu *et al.*, 1983.

which is controlled at the level of transcription, and that a similar switch from NNE to NSE expression may occur during the differentiation of at least some classes of neuron; these studies are discussed under the headings of the relevant tissue-specific enolases. There have been few studies of mammalian NNE expression outside the contexts of neurogenesis and myogenesis. The *NNE* gene is expressed in the majority of proliferating human cell lines, although mRNA levels are low in quiescent lymphoblasts (Giallongo *et al.*, 1986). In these cells, and others, *NNE* gene expression can be induced by mitogenic stimulation, and a peak of *NNE* mRNA accumulation occurs about 24 hours after treatment (Giallongo *et al.*, 1986). Previously, it had been reported that cDNA clones corresponding to five mRNAs induced by the mitogenic stimulation of quiescent rat fibroblasts represented five glycolytic enzymes including enolase (Matrisian *et al.*, 1985). These data suggested that activation of glycolysis may herald re-entry into the cell cycle (Rubin and Fodge, 1974) and it is therefore interesting to note that expression of the *Saccharomyces*

cerevisiae enolase genes is also regulated globally by the growth status of the cells (see Twyman and Jones, 1995c). Unlike *S. cerevisiae ENO1*, human *NNE* is not inducible by heat shock, at least at the level where other human heat shock proteins can be easily detected (Giallongo *et al.*, 1986).

In birds, NNE is expressed in a spatial and temporal pattern broadly similar to mammalian NNE. However, in certain species, high levels of the protein accumulate specifically in the lens, a property not displayed by the mammalian homologues. The components of lenses which enable them to transmit and refract light are highly abundant soluble proteins termed *crystallins*. Although these proteins perform a very specialised function, it has been shown that many are in fact common, housekeeping enzymes which are expressed to extraordinary high levels in a lens-specific manner (reviewed by Wistow and Piatigorsky,1987; 1988). The initial suggestion that enolase might be among these enzymes came from partial sequences of turtle and lamprey τ-crystallin and when the complete amino acid sequence of Peking duck τ-crystallin was deduced from a full length cDNA clone, it demonstrated 92.5% identity to human NNE (Wistow *et al.*, 1988). The authors then provided convincing evidence to show that both the glycolytic enzyme and the lens crystallin were encoded by a single gene, α*ENO*/τ*CRY* (Wistow *et al.*, 1988). Northern analysis showed that the transcripts encoding each protein were identical and that levels of the common α*ENO*/τ*CRY* message were 25 times higher in lens than in liver, indicating that regulation occurred at the level of transcription (Wistow *et al.*, 1988). α*ENO*/τ*CRY* mRNA accumulated in the duck lens between E12 and E14, and levels were higher in the epithelial cells than the fibre cells (Kim *et al.*, 1991). Although there was no evidence to suggest any differences between the tertiary structures of the two proteins, τ-crystallin has been shown to exist as a 48 kDa monomer with little enolase activity (Stapel and de Jong, 1983; Williams *et al.*, 1985; Rudner *et al.*, 1988), whilst NNE in mammals, in common with eukaryotic enolases generally, has been shown to be dimeric (Rider and Taylor, 1974). Immunohistological studies of lens τ-crystallin in turtles revealed a background staining in all tissues, persumably representing NNE expression; it is not known whether the difference in staining intensity was completely attributable to differing protein levels or perhaps reflected some antigenic discrimination between the proteins. Although τ-crystallin has been detected in many lower vertebrates and in ducks, it appears to be absent in chickens (Stapel and de Jong, 1983). The levels of chicken NNE have been investigated during development at both the protein and mRNA levels (Tanaka *et al.*, 1985a; 1985b; 1995) and in neither case does lens accumulate significantly more gene product than liver. Furthermore, gel filtration analysis showed that all the chicken lens NNE existed as an

enzymatically active dimer and not as a monomer (Tanaka *et al.*, 1995). An interesting question raised by the above studies is why, in at least some birds and other lower vertebrates, should enolase have been recruited as a lens crystallin? It is unlikely that its catalytic properties would be valued in the lens, as the variety of independently recruited enzymes making up the crystallin population indicates a programme of neutral selection (Wistow *et al.*, 1990). It has been suggested that, as enzymes (including enolase) are often found in high concentrations to enhance substrate processing (Srivastava and Bernhard, 1986), they may have become pre-adapted to high protein environment found in the lens and therefore suitable for recruitment (Wistow *et al.*, 1988).

1.4 Expression and ontogeny of β-enolase (muscle-specific enolase)

1.4.1 Cell-type specificity

As described above, the early studies of rat enolase showed that expression of β-enolase (muscle-specific enolase, MSE) was restricted to skeletal muscle and heart (Rider and Taylor, 1974). In the former, almost all enolase activity was due to the ββ-enolase isoenzyme whilst in the latter, where the NNE and MSE subunits were coexpressed, the αβ-enolase heterodimer was shown to predominate. In adult rat, mouse and human skeletal muscle, immunohistochemical and *in situ* hybridisation studies have shown that MSE is preferentially expressed in fast twitch (type II) muscle fibres (Ibi *et al.*, 1983; Kato *et al.*, 1985; Keller *et al.*, 1992) whilst residual NNE is evenly distributed between fast and slow twitch fibres (Keller *et al.*, 1992). Studies in rat and mouse (Fletcher *et al.*, 1978; Kato *et al.*, 1985) showed that moderate levels of MSE were also found in cartilagenous tissue (again with the heterodimer predominating) and low levels of the protein could be detected in organs such as stomach and bladder which contain smooth muscle. Insignificant levels of MSE were found in other tissues.

In a number of mammals, the level of MSE protein in adult skeletal muscle has been shown to depend upon the functional state of the muscle and its innervation (Kato *et al.*, 1985; Matsushita *et al.*, 1986; 1991; Satoh *et al.*, 1991; Keller *et al.*, 1992a). Thus, MSE levels have been shown to decline following denervation, and this reflects a general decrease in the levels of enolase and other glycolytic enzymes (Prewitt and Salafsky, 1970; Shackelford and Lebherz, 1981). A moderate increase in NNE protein expression also accompanies denervation, and this may help to explain the

foetal enolase isoenzyme profiles observed in some neuromuscular disorders (Edwards *et al.*, 1982).

1.4.2 Developmental regulation *in vivo* and *ex vivo*

In rats, only the postnatal ontogeny of MSE has been considered in any detail (Rider and Taylor, 1974; Kato *et al.*, 1985; Sakimura *et al.*, 1989). By studying the relative amounts of the three muscle isoenzymes, a clear difference between heart and skeletal muscle ontogeny was demonstrated (Rider and Taylor, 1974; 1975a). In the heart, MSE was first detected postnatally and its contribution to total enolase activity rose from nothing to 30% by postnatal day 80. The profile of the three isoenzymes conformed to a best fit binomial distribution based on the abundance of the NNE and MSE subunits, indicating that the subunits were coexpressed, the isoenzymes being generated by random dimerisation. In contrast, MSE was already detectable in foetal skeletal muscle, where it contributed 20-40% of total enolase activity. The prevalence of MSE increased until postnatal day 30 when none of the NNE subunit could be detected. During this switchover, the profile of the three isoenzymes failed to fit a best fit binomial distribution, revealing a deficiency for the heterodimer. These data suggested that a rapid switch from NNE to MSE expression occurred during development and that the heterodimer formed only during the transient stage when both subunits were expressed.

In the mouse, isoenzyme analysis showed that postnatal accumulation of MSE protein was similar to the profile observed in rats (Fletcher *et al.*, 1978). The mouse studies have been more informative, however, because the investigators have considered earlier stages of development and have looked at the relative levels of *MSE* and *NNE* gene expression at both the protein and mRNA levels. Fletcher and colleagues found that MSE protein was already expressed in skeletal muscle, heart and tongue of the earliest stage mouse embryos they examined (E13) although in hind limb skeletal muscle, significant accumulation of the MSE protein did not occur until E17. Northern analysis showed that *MSE* mRNA could not be detected prior to E15 in hindlimb skeletal muscle (Barbieri *et al.*, 1990; Lucas *et al.*, 1992). The study by Lucas and colleagues showed that from E17, *MSE* became the predominant message; the accumulation was shown to be biphasic, the first steep rise occurring prenatally, and coinciding with the formation of secondary myofibres, the second beginning at P5, and coinciding with their definitive specialisation. The levels of *NNE* mRNA decreased over the entire developmental period studied, but the greatest decrease

occurred postnatally. Quantitative western analysis carried out in parallel showed that the transition from NNE to MSE in the mouse was controlled primarily at the level of transcription. The biphasic accumulation of *MSE* mRNA was shown to match that of another muscle-specific protein, α-skeletal actin, and the second phase of *MSE* mRNA accumulation coincided with the accretion of fast type IIB myosin heavy chain transcripts. No correlation between the increase in *MSE* message and the decline of *NNE* message could be detected, indicating that the two processes, whilst physiologically related, were regulated independently.

In vivo experiments, showing the onset of *MSE* gene expression in the hindlimb buds to be coincident with the formation of secondary myofibres, suggested that the gene could be used as a marker of late myogenesis. However, analysis of myoblast differentiation *ex vivo* indicated that gene expression commenced at a much earlier stage. As a model for myogenesis, Lamandé *et al.*, (1989) investigated the modulation of *NNE* and *MSE* mRNAs in premyogenic C3H10T½ cells and their myogenic derivatives and also in permissive and inducible C2.7 myoblasts. The *MSE* message was already detectable in both proliferating and quiescent myoblasts and accumulated further during terminal differentiation. The ratio of *MSE* to *NNE* mRNA increased about threefold and a recent study has shown that the increase in the abundance of *MSE* mRNA was due to upregulation of transcription and not to an increase in RNA stability (Lamandé *et al.*, 1995). Other muscle-specific messages, such as the mRNA for α-skeletal actin, were not detected in myoblasts (Lamandé *et al.*, 1989). C3H10T½ cells can be induced to differentiate into myoblasts or other cell types (e.g. adipocytes) by different chemical treatments. *MSE* was absent from undifferentiated C3H10T½ cells, but present in myogenic derivatives generated by treatment with hypomethylation agents or transfection with *MyoD1* cDNA. Taking the results from the *in vivo* and *ex vivo* experiments together, it was suggested that *MSE* could be expressed in particular subsets of myoblasts, specifically the adult myoblasts (also called satellite cells) which accumulate during late foetal development and give rise to secondary myofibres, but not in embryonic myoblasts which give rise to primary myofibres (Barbieri *et al.*, 1990). It is possible to discriminate between the two types of myoblast in culture on the basis of their response to various differentiating agents and their accumulation of myosin isoforms. This theory was therefore tested by assaying cultured embryonic and foetal myoblasts for the *MSE* message; this has been done in mouse (Barbieri *et al.*, 1990) and human cells (Peterson *et al.*, 1992). In the case of the mouse, *MSE* message was detected in foetal but not embryonic myoblasts as expected. Furthermore, when the myoblasts were differentiated *in vitro*, the expression of *MSE* mRNA in the secondary myotubes

was tenfold higher than that observed in the primary myotubes. In humans, undifferentiated embryonic and foetal myoblasts showed levels of *MSE* expression similar to the murine myoblasts, however, upon differentiation, both primary and secondary myotubes accumulated comparable levels of the *MSE* transcript. The authors argued that the apparent discrepancy between these results was attributable to differences in the developmental stage from which the embryonic myoblasts were obtained (Peterson *et al.*, 1992), the mouse embryonic myoblasts being derived from an earlier stage than the human cells. However, the more sensitive *in situ* hybridisation technique has been used to investigate *MSE* expression during very early myogenesis (Keller *et al.*, 1992a) and this analysis showed that a more limited accumulation of the message occurred in *primary* myofibres, starting as early as E7.8. *MSE* mRNA was first detected in the cardiac tube, the earliest myogenic structure to form, and expression of the transcript was also observed in the myotomes of rostral somites from E8.75. By E11.5, most developing skeletal muscles expressed detectable levels of *MSE* mRNA and MSE protein, but there was still no detectable expression in the limb buds. *MSE* transcripts were shown to start accumulating in the forelimb buds at E12.5, and in the hindlimb buds at E13.5, much earlier than results from previous northern analyses had suggested (Barbieri *et al.*, 1990; Lucas *et al.*, 1992). These experiments showed that the ontogeny of *MSE* was triphasic, the first (embryonic) stage marked by accumulation of the message and protein in primary myofibres at levels detectable by *in situ* hybridisation and *in situ* immunohistological assay but not by biochemical analysis, the second stage marked by a more pronounced accumulation in secondary (foetal) myofibres at levels detectable by northern and western procedures and the third (postnatal) stage marked by rapid replacement of embryonic enolase isoenzymes with MSE, coincident with final differentiation of the myofibres.

1.5 Expression and ontogeny of γ-enolase (neuron-specific enolase)

γ-enolase is known as neuron-specific enolase (NSE) because its expression is largely restricted to neuronal and neuroendocrine cells (Marangos *et al.*, 1979). Of the three mammalian enolases, NSE has accumulated the most literature, a) because of its use as a neuronal marker, based on the early studies of 14-3-2 protein (also known as *neuron-specific protein*); b) because it has found many clinical applications, specifically in the diagnosis of various tumours and diseases/injuries of the nervous system, and c) because it provides an insight into the mechanism of neuron-specific gene expression (Twyman and Jones, 1995b; *see* Chapter 2). Whilst this chapter

concentrates on the characteristics of *NSE* gene expression and regulation, the clinical uses of the enolases are outside its scope, however the interested reader can refer to several excellent reviews on the subject for further information (Marangos *et al.*, 1982; Zomzely-Neurath, 1983; Marangos and Schmechel, 1987).

1.5.1 Cell-type specificity

The first studies of NSE expression involved isoenzyme resolution and immunological analysis of crude tissue extracts. These investigations showed that NSE was abundant in mammalian brain (accounting for about 1.5% of soluble protein) but that it was also expressed, albeit at much lower levels, in all manner of peripheral tissues (Marangos *et al.*, 1975; Hullin *et al.*, 1980; Kato *et al.*, 1982; Jorgensen and Centervall, 1982; Haimoto *et al.*, 1985). In many glandular tissues the moderate levels of NSE protein were thought to reflect its expression in neuroendocrine cells, whilst the low amounts of NSE observed in nonneuronal tissue such as liver and muscle were attributed to innervation of these organs. In the brain, most NSE was found as the $\gamma\gamma$-enolase homodimer although the heterodimer accounted for about 30% of enolase activity (Fletcher *et al.*, 1978; Lucas *et al.*, 1988); in peripheral tissues, the heterodimer was predominant. Regional studies of the brain showed grey matter to be enriched for NSE whilst white matter contained mostly NNE (Marangos *et al.*, 1979; Zaiko and Burbaeva, 1986). Generally, levels of NSE protein were found to be higher in the central nervous system compared to the peripheral nervous system and neuroendocrine tissue, whilst the levels of NNE were similar in each. In some peripheral tissues, the presence of NSE was thought to reflect not innervation, but perhaps a genuine level of nonneuronal NSE expression. For instance, a significant amount of NSE was detected in platelets, which are neither innervated nor derived from the neurectoderm (Marangos *et al.*, 1980).

Whilst the analysis of bulk tissue extracts allowed the investigator to compare the abundance of the enolase subunits and the relative proportions of different isoenzymes, the use of this type of experiment was somewhat limited by its poor resolution. In the nervous system, which characteristically contains numerous cell types in a common tissue, the detection of NSE and NNE *in situ* was a more informative approach because such a strategy could discriminate between these disparate cell types. Such experiments showed that NSE was found only in the neurons of the nervous system, not in the glial cells or the vascular epithelial cells which instead expressed NNE. NSE was localised to neurons in the brain, spinal

cord, ganglia and retina (Pickel *et al.*, 1976; Schmechel *et al.*, 1978a; Marangos *et al.*, 1979). It was also localised to neuroendocrine cells of peripheral glandular tissue such as pinealocytes, adrenal chromaffin cells, Islets of Langerhans cells of the pancreas and parafollicular cells of the thyroid gland (Schmechel *et al.*, 1978b). Early investigations also provided evidence that NNE was *not* expressed in neurons (Schmechel *et al.*, 1978a; Marangos *et al.*, 1979; Ghandour *et al.*, 1981; Vinores *et al.*, 1984) thus the two enolase subunits were regarded as discrete markers of the two cell lineages within the nervous system, and hence their names.

Unfortunately, further investigations soon showed that the neuronal/nonneuronal enolase dichotomy described by Marangos and Schmechel was not so clear cut as was at first suggested. Various immunological studies provided evidence for the expression of NNE in at least some classes of neuron: for example, cerebellar stellate/basket cells were shown to contain both NNE and NSE subunits, although the hybrid αγ-enolase isoenzyme could not be detected in this assay (Schmechel *et al.*, 1980), and single cell resolution radioimmunoassay and immunocytochemical staining showed that Purkinje cells contained all three brain isoenzymes (Kato *et al.*, 1981). A consistent problem with many of these early experiments was that preparations of antisera were often quite crude, making it difficult to detect nonabundant isoenzymes. Perhaps the most convincing evidence against the mutually exclusive expression of NSE and NNE came from the prevalence of the hybrid αγ-enolase in the brain and other nervous tissue. Biochemical studies have argued strongly against the formation of artefactual heterodimers *in vitro* as a consequence of extraction techniques (Keller *et al.*, 1981; Shimizu *et al.*, 1983) indicating that the αγ-enolase must form *in vivo*, thus requiring a moderate number of cells to express both subunits. More recent analysis of *NSE* and *NNE* mRNA expression in the brain by *in situ* hybridisation has shown that most neurons do express both genes (Schmechel *et al.*, 1987; Watanabe *et al.*, 1990; 1993; Katagiri *et al.*, 1993; Keller *et al.*, 1994), whilst glial and other nonneuronal cells may express the *NNE* message but never the *NSE* message. Within the neuronal lineage, it is apparent that the relative amounts of the two gene products vary considerably depending upon cell type (Frikke *et al.*, 1987; Katagiri *et al.*, 1993; Keller *et al.*, 1994); this is similar to the heterogeneity of *MSE* and *NNE* gene expression in differentiating myoblasts (Barbieri *et al.*, 1990; Peterson *et al.*, 1992). In the most recent study, Keller and colleagues reported that many neurons, e.g. those of the hippocampus and lateral vestibular nucleus, appeared to contain similar amounts of each transcript. However, in some cases, e.g. neurons of the peripeduncular nucleus, high levels of *NSE* message were observed whilst *NNE* mRNA was undetectable. In these particular neuronal cells, therefore, it is possible

that a complete switchover from *NNE* to *NSE* gene expression may occur, akin to the switch from *NNE* to *MSE* in skeletal muscle. Furthermore, neurons of the solitary nucleus appeared to demonstrate opposite properties to those above, accumulating high levels of the *NNE* message, greatly in excess of the observed *NSE* mRNA. A number of investigators have studied enolase gene expression in Purkinje cells of the cerebellar cortex and the conclusions of these studies have varied, some authors reporting that such cells are immunopositive for NSE (Langley *et al.*, 1980; Schmechel *et al.*, 1980; Kato *et al.*, 1981) whilst others have reported that the same cells are immunonegative (Vinores *et al.*, 1984) or immunopositive only during a particular stage of development (Whitehead *et al.*, 1982). In an investigation involving both immunocytochemical staining and *in situ* hybridisation (Watanabe *et al.*, 1990), NSE immunoreactivity was observed in rat Purkinje cells from postnatal day 3. There was a striking increase in the level of detectable protein from P3 to P9 and this was reflected by a similar increase in the level of *NSE* mRNA, indicating that regulation of the *NSE* gene in these cells occurred at the level of transcription. From P9 onwards, the number of NSE immunopositive Purkinje cell bodies decreased and none were observed in adult brain, however, NSE immunopositive Purkinje axons were still detectable in adult rats. Conversely, the *NSE* mRNA was still present in Purkinje cell bodies from P9 to adulthood. The expression of *NNE* mRNA in Purkinje cells has also been documented (Katagiri *et al.*, 1991).

Two reports have indicated that oligodendrocytes lack detectable NNE (Langley and Ghandour, 1981; Ghandour *et al.*, 1981) and may therefore not express enolase at all. Although these data conflict with the earliest immunohistochemical investigations (Schmechel *et al.*, 1978a; 1980), recent *in situ* hybridisation studies have also provided evidence for the absence of *NNE* expression in white matter cells of the brain. The authors suggested that oligodendrocytes, which synthesise large amounts of lipid and fatty acids, may have dispensed with glycolysis and use an alternative oxidation pathway (Ghandour *et al.*, 1981) although this remains to be demonstrated.

1.5.2 Developmental regulation *in vivo*

Prior to the discovery of its enolase activity, the ontogeny of 14-3-2 protein (neuron-specific protein) was studied extensively in order to help determine its (at the time unknown) biological function. Although these investigations (reviewed by Moore, 1975) failed to determine a biological role for the protein, they concluded that the onset of expression coincided with neuronal differentiation *in vivo*. The discovery of

the NSE subunit in the rat prompted renewed investigation of the ontogeny of this protein (Fletcher *et al.*, 1976): the γγ-enolase isoenzyme was shown to be absent from the foetus, first becoming detectable at postnatal day 10. The heterodimer αγ-enolase was, however, already detectable in the foetus, indicating the earlier onset of NSE expression. Isoenzyme and immunological analysis, and biochemical studies of mRNA expression demonstrated a biphasic accumulation of NSE in the rat. By immunohistochemical staining, NSE protein was first detected at embryonic day 13, increasing to approximately 100-fold its initial concentration by P0 (Marangos *et al.*, 1980). By northern analysis, a similar pattern of *NSE* mRNA expression was revealed, although using this less sensitive technique, the *NSE* message was first detectable at E16, increasing threefold by P0. There followed a plateau, where no significant change in *NSE* gene expression occurred, then a subsequent rise in protein and mRNA levels lasting until P30 where gene expression remained at the same maximum level into adulthood (Fletcher *et al.*, 1976; Forss-Petter *et al.*, 1986; Di Liergo *et al.*, 1991). During this time, the levels of *NNE* mRNA and NNE protein remained steady (Marangos *et al.*, 1980; Di Liergo *et al.*, 1991). The parallel expression of mRNA and protein for each subunit indicated that the genes encoding them were regulated primarily at the level of transcription. In the mouse, immunological analysis of bulk tissue extracts has shown that NSE protein could first be detected at E 15 (Fletcher *et al.*, 1978). More sensitive immunohistochemical assays carried out by Forss-Petter and coworkers (Forss-Petter *et al.*, 1990) and during the course of this project (*see* Chapter 7) have demonstrated the presence of immunoreactive neurons in the ventral horn of the rostral neural tube as early as E10.5; it has also been claimed that NSE is present in the neuronal-glial precursor cells of embryos which contain no differentiated neurons at all (De Vitry *et al.*, 1980; Schubert *et al.*, 1985). Generally, experiments such as those described above have shown that in both mammalian and avian embryos, the levels of NSE protein are low pre- and perinatally, most accumulation occurring postnatally, whilst the levels of NNE protein are high in the embryo and remain so throughout development (Zomzely-Neurath and Keller 1977; Zomzely-Neurath, 1983; Marangos *et al.*, 1980; Secchi *et al.*, 1980; Ledig *et al.*, 1982; 1985; Maxwell *et al.*, 1982; Kato *et al.*, 1985; Lucas *et al.*, 1988; Gross *et al.*, 1990). The ontogeny of NSE is thus characterised by an increase in the NSE:NNE ratio, a developmental process which is more rapid in brain areas which develop quickly, such as the brainstem, compared to those which develop more slowly, such as the cerebral cortex (Marangos *et al.*, 1980; Zomzely-Neurath and Keller, 1977; Zomzely-Neurath and Walker, 1980).

In the developing nervous system, *NSE* mRNA and NSE protein could not be detected in the proliferative zones, which were immunopositive for NNE. *NSE* gene expression begins in postmitotic, postmigratory neurons, probably at the time when synaptic associations are made (Schmechel *et al.*, 1980). Because *NNE* gene expression in neuronal cells was not established until recently, the authors of this report concluded that a switchover from *NNE* to *NSE* gene expression occurred during neuronal differentiation, similar to the switch from *NNE* to *MSE* gene expression during myogenesis. As discussed above, recent data from *in situ* hybridisation studies has indicated that a complete switchover may occur in only a few neuronal cell types whilst the differentiation of most is characterised by the *onset* of *NSE* expression without significant effects upon the expression of *NNE*. Notwithstanding these results, NSE remains a useful marker of neuronal differentiation and neuronal/neuroendocrine cells generally. NSE has therefore been used to determine the innervation and neuronal architecture of various developing and adult peripheral tissues and organs including the chick eye (Zwaan *et al.*, 1994), human and rodent gut (Bishop *et al.*, 1982; Frykberg *et al.*, 1985), cutaneous *Merkel* cells (Gu *et al.*, 1981), muscles (Hachisuka *et al.*, 1984), mammalian respiratory tract (Sheppard *et al.*, 1982), Leydig cells of the testis (Angelova *et al.*, 1991) and avian and rodent organs of Corti in the developing inner ear (Whitehead *et al.*, 1982; Whilton and Sobkowicz, 1988; Altschuler *et al.*, 1985). It has also been used as an investigative tool in human development (Parsons *et al.*, 1981; Shinohara *et al.*, 1986)

1.5.3 Developmental regulation and induction *ex vivo*

Studies of NSE ontogeny using primary cultures of neurons dissociated from embryonic or foetal nervous tissue have generally supported the results from *in vivo* experiments where the levels of NSE reflected the extent of neuronal differentiation (Secchi *et al.*, 1980; Bock *et al.*, 1980; Schmechel *et al.*, 1980; Ledig *et al.*, 1982; 1985; Jirikowski *et al.*, 1983; Weyhenmeyer and Bright, 1983; Di Liergo *et al.*, 1991). Thus, the amount of gene product has usually been shown to increase with time in culture, concomitant with the extent of differentiation as judged by neurite outgrowth and other physiological characteristics. However, Bock *et al.* (1980) found that NSE could be detected only in trace amounts after culturing neurons for seven days whilst Secchi *et al.* (1980) found that NSE was already expressed in undifferentiated embryonic rat neurons after five days in culture. Primary cultures of neurons from foetal mouse spinal cord, dorsal root ganglia and brain have all been shown to be immunopositive for NSE (Schmechel *et al.*, 1980). Although such studies are broadly

in agreement, the different investigators have found varying levels of the protein or mRNA in primary neuronal cell cultures. Such discrepancies probably reflect differences in the cell type, location and developmental stage from which the cells were isolated and the levels of differentiation they attained in culture; this is similar to the enolase heterogeneity observed in cultured myoblasts (Barbieri *et al.*, 1990; Peterson *et al.*, 1992).

NSE expression has also been investigated in established cell lines. Immunological and isoenzyme profile analysis in various clonal cell lines has shown that NSE levels are low in proliferating neuroblastoma cells (contributing less than 3% of the total enolase activity) but higher in neuronal cell lines (contributing 10% of the total enolase activity, similar to levels in foetal brain) consistent with the relatively more differentiated phenotype of the neuronal cells (Zomzely-Neurath and Keller, 1977; Marangos *et al.*, 1978). In confirmation, the levels of *NSE* mRNA in various proliferating neuroblastoma cell lines are very low compared to primary cultures of rat neurons (Sakimura *et al.*, 1995). A number of investigators have shown that the levels of NSE protein and *NSE* mRNA in various neuroblastoma cell lines increase in response to differentiating agents (Marangos *et al.*, 1978; Legault-Demare *et al.*, 1982; Kornblatt *et al.*, 1983; Zeltzer *et al*, 1986; Cervello *et al.*, 1993; Matranga *et al.*, 1993) whilst the levels of NNE protein and *NNE* mRNA remain more or less constant (Kornblatt *et al.*, 1983; Matranga *et al.*, 1993). NSE expression can be induced by a number of chemical agents (dimethyl sulphoxide, retinoic acid, dibutyryl cyclic AMP (db-cAMP) and certain growth factors have been investigated) and by imposing growth conditions including serum withdrawal and increasing cell density. The inductive effects of these agents and conditions vary in potency, but the accumulation of NSE once again appears to correlate to the extent of physiological differentiation (as assessed by neurite outgrowth) and arrest of cell division, both of which mirror the maturation of neurons *in vivo*. Different reports of NSE induction have not always been in agreement, for example treatment of a neuroblastoma cell line with dbcAMP generated a twofold increase in NSE protein expression according to Marangos *et al.* (1978) whilst Matranga *et al.* (1993) showed that the same treatment generated a twentyfold increase in the levels of *NSE* mRNA. Such discrepancies might be attributable to different growth conditions, and the confluence of the cells when harvested would be a critical parameter in such studies. Furthermore, different agents promote the differentiation of human neuroblastoma cell lines into mixed populations of cells including neurons, Schwaan cells and melanocytes (Tsokos *et al.*, 1987). Slight differences in the treatments administered to proliferating neuroblastoma cells could therefore generate different mixtures of cells which would express varying

amounts of the induced genes (Matranga *et al.*, 1993). Density-dependent induction of *NSE* gene expression has been demonstrated (Legault-Demare *et al.*, 1980; Zeltzer *et al.*, 1986; Matranga *et al.*, 1993); the levels of NSE protein were reported to increase 20-25-fold during the slowing down of growth (Legault-Demare *et al.*, 1980) although no quantifiable data concerning the cell densities was provided in this report. The levels of *NSE* mRNA were shown to increase approximately eightfold given an eightfold increase in cell density (Matranga *et al.*, 1993) whilst the levels of mRNA for *NNE* remained constant. Induction of *NSE* gene expression by nerve growth factor has been reported for the pheochromocytoma cell line PC12 (Vinores *et al.*, 1981). PC12 cells are derived from (neuroendocrine) adrenal chromaffin cells, but they are stimulated by nerve growth factor (NGF) to differentiate *in vitro* towards a neuronal phenotype as judged by neurite outgrowth and other criteria (Green and Tischler, 1976). Vinores and colleagues showed that as little as 1ng/ml NGF could induce the maximal increase in *NSE* gene expression, a response which could not be elicited by insulin, growth hormone or epidermal growth factor (EGF), although the latter did cause a moderate induction of the gene. The developmental studies *in vivo* and *ex vivo* as well as the inductive studies using clonal cell lines have all provided evidence supporting the role of NSE as a marker of neuronal differentiation. Additionally, NSE can be used as a model for the analysis of inductive events caused by various chemical stimuli and growth conditions.

1.6 Mammalian and avian enolases - structure, function and evolution

In the preceding sections, the discovery of the mammalian enolases, and their expression and ontogeny have been discussed . A large body of evidence has established that the three subunits are encoded by three dispersed single-copy genes: this includes data from genomic Southern analysis, comparison of cDNA sequences and the mapping of each cytogenetic locus to separate chromosomes in man, rat and mouse (Khan *et al.*, 1974; Grzeschik, 1974; Van Cong *et al.*, 1977; Cook and Hamerton, 1979; Law and Kao, 1982; Craig *et al.*, 1989; Feo *et al.*, 1990a; Mitchell *et al.*, 1991; Göran Levan, pers. comm.); there is also a *NNE* pseudogene in the human genome (Feo *et al.*, 1990b). When enolase isoenzyme heterogeneity in the rat was first discovered, the authors asked why different subunits, with indistinguishable kinetic properties, should coexist (Rider and Taylor, 1974; Fletcher *et al.*, 1976). This question has remained pertinent, given the specific and independent regulation of the enolase genes as described above.

In recent years, a large number of enolase sequences has been published (see Table 1.2) and this has facilitated comparisons between the three isoproteins to reveal differences in structure which may in turn provide some clues about their individual functional roles. The number of independently verified clones has virtually excluded

Enolase	Species	Sequence	References	Comments
α (NNE)	rat	cDNA	Sakimura *et al.*, 1985a	
	mouse	cDNA	Kaghad *et al.*, 1990	
	human	cDNA genomic cDNA	Giallongo *et al.*, 1986 Giallongo *et al.*, 1990 Verma and Kurl, 1990	Lung enolase (1)
	duck	cDNA genomic	Wistow *et al.*, 1988 Kim *et al.*, 1991	α-enolase/τ-crystallin (2)
	chick	cDNA	Tanaka *et al.*, 1995	
β (MSE)	rat	cDNA genomic	Ohshima *et al.*, 1989 Sakimura *et al.*, 1990	
	mouse	cDNA genomic	Lamandé *et al.*, 1989	Unpublished (3)
	human	cDNA genomic	Calì *et al.*, 1990 Peshavaria *et al.*, 1989 Peshavaria and Day, 1991	
	rabbit	protein	Chin, 1990	
	chick	protein cDNA	Russel *et al.*, 1986 Tanaka *et al.*, 1995	
γ (NSE)	rat	cDNA cDNA genomic	Sakimura *et al.*, 1985b Forss-Petter *et al.*, 1986 Sakimura *et al.*, 1987	
	mouse	cDNA	Kaghad *et al.*, 1990	
	human	cDNA/protein cDNA cDNA cDNA genomic	McAleese *et al.*, 1988 Day *et al.*, 1987 Van Obberghen *et al.*, 1988; Oliva *et al.*, 1989 Oliva *et al.*, 1991	3' UTR only

Table 1.2: Origin of the known mammalian and avian enolase sequences. (1) Verma and Kurl (1990) have reported the sequence of a cDNA encoding enolase which they isolated from a human lung library. The lung enolase is most similar to NNE (Giallongo *et al.*,1986) but not identical; most remarkably, the deduced amino acid sequence is 458 residues in length, 25 residues longer than all the other reported mammalian sequences. (2) The duck α-enolase gene encodes a bifunctional protein also known as τ-crystallin (see section 1.3). (3) The mouse *MSE* gene sequence (N. Lamandé, S. Brosset, A. Keller, M. Lucas, and M. Lazar) is unpublished in the literature but is available from the databases under accession number X61600.

the problem of sequencing errors and it is therefore possible to compare the sequences of each subunit from mouse, rat and man without such errors confounding the observed variation. Each polypeptide is 433 amino acid residues in length and perfect alignment between all nine sequences is possible; this allows both paralogous (within species between unlike subunits) and orthologous (across species between like subunits) comparisons to be made in all possible pairwise combinations (see Table

1.3). It is also possible to align each mammalian sequence with that of *S. cerevisiae* enolase 1 (Holland *et al.*, 1981), allowing any substitutions found between subunits to be assessed with respect to the secondary and tertiary structure predicted for the yeast protein (Lebidoa and Stec, 1988; Lebidoa *et al.*, 1989; Stec and Lebidoa, 1990).

Species/ enolase	rNNE	rNSE	rMSE	mNNE	mNSE	mMSE	hNNE	hNSE	hMSE
rNNE	100	82.5 p	82.5 p	96 o	82.5	83	94 o	82	84
rNSE		100	83 p	83	98.5 o	84	84	83.5	83.5
rMSE			100	82.5	81.5	98.5 o	82.5	82	97 o
mNNE				100	83 p	84 p	83.5	83.5	83
mNSE					100	84 p	83	83.5	82.5
mMSE						100	83	82	97.5 o
hNNE							100	83 p	83 p
hNSE								100	83.5 p
hMSE									100

Table 1.3: Comparison of the primary amino acid sequences of each enolase isoprotein deduced from rat (r), mouse (m) and human (h) cDNA clones. Figures represent percent identity over entire amino acid sequences excluding the initiator methionine (432 amino acids). Paralogous comparisons (p) are highlighted in light grey. Orthologous comparisons (o) are highlighted in dark grey. Where multiple cDNA sequences exist, the following are used: human NSE - Oliva *et al.*, 1990; rat NSE - Sakimura *et al.*, 1985a. The lung enolase isolated by Verma and Kurl (1990) is ignored in this table.

The results of such comparisons show that there is greater identity between like subunits across species, than there is between unlike subunits within species. This underscores biochemical and immunological evidence which has shown that, between species, like isoenzymes have similar pI values and like subunits are immunologically cross-reactive (Cardenas and Wold, 1971; Moore, 1975; Rider and Taylor, 1974; 1975a; Clark-Rosenberg and Marangos, 1980; Jackson *et al.*, 1985; reviewed in Twyman and Jones, 1995c). Comparisons with the secondary structure predicted from crystallised yeast enolase showed that the major paralogous substitutions occurred at sites equivalent to yeast enolase 1 α-helices B, C, D, I and J which are presented on the surface of the protein and are not predicted to take part in substrate or cofactor binding (Day *et al.*, 1993); the eight β-strands which make up the active site of the enzyme are invariant between the human subunits (Peshavaria *et al.*, 1989). The kinetic similarity of the mammalian enolase isoenzymes is therefore thought to

arise from the invariant core structure of the polypeptides, whilst functional differences are thought to arise from surface properties which reflect interaction with other cellular components. Enolases throughout nature are well-known for secondary functions which are unrelated to catalysis: in the bacterium *Clostridium difficile,* enolase is thought to act as a toxin whilst in the yeast *S. cerevisiae*, enolase 1 is a heat shock protein (Green *et al.*, 1993; Iida and Yahara, 1985); the role of α-enolase in certain birds and reptiles has already been discussed (Wistow *et al.*, 1988). Compared to NNE, the expression of the tissue-specific enolases MSE and NSE is highly regulated and secondary functions are likely to reflect adaptations to specific intracellular environments. Hence, it has been shown that NSE is more resistant to chloride ion inactivation than NNE, and this might reflect an adaptation to the high intracellular chloride ion concentration of electrophysiologically active neurons (Marangos *et al.*, 1978). Both NSE and MSE have been shown to be more thermotolerant than NNE although the physiological relevance of this is not clear (Marangos *et al.*, 1978; Tanaka *et al.*, 1985a). NSE has been shown to undergo slow component axonal transport and to be associated both with other enzymes and the membrane at the synaptic terminal (Brady and Lasek, 1981; Batke et al., 1988; Lim *et al.*, 1983); such interactions would certainly require modifications to the surface structure of the protein. NSE has also been shown to act as a neuronal survival factor (Takei *et al.*, 1991); these and other observations provide some suggestions as to why three enolase isogenes have evolved and have come to be expressed in the manner discussed above, however, there is still much to learn about the roles of these proteins.

As well as providing data for functional autonomy amongst the enolases, sequence comparisons can provide some information about the evolution of the enolase gene family. Paralogous comparisons in man, rat and mouse show that the divergence between isoproteins is approximately 17% in all pairwise combinations, suggesting that all three genes were created during a single evolutionary event (Day *et al.*, 1993). The existence of an ancestral enolase gene is confirmed by the identical intron/exon architecture within the nine coding regions, with boundaries occurring at homologous positions in each sequence. Orthologous comparisons demonstrate that the burst event must have occurred before man/rodent speciation and the level of sequence identity observed between the limited bird enolase sequences and those of mammals indicate that it predated the divergence of birds and mammals (about 200 M yr ago); bird enolase genes also share the same intron/exon boundaries as their mammalian counterparts. Several authors have deduced that the event occurred approximately 300 M yr ago (Segil *et al.*, 1984; Clark-Rosenberg and Marangos, 1980). This timescale would indicate that three enolases should exist in most tetrapods, although

the *specialisation* seen in present day mammals and birds might not have arisen in all branches of the phylogenetic tree (see Twyman and Jones, 1995c). Orthologous comparisons also show how quickly each subunit is evolving: during man/rat speciation, only 8 amino acid substitutions occurred in the NSE subunit, 13 in the MSE subunit and 26 in the NNE subunit (Day *et al.*, 1993); once again, the majority of these substitutions occurred on the surface of the protein. These data show that in mammals, NNE is evolving most quickly whilst the two tissue-specific subunits are evolving slowly, probably due to additional constraints on surface residues imposed by their probable secondary functions.

1.7 The molecular basis of enolase gene regulation

1.7.1 The human *NNE* gene

Sites of interest	Character of human *NNE* gene
Basal Transcription	No TATA box GC rich, CpG:GpC ratio 0.95
Upstream promoter	No CCAAT boxes 5x CACCC (UPE) motifs
Consensus binding sites	AP1, AP2, AP3, AP4, AP5, ATF, CREB, C2, CTF/NF1, E2AE-Cβ, E2F, E4TF1, EF.C, HIF-1, MLTF/USF, Oct-1, PEA2 and Sp1 (3x).
Other consensus motifs	Viral core sequence GTGGAAAG
Other features of interest	Paired direct repeats: GGTGAAATCAC, GGCAGGAGG, CGGAGCCCCG and CCCCTTTCC Inverted repeat with the half sequence TGAATTTAAT

Table 1.4: Characteristics of the 5' putative reguatory region of the human *NNE* gene.

Very little is known about the regulation of mammalian *NNE* because no functional analysis has been carried out. About 2 kbp of the human *NNE* gene 5' flanking region has been sequenced and analysed for putative regulatory motifs (Giallongo *et al.*, 1990), and some characteristics of the gene are shown in Table 1.4. It has recently been reported that low blood oxygen tension (hypoxia) induces the expression the human glycolytic enzymes aldolase A, phosphoglycerate kinase 1 and pyruvate kinase M (Semenza *et al.*, 1994). A *trans*-acting factor termed hypoxia inducible factor 1 (HIF-1) has been identified which binds upstream of all three genes and transient transfection assays, in which each of these putative HIF-1 binding sites was used to drive a reporter gene, showed that the motif was sufficient in each case to confer

hypoxia-inducible reporter expression. HIF-1 binding sites are present upstream of other human glycolytic genes including those for phosphofructokinase L and nonneuronal enolase. Although the HIF-1 site in the *NNE* gene has not been tested by transfection analysis, synthetic oligonucleotides corresponding to the HIF-1 binding site of all five human genes, and the mouse gene for lactate dehydrogenase A, have been shown to bind HIF-1 in crude nuclear extracts and affinity purified preparations (Semenza *et al.*, 1994). These results strongly suggest that *NNE* may also be regulated by HIF-1.

1.7.2 The Peking duck α*ENO/*τ*CRY* gene

The duck α*ENO/*τ*CRY* gene has been cloned and about 1 kbp of its 5' flanking region has been sequenced and analysed for putative regulatory elements (Kim *et al.*, 1991; see Table 1.5). The authors noted that three of the potential binding sites upstream of α*ENO/*τ*CRY* had been implicated in the lens-specific expression of other crystallins: An NF-κB like motif found upstream of the murine α*A-CRY* gene was shown to be critical for lens-specific expression in transfection experiments and to bind a zinc finger transcription factor known as αA-CRYBP1 (Nakamura *et al.*, 1990); octamer-like motifs present upstream of the chicken β*B1-CRY* gene and the mouse γ*F-CRY* gene have also been shown to be important for lens-specific expression in transfection studies (Lok *et al.*, 1989; Roth *et al.*, 1991); finally, GC-rich motifs, including a putative Sp-1 site, have been shown to be important for the transcription of the chicken δ*1-CRY* gene (Das and Piatigorsky, 1986; 1988). However, transfection studies, in which about 800 bp of the α*ENO/*τ*CRY* 5' sequence was used to drive reporter gene expression in cultured liver, lens and fibroblast cells, showed no preferential gene expression in lens (Kim *et al.*, 1991). There is also evidence to suggest that the duck α*ENO/*τ*CRY* gene may be a candidate for regulation by c-myc (Warwar *et al.*, 1992). A comparison between the human *NNE* and duck α*ENO/*τ*CRY* 5' flanking regions showed that although the sequences differed significantly, two regions of homology could be identified (Kim *et al.*, 1991). The first, a sequence about 40 bp in length was located close to the start of transcription in both flanking regions; in the duck, this sequence appeared just once whilst in humans, another similar element was found about 350 bp upstream from the first. A second region of homology was found between positions -155 and -189 in the duck promoter and between positions -718 and -750 in the human promoter. In each case, the sequences demonstrated about 90% identity, however, their functional significance has not been tested.

Sites of interest	Character of αENO/τCRY gene
Basal Transcription	TATA box
Upstream promoter	3X CCAAT boxes
Putative lens-specific motifs	NF-κB, Oct-1, and Sp1
Other features of interest	Several GC-rich areas AT-rich region between -488/-605 Many repeats of ATTT motif Two regions of homology with human *NNE* 5' flanking region

Table 1.5: Characteristics of the 5' putative reguatory region of the duck *αENO/τCRY* gene. The relevance of the lens-specific motifs is discussed in the text.

Transgenic mice carrying the entire 13 kbp *αENO/τCRY* gene plus 3 kbp of 5' flanking region and 4 kbp of 3' flanking region have been generated to investigate how evolving lenses deal with sudden increases in the concentration of novel proteins and whether this affects their refractive properties (Kim and Wistow, 1993). However, the mice expressed duck *αENO/τCRY* in the same manner as endogenous *NNE* with no obvious accumulation of the message in the lens, suggesting that the *cis*-acting elements responsible for lens-specific control in the duck were either nonfunctional in the mouse or located outside the region covered by the transgene. The fact that τ-crystallin is not a prevalent lens crystallin in mammals supports the former explanation. Although lens preferred expression of the transgene did not occur, a sudden increase in protein concentration within the lens was evident simply due to the effects of gene dosage. Transgenic lenses were, however, still transparent and remained so well into old age, thus showing that the lens demonstrates considerable flexibility with respect to acceptable levels of intracellular protein and that the stepped increases in protein concentration which occur as enzymes are recruited during evolution are probably well-tolerated.

1.7.3 The rat, mouse and human *MSE* genes

Through studies of mRNA and protein expression, it has become well established that regulation of the enolase genes occurs primarily at the level of transcription. It is very likely that, in the case of *MSE*, such regulation involves the helix-loop-helix family of myogenic regulatory proteins. Evidence to support this statement is plentiful: in the embryo, *MSE* transcripts are first detected just after the early HLH regulators are expressed (Keller *et al.*, 1992a); undifferentiated C3H10T½ cells transfected with cDNAs corresponding to each member of the MyoD1 family differentiate into

myoblasts expressing high levels of the *MSE* transcript, demonstrating that *MSE* gene expression accompanies myogenic determination whichever factor is responsible (Lamandé *et al.*, 1989; Keller *et al.*, 1992b); and a survey of putative transcription factor binding sites in the 5' flanking region and introns of the human, rat and mouse *MSE* genes has revealed numerous myogenic binding motifs, including MyoD1-binding consensus sequences (Sakimura *et al.*, 1990; Peshavaria and Day, 1991; Keller *et al.*, 1992b; see Table 1.6). Comparitive analysis of the human and rat *MSE* 5' flanking regions has shown that the muscle-specific *cis*-acting elements occur at homologous positions suggesting a regulatory mechanism conserved across species (Giallongo *et al.*, 1993).

Sites of interest	**Human *MSE* gene**	**Rat *MSE* gene**
Basal Transcription	Canonical TATA box Single transcriptional start CpG:GpC ratio 0.54	Cannonical TATA box Single transcriptional start CpG:GpC ratio 0.47
Upstream promoter	No CCAAT boxes	No CCAAT boxes
Myogenic motifs	Within 800 bp of transcriptional start site: 2 binding sites for MyoD family proteins, M-CAT, CCArGG box	Within 1.8 kbp of transcriptional start site:10 binding sites for MyoD family proteins, CCArGG box
Other features of interest	Direct repeat CTGTCCCAGC Alternatively spliced 5' exon Muscle-specific methylation	Probably alternatively spliced 5' exon

Table 1.6: Characteristics of the putative reguatory region of the human and rat *MSE* genes. The CC(AT-rich)GG-box is also present in actin gene promoters (Gustafson and Kedes, 1989; Ng *et al.*, 1989). The M-CAT element has been shown to be responsible for the muscle-specific activation of the troponin T gene (Mar and Ordahl, 1990). The muscle-specific methylation site in the human *MSE* gene is a CpG dinucleotide which is fully methylated in sperm and brain but unmethylted in muscle (Peshavaria and Day, 1993).

Although *MSE* expression may be controlled by the myogenic HLH family of regulatory proteins following differentiation, it is unlikely that the same factors regulate the gene in proliferating myoblasts. HLH family proteins are present in myoblasts, but they have been shown to be inactive as transcription factors for muscle-specific genes in these cells (Vaidya *et al.*, 1989). Consistent with this theory is the high level of *MSE* expression in mutant C2C12 myoblasts in which expression of the entire MyoD1 family of regulators has been abolished (Peterson *et al.*, 1992). These data indicate that *MSE* is regulated by an alternative pathway in undifferentiated cells, and a recent investigation of the human *MSE* 5' flanking region using a deletion-transfection strategy has identified a 79 bp myoblast-specific enhancer element approximately 500 bp upstream of the start of transcription (Taylor *et al.*, 1995). As well as reducing reporter gene expression in cultured myoblasts,

deletion of this element resulted in elevated transcription of the *MSE*-luciferase construct in fibroblasts, suggesting that it also acts as a silencer in nonmyogenic cells. Gel retardation assays showed that protein(s) present in myoblast nuclear extract bound specifically to the 3' region of the enhancer, which contains an *ets* motif. However, transfection experiments indiciated that the *ets* motif alone was insufficient for myoblast-specific gene expression, indicating that other sequences within the enhancer were also required. The *MSE* enhancer shows homology to the myoblast-specific enhancer found upstream of the desmin gene (Li and Paulin, 1993) suggesting that myoblast gene expression might be coordinately regulated.

1.7.4 The rat and human *NSE* genes

Whilst mechanisms of muscle-specific gene expression are relatively well-understood, the basis of gene expression in neurons is less clear (Twyman and Jones, 1995b; *see* Chapter 2). In both cases, *cis*-acting elements and *trans*-acting factors are known to participate, but in the case of neuronal gene expression, much less is known about these participants. *NSE* represents a good model for the study of neuronal gene expression because it is tightly regulated and panneuronal, whilst many other neuronal genes are also expressed outside the nervous system or are restricted to particular subsets of neuronal cell types (Twyman and Jones, 1995b; *see* Chapter 2). Both the human and rat *NSE* genes have been cloned (Sakimura *et al.*, 1987; Oliva *et al.*, 1990) and extensive 5' flanking material has been sequenced in each case. A search for *cis*-acting elements has revealed a number of neuronal motifs and other elements which may be involved in the induction of the *NSE* gene by various differentiating agents (see Table 1.7). A comparison of the human and rat 5' flanking regions demonstrated 70% identity over about 1 kbp of sequence and many of the abovementioned *cis*-acting elements are conserved in both species, suggesting that the regulatory mechanisms may be shared (Oliva *et al.*, 1991).

Of the three mammalian enolase genes, functional analysis of the *NSE* gene has been most thorough. The studies can be divided into three groups: those involving transgenic mice, those based upon transduction using recombinant herpesvirus vectors, and those based upon deletion-transfection analysis.

Sites of interest	Human *NSE* gene	Rat *NSE* gene
Basal Transcription	Nonconsensus TATA (CCTATAGG) CpG:GpC ratio 0.54	Nonconsensus TATA (TCTATAGG) CpG:GpC ratio 0.6
Upstream promoter	No CCAAT boxes	No CCAAT boxes 5x CACCC (UPE) motifs
Neuronal motifs	CCAGG..CTG motif 2x in 5' region	CCAGG..CTG motif 3x in 5' region and 1x in intron 1. Neuronal ID element in 3' region Peptide hormone octamer
Relevant response elements		RARE, C/EBP, GRE, MTF-1, Octamer
Other features of interest	327nt *Alu* element at approx. position -800	Seven classes of repeated sequences of unknown function

Table 1.7: Characteristics of the putative regulatory regions of the human and rat *NSE* genes. Three elements known to be associated with neuronal gene expression are observed. A neuronal ID element is found 3' to the final exon of the rat *NSE* gene (Sutcliffe *et al.*, 1982; McKinnon *et al.*, 1986). An octameric motif, GCCCAGCC, which is present in several genes encoding peptide hormones (Haberner *et al.*, 1989) and is required for the specific expression of the gastrin gene in neuroblastoma cells (Thiel *et al.*, 1987) is found just downstream of the rat *NSE* TATA-like box, homologous to its position in other genes. This is particularly interesting because *NSE* is also expressed in the neuroendocrine system, however, in the human *NSE* gene, the central adenosine residue is replaced by a guanidine residue and it is not clear if this modified sequence would be functional. Both *NSE* gene 5' flanking regions contains several copies of a bipartite consensus motif CCAGG(AT-rich)CTG, which is present in the regulatory regions of many other neuronal genes (Twyman and Jones, 1995b; *see* Chapter 2). A fourth such element in the first intron of the rat *NSE* gene may be responsible for elevated neuron-specific gene expression (Sakimura *et al.*, 1995). *Ex vivo*, *NSE* is induced by various agents and growth conditions (see text). Response elements specific for some of those agents (e.g. retinoic acid) are found in the 5' flanking region of the rat gene.

Transgenic mice, carrying 1.8 kbp of the rat *NSE* 5' flanking region (including the first noncoding exon but not the first intron) fused to *Escherichia coli lacZ,* expressed the transgene almost specifically in the nervous system (Forss-Petter *et al.*, 1990). Of seven transgenic lines, the two which expressed the transgene most strongly were chosen for more extensive analysis and in each case, northern blots also showed that a number of aberrant *lacZ* transcripts were present in testis although no β-galactosidase activity could be detected. There *was*, however, transient β-galactosidase expression in the (nonneuronal) pigmented layer of the retina during development. Expression of the transgene was compared to endogenous NSE using immunohistochemical techniques, and as expected, NSE and β-galactosidase expression were both found only in neuronal cells of the brain, spinal cord and retina. Both the transgene and endogenous gene were expressed at different levels in distinct neuronal populations: for instance, stellate/basket cells were shown to express the transgene and endogenous gene at a relatively low level, in agreement with earlier immunohistological studies (Schmechel *et al.*, 1980). The transgenic lines which expressed the transgene weakly

were also analysed and in these cases, both the level and extent of reporter gene activity were less, thus β-galactosidase activity could not be detected in all classes of neuron. During development, there was parallel onset of reporter gene and endogenous gene expression, however, whilst endogenous mRNA accumulated in postnatal mice, the reporter transcript remained at embryonic levels. These results showed that the 1.8 kbp regulatory element contained all the *cis*-acting information required for correct spatial and early temporal regulation of the *NSE* gene but that additional elements, probably lying outside the region analysed, were responsible for the high level of gene expression in postnatal mice. The *NSE* 5' flanking region was also used in a recent study to drive the human *BCL-2* gene in transgenic mice (Martinou *et al.*, 1994). Although this study was concerned with the overexpression of BCL-2 protein and its effects on naturally occurring cell death in the developing nervous system, and not particularly with the specificity and efficiency of the *NSE* promoter, it also served to demonstrate that *NSE*-driven transgenes could vary in their modes of expression, with different transgenic mice showing onset of *NSE-BCL-2* at different stages (the earliest being at E13, much later than shown in the original study by Forss-Petter and coworkers). Martinou *et al.* also reported the presence of *NSE-BCL-2* transcripts in uterus, kidney, testis and heart, but not in vagina or liver, however, no human BCL-2 protein could be detected by immunohistochemical methods in any of these ectopic sites, suggesting that the transcripts were aberrant or unstable. Full expression of reporter genes driven by the *NSE* promoter was therefore found to be almost completely neuron-specific in two independent studies, however, transcription of the construct was somewhat leaky, leading to the observed ectopic transcription in various nonneuronal tissues.

Similar or identical expression cassettes have been subcloned into herpesvirus vectors for the purpose of transducing genes into cultured cells and into the central nervous system of live animals (Andersen *et al.*, 1992; 1993; Roemer *et al.*, 1995). In the first such experiment, the *NSE-lacZ* fusion gene (Forss-Petter *et al.*, 1990) was inserted into the *tk* locus of the wild-type HSV-I genome. Transduction of neuronal and nonneuronal cells in culture showed that β-galactosidase activity was neuron-specific, although no expression was detected in PC12 cells which *do* express endogenous NSE. Infection of live rats by injection of the recombinant virus into the right frontal lobe resulted in extended expression of the reporter gene in neurons, however, the numbers of transduced, expressing cells were limited and the authors concluded that although the *NSE* promoter was highly specific, it was not particularly efficient and was therefore not an ideal system for therapeutic use. Some β-galactosidase activity was also detected in immune cells, a phenomenon which the authors attributed to

phagocytosis of other transduced cells (Andersen *et al.*, 1993) and not to ectopic expression. In a more recent study, the 1.8 kbp *NSE* 5' regulatory sequence was fused to the firefly luciferase gene and inserted into an intergenic site in the genome of a replication deficient HSV-I (Roemer *et al.*, 1995). In this investigation, the reporter gene was expressed constitutively in all transduced cell lines, including PC12 and the nonneuronal line BHK. It is not clear why the cell-type specificity of the *NSE* promoter was lost in this series of experiments, but it could reflect a number of technical differences such as site of insertion or the use of a replication defective rather than a replication competent vector; several foreign promoters have been reported to be regulated in an unusual manner in the context of the herpesvirus genome and the position of integration has previously been shown to affect promoter activity (Roemer *et al.*, 1995 and references therein).

Although transgenic mice carrying an *NSE-lacZ* reporter construct were shown to express the transgene exclusively in neuronal cells (Forss-Petter *et al.*, 1990), undifferentiated ES cells stably transfected with the same expression cassette unexpectedly diplayed β-galactosidase activity (Alouani *et al.*, 1993). Further analysis showed that *NSE* mRNA was also present in undifferentiated ES cells, morulae and blastocysts, however the endogenous NSE protein could not be detected. These data suggested that factors resposible for the neuron-specific transcriptional regulation of *NSE* were already present in the very early embryo, however, these factors were presumably lost later on in development as RNA analysis experiments have shown that the *NSE* transcript cannot be detected in more advanced rat and mouse embryos until the biphasic accumulation associated with neurogenesis occurs (Forss-Petter *et al.*, 1986; Zeitoun *et al.*, 1983; Yoshida *et al.*, 1983). Consistent with this theory was the transient drop in both β-galactosidase activity and *NSE* mRNA levels accompanying the initiation of neuronal differentiation in the stably transfected cells (Alouani *et al.*, 1993). However, in long term culture, the levels increased once again and were positively regulated by attachment factors such as laminin and treatment with nerve growth factor (NGF). These data indicated that ES cells could provide an important model for the investigation of neuronal differentiation and the regulation of the genes involved in this process. The parallel behaviour of endogenous *NSE* and integrated *lacZ* also demonstrated that the 1.8 kbp *NSE* regulatory element was likely to contain not only the *cis*-acting elements responsible for spatial and temporal regulation of the gene, but also response elements for induction by NGF and other agents.

Deletion-transfection analysis is a very direct approach to identifying *cis*-acting elements responsible for gene regulation (Twyman and Jones, 1995b; *see* Chapter 2). Very recently, Sakimura and colleagues have reported an extensive study of rat *NSE* gene regulation based upon such a deletion-transfection strategy using primary cultured rat neurons, neurobastoma cell lines, PC12 cells, glial cells and nonneuronal HeLa cells (Sakimura *et al.*, 1995). A 4.5 kbp segment of the 5' flanking region (including the first exon and the proximal half of intron 1) was investigated by generating numerous stepwise and internal deletions, inversions and rearrangements and fusing the products to the *cat* reporter gene. Comparisons of normalised reporter activities in neurons showed that deletion to the *Sac* I site corresponding to the start of the 1.8 kbp regulatory element used in previous studies caused only a slight reduction in reporter activity, whilst external deletion to a proximal *Xho* I site just 250 bp upstream of the transcriptional start site only reduced reporter expression to 70% of its maximum value. However, removal of the proximal half of the first intron reduced CAT activity by at least twentyfold, regardless of the presence or absence of 5' flanking sequences; similar results were obtained for NGF treated PC12 cells. These results indicated that *cis*-acting elements present in the proximal half of the first intron were crucial for high level gene expression in neurons and PC12 cells, thus it is interesting to note that transgenic mice lacking the intron are still capable of expressing a reporter gene driven by the *NSE* 5' flanking sequence in a neuron-specific manner (Forss-Petter *et al.*, 1990). When the short *Xho* I external deletion construct lacking intron 1 was transfected into nonneuronal cells, low but significant CAT activity, about fiftyfold less than the level seen in neurons, was observed. Addition of intron 1 and 2.7 kbp of 5' flanking sequence separately and in combination made little difference to the levels of CAT activity, indicating that elements in the intron and 5' flanking region were neuron-specific and not constitutive enhancers of gene expression. It is possible that the 5' flanking region of the *NSE* gene contains spatial and temporal controls whilst the intron contains strong neuronal enhancers; this might explain why transgenic mice carrying the *NSE-lacZ* transgene express β-galactosidase correctly, but are unable to match the high levels of endogenous gene expression in adult animals.

1.7.5 Posttrancriptional regulation of enolase

In certain eukaryotes, it is apparent that enolase gene expression is regulated in a complex manner, often at the levels of transcription, RNA processing, protein synthesis and beyond (Twyman and Jones, 1995c). It has been reported that chicken

NNE is phosphorylated in Rous Sarcoma Virus (RSV) transformed chick fibroblast cells (Cooper *et al.*, 1983) and further *in vitro* experiments have shown that chicken NNE and rabbit MSE, but not chicken MSE are phosphorylated on the same tryptic peptide fragment by RSV tyrosine kinase (Cooper *et al.*, 1984). Recent sequence data has shown that a tyrosine residue at position 44 in the chicken NNE sequence and in the equivalent position in all mammalian enolases is replaced by histidine in chicken MSE (Tanaka *et al.*, 1995), however, no kinetic differences between phosphorylated and nonphosphorylated chicken NNE have been observed and the significance of this obscure posttranslational modification, if any, remains to be determined (Eigenbrodt *et al.*, 1983).

In mammals, there is evidence that both *MSE* and *NSE* genes are regulated posttranscriptionally although transcription appears to be the most important level of control. Orthologous comparisons of cDNA sequences has shown that the 5' and 3' untranslated regions (UTRs) of the genes are highly conserved. This is particularly striking in the case of *NSE* because, in common with many other neuronal genes, the 3' UTR is very long (approximately 1 kbp) yet there is still over 70% identity between rat, mouse and human sequences. It is apparent that the long *NSE* 3' UTR came into existence by an evolutionary insertion event, as there is a long sequence of consecutive adenosine residues approximately 150 bp from the 3' end of the coding region, a position homologous to the polyadenylation sites of the yeast *ENO1* and *ENO2* and the mammalian *NNE* genes (Day *et al.*, 1987). There are also numerous tandem repeats of the sequence ATTT about 400 bp from the 3' end of the coding region (Day *et al.*, 1987), which have been shown to influence mRNA stability in other genes (Shaw and Kamen, 1986). A further repetitive motif, CCACCG, is found in the short *NSE* 5' UTR although its significance is unknown. Posttranscriptional negative regulation of *NSE* has been proposed on the basis of evidence showing that the message accumulates faster than the encoded protein during neuronal differentiation both *in vivo* and *ex vivo* (Forss-Petter *et al.*, 1986; Di Liergo *et al.*, 1990). The differential expression of NSE protein and *NSE* mRNA in Purkinje cells (Watanabe *et al.*, 1990) and the recent demonstration that *NSE* mRNA but not NSE protein accumulates in murine ES cells and preimplantation embryos (Alouani *et al.*, 1993) provides further support. Finally, in two studies of *NSE*-transgenic mice, transcripts were found in both neuronal and nonneuronal tissue, whilst reporter protein was found only in neuronal tissue (Forss-Petter *et al.*, 1990; Martinou *et al.*, 1994).

Heterogeneity at the 5' end of human *MSE* mRNA provided the first evidence for posttranscriptional regulation of the *MSE* gene (Peshavaria and Day, 1991). RACE cloning confirmed that the *MSE* gene gives rise to two alternatively spliced products by differential utilisation of two splice donor sites and one splice acceptor site within exon 1 (Giallongo *et al.*, 1993). The two mRNAs differed from each other in the presence or absence of a 42 base leader sequence and alternatively spliced *MSE* messages of similar structure have been found in mouse (S. Ventura, unpublished) and, based upon cDNA sequence comparisons, probably also exist in rat (Ohshima *et al.*, 1989; Giallongo *et al.*, 1993). Although each splice product encodes the same protein, the secondary structures predicted from the primary sequence data suggested that differential translational controls may be operative, as has been described for other eukaryotic genes (Alberts *et al.*, 1994). Although the role of alternatively spliced *MSE* transcripts is not known, their cross-species conservation argues for an important regulatory function.

1.8 Concluding comments

In this Chapter, we have discussed the expression, ontogeny and regulation of the three enolases in mammals and birds, with particular emphasis on recent investigations into the molecular basis of enolase gene regulation. The present study, which examines regulation of the rat neuron-specific enolase gene, will hopefully contribute to the growing literature on this important subject.

Chapter 2 - The Molecular Basis of Neuron-Specific Gene Expression in the Mammalian Nervous System

As discussed in the previous chapter, one of the major reasons for studying neuron-specific enolase is to find out more about neuron-specific gene regulation in general, a subject which is still poorly understood (Mandel and McKinnon, 1993). The purpose of this second introductory chapter is therefore to summarize the current litereature embracing the molecular basis of neuronal gene expression in the mammalian nervous system and as such, it has been published as a review (Twyman and Jones, 1995b).

2.1 Gene expression in the mammalian nervous system.

The development of a multicellular organism from a fertilised egg involves the progressive and hierarchical restriction of gene expression in time and space. Eventually, each differentiated cell comes to express a characteristic set of gene products, conferring upon it specific biochemical and physiological properties which can be termed its phenotype. In mammals, many genes are expressed only in the nervous system and a great number of these are restricted to the neuronal cell lineage. The gene encoding neuron-specific enolase is an example of a *panneuronal* gene, a gene expressed in all cells of neuronal origin. Panneuronal genes encode proteins which are responsible for those characteristics general to all neuronal cell types (e.g. electrophysiologically excitable membranes, exit from the cell cycle, neurite outgrowth and formation of synaptic junctions). Other neuronal genes may be described as *subneuronal* because they are expressed in a subset of neuronal cell types and encode proteins which are responsible for the individual characteristics of particular subpopulations of cells (e.g. neurotransmitter phenotype).

The mammalian nervous system originates from two major embryonic tissues. The central nervous system (CNS) is derived from the neural tube whilst the majority of the peripheral nervous system (PNS) is derived from the neural crest, the remainder originating from placodes of ectodermal origin. Within the adult nervous system, there is an incredible variety of cell types, the origins of which are considered in two excellent reviews concentrating on the CNS and PNS lineages respectively (Anderson, 1989; McKay, 1989). In the last few years, much attention has been directed towards the function and regulation of genes involved in the developing nervous system, specifically to those genes responsible for the determination of cell fates (reviewed by Lemke, 1993). Other groups have aimed to explain the effects of

neurotrophic factors, a family of polypeptides whose members exert development-related effects upon neurons (see Barde, 1991); of these, the best characterised is nerve growth factor (NGF) (Levi-Montalclini, 1987). Neurotrophic factors are thought to exert their effects by stimulating the expression of *early response* or *immediate early genes* (Sheng and Greenberg, 1990), a class of genes encoding transcription factors which directly or indirectly regulate the expression of the *terminal* or *late response genes* in the nervous system, those responsible for neuronal phenotype. Although such studies have already provided much information concerning the genetic control of neural development, it is apparent that there is still a 'missing step' between the early stages of neurogenesis and the maintenance of the neuronal phenotype in the mature animal. At present, investigators are attacking this problem from both ends, i.e. by studying the regulation of neuron-specific genes and the downstream targets of neurogenic genes and immediate early genes. The present study of neuron-specific enolase gene regulation contributes to the former.

2.2 Strategies for studying gene regulation.

Most genes are regulated at the level of transcription, primarily by interaction between diffusible *trans*-acting factors and *cis*-acting DNA elements located near to the transcribed region of the gene (reviewed by Maniatis *et al.*, 1987). Generally, the *cis*-acting elements consist of a core *basal promoter*, which is absolutely required for minimal gene expression, and any number of additional upstream regulatory elements which modulate that expression either constitutively (i.e. in all environments) or confer upon the gene its spatial, temporal and inducible specificity. It is desirable to identify particular functional elements within this upstream region as such elements often represent sites where *trans*-acting factors bind to the DNA.

Genes may be studied as intact units, in which case a suitable assay must be available to detect and measure the gene product. In such cases, the gene is usually studied in a surrogate environment, e.g. a transgenic mouse containing an integrated human gene. It is usually more convenient, however, to study gene regulation indirectly by fusing the putative control elements of the gene under investigation to a *reporter gene*, a heterologous gene whose product can be assayed easily and quantitatively. Common reporter genes used in animal studies include those encoding the enzymes β-galactosidase (β-gal), chloramphenicol acetyltransferase (CAT) and luciferase (luc). The advantage of using reporter constructs, rather than intact genes, is that assays can

easily be carried out in cell lines or *in vivo* where the endogenous gene is also expressed.

A general strategy for the analysis of gene regulation is to identify important *cis*-acting elements in the flanking region of a given gene by deleting, rearranging, substituting or otherwise modifying specific regions of the putative regulatory sequence and comparing the performance of the modified and unmodified constructs. Preliminary results may be obtained by simple stepwise deletions but these may need to be refined and reinforced by observing the effects of internal deletions, linker scanning mutations and finally, specific point mutations. There are two major approaches to the analysis of gene regulation: a cell line approach, involving the transfection of reporter constructs into a variety of permissive and nonpermissive cell lines, and a transgenic approach, involving the analysis of gene expression *in vivo*. Each has its advantages and disadvantages (see Table 2.1). Gene expression may also be analysed *in vitro* using protein extracts from cell lines and organs; *in vitro* transcription assays may succeed where the transfection approach has failed (e.g. Schwartz *et al.*, 1994). Usually, the *in vitro* approach is used to identify protein binding sites, e.g. by using gel retardation and footprinting assays.

Cell line approach:	
Advantages:	Easy technique with rapid results.
	Many constructs can be studied during a single experiment.
	Can study specific inductive responses and *trans*-activation/repression.
Disadvantages:	No indication of temporal or spatial regulation.
	Often limited by properties of available cell lines; sometimes difficult to identify cell lines with appropriate properties.
	Established cell lines may not accurately represent conditions *in vivo*.
	Introduction of too much DNA may titrate out available transcription factors.
	Transfected DNA does not respond to endogenous *cis*-acting factors such as distant enhancers, chromatin effects, replication timing and methylation.
Transgenic approach:	
Advantages:	Spatial and temporal gene regulation can be observed, often at single cell resolution.
	Transgenes respond to true *in vivo* conditions.
	Usually only a limited number of copies integrated so that transcription factors will not be titrated out.
Disadvantages:	Technique more difficult and time-consuming, making it less easy to study many constructs at once.
	Integrated gene may be subjected to unfavourable position effects.

Table 2.1: Advantages and disadvantages of the cell line and transgenic approaches to the analysis of gene regulation.

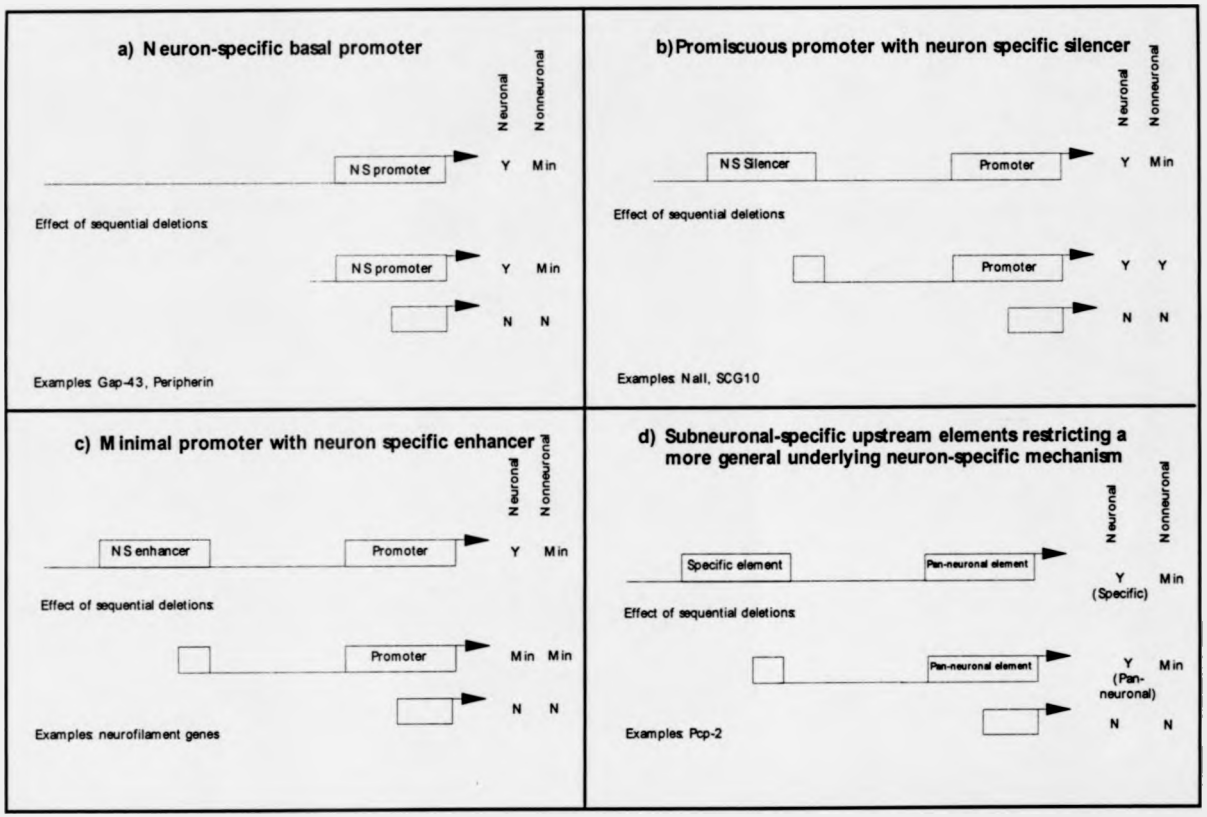

Figure 2.1. Principle mechanisms of neuron-specific gene expression based upon the results of hypothetical transfection experiments using neuronal and nonneruonal cells (see text for details). Example genes for each mechanism are given. Abbreviations Y/N - Yes/No to gene expression in the cell line shown. NS = neuron-specific; Min = minimal gene expression

2.3 Mechanisms of neuron-specific gene expression

For many eukaryotic cells, the *cis*-acting elements responsible for cell type specific gene transcription have been identified and well-characterised. For instance, the molecular basis of muscle-specific gene regulation is now understood in detail (reviewed by Buckingham, 1994). Although neuron-specific gene regulation has been under study for the last ten years, its molecular basis remains largely unclear. Many neuronal genes possess a GC-rich, housekeeping type promoter although just as many have typical TATA box-containing class II promoters or intermediate type promoters; in each case, transcription may be initiated at single or multiple start sites. A number of motifs have been identified which appear to be important for the cell type specific expression of small groups of neuronal genes, but no panneuronal mechanism of gene control has emerged. It is possible that both the promoter and regulatory element heterogeneity reflect the variety of distinct neuronal cell types in the nervous system, which, in addition to a ubiquitous control mechanism, would require distinct developmental programmes. Recent studies indicate that neuronal gene expression can be achieved by three principle mechanisms (Figures 2.1a-2.1c) which may operate alone or in combination. In each case, the *cis*-acting elements responsible for cell-type specificity may be supported by further elements which act constitutively. Genes expressed in specific neuronal subpopulations (rather than panneuronally) are often regulated by modular elements which act to restrict expression driven by a more promiscuous underlying programme (Figure 2.1d). In the following sections, these four mechanisms are examined in detail with examples taken from the recent literature. There is then a brief discussion of some putative regulatory motifs which are common to several neuronal genes and finally a gene table which summarises the studies of neuron-specific gene expression to date.

2.3.1 Neuron-specific gene expression conferred by a basal promoter

The analysis of a number of neuronal genes has shown that the functional cell type-specific regulatory elements lie very close to the transcriptional start site meaning that most of the 5' flanking region can be deleted without affecting the specificity of gene expression. The smallest functional regulatory element is often less than 300 bp in length, which suggests either that the basal transcriptional apparatus may be preferentially active in neuronal cells (as shown in Figure 2.1a) or that neuronal control elements are located very close to the basal promoter (as shown in Figures 2.1b and 2.1c).

The existence of a neuron-specific basal promoter has been proved beyond doubt in the case of the mouse peripherin gene which encodes a panneuronal but PNS-preferred neuronal intermediate filament protein. The 5' flanking region was dissected by Desmaris *et al.* (1992) who showed that as little as 98 bp of sequence upstream from the transcriptional start site was sufficient for cell-type specific reporter gene activity following transfection. Minute analysis of this region by DNase footprinting identified three protected fragments: PER1, PER2 and PER3. Targeted mutation of these regions showed that PER1, which overlapped the TATA box, was required for cell-type specific expression whilst PER2 and PER3 were required for general, constitutive upregulation. The neuron-specific element PER1 probably interacts with the basal transcription apparatus as deletion experiments have shown that it cannot be removed without the loss of expression in *all cells*; this is the essential point of Fig 2.1a. Two possible mechanisms of core promoter specificity have been reported: Tamura *et al.* (1990) have shown that different forms of the basal transcription factor TFIID exist in extracts of brain and liver, and that these factors differentially support expression of the myelin basic protein gene. Thus, neuronal specificity could be brought about by the existence or activity of a basal transcription factor only in neuronal cells. Secondly, Wefald *et al.* (1990) have shown that the context of the TATA box may influence the way in which ubiquitous transcription factors interact with tissue-specific factors located elsewhere in the gene and this is another possible explanation for cell type-specific expression of peripherin.

Neuron-specific core promoters are also thought to control transcription of the rat GAP-43, synapsin I and calmodulin II-encoding genes as well as the mouse gene encoding synapsin II. However, although cell type-specific expression has been observed for short reporter constructs in all cases, the proximal regulatory sequences have not been studied by footprinting and might conceivably contain independant enhancers or silencers upstream of a nonspecific promoter, as shown in Figures 2.1b and 2.1c. *GAP-43* encodes a panneuronal axonal growth-associated protein (neuromodulin, B-50) which is expressed preferentially in immature and regenerating neurons. Dissection of the 5' flanking region (Nedivi *et al.*, 1992) revealed a neuron specific promoter extending 386 bp upstream of the transcriptional start site. Interestingly, this core sequence was flanked by two unusual DNA elements; one, a short sequence of alternating purines and pyrimidines with the potential to form left-handed Z-DNA (Rich *et al.*, 1984) and the other, a long polypurine sequence with the potential to form triple stranded H-DNA by Hoogsteen base pairing

(Htun and Dahlberg, 1989). In transfection experiments, deletion of either of these unusual elements resulted in the severe repression of transcription, but if both were present, there were no adverse effects. It is therefore possible that *GAP-43* gene expression is mediated by countermodulation, involving interaction between the elements.

Synapsins are membrane-associated phosphoproteins localised in the presynaptic termini throughout the nervous system. There are four synapsin proteins, (Ia and Ib, IIa and IIb) which are produced by alternative splicing of the two synapsin genes. Neuron-specific core promoters are thought to be present in the rat synapsin I and mouse synapsin II genes (Saurwald *et al.*, 1990; Chin *et al.*, 1994; Howland *et al.*, 1991) but not in the human synapsin I gene (G. Thiel *et al.*, 1991). All the promoters appear to be of the housekeeping type, with no canonical TATA box, and there is only one transcriptional start site for each of the genes. The 5' flanking region of the rat synapsin I gene was dissected by Saurwald *et al.* (1990) who found that 225 bp of upstream sequence and 105 bp downstream from the transcriptional start site was sufficient to drive cell type-specific expression in transfection experiments. Thiel *et al.* (1991) showed, however, that the human synapsin I gene was driven by a nonspecific basal promoter, which extended 115 bp upstream of the transcriptional start site, and one or more neuron-specific enhancer elements located further upstream but within 422 bp of the start. The 5' region of the rat synapsin II gene was analysed by Chin *et al.* (1994) and was shown to comprise a neuron-specific promoter extending 153 bp upstream of the transcriptional start site and a number of neuron-specific positive and negative elements located further upstream. The synapsin genes therefore demonstrate that gene regulation is often more complex than shown in Fig 2.1, and may involve a combination of alternative mechanisms.

2.3.2 Promiscuous transcription repressed by a neuron-specific negative modulator

A neuron-specific *negative modulator* would function in nonneuronal cells and would confer cell type-specificity upon a nonspecific basal promoter. By sequential deletion, it should be possible to remove the modulator and allow the expression of a reporter minigene in a wider variety of cell types; these are the essential features of Fig 2.1b. Should such an element function in an orientation and position independent fashion, and be capable of conferring neuronal specificity upon a heterologous promoter, it would then constitute a *silencer* (Brand *et al.*, 1985).

The first gene discovered to be regulated by a neuron-specific negative element was the rat *NaII* gene encoding the type II sodium channel (NaII). Sodium channels are transmembrane-gated ion channels which confer upon neurons and other cells the property of electrical excitability. The type II sodium channel is one of four such proteins differentially expressed in neurons and it belongs to a large protein family, other members of which are expressed in muscles and glia (for a review, see Mandel, 1992). Of the neuronal sodium channel genes, the type II gene is the best candidate for the study of neuron-specific gene regulation because it is the only gene expressed strongly and panneuronally in the adult nervous system. A reporter gene, driven by 1051 bp of *NaII* 5' flanking sequence was generated by Maue *et al.* (1990). In transfection experiments, this construct was expressed in cells of neuronal origin but neither in excitable nor nonexcitable cells of nonneuronal origin. Stepwise 5' deletions identified a number of negative regulatory elements, the strongest of which was located between 983 and 1051 bp upstream of the transcriptional start site; when this region was deleted, a ninefold upregulation of reporter expression in nonneuronal cells was observed. The functional element (then called repressor element 1, RE1) was identified by footprinting as a 28 bp motif with the sequence ATTGGGTTTCAGAACCACGGACAGCACC (Kraner *et al.*, 1992). This element fulfilled all the properties of a silencer and was later renamed the neuronal restrictive silencer element (NRSE) (Mori *et al.*, 1992). Kraner and colleagues also performed gel retardation assays and identified a protein present only in nonneuronal cell extracts which bound specifically to the NRSE.

The regulation of the rat neuron-specific *SCG10* gene was studied by transfection (Mori *et al.*, 1990) and in transgenic mice (Wuenschell *et al.*, 1990). SCG10 is another axonal growth-associated protein which is homologous to the ubiquitously expressed protein strathmin but unrelated to GAP-43 (for a review, see Okazaki *et al.*, 1993). 500 bp of the 5' flanking sequence was shown to confer no cell type-specificity either in cell lines or *in vivo*, although a number of constitutive enhancer elements were identified. However, a construct containing 4 kbp of upstream sequence was neuron-specific. Further characterisation of this upstream region (Mori *et al.*, 1992) revealed an element which was very similar in sequence and function to the *NaII* silencer, and bound a similar sized protein, which was termed the neural-restrictive silencer [binding] factor (NRSBF, NRSF).

The discovery of similar functional *cis*-acting elements in two neuron-specific but otherwise unrelated genes prompted a search for conserved elements in other neuronal promoters, some of which are shown in Table 2.2. Homologous elements have now been identified in 18 neuronal genes demonstrating a mean identity of 93% to the consensus (Schoenherr and Anderson, 1995). In addition to the *NaII* and *SCG10* NRSEs, two further elements - those in the synapsin 1 (Saurwauld *et al.*, 1990; G. Thiel *et al.*, 1991; 1994; L. Li *et al.*, 1993) and Na,K-ATPase subunit genes (Pathak *et al.*, 1994) - have been shown to be functional. Analyses of the putative NRSEs upstream of the human and rat synapsin 1 genes (Saurwald *et al.*, 1990; G. Thiel *et al.*, 1991) at first failed to demonstrate their neuron-specific silencer activities. L. Li *et al.* (1993) reported that the putative silencer element located in the human synapsin I promoter was indeed functional and that deletion of the element caused an upregulation of synapsin I-reporter expression in nonneuronal cell lines, however, statistical analysis of the results suggested that the observed upregulation was not significant. G. Thiel and colleagues have shown that the NRSE in the human synapsin I promoter overlaps a binding site for the positive transcriptional activator Krox-24 (G. Thiel *et al.*, 1994). They have shown that the

Rat *BDNF*	TTCAGCACCTTGGACAGAGCCa I IIIII IIIII I II g TGATGGTGGAGCCTGTTTAGGc
Human *DBH*	gGTCAG..CGCTGGACAGCTCCtcg
Rat *NaII*	catTTCAGCACCACGGAGAGTGCCtctgct
Rat *SCG10*	ggtTTCAGAACCACGGACAGCACCagagt
Human synapsin I	ggaTTTAGTACCGCGGACAGAGCCttcgc
Rat synapsin I	agcTTCAGCACCGCGGACAGTGCCttcgc
Consensus	**...TTYAGNACCRCGGASAGNRCC....**

Table 2.2: Comparing the sequences of some of the known neural restrictive silencer elements (adapted from Fig 4 in Mori *et al.*, 1992). In the human *DBH* element, maximum alignment has been achieved by inserting gaps (represented by stops). Base pair complementarity is shown between the two contiguous sequences present in the *BDNF* promoter. Nomenclature for ambiguous nucleotides: R = G or A (puRine), Y = C or T (pYrimidine), S = G or C (three bondS), N = any Nucleotide.

NRSF can prevent transactivation of synapsin I reporter constructs by Krox-24 *in vitro* and propose that interaction between Krox-24 and the NRSF mght therefore play a pivotal role in the regulation of this gene.

A cDNA encoding the NRSF has recently been isolated from a HeLa λgt11 library using a probe comprising three tandem repeats of the *Na11* NSRE (Schoenherr and Anderson, 1995). A partial cDNA was isolated which encoded a novel protein containing eight zinc finger motifs. *NRSF* mRNA was absent from neuronal cell lines, including PC12 cells, but present in glia and fibroblast cells. *In situ* hybridisation to mouse embryos showed that *NRSF* transcripts could be detected in the proliferative ependymal layer of the neural tube, but not in the mantle zone which is rich in postmitotic neuronal cell bodies. The expression domains of *SCG10* and *NRSF* mRNA in the neural tube were mutually exclusive and complementary. Northern and RNase protection analysis showed that, excluding the nervous system, expression of *NRSF* mRNA was nearly ubiquitous throughout the mouse embryo, supporting the role of NRSF as a widespread inhibitor of neuronal gene expression in nonneuronal tissue.

Although only four of the NRSEs have been shown to be functional as neuronal silencers, those from six other genes bind specifically to recombinant NRSF *in vitro* (Schoenherr and Anderson, unpublished observations). Similar elements have also been observed in the flanking regions of several nonneuronal genes, although they demonstrate only 84% identity to the consensus NRSE compared to 93% for those in neuronal genes. NRSF activity has also been reported in neuronal as well as nonneruonal tissue (Thiel *et al.*, 1994) although this conflicts with earlier reports (Mori *et al.*, 1992; Kraner *et al.*, 1992). The BDNF gene locus contains two NRSEs, inverted with respect to each other, between two brain-specific promoters (Timmusk *et al.*, 1992). A homologous element has also been identified in the 5' flanking region of the human dopamine β-hydroxylase (*DBH*) gene which has been shown to possess a relatively promiscuous basal promoter (Ishiguro *et al.*, 1993). If functional, however, the silencer must work in concert with a cAMP responsive neuron-specific enhancer which was shown by Ishiguro *et al.* to be essential for cell type specific expression. The equivalent region in the rat *DBH* promoter does not contain a silencer element (Shaskus *et al.*, 1992). Putative neuron-specific negative modulators have been identified upstream of genes encoding other neuronal proteins including synaptophysin (Bargou and Leube, 1991) but these have not been further characterised and it is not known if they correspond to the NRSE consensus.

2.3.3 Minimal nonspecific basal transcription activated by a neuron-specific positive modulator

A neuron-specific *positive modulator* would function in neuronal cells and would upregulate transcription from a constitutive minimal promoter. By sequential deletion, it should be possible to remove such an element and return the expression of a reporter minigene to a minimal level in all cell types; these are the essential features of Fig 2.1c. Should such an element function in a position and orientation independent fashion and be capable of conferring neuronal-specificity upon a heterologous basal promoter, it would then constitute an *enhancer* (see Maniatis *et al.*, 1987).

As positive regulation is a common feature of eukaryotic gene function, it is not surprising that a number of neuron-specific genes should possess binding sites for specific transcriptional activators. In some cases, however, such elements have been difficult to isolate. A number of filament proteins are expressed specifically in neuronal cells including the intermediate neuronal filament proteins NF-H (heavy chain), NF-M (mid range chain) and NF-L (light chain). Early reporter-transfection studies, using considerable lengths of 5' and 3' flanking DNA from various neurofilament genes, identified a number of constitutive positive and negative regulatory elements but failed to isolate elements required for cell type-specificity. Thus, reporter constructs were found to be expressed with equal efficiency in neuronal and nonneuronal cell lines alike (Julien *et al.*, 1987; Monteiro and Cleveland, 1989; Nakahira *et al.*, 1990; Pleasure *et al.*, 1990; Schneidman at al., 1992; Zopf *et al.*, 1990). This was also found to be true for the α-internexin gene, which encodes another neuron-specific intermediate filament protein (Ching and Liem, 1991). Evidence from transgenic mouse experiments showed, however, that reporter transgenes driven by relatively short regions of 5' and 3' flanking sequence were properly regulated, indicating that all the required *cis*-acting elements were present near to the transcriptional start site (Byrne and Ruddle; 1989; Julien *et al.*, 1988;1990; Beaudet *et al.*, 1992; Lee *et al.*, 1992; Reeben *et al.*, 1993; Yazdanbakhsh *et al.*, 1993). This discrepancy was attributed to the artificial nature of the transfection assay (see Table 2.1) but deletion analysis in transgenic mice also failed to identify specific functional control elements. In conflicting reports, Yazdanbakhsh *et al.* (1993) claimed to have identified a neuron-specific positive element in the flanking region of the human *NF-L* gene, located between 190 and 300 bp upstream of the transcriptional start site whilst Beaudet *et al.* (1992) claimed that 300 bp of upstream sequence was

insufficient to confer neuronal-specificity upon a reporter transgene but that 4.6 kbp of *downstream* information, combined with the minimal promoter, could confer cell type specificity in transfection experiments. To overcome the limitations of the transfection assay, Schwartz *et al.* (1994) have analysed the regulation of the mouse *NF-H* gene by *in vitro* transcription using protein extracts from brain and liver. They found that a minimal promoter extending 65 bp upstream of the transcriptional start site was capable of sponsoring relatively strong reporter expression using extracts from both tissues but that a region located between 65 and 115 bp upstream of the start site was responsible for brain-specific enhancement of transcription. Within this region, a sequence displaying perfect dyad symmetry was shown to be essential: GGGGAGGAGG N_{15} CCTCCTCCCC. Interestingly, deletion experiments showed that only the pyrimidine-rich repeat was essential and that the complementary, purine-rich element could be mutated or deleted without effect. Identical or highly conserved elements have been found near to the transcriptional start sites in all three human and murine neurofilament genes suggesting a common overall mechanism of spatial regulation, however, as the genes are differentially regulated during development (Julien *et al.*, 1986) further controls may be superimposed upon this general regime. In the human and murine *NF-L* genes, the enhancer is found downstream of the transcriptional start site, supporting the conclusions of Beaudet *et al.* (1992). The NF enhancer has not been found in the flanking regions of any other genes and is presumed to be unique to this closely related gene family.

Cell-specific transcription of the rat tyrosine hydroxylase gene has also been traced to a neuron-specific enhancer. Transfection analysis in PC8b cells located the enhancer just upstream of the transcriptional start site (Yoon *et al.*, 1992). The *TH* enhancer comprises an AP-1 binding motif (TGATTCA) with an overlapping 20 bp element displaying imperfect dyad symmetry. This element has an E-box core, which features in other tissue-specific enhancers such as the exocrine specific *Pan* element and the immunoglobulin light chain enhancer kE2 (Nelson *et al.*, 1990; Murre *et al.*, 1989). Mutational analysis carried out by Yoon *et al.* has shown that both the E-box motif and the AP-1 binding site are required for enhancer function and that their spatial relationship is also important, indicating a close interaction between them. More recently, Wong *et al.* (1994) have shown that the AP-1/ E-box dyad motif is both insufficient and nonessential for neuron-specific expression of rat *TH* reporter constructs in PC12 cells. Instead, a functional enhancer sequence was located 500 bp upstream of the transcriptional start site.

2.3.4 Gene expression in subsets of neurons involving combinatorial controls superimposed upon a more promiscuous mechanism

Many neuron-specific genes have been analysed in transgenic mice but these studies are usually limited to showing that a particular length of flanking DNA is capable of conferring correct spatial and temporal expression. Relatively few genes have been dissected in a rigorous manner, to identify elements responsible for spatiotemporal control, but those encoding enzymes of the catecholamine synthesis pathway are an exception. The genes involved in neurotransmitter synthesis and function are prime examples of subneuronal-specific genes. The transmitter phenotype of a particular neuron depends upon the combination of enzymes made in the cell (for example, the pathway to catecholamine synthesis is shown in Figure 2.2) and neurons which synthesise particular neurotransmitters are located in characteristic parts of the nervous system. One would expect that the enzymes involved in neurotransmitter synthesis, activity and degradation would be synthesised in specific overlapping spatial domains, and this would be reflected in the promoters of the corresponding genes.

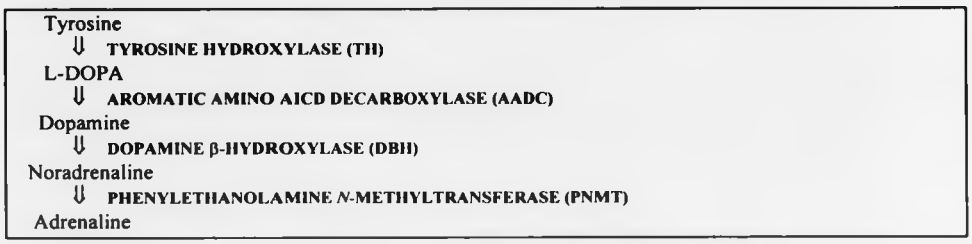

Figure 2.2. Catecholamine synthesis in the mammalian nervous system. The pathway is shown to the left with the enzymes to the right.

Hoyle and colleagues have recently investigated the regulation of the human *DBH* gene in transgenic mice using a nested set of 5' deletions (Hoyle *et al.*, 1994). Endogenous *DBH* expression is restricted to noradrenergic neurons (i.e. most sympathetic and parasympathetic neurons) and adrenal chromaffin cells whilst transgenic mice carrying 5.8 kbp of the human *DBH* 5' flanking region express the reporter-transgene in those cells where endogenous *DBH* mRNA is detected but also in ectopic tissues such as the dorsal root ganglia and dopaminergic and noncatecholaminergic neurons of the brain. Transient ectopic expression is also observed during development in the spinal cord and facial

mesenchyme (Mercer *et al.*, 1991; Kapur *et al.*, 1991; Hoyle *et al.*, 1994). The ectopic expression was thought to be due to the absence of negative modulators located outside the limited regulatory DNA flanking the reporter gene. Deletion of 5' flanking sequence to 1.1 kbp upstream of the transcriptional start site allowed further ectopic expression in the hypothalamus, septum and olfactory bulb, however neither this expression, nor the ectopic expression observed for the 5.8 kbp 5' sequence, was observed if 1.5 kbp of flanking DNA was present. Hoyle *et al.* therefore suggested that the region between 1.1 and 1.5 kbp upstream of the transcriptional start site was responsible for restricting the pattern of expression conferred by the more promiscuous 1.1 kbp sequence but that further elements, located between 1.5 and 5.8 kbp upstream were able to allow expression in other cells and that these permissive elements were repressed by sequences elsewhere. Finally, deletion of the 5' flanking sequence to within 600 bp of the transcriptional start site abolished reporter gene expression altogether suggesting the presence of an essential positive element between -600 and -1100 bp. Transfection analysis using the same promoter (Ishiguro *et al.*, 1993) identified a functional NRSE 500 bp upstream of the transcriptional start site and an essential cAMP responsive element (CRE) less that 300 bp from the transcriptional start site. The loss of expression in transgenic mice could not be due to the removal of either of these elements and might be caused by unfavourable position effects.

Because all cells expressing *DBH* should also express *TH*, Hoyle *et al.* put forward the idea that the ectopic expression from the *DBH* minigene might correspond to the endogenous expression of *TH*. This would further suggest that the genes involved in catecholamine synthesis could be regulated according to a common paradigm with extra levels of restriction imposed upon those genes encoding downstream enzymes. Although this was an attractive proposal, comparison of promiscuous *DBH* reporter expression with endogenous *TH* mRNA showed that some populations of cells expressed the *DBH*-reporter message but not *TH*, and that the domains of expression of the two genes did not match. Furthermore, Shaskus *et al.* (1992) has compared the proximal flanking regions of the rat *DBH* and *TH* genes and although two conserved regions were found, deletion analysis showed that neither were required for cell type-specific expression and that the conserved region was not present in the human *TH* promoter.

A striking example of subneuronal-specific gene regulation imposed upon an underlying panneuronal mechanism comes from study of the Purkinje cell protein 2 (*Pcp-2*) gene (Vandaele *et al.*, 1991). *Pcp-2* is expressed specifically in cerebellar Purkinje cells and

retinal bipolar neurons, and transgenic mice carrying 4 kbp of 5' flanking sequence express the reporter gene faithfully in the Purkinje cells (Oberdick *et al.*, 1990). Vandaele *et al.* showed that a transgene driven by only 400 bp of the flanking sequence was expressed in a multitude of neuronal cell types whilst a transgene driven by 3.5 kbp was expressed in the same manner as the endogenous gene. This showed that negative elements, located between -400 and -3500 bp, were responsible for the restriction of expression to certain subneuronal cell types and that this restriction had been imposed upon a more promiscuous (but still neuron-specific) core region.

2.4 Other conserved features of neuron-specific genes

The studies outlined above have identified a number of *cis*-acting motifs which appear to confer neuronal cell type specificity; these include the neuronal restrictive silencer element or NRSE (Mori *et al.*, 1992) and the neurofilament enhancer (Schwartz *et al.*, 1994). A number of further motifs, described below, have been found to be conserved between otherwise unrelated neuronal genes, however, their functional significance is less clear.

2.4.1 A neuronal consensus with unknown function

Maue *et al.* (1990) first noted a conserved sequence with the core motif CCAGG within the flanking regions of four neuronal genes: the rat type II sodium channel and peripherin genes, the mouse *NF-L* gene and the *Drosophila* dopamine decarboxylase gene. The sequence has been found to be required but not sufficient for CNS expression in *Drosophila* (Scholnick *et al.*, 1986) and was termed element 1, however, in the sodium channel gene, its deletion was shown to have no effect (Maue *et al.*, 1990). Later, the list of neuronal genes carrying the consensus sequence within their flanking sequences was expanded by Vandaele *et al.* (1991). Some genes were shown to possess multiple copies of the sequence either dispersed or arranged in tandem. For instance, the rat neuron-specific enolase gene contains four such sequences, three located upstream of the transcriptional start site (Vandaele *et al.*, 1991) and one located within the first intron (Sakimura *et al.*, 1995). Homologous elements are also present upstream of the mouse synapsin II gene (Chin *et al.*, 1994), the rat *GAP-43* gene (Nedivi *et al.*, 1992), the mouse *OMP* gene (Kudrycki *et al.*, 1993) and the rat *PPT* gene (Quinn and McAlister, 1993); all

the known sequences are aligned for comparison in Table 2.3. In those cases where the sequence has

Sequence			Species/Gene	Position
AGTGTTTGCCCCAGG	GCAT.	. . GGGCTG	Rat *DBH*	(-136/-111)
CCAGG	AGAT		Rat *GAP-43*	(-279/-286)
GCT. . GAGCCAGG	A.	GCTGGCTG	Rat $G_{olfα}$	(-252/-232)
GAACTgggtggggCCAGG	AA.	GAAGGCTG	Mouse *OMP*	(-61/-86)
AGCTT. . G. . CCAGG	. . . . .	AGAGCCTG	Rat *NaII*	(-1050/-1026)
A. CTT. GTGACCAGG	AGAT.	GGA. GCTG	Rat *NaII*	(-60/-34)
AGC. . . . . GGCCAGG	CT.	GGAGCC. G	Mouse *NF-L*	(-184/-161)
. GCT. . GGGCCCAGG	GCAGAAAAGT.	. . . . .	Human *NF-M*	(502/543)
. . . . . CCAGG	TTCCCAT.	GCGGCCTG		
	GAG	AGAGGCTC	Rat *NSE*	(-995/-986)
AGCT. . GGGGCCAGG	GAAA.	AGATCCTG	Rat *NSE*	(-823/-771)
CCAGG	AGGCCAA.	AGATGCTG	Rat *NSE*	(-662/-641)
A. CTT. GTGACCAGG	AGAT	GGA. GCTG	Rat *NSE*	(372/378)
CCAGG	AGATCAA.	AGACGCTG	Human *NSE*	(-763/-782)
AGGTcaGAGACCAGG	AGAAAAGTATAGGAGAG	. . . . .	Mouse *Pcp-2*	(-285/-210)
atacacaatGGACCAGG	AAGAAGAAAAGGGAGAG	GGAGGCTC		
GCTT. AGGCCAGG			Rat peripherin	(-404/-393)
AGC. . . . AACCAGG	. . . . . AGAG	GGAGGGTG *	Rat peripherin	(-167/-151)
	GGGA. . .	GGA. GCTG	Rat peripherin	(-77/-64)
TGTGCCtGG	. . . . . GA.	AGAAGCTG	Rat *PPT*	(-761/-741)
AGCTT. . . . CCAGG	CA.	AGA. GCTG	Rat *SCG10*	(-226/-204)
AACCAGG	AG		Mouse synapsin II	(-130/-139 opp)
A. CTT. . GGCCAGG	ACGCCTAACCGTGCGA.	CGA. CCTG	*Drosophila Ddc*	(-61/-96 opp)
AGCTTGNGVCCAGG	AG-RICH	RGA(N)SCTG	CONSENSUS	

Table 2.3: Comparing the flanking regions of various neuron-specific genes containing a conserved motif with the consensus sequence shown on the bottom row of the table. Sequences are shown with gaps (indicated by stops) or condensed sequence (subscript lower case letters) introduced for maximum alignment. The core sequences CCAGG and GA.. CTG are emphasised in bold. The GAAAAG motif, which appears in three of the genes, is underlined. In the right hand column of the table, numbers indicate the positions, within the respective genes, where the sequences occur. In the mouse *Pcp-2* and human *NF-M* genes, the consensus occurs twice and the two sequences are contiguous. In the other genes where the consensus is present as multiple copies, each sequence occurs at a distinct position as indicated. The sequence usually appears on the sense strand, except where opposite orientation is indicated (opp). The asterisk indicates that the peripherin sequence has been condensed to show maximum alignment; the correct sequence of the distal element is GGAaGgGGTG. Adapted from Fig 4 in Vandaele *et al.*, 1991; original consensus described for type II Na^+ channel gene, peripherin, *NF-L* and *Drosophila Ddc* by Maue *et al.*, 1990.

been manipulated in mammalian genes, it has proved both insufficient and nonessential to confer neuronal specificity upon a reporter construct. Its existence in the promoters of so many neuronal genes is therefore a mystery, but the observed conservation with the essential *Drosophila* element 1 would suggest an important function. Quinn and McAlister (1993) have shown that the neuronal element in the rat *PPT* gene binds a protein of approximately 40 kDa in brain extracts but not in extracts of various cell lines (neuronal and nonneuronal). Remarkably, the protein binds to only one strand of the element and binding is not competed by the duplex. The authors noted that there is some homology between the *PPT* neuronal element and single-stranded binding elements in other genes (adipsin, growth hormone) and the TAR region of HIV which interacts with the TAT protein at the RNA level. Molecular modelling has shown that the TAR region can form a stem loop structure, with the TAT protein interacting with a single-stranded portion of the stem. The neuronal consensus is included within this stem-loop structure and it is therefore possible that DNA secondary structures may be involved in the neuronal regulation of *PPT* and other genes containing the motif. However, as no studies have shown the neuronal element to be necessary for cell type-specific gene expression, its relevance remains to be determined.

2.4.2 The SNN motif

Another bipartite motif, identified by Saurwald *et al.* (1990), was termed the SNN motif because it is found in the rat and human Synapsin I promoters, the mouse *NF-M* promoter (Lewis and Cowan, 1986) and the human NGF receptor gene promoter (Sehgal *et al.*, 1988). Although the SNN motif itself has not been functionally tested, a cAMP response element, shown to be essential for transcription overlaps the motif in both synapsin I promoters and the upstream moeity forms a consensus Krox-24 binding site which may be required for proper gene regulation in the synapsin and neurofillament promoters. The kown SNN motifs are shown in Figure 2.3.

2.4.3 The neuronal identifier (ID) sequence

In the early 1980s, Sutcliffe *et al.* identified two small cellular RNA (scRNA) molecules, called BC1 and BC2 respectively, which were expressed specifically in the rat brain and

peripheral nervous system by RNA polymerase III (Sutcliffe *et al.*, 1982; 1984). A middle repetitive DNA element dispersed throughout the rat genome was found to

Sequence	Species/gene	Position
CCTTCGCCCCCGC - N_{36} - CGGGCTGAC	Rat synapsin I	-212
CCTTCGCCCCCGC - N_{37} - CGCGCTGAC	Human synapsin I	-213
CGTTCGCCCCCGC - N_{39} - CGCGCTGCC	Mouse neurofilament	-150
CCTTTGCCTCTGC - N_{47} - CGGGCTGGC	Human NGF receptor	-117
CSTTYGCCYCYGC -N_{36-47}- CGSGCTGNC	**Consensus**	

Figure 2.3: SNN motifs in neuronal genes (adapted from Sauerwald *et al.*, 1990). Underline shows position fo overlap with cAMP response element in synapsin promoters. Double underline shows Krox 24 binding sites. Positions relative to transcriptional start site. Nomenclature for ambiguous nucleotides: R = G or A (puRine), Y = C or T (pYrimidine), S = G or C (three bondS), N = any Nucleotide

hybridise to these scRNA molecules and it was later discovered that the sequences were preferentially located near to or within postnatally expressed neuronal and neuroendocrine genes (Milner *et al.*, 1984), e.g. there is an ID element 3' to the final exon of the rat *NSE* gene (Sakimura *et al.*, 1987). A model was proposed in which neuron-specific polymerase III transcription of the ID element would produce the scRNAs and at the same time generate an open chromatin domain which could be exploited by RNA polymerase II (Sutcliffe *et al.*, 1984). Although this model has not been experimentally proven, such a mechanism would have to work in concert with the gene-specific transcriptional regulation described in the preceding sections. The 75 bp ID element has been shown to work as a *cis*-acting positive modulator of neuronal gene expression in transfection experiments (McKinnon *et al.*, 1986).

2.4.4 The peptide hormone downstream octamer

An octamer motif with the sequence 5' GCCCAGCC 3' was reported to confer cell-type specificity upon the human gastrin gene when transfected into neuroblastoma cells (Thiell *et al.*, 1987). Unlike many of the functional *cis*-acting elements discussed in this Chapter, the peptide hormone gene octamer is always located between the TATA box and the transcriptional start site. Homologous motifs are found in similar positions in the genes

for other peptide hormones including cholecystokinin, gastrin-releasing hormone, neuropeptide Y, thyrotropin-releasing hormone, vasoactive intestinal peptide and vasopressin (Habener *et al.*, 1989) and in at least one case, the sequence has been shown to direct reporter gene expression to certain populations of neurons (Habener *et al.*, 1989). It is interesting to note that an identical element is found between the TATA-like box and the first exon in the rat *NSE* gene (Sakimura *et al.*, 1987).

2.4.5 Purine-rich sequence elements

A 22 bp purine-rich repetitive element with the consensus sequence GAGAGGGGAGAGGRGRGAGRRG was identified upstream of the rat gene for $GABA_A$ receptor δ and was shown to bind a brain-specific protein factor termed BSF-1 (Motejlek *et al.*,1994). Analysis of the sequences of other promoters showed that homologous elements were located upstream of other neuronal genes including three further $GABA_A$ receptor subunit genes, *Pcp-2*, and several neurofilament genes. These purine-rich elements within the human neurofilament gene promoters had previously been identified as binding sites for a ubiquitous protein factor, PAL (Elder *et al.*, 1992a; 1992b). An element showing limited homology was also found within the astrocyte-specific GFAP (glial fibrillary acidic protein) gene. Overall, these elements demonstrated 50-60% identity to the B site found in the immunoglobulin κ3 light chain enhancer (Sen and Baltimore, 1986) which is recognised by a brain-specific transcription factor termed BETA (Korner *et al.*,1989). Purine rich elements with little homology to the above have been identified in the promoters for rat *GAP-43* (Nedevi *et al.*, 1992), human synapsin I (Saurwauld *et al.*, 1990) and in the first intron of rat *NSE* (Sakimura *et al.*, 1995). None of these sequences have been shown to demonstrate protein-binding activity although in both *GAP-43* and *NSE*, these elements lie close to other unusual DNA structures which may cooperate with them to regulate gene expression.

2.5 Neuronal Gene Table

Gene	Species	Promoter type	Expression	Relevant Studies	References
AADC (Aromatic L-amino acid decarboxylase)	Human	GC-rich Atypical TATA	Catecholaminergic and serotonergic neurons, adrenal gland. Some nonneuronal tissues e.g. liver, kidney (function unknown)	Transfection analysis: Deletion analysis identifies 560bp cell type specific promoter. Constitutive elements located further upstream. Second promoter identified 10kb upstream which directs nonneuronal expression	le van Thai *et al.*, 1993 Albert *et al.*, 1992
ACH receptor (nicotininc receptor subunits)	Rat Chick	GC-rich No TATA	Certain subpopulations of neurons	Transfection analysis: Analysis of intergenic region between α3 and β4 subunit genes reveals a 600bp promoter for a3. A cell type specific AT-rich silencer is present upstream (in the β4 transcription unit). Promoter shown to be activated in neuronal context by SCIP/Tst1. *In vitro* analysis: constitutive silencer found upstream of gene for α2 subunit. Consists of octamer repeats and can be changed to enhancer by reducing copy number. Transfection analysis: Deletion analysis shows that region between -188 and -406bp upstream of the α7 subunit gene transcriptional start site is sufficient for cell type specific expression.	Duvoisin and Heinemann, 1993 Boyd, 1994 Bessis *et al.*, 1993 Matter-Sadzinski *et al.*, 1992
Aldolase C	Human	Housekeeping Type	Adult and foetal brain (neurons & astrocytes) Lower levels in other foetal tissue	Transfection analysis: 420bp 5' seq. sufficient for high level reporter expression in human neuroblastoma cells. Deletion of region between -420 and -164 results in 60% loss of activity. 115bp 5' seq. confers neural specificity, contains overlapping Sp1 and Krox 24 binding sites. Transgenic analysis: 115bp 5' seq. sufficient for tissue-specific transgene expression although level of expression very low. This level greatly increased by 5.5kb of flanking sequence	Buono *et al.*, 1990; 1993 Thomas *et al.*, 1993 Makeh *et al.*, 1994
Amyloid precursor protein	Mouse Rat Human	GC-rich Multiple starts	Neuronal. Accumulates during Alzheimer's disease	Transfection analysis: APP gene expression is methylation dependent. Transfection analysis: 375bp of 5' sequence direct high level reporter expression in PC12 cells. Two important positive elements located within this region, one of which interacts with a brain protein. Transgenic analysis: 4.5kb 5' sequence drives correct neuron-specific expression in transgenic mice.	Ledoux *et al.*, 1994 Hoffman and Chernak, 1994 Wirak *et al.*, 1991

Gene	Species	Promoter type	Expression	Relevant Studies	References
BDNF (Brain Derived Neurotrophic Factor)	Rat	Four promoters	Brain	Transfection analysis: Two promoters are neuron-specific. Inverted repeat of NRSE lies in the intergenic region between these promoters. Transgenic analysis: Various transgenes demonstrate independent activity of BDNF promoters	Timmusk *et al.*, 1993 Nakayama *et al.*, 1994 Timmusk *et al.*, 1995
CaII (Calmodulin II)	Rat	Typical Class II	Panneuronal	Transgenic analysis: 294bp promoter and 68bp leader sufficient for neuron-specific reporter expression in transgenic mice. Transfection studies: Same construct allows basal expression in fibroblasts.	Matsuo *et al.*, 1993
ChAT (Choline acetyltransferase)	Human Porcine Rat	No TATA TATA present TATA present Single start	Cholinergic neurons	Transfection studies: Essential constitutive enhancer present at homologous regions in human and porcine 5' seq (-900, -750). Second enhancer in porcine gene downstream of transcriptional start site. Human and rat genes regulated by cell-type specific silencer elements.	Hersh *et al.*, 1993 Ibanez and Persson, 1991 Y-P Li *et al.*, 1993 Hahn *et al.*, 1992 Benjamin *et al.*, 1992
α1-chimaerin	Human	Housekeeping type, multiple starts	Neuron-specific. In brain, localised to cerebellum, cerebral cortex, hippocampus.	Transfection studies: Minimal promoter is no neuron-specific. 4.4kb upstream sequence demonstrates neuron-specific silencer activity. However, only 3-fold difference between neuronal and nonneuronal cells, may indicate neuroblastoma cells used not fully permisive for expression.	Dong *et al.*, 1995
D_{1A} dopamine receptor	Human	Housekeeping type	Mainly in striatum	Transfection analysis: Deletion analysis shows that all elements responsible for cell-type specific regulation are located within 1kb of transcriptional start site. Other constitutive elements located further upstream.	Minowa *et al.*, 1992
DBH (Dopamine β-hydroxylase)	Human Rat Mouse	Typical Class II Atypical TATA	Adrenergic neurons Adrenal gland	Transgenic analysis: 5.8kb 5' seq. drives reporter expression in DBH expressing cells and ectopic sites. Deletion analysis identifies several spatial control elements. Transfection analysis: Deletion analysis identifies CRE element as essential enhancer and NRSE as silencer. 395bp promoter sufficient for cell-type specific expression. Enhancer (DB1) within this region contains CRE element which also mediates second messenger response. Transgenic analysis: *PNMT* coding region under *DBH* promoter results in accumulation of adrenergic sympathetic neurons.	Mercer *et al.*, 1991 Kapur *et al.*, 1991 Hoyle *et al.*, 1994 Ishiguro *et al.*, 1993 Lamouroux *et al.*, 1993 Shaskus *et al.*, 1992 Cadd *et al.*, 1992

Gene	Species	Promoter	Expression	Relevant studies	References
FE65	Rat	GC-rich No TATA	Somatic and visceral ganglia	Transfection analysis: Two elements revealed in proximal promoter. Constitutive enhancer Sp1 site and tissue-specific core element overlapping initiator. Gel retardation identifies a number of neuron-specific complexes.	Faraonio *et al.*, 1994
$GABA_A$-Rδ	Rat	Housekeeping Type	Brain - specifically cerebellum, dentate gyrus, thalamic nuclei	*In vitro* studies: Tandemly repeated purine-rich element which demonstrates brain-specific protein binding activity implicated in tissue-specific control.	Motejlek *et al.*, 1994
GAP-43 (*B-50*, neuromodulin)	Rat	Typical Class II with unusual DNA flanking elements. Multiple starts	Panneuronal Axonal growth cones Transient expression in nonneuronal cells of chick limb bud.	Transfection analysis: Deletion analysis shows 386bp core promoter is cell type specific. Negative countermodulation by unusual DNA elements flanking this region. Function of minimal promoter almost fully conserved in transgenic zebra fish. 8.4kb 5' seq. drives neuron-specific reporter expression in transient *Xenopus* DNA microinjection assays. Second promoter identified downstream of neuron-specific core promoter which is active during development.	Nedevi *et al.*, 1992 Starr *et al.*, 1994 Reinhardt *et al.*, 1994 Verhaagen *et al.*, 1993 Eggen *et al.*, 1994
HSV Immediate Early Genes			Inactive in neurons Active in nonneuronal cells	Failure of viral IEG expression in neuronal cells traced to octamer-like TAATGARAT motif in the IEG promoters.	Kemp *et al.*, 1990
α-Internexin	Rat	GC-rich Atypical TATA	CNS	Transfection analysis: 5kb 5' seq. insufficient for cell type specificity.	Chin and Liem, 1991
NaII (Type II sodium channel)	Rat	AT-rich No TATA Multiple starts	Panneuronal Pref. in adult brain	Transfection analysis: Deletion analysis shows promiscuous basal promoter restricted by distant, cell type specific silencer element, prototype NRSE.	Maue *et al.*, 1990 Kraner *et al.*, 1992 (Mori *et al.*, 1992)
NGF receptor	Human Mouse	Housekeeping type	Panneuronal and nonneuronal descendants of neural crest	Transfection analysis: 1.2kb of 5' seq. allows expression in fibroblasts. Cell type specific negative regulatory element located 1.7kb upstream of transcriptional start site contains E-box motif.	Sehgal *et al.*, 1988 Neuman *et al.*, 1993b

Gene	Species	Promoter	Expression	Relevant studies	References
Neurofilament genes (*NF-H, NF-M, NF-L*)	Rat (r) Mouse (m) Human (h) Chicken (ch)	Typical Class II	Panneuronal	Transfection analysis: Various NF genes with extensive flanking seq. are expressed with equal efficiency in neuronal and nonneuronal cell lines. Most deletion studies fail to identify cell type specific elements although a number of constitutive elements are found. Yazdanbakhsh *et al.* (1993) claim to have identified cell type specific enhancer in human *NF-L* gene.	Julien *et al.*, 1987 (h*NF-L*) Nakahira *et al.*, 1990 (m*NF-L*) Monteiro and Cleveland, 1989 (m*NF-L*) Pleasure *et al.*, 1990 (h*NF-M*) Schneidman *et al.*, 1992 (m*NF-H*, *NF-M* and *NF-L*) Yazdanbakhsh *et al.*, 1993 (h*NF-L*) Zopf *et al.*, 1990 (ch*NF-M*)
				Transgenic analysis: Homologous and heterologous NF genes overexpressed in transgenic mice cause recognisable neuropathological disorders.	Coté t al., 1993 (h*NF-H*) Xu *et al.*, 1993 (m*NF-L*)
				Various NF genes with limited flanking seq. are correctly regulated in transgenic mice indicating that all relevant *cis*-acting sequences are present. Deletion analyses fail to identify neuron-specific elements, although Beaudet *et al.* (1992) identify downstream neuron-specific elements in human *NF-L*.	Beaudet *et al.*, 1992 (n*HF-L*) Lee *et al.*, 1992 (h*NF-M*) Reeben *et al.*, 1993 (r*NF-L*) Julien *et al.*, 1988; 1990 (h*NF-L*) Monteiro *et al.*, 1990 (m*NF-L*) Byrne and Ruddle, 1989 (m*NF-L*) Vidal-Sanz *et al.*, 1991 (h*NF-L*)
				In vitro analysis: *In vitro* transcription using brain and liver extracts identifies tissue-specific enhancer in mouse *NF-H* gene; homologous elements in all other NF genes. A number of transcription factor binding sites are identified, including those for Krox-24.	Schwartz *et al.*, 1994 (m*NF-H*) Elder *et al.*, 1992a; b (h*NF-H* and *M*) Ivanov and Brown, 1992 (m*NF-L*) Pospelov *et al.*, 1994 (h*NF-L*)

Gene	Species	Promoter type	Expression	Relevant Studies	References
NSE (neuron-specific enolase)	Rat	GC-rich Atypical TATA	Panneuronal and neuroendocrine	Transgenic analysis: 1.8kb 5' seq. drives correctly regulated reporter expression in transgenic mice and can restrict gene expression to neurons in brains transduced with recombinant herpesvirus vectors. Stable transfection study: 1.8kb 5' seq. responds to NGF and retinoic acid in parallel to endogenous gene. Transient transfection study: 500bp proximal segment of first intron confers enhanced neuron-specific expression in cultured neurons and NGF-treated PC12 cells.	Forss-Petter *et al.*, 1990; J Andersen *et al.*, 1992; 1993 Roemer *et al.*, 1995 Alouani *et al.*, 1993 Sakimura *et al.*, 1995 For review see section 1.7.4
Oxytocin/ Vasopressin	Rat Bovine		Hypothalamus	Transgenic analysis: 5.2kb transgene including oxytocin and vasopressin genes allows tissue-specific expression of oxytocin but not vasopressin in transgenic mice. Transgenic analysis: 1.25kb of 5' Vasopressin sequence insufficient for tissue-specific expression. Construct containing 9kb 5' sequence and 1.5kb 3' sequence is expressed in a tissue-specific manner	Young *et al.*, 1990 Ang *et al.*, 1993
OMP (Olfactory Marker Protein)	Mouse	GC-rich No TATA	Olfactory neuroepithelium	Transgenic analysis: 0.3kb 5' seq. sufficient for tissue-specific reporter expression in transgenic mice. This sequence contains one Olf-1 binding site which is also present in several other olfactory neuron-specific genes.	Kudrycki *et al.*, 1993 Wang *et al.*, 1993 Danciger *et al.*, 1989
Pcp-2/L1 (Purkinje cell protein 2)	Mouse	Typical Class II Two start sites	Retinal bipolar neurons. Cerebellar Purkinje cells.	Transgenic analysis: 3.5kb of 5' seq. drives correctly regulated reporter expression in transgenic mice. 400bp of 5' seq. drives expression in a variety of neuronal cell types.	Oberdick *et al.*, 1990 Vandaele *et al.*, 1992
PEP-19	Mouse		Panneuronal	Transgenic analysis: 1.35kb 5' seq insufficient for expression in transgenic mice but this element does specifically bind proteins from cerebellar extract.	Sangammeswand and Morgan, 1993
Peripherin	Mouse	Typical Class II	PNS	Transfection analysis: Deletion analysis shows 98bp promoter sufficient for cell type specific expression. Three footprints in this region; one (PER1) is required but insufficient for specificity. PER2 and 3 are essential constitutive elements.	Desmaris *et al.*, 1992 Karpov *et al.*, 1992 Thomson *et al.*, 1992

Gene	Species	Promoter type	Expression	Relevant Studies	References
PPT (Preprotachykinin A) - Substance P, Neurokinin A, Neuropeptides K and γ	Rat	Three TATA boxes	Dorsal root ganglia	Transfection analysis: 865bp 5' seq. confers neuron-specificity to reporter gene but expression is not restricted to those neuronal populations expressing substance P, nor is reporter NGF inducible. Neuron-specific binding site identified on border between intron 1 and exon 1. *In vitro* analysis: CCAGG element binds to single-stranded DNA binding protein	Mulderry *et al.*, 1993 Quinn, 1992 Quinn and McAlliste 1993
PNMT (Phenylethanolamine *N*-methyltransferase)	Human	GC-rich Atypical TATA	Inner nuclear layer of retina. Adrenal gland	Transgenic analysis: 2kb of 5' seq. drives correct expression of reporter gene in transgenic mice.	Baetge *et al.*, 1988
RC3 (Neurogranin)	Rat	No TATA Multiple starts	neuron-specific, enriched in striatum, neocortex, hippocampus	Transfection analysis: largest reporter construct (1500nt) still expressed at high levels in nonneuronal cells. Retinoic acid and glucocorticoid response elements shown to be functional in heterologous context.	Sato *et al.*, 1995 Iñiguez *et al.*, 1994
SCG10	Rat	Typical Class II Multiple starts	Panneuronal Axonal growth cones	Transfection analysis: Deletion analysis shows promiscuous basal promoter restricted by distant, cell type specific silencer element (NRSE). Transgenic analysis: 4kb 5' seq. drives correctly regulated reporter expression. 300bp 5' seq. drives expression in many nonneuronal tissues.	Mori *et al.*, 1990 Mori *et al.*, 1992 Wuenschell *et al.*, 1990
Serotonin-2 (*5-HT2*)	Mouse	GC-rich Multiple starts	Neuron-specific	Transgenic analysis: 5.6kb 5' flanking DNA sufficient for brain specific expression Transfection analysis: Basal nonspecific promoter plus two neuron-specific repressor elements	Toth *et al.*, 1994
Synapsin I	Rat Human	Housekeeping type Single start	Panneuronal	Transfection analysis: Deletion analysis shows 225bp promoter and 105bp leader sufficient for cell type specific expression. CRE element found at -155. Transgenic analysis: 4.3kb 5' seq. sufficient for correct tissue-specific expression. Transfection analysis: Deletion analysis reveals functional silencer element (NRSE) although activity not significant. Region from -115 to +44 shown to act as basal promoter. Region from -22 to -422 contains cell type specific enhancer. This region contains NRSE and binding site for Krox-24; NRSBF and Krox-24 thought to interact to regulate expression.	Saurwald *et al.*, 1990 Howland *et al.*, 1991 Hoesche *et al.*, 1993 L Li *et al.*, 1993 G Thiel *et al.*, 1991 G Thiel *et al.*, 1994
Synapsin II	Mouse	Housekeeping type Single start	Panneuronal	Transfection analysis: Deletion analysis reveals cell type specific core promoter between -79 and +153. Cell type specific silencers and enhancers also located further upstream.	Chin *et al.*, 1994

Gene	Species	Promoter type	Expression	Relevant Studies	References
Synaptophysin	Rat	Housekeeping type Multiple starts	Panneuronal and neuroendocrine	Transfection analysis: 1.2kb of 5' seq insufficient for cell type specific expression. Two upstream regions capable of conferring specificity.	Bargou and Leube, 1991
TH (Tyrosine Hydroxylase)	Rat	Typical Class II	CNS- Mainly olfactory bulb Sympathetic ganglia Adrenal gland	Transfection analysis: Deletion analysis shows 212bp promoter sufficient for cell type specific expression. Region between -187 and -212 essential. AP-1/ E box dyad motif in this region shown to act as essential enhancer in PC8b cells. Same region showed to be both insufficient and nonessential for expression in PC12 cells, instead functional enhancer lies about 500bp upstream of transcriptional start site.	Cambi *et al.*, 1989 Fung *et al.*, 1992 Yoon and Chikaraishi, 1992 Wong *et al.*, 1994 Gandleman *et al.*, 1990
				Transgenic analysis: Reporter transgenes with 2.5-3.5kb 5' seq. insufficient for tissue-specific expression. Reporter expression incomplete and ectopic. 4.8kb 5' sequence gives correct expression in crude CAT analysis and correct expression with single cell resolution using human growth hormone as reporter.	Banerjee *et al.*, 1992; 1994 Kaneda *et al.*, 1991 Suri and Chikaraishi, 1991 Morgan and Sharpe, 1991 Dupin *et al.*, 1993
	Quail			Transfection analysis: 77bp promoter, including CRE, sufficient for high level expression in cultured neural crest cells.	Stachowiak *et al.*, 1990 Goc and Stachowiak, 1994
	Cow			Transfection and *in vitro* analysis shows that AP-1-like factors and other inducible proteins are probably involved in response to angiotensin and nicotine. Response element identified between -194 and -269.	Huang *et al.*, 1991
	Human			Transfection analysis: Transfection into a variety of cell lines demonstrates that cAMP response in *TH* depends upon its context in the promoter.	Nagatsu *et al.*, 1991; 1994 Kim *et al.*, 1993 Kobayashi *et al.*, 1992
vgf	Rat	Typical Class II	Neuronal, neuroendocrine	Transfection analysis: Deletion analysis shows 180bp promoter is cell type specific. This region contains CRE element and (unidentified) NGF inducible site.	Possenti *et al.*, 1989

2.6 Transcription factors in the mammalian nervous system - approaches to isolation and identification of function.

Although the expression of many neuronal genes has been studied, relatively little is known about the transcription factors which regulate them. This lack of knowledge reflects the major approaches used to identify such factors, approaches which exploit their structural or functional similarity to those expressed outside the nervous system or in other animals, rather than their participation in the regulation of specific genes. For example, a large family of neuronal POU domain-containing factors has been identified using the popular approach of homology-based PCR amplification, where degenerate primers are synthesised to match the most highly conserved sequences of a given DNA-binding domain and used to isolate novel factors of the same family (He *et al.*, 1988). An alternative approach exploits known transcription factor binding sites and traps novel proteins which bind to them. The brain-specific DNA binding proteins BETA and BSF1 have been isolated in this manner (Korner *et al.*, 1989; Motejlek *et al.*, 1994). Both these methods are limited by their inability to identify downstream genes although, in the latter case, consensus binding sites may be sought in appropriate genes and candidates containing such sites may be analysed for binding activity. The homology search approach has the major advantage that *genes* encoding novel putative transcription factors may be isolated and cloned, thereby allowing domains of expression to be determined by *in situ* hybridisation and downstream candidate genes with overlapping expression patterns may then be sought. Perhaps the greatest disadvantage of the homology search approach is that only novel factors belonging to well-characterised families can be isolated. The opposite approach involves the characterisation of putative transcription factors based on their ability to bind *cis*-acting elements which have been shown to be involved in neuronal gene expression. This strategy was used to identify the NRSBF (Mori *et al.*, 1992) and has the advantage that natural downstream target genes are already known. However, most such factors are only poorly characterised because it is more difficult to move from this stage to then isolate the corresponding gene. An interesting and novel way to isolate putative neuronal transcription factors was reported by Mullen *et al.* (1992). These investigators raised a battery of monoclonal antibodies against brain cell nuclei in an attempt to isolate neuronal nuclear proteins. One such antibody recognised a neuron-specific and almost panneuronal nuclear protein, named NeuN, which bound to DNA *in vitro*. Once an interesting protein has been identified, this approach becomes very powerful, allowing purification and *in situ* localisation of the protein, and isolation of cDNA sequences from an expression library.

2.7 Transcription factors in the mammalian nervous system - regulation of neuronal genes

2.7.1 Regulation of neuronal genes by immediate early gene products

A number of neuronal genes have been shown to be regulated at the transcriptional level by the products of the cellular immediate early genes (Sheng and Greenberg, 1990). The immediate early genes (IEGs) encode transcription factors which are expressed promptly and transiently following certain extracellular stimuli (e.g. electrical polarisation or the presence of growth factors). Most of the IEG products are not specific to neuronal cells and mediate their effects in other tissues as well as the nervous system, however, such factors may provide an important constitutive regulatory function or may co-operate with tissue-specific factors to mediate specific regulatory controls. The Krox-24 factor (Lemaire *et al.*, 1988), also known as NGFI-A (Milbrandt, 1987) and zif268/egr-1 (Christy *et al.*, 1988) has been shown to transactivate at least one neuronal gene, synapsin I, probably in concert with the NRSBF which binds an adjacent silencer element (G. Thiel *et al.*, 1994). The binding site for Krox-24 (Christy and Nathans, 1989; Lemaire *et al.*, 1990; Cao *et al.*, 1990) has been found upstream of a number of other neuronal genes including those of the neurofilament family, synapsin II, synaptophysin and synaptobrevin II (Archer *et al.*, 1990; Özcelik *et al.*, 1990; Südhof *et al.*, 1990). At least one IEG product, NGFI-C, *is* restricted to neuronal cells, mostly those of the cortex, dorsal root and superior cervical ganglia and sciatic nerve.

2.7.2 Putative regulatory factors containing a POU domain

At present, most of the transcription factors which have been identified in the mammalian nervous system belong to the POU-domain class of helix-turn-helix proteins, so called because they share a consensus domain common to the mammalian transcription factors Pit-1, Oct-1/Oct-2 and the *Caenorhabditis elegans* protein unc 86 (Herr *et al.*, 1988; for reviews, see Robertson, 1988; Ruvkin and Finney, 1991; Schöler, 1991; Rosenfeld, 1991; Wegner *et al.*, 1993). In *C. elegans* and *Drosophila melanogaster*, POU-domain proteins have been shown to play a pivotal role in the control of neuronal cell fate during development (Campos-Ortega and Jan, 1991; Finney *et al.*, 1988). Given the premise

that such factors could play an equally important role during mammalian development, He and colleagues carried out a homology-based PCR search for novel POU factors in the mammalian brain (He *et al.*, 1989). Four new factors were identified, named Brn-1, Brn-2, Brn-3 and Tst-1 (see also Hara *et al.*, 1992). The Brn factors were brain specific and restricted to discrete populations of cells, supporting the notion that they might influence neuronal cell fate and regulate discrete sets of neuronal genes. Tst-1 (which is also known as Oct-6 and SCIP (suppressed cAMP inducible POU)) was expressed in both brain and testis. Since that early report, a number of additional nervous system-specific POU domain proteins have been identified and characterised (see section 2.8).

Although the differential and overlapping distribution of these POU domain proteins suggested an important regulatory role in the nervous system, proof that such factors directly interact with neuronal genes has been slow in coming. Tst-1/SCIP has been shown to downregulate the glial gene P_0 (which encodes protein zero, the major protein component of myelin) in Schwann cells transiently cotransfected with *Tst-1/SCIP* cDNA (He *et al.*, 1991; Monuki *et al.*, 1993), whilst Yang *et al.* (1994) have recently shown that the same factor is able to activate the gene for the acetylcholine receptor α3 in neuronal cells, even in the absence of its characteristic binding site. This more recent study suggests that the factor mediates its effect by binding to other proteins and not necessarily by binding to the upstream promoter. Kemp *et al.* (1990) have shown that the replication deficiency of Herpes Simplex Virus type I in neuronal cells can be traced to octamer motifs located upstream of the viral immediate early genes. In their study, the octamer motif upstream of the *IE3* gene was shown to bind a repressor protein present only in neuronal cell lines; the nature of the repressor is unknown but any one of the neuronal POU domain proteins could well fill this role. *Oct-2* is a POU gene expressed both in the nervous system and in B-cells. The gene encodes numerous splice variants (Writh *et al.*, 1990) two of which (Oct-2.4 and 2.5) are expressed preferentially in neuronal cells (Lillycrop and Latchman, 1992). Recently, Dawson *et al.* (1994) have shown that the tyrosine hydroxylase gene can be repressed in a cell-specific manner by neuronal isoforms of Oct-2 and that the *cis*-acting element responsible for this repression is the heptamer component of adjacent heptamer-octamer motifs located in the proximal *TH* promoter. Most recently, the Brn factors Brn-3a, Brn-3b and Brn3c have been shown to differentially regulate at least two neuronal genes, and domain swap experiments have been carried out to determine the regions of each protein required for the specificity of regulation (Milton *et al.*, 1995; Budhram-Mahadeo *et al.*, 1995).

More direct proof of neuronal POU protein function comes not from mammals, but from *Drosophila*. The *D. melanogaster* gene *Ddc* encodes the enzyme L-dopa decarboxylase, which is required for catecholamine synthesis (see Fig. 2.2). A POU domain transcription factor termed Cf1-a, which is homologous to the *C. elegans* factor unc 86, binds upstream of the *Ddc* transcriptional start site and has been implicated as a mediator of dopaminergic/serotonergic neuronal differentiation (Johnson and Hirch, 1990). In *C. elegans*, unc 86 also functions to specify dopaminergic and serotonergic neuronal differentiation during development. Treacy *et al.* (1991) have identified a *Drosophila* POU protein which lacks a DNA-binding domain but can form heterodimers with Cf1-a and hence repress *Ddc*. The suggestion is that this factor, named I-POU, may be expressed in nondopaminergic neurons and may repress *Ddc* through the formation of inactive heterodimers although this has yet to be proven experimentally.

2.7.3 Factors containing an HLH domain

An additional class of neuronal transcription factors has been isolated from mammalian brain due to homology with the *Drosophila achaete-scute* complex, a group of *proneural genes* so-called because they confer upon cells the potential to become neurons (Glysen and Dambly-Chaudiere, 1988). Two cDNAs were isolated, termed *Mash-1* and *Mash-2* (for murine achaete-scute homologue) and whilst *Mash-2* was expressed only in the trophectoderm, the *Mash-1* product was shown to be restricted to neuronal precursors (Johnson *et al.*, 1990; Guillemot and Joyner, 1993) suggesting that the role in neuronal development was also preserved. Accordingly, homozygous *Mash-1* knockout mice showed normal development of the central nervous system but defects in the sympathetic, parasympathetic and enteric ganglia, and death of neuronal progenitor cells in the olfactory epithelium (Guillemot *et al.*, 1993). *Neurogenic genes* act later than the proneural genes and their expression contributes to the decision of whether or not a competent proneual cell becomes a neuron. The *Drosophila* homeobox gene *Prospero* and its mammalian homologue *Prox-1* are expressed specifically in newborn postmitotic neurons and may act as transcription factors controlling genes involved in the early processes of neuronal differentiation (Oliver *et al.*, 1993). A number of additional HLH family transcription factors have been identified in the mammalian nervous system, some of which are restricted to the nervous system whilst others are also expressed elsewhere (*see* Section 2.8). Perhaps the most interesting of these is NeuroD (Lee *et al.*, 1995), a bHLH protein which is expressed during the terminal differentiation of a subset of central

and peripheral neurons and which, when expressed ectopically, can cause the premature differentiation of neuronal precursors.

2.7.4 Factors containing an Sry-like box

The Sry-like box is a sequence-specific DNA-binding motif first identified in the human sex determining gene *SRY*. A number of autosomal genes containing similar motifs have recently been identified which are developmentally regulated (Laudet *et al.*, 1993) and these genes have been named the SRY-like box or *Sox* genes. Several chicken (Uwanogho *et al.*, 1995) and mouse (R. Lovell-Badge, unpublished observations; P. Koopman, unpublished observations) *Sox* genes have recently been identified whose expression patterns suggest a role in nervous system development. *Sox-2* and *Sox-3* are expressed in the proliferative neural epithelium, like the proneural gene *Mash-1*. The deposition of postmitotic neurons in the mantle layer of the nervous system is marked by downregulation of *Sox-2* and *Sox-3* and the onset of *Sox-11* expression. Sox-11 is absent from the proliferative layer. Like the proneural and neurogenic HLH factors, therefore, the Sox proteins may also play a role in the progressive determination of neuronal cell fate, a process which necessarily involves the regulation of numerous downstream genes.

2.8 Transcription factor Table

Factor	Alternative Products	Class	Expression (Embryo)	Expression (Adult)	Target site	Known target genes (neural/neuroendocrine)	References
BETA		Unknown		Brain	KB site	Proenkephalin? *Pcp-2*?	Korner *et al.*, 1989
BGC		Unknown		Brain-enriched	Sp1 site	Tissue plasminogen activator	Pecorino *et al.*, 1993
Brn-1		POU III	Widespread in nervous system	Widespread in nervous system. Expression also in kidney	Octamer		He *et al.*, 1989
Brn-2 (N-Oct3/5)	N-Oct 3/N-Oct5A/ N-Oct5B	POU III	Widespread in nervous system	Widespread in nervous system. No expression in kidney	Octamer		He *et al.*, 1989 Schreiber *et al.*, 1993
Brn-3.0 (Brn-3/Brn-3a/ RDC 1)	Brn-3a(l)/Brn-3a(s)	POU IV	Widespread in nervous system	Sensory neurons of brain and ganglia, thalamus, posterior hypothalamus, inferior olive	Octamer	α-internexin (upregulation)	He *et al.*, 1989 Gerrero *et al.*, 1993 Collum *et al.*, 1992 T Thiel *et al.*, 1994 Budhram-Mahadeo *et al.*, 1995
Brn 3.1 (Brn-3c)		POU IV	Widespread in nervous system	None	Octamer	α-internexin (upregulation)	Ninkina *et al.*, 1993 Budhram-Mahadeo *et al.*, 1995
Brn 3.2 (Brn-3b)		POU IV	Widespread in nervous system	None	Octamer	Neuronal nicotinic acetylcholine receptor α2 (upregulation); α-internexin (downregulation)	Lillycrop *et al.*, 1992 Ring and Latchman, 1993 Milton *et al.*, 1995
Brn-4 (RHS-2/ N-Oct4)		POU III	Neural tube but weak in telencephalon	CNS (hypothalamus, media habenula, subependymal zone)	Octamer		Mathis *et al.*, 1992 Le Moine and Young, 1992
Brn-5 (Emb)	Two splice variants in nervous system. Two smaller variants in testis	POU VI	Widespread in nervous system	CNS (particularly in hippocampus)	Octamer		Okamoto *et al.*, 1993 B Andersen *et al.*, 1994

Factor	Alternative Products	Class	Expression (Embryo)	Expression (Adult)	Target site	Known target genes (neural/neuroendocrine)	References
BSF1		Unknown		Brain-specific, primarily in neurons	KB site	*$GABA_A$-R*δ, *Pcp-2*?, *GFAP*?	Motejlek *et al.*, 1994
Cns-1		POU VII		Panneuronal in CNS	Octamer		Bulleit *et al.*, 1994
HES-3		bHLH		Cerebellar Purkinje neurons	E box		Campos-Ortega and Knust, 1990
HES-5		bHLH	Ventricular zone of CNS, neural retina	Low level in mature neurons	N box	*Pcp-2*	Akazawa *et al.*, 1992
hMEF2C	Brain and muscle-specific alternative transcripts	MADS-box (MEF2-like)		Subset of cortical neurons in brain	MEF2 consensus		McDermott *et al.*, 1993
Id-1		HLH	Many tissues, but restricted to ventricular zone within CNS	None	Inhibitory: No DNA-binding domain		Duncan *et al.*, 1992
Id-2		HLH	Many tissues, but restricted to ventricular zone within CNS	None	Inhibitory: No DNA-binding domain		Neuman *et al.*, 1993a
MASH-1		bHLH	Neuroepithelial cells of brain and spine, sympathetic precursors	Pan neuronal, including olfactory epithelium and neural retina			Guillemot *et al.*, 1993 Guillemot and Joyner, 1993 Johnson *et al.*, 1990 Anderson, 1993 Lo *et al.*, 1991
mKr2		Finger	Neuron specific and panneuronal				Chowdhury *et al.*, 1988
NeuN		Unknown		Neuron-specific, panneuronal except cerebellar Purkinje cells and certain sensory neurons	Unknown, but does bind DNA *in vitro*		Mullen *et al.*, 1992

Factor	Alternative Products	Class	Expression (Embryo)	Expression (Adult)	Target site	Known target genes (neural/neuroendocrine)	References
NeuroD		bHLH	CNS and PNS neurons at terminal differentiation		E-box		Lee *et al.*, 1995
neuro-d4	Four splice variants	Finger	Neuron-specific. Expressed in dorsal root ganglia, hippocampus, cerebellar cortex	Strong expression in Purkinje cells			Buchman *et al.*, 1992
NEX-1		bHLH	Marker of neuronal differentiation	Maintained throught adult life. High levels in hippocampus, cerebellum.	E-box	Autoregulates its own gene. Other targets unknown	Bartholomä and Nave, 1994
NGFI-C		Finger	Neuron-specific		GCGGGGGCG		Crosby *et al.*, 1992
NHLH1 (HEN1/NSCL1)		bHLH	Proliferating neurons (subependymal layer)	None	E-box		Brown *et al.*, 1992 Brown and Baer, 1994
NRL (D14546E)		bZIP	Neural retina		E-box		Farjo *et al.*, 1993
NRSEF (NRSBF)		Finger	Ubiquitous in nonneruonal tissues, including proliferative layer of CNS. Also present in various nonneuronal cell lines.		NRSE	*NaII, SCG10,* synapsin I, Na,K-ATPase subunit 14 other candidate genes	Mori *et al.*, 1992 Kraner *et al.*, 1992 Schoenherr and Anderson, 1995
Nurr1		Nuclear receptor	Already detectable in E19 brain, probably neuronal as expressed in PC12 cells	High levels in neonatal brain but less in adult brain	Unknown		Law *et al.*, 1992

Factor	Alternative Products	Class	Expression (Embryo)	Expression (Adult)	Target Site	Known Target Genes (Neural, Neuroendocrine)	References
Oct-1 (OTF-1/ NF-A1/NFIII/ OBP100)	Oct-1A/1B/1C	POU II	Many tissues	Many tissues. In nervous system, expression restricted to thalamus, hypothalamus and cerebellar granule cells	Octamer		He *et al.*, 1989
Oct-2 (OTF-2/ NF-A2)	Oct-2.1 to 2.6 and mini-Oct; (former names Oct-2a-d) Oct 2.4 and 2.5 are neuronal isoforms	POU II	Neural tube, but weak in telencephalon	Lymphoid system, Nervous system (predominantly in hypothalamus and cerebellum)	Octamer	Tyrosine hydroxylase	Clerc *et al.*, 1988 Wirth *et al.*, 1990 Lillycrop and Latchman, 1992 He *et al.*, 1989 Dawson *et al.*, 1992
Olf-1		Unknown	Olfactory neuroepithelium		YTCCCY RGGGAR	*OMP, OcNG,* $G_{olf\alpha}$, Type III cyclase, 50.06, 50.11	Kudrycki *et al.*, 1993 Wang *et al.*, 1993
Pit-1 (GHF-1)	Pit 1/1a (GHF-1/2)	POU I	Neural tube and pituitary	Anterior pituitary	Octamer	Prolactin Growth Hormone	Bodner *et al.*, 1988 Mangalam *et al.*, 1989
Prox-1		Homeobox	Young postmitotic neurins				Oliver *et al.*, 1993
Sox-2, cSox2		SRY-box	Proliferative layer		WWCAAAG		Uwanogho *et al.*, 1995
Sox-3, cSox3		SRY-box	Proliferative layer		WWCAAAG		
Sox-11, cSox11		SRY-box	Young postmitotic neurons		WWCAAAG		
Tst-1 (Oct-6/ SCIP)		POU III	Embryonic brain ES/EC cells	Neurons, myelinating glia, testis	Octamer	P_0, α3 ACH receptor, JCV immediate early genes	He *et al.*, 1989; 1991 Monuki *et al.*, 1993 Yang *et al.*, 1994 Renner *et al.*, 1994

2.9 Neuron-specific gene expression in the mammalian nervous system - concluding comments

Gene expression in the mammalian nervous system has been shown to follow the same basic rules that govern those genes expressed in all other tissues, i.e. mechanisms involving the interaction between specific *cis*-acting elements and diffusible *trans*-acting factors. With a number of notable exceptions, neuronal expression appears to be regulated primarily by positive *cis*-acting elements which, by binding transcriptional activators, allow high level gene expression specifically in neuronal cells. This paradigm is common to eukaryotic genes generally, with negative regulation playing an important role in the tissue-specific expression of only a few genes. Although neuronal gene expression *per se* is mediated principally by positive interactions, the expression of genes in restricted subsets of neuronal cells appears to be controlled essentially by negative interactions. For example, the studies of Ishiguro *et al.* (1993) and Shaskus *et al.* (1992) have shown that the human and rat dopamine β-hydroxylase genes require a cAMP response element as an essential enhancer of gene activity, however, to achieve the correct subneuronal expression pattern, a number of negative modules are required further upstream to progressively restrict the expression domain (Hoyle *et al.*, 1994). It has been suggested that the disproportionate frequency of negative regulatory mechanisms in the mammalian nervous system may reflect the unusually large number of distinct cellular phenotypes which exist and interact within what is commonly regarded a single tissue (Mandel and McKinnon, 1993). Thus the importance of negative modulation may have increased in order to potentiate the maximum number of modes of interaction for a limited number of transcription factors (Mandel and McKinnon, 1993). This is supported by experiments which have shown the same transcription factor can act as both a positive and negative modulator of gene expression (e.g. Tst-1, compare Monuki *et al.*, 1993 and Yang *et al.*, 1994) and that minor modifications to *cis*-acting elements located in a gene promoter can convert them from enhancers to suppressers of gene activity (e.g. see Bessis *et al.*, 1993).

Although a relatively small number of mammalian neuronal genes have been cloned and characterised (there are estimated to be 3×10^4 brain specific genes in the rat genome (Milner *et al.*, 1984)), a number of encouraging similarities are now emerging. It is very likely that, in such a complex tissue as the mammalian nervous system, the number of *cis*-acting elements and *trans*-acting factors which regulate its intricate development, interaction and adaptation to the environment is much larger than the selection that has

been identified thus far. It remains for further studies to shed more light upon this most intricate and elaborate biological phenomenon.

Aims

The two introductory chapters have placed the study of neuron-specific enolase in the context of neuronal gene regulation as a field of research. Particularly, the last sections of Chapter 1 discussed the recent molecular studies of neuron-specific enolase gene regulation, and indicated the limits of those studies and work which could be carried out to further them. The major aims of this project were therefore as follows:

- To develop a system for the analysis of *NSE* gene regulation in cell lines.
- To identify *cis*-acting elements responsible for cell type-specific expression of *NSE ex vivo*, using a deletion-transfection strategy.
- To investigate *NSE* regulation in the context of neuronal differentiation, using the deletion-transfection strategy and established *ex vivo* models such as EC cells and the PC12 cell line.
- To investigate *NSE* regulation *in vivo* by generating transgenic mice carrying parts of the *NSE* 5' flanking region linked to *lacZ*.
- To use information from both *in vivo* and *ex vivo* experiments to delineate gel retardation assays to characterise binding activity on the *NSE* 5' flanking region.

Section II - Materials and Methods

Chapter 3 - Materials

3.1 Equipment

3.1.1 Centrifuges

For routine laboratory procedures involving small sample volumes in Eppendorf microfuge tubes, an MSE MicroCentaur was used at 13 000 x *g*. Where protocols especially recommended cooling, a temperature-controlled IEC Centra MP4R fitted with a microfuge rotor was used as above. Larger samples were centrifuged in 20ml Sterilin universal tubes using an MSE Mistral 2000 or IEC Centra MP4R fitted with a swing bucket rotor. An MSE Mistral 2000 dedicated for cell culture applications was used for pelleting cells during routine cell culture procedures. For greater volume applications such as large scale plasmid preparations, a Beckman J2-21 M/E centrifuge, fitted with a JS 13.1 or JA 14 rotor as appropriate, was used. Caesium chloride equilibrium gradient centrifugation was carried out using a Beckman L8-70M ultracentrifuge fitted with a Vti-50 rotor. For double centrifugations, a Vti-65 rotor was used for the second step.

3.1.2 Microscopes and photography

Embryo dissections were carried out using a Zeiss Stemi SV6 dissecting microscope. This instrument was also used for the photography of wholemount embryos subjected to β-galactosidase staining, *in situ* hybridisation or wholemount immunohistochemical staining. Embryos were photographed on a white tile background with incident light from a Schott KL 1500 electronic fibre optic source using an Olympus SLR OM10 camera and Kodak Ektachrome 160T colour slide film. Cultured cells were observed using a Wild M40 inverted phase microscope. Cells and tissue sections stained with fluorescent antibodies were observed using a Nikon Optiphot epifluorescence microscope and photographed using a Nikon FX-35A camera with Kodak Ektachrome 160T colour slide film.

3.1.3 Incubators and ovens

For hybridisation reactions, membranes were dried in a Gallenkamp 80°C oven and hybridised and washed in a Hybaid minioven. A Gallenkamp size 1 incubator at 37°C was used for the static incubation of agar plates, whilst a New Brunswick Scientific G25 incubator/shaker at 37°C, 250 rpm was used for growing bacterial cultures. A variable temperature Gallenkamp size 1 incubator was used for *in situ* hybridisation protocols and various other incubations. Cultured eukaryotic cells were maintained in a Heraeus CO_2 incubator at 37°C, 5% CO_2, whilst following calcium phosphate transfection, cells were moved to a Flow CO_2 incubator 220 at 35°C, 3% CO_2. Low temperature reactions were carried out in Sadia Airofreeze refrigerators and similar instruments were used for storage of reagents and samples at 4°C and -20°C. For ultralow temperature storage, a Kelvinator 100 series -70°C freezer was used. For sterilisation, a Gallenkamp 180°C OV-330 size 2 oven was used for glassware, and a Victor UV plate dryer was used for drying and sterilising fresh agar plates.

3.1.4 Electrophoresis apparatus

Agarose gels for routine preparative and analytical procedures were run in Horizon 58 horizontal gel tanks (Gibco BRL). Agarose gels for Southern and northern analysis were run in Horizon 11.14 horizontal gel tank (Gibco BRL). Gels were photographed using ISO3000 black and white Polaroid film. Denaturing polyacrylamide gels for resolving nucleic acids (e.g. sequencing gels) were run on a Raven vertical slab gel tank. Nondenaturing gels for electrophoretic mobility shift assays were run on a V15.17 vertical gel tank (Gibco BRL), fitted with a cyclical buffer pump. SDS polyacrylamide gels for resolving proteins were run using a Mini-Protean II system (Bio-Rad). Gels for resolving nucleic acids were run using an LKB 2197 power source. A Bio-Rad model 200 power source was used in conjunction with the Mini-Protean II system. Gels were dried using a Bio-Rad 583 Slab gel dryer and autoradiography was carried out using Fuji X-ray film in cassettes supplied by X-ray Accessories Ltd., Bushey, UK.

3.1.5 Cell culture equipment

Cell culture experiments were carried out in a Gelaire BSB4 containment cabinet. A Bibby rechargeable automatic pipetter was used for aseptic transfer of cells and media.

3.1.6 Miscellaneous equipment

Waterbaths were supplied by Grant Instruments, Cambridge, UK. Microwave ovens were supplied by Phillips, Germany. Heating blocks were supplied by Jennings Laboratory Supplies, Bridgeford, UK. Geiger counters were supplied by Mini-Instruments Ltd., Essex, UK. The vacuum dryer, model EF-03, was supplied by Edwards High Vacuum Ltd., Crawley, UK. Heated stirrers were supplied by A. Gallenkamp & Co. and Vortex machines by Fisons. Rotating platforms and mixers were supplied by Luckham Ltd., Burgess Hill, UK. The cryostat used in this project was a Reichert-Jung Frigocut model 2700. PCRs were carried out on Hybaid Omn-E thermal cyclers. DNA and RNA concentrations were determined using a Pharmacia Ultraspec III UV/visible spectrophotometer.

3.2 Reagents

3.2.1 General chemicals and solvents

Chemicals and solvents used to make common laboratory solutions were usually supplied by Analar BDH or Fisons depending upon availability. Deionised formamide was supplied by Fluka. The detergents Triton X-100 and Tween 20 were supplied by Sigma Chemical Co., St. Louis, USA. For general applications, distilled water was made in the laboratory using a Purite Labwater system and solutions were autoclaved for 20 minutes at 15 psi in a Rosamon electric autoclave. Solutions which could not be autoclaved were made up in sterile redistilled water purified centrally by the department. For RNase-free work, solutions were made up in sterile redistilled water and treated with DEPC according to Sambrook *et al.* (1989). Tris-containing solutions for RNase-free work, which cannot be treated with DEPC, were made up in DEPC-treated, autoclaved water using dedicated Tris-base crystals and baked glassware.

3.2.2 Reagents for specific applications

Agarose and low melting point agarose were supplied by Gibco BRL. Acrylamide was supplied by Fisons and *bis*-acrylamide by Kodak. Tris-buffered phenol was supplied by Fisons. The following reagents, used in several applications, were supplied by Sigma Chemical Co., St. Louis, USA: unlabelled nucleotide triphosphates, gel loading dyes (bromophenol blue, xylene cyanol FF), ethidium bromide, dithiothreitol (DTT), β-mercaptoethanol, guanidine isothiocyanate, protease inhibitors (aprotinin, bestatin, leupeptin, PMSF), sodium azide, paraformaldehyde powder and bovine serum albumin. The suppliers of other reagents intended for use in specific methods are indicated in the appropriate section of the methods chapter.

3.2.3 Radioisotopes

α-^{32}P-dGTP and α-^{35}S-dATP were supplied by Amersham International with specific activities of 3000 and 1000 Ci mmol^{-1} respectively. D-threo-[1, 2-^{14}C]-chloramphenicol was supplied by ICN Radiochemicals with a specific activity of 98 Ci mmol^{-1}.

3.2.4 Bacteriological media and fine chemicals

Materials for bacterial growth media were supplied by Difco laboratories (Michigan, USA) and Oxoid Ltd. (England). Antibiotics were supplied by Sigma Chemical Co., St. Louis, USA. Petri dishes were supplied by Falcon.

3.2.5 Cell culture media and fine chemicals

DMEM (Dulbeccos Modified Eagles Medium) and L-glutamine, penicillin/streptomycin, Versene and trypsin stock solutions were made in the department (see Table 3.1). Ham's F10 medium, RPMI 1640 medium and OptiMEM serum reduced medium were obtained from Gibco BRL. FBS (Foetal Bovine Serum), myoclone FCS (Foetal Calf Serum), Horse Serum and 100x MEM (Minimal Essential Medium) were also obtained from Gibco BRL. Tissue culture grade plastic ware was

obtained from Nunc and Costar. Rat tail collagen and poly-L-lysine for attaching neuronal type cells were obtained from Sigma Chemical Co., St. Louis, USA. The mitogenic inhibitors uridine, cytosine arabinoside and 5'-fluoro-2'-deoxyuridine, and the differentiation inducing agents NGF-β (nerve growth factor β) and all-*trans* retinoic acid were also obtained from Sigma Chemical Co., St. Louis, USA. For transfection, DEAE-dextran was obtained from Pharmacia BioProcesses, Uppsala, Sweden; BES (*N,N-bis*[2-hydroxyethyl]-2-aminoethanesulphonic acid) was obtained from Sigma Chemical Co., St. Louis, USA; TransfectACE, Lipofectin and LipofectAMINE were obtained from Gibco BRL; Transfectam and Tfx-50 were obtained from Promega and DOTAP was obtained from Boehringer Mannheim. Assays for β-galactosidase and CAT (chloramphenicol acetyltransferase) were carried out using acetyl coenzyme A, ONPG (*o*-nitrophenyl-β-galactopyranoside) and β-glactosidase obtained from Sigma Chemical Co., St. Louis, USA. 200 x 200 mm TLC (thin layer chromatography) plates for CAT assays were obtained from Merck, Darmstadt, Germany.

Reagent (Manufacturer)	Stock composition	Used
L-Glutamine (Flow)	200m*M* in water	1/100
Penicillin/Streptomycin (Sigma)	10 000 U ml^{-1} penicillin, 0.1g ml^{-1} streptomycin in PBS	1/1000
Trypsin (Difco)	0.25% w/v in TBS (pH 7.7) + 0.1% w/v phenol red	neat
Versene (Analar)	0.02% w/v EDTA in PBS (pH 7.2) + 0.1% w/v phenol red	neat

Table 3.1: Composition of cell culture reagents made in the department. Abbreviations: PBS - Phosphate Buffered Saline; TBS - Tris Buffered Saline; EDTA - ethylenediaminetetraacetic acid; U - units; w/v - weight solute per volume solvent.

3.3 Enzymes

All enzymes and buffers (excluding those obtained as part of kits) were supplied by Gibco BRL except *Bsa* I and *Hph* I restriction endonucleases and β-agarase I which were supplied by New England Biolabs, and calf intestinal alkaline phosphatase, DNase I and proteinase K which were supplied by Boehringer Mannheim.

3.4 Kits

Geneclean II and Qiaex DNA preparation kits were supplied by Bio 101 Inc, La Jolla CA, USA and Qiagen, Chatsworth CA, USA respectively. The Sequenase version 2.0

DNA sequencing kit was obtained from USB, Cleveland Ohio, USA. The DIG-RNA (T7/SP6) labelling kit and the DIG detection kit were obtained from Boehringer Mannheim, Mannheim, Germany.

3.5 Antisera

A polyclonal antiserum against human NSE (neuron-specific enolase) was obtained from INCstar Corporation, Stillwater MN, USA. Secondary goat anti-rabbit IgG FITC and horseradish peroxidase conjugated antibodies were obtained from Sigma Chemical Co., St. Louis, USA. Polyclonal anti-β-galactosidase antiserum was a kind gift from Mr Dylan Sweetman. Monoclonal anti-DIG antiserum was a kind gift from Mr S S Bhamra. Tissue-specific antisera 2G-9, Ep-A and 4G6 were kind gifts from Dr E A Jones (Jones and Woodland, 1987; Jones and Woodland, 1989; Jones *et al.*, 1993).

3.6 Plasmids

3.6.1 Commercially available plasmids

The following commercially available plasmids were used during this project: pBluescriptIIKS-, pBluescriptIISK- (Stratagene, La Jolla CA, USA) and pCAT-Control, pCAT-Basic, pSV-β-galactosidase (Promega Biotech, UK).

3.6.2 Recombinant plasmids obtained as gifts

pNSElacZ contains 1.8kb of the rat *NSE* 5' flanking region upstream of the *E. coli lacZ* gene allowing expression of β-galactosidase under *NSE* promoter control (Forss-Petter *et al.*, 1990). pcD169 contains the rat *NSE* cDNA including 5' and 3' untranslated regions and a small insert within the coding region, probably representing part of an unexcised intron (Forss-Petter *et al.*, 1986). Both plasmids were kind gifts from Drs. Sonja Forss-Petter and Patria Danielson. pcD-cSox2 and pcD-cSox3 contain the cDNA sequences of the chick Sry-like box transcriptional regulators Sox2 and Sox3 respectively. These were kind gifts from Dr Maria Rex.

3.7 Bacterial strains.

For cloning, four strains of *Escherichia coli* have been used in this project (see Table 3.2). Strains DH5α, JM101 and MC1061 were used for general cloning purposes according to their availability and these were kind gifts from Dr S Burbidge. Strain HB101 was recommended by the suppliers of the pCAT series of vectors for cloning these plasmids and their derivatives. This strain was a kind gift from Dr D P Smith.

Strain	Genotype	Uses
DH5α	*sup*E44 Δ*lac*U169 (Φ80 *lac*Z ΔM15) *hsa*R17 *rec*A1 *end*A1 *gyr*A96 *thi*1 *rel*A1	General cloning
JM101	*sup*E *thi* Δ(*lac-pro*AB) [F' *tra*D36 *pro*AB *lac*I^q ZΔM15]	General cloning
HB101	F$^-$ *leu*36 *pro*A2 *rec*A13 *thi*1 *ara*14 *lac*Y1 *gal*K2 *xyl*5 *mtl*1 *rps*L20 λ$^-$ *sup*E44 *hsd*S20r$_B^-$m$_B^-$	Cloning pCAT vectors
MC1061	Δ(*lac*IPOZYA) X74 *gal*U *gal*K *str*A	General cloning

Table 3.2: Strains of bacteria used in this project with their genotypes and applications.

3.8 Eukaryotic cell lines

The mouse Ltk$^-$ line was a gift from Dr E A Jones. Mouse U-138 MG astrocytoma and U-373 MG glioblastoma lines were gifts from Dr A G Morris. HeLa cells were a gift from Mrs S Corden. The mouse P19 EC (embryonal carcinoma) line was a gift from Dr D Clements. Two PC12 lines have been used during this project. The first was a gift from Glaxo Institute for Molecular Biology, Geneva, Switzerland whilst the second was a gift from Dr P W Andrews; these are termed PC12 (Geneva) and PC12 (Sheffield) in the text. Mouse Neuro-2A and NB4-1A3 neuroblastoma lines were obtained from the American Type Culture Collection.

3.9 Animals

Mice for immunological and *in situ* hybridisation studies were strain TO. For transgenic studies, DNA fragments were microinjected into the pronuclei of one-cell stage C57Bl/6 x CBA F_2 embryos. All mice were supplied by Bantin and Kingsman Ltd., Hull, UK.

Chapter 4 - Methods

4.1 Routine procedures

Most of the procedures in this section are either modified from those published in *Molecular Cloning: a Laboratory Manual* (Sambrook *et al.*, 1989) or taken directly from manufacturers' instructions. I have therefore refrained from lengthy reiteration of readily available information and have restricted the material presented below to the description of deviations from the published protocols.

4.1.1 Routine preparation of plasmid DNA

Depending upon the amount of DNA required and its purpose, a number of different plasmid preparation methods were used.

For routine diagnostic procedures, plasmid DNA was prepared by the TELT method (D Stott, pers. comm.). The DNA obtained using this protocol was unsuitable for many applications due to the presence of impurities but it was of sufficient quality to be cleaved by the majority of restriction endonucleases. From small scale cultures (5ml), 1.5ml was removed to a fresh microcentrifuge tube and centrifuged at 13 000 x *g* for 30 seconds. The supernatant was removed and the pellet of bacterial cells resuspended in 100µl TELT (2.5*M* LiCl, 50m*M* Tris.Cl (pH 8.0), 63.5m*M* EDTA, 4% v/v Triton X-100). To this suspension was added 50µl Tris-buffered phenol and 50µl chloroform:isoamyl alcohol (24:1, v/v). The tube was vortexed for 30 seconds to facilitate thorough mixing of the aqueous and organic phases, and centrifuged as above for 5 minutes. The upper, aqueous layer was transferred to a fresh microcentrifuge tube and precipitated immediately with 2 volumes of ethanol. The tube was vortexed briefly, then centrifuged for 10 minutes as above. The supernatant was removed and the pellet, containing the plasmid DNA, was washed with 70% v/v ethanol, dried and resuspended in 40µl TE (pH 8.0) containing DNase-free RNaseA at a final concentration of 50µg ml^{-1}. The DNA could then be used directly for digestion with restriction endonucleases, as the RNase worked during this subsequent reaction. The yield of plasmid DNA was enough for 5-6 restriction digests.

Where small quantities of plasmid DNA were required for further manipulation, the alkaline lysis method found in Sambrook *et al.* (1989), pp 1.25-1.28 was followed exactly, including the optional step in which the bacterial pellet is resuspended in 500

µl STE (0.1*M* NaCl, 10m*M* Tris.Cl (pH 8.0), 1m*M* EDTA) to avoid enzyme inhibition by components of the bacterial cell walls. This protocol was based on original methods from Birnboim and Doly (1979) and Ish-Horowicz and Burke (1981). The alternative 'boiling method' for small scale plasmid preparation, also found in Sambrook *et al.* (1989), pp1.29-1.30 was tried as well, although it was found to be less satisfactory. This method was adapted from a procedure first published by Holmes and Quigley (1981).

Where large quantities of high quality plasmid DNA were required, the alkaline lysis method (Sambrook *et al.*, 1989), pp 1.38-1.39 was used, followed by purification of supercoiled plasmid DNA by equilibrium centrifugation in a continuous CsCl/ethidium bromide gradient (Sambrook *et al.*, 1989), pp 1.42-1.43. The impure DNA was centrifuged for 22 hours at 45 000 rpm in a fixed angle Vti50 rotor. The lower (supercoiled) band was removed with a wide bore syringe and the DNA purified by extraction with butan-1-ol, followed by extensive dialysis against several changes of 5l TE, followed by ethanol precipitation. Plasmid DNA for transfection of eukaryotic cells was put through two rounds of centrifugation as recommended (Sambrook *et al.*, 1989). Following the first step described above, the supercoiled band was transferred to a fresh 6ml Beckman ultracentrifuge tube and topped up with 1.55 g ml^{-1} CsCl containing 600µg ml^{-1} ethidium bromide. The sample was then centrifuged for 6 hours at 65 000 rpm in a Vti65 fixed angle rotor. The (major) supercoiled band was then removed and purified as described above. The yield of plasmid DNA from this procedure was usually 1-2mg, although it was reduced somewhat by a second centrifugation.

Where the presence of nicked circular DNA and small amounts of linear DNA did not present a problem, the nucleic acid pellet remaining at the final stage of the lysis procedure was resuspended in 2ml of water and the RNA selectively precipitated by adding 2.5ml 5*M* LiCl. The mixture was incubated on ice for 15 minutes then centrifuged at 10000 rpm using a Beckman J2-21M/E centrifuge precooled to 4°C . The DNA (remaining in solution) was transferred to a fresh Corex tube and precipitated with 10ml of cold absolute ethanol; the tube was incubated at -20°C for 10 minutes then centrifuged as above. The DNA pellet was redissolved in 400µl TE (pH 8.0) and transferred to a microcentrifuge tube. DNase free RNaseA was added to a final concentration of 50µg ml^{-1} and the tube was incubated at 37°C for 30 minutes. Residual protein was removed by extraction with phenol, then phenol:chloroform: isoamyl alcohol. Residual phenol was removed by extraction with chloroform:

isoamyl alcohol and the DNA precipitated with ethanol as described in (Sambrook *et al.*, 1989). The yield of this method was 2-3mg DNA.

4.1.2 Routine subcloning

4.1.2.1 Diagnostic and preparative use of restriction endonucleases.

Restriction endonucleases were supplied by their manufacturers with the appropriate buffers and were used according to manufacturers' instructions. The progress of each reaction was assessed by agarose gel electrophoresis as described in section 4.1.3.1. Partial digests were assessed by taking samples from the reaction at various times until completion and comparing the reaction products to the uncut plasmid. For full digests, completion of the reaction was verified by ensuring the absence of uncut plasmid bands in each lane. DNA markers (1kb ladder, Gibco BRL) were always used as a reference. In the case of double digests, the route chosen to achieve the desired reaction depended upon the properties of the enzymes involved. If both enzymes worked with greater than 80% efficiency in the same buffer at the same temperature, the reactions were carried out concurrently. If both enzymes worked with greater than 80% efficiency in the same buffer, but the optimal temperature varied, the reactions were carried out consecutively with an intermediate heat inactivation step if necessary. If the enzymes could not work with greater than 80% efficiency in the same buffer, but one buffer could be converted into the other e.g. by increasing the salt concentration, the reactions were carried out consecutively with the necessary supplementation step and an intervening heat inactivation step if necessary. If the enzymes were totally incompatible, and no route could be found to combine them, the products of the first digest were purified using the Geneclean II kit according to the manufacturer's instructions and redissolved in the buffer appropriate for the subsequent reaction.

4.1.2.2 Filling recessed 3' ends with the Klenow fragment of *E. coli* DNA polymerase I

To facilitate the joining together of incompatible sticky ended DNA fragments, the recessed 3' ends of certain restriction digestion products were filled using the 5'->3' polymerase activity of the Klenow fragment of *E. coli* DNA polymerase I. The procedure followed was similar to that presented in Sambrook *et al.* (1989), appendix

F2-F3, although the final concentration of each dNTP in the reaction was 1m*M*, not 0.5m*M* as suggested.

4.1.2.3 Removing overhanging 3' ends with T4 DNA polymerase

Recessed 5' termini cannot be filled in the same manner as recessed 3' termini because of the polarity of all DNA polymerases and their inability to initiate DNA synthesis *de novo*. To generate blunt ends from overhanging 3' termini the 3'⇒5' exonuclease activity of bacteriophage T4 DNA polymerase was exploited. This enzyme is more suitable than the Klenow fragment for this particular application because it's exonuclease activity is 2-300 fold greater than that of the other enzyme. Whilst trimming overhanging 3' termini, the enzyme simultaneously fills in recessed 3' termini.. The Klenow fragment of DNA polymerase I was chosen when end-filling alone was required simply on the basis of its cost. The procedure followed was similar to that presented in Sambrook *et al.* (1989), appendix F4-F5, although the final concentration of each dNTP in the reaction was 0.1m*M*, not 2m*M* as suggested.

4.1.2.4 Removing 5'-terminal phosphate groups with calf intestinal alkaline phosphatase

The removal of 5'-terminal phosphate groups from linearised plasmids with compatible ends helps to limit intramolecular ligation. The method used was similar to that presented in Sambrook *et al.* (1989), pp 1.60-1.61, although the same amount of enzyme (1 unit per 2 pmoles 5'-terminal phosphate residues) was used for both protruding 5' termini and blunt or recessed 5' termini, resulting in a great excess of enzyme for the former reaction. Following restriction digestion, 10x dephosphorylation buffer (supplied by the manufacturer) and enzyme were added directly to the reaction mixture with no intermediate phenol:chloroform extraction and ethanol precipitation step which is advised in the method of Sambrook and colleagues. A phenol:chloroform extraction step followed by ethanol precipitation was carried out after the reaction was complete in order to remove all traces of the enzyme. This was necessary because even small amounts of phosphatase activity in the subsequent ligation reaction could dramatically reduce its efficiency.

4.1.2.5 Ligation

Ligations (involving cohesive and blunt-ended fragments) were carried out using bacteriophage T4 ligase according to the method of Sambrook *et al.* (1989), pp 1.68-1.70. Bacteriophage T4 ligase buffer was supplied by the manufacturer as a 5x concentrate and was used according to manufacturer's instructions. For the majority of ligations, a recombinant plasmid containing an insert of foreign DNA was generated. Under these circumstances, a threefold molar excess of insert over vector fragments was used in the reaction and the vector fragment was pretreated with CIAP to limit intramolecular ligation (see section 4.1.2.4). No condensing agents were used in blunt-ended ligation reactions, but the concentration of vector fragments was increased from 10μg ml^{-1} to 100μg ml^{-1} with a proportionate increase in the concentration of insert. The concentration of bacteriophage T4 DNA ligase used was 50 Weiss units ml^{-1} (Weiss *et al.*, 1968) for both cohesive and blunt-ended ligations. To verify the various stages of the subcloning procedure, several control ligations were carried out in parallel as shown in table 4.1. These controls were still carried out if subcloning was directional (i.e. the vector ends were incompatible) as they then gave some indication of the performance of the restriction endonuclease digestions.

Control	Contents	Purpose
A	Dephosphorylated vector No insert	Tests for success of dephosphorylation
B	Untreated vector No insert	Tests for integrity of vector sequence and indicates maximum transformation efficiency
C	No vector Untreated insert	Tests for purity of insert
D	No DNA	Tests for purity of reaction components and integrity of bacteria

Table 4.1: Controls used to verify ligation reactions

4.1.2.6 Transformation of competent *Escherichia coli* cells with plasmid vectors

Competent *Escherichia coli* cells were prepared freshly for each transformation according to the method of Cohen *et al.* (1972). An additional step was included in which the cells were resuspended in cold 100m*M* $MgCl_2$ then pelleted at 2000 rpm prior to resuspension in cold 100m*M* $CaCl_2$ as described in the published method. This step was reported to increase the transformation efficiency (C. Mason, pers. comm.). Transformation was carried out with 200μl competent cells using approximately 50ng DNA (from a ligation reaction or freshly diluted from plasmid stock) according to the method of Cohen *et al* (1972). All plasmids used in this study

conferred ampicillin resistance upon their hosts and it was therefore unnecessary to allow the cells to recover following transformation. Transformed cells were plated on LB-agar supplemented with 100µg ml-1 ampicillin, incubated at 37°C overnight and transferred to 4°C before satellite colonies were able to grow.

4.1.3 Gels for resolving nucleic acids

4.1.3.1 Nondenaturing agarose gels for diagnostic applications

For the separation of DNA fragments between 100bp and 12kbp for diagnostic applications, 0.2 volumes of Type III loading buffer (50% v/v glycerol, 0.25% w/v bromophenol blue, 0.25% w/v xylene cyanol FF) was added to each sample and they were loaded and run on 0.6 to 2.0% w/v agarose gels made in 1x TBE buffer, supplemented with 0.2µg ml^{-1} ethidium bromide (made up as a stock in 1x TBE buffer). Gels were run at 80mA in 1x TBE buffer supplemented with 0.5µg ml^{-1} ethidium bromide. At the appropriate time, they were examined over a UV transilluminator and photographed using ISO3000 black and white Polaroid film. The use of nondenaturing agarose gels for Southern and northern hybridisation analysis is described in section 4.1.7.

4.1.3.2 Low melting point agarose gels for preparative applications

For the isolation of DNA fragments generated by restriction endonuclease digests, samples were mixed with Type III loading buffer as described in the preceding section and run on 0.8-1.2% w/v low melting point agarose gels made in 1x TBE buffer supplemented with 0.5µg ml^{-1} ethidium bromide. Gels were run at a maximum of 40mA in 1x TBE buffer supplemented with 0.5µg ml^{-1} ethidium bromide. Appropriate bands were excised as a small gel slice using a fresh razor blade and transferred to a microcentrifuge tube. The DNA was then purified as described in section 4.1.4.

4.1.3.3 Denaturing polyacrylamide gels for high resolution electrophoresis.

Where it was necessary to resolve DNA fragments of similar length (e.g. sequencing reactions), 6% or 8% polyacrylamide gels (19:1 acrylamide:*bis*-acrylamide)

containing 42% w/v urea in 1x TBE were poured between 20 x 40cm glass plates according to the method described in Sambrook *et al.* (1989), pp 6.39-6.43. Samples in denaturing gel loading buffer (90% v/v deionised formamide, 10m*M* EDTA (pH 8.0), 0.01% w/v bromophenol blue, 0.01% w/v xylene cyanol FF) were heated to 100°C on a heating block for 5 minutes, loaded onto the gel and run at 38W in 1x TBE. Gels with ^{35}S-containing samples (e.g. sequencing gels) were fixed by immersion in 10% v/v ethanol, 10% v/v acetic acid for 15 minutes, transferred to Whatmann 3MM paper, dried under vacuum at 80°C and exposed to X-ray film in an autoradiograph cassette without an intensifying screen at room temperature. Gels with ^{32}P-containing samples were left on the lower gel plate, wrapped in cling film and exposed to X-ray film in an autoradiograph cassette with an intensifying screen at -70°C.

Polyacrylamide gels for protein resolution and gel retardation assays are discussed in sections 4.1.8 and 4.6.4 respectively.

4.1.4 Isolating DNA from agarose gels

DNA fragments generated by restriction endonuclease digestion were excised from low melting point agarose gels as a small gel slice according to the method of Sambrook *et al.* (1989), pp 6.30-6.31. The fragment was then purified by one of three methods depending upon its subsequent use. For routine subcloning, fragments were purified using the Geneclean II kit (Bio 101 Inc.) according to manufacturer's instructions. For the purification of particularly small fragments, with which the Geneclean II system was unable to cope, the Qiaex Gel Extraction kit (Qiagen) was used according to manufacturer's instructions. For the purification of particularly large fragments, which tend to be sheared by the vortexing steps required in the above procedures, β-agarase I (New England Biolabs) was used according to manufacturer's instructions.

4.1.5 dsDNA sequencing

Double stranded DNA sequencing was carried out using the Sequenase kit version 2.0 (Promega) according to the manufacturer's instructions. The protocol is based on the dideoxy chain terminator method first proposed by Sanger *et al.* (1977). 2μg of plasmid DNA (prepared using the CsCl equilibrium centrifugation method described

in section 4.1.1) was dissolved in 100µl water and denatured by adding 10µl 2*M* NaOH, 2m*M* EDTA and incubating at 37°C for 30 minutes. The DNA was then precipitated with ethanol and resuspended in 10µl Sequenase 1x react buffer prior to the sequencing reaction.

4.1.6 Isotopic and nonisotopic labelling of nucleic acids

4.1.6.1 Nick translation

Nick translation, to generate isotopically labelled DNA probes for filter hybridisation analysis, was carried out essentially as described in Sambrook *et al.* (1989), pp 10.8-10.9. This was based on methods originally presented by Maniaitis *et al.* (1975) and Rigby *et al.* (1977). The amounts of the various components of the nick translation mix varied between the method of Sambrook *et al.* and the one used during this project. The nick translation mix used in the present study comprised 50-100ng DNA in 1x nick translation buffer (50m*M* Tris.Cl (pH 7.5), 10m*M* $MgSO_4$, 0.1m*M* DTT, 50 µg ml^{-1} bovine serum albumin), 0.75m*M* dATP, 0.75m*M* dCTP, 0.75m*M* dTTP, 1µl DNase 1 (10^5-fold dilution from 10U μl^{-1} stock), 20U DNA polymerase I and 40µCi α^{32}P-dGTP in a total volume of 20µl. The reaction was incubated for 3 hours at 16°C and stopped by adding 80µl 0.3*M* sodium acetate, 1m*M* EDTA. Labelled probe was separated from unincorporated nucleotides by chromatography through a small column of Sephadex G-50 (Sigma Chemical Co., St. Louis, USA). Aliquots of the probe were eluted from the column and those with the highest specific activity were denatured by floating on boiling water for 5 minutes, quenched on ice to prevent reannealing and added to the hybridisation stage of the appropriate reaction (see section 4.1.7).

4.1.6.2 Labelling 3' termini by end-filling

Probes for the electrophoretic mobility shift assay were prepared by end-filling small (50-200bp) DNA restriction fragments, with 5' overhangs, using a nucleotide mix containing α^{32}P-dGTP. The fragments used in this study were generated by restriction endonucleases which left unpaired cytidine residues in the template strand, therefore only one labelled nucleotide was required. The protocol is modified from Sambrook *et al.* (1989), pp 1052-1053. 50-100ng of DNA was labelled in a total reaction volume of 20µl. The reaction mixture comprised 50m*M* Tris.Cl (pH 7.6),

7m*M* $MgCl_2$, 0.1m*M* DTT, 0.1% v/v β-mercaptoethanol, 0.3m*M* dATP, 0.3m*M* dCTP, 0.3m*M* dTTP, 0.5mg ml^{-1} BSA, 20μCi α^{32}P-dGTP and 1-2 units of the Klenow fragment of DNA polymerase I. The reaction was incubated at room temperature for one hour, and stopped by adding 80μl TE and 3μg *Escherichia coli* tRNA (Sigma Chemical Co., St. Louis, USA). The mixture was extracted three times with phenol:chloroform then ammonium acetate was added to a final concentration of 2.5*M* and the DNA was precipitated overnight with ethanol. The probe was recovered by centrifugation at 13 000 x g for 10 minutes at 4°C. It was washed with 70% v/v ethanol, dried and resuspended in 100μl water.

4.1.6.3 Generation of hapten-labelled antisense RNA probes by *in vitro* transcription

The synthesis of RNA probes was facilitated by the use of vectors designed specifically for the *in vitro* transcription of inserted DNA. Such vectors generally contain a polylinker flanked by promoters specific for different bacteriophage RNA polymerases. The pBluescriptII transcription vectors, which were used in this project, contained promoters specific for bacteriophage T3 and bacteriophage T7 RNA polymerases. Linearisation of the recombinant plasmid by restriction endonuclease digestion within the insert allowed the synthesis of 'run-off' sense and antisense transcripts of defined length. The presence of digoxigenin-labelled UTP in the nucleotide mix allowed the synthesis of probes which could be detected using an enzyme-linked immunoassay (Höltke and Kessler, 1990). 2μg of plasmid DNA was linearised with the appropriate restriction endonuclease as described in section 4.1.2.1 and the linear DNA was purified by phenol:chloroform extraction followed by ethanol precipitation. Sense and antisense probes were synthesised using the DIG RNA labelling kit (SP6/T7) (Boehringer Mannheim) according to the manufacturer's instructions, excepting that bacteriophage T3 RNA polymerase (Gibco BRL) was used, in the buffer supplied by the manufacturer, instead of bacteriophage SP6 RNA polymerase. Aliquots of probe were taken from the reaction prior to and following DNase treatment. The success of the reaction was assessed by running samples of DNA template, pre-DNase probe and post-DNase probe against DNA and RNA markers (DNA 1kb ladder and RNA ladder, Gibco BRL) on a 2% w/v agarose gel made in 1x TBE supplemented with 0.2μg ml^{-1} ethidium bromide. 0.2 volumes of Type III loading buffer (50% v/v glycerol, 0.25% w/v bromophenol blue, 0.25% w/v xylene cyanol FF) was added to each sample prior to loading and the gel was run in 1x TBE supplemented with 0.5μg ml^{-1} ethidium bromide for 15 minutes at 100mA.

The probe was precipitated with LiCl and ethanol according to manufacturer's instructions and stored at -20°C in 50µl DEPC-treated sterile distilled water containing 20 units RNase inhibitor.

4.1.7 Filter hybridisation

4.1.7.1 Analysis of genomic DNA by Southern hybridisation

Aliquots of mouse genomic DNA (a gift from Dr David Stott) were digested with three common restriction endonucleases (*Eco*R 1, *Hin*d III and *Bam*H 1) according to manufacturers' instructions, separated by agarose gel electrophoresis and transferred to a nylon membrane (Hybond N+, Amersham) under denaturing conditions as described by Sambrook *et al.* (1989) p 9.45. 20µg of genomic DNA was used per reaction. At completion, the entire contents of each reaction was mixed with 0.2 volumes of Type III loading buffer and loaded onto a 0.6% w/v agarose gel made as described in section 4.1.3.1. Overnight electrophoresis was carried out at 10mA in 1x TBE buffer supplemented with 0.5µg ml^{-1} ethidium bromide. As controls for the subsequent hybridisation reaction, defined quantities of plasmid DNA (1ng, 100pg and 10pg) containing the probe sequence were run alongside the genomic DNA. DNA markers (1kb DNA ladder, Gibco BRL) were used as a reference. After electrophoresis, the gel was photographed as described in section 4.1.3.1 against a fluorescent ruler for future reference.

Following transfer, the nylon membrane was baked for 2 hours at 80°C then immediately cross-linked by placing face-down over a UV transilluminator for 2 minutes. For the subsequent procedures, the membranes were placed in Hybaid C4 glass tubes and were kept wet by constant rotation in a Hybaid mini-oven. Hybridisation reactions and washing steps were carried out according to the phosphate-buffer method of Church and Gilbert (1984). By using this method, prehybridisation was unnecessary and the washing stringency could controlled entirely by temperature. High stringency washes were carried out at 65°C for 15-20 minutes. By varying the temperature between 40°C and 60°C, a range of low and moderate stringency conditions could be generated. Following the washing steps, membranes were removed from the Hybaid tubes, wrapped in cling-film whilst still wet and exposed to X-ray film in a cassette with intensifying screen at -70°C. If kept wet, membranes could be stripped and reused by washing for 10 minutes in 0.2*M* NaOH at room temperature and rinsing in distilled water.

4.1.7.2 Extraction of cellular RNA

Total RNA was extracted from cultured cells using 4*M* guanidine isothiocyanate according to the method of Chirgwin *et al.* (1979). The quality and yield of each extraction was determined by UV spectrophotomertry at 260 and 280nm.

4.1.7.3 Northern hybridisation

Northern hybridisation was carried out according to the method of Thomas *et al.* (1980) using nick translated DNA corresponding to the 3' UTR of the rat *NSE* gene.

4.1.8 Immunoblotting

4.1.8.1 Preparation and electrophoresis of protein extracts

Samples for protein electrophoresis were prepared as described in Sambrook *et al.* (1989), pp 18.62-18.63 although leupeptin and bestatin protease inhibitors were added to the suspension buffer, at final concentrations of 0.5μg ml^{-1} and 40μg ml^{-1} respectively, in addition to the aprotinin and PMSF mentioned in the published protocol. Sonication to shear chromosomal DNA was not performed and did not appear to affect subsequent steps in the procedure. Proteins were separated by SDS-polyacrylamide gel electrophoresis using a discontinuous Tris-glycine buffer according to the method described by Sambrook *et al.* (1989), pp 18.47-18.54. Lanes were equalised for total protein loading using the Bio-Rad protein assay system. Protein size markers were used as a reference and electrophoresis was carried out using the Mini-PROTEAN II gel system (Bio-Rad) according to manufacturer's instructions.

4.1.8.2 Analysis of proteins following electrophoresis

Generally, two identical gels were run in parallel, allowing one to be used for immunoblotting and the other to be stained for total protein. Gels were stained with Coomassie Brilliant Blue R250 (Sigma Chemical Co., St. Louis, USA) according to the method of Sambrook *et al.* (1989), p18.55. Gels were photographed over a light box using an Olympus SLR OM10 camera and Kodak ISO 400 black and white film.

4.1.8.3 Transfer of proteins to nitrocellulose membrane

Proteins were transferred from the gel to a nitrocellulose membrane (Hybond C, Amersham) according to the method of Sambrook *et al.* (1989), pp 18.64-18.66. The transfer was carried out using a Trans-Blot tank (Bio-Rad Laboratories, Richmond CA, USA) for 3 hours at 60V (≈200mA) with the tank immersed in ice.

4.1.8.4 Analysis of proteins following transfer

Following transfer, nitrocellulose filters were stained with Ponceau S (Sigma Chemical Co., St. Louis, USA) according to the method of Sambrook *et al.* (1989), p 18.67. Although the published protocol suggested that the solution should be discarded after use, recycled Ponceau S was found to be perfectly satisfactory.

4.1.8.5 Immunological detection of proteins

Immunological detection of proteins bound to nitrocellulose filters was carried out according to the method of Sambrook *et al.* (1989), pp 18.69-18.75. After blocking in 5% w/v Marvel milk, 0.02% w/v sodium azide in PBS for two hours, the filter was sealed into a plastic bag with 1ml primary antiserum at manufacturers' recommended working dilution and incubated on a tilting platform under foil overnight. Once- or twice-used primary antiserum recovered from immunohistological staining procedures was also found to be perfectly adequate for immunoblot applications. Before incubation with the secondary, horseradish peroxidase-conjugated antiserum, the filter was washed several times in PBS then extensively in phosphate-free, azide-free saline (150m*M* NaCl, 50m*M* Tris.Cl (pH 7.5)). The optimal working dilution for

the secondary antiserum was determined empirically by titration. The filter was sealed into a second plastic bag and incubated on a tilting platform under foil for 2 hours with 1ml of the secondary antiserum at the optimal concentration in phosphate-free, azide-free saline without block. The filter was then washed extensively in phosphate-free, azide-free saline and stained with diaminobenzidine tetrahydrochloride (Sigma Chemical Co., St. Louis, USA) without metal ions as described by Sambrook *et al.* (1989), p 18.75. Filters were photographed over a light box whilst still wet, using an Olympus SLR OM10 camera and Kodak Gold colour film.

4.2 Cell culture techniques

4.2.1 Routine maintenance of cell lines

Cells were maintained in T75 Costar tissue-culture grade flasks in a 37°C humidified incubator with 5% CO_2. Cultures were split when subconfluent, the harshness of the split ranging from 1:5 to 1:20 depending upon the cell line and experimental requirements. The media used to maintain each cell line are shown in table 4.2. To facilitate attachment of the PC12 cells, flasks were coated with rat tail collagen according to the method of Green *et al.* (1987). All cell lines were split using trypsin and Versene. Briefly, the medium was removed from a flask by aspiration and replaced with 5ml Versene, prewarmed to 37°C. The Versene was left in contact with the cells for five minutes to chelate divalent cations, specifically calcium and magnesium. The Versene was then removed by aspiration and replaced with 5ml 0.25% w/v trypsin, also prewarmed to 37°C. The trypsin was left in contact with the cells for up to 5 minutes and then the cells were removed from the surface of the flask by gentle agitation. 10ml complete medium, prewarmed to 37°C, was then added to the flask and the cell suspension collected into a 20ml Sterilin tube. The cells were pelleted by a 3 minute centrifugation at 1000 rpm and resuspended in 10ml fresh medium. 0.5ml - 2ml of the suspension was used to reseed a fresh flask containing 15ml medium prewarmed to 37°C. Cells which tended to clump together, such as the PC12 (Geneva) and P19 cells. were removed from the plastic surface using a Costar cell scraper and a small volume of medium. The cells were then collected into a 20ml Sterilin tube and monodispersed by pipetting up and down a number of times.

Cell line	Maintenance Medium
Ltk-	DMEM + 10% FBS
HeLa	DMEM + 10% FBS
U138MG	DMEM + 10% FBS
U373MG	DMEM + 10% FBS
Neuro 2A	DMEM + 10% FBS, 1% NAA
NB4-1A3	Ham's F10 + 12.5% HS, 2.5% FBS
PC12 (Geneva)	RPMI1650 + 10% HS, 5% FCS
PC12 (Sheffield)	DMEM + 10% FBS
P19 (stem cells)	DMEM + 10% FBS
NTERA-2 (stem cells)	DMEM + 10% FBS

Table 4.2 - Maintenance media required for cell lines used in the present study. All media were also supplemented with 2m*M* L-glutamine and 10 U ml^{-1}/0.1mg ml^{-1} penicillin/streptomycin. Abbreviations: DMEM - Dulbecco's Modified Eagle's Medium, FBS - Foetal Bovine Serum, NAA - Nonessential Amino Acids, HS - Horse Serum, FCS - Myoclone Foetal Calf Serum.

4.2.2 Storing cell lines

For long term storage, cells were dissociated and pelleted as described in the preceding section. They were then dispersed in 10ml fresh medium, in order to dilute out the trypsin and ensure that all clumps were separated, and pelleted once again. The cells were then dispersed in 5ml freezing mix (90% v/v serum, 10% v/v DMSO) and divided into 1ml aliquots in freezing vials. The serum in the freezing mix was made up to reflect the requirements of the proliferating cells, thus for Ltk- cells a mixture containing 90% v/v foetal bovine serum and 10% v/v DMSO was used whilst for PC12 (Geneva) cells, a mixture containing 60% v/v horse serum, 30% v/v myoclone foetal calf serum and 10% v/v DMSO was used. The cells were immediately transferred to a storage box at -70°C and left overnight. They were then stored indefinitely under liquid nitrogen.

4.2.3 Differentiation of PC12 cells using nerve growth factor

PC12 cells were induced to differentiate with NGF-β from mouse submaxillary gland (Sigma, St. Louis MO, USA). PC12 (Geneva) cells were differentiated with complete medium supplemented with 50ng ml^{-1} NGF according to the method of Green *et al.* (1987). PC12 (Sheffield) cells were differentiated according to the same method but using 100ng ml^{-1} NGF (R Gibson, pres. comm.). Differentiated cells for transfection were seeded at a density of 5×10^5 into collagen-coated Nunc 35mm plates.

4.2.4 Differentiation of EC cells using retinoic acid

P19 mouse EC cells were induced to differentiate with retinoic acid according to the method of Rudnicki and McBurney (1987). Differentiated neuronal cells were selected by supplementing the growth medium with 5 μg ml^{-1} cytosine arabinoside 48 hours after retinoic acid treatment was discontinued, thus inhibiting the growth of proliferative cells (Rudnicki and McBurney, 1987).

4.2.5 Transfection of eukaryotic cells - general strategy

Transfections were carried out in triplicate using Nunc 35mm 6-well plates. Each experiment was performed at least twice (lipofections) or three times (other transfection methods). Two independent preparations of each construct were tested (plasmids were prepared using the double caesium chloride equilibrium centrifugation method described in section 4.1.1). In pilot experiments designed to optimise transfection efficiency, cells were transfected with pSV-β-galactosidase, a plasmid which contains the *E. coli lacZ* gene under the control of the SV40 early promoter, and transfection efficiency was determined by soluble β-glactosidase assay. To analyse transcriptional regulation of the rat *NSE* gene, constructs containing parts of the *NSE* 5' flanking region joined to the *E. coli cat* gene were transfected into a variety of neuronal and nonneruonal cell lines and the transcriptional activity of each construct was determined by CAT assay. As internal controls, pCAT-Control, a plasmid which contains the *E. coli cat* gene under the control of the SV40 early promoter, and pCAT-Basic, a plasmid which contains the *E. coli cat* gene but lacks a eukaryotic promoter, were transfected into parallel cultures as standards to compare promoter function. Each construct was cotransfected with an equal amount (by mass) of pSV-β-galactosidase to control for transfection efficiency across all constructs. The cotransfection control plasmid allowed the data from CAT assays to be normalised for transfection efficiency as shown in section 5.5.1.

4.2.6 Transfection using DEAE-dextran

DEAE-dextran mediated transfection was used successfully for Ltk- cells but was found unsatisfactory for other cell types. The method used was that of Selden (1987) and after careful optimisation, 2μg DNA and 200μg DEAE-dextran (added as a 10mg

ml^{-1} solution in TBS) made up in 1.5ml OptiMEM serum-reduced medium were used per 35mm well. Transfection was carried out at 50-60% confluence with a duration 4 hours followed by 2 minute 10% v/v DMSO/PBS shock at room temperature. Chloroquine treatment, which has been reported to increase transfection efficiency (Luthman and Magnusson, 1983) was not attempted.

4.2.7 Transfection using calcium phosphate

Transfection by calcium phosphate was carried out according to the modified procedure of Chen and Okayama (1987; 1988) as described in Sambrook *et al.* (1989), pp16.39-16.40 Several batches of 2x BES-buffered saline were prepared and tested for transfection efficiency using mouse Ltk- cells. The optimal buffer was stored and used as a reference for the preparation of further buffer stocks. Coprecipitates were prepared in 1ml volumes which were divided equally between triplicate wells. The optimal amount of DNA used per transfection was carefully optimised for each individual cell line.

4.2.8 Transfection using liposome formulations

Several different liposome formulations have been used to transfect cells during this project (see Table 4.3). Liposome-mediated transfection was carried out in the first instance according to the manufacturers' general guidelines and then carefully optimised for each cell line by modulation of the transfection parameters according to the manufacturers' instructions. The choice of liposome formulation itself appeared to be critical for the efficient transfection of some cell lines and a number of different products were compared wherever possible. The critical parameters for liposome mediated transfection were transfection duration, concentration of lipid, concentration of DNA and the presence or absence of serum in the transfection medium. Table 4.4 shows the optimum parameters for the cell lines used in this project.

Liposome formulation	Manufacturer
DOTAP	Boehringer Mannheim
Lipofectin	Gibco BRL
LipofectAMINE	Gibco BRL
Tfx-50	Promega
TransfectACE	Gibco BRL
Transfectam	Promega

Table 4.3: Liposome formulations used during this project and their manufacturers

Cell line	Lipid / amount (µl)	DNA (µg)	Duration (hrs)	Medium
Ltk-	LipofectAMINE 5	2	5-8	OptiMEM
NB4-1A3	LipofectAMINE 5	1.5	5	OptiMEM
HeLa	LipofectAMINE 6	2	8-10	OptiMEM
P19 (stem cells)	LipofectAMINE 10	2	4	OptiMEM
PC12 (-NGF)	LipofectAMINE 6-10	2	5	OptiMEM

Table 4.4: Optimal conditions for liposome-mediated transfection of a number of cell lines. Amounts for lipid and DNA are totals per 35mm well with 1ml medium. LipofectAMINE is supplied at 2mg ml^{-1}. OptiMEM is serum reduced medium developed for transfection (Gibco BRL). PC12 cells require collagen coated flasks for attachment (see section 4.2.1).

4.2.9 Preparation of cell lysates

Transfected cells were scraped into microfuge tubes using a Costar disposable scraper, pelleted by 30 second pulse centrifugation and resuspended in 100µl 0.25*M* Tris.Cl (pH 7.5). The cells were lysed by three freeze-thaw cycles, and the debris pelleted by centrifugation at 13 000 x *g* for 10 minutes. 30µl of the cleared lysate was transferred to a fresh microfuge tube and assayed for β-galactosidase activity as described in section 4.2.10 whilst 50µl of the remaining lysate was transferred to a second fresh microfuge tube and assayed for CAT activity as described in section 4.2.11.

4.2.10 Soluble β-galactosidase assay

Assays for β-galactosidase activity in mammalian cell extracts were carried out exactly as described in Sambrook *et al.* (1989), pp 16.66-16.67.

4.2.11 CAT assay

CAT activity was assayed by thin layer chromatography, essentially as described by Gorman *et al.* (1982) although there were minor differences between the method used in this project and the published protocol. The CAT reaction mixture comprised 50µl cell lysate, 5µl 25µCi ml^{-1} D-threo-[1, 2-^{14}C]-chloramphenicol, 5µl 66mg ml^{-1} acetyl coenzyme A and 40µl sterile redistilled water. Reactions were carried out for 1 hour at 37°C. Following chromatography, the plates were dried and exposed to X-ray film in an autoradiograph cassette without intensifier screen at room temperature. Quantification was carried out by wrapping TLC plates in cling film and exposing them to a phosphorimager screen (Molecular Dynamics) for 4 hours. Phosphorimager analysis was facilitated by using the ImageQuant programme (Molecular Dynamics) according to manufacturer's instructions.

4.3 Immunological techniques

4.3.1 Preparation of cultured cells for immunocytochemical staining

Adherent cells were grown on high grade microscope coverslips (Chance Proper Ltd., Warley, UK) according to the method of Harlow and Lane (1988). Coverslips were sterilised by dipping in 70% v/v ethanol and flaming, then they were aseptically transferred to petri dishes under a flow hood. Cells were seeded into the petri dishes at a density of 10^5 ml^{-1}, transferred to a humidified incubator at 37°C, 5% CO_2 and allowed to attach to the coverslips for 24 hours. For nonadherent or partially adherent cells such as PC12 cells, the coverslips were treated with poly-L-lysine and sterilised by overnight exposure to UV light under a flow hood prior to seeding. Cells were fixed by rinsing the coverslips in PBS and incubating in 4% w/v paraformaldehyde (pH 8.0) in PBS for 10 minutes at room temperature. The cells were then washed twice with PBS and permeabilised by dipping into 0.2% v/v Triton X-100 in PBS for 2 minutes. Prior to staining with antibodies, the coverslips were washed in PBS, 3x 5 minutes.

4.3.2 Preparation of mouse embryos and adult tissue for immunohistological staining

Pregnant female mice were sacrificed by cervical dislocation and embryos were dissected into cold PBS. After rinsing, litters were transferred to 20ml Sterilin tubes and fixed in 4% w/v paraformaldehyde/PBS (pH 8.0) on ice. The fixation time was varied from 30 minutes to 12 hours according to the size of the specimens and embryos more advanced than E12.5 were pierced to facilitate penetration of the fixative. After fixation, litters were transferred to fresh 20ml Sterilin tubes and equilibrated first in 5% then 15% w/v sucrose/PBS on ice. Meanwhile, a solution of 7% gelatin, 300 Bloom (Sigma Chemical Co., St. Louis, USA.) in 15% w/v sucrose/PBS was prepared by boiling in a microwave oven and cooling to 37°C in a waterbath. The embryos were transferred to fresh 20ml Sterilin tubes containing 10ml gelatin solution at 37°C and incubated for 30 minutes. They were then transferred to plastic moulds, oriented and embedded in gelatin overnight at 4°C. The blocks were trimmed into trapezoid shapes to emphasise orientation and frozen by immersion in isopentane over liquid nitrogen. They were stored in Sterilin tubes at -70°C prior to sectioning. Adult tissues were dissected, cut into blocks approximately $5mm^3$ if necessary and prepared in the same manner as embryos.

4.3.3 Sectioning of mouse tissue

Blocks stored at -70°C were transferred to the cryostat cabinet at -20°C, mounted onto the chuck using Tissue-Tek O.C.T. compound (Miles Inc.) and trimmed. Sections were cut at 10μm and collected onto gelatin-subbed slides stored at room temperature. 10-20 sections were collected onto each slide. They were briefly air dried and used immediately for immunohistological staining.

4.3.4 Immunological staining - general strategy

Specimens subjected to immunological staining for specific proteins were also subjected to control reactions in order to verify the results. As a negative control, specimens were incubated in blocking agent whilst the experimental specimens were exposed to the primary antiserum. Both the experimental and control specimens were then exposed to the secondary antiserum. This strategy controlled for nonspecific

binding of the secondary antiserum and autofluorescence. As a positive control, a number of antisera known to bind to specific tissues were used. Control specimens were incubated with these antisera whilst the experimental specimens were exposed to their primary antiserum. Both the experimental and control specimens were then exposed to the secondary antiserum. This strategy controlled for failure of primary or secondary binding and allowed nonambiguous identification of specific cell types.

4.3.5 Immunocytochemical staining of cells

Cell staining was carried out according to the method of Harlow and Lane (1988), pp 392-393. Coverslips were transferred to a damp chamber lined with water repelling film (Nescofilm) and blocked with 3% w/v BSA/PBS. Primary antisera were used at manufacturers' recommended working dilutions and coverslips were incubated in the foil-wrapped chamber for 3 hours. The coverslips were then rinsed in three changes of 100ml PBS containing 1% v/v Triton X-100, blotted on a tissue to remove excess liquid and incubated with the secondary, FITC-conjugated antiserum. The optimal working dilution for the secondary antiserum was determined empirically by titration and incubation was carried out as above. The cells were washed and dried as above then mounted on clean glass slides with 50% v/v glycerol/PBS. No anti-quenching additives were used as the stained sections were observed and photographed immediately, as described in section 3.1.2.

4.3.6 Immunohistochemical staining of tissue sections

Sections were blocked and stained according to the method of Hogan *et al.* (1986), pp 243-4. Primary antisera were used at the manufacturers' recommended working dilutions, 250µl per slide. Incubation was carried out for 1 hour in a foil-wrapped damp chamber on a tilting platform. Slides were then transferred to a rack which was placed in a staining jar containing a small magnetic stirrer and washed for 5 minutes each in three changes of 400ml PBS. The optimal concentration of the secondary, FITC-conjugated antiserum was determined empirically by titration. Tissue paper was used to dry as much of the slides as possible without disturbing the sections and the secondary antisera were added, 250µl per slide. Incubation was carried out for 30 minutes as above. The slides were washed and dried as above and the sections were mounted in 50% v/v glycerol/PBS. No anti-quenching additives were used in the

mountant and the stained sections were observed and photographed immediately, as described in section 3.1.2.

4.4 *In situ* hybridisation techniques

4.4.1 *In situ* hybridisation - General strategy

Analysis of *NSE* expression at the mRNA level during mouse development was facilitated by the use of antisense RNA probes corresponding to a distal portion of the rat *NSE* 3' UTR. The UTRs of the three mammalian enolase genes are highly divergent, allowing isogene-specific probes to be generated (see section 1.6), however, there is strong orthologous conservation of the UTRs between species allowing heterologous probes to be used with success. *NSE* mRNA expression was studied by wholemount *in situ* hybridisation using digoxigenin-UTP-labelled antisense RNA probes synthesised as described in section 4.1.6.3. Sense probes generated from the same construct were used as controls for non-specific hybridisation. Further controls, where no probe was included in the hybridisation step, were used to detect nonspecific binding of the antibody or accumulation of colouring reagents.

4.4.2 Preparation of embryos

Wholemount *in situ* hybridisation was carried out according to the procedure described in the following sections. This was optimised by Dr D Stott from standard *in situ* hybridisation protocols (Wilkinson, 1992). Embryos were dissected into cold PBS and the extraembryonic membranes were removed with fine forceps. The embryos were transferred to 20ml Sterilin tubes and fixed on ice in 4% w/v paraformaldehyde/ PBS (pH 8.0) overnight. All following steps were carried out in microcentrifuge tubes at room temperature for 5 minutes using 1ml of solution and gentle end over end rotation, unless stated otherwise. Following fixation, the embryos were washed twice in PBS, refixed in 4% w/v paraformaldehyde/PBS (pH 8.0) at 4°C for 20 minutes, washed twice in PBST (1% v/v Tween 20/PBS) and then incubated with proteinase K (20 μg ml^{-1} in PBST). The duration of proteinase K treatment depended upon the size of the specimen: embryos at E9 or earlier were incubated for 3 minutes, those at E9.5-E10.5 for 5 minutes. The embryos were then rinsed briefly in PBST, washed in PBST then postfixed for 10 minutes in 4% w/v

paraformaldehyde/PBS (pH 8.0). After a brief rinse in distilled water, the embryos were treated for 10 minutes with 0.1*M* triethanolamine (pH 8.0) (Analar BDH) containing 2.5 μl ml^{-1} acetic anhydride (Analar BDH), to reduce background staining. The embryos were transferred to glass vials, washed twice in PBST and were then ready for hybridisation. If storage of the embryos was required, they were transferred to glass vials containing 50% v/v ethanol after the first fixation and wash step. They were then equilibrated in several changes of 70% v/v ethanol and stored at 4°C in the dark. Stored embryos were stable for at least three months and were rehydrated by incubating in 50% v/v ethanol, 30% v/v ethanol/PBS followed by two washes in PBST before further processing.

4.4.3 Wholemount *in situ* hybridisation to mouse embryos

The following steps were carried out at 50°C in a waterbath without rotation. The embryos were equilibrated for 1 hour in hybridisation solution without blocking agents (50% v/v deionised formamide, 5x SSC, 20m*M* Tris.Cl (pH 8.0), 5m*M* EDTA, 0.1% v/v Tween 20). The hybridisation solution was removed and replaced with fresh, plus an equal volume of hybridisation solution with blocking agents (50% v/v deionised formamide, 5x SSC, 20m*M* Tris.Cl (pH 8.0), 5m*M* EDTA, 0.1% v/v Tween 20, 0.2% w/v polyvynilpyrrolidone, 0.2% w/v Ficoll type 400, 2mg ml^{-1} heparin, 2mg ml^{-1} yeast RNA; all blocking agents obtained from Sigma Chemical Co., St. Louis, USA.) and prehybridisation was carried out for at least 2-6 hours. The probe was added to the hybridisation mix to a final concentration of 0.1 μg ml^{-1} and hybridisation was carried out overnight.

4.4.4 Posthybridisation washes

Following hybridisation, the embryos were washed at 50°C for 20 minutes in 50% v/v deionised formamide, 2x SSC, then at 37°C for 3x 10 minutes in NTET (0.5*M* NaCl, 10m*M* Tris.Cl (pH 7.5), 5m*M* EDTA, 0.1% v/v Tween 20). The embryos were then treated with RNase for 30 minutes at 37°C (final concentrations 20μg ml^{-1} RNase A, 100U ml^{-1} RNase T1 in NTET) and washed again in NTET for 10 minutes. The embryos were then washed in 50% v/v deionised formamide, 2x SSC, 50°C for 1 hour; 2x SSC, 0.1% v/v Tween 20, 50°C for 1 hour and 0.2x SSC, 0.1% v/v Tween 20, 50°C for 1 hour. They were then equilibrated with PBST.

4.4.5 Signal detection

Signal detection was carried out using the DIG detection kit (Boehringer Mannheim, Mannheim, Germany) according to manufacturer's instructions. Briefly, nonspecific binding sites were blocked by incubating the embryos with 1ml 0.5% w/v Boeringher blocking compound in PBST for 1 hour at room temperature. 0.5µl of Boehringer antidigoxigenin antiserum was then added (final concentration 1:2000 dilution from stock) and the reaction was incubated overnight at 4°C. The next day, the embryos were washed in PBST at room temperature, 6x 1 hour. The colour reaction was then set up by washing the embryos twice, for 5 minutes each time, in 1ml colour buffer (0.1*M* Tris.Cl (pH 9.5), 50m*M* $MgCl_2$, 0.1*M* NaCl, 0.1% v/v Tween 20, 5m*M* levamisole (Sigma Chemical Co., St. Louis, USA)) and then adding 4.5µl nitroblue tetrazolium and 3.5µl X-phosphate (5-bomo-4-chloro-3-indolyl phosphate) from the kit. The reaction was left to colour for 24 hours, then the embryos were cleared in Murray's reagent (50% v/v benzyl alcohol/benzyl benzoate) and photographed as described in section 3.1.2.

4.5 Transgenic mice

4.5.1 Preparation of transgene DNA

Transgene DNA was prepared according to the method of Hogan *et al.* (1986) without prokaryotic vector sequences, which have been shown to inhibit the expression of integrated genes (e.g. see Chada *et al.*, 1985). Plasmid DNA was prepared by caesium chloride equilibrium centrifugation as described in section 4.1.1 and the transgene excised by digestion with restriction endonucleases as described in section 4.1.2.1. The restriction fragments were separated by agarose gel electrophoresis as described in section 4.1.3.2 and the desired band isolated using β-agarase 1 as described in section 4.1.4. The washed DNA pellet was resuspended at a concentration of 1µg ml^{-1} in 5m*M* Tris.Cl (pH 7.4), 0.1m*M* EDTA.

4.5.2 Generation of transgenic mice

Transgenic mice were generated by pronuclear injection according to the method of Hogan *et al.* (1986). Vasectomisation of stud males, superovulation of donor females,

embryo retrieval, pronuclear microinjection and embryo transfer were carried out by Dr D Stott.

4.5.3 Identification of transgenic embryos

4.5.3.1 Preparation of genomic DNA.

Genomic DNA was isolated from tail tips or extraembryonic membranes according to the method of Gendon-Maguire and Gridley (1993). The tissue was dissected into cold PBS, transferred to a clean microfuge tube and pelleted by brief centrifugation at 13 000 x g. The supernatant was removed and the tissue digested overnight at 55°C with proteinase K. The proteinase K incubation mixture comprised 10m*M* Tris.Cl (pH 7.5), 1m*M* EDTA, 1% w/v SDS and 200 μg ml^{-1} proteinase K (Boehringer Mannheim, Mannheim, Germany). The digested tissue was extracted once with phenol:chloroform and the aqueous phase, containing the DNA, was transferred to a fresh microfuge tube.

4.5.3.2 PCR test to identify transgenic embryos

The presence of transgene sequences was established by PCR using 100ng each of primers LC1 and LC2 which anneal to the *lacZ* coding region (Stott *et al.*, 1993). Three control reactions were performed alongside each experiment, one using DNA from a known *lacZ* transgenic mouse, one using DNA from a known wild type mouse and one using no DNA at all, to control for contamination. The primers and control DNAs were a gift from Miss H Taylor.

4.5.3.3 Southern analysis of transgenic embryos

Following PCR analysis, embryo genomic DNA was investigated by Southern analysis to estimate transgene copy number and check for any rearrangements. Southern analysis was carried out as described in section 4.1.7.1. 20μl genomic DNA, was prepared as described in section 4.5.3.1 by digestion with *Bam*H 1, which cuts within the *lacZ* gene. The DNA was transferred to a nylon membrane and hybridised with a nick translated probe containing the *lacZ* sequence. The results were analysed by autoradiography as described in section 4.1.7.1.

4.5.4 Staining whole mouse embryos for β-galactosidase activity

For wholemount β-galactosidase staining, embryos were prepared and stained according to the method of Bonnerot and Nicholas (1993); they were then equilibrated in absolute methanol and stored at -20°C. As a positive control for the staining reaction, salivary glands were dissected from transgenic homozygous ULZ:307 *Drosophila* and incubated alongside the mouse embryos (dissections carried out by J. Drummond). P[GAL4] enhancer trap lines tend to strongly express ectopic β-galactisidase in the salivary glands due to a poorly understood intrinsic effect of the insert, possibly relating to properties of the polytene chromosomes (M. Allen, pers. comm.) Generally, a blue colour developed in the salivary glands within one minute. Embryos were first photographed uncleared, then after clearing in Murray's reagent (50% v/v benzyl alcohol, 50% v/v benzyl benzoate). Mouse embryos stained for β-galactosidase activity were suitable for cryostat sectioning and were prepared by equilibration in methanol (to remove the clearing agent) followed by incubation in a series of methanol/water mixtures with a decreasing proportion of methanol, followed by equilibration sucrose, embedding in gelatin and freezing in isopentane over liquid nitrogen as described in section 4.3.2. The sections were restained for β-galactosidase activity according to the method of Bonnerot and Nicholas (1993) prior to observation and photography.

4.6 Gel retardation assay.

4.6.1 Preparation of protein extracts from cell lines, embryos and adult organs.

Attached cells were removed from culture vials in a small volume of cold PBS using Costar disposable plastic scrapers. Embryos and adult organs were dissected into cold PBS and cut into small blocks of approximately $5mm^3$ if necessary. Protein extracts were prepared from the above material according to the method of Dent and Latchman (1993).

4.6.2 Preparation of probes for the gel retardation assay

Probes were prepared by end-filling as described in section 4.1.6.2. 1µl of redissolved probe was used for each assay.

4.6.3 DNA - protein interaction *in vitro*.

Binding reactions were carried out in a total volume of 15µl. The components were mixed on ice and were added in the following order: water, 5x gel retardation assay buffer, nonspecific competitor, specific competitor (if appropriate), protein extract. Generally, the components were allowed to equilibrate at 37°C for 10 minutes. The probe was then added and the reaction incubated at 37°C for a further 10 minutes. Different reaction temperatures and incubation times were also tried for individual assays, where appropriate, as described in Chapter 8.

4.6.4 Gels for the gel retardation assay

After incubation, the components of the gel retardation assay reaction were placed on ice. They were then transferred to the cold room and loaded onto a 6% nondenaturing polyacrylamide gel, which had been prerun at 200V, 4°C for 30 minutes. Type III loading buffer (see section 1.4.3.1), diluted with an equal volume of water, was loaded into the first lane as a reference. The gel was run at 500V for 2 minutes then at 200V, 4°C for 2-3 hours in 1x TAE buffer which was recirculated using a cyclical pump. After electrophoresis, the upper glass plate was removed and the gel was fixed by immersion in 10% v/v ethanol, 10% v/v acetic acid for 15 minutes. It was then transferred to Whatmann 3MM paper, dried under vacuum at 80°C and exposed to X-ray film in an autoradiograph cassette with an intensifying screen at -70°C.

Experimental Overview

Studies of gene regulation which involve the identification of specific sequence elements and protein factors required for particular modes of expression are often grouped under the phrase *promoter analysis*, despite the loose use of the term promoter in this context. Promoter analysis may be approached from three directions: firstly, by the *in vivo* route, which requires the generation of transgenic animals; secondly, by the *ex vivo* route, which requires the transfection of suitable cultured cells; and finally, by the *in vitro* route, for which binding activities are sought in purified cell extracts. Generally, the *in vivo* and *ex vivo* approaches are used to establish the position of specific regions of regulatory information, whilst the *in vitro* approach is used to characterise protein binding activities following the location of such regulatory elements. Exceptionally, *in vivo* and *ex vivo* analysis may fail to identify the position of relevant *cis*-acting elements and an *in vitro* transcription assay may be preferred (see Schwartz *et al.*, 1994).

The *in vivo* and *ex vivo* approaches to promoter analysis have relative advantages and disadvantages (see Table 2.1) and for this reason, studies of neuronal gene regulation based upon one or the other alone have sometimes been inconclusive (see section 2.2). It was therefore desirable to investigate the regulation of *NSE* using both transgenic animals and cell lines, allowing the advantages of both strategies to be exploited (Chapters 6 and 7). Before such analysis could take place, however, it was necessary to establish the nature of endogenous *NSE* gene expression in each of the systems used. This preliminary work was essential because no firm conclusions could be drawn from experiments involving the analysis of reporter genes driven by specific regions of the rat *NSE* 5' flanking region, without using the expression of the endogenous (wild type) gene as a reference (Chapters 5 and 7). Finally, the results from *in vivo* and *ex vivo* analysis of the *NSE* 5' flanking region were used to plan *in vitro* experiments to characterise protein binding activities (Chapter 8).

Chapter 5 - Ex vivo *analysis of the rat* NSE *gene 5' flanking region: development of an experimental system*.

5.1 Chapter summary

For *ex vivo* analysis of *NSE* gene regulation, four preliminary factors had to be considered before experiments began. Firstly, it was necessary to consider which cell lines would be most informative for the study. Previous investigators of neuronal gene regulation have often used a range of cell lines, usually including at least one of neuronal and one of nonneuronal origin. The most important aspect of this choice is that cell lines should be available which either do or do not express the gene under investigation. Secondly, it was necessary to consider the manner in which the 5' flanking region should be dissected. Once again, previous studies of neuronal gene expression offer plenty of examples of how such analysis should be undertaken: for some studies, simple external deletions were sufficient. Others required internal deletions, linker-scanning mutations and point mutations. Thirdly, an essential preliminary step was to optimise the parameters for transient transfection. Experience has shown that different cell lines vary widely in their ability to take up DNA, and the most efficient transfection method had to established in each case. Finally, it was important to determine how the results from the transfection experiments would be analysed and used to draw conclusions for further investigation. The purpose of this first results chapter is to describe these preliminary experiments and set the scene for the *ex vivo* analysis proper, which is discussed in Chapter 6.

5.2 Choice of cell lines

5.2.1 Initial considerations

The choice of cell lines for transfection was based upon the ability of each cell type to express *NSE* mRNA and NSE protein. Cells which expressed the endogenous gene were said to be *permissive* whilst those lacking this property were termed

nonpermissive. Before discussing the cells lines in detail, it is worth considering how endogenous gene expression was established and which methods of detection were used.

To establish the expression of NSE protein, protein extracts were resolved by SDS-polyacrylamide gel electrophoresis, electroblotted onto a nitrocellulose membrane and exposed to a polyclonal antiserum raised against human NSE. Because the protein extracts used in this study originated from either murine or rat sources (or cell lines originally derived therefrom), it was essential to ascertain whether or not the antiserum would cross-react with the mouse and rat NSE proteins and therefore be useful as a detection tool. Previous studies have indicated that antigenic determinants on the surface of the NSE protein are highly conserved throughout mammals and birds (Clarke-Rosenberg and Marangos, 1980) and probably other vertebrates (Jackson *et al.*, 1985) therefore cross-reactivity of the antiserum was anticipated. It has also been reported that NSE is an abundant protein in adult mouse, rat, human and monkey brains, accounting for 1-2% of total soluble protein. This preliminary investigation therefore also served to establish the optimal amounts of total protein required to detect NSE.

The concentration of protein in extracts of various cells, adult organs and embryos was determined using the Bio-Rad protein assay according to manufacturers instructions. The assay was calibrated using bovine serum albumin as shown in Figure 5.1. Next, mouse brain protein and PC12 cell protein (of rat origin) were loaded in the following amounts: 10μg, 1μg, 100ng, 10ng, 1ng, resolved and subjected to western analysis as described in section 4.1.8. The results of this analysis are shown in Figure 5.2. In both mouse brain and PC12 extracts, single bands were observed which comigrated with the 45kDa ovalbumin marker, corresponding to the expected size of the NSE monomer (Rider and Taylor, 1975b). This showed that the antiserum raised against human NSE was indeed capable of detecting both the mouse and rat isoproteins. Also in both cases, NSE protein could be detected in as little as 100ng total protein. As the limits of detection in the western procedure lie between 1-

5ng specific protein (Maniatis *et al.*, 1989), this result suggested than in mouse brain and PC12 cells, NSE accounts for approximately 1% of total soluble protein.

To establish the expression of *NSE* mRNA, total RNA was resolved by electrophoresis, transferred to a nylon membrane and hybridised to a probe corresponding to part of the long 3' untranslated region of the rat *NSE* gene. Whilst the coding regions of the three enolase genes are highly conserved and virtually useless as specific probes in cross-species hybridisation studies, the untranslated regions enjoy the status of isogene-specificity and probes corresponding to such regions can discriminate between the three isogenes even across species barriers. These differences form the basis of a major strategy which has been used for the isolation and cloning of enolase sequences, and for the detection of specific sequences in filter and *in situ* hybridisation experiments (see Sakimura *et al.*, 1995 for an example of UTR hybridisation in northern analysis and Keller *et al.*, 1994 for an example in *in situ* hybridisation analysis). Because many of the RNA samples used in the present study were of murine origin, it was essential to establish whether or not the rat *NSE* 3' untranslated region could hybridise with the mouse *NSE* sequence. Alignment using the BESTFIT subroutine of the GCG database showed a high degree of conservation between the mouse and rat 3' untranslated regions, although a number of large gaps were evident in the middle of the rat sequence (Figure 5.3). Convenient restriction endonuclease sites within the rat *NSE* 3' UTR allowed a 300 bp *Nco* I - *Sma* I fragment to be excised and labelled as a probe. This probe was tested by hybridisation to mouse genomic DNA as shown in Figure 5.4. Single hybridising bands were observed in each lane, corresponding to the single copy of the mouse *NSE* gene. This experiment showed that despite some gaps, the rat *NSE* 3' UTR could indeed be used to identify the murine *NSE* sequence in hybridisation studies and was used for all subsequent analysis.

Numerous Originals in Colour

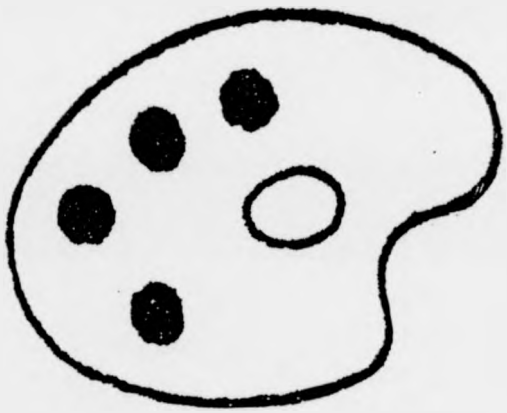

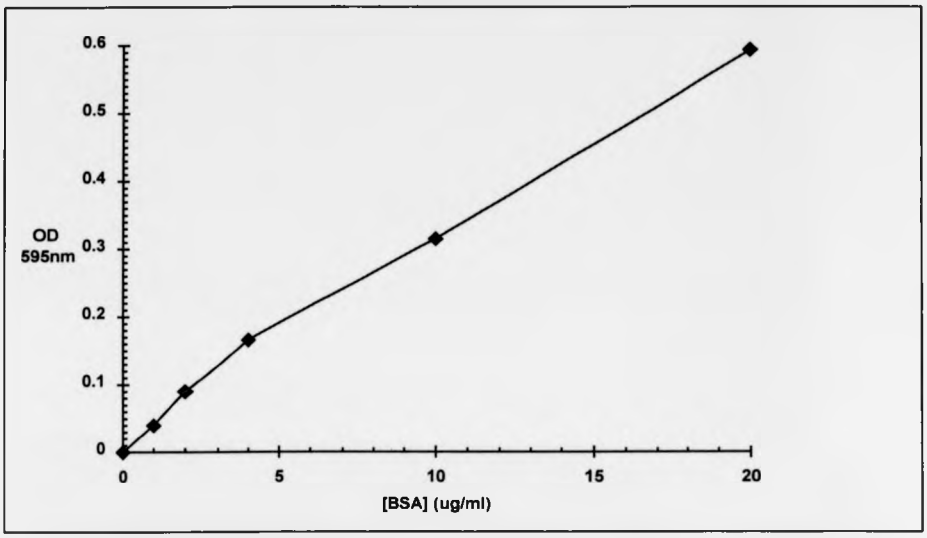

Figure 5.1: Bovine serum albumin (BSA) reference curve for the determination of protein concentrations. Different *known* concentrations of BSA ([BSA], shown on *x*-axis) were used to calibrate the Bio-Rad protein assay, each preparation producing a certain optical density at 595nm (OD_{595}, shown on *y*-axis) when the assay was carried out according to manufacturer's instructions. By plotting OD_{595} values against [BSA], a straight line graph was generated. This represented a linear range over which known values on one axis could be used to predict the unknown values on the other, using the universal equation for a straight line, $y = mx + c$. Protein concentrations were therefore calculated using the equation [protein] = OD/0.032, which is a simple substitution and rearrangement of the above, where x = [protein], $y = OD_{595}$, $m = 0.032$ (a constant determined in this experiment representing the gradient of the straight line) and $c = 0$ (c is the intercept and the line passes through the origin).

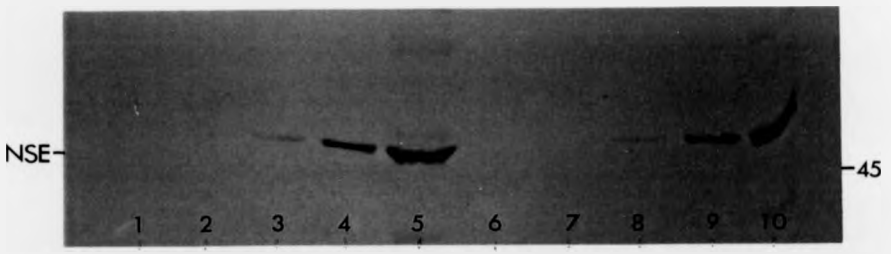

Fig 5.2: Western blot titration to show the sensitivity of polyclonal anti-human NSE antiserum for NSE from mouse brain and PC12 cells (of rat origin). Bound antibody was detected using horseradish peroxidase-conjugated goat anti-rabbit IgG secondary antiserum and bands were revealed by staining with diaminobenzidine tetrahydrochloride without metal ion enhancement. Lanes 1-5 contain total mouse brain protein in 1ng, 10ng, 100ng, 1μg and 10μg amounts respectively. Lanes 6-10 contain total protein from proliferating PC12 cells in 1ng, 10ng, 100ng, 1μg and 10μg amounts respectively. A single band is detected in each lane with a size of approximately 45kDa. This corresponds to the expected size of the NSE monomer. Extra bands observed in lanes 5 and 10 probably reflect overloading of the gel. The 45kDa protein marker was ovalbumin.

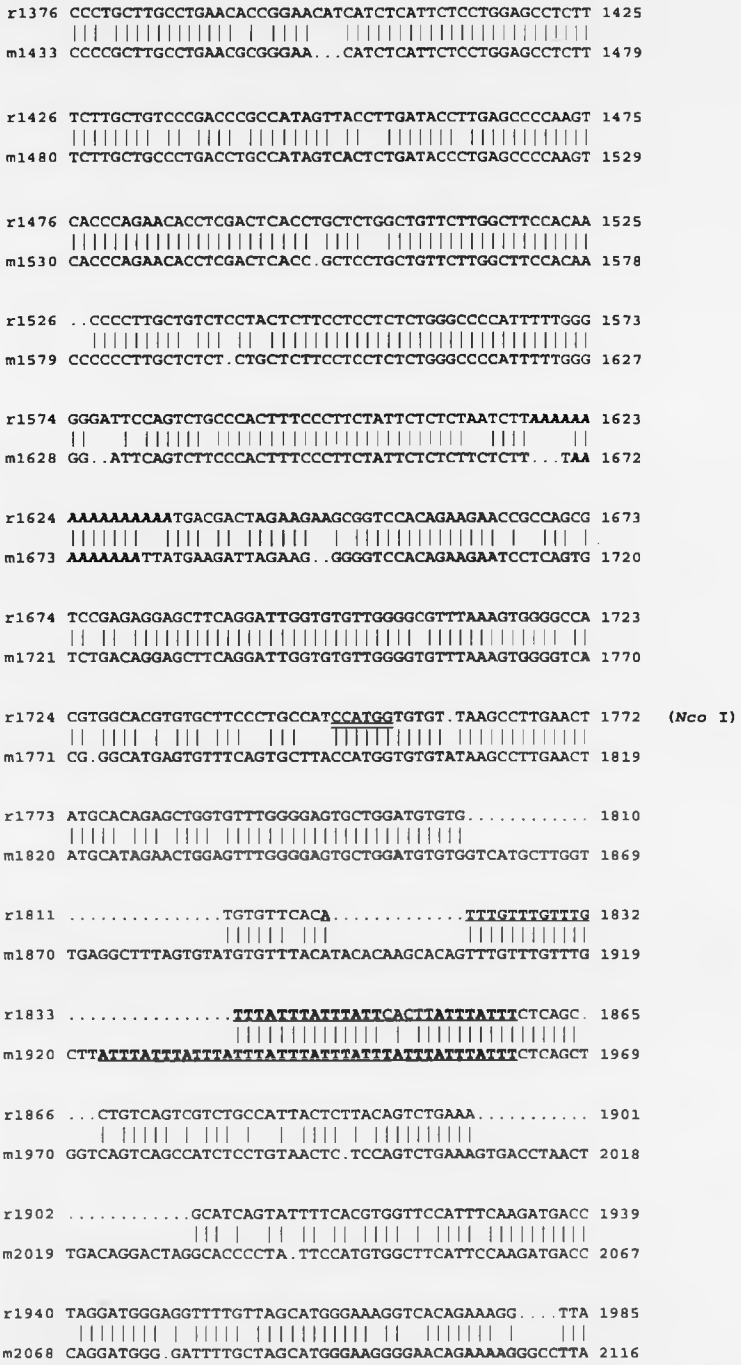
r1376 CCCTGCTTGCCTGAACACCGGAACATCATCTCATTCTCCTGGAGCCTCTT 1425
m1433 CCCCGCTTGCCTGAACGCGGGAA...CATCTCATTCTCCTGGAGCCTCTT 1479
r1426 TCTTGCTGTCCCGACCCGCCATAGTTACCTTGATACCTTGAGCCCCAAGT 1475
m1480 TCTTGCTGCCCTGACCTGCCATAGTCACTCTGATACCCTGAGCCCCAAGT 1529
r1476 CACCCAGAACACCTCGACTCACCTGCTCTGGCTGTTCTTGGCTTCCACAA 1525
m1530 CACCCAGAACACCTCGACTCACC.GCTCCTGCTGTTCTTGGCTTCCACAA 1578
r1526 ..CCCCTTGCTGTCTCCTACTCTTCCTCCTCTCTGGGCCCCATTTTTGGG 1573
m1579 CCCCCCTTGCTCTCT.CTGCTCTTCCTCCTCTCTGGGCCCCATTTTTGGG 1627
r1574 GGGATTCCAGTCTGCCCACTTTCCCTTCTATTCTCTCTAATCTTAAAAAA 1623
m1628 GG..ATTCAGTCTTCCCACTTTCCCTTCTATTCTCTCTTCTCTT...TAA 1672
r1624 AAAAAAAAAATGACGACTAGAAGAAGCGGTCCACAGAAGAACCGCCAGCG 1673
m1673 AAAAAAATTATGAAGATTAGAAG..GGGGTCCACAGAAGAATCCTCAGTG 1720
r1674 TCCGAGAGGAGCTTCAGGATTGGTGTGTTGGGGCGTTTAAAGTGGGGCCA 1723
m1721 TCTGACAGGAGCTTCAGGATTGGTGTGTTGGGGTGTTTAAAGTGGGGTCA 1770
r1724 CGTGGCACGTGTGCTTCCCTGCCATCCATGGTGTGT.TAAGCCTTGAACT 1772 (Nco I)
m1771 CG.GGCATGAGTGTTTCAGTGCTTACCATGGTGTGTATAAGCCTTGAACT 1819
r1773 ATGCACAGAGCTGGTGTTTGGGGAGTGCTGGATGTGTG..... 1810
m1820 ATGCATAGAACTGGAGTTTGGGGAGTGCTGGATGTGTGGTCATGCTTGGT 1869
r1811 .....TGTGTTCACA.....TTTGTTTGTTTG 1832
m1870 TGAGGCTTTAGTGTATGTGTTTACATACACAAGCACAGTTTGTTTGTTTG 1919
r1833 .....TTTATTTATTTATTCACTTATTTATTTCTCAGC. 1865
m1920 CTTATTTATTTATTTATTTATTTATTTATTTATTTATTTCTCAGCT 1969
r1866 ...CTGTCAGTCGTCTGCCATTACTCTTACAGTCTGAAA..... 1901
m1970 GGTCAGTCAGCCATCTCCTGTAACTC.TCCAGTCTGAAAGTGACCTAACT 2018
r1902 .....GCATCAGTATTTTCACGTGGTTCCATTTCAAGATGACC 1939
m2019 TGACAGGACTAGGCACCCCTA.TTCCATGTGGCTTCATTCCAAGATGACC 2067
r1940 TAGGATGGGAGGTTTTGTTAGCATGGGAAAGGTCACAGAAAGG....TTA 1985
m2068 CAGGATGGG.GATTTTGCTAGCATGGGAAGGGGAACAGAAAAGGGCCTTA 2116

```
r1986 GCAATGGTTTTTCATTTGGTGCACTAACTGAAGCTCGGTACTTTACAGAA 2035
      |||||  |  ||||||  |||||||||||  |||||||||  ||||||||||
m2117 GCAAT..TGCTTCATTCGGTGCACTAACCGAAGCTCGGAACTTTACAGAA 2164

r2036 TGGGGCTGTGTACCCGGGGA..CTTTTCTCCTATAACTCTCTCCCCCAGC 2083  (Sma I)
      ||||||||||| ||| ||||  ||||||||||  ||||  ||||  |||||||
m2165 TGGGGCTGTGGACCTGGGGAGGCTTTTCTCCTCTAACCCTCT.CCCCAGC 2213

r2084 CCTAGGTTCCTCAGTCTTTTTCTCCGGCTGCACCAGAGCGCTGCCTCATT 2133
      ||||||  |||||  |||  |||||||||||||||||||||||||||||  |
m2214 CCTAGGCTCCTCCGTC..TTTCTCCGGCTGCACCAGAGCGCTGCCTCACT 2261

r2134 CCCCCGTGCCATGTCCCACAGTTGCCACTGTCTCTGTGGCTTTGAAATGA 2183
      ||||  | ||||||||||||||||||||||  ||||  ||||||||||||||||
m2262 CCCCTGCGCCATGTCCCACAGTTGCCACCATCTCCGTGGCTTTGAAATGA 2311

r2184 CCACCACTATTAAAGTCTGAACCACAGTGC                    2213
      |||||||  ||||||||||||||  |||||  ||
m2312 CCACCACCATTAAAGTCTGAATCACAGCGC                    2341
```

Fig 5.3 (above and opposite page): Alignment of the rat (r) and mouse (m) *NSE* 3' UTRs. Numbers refer to the positions within each respective cDNA sequence (Sakimura *et al.*, 1985a; Kaghad *et al.*, 1990) and bear no significance to the numbering system used to describe the rat *NSE* 5' flanking sequence throughout this thesis. An internal A-rich region, which is thought to represent the site of an obsolete poladenylation sequence (Day *et al.*, 1993), is shown in bold italic. A conserved element, characterised by numerous repeats of the motif ATTT(Day *et al.*, 1993) is shown in bold underlined. These motifs are discussed in section 1.7.5. In the rat sequence, the positions of restriction endonucelase sites for *Nco* I and *Sma* I are identified by double underlining with the endonuclease identified in the right hand margin. These sites are the boundaries of the segment used as a probe for hybridisation experiments.

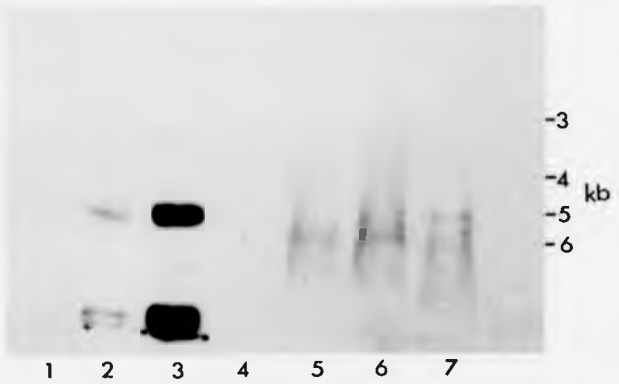

Figure 5.4: Southern blot showing mouse genomic DNA, digested with three common restriction endonucleases and probed with a *Sma* I - *Nco* I fragment of the rat *NSE* 3' untranslated region. Lanes 1, 2 and 3 loaded with plasmid pcD169, containing the rat *NSE* cDNA (Forss-Petter *et al.*, 1986) in 10pg, 100pg and 1ng amounts respectively, as positive controls for hybridisation. Lane 4 was empty. Other lanes loaded with 20µg genomic DNA, lane 5 - digested with *Bam*H I; lane 6 - digested with *Eco*R I; Lane 7 - digested with *Hin*d III. Blot was hybridised overnight, washed at a final stringency equivalent to 0.4x SSC at 55°C and exposed overnight. Markers are Gibco BRL 1kb DNA ladder.

5.2.2 Analysis of cell lines

In previous *ex vivo* studies of gene regulation, the investigators have tended to use permissive and nonpermissive cells to distinguish between positive and negative aspects of cell type-specific regulation. Thus the deletion of a positive cell type-specific regulatory element would generate a fall in reporter gene activity specifically in the permissive cell line, whilst the removal of a negative cell type-specific element would cause a rise in reporter gene activity in the nonpermissive cells. Neuron-specific gene regulation can be achieved by positive or negative regulation, as discussed in Chapter 2. It was therefore desirable to study *NSE* gene regulation in both permissive and nonpermissive backgrounds.

The choice of cell lines for this project is discussed in the following sections. In each case, endogenous expression of *NSE* mRNA and NSE protein was established by northern and western analysis using RNA and protein from mouse brain and liver as positive and negative controls, respectively. For those cells where the expression of NSE was confirmed by western analysis, immunocytochemical staining was used to investigate intracellular localisation of the protein.

5.2.3 Endogenous *NSE* gene expression in Ltk- and PC12 cells

For the preliminary studies of *NSE* gene regulation, PC12 (Geneva) and Ltk- cells were chosen as candidate neuronal and nonneuronal lines. The expression of *NSE* mRNA and NSE protein has been reported previously in undifferentiated and NGF-treated PC12 cells (Vinores *et al.*, 1981; Sakimura *et al.*, 1995) and this cell line was recently used for analysis of *NSE* gene regulation (Sakimura *et al.*, 1995). *NSE* gene expression in Ltk- cells has not been reported, and it was important to establish the nonpermissive status of these cells. For RNA analysis, total RNA (10μg per lane) was resolved by electrophoresis and subjected to northern hybridisation as described in section 4.1.7.3. Figure 5.5a shows the results of this analysis. In the brain and

PC12 cell lanes, a single intense hybridising band could be seen comigrating with the 2.37 kb marker, corresponding to the expected size of the mouse and rat *NSE* messages. A second, weakly hybridising band, which was estimated to be approximately 600 b in length, could also be observed in the same lanes. The nature of this band was unknown: it was unlikely to be an unrelated transcript because in this experiment and those presented later in the chapter, its specificity and intensity mirrored those of the major band. Furthermore, Southern analysis carried out at the same stringency revealed only a single hybridising sequence in the mouse genome (Figure 5.4). Some heterogeneity in the transcriptional start site of the *NSE* gene generates transcripts with a range of sizes, but all such products have been reported to be over 2 kb in length. It was very unlikely that the 600 b band represented a novel alternative splice product as this would surely have been identified by other authors (Sakimura *et al.*, 1985b; Forss-Petter *et al.*, 1986). The weak band may correspond to a more stable degradation product, as a smeared 'tail' of such products can be seen running ahead of the major band. Neither the major *NSE* band, nor the minor band was observed in the liver or Ltk- cell lanes. For protein analysis, total protein (5μg per lane) was resolved by electrophoresis and subjected to immunoblotting as described in section 4.1.8. The results of this experiment are shown in Figure 5.5b. In the brain and PC12 cell lanes, a single band was detected which was slightly retarded with respect to the 45kDa ovalbumin marker. The position of this band corresponded to the expected size of the *NSE* monomer (47kDa). It is clear from these experiments that the PC12 (Geneva) cell line expresses levels of *NSE* mRNA and NSE protein which are comparable to or greater than those found in adult brain. This may reflect the large population of glial cells in the whole brain, which dilute the *NSE*-expressing neuronal cells. *NSE* mRNA and NSE protein were undetectable in the Ltk- cell line, confirming its proposed role as a nonpermissive system for the analysis of *NSE* gene regulation. *In situ* detection of NSE protein in PC12 cells was carried out as described in section 4.3.5. The results are shown in Figure 5.5c and demonstrate that the protein is dispersed throughout the cytoplasm.

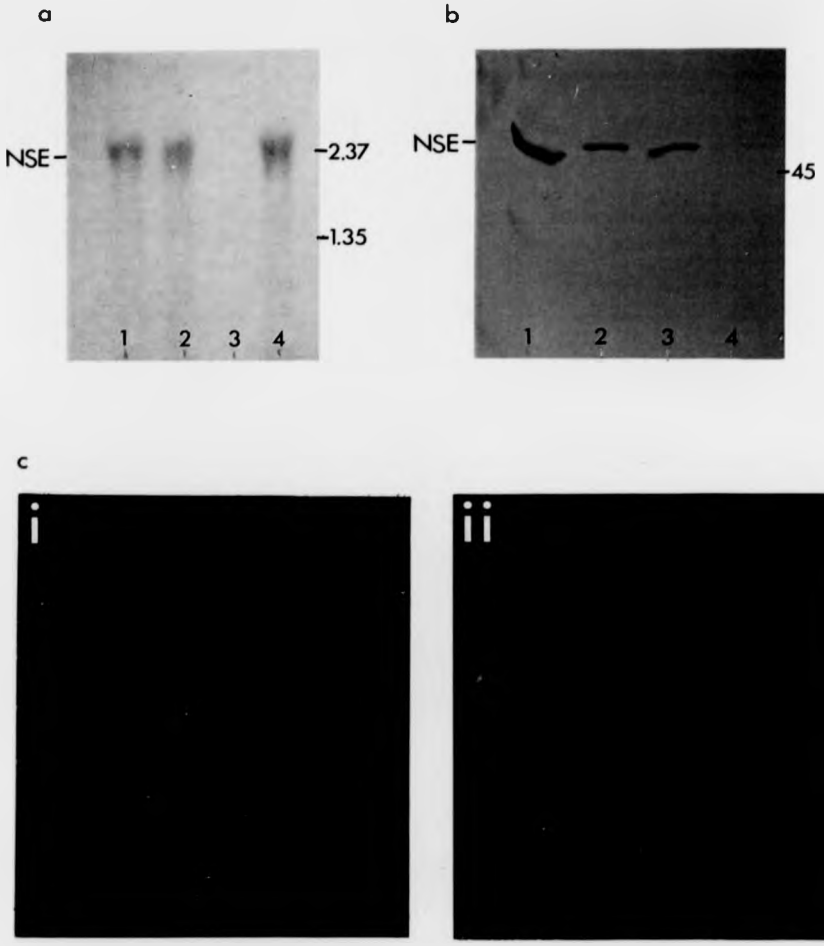

Figure 5.6: Northern, western and immunocytochemical analysis of U138MG glioma and U373MG astrocytoma cells. a) Northern analysis using the *Sma* I - *Nco* I fragment of the rat *NSE* 3' UTR as a probe - lanes loaded equally for total RNA, 10μg per lane: 1 - U373MG, 2 - U138MG, 3 - mouse liver, 4 - mouse brain. Markers are Gibco BRL RNA ladder. b) Western analysis using anti-human NSE, detected with horseradish peroxidase-conjugated goat anti-rabbit IgG and revealed by staining with diaminobenzidine tetrahydrochloride without metal ion enhancement - lanes loaded equally for total protein, 5μg per lane: 1 - mouse brain, 2 - U138MG, 3 - U373MG, 4 - mouse liver. 45kDa marker is ovalbumin. c) Immunocytochemical analysis of (i) U138MG and (ii) U373MG cells using anti-human NSE, detected with FITC-conjugated goat anti-rabbit IgG, x40 under epifluorescence microscopy. Staining observed throughout cell bodies of both cell types, but only limited staining was observed for the glioma line U138MG.

5.2.5 *NSE* gene expression in neuroblastoma cells

Following the preliminary transfection studies described in the first part of the next chapter, two neuroblastoma cell lines, Neuro-2A and NB4-1A3, were obtained. Whilst the glioma cell lines described in the preceding section proved satisfactory as permissive cells, it was preferable to study *NSE* gene regulation in a truly neuronal background for the following reason: as endogenous glial cells do not express *NSE*, the expression observed in cell lines of glial origin must reflect some aspect of the genetic change which accompanies growth transformation and it is therefore possible that *NSE* gene expression in such cell lines is mediated by an unusual or aberrant pathway; dissection of the 5' flanking sequence in such a background might not, therefore, reveal the mechanism of gene regulation which occurs normally.

Previous studies have shown that proliferating neuroblastoma cells express *NSE* at very low levels, and that in some cases, the mRNA and protein may be barely detectable (Zomzely-Neurath, 1983; Sakimura *et al.*, 1995). However, if cells are allowed to become confluent, the slowing down of growth induces *NSE* gene expression and levels of the gene product rise (see section 1.5.3 and references therein). It was important to establish the characteristics of *NSE* gene expression in proliferating and confluent neuroblastoma cells because this crowding factor would also influence the behaviour of reporter constructs containing fragments of the *NSE* 5' flanking region. Generally, in the transfection experiments described in this and the following Chapters, transfection was carried out using semi-confluent proliferating cells and posttransfection cells were collected 48 hrs later when fully confluent. In the first instance, total RNA and protein was isolated from proliferating Neuro-2A and NB4-1A3 cells and subjected to northern, western and immunocytochemical analysis as described in section 5.2.3. As reported previously for other neuroblastoma lines, the levels of *NSE* mRNA and NSE protein were almost undetectable by biochemical means although staining was observed in the perikarya and neurites of isolated cells of both types subjected to immunocytochemical analysis. These results are shown in Figures 5.7a-c. Total RNA and protein was then isolated from proliferating Neuro-2A

cells seeded at 10^5 cells ml^{-1} after 0, 1, 2 and 3 days in culture (by day 3, the cells were fully confluent). The results, shown in in Figures 5.8a and 5.8b, showed that the levels of mRNA and protein increased with time in culture, and that the upregulation correlated to the confluence of the cells. Fully confluent cells expressed *NSE* mRNA and NSE protein at similar levels to those observed in adult brain, suggesting that posttransfection cells represented an excellent permissive system for the analysis of *NSE* gene regulation. The 600 b RNA band observed in the brain control lane (as discussed in section 5.2.3) was also evident in the Neuro-2A cell lanes, and its intensity increased in parallel with the major *NSE* mRNA band. This observation in particular suggested that the 600 b RNA band was not an independent transcript, but a degradation product of the full length *NSE* message. Western analysis suggested that NSE protein accumulation lagged behind that of the transcript, as the intensity of the NSE protein signal by day 2 in culture did not match that in adult brain (Figure 5.8b, lane 5) whereas the *NSE* message had already accumulated to such levels (Figure 5.8a, lane 5); evidence for posttranscriptional downregulation of the *NSE* gene has already been discussed (see section 1.7.5).

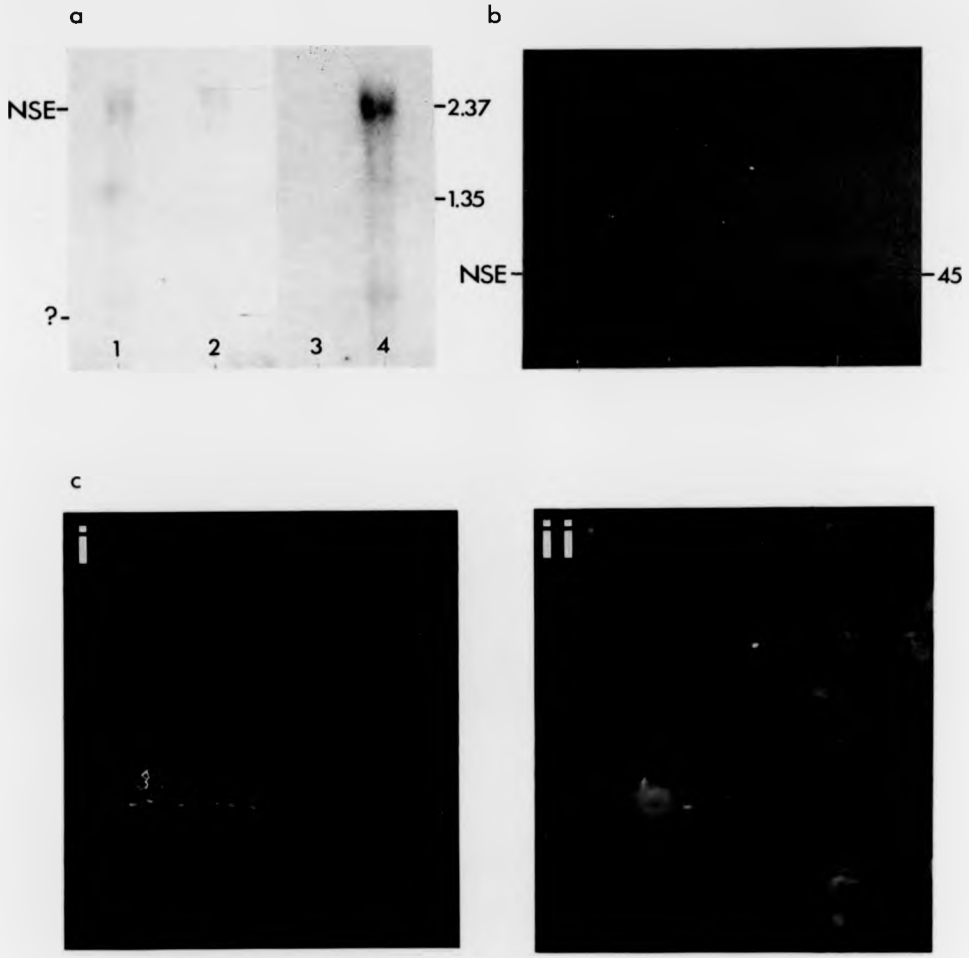

Figure 5.7: Northern, western and immunocytochemical analysis of Neuro-2A and NB4-1A3 neuroblastoma cells. a) Northern analysis using the *Sma* I - *Nco* I fragment of the rat *NSE* 3' UTR as a probe - lanes loaded equally for total RNA, 10μg per lane: 1 - NB4-1A3 cells, 2 - Neuro-2A cells, 3 - mouse liver, 4 - mouse brain. Markers are Gibco BRL RNA ladder. b) Western analysis using anti-human NSE, detected with horseradish peroxidase-conjugated goat anti-rabbit IgG and revealed by staining with diaminobenzidine tetrahydrochloride without metal ion enhancement - lanes loaded equally for total protein, 5μg per lane: 1 - NB4-1A3 cells, 2 - Neuro-2A cells, 3 - mouse liver, 4 - mouse brain. 45kDa marker is ovalbumin. c) Immunocytochemical analysis of (i) Neuro-2A cells and (ii) NB4-1A3 cells using anti-human NSE, detected with FITC-conjugated goat anti-rabbit IgG, x40 under epifluorescence microscopy. Staining observed throughout cell bodies and neurites of both cell types.

a

b

Figure 5.8: Northern and western analysis of *NSE* gene expression in cultured Neuro-2A cells. a) Northern analysis using the *Sma* I - *Nco* I fragment of the rat *NSE* 3' UTR as a probe - lanes loaded equally for total RNA, 10μg per lane: 1 - mouse liver, 2 - mouse brain, 3-6 - Neuro-2A cells after 0, 1, 2 and 3 days in culture. Markers are Gibco BRL RNA ladder. b) Western analysis using anti-human NSE, detected with horseradish peroxidase-conjugated goat anti-rabbit IgG and revealed by staining with diaminobenzidine tetrahydrochloride without metal ion enhancement - lanes loaded equally for total protein, 5μg per lane: 1 - mouse liver, 2 - mouse brain, 3-6 - Neuro-2A cells after 0, 1, 2 and 3 days in culture. 45kDa marker is ovalbumin. Cells were 90% confluent after 2 days and fully confluent by three days.

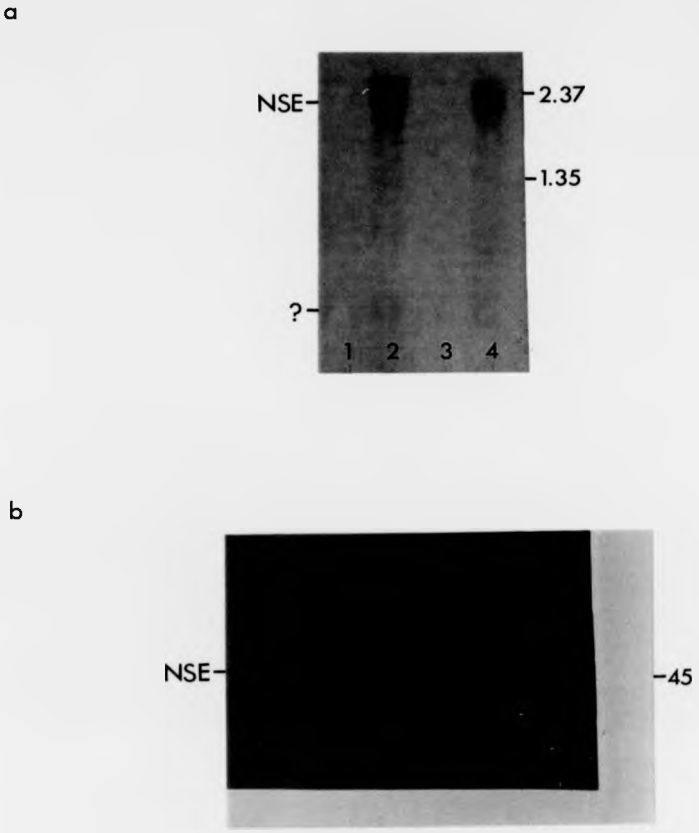

Figure 5.11: Northern and western analysis of differentiating P19 EC cells. a) Northern analysis using the *Sma* I - *Nco* I fragment of the rat*NSE* 3' UTR as a probe - lanes loaded equally for total RNA, 10μg per lane: 1 - P19 stem cells, 2 - P19 neurons, 3 - mouse liver, 4 - mouse brain. Markers are Gibco BRL RNA ladder. b) Western analysis using anti-human NSE, detected with horseradish peroxidase-conjugated goat anti-rabbit IgG and revealed by staining with diaminobenzidine tetrahydrochloride without metal ion enhancement - lanes loaded equally for total protein, 5μg per lane: 1 - P19 stem cells, 2 - P19 neurons, 3 - mouse liver, 4 - mouse brain. 45kDa marker is ovalbumin. P19 stem cells were proliferating cells equivalent to stage (a) in Figure 5.10. P19 neurons were fully differentiated, equivalent to stage (c) in Figure 5.10.

5.2.8 *NSE* gene expression in PC12 cells and their neuronal derivatives

PC12 cells present a classic *ex vivo* model of neuronal differentiation. It is well established that these cells can differentiate into neurons when treated with low doses (1ng ml^{-1}) of nerve growth factor (Green *et al.*, 1987), and other investigators have demonstrated that the induction of *NSE* gene expression accompanies this process (Vinores *et al.*, 1981). Undifferentiated PC12 cells have been shown to express *NSE* mRNA and NSE protein at relatively high levels (see sections 5.2.1 and 5.2.3) thus an investigation of *NSE* induction by NGF was made. Northern and western analysis were used to determine the levels of *NSE* gene products in both proliferating and differentiating PC12 cells as described in section 5.2.3. However, under the conditions employed in this project, only a slight increase in *NSE* mRNA and NSE protein expression was observed in differentiated verses undifferentiated PC12 cells. It is interesting to note that almost identical results were obtained from both PC12 clones used in this study as shown in Figures 5.12 (PC12 (Geneva)) and 5.13 (PC12 (Sheffield)).

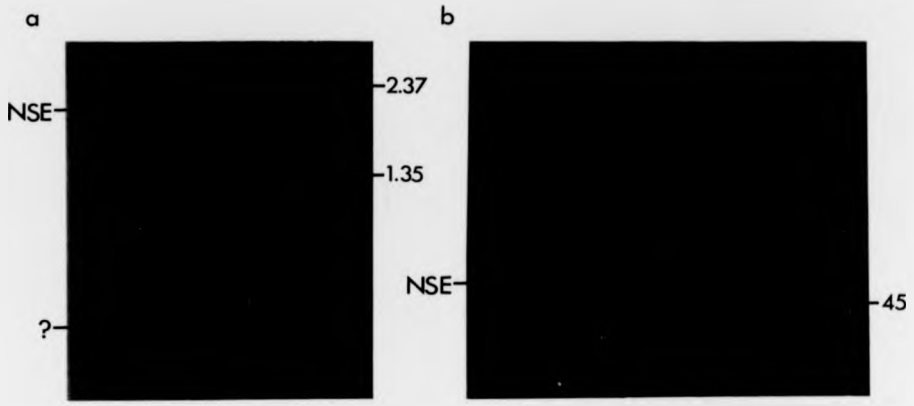

Figure 5.12: Northern and western analysis of differentiating PC12 (Geneva) cells. a) Northern analysis using the *Sma* I - *Nco* I fragment of the rat *NSE* 3' UTR as a probe - lanes loaded equally for total RNA, 10μg per lane: 1 - mouse brain, 2 - mouse liver, 3 - undifferentiated PC12 cells, 4 - differentiated PC12 cells. Markers are Gibco BRL RNA ladder. b) Western analysis using anti-human NSE, detected with horseradish peroxidase-conjugated goat anti-rabbit IgG and revealed by staining with diaminobenzidine tetrahydrochloride without metal ion enhancement - lanes loaded equally for total protein, 5μg per lane. During immunoblotting, gel was placed upon the filter in the normal rather than inverted orientation. Consequently, the order of lanes was reversed with respect to the northern blot: 1 - differentiated PC12 cells, 2 - undifferentiated PC12 cells, 3 - mouse liver, 4 - mouse brain. 45kDa marker is ovalbumin.

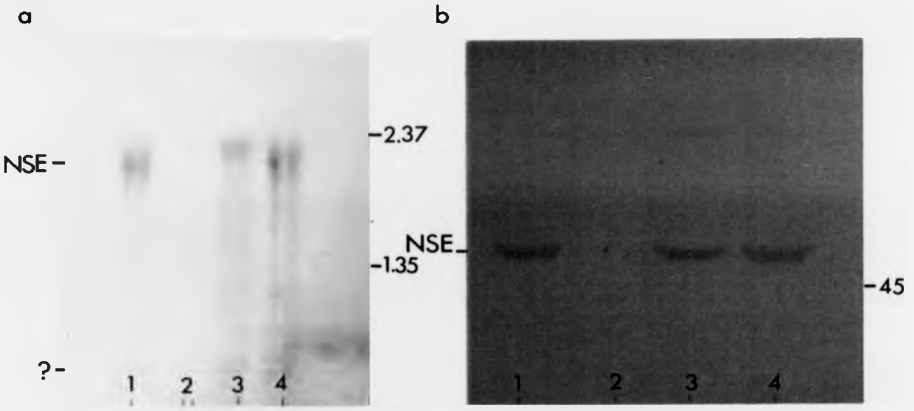

Figure 5.13: Northern and western analysis of differentiating PC12 (Sheffield) cells. a) Northern analysis using the *Sma* I - *Nco* I fragment of the rat *NSE* 3' UTR as a probe - lanes loaded equally for total RNA, 10μg per lane: 1 - mouse brain, 2 - mouse liver, 3 - undifferentiated PC12 cells, 4 - differentiated PC12 cells. Markers are Gibco BRL RNA ladder. b) Western analysis using anti-human NSE, detected with horseradish peroxidase-conjugated goat anti-rabbit IgG and revealed by staining with diaminobenzidine tetrahydrochloride without metal ion enhancement - lanes loaded equally for total protein, 5μg per lane: 1 - mouse brain, 2 - mouse liver, 3 - undifferentiated PC12 cells, 4 - differentiated PC12 cells. 45kDa marker is ovalbumin.

5.3 Strategy for the generation of deletion constructs

5.3.1 Starting material

At the time this project was initiated, the only published information concerning the regulation of *NSE* was that of Forss-Petter *et al.* (1990). As discussed in section 1.7.4, these researchers found that a 1.8 kbp fragment of the rat *NSE* 5' flanking region, up to and including the first (noncoding) exon but not the first intron, was sufficient to direct the expression of a reporter transgene in the same manner as that of endogenous *NSE* in transgenic mouse embryos, but was unable to support postnatal accumulation of the reporter message, a feature characteristic of the endogenous *NSE* gene in both rats and mice.

The major aims of this project were to investigate the mechanisms of cell type-specific and inducible expression of the rat *NSE* gene. As the 1.8 kbp regulatory sequence described by Forss-Petter and coworkers appeared to be sufficient to confer the developmental stage- and cell type-specific properties of *NSE* upon a heterologous reporter gene, it was chosen as the starting point for the study. The 1.8 kbp regulatory element is referred to as the *complete NSE regulatory sequence* in this thesis because of its properties in transgenic mice, although the more recent study by Sakimura and colleagues suggests that additional regulatory material, both upstream and downstream of the complete *NSE* regulatory sequence, may be involved in the expression of this gene (Sakimura *et al.*, 1995). No information was initially available concerning the molecular basis of *NSE*-induction by the various agents and growth conditions described in section 1.5.3, however, a recent investigation has shown that the complete *NSE* regulatory sequence is able to respond to retinoic acid, nerve growth factor and attachment factor treatments in a manner similar to the endogenous *NSE* gene when stably transfected into ES cells (Alouani *et al.*, 1993; *see* section 1.7.4). The complete *NSE* regulatory sequence was therefore a prudent starting point for the study of both cell type-specific and inducible regulatory elements.

5.3.2 Sequence and numeration of the rat *NSE* 5' flanking region

The rat *NSE* 5' flanking region has been independently cloned and partially sequenced by two groups (Sakimura *et al.*, 1987; Forss-Petter *et al.*, 1990). The published sequence data from Sakimura and colleagues extends 1157 bp upstream from the start of the first intron and has been submitted to the GenBank database under the accession number M22565. The published sequence data from Forss-Petter and colleagues extends 354 bp upstream from the start of the first intron and has not been submitted. The two sequences are in excellent agreement over the area available for comparison, differing at only two positions as shown in Figure 5.14.

Although the sequences are all but identical, the two groups have presented evidence for different major transcriptional start sites and their numbering systems have been based upon this data (Sakimura *et al.*, 1987; Forss-Petter *et al.*, 1990; Sakimura *et al.*, 1995). To avoid confusion, only one of the numbering systems has been used in this thesis and the one originally employed by Forss-Petter and colleagues was chosen. This choice was made on the basis that the material used in this project was the same as that used by these investigators in their earlier study (Forss-Petter *et al.*, 1990) and also because position +1 refers to the start of transcription corresponding to the first nucleotide found in three independent cDNA clones (Sakimura *et al.*, 1985b; Forss-Petter *et al.*, 1986) as well as a prominent site identified by primer extension analysis (Forss-Petter *et al.*, 1990).

5.3.3 Subcloning strategy

Plasmid pNSElacZ, which contains the complete *NSE* regulatory sequence linked to the *E. coli lacZ* gene and the SV40 polyadenylation sequence, was the source of all material used in this study (Figure 5.15). Although it would have been possible to manipulate this vector to generate suitable deletion constructs for transfection

```
-1102                                                                AG

-1100 TAAAGGTGAT GGCAGGAAGG CAGCCCCCGG AGGCAAAGGC TGGGCACGCG  Hph 1

-1050 GGAGGAGAGG CCAGAGTCAG AGGCTGCGGG TATCTCAGAT ATGAAGGAAA

-1000 GATGAGAGAG GCTCAGGAAG AGGTAAGAAA AGACACAAGA GACCAGAGAA  Bsa 1

-950  GGGAGAAGAA TTAGAGAGGG AGGCAGAGGA CCGCTGTCTC TACAGACATA

-900  GCTGGTAGAG ACTGGGAGGA AGGGATGAAC CCTGAGCGCA TGAAGGGAAG

-850  GAGGTGGCTG GTGGTATATG GAGGATGTAG CTGGGGCCAG GGAAAAGATC

-800  CTGCACTGGG GATCTGAAGC TGGGGAGAAC AGGACACGGGG TGGAGAGGC  Dra III

-750  GAAAGGAGGG CAGAGTGAAG CAGAGAGACT GAGGCCTGGGG ATGTGGGCA  Stu 1

-700  TTCCGGTAGG GCACACAGTT CACTTGTCTT CTCTTTTTCCA GGAGGCCAA

-650  AGATGCTGAC GTCAAGAACT CATAATACCC CAGTGGGGACC ACCGCATTC

-600  ATAGCCCTGT TACAAGAAGT GGGAGATGTT CCTTTTTGTCC CAGACTGGA

-550  AATCCATTAC ATCCCGAGGC TCAGGTTCTG TGGTGGTCATC TCTGTGTGC

-500  CTTGTTCTGT GGGCCTACCT AAAGTCCTAA GCACAGCTCTC AAGCAGATC

-450  CGAGGCGACT AAGATGCTAG TAGGGGTTGT CTGGAGAGAAG AGCCGAGGA

-400  GGTGGGCTGT GATGGATCAG TTCAGCTTTC AAATAAAAAGG CGTTTTTAT
                                                          ⇒
-350  ATTCTGTGTC GAGTTCGTGA ACCCCTGTGG TGGGCTTCTCC ATCTGTCTG
                          *          *
-300  GGTTAGTACC TGCCACTATA CTGGAATAAG GUGACGCCTGC TTCCCTCGA  Xho 1

-250  GTTGGCTGGA CAAGGTTATG AGCATCCGTG TACTTATGGGG TTGCCAGCT

-200  TGGTCCTGGA TCGCCCGGGC CCTTCCCCCA CCCGTTCGGTT CCCCACCAC

-150  CACCCGCGCT CGTACGTGCG TCTCCGCCTG CAGCTCTTGAC TCATCGGGG  Pst 1
                                          ⇓
-100  CCCCCGGGTC ACATGCGCTC GCTCGGCTCT ATAGGCGCCGC CCCCTGCCC  Sma 1, Nar 1
      ⇓     ⇓                    ↓  ↓     ↓
-50   ACCCCCCGCC CGCGCTGGGA GCCGCAGCCG CCGCCACTCCT GCTCTCTCT
      ↓        ↓
+1    GCGCCGCCGC CGTCACCACC GCCACCGCCA CCGGCTGAGTC TGCAGTCCT

+51   CGAGgtgagg.......
```

Figure 5.14: Sequence of the rat NSE 5' flanking region (data taken from Sakimura *et al.*, 1987 and Forss-Petter *et al.*, 1990). Double underlined motifs are restriction endonuclease sites (with the appropraite enzyme identified in the right hand margin) used in the present study to generate deletion constructs. The putative TATA box is shown in bold italic. Transcriptional start sites are shown with vertical arrows - double arrows refer to sites identified by both authors, single arrows to those sites detected only by Forss-Petter *et al.* The site at position -65 is position +1 in Sakimura *et al.* (1995). Asterisks refer to positions where sequence data do not agree - at position -269, Sakimura *et al.* reported A and Forss-Petter *et al.* G; The G at position -277 is absent from the sequence of Forss-Petter *et al.* Horizontal arrow indicates beginning of the sequence data from Forss-Petter *et al.* (1990). Intron I begins at position +55, shown by lower case letters.

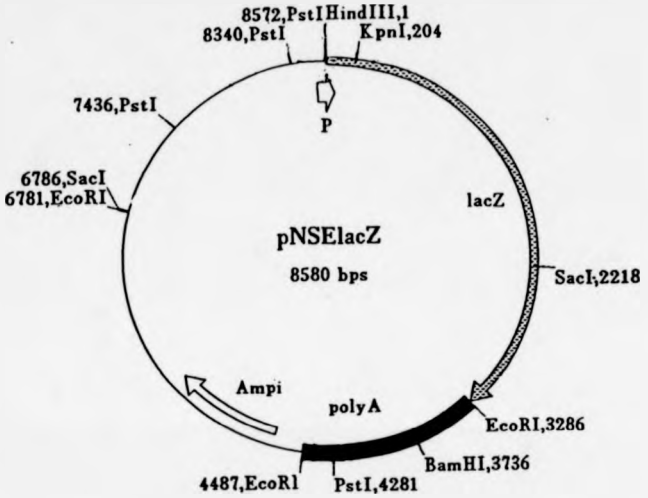

Figure 5.15: Plasmid map of pNSElacZ, a hybrid of three vectors (pSV-cat, pCH110 and pUC18) which contains the 1.8kb full *NSE* regulatory region (P) upstream of the *E. coli lacZ* gene (lacZ) and the SV40 polyadenylation site (polyA). The ampicillin resistance gene (Ampi) and various restriction endonuclease sites are also shown. This plasmid was the source of all *NSE* regulatory sequences used in this study and is redrawn from Forss-Petter *et al.* (1990), wherein details of its construction can also be found.

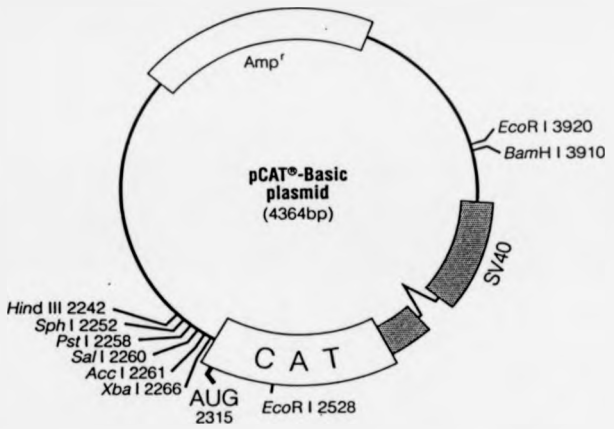

Figure 5.16: Plasmid map of pCAT-Basic, containing a promoterless *E. coli cat* gene downstream of a multiple cloning site. This vector is used as a negative control in transfection experiments and as the source vector to construct recombinants in which *cat* is driven by exogenous regulatory elements. The map shows the ampicillin resistance gene (Amp^r), the *cat* gene (CAT), the translational initiation site (AUG), the SV40 large T antigen region (SV40) and restriction endonuclease sites in the polylinker. Taken from Promega Protocols and Application Guide, second edition, 1991.

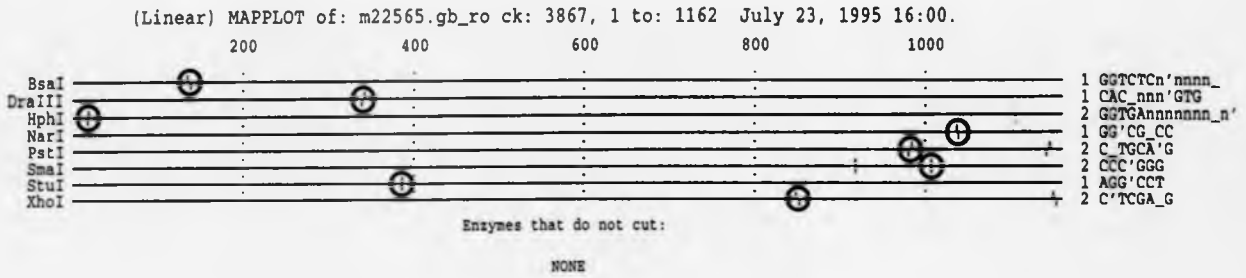

Figure 5.17: Linear MAPPLOT of the sequenced portion of the rat *NSE* 5' flanking region. Sequence data taken from Sakimura *et al.* (1985a). Restriction endonuclease sites chosen for subcloning procedures are circled.

analysis, the ungainly size of the plasmid (≈9 kbp), its hybrid nature and lack of unique restriction endonuclease sites made it an inconvenient subcloning system. Therefore, the complete *NSE* regulatory sequence was excised as a 1.8 kbp *Eco*R I - *Hin*d III fragment, blunted by end-filling using the Klenow fragment of DNA polymerase I and inserted into the more suitable pCAT-Basic vector for subsequent analysis. The pCAT-Basic vector (Figure 5.16) contains a promoterless *E. coli cat* gene downstream of a polylinker and was developed specifically for transient transfection analysis. A major advantage of pCAT-Basic over pNSElacZ was the availability of its complete sequence, allowing a computer-generated restriction map to be obtained using the circular MAPPLOT subroutine of the GCG database. The 1.8 kbp regulatory fragment was inserted into the (blunt) *Xba* I site in the pCAT-Basic polylinker to generate a recombinant vector named pNSE1800CAT. As a byproduct of this subcloning strategy, a second recombinant was obtained with the 1.8 kbp regulatory region in the reverse orientation. This vector was named pNSEinv1800CAT.

pNSE1800CAT represented a logical starting point for transfection analysis, as the regulatory information driving the reporter gene had been shown to confer correct spatial and temporal expression of *lacZ* in transgenic mice (Forss-Petter *et al.*, 1990). Earlier investigation had also shown that 255 bp of the rat *NSE* 5' flanking sequence was capable of driving *in vitro* transcription using HeLa cell extracts (Sakimura *et al.*, 1987) and the authors suggested that this fragment of the flanking sequence constituted the basal promoter of the gene. For preliminary analysis, therefore, the aim was to generate deletion constructs with 200-600 bp blocks of sequence removed in a stepwise fashion between positions -1800 and -255.

To choose suitable restriction endonuclease sites for the production of such constructs, a computer-generated restriction map of the sequenced portion of the rat *NSE* 5' flanking region was obtained using the linear MAPPLOT subroutine of the GCG database (Figure 5.17). Four candidate sites were identified: these were the *Hph* I site at -1084, the *Bsa* I site at -950, the *Stu* I site at -717 and the *Xho* I site at -255, the latter representing the minimal fragment investigated previously (Sakimura *et al.*,

1987). In each case, recombinant vectors were generated by excising the appropriate fragments (of 1205 bp, 1072 bp, 839 bp, and 376 bp respectively) from pNSElacZ using one of the endonucleases named above in combination with *Hin*d III. Each fragment was then blunted and inserted into the *Xba* I site of pCAT-Basic. Fortunately, the *Hph* I site was located only 10 bp downstream from the beginning of the published sequence, which allowed the removal of the entire unsequenced portion of the insert. This strategy permitted experiments to be carried out in which only the sequenced portion of the *NSE* flanking region was used to drive reporter expression. Comparison of this construct with that containing the complete *NSE* regulatory element showed whether the unsequenced portion of the flanking region was worthy of further study.

Due to the presence of an overlapping *dam* methylase site, the *Stu* I digest was unsuccessful. Unfortunately, the suitable alternative (a unique *Dra* III site at position -760), also failed to cleave. Control experiments showed that the enzyme was working efficiently and it was concluded that the *Dra* III site shown on the restriction map was there due to a discrepancy between the sequences of the independent clones (Sakimura *et al.*, 1987; Forss-Petter *et al.*, 1990) or a sequencing or clerical error. The remaining strategies were successful and the recombinant plasmids were named pNSE1200CAT, pNSE1000CAT and pNSE300CAT respectively (Figure 5.18).

The first series of transfections showed that the smallest construct, pNSE300CAT, was still capable of cell type-specific reporter activity. Further deletion constructs were therefore required in which more of the *NSE* flanking sequence had been removed. Because of the small size of the inserts required, a different subcloning strategy was used. Vector pNSE1800CAT was used as the starting material and variable sized distal portions of the original insert were removed; the vector was then reclosed. The sites within the pCAT-Basic polylinker were found to be very convenient for this purpose. pNSE120CAT was generated by partial digestion with *Pst* I, releasing an internal fragment from the *Pst* I site at position -119 in the insert to the *Pst* I site in the polylinker (upstream of the *Xba* I site originally used to accommodate the larger insert) and the vector was then reclosed.

6.5.3 Conclusions from transfection studies involving *ex vivo* neuronal differentiation

Transient transfection analysis of PC12 cells revealed remarkably little difference between undifferentiated and differentiated cells with respect to the regulation of *NSE*. In both cultures, cells transfected with the longest construct, pNSE1800CAT, yielded mean Relative CAT Activities of approximately 100%. Slightly greater CAT activity was observed for the NGF-treated cells. Cells transfected with pNSE120CAT and the more truncated construct pNSE95CAT demonstrated very low mean Relative CAT Activities (10% or less) and these results indicated that strong positive regulatory elements were located in the 5' flanking sequence, 5' to position -120 (the upstream boundary of pNSE120CAT). In the undifferentiated cells, a biphasic stepped decrease in reporter activity was observed. When the 5' flanking region was truncated to 1000 bp, a twofold reduction in mean Relative CAT Activity was evident. There was no significant modulation following truncation to 255 bp, but a fivefold reduction occurred following truncation to 120bp. These results indicated the presence of at least two positive regulatory elements in the 5' flanking region, one located between 1800 and 1000 bp upstream of the transcriptional start site and one located between 255 and 120 bp upstream of the transcriptional start site. In differentiated cells, there was no significant difference in levels of reporter activity when comparing cells transfected with pNSE1800CAT, pNSE1000CAT and pNSE300CAT. However, truncation to 120 bp resulted in a seven to tenfold reduction in reporter expression, indicating the presence of a very strong enhancer located between 255 and 120 bp upstream of the transcriptional start site. It is interesting to note that the same small region of the promoter was found to be important for regulation of *NSE* in the Ltk- and Neuro-2A cell lines. P19 stem cells demonstrated very low mean Relative CAT Activities (less than 5%) regardless of the construct transfected into them. However, P19 neurons transfected with all constructs except the highly truncated pNSE65CAT demonstrated very high levels of reporter expression. The mean values fell within a range 90-170%, although this may have been underestimated due to poor transfection efficiency in one experiment as discussed above. There was a slight

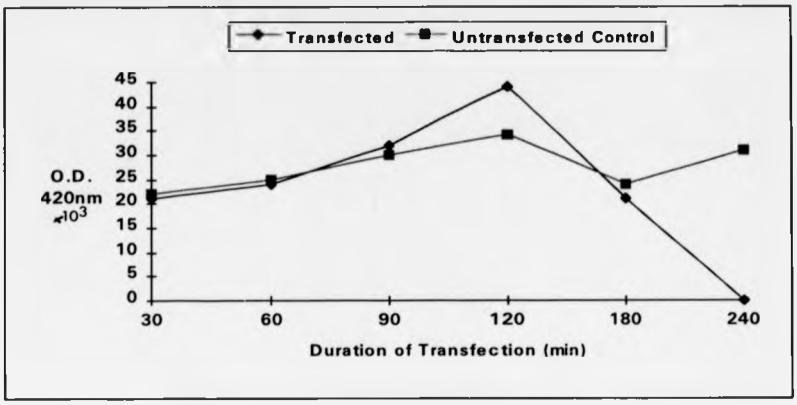

Figure 5.20: Graph to show effect of duration upon transfection efficiency. Cells were transfected using DEAE-dextran according to the method of Selden (1987). Control cells were not transfected, but were exposed to OptiMEM serum-free medium for the appropriate time.

Thus, although shortening the transfection time did increase transfection efficiency slightly above background, the results were not in the linear range of the β-galactosidase assay and were therefore not useful.

Attempts were next made to optimise DEAE-dextran mediated transfection from first principles. Initially, 0.5μg DNA was used per 35mm well and the concentration of DEAE-dextran in the medium was varied through the range 0 - 200μg ml^{-1}. It was found that, using these parameters, transfection efficiency showed a linear response to increasing doses of the reagent up to an optimal value of 133μg ml^{-1} For values above this dose, there was a fall in transfection efficiency and at doses greater than 166μg ml^{-1} significant cell death became apparent. These results are shown in Figure 5.21. The concentration of DEAE-dextran was then held at its optimal level and the amount of DNA was varied between 0 and 5μg per 35mm well. It was observed that transfection efficiency demonstrated a linear relationship to increasing amounts of DNA up to 2μg per 35mm well. Higher doses appeared neither to increase nor decrease the efficiency of transfection although the highest dose of DNA caused a heavy precipitate to form in the medium which resulted in some cell death. These results are shown in Figure 5.22.

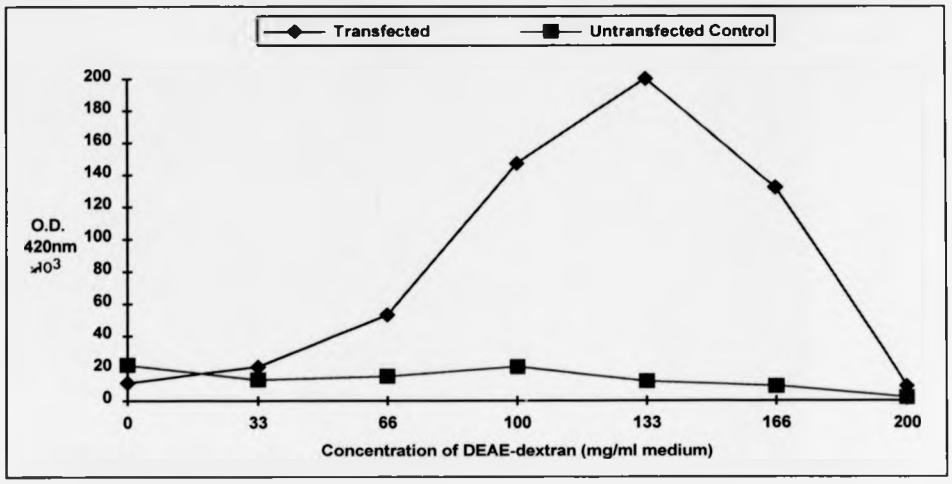

Figure 5.21: Optimisation of DEAE-dextran transfection of Ltk- cells by varying the dose of DEAE-dextran in the medium. Other parameters: cells transfected at 50% confluence, 0.5 µg DNA used per 35mm well, duration of transfection 4 hours followed by 2 minute 10% v/v DMSO/PBS shock. Untransfected cells were exposed to the same experimental conditions as the transfected cells with the exception that no DNA was included in the transfection mixture.

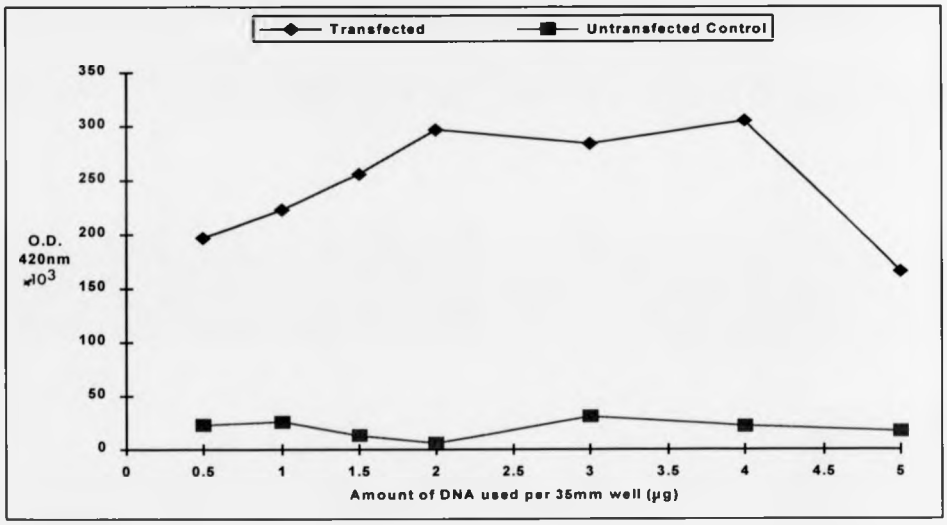

Figure 5.22: Optimisation of DEAE-dextran transfection of Ltk- cells by varying the amount of DNA: Other parameters: cells transfected at 50% confluence, 133µg ml^{-1} DEAE-dextran used per 35mm well, duration of transfection 4 hours followed by 2 minute 10% v/v DMSO/PBS shock. Untransfected cells were exposed to the same experimental conditions as the transfected cells with the exception that no DEAE-dextran was included in the transfection mixture.

5.4.1.2 Optimisation of transfection of Ltk- cells using calcium phosphate

When it became clear that other cell types used in this project, specifically the Neuro-2A neuroblastoma cell line and the U-138 MG and U-373 MG glioma lines, were refractory to DEAE-dextran-mediated transfection, it was decided to transfect Ltk- cells using calcium phosphate. As Ltk- cells were used as nonneuronal controls against each of these cell lines, it was convenient to carry out parallel transfections by the same method. Also, it was useful to compare the results of *NSE-cat* experiments from cells transfected by different methods to ensure that different transfection methods did not affect the results obtained.

Ltk- cells were transfected using BBS under conditions optimised for the U-138 MG and U-373 MG lines as described in section 5.4.3. Initially, it was decided to hold all other parameters at the same values optimised for U-138 MG and U-373 MG and vary the amount of DNA used in the transfection between 0 - 25μg per triplicate. A low transfection efficiency was observed when using 5-10μg DNA per triplicate and then a linear increase in transfection efficiency was evident with increasing amounts of DNA up to a peak value of 25μg. The transfection efficiency was observed to drop if greater amounts of DNA were used. These data are shown in Figure 5.23.

5.4.1.3 Optimisation of liposome-mediated transfection of Ltk- cells

Liposome-mediated transfection of Ltk- cells was carried out to allow this cell line to be used as a nonneuronal control against cell lines which could only be transfected using this method (e.g. NB4-1A3 and PC12 (Sheffield) cells). Transfections were optimised according to manufacturers' recommendations starting with the following parameters: cells transfected at 80% confluence, duration of transfection 5 hours, 2μg DNA per 35mm well in OptiMEM serum reduced medium. Four different liposome formulations were tried and the results are shown in Figure 5.24. It was clearly found that LipofectAMINE was the superior reagent for liposome-mediated transfection of Ltk- cells and 5μl of the reagent per 35mm well was the optimal amount. It was also

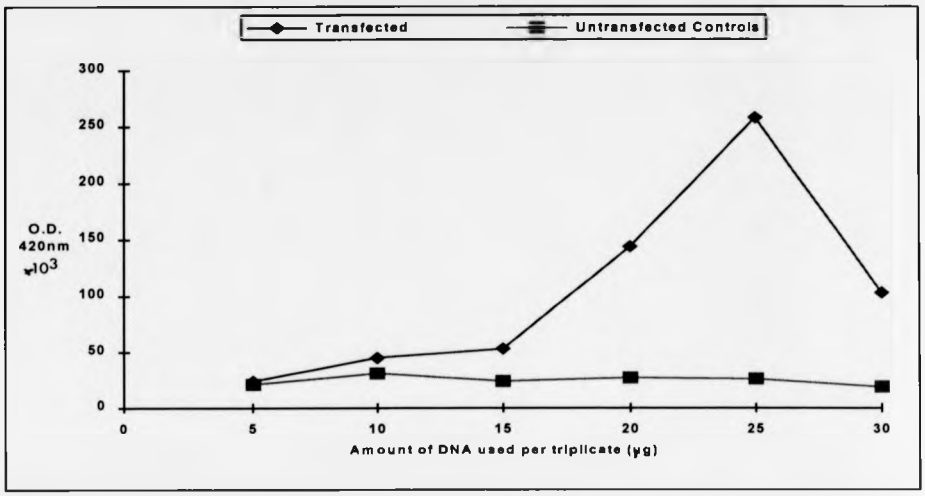

Figure 5.23: Optimisation of calcium phosphate-mediated transfection of Ltk- cells by varying the amount of DNA: Other parameters: cells transfected at 70% confluence, duration of transfection 18 hours. Untransfected cells were exposed to the same experimental conditions as the transfected cells with the exception that no $CaCl_2$ was included in the transfection mixture.

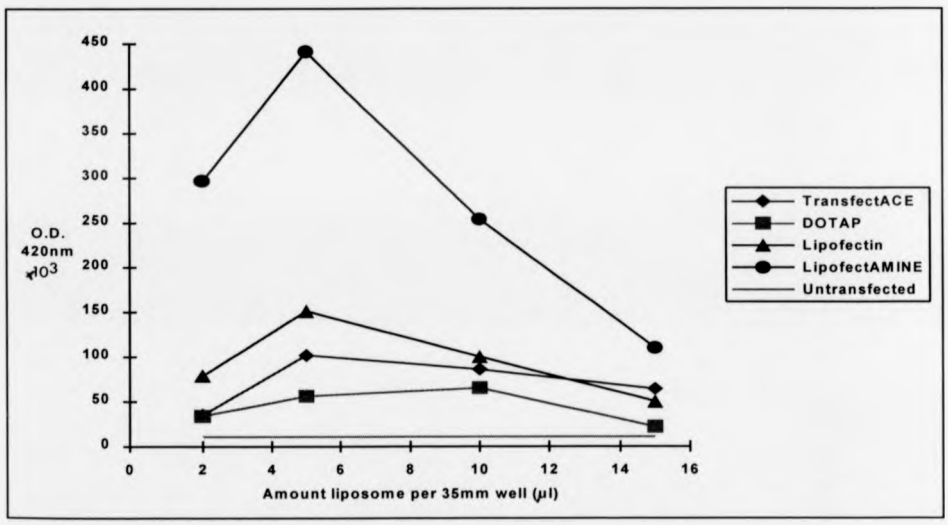

Figure 5.24: Optimisation of liposome-mediated transfection of Ltk- cells by varying the amount of liposome. Other parameters: cells transfected at 80% confluence, duration of transfection 5 hour, 2µg DNA per 35mm dish. Because of the cost of liposome formulations, negative control lacking DNA but containing the same amount of each liposome as the experimental transfections were not carried out. The untransfected cells in this experiment were not treated with DNA or liposomes, but were exposed to serum-reduced medium for the same duration as the transfected cells

noted that the highest doses of Lipofectin, TransfectACE and LipofectAMINE caused regional cell death, generating patches of lysed cells, often at the periphery of each dish. Next, the amount of DNA used per transfection was optimised, using the LipofectAMINE reagent at its optimal dose. Keeping the other parameters unchanged, the amount of DNA was varied between 0.5 and 3 μg per 35mm well. It was found that 2μg DNA per transfection was, in fact, the optimal amount. These results are shown in Figure 5.25.

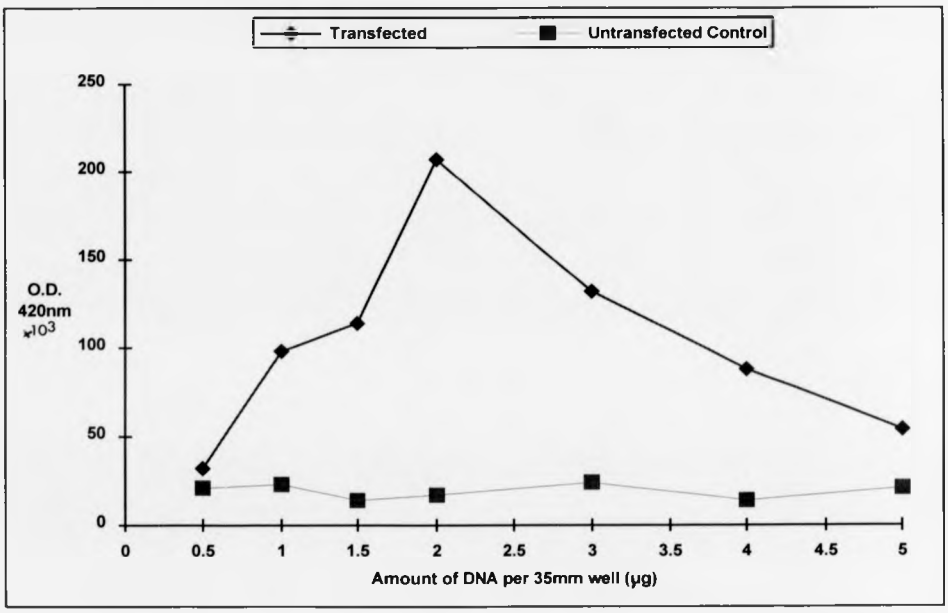

Figure 5.25: Optimisation of LipofectAMINE-mediated transfection of Ltk- cells by varying the amount of DNA. Other parameters: cells transfected at 80% confluence, duration of transfection 5 hour, 5μl LipofectAMINE per 35mm dish. Untransfected cells were exposed to the same experimental conditions as the transfected cells with the exception that no LipofectAMINE was included in the transfection mixture.

5.4.2 Optimisation of transfection of PC12 cells

5.4.2.1 Attempts to transfect PC12 (Geneva) cells

PC 12 (Geneva) cells were first transfected using the DEAE-dextran protocol optimised for Ltk- cells. This attempt to introduce DNA into the cells failed to generate detectable levels of β-galactosidase above the background of untransfected cells even after an 18 hour assay for β-galactosidase activity (data not shown). Whilst keeping the other parameters constant, attempts were made to optimise the transfection of these cells by varying the dose of DEAE-dextran, the amount of DNA, the duration of transfection and the method of posttransfection shock. In all cases, no detectable levels of β-galactosidase activity were found. Transfection of PC12 cells by this approach was then abandoned.

PC12 cells were next transfected using calcium phosphate coprecipitation. In the first instance, the parameters optimised for U-138 MG and U-373 MG glioma cell lines were used although the amount of DNA per triplicate was varied between 5 and 50μg. As before, no β-galactosidase activity above untransfected background was observed (data not shown). The duration of transfection was extended up to 24 hours, but this approach merely resulted in extensive cell death. In the case of difficult cell lines, it has been demonstrated that the pH of the BES buffered saline can play a critical role in the success of transfection. A series of alternative buffers, ranging from pH 6.95 to 6.98 inclusive, were therefore prepared and tested with a range of DNA concentrations. Once again, no β-galactosidase activity was evident (data not shown) and transfection of PC12 cells by this approach was also abandoned.

Next, a range of liposome formulations was investigated. The following products were used according to the manufacturers' instructions but failed to yield any posttransfection β-galactosidase activity above background: Lipofectin, TransfectACE and Transfectam (data not shown). Two formulations, LipofectAMINE and Tfx-50, generated posttransfection β-galactosidase activities slightly above background, yet still not in the linear range of the soluble assay even after 18 hour incubations (results

not shown). Also no CAT activity was evident in cells contransfected with pCAT-Control (results not shown). Following the failure of this approach, PC12 (Geneva) cells were abandoned as an experimental system.

5.4.2.2 Optimisation of liposome-mediated transfection of PC12 (Sheffield) cells

Having failed to transfect the PC12 (Geneva) cells using all available means, a different solution to the problem was sought. It has been reported that PC12 subclones with different characteristics can be propagated by selection and modification of growth conditions (Green *et al.*, 1987). For instance, it is easy to produce a clone of PC12 cells which attach relatively well to plastic surfaces simply by discarding those cells which are less adherent (Twyman and Jones, unpublished observations) and presumably these cells differ according to their expression of various extracellular matrix proteins and cell adhesion molecules. Transfection of PC12 cells by calcium phosphate and liposome methods had been reported elsewhere (e.g. Sakimura *et al.*, 1995) and there was therefore no reason why these experiments should be so difficult to carry out unless there was a characteristic of the cells in our possession which made them refractory to DNA uptake. The PC12 (Geneva) cells displayed many characteristics which would suggest transfection difficulty - they attached poorly, were rounded and grew as large aggregates, masking many of the cells from exogenously applied DNA. A different PC12 line was therefore obtained, whose characteristics were more suitable. The PC12 (Sheffield) cells grew as a monolayer, spread out in a fibroblastoid manner and attached well to plastic surfaces coated in collagen. The two PC12 lines required drastically different growth conditions (see section 4.2.1.) which might partially explain their different characteristics. Transfections were optimised with LipofectAMINE according to manufacturers' recommendations starting with the following parameters: cells transfected at 70% confluence, duration of transfection 5 hours, 2μg DNA per 35mm well in OptiMEM serum reduced medium. It was found that 6-10μl of the reagent per 35mm well gave the optimum transfection efficiency (Figure 5.26) and that 2μg of DNA per 35mm well was ideal (Figure 5.27).

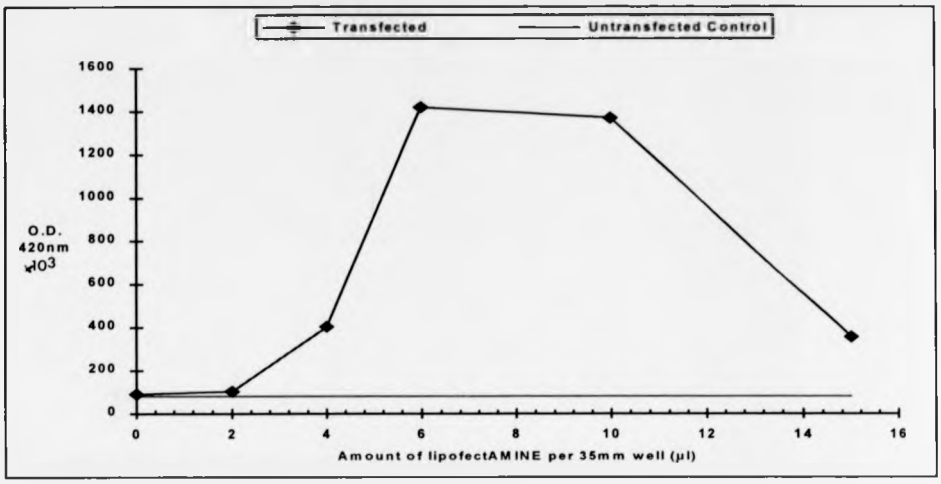

Figure 5.26: Optimisation of LipofectAMINE-mediated transfection of PC12 (Sheffield) cells by varying the concentration of liposome. Other parameters: cells transfected at 70% confluence, duration of transfection 5 hours, 2µg DNA per 35mm dish. Because of the cost of liposome formulations, negative controls lacking DNA but containing the same amount of each liposome as the experimental transfections were not carried out. The untransfected cells in this experiment were not treated with DNA or liposomes, but were exposed to serum-reduced medium for the same duration as the transfected cells. The very large OD readings in this experiment are outside the linear range of the assay and occurred because the assay was left for 18 hours. The success of the transfection was unexpected, as reflected by the long assay time.

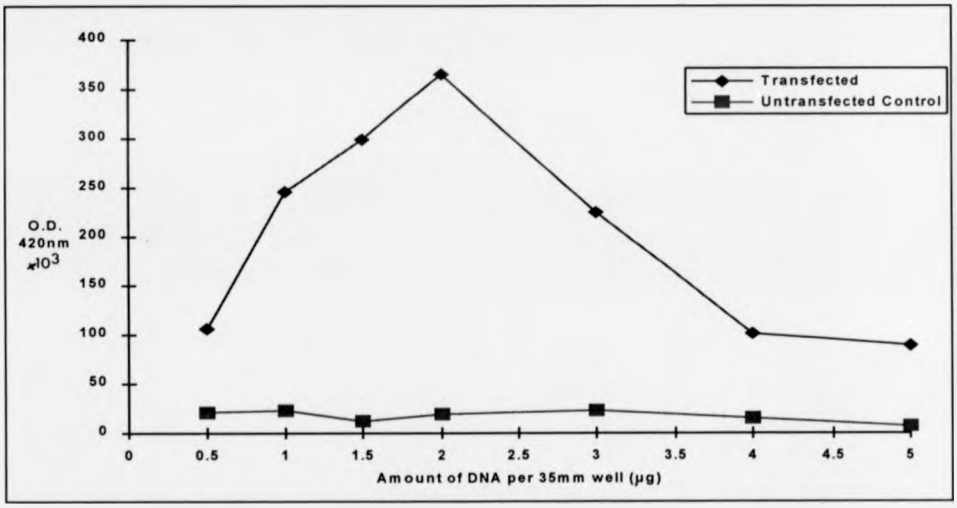

Figure 5.27: Optimisation of LipofectAMINE-mediated transfection of PC12 (Sheffield) cells by varying the amount of DNA. Other parameters: cells transfected at 70% confluence, duration of transfection 5 hour, 6µl LipofectAMINE per 35mm dish. Untransfected cells were exposed to the same experimental conditions as the transfected cells with the exception that no LipofectAMINE was included in the transfection mixture. Duration of the soluble β-galactosidase assay was 2 hours as usual.

It is notable that whilst 6-10µl of LipofectAMINE was optimal for PC12 (Sheffield) cells but insufficient for the transfection of PC12 (Geneva cells), 15µl of LipofectAMINE was the stated optimal amount for a PC12 clone transfected by another group (Hawley-Nelson *et al.*, 1994), whilst 15µl was toxic to both clones used in this project. This data supports our conclusions concerning the variability of PC12 cells and indicates that careful optimisation of transfection parameters must be carried out before such cells are used.

5.4.3 Optimisation of transfection of U-138 MG and U-373 MG cells using calcium phosphate

Attempts to transfect U-138 MG and U-373 MG glioma cells using DEAE-dextran failed although the same optimisation procedure was followed as for Ltk- cells. It was noted that doses of DEAE-dextran above 133mg ml^{-1} medium were toxic for a 4 hour transfection (data not shown). Transfection using calcium phosphate was then attempted, following the recommendations of Sambrook *et al.* (1989) and using 20µg DNA per triplicate as a starting parameter. Several batches of BES buffered saline with pH ranging from 6.95-6.98 were then made and each of these solutions was tried in parallel transfections. The BBS at pH 6.96 was found to be optimal, although the superiority of this batch over the others was not particularly marked (Figure 5.28). The amount of DNA per triplicate transfection was then optimised, using a range from 5-30µg. It was found that 25µg DNA per triplicate was ideal for both cell lines (Figure 5.29).

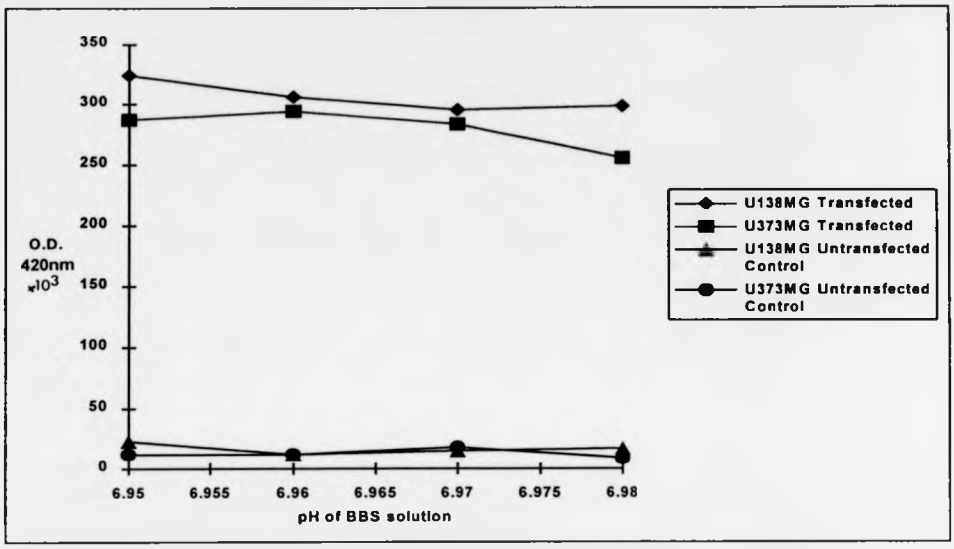

Figure 5.28: Optimisation of calcium phosphate-mediated transfection of U-138 MG and U-373 MG cells by varying the pH of the BES buffered saline: Other parameters: cells transfected at 70% confluence, duration of transfection 18 hours, 20μg DNA per triplicate. Untransfected cells were exposed to the same experimental conditions as the transfected cells with the exception that no $CaCl_2$ was included in the transfection mixture.

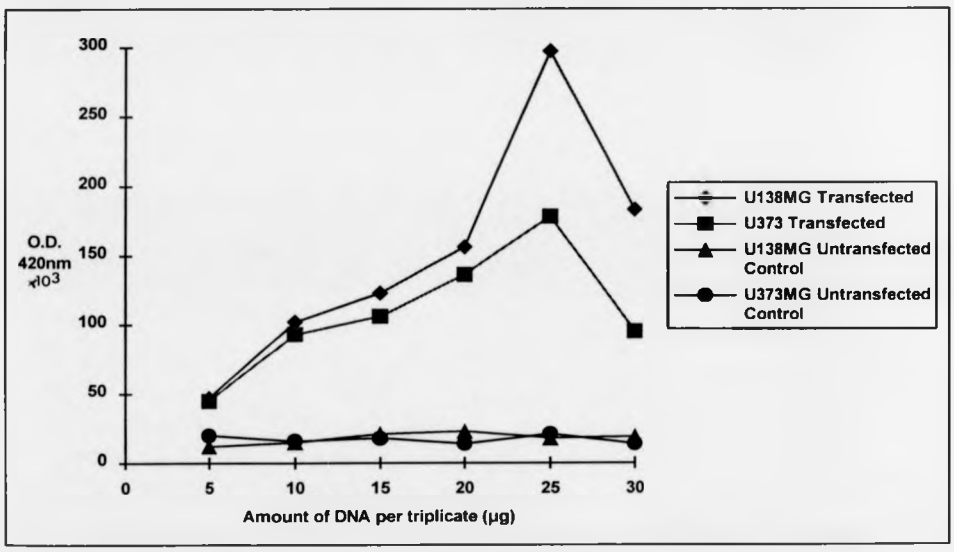

Figure 5.29: Optimisation of calcium phosphate-mediated transfection of U-138 MG and U-373 MG cells by varying the amount of DNA: Other parameters: cells transfected at 70% confluence, duration of transfection 18 hours, BBS at pH 6.95. Untransfected cells were exposed to the same experimental conditions as the transfected cells with the exception that no $CaCl_2$ was included in the transfection mixture.

bacteria or fungi. It is possible that specific vector sequences in the *NSE-cat* constructs either interfered with the expression of the pSV-β-galactosidase plasmid or generally reduced transcription in the cells, but it was thought unlikely that this should occur specifically in one cell type. Furthermore, the immunity of construct pNSE95CAT suggested that vector sequences were not responsible for the observed effects. Eventually, it was decided to carry out the experiments notwithstanding this phenomenon, and to increase the assay times accordingly. The results showed that P19 stem cells expressed all constructs at $< 10\%$ of the control levels. The highest level of reporter activity was demonstrated by pNSE95CAT in the first transfection, but as discussed above, this elevation of gene expression might reflect the peculiar transfection efficiency of this construct. Notwithstanding the high transfection efficiency of pNSE95CAT, the second transfection experiment showed the lowest Relative CAT Activities for this construct. Reduction of the *NSE* 5' flanking region from 255 bp to 120 bp did not reveal a silencer element similar to that observed in Ltk- cells.

5.4.5 Optimisation of transfection of NB4-1A3 cells

Despite careful modulation of transfection parameters, NB4-1A3 cells could not be transfected using either DEAE-dextran or calcium phosphate (data not shown). Liposome-mediated transfection was attempted using DOTAP, LipofectAMINE, Lipofectin and TransfectACE. Transfections were optimised according to manufacturers' recommendations starting with the following parameters: cells transfected at 50-60% confluence, duration of transfection 5 hours, 2μg DNA per 35mm well in OptiMEM serum reduced medium; the results are shown in Figure 5.31. As with the Ltk- cells, LipofectAMINE was found to be the superior reagent for liposome-mediated transfection and 5μl of the reagent per 35mm well was found to be the ideal dose. The regional cell death, characterised by patches of lysed cells was not observed for NB4-1A3 cells as it was for other cell lines. The amount of DNA used per transfection was then optimised, using the LipofectAMINE reagent at its optimal dose. Keeping the other parameters unchanged, the amount of DNA was varied between 0.5 and 3 μg per 35mm well and 1.5μg DNA per transfection was found to be the optimal amount. These results are shown in Figure 5.32.

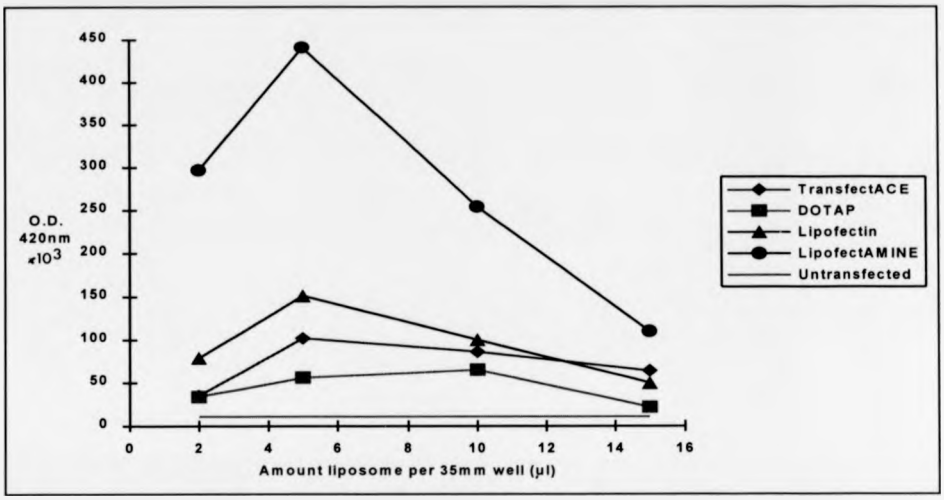

Figure 5.31: Optimisation of liposome-mediated transfection of NB4-1A3 cells by varying the amount of liposome. Other parameters: cells transfected at 50% confluence, duration of transfection 5 hour, 2 µg DNA per 35mm dish. Because of the cost of liposome formulations, negative controls lacking DNA but containing the same amount of each liposome as the experimental transfections were not carried out. The untransfected cells in this experiment were not treated with DNA or liposomes, but were exposed to serum-reduced medium for the same duration as the transfected cells

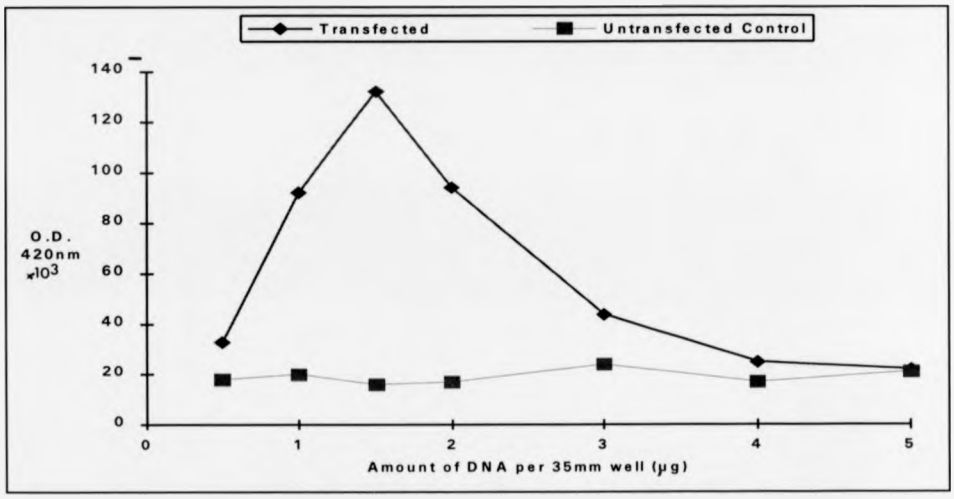

Figure 5.32: Optimisation of LipofectAMINE-mediated transfection of NB4-1A3 cells by varying the amount of DNA. Other parameters: cells transfected at 50% confluence, duration of transfection 5 hour, 5µl LipofectAMINE per 35mm dish. Untransfected cells were exposed to the same experimental conditions as the transfected cells with the exception that no LipofectAMINE was included in the transfection mixture.

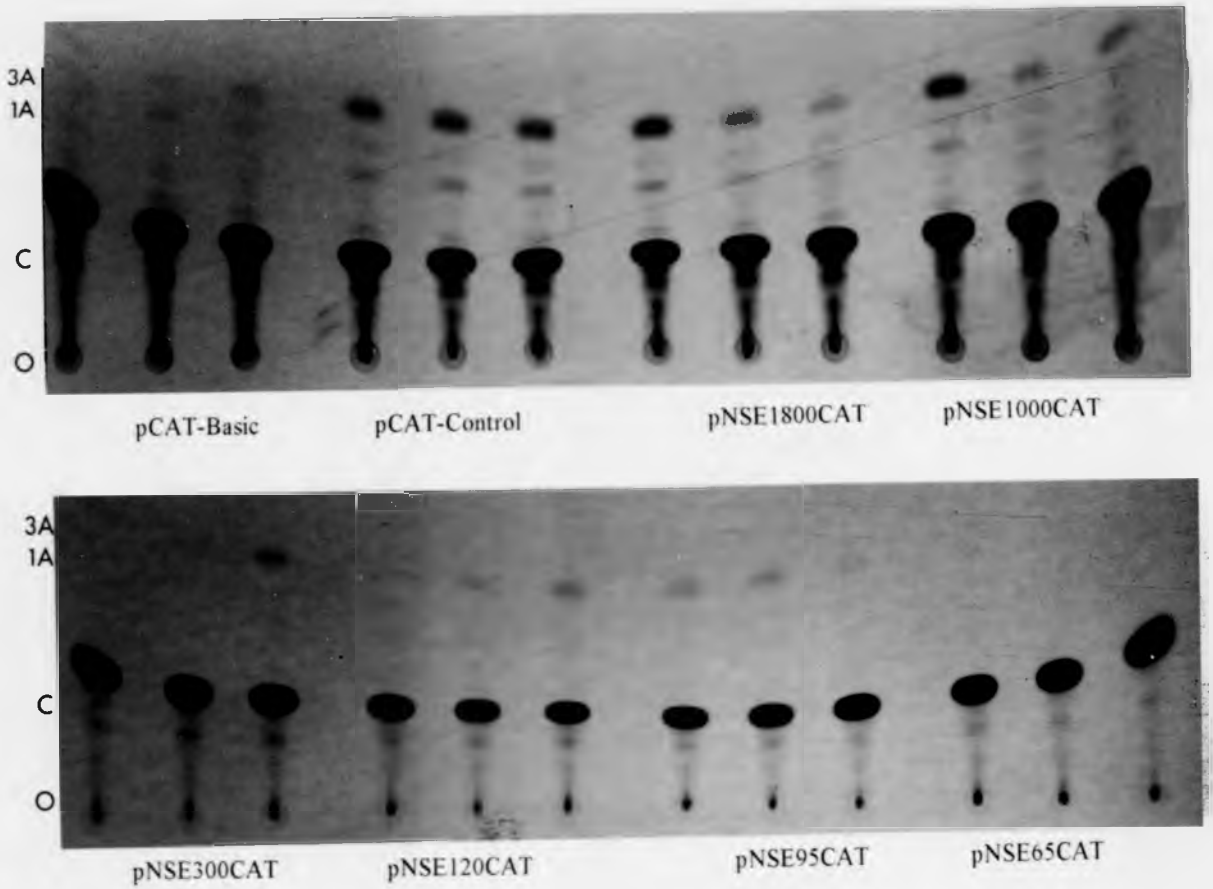

Figure 6.41: Representative CAT assay from the differentiated PC12 cells series of transfections with the full set of *NSE-cat* constructs. Each construct was transfected in triplicate and the lanes of the TLC plate were grouped accordingly. The assay shown above corresponds to the experiment shown in Figure 6.39. Abbreviations: O = origin; C = chloramphenicol; 1A = 1-acetyl-chloramphenicol; 3A = 3-acetylchloramphenicol.

Construct	RCA1	RCA2	xRCA12	semRCA12
Control	88.03	87.25	100.00	5.28
	119.07	110.55		
	92.90	102.19		
Basic	-0.69	-1.08	0.00	0.37
	N/A	1.10		
	0.69	-0.02		
NSE1800	122.46	157.71	116.73	10.68
	129.86	102.59		
	106.01	81.75		
NSE1000	92.31	153.65	97.26	13.54
	119.37	71.14		
	73.83	73.24		
NSE300	150.40	4.60	79.37	27.27
	134.58	5.92		
	129.05	51.69		
NSE120	1.98	11.89	10.50	3.34
	3.87	13.84		
	7.05	24.37		
NSE95	0.68	19.88	10.13	4.02
	3.21	20.35		
	-0.06	16.74		
NSE65	-1.72	-0.62	-1.19	0.21
	-1.65	-1.09		
	-1.52	-0.52		

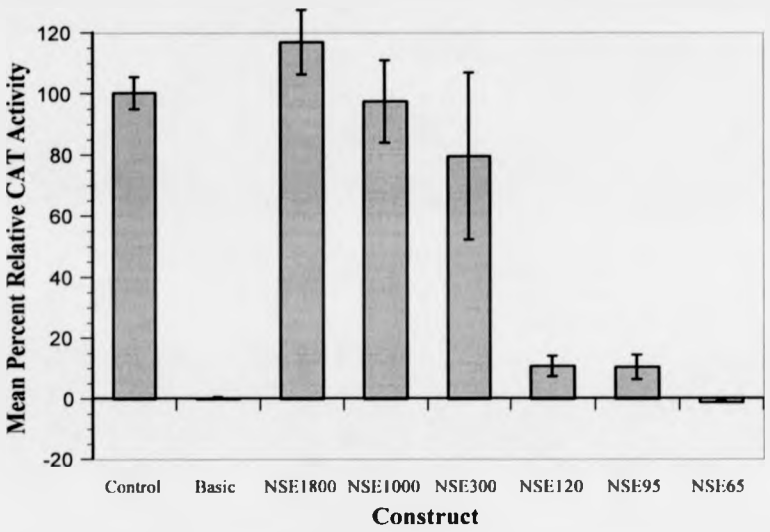

Figure 6.40: Table and histogram showing combined data from the transfection of NGF-treated PC12 cells with the full series of *NSE-cat* deletion constructs. Abbreviations used in the table: RCA1 and RCA2 - Relative CAT Activities from the two individual experiments (as shown in Figures 6.38 and 6.39); xRCA12 - combined mean Relative CAT Activity for each construct over two experiments (six transfections); semRCA12 - standard error of the combined mean Relative CAT Activities. A brief explanation of these terms can be found in Figure 6.1, a fuller explanation in section 5.5. The histogram shows combined mean relative CAT activity for each construct and illustrates the trend in reporter gene activity for reporter constructs containing stepwise deletions of the rat *NSE* 5' flanking region. Error bars represent standard errors of the combined mean Relative CAT Activities.

Construct	Name and Size of source vector	Size of insert	Size of recombinant	MEC
pNSE1800CAT	pCAT-Basic 4364	1799	6163	1
pNSE1200CAT	pCAT-Basic 4364	1205	5569	1.11
pNSE1000CAT	pCAT-Basic 4364	1072	5436	1.13
pNSE300CAT	pCAT-Basic 4364	376	4740	1.30
pNSE120CAT	pCAT-Basic 4364	240	4604	1.34
pNSE95CAT	pCAT-Basic 4364	216	4580	1.35
pNSE65CAT	pCAT-Basic 4364	186	4550	1.35
pCAT-Control	pCAT-Control 4752	-	4752	1.30
pCAT-Basic	pCAT-Basic 4364	-	4364	1.41

Table 5.1: Calculated Molar Equivalence Constants (MECs) for the constructs used during this project. All sizes are in nucleotides.

To directly compare the performance of different constructs within an experiment, CAT activity was normalised for transfection efficiency and corrected for molar equivalence to yield a value termed the Actual CAT Activity (ACA). The ACA was calculated as shown below, where CAT = CAT activity, GAL = β-galactosidase activity and MEC = molar equivalence constant:

$$ACA = \frac{CAT}{1000GAL.MEC}$$ Units CAT activity per Unit β-galactosidase activity

Generally, CAT activities fell within the range 1000 to 100 000, whereas β-galactosidase activities fell within the range 0.1 to 1.0. Each β-galactosidase activity was multiplied by 1000 so that ACA values could be written without the use of exponents. MEC was placed as a divisor in the above equation because for smaller constructs, a relatively greater molar quantity of plasmid was introduced into the cells, thus the CAT activity had to be *reduced* by the appropriate amount.

The calculation of ACA values allowed the performance of different constructs to be compared *within* each experiment (i.e. where transfections were carried out in parallel) but due to variations in experimental technique, and the need to vary assay times in different cell lines, meaningful comparison *between* experiments was not possible. To allow intraexperimental comparisons to be made, the ACA of each construct was expressed as a percentage of the ACA of the positive control vector, pCAT-Control, corrected for the background CAT activity of the negative control

vector, pCAT-Basic and this value was termed the Relative CAT Activity (RCA). Because transfections were carried out in triplicate within each experiment, the RCA values for each construct were based on the *mean* ACAs of the control vectors. Obviously, a large variation in the ACA values of the control vectors themselves would render the RCA calculations meaningless and, as an arbitrary condition, a maximum standard error of 15% was permitted for the control vector ACAs. The RCA for each construct was therefore calculated as follows where ACA = Actual CAT Activity of the construct under investigation and xACA = mean Actual CAT Activity for the control vectors as shown in parenthesis. The RCA is a relative value and has no units:

$$\text{RCA(construct)} = \frac{\{\text{ACA(construct)} - \text{xACA(pCAT-Basic)}\}}{\{\text{xACA(pCAT-Control)} - \text{xACA(pCAT-Basic)}\}} \times 100\%$$

From each triplicate transfection, mean RCA values were calculated. Whilst presenting the results in this manner allowed direct comparisons between experiments using the same cell line, such comparisons between different cell lines were made with caution because the tacit assumption has to be made that the SV40 promoter, which drives the control plasmids, functions in a similar manner in all cells. If this were not so, differences noted and attributed to the function of the *NSE* promoter could in fact reflect differences in both the *NSE* promoter and SV40 early promoter. Having said this, however, the calculation of RCA values allows one to legitimately compare *trends* in activity as the *NSE* flanking region is reduced in different cell lines, because this reflects only upon the function of the *NSE* promoter, and not upon its relationship with the SV40 early promoter.

Chapter 6 - Cell type-specific and inducible expression of the rat NSE *gene* ex vivo.

6.1 Chapter summary

The previous chapter showed how an *ex vivo* system for promoter analysis of the rat *NSE* gene was developed. The present chapter turns to the *ex vivo* analysis itself, showing how this system was put into practice. The initial experiments, involving one permissive and one nonpermissive cell line, and four deletion constructs, aimed to determine the position of cell type-specific regulatory elements in the upstream region of the *NSE* gene. The results showed, however, that even the shortest construct was capable of full cell type-specific reporter activity in the system chosen for analysis, and that it was necessary to truncate the flanking region further still to identify functional elements. Subsequent analysis was carried out in two permissive and two nonpermissive cell lines. The regulation of *NSE* was also investigated in the context of *ex vivo* neuronal differentiation, involving PC12 and P19 cell lines as described in sections 4.2.3 and 4.2.4. Finally, *NSE* expression was investigated in cells expressing cSox2 and cSox3 transcription factors, which are expressed in the developing nervous system at about the time of neuronal differentiation and whose pattern of expression has been shown to be complementary to that of NSE (Uwanogho *et al.*, 1995; R. Lovell-Badge, unpublished observations).

6.2 Methodology and data presentation

As discussed in section 4.2.5, convention dictates that transient transfection studies are carried out at least three times, using two or more independently derived preparations of plasmid DNA. The rationale behind such a strategy is obvious: by carrying out each experiment a number of times, one increases the statistical reliability of the results; and by using more than one source of DNA, one can identify artefactual effects caused by specific plasmid preparations. During the project, transfections mediated by DEAE-dextran or calcium phosphate were routinely carried out nine times (three experiments in which each construct was transfected into triplicate parallel cultures). In the case of transfections mediated by liposomes, the constancy and repeatability of the method was greater and six transfections were sufficient (two triplicate experiments). Two preparations of each plasmid were made, both by double CsCl gradient centrifugation as described in section 4.1.1. To save time and minimise expense, the plasmids were tested for

transfection efficiency and expression in only one cell line (Neuro-2A) and were found to give similar results (data not shown). Given the supposition that any preparation-specific properties of plasmid DNA would be manifest in all cell lines, this single test was judged to be a sufficient confirmation of the suitability of plasmids for use in transfection assays.

For each series of experiments, the raw and processed data are presented in tables, one per experiment, with histograms to illustrate the results graphically. A full explanation of the terms used in this chapter can be found in section 5.5, but a brief glossary is provided in Figure 6.1 for quick reference by the reader. Following the individual experiments, a combined table summarises the data over the whole experimental series and a histogram is shown to illustrate the overall trend of reporter construct activity in the particular cell line under investigation. There is also a representative CAT assay for each group of transfections to exemplify the calibre of the primary data.

6.3 Transfection with initial *NSE-cat* constructs

The first series of *NSE-cat* constructs, comprising pNSE1800CAT, pNSE1200CAT, pNSE1000CAT and pNSE300CAT, was transfected into permissive U-138 MG glioma and nonpermissive Ltk- fibroblast cells, both of murine origin. As discussed in the previous chapter, the longest construct contained sufficient regulatory information to confer correct spatial and temporal properties upon the heterologous *lacZ* gene in transgenic mice (Forss-Petter *et al.*, 1990), whilst the regulatory information in the shortest construct was, at the time the study was initiated, thought to comprise the minimal *NSE* promoter (Sakimura *et al.*, 1987). These constructs were transfected into permissive and nonpermissive cells to investigate both positive and negative aspects of gene regulation.

Construct	CAT	GAL	MEC	ACA	xACA	RCA	xRCA	semRCA
Control	65834	255	1.30	198.59	204.61	97.05	100.00	6.24
	79412	328		186.24		90.98		
	63111	212		228.99		111.97		
Basic	441	455	1.41	0.69	0.93	-0.12	0.00	0.17
	347	507		0.49		-0.22		
	508	224		1.61		0.33		
NSE1800	65734	341	1.00	192.77		94.19	97.04	3.28
	79886	377		211.90		103.58		
	62101	325		191.08		93.36		
NSE1000	88452	551	1.11	144.62		70.55	57.71	6.81
	75912	603		113.41		55.23		
	83752	775		97.36		47.34		
NSE300	82108	566	1.30	111.59		54.33	52.47	2.88
	93555	623		115.51		56.26		
	80356	642		96.28		46.81		
NSE120	12674	623	1.34	15.18		7.00	9.91	2.14
	22898	577		29.62		14.08		
	10047	405		18.51		8.63		
NSE95	9856	575	1.35	12.70		5.78	6.79	0.82
	11597	475		18.08		8.42		
	10234	561		13.51		6.18		
NSE65	520	465	1.35	0.83		-0.05	-0.06	0.04
	473	525		0.67		-0.13		
	732	583		0.93		0.00		

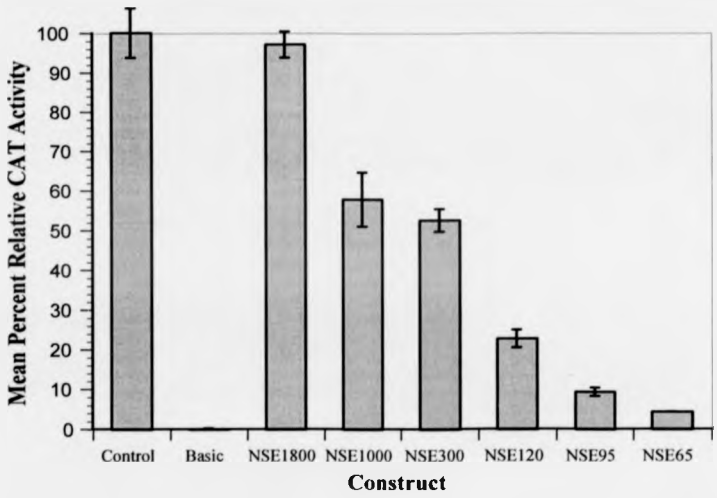

Figure 6.35: Table and histogram showing data from the second transfection of undifferentiated PC12 (Sheffield) cells with the full series of *NSE-cat* deletion constructs. Transfection was carried out using LipofectAMINE. Abbreviations used in table headings: CAT - CAT (chloramphenicol acetyltransferase) activity; GAL - β-galactosidase activity; MEC - Molar Equivalence Constant; ACA - Actual CAT Activity, xACA - mean Actual CAT Activity of control constructs; RCA - Relative CAT Activity; xRCA - mean Relative CAT Activity; semRCA - standard error of the mean Relative CAT Activity. A brief explanation of these terms can be found in Figure 6.1, a fuller explanation in section 5.5. The histogram shows mean Relative CAT Activities for each construct with error bars representing standard errors.

Glossary

(a) Abbreviations used in data tables and histograms -

Construct - The plasmid transfected into the cells.

CAT - The **CAT** (chloramphenicol acetyltransferase) activity of the posttransfection cells, reflecting the activity of the *NSE-cat* reporter construct transfected into them. These values were obtained by phosphorimaging and lie within the range 10^4-10^6.

GAL - The β-**gal**actosidase activity of the posttransfection cells. A vector expressing *lacZ* under the control of the SV40 early promoter was cotransfected into all cultures to provide an internal control for transfection efficiency and cell number. These values were obtained by colourimetric assay and lie within the range 0.1 - 1.0; they were multiplied by 1000 so that they might be represented by integers.

MEC - The **M**olar **E**quivalence **C**onstant: a dimensionless number introduced into the calculations to account for the molar ratio of the various constructs introduced during transfection, the constructs being of unequal size but the *mass* of DNA introduced into the cells remaining the same.

ACA - The **A**ctual **C**AT **A**ctivity, a measure of CAT activity corrected for transfection efficiency and molar ratio of plasmid DNA. This allows direct comparisons between the performance of the various *NSE-cat* constructs *within a single experiment*. The Actual CAT Activity is calculated using the following equation: ACA = CAT/(GAL x MEC).

xACA - Mean Actual CAT Activity. xACAs are calculated for the *control constructs only* (pCAT-Basic, pCAT-Control) and allow calculation of the Relative CAT Activity (RCA).

RCA - **R**elative **C**AT **A**ctivity, the CAT activity of each construct expressed as a percentage of that of the positive control construct, pCAT-Control, corrected for the background level of the negative control construct, pCAT-Basic. The Relative CAT Activity, which is calculated using the following equation, allows comparisons between the performance of various *NSE-cat* constructs *across experiments*.

$$RCA = \frac{ACA(construct) - xACA(pCAT\text{-}Basic)}{xACA(pCAT\text{-}Control) - xACA(pCAT\text{-}Basic)} \times 100\%$$

xRCA - Mean Relative CAT Activity. xRCAs are calculated for each construct from the individual RCAs and are the values shown on the histograms; for individual experiments, the means are from a sample of three whilst for the combined results the means are generally from a sample of six or nine. Note that, the xRCA of pCAT-Control is always 100% and that of pCAT-Basic is always 0%. These arbitrary values arise from use of the above equation.

semRCA - Standard error of the mean Relative CAT Activity, calculated for each construct and represented by error bars on the histograms.

(b) Abbreviation used in CAT assay figures -

O - Origin

C - Position of chloramphenicol

1A - Position of 1-acetylchloramphenicol

3A - Position of 3-acetylchloramphenicol

Figure 6.1: A glossary to explain the data presentation style used throughout this chapter.

Construct	CAT	GAL	MEC	ACA	xACA	RCA	xRCA	semRCA
Control	106802	109	1.30	753.72	682.58	110.49	100.00	31.47
	186699	142		1011.37		148.50		
	93334	254		282.66		41.01		
Basic	909	155	1.41	4.16	4.63	-0.07	0.00	0.06
	857	142		4.28		-0.05		
	1891	246		5.45		0.12		
NSE1800	125850	152	1.00	827.96		121.44	85.24	27.05
	172533	248		695.70		101.93		
	87523	391		223.84		32.33		
NSE1000	220404	581	1.11	341.76		49.73	49.10	14.18
	149032	795		168.88		24.23		
	206669	371		501.86		73.34		
NSE300	136481	520	1.30	201.89		29.10	58.71	27.60
	262488	260		776.59		113.87		
	161761	542		229.58		33.18		
NSE120	39695	753	1.34	39.34		5.12	8.19	1.77
	48950	452		80.82		11.24		
	13476	167		60.22		8.20		
NSE95	8881	247	1.35	26.63		3.25	4.72	0.74
	27278	475		42.54		5.59		
	9169	167		40.67		5.32		
NSE65	766	765	1.35	0.74		-0.57	-0.55	0.02
	573	525		0.81		-0.56		
	891	583		1.13		-0.52		

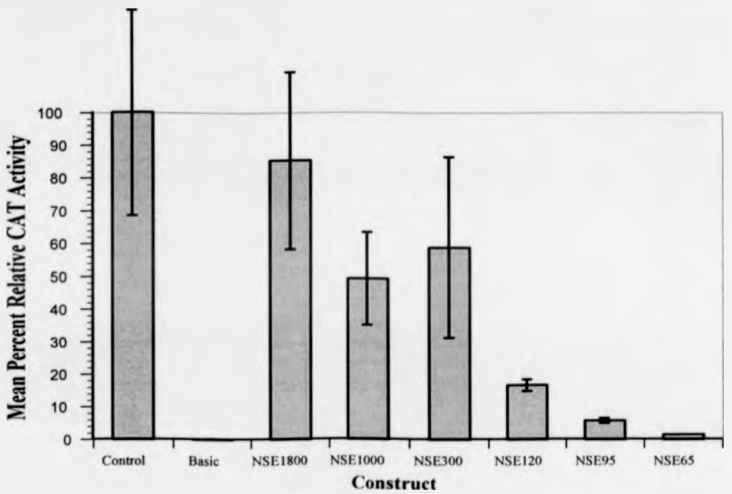

Figure 6.34: Table and histogram showing data from the first transfection of undifferentiated PC12 (Sheffield) cells with the full series of *NSE-cat* deletion constructs. Transfection was carried out using LipofectAMINE. Abbreviations used in table headings: CAT - CAT (chloramphenicol acetyltransferase) activity; GAL - β-galactosidase activity; MEC - Molar Equivalence Constant; ACA - Actual CAT Activity, xACA - mean Actual CAT Activity of control constructs; RCA - Relative CAT Activity; xRCA - mean Relative CAT Activity; semRCA - standard error of the mean Relative CAT Activity. A brief explanation of these terms can be found in Figure 6.1, a fuller explanation in section 5.5. The histogram shows mean Relative CAT Activities for each construct with error bars representing standard errors.

6.3.1 Transfection of Ltk- cells

Under the conditions described in section 5.4.1, Ltk- fibroblasts were transfected with the initial series of *NSE-cat* constructs and controls using DEAE-dextran. Data from three individual experiments are presented in Figures 6.2-6.4, followed by combined results in Figure 6.5. A representative CAT assay is shown in Figure 6.6. The results showed that constructs containing over 1 kbp of the *NSE* 5' flanking sequence displayed a mean Relative CAT Activity of approximately 10-15%, whilst the most truncated construct, pNSE300CAT, displayed a mean Relative CAT Activity of approximately 20%. The individual values varied from transfection to transfection but were highly repeatable; this is demonstrated by the similar trends in Relative CAT Activity for each experiment and the generally low standard errors (i.e. less than 10% of the mean) for the combined results.

previous experiments, the most truncated construct, pNSE65CAT, gave no expression above the background level of pCAT-Basic.

Construct	CAT	GAL	MEC	ACA	xACA	RCA	xRCA	semRCA
Control	312734	113	1.30	2128.89	1535.74	139.68	100.00	21.42
	289845	154		1447.78		94.12		
	226411	169		1030.55		66.20		
Basic	10034	144	1.41	49.42	41.02	0.56	0.00	0.57
	9669	138		49.69		0.58		
	4661	138		23.95		-1.14		
NSE1800	21995	103	1.00	213.54		11.54	10.15	1.16
	24545	155		158.35		7.85		
	29111	141		206.46		11.07		
NSE1200	22645	113	1.11	180.54		9.33	12.63	4.11
	63656	163		351.83		20.79		
	32746	188		156.92		7.75		
NSE1000	35923	111	1.13	286.40		16.42	11.45	2.49
	29622	145		180.79		9.35		
	33893	177		169.46		8.59		
NSE300	45619	101	1.30	347.44		20.50	18.26	1.12
	40023	103		298.90		17.25		
	44197	115		295.63		17.03		

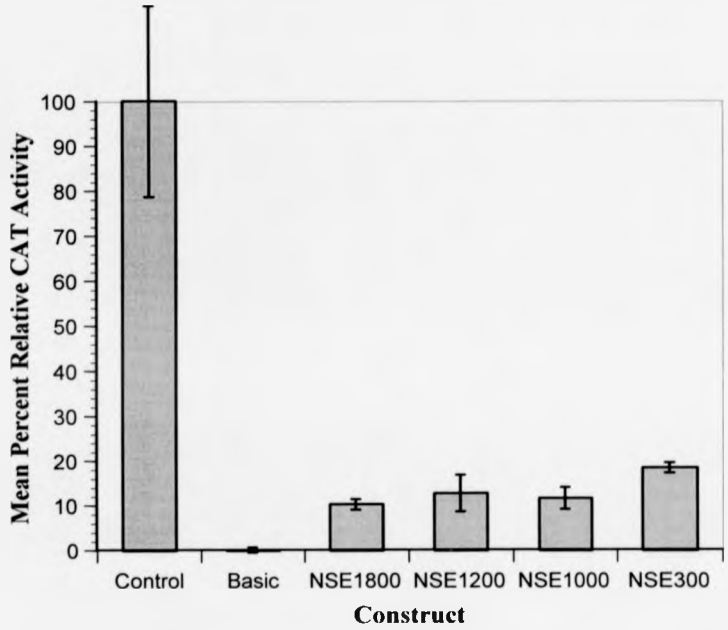

Figure 6.4: Table and histogram showing data from the third transfection of Ltk- cells with the initial series of *NSE-cat* deletion constructs. Abbreviations used in table headings: CAT - CAT (chloramphenicol acetyltransferase) activity; GAL - β-galactosidase activity; MEC - Molar Equivalence Constant; ACA - Actual CAT Activity, xACA - mean Actual CAT Activity of control constructs; RCA - Relative CAT Activity; xRCA - mean Relative CAT Activity; semRCA - standard error of the mean Relative CAT Activity. A brief explanation of these terms can be found in Figure 6.1, a fuller explanation in section 5.5. The histogram shows mean Relative CAT Activities for each construct with error bars representing standard errors.

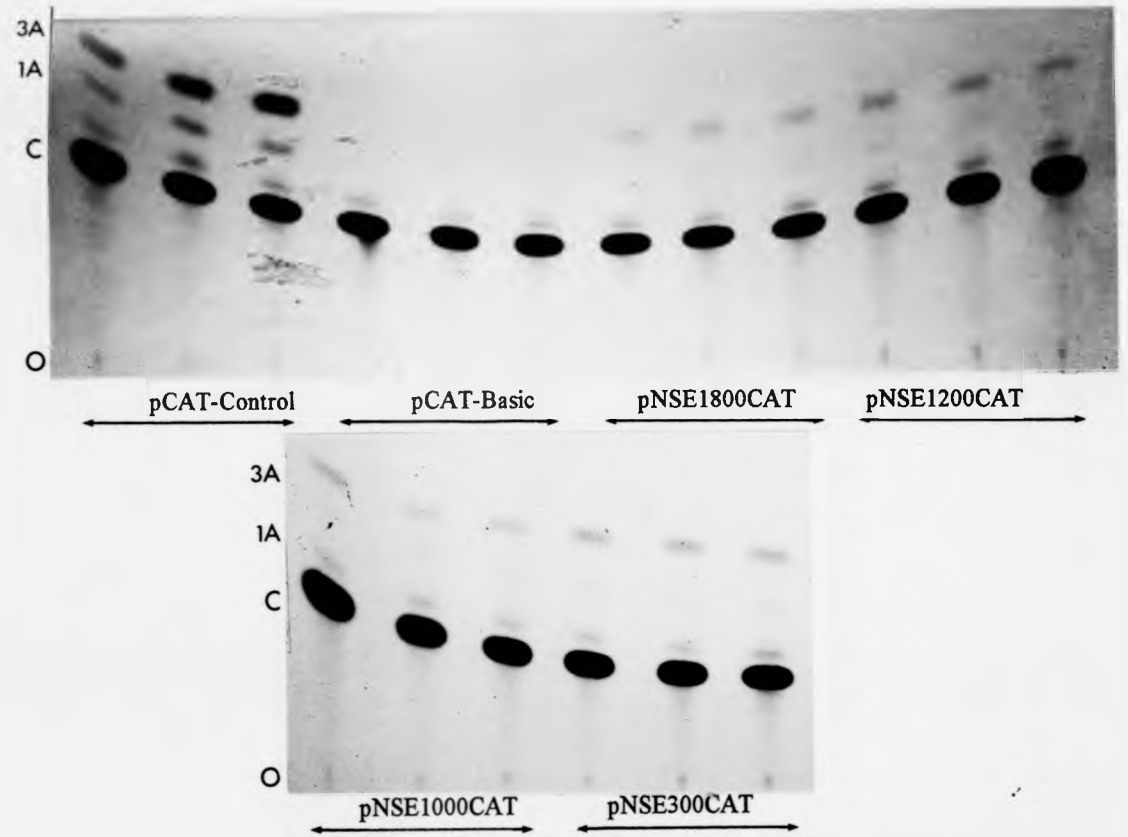

Figure 6.6: Representative CAT assay from the Ltk- series of transfections with the initial set of *NSE-cat* constructs. Each construct was transfected in triplicate and the lanes on the TLC plate were grouped accordingly. The assay above corresponds to the experiment described in Figure 6.2. Abbreviations: O = origin; C = chloramphenicol; 1A = 1-acetylchloramphenicol; 3A = 3-acetyl-chloramphenicol

6.3.2 Transfection of U-138 MG cells

Under the conditions described in section 5.4.3, U-138 MG glioma cells were transfected with the first series of *NSE-cat* constructs and controls using calcium phosphate. Data from three individual experiments are presented in Figures 6.7-6.9, followed by combined results in Figure 6.10. A representative CAT assay is shown in Figure 6.11. The results showed that all four constructs displayed mean Relative CAT Activities of approximately 100%-110%. The individual values varied from transfection to transfection but were in most cases repeatable; this was demonstrated by the similar trends in mean Relative CAT Activity for each experiment and the generally low standard errors (i.e. less than 10% of the mean) for the combined results. For the most truncated construct, pNSE300CAT, an uncharacteristically low mean Relative CAT Activity was observed for the third transfection experiment (Figure 6.8). Although this may have reflected a genuine fall in reporter activity caused by removal of the ≈700 bp separating the upstream boundaries of pNSE300CAT and pNSE1000CAT, the absence of this trend in the previous transfection experiments and the high standard error (30% of the mean), indicated that at least one of the data points in this experiment was nonrepresentative. The third transfection experiment showed generally higher standard error values than the previous two in the series, perhaps reflecting an undetected problem with the cultured cells or the transfection process itself. It has been observed that calcium phosphate-mediated transfection can produce less repeatable results than other transfection methods, even using carefully controlled parameters (Kingston *et al.*, 1990). It was also notable that the standard error for the positive control vector, pCAT-Control, was greater than 15% of the mean. In section 5.5, the knock-on effect of highly variable control transfections upon the *NSE-cat* constructs was discussed and a maximum standard error value of 15% was allowed. As this limit was transcended, less confidence must be placed in the conclusions from this particular experiment.

Construct	CAT	GAL	MEC	ACA	xACA	RCA	xRCA	semRCA
Control	294400	304	1.30	744.94	667.83	111.95	100.00	6.01
	240339	297		622.48		92.97		
	266264	322		636.08		95.08		
Basic	10765	402	1.41	18.99	22.67	-0.57	0.00	0.45
	11462	287		28.32		0.88		
	9477	325		20.68		-0.31		
NSE1800	202647	288	1.00	703.64		105.55	102.17	2.15
	215984	315		685.66		102.76		
	193564	295		656.15		98.19		
NSE1200	221754	310	1.11	644.45		96.38	109.36	6.77
	238981	272		791.54		119.17		
	223563	269		748.73		112.54		
NSE1000	232656	265	1.13	776.94		116.91	103.86	6.53
	116563	158		652.87		97.68		
	111372	152		648.42		96.99		
NSE300	199543	177	1.30	867.20		130.90	108.88	12.10
	212736	248		659.85		98.76		
	245527	308		613.20		91.53		

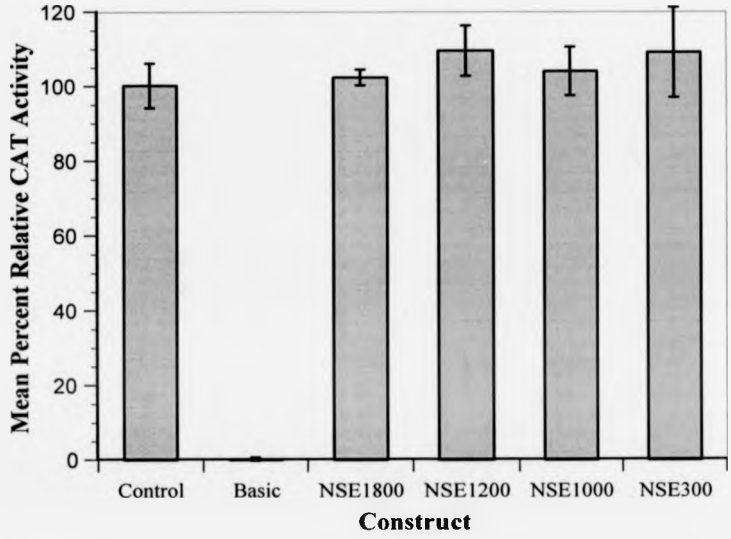

Figure 6.7: Table and histogram showing data from the first transfection of U-138 MG cells with the initial series of *NSE-cat* deletion constructs. Abbreviations used in table headings: CAT - CAT (chloramphenicol acetyltransferase) activity; GAL - β-galactosidase activity; MEC - Molar Equivalence Constant; ACA - Actual CAT Activity, xACA - mean Actual CAT Activity of control constructs; RCA - Relative CAT Activity; xRCA - mean Relative CAT Activity; semRCA - standard error of the mean Relative CAT Activity. A brief explanation of these terms can be found in Figure 6.1, a fuller explanation in section 5.5. The histogram shows mean Relative CAT Activities for each construct with error bars representing standard errors.

Construct	CAT	GAL	MEC	ACA	xACA	RCA	xRCA	semRCA
Control	441524	180	1.30	1886.85	1885.32	99.83	100.00	15.66
	414119	232		1373.07		72.96		
	460997	148		2396.03		127.21		
Basic	1318	175	1.41	5.34	4.27	0.06	0.00	0.03
	857	179		3.40		-0.05		
	943	164		4.08		-0.01		
NSE1800	185090	110	1.00	1682.63		89.43	109.51	10.22
	101426	46		2204.91		116.21		
	222994	97		2298.90		122.89		
NSE1200	298754	146	1.11	1843.48		98.07	114.52	8.24
	256820	101		2290.79		121.92		
	249991	97		2321.83		123.57		
NSE1000	261361	108	1.13	2141.60		113.96	112.57	24.14
	254381	78		2886.10		153.66		
	239919	161		1318.74		70.09		
NSE300	234923	118	1.30	1531.44		81.43	70.75	22.41
	74326	50		1143.48		60.74		
	43144	13		2552.90		135.89		

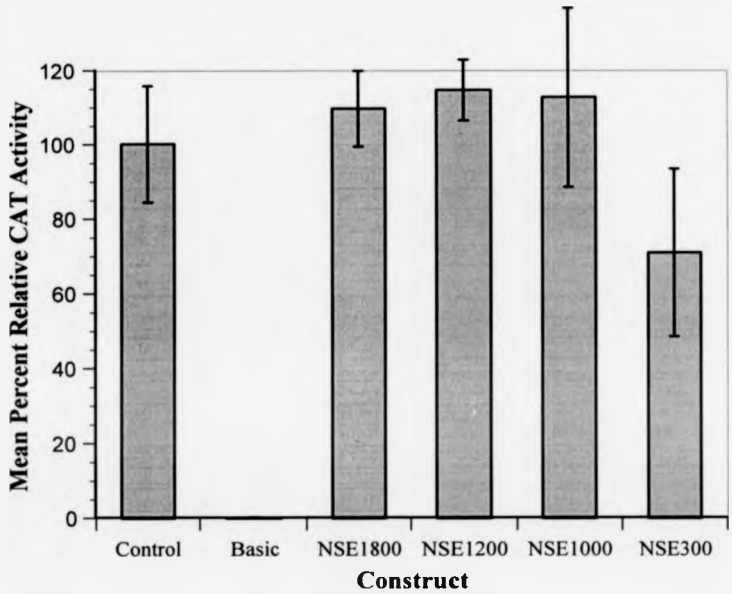

Figure 6.8: Table and histogram showing data from the second transfection of U-138 MG cells with the initial series of *NSE-cat* deletion constructs. Abbreviations used in table headings: CAT - CAT (chloramphenicol acetyltransferase) activity; GAL - β-galactosidase activity; MEC - Molar Equivalence Constant; ACA - Actual CAT Activity, xACA - mean Actual CAT Activity of control constructs; RCA - Relative CAT Activity; xRCA - mean Relative CAT Activity; semRCA - standard error of the mean Relative CAT Activity. A brief explanation of these terms can be found in Figure 6.1, a fuller explanation in section 5.5. The histogram shows mean Relative CAT Activities for each construct with error bars representing standard errors.

Construct	CAT	GAL	MEC	ACA	xACA	RCA	xRCA	semRCA
Control	323422	178	1.30	1397.68	1451.78	96.25	100.00	2.09
	249763	132		1455.50		100.26		
	283157	145		1502.16		103.49		
Basic	2154	109	1.41	14.02	8.55	0.38	0.00	0.20
	1653	167		7.02		-0.11		
	1003	154		4.62		-0.27		
NSE1800	308753	177	1.00	1744.37		120.27	125.62	7.22
	284372	168		1692.69		116.69		
	312267	154		2027.71		139.91		
NSE1200	229452	154	1.11	1342.30		92.41	117.43	16.63
	287421	120		2157.82		148.92		
	216230	121		1609.93		110.96		
NSE1000	263211	148	1.13	1573.85		108.46	127.74	14.48
	321953	126		2261.22		156.09		
	237293	122		1721.26		118.67		
NSE300	342839	156	1.30	1690.53		116.54	120.89	8.45
	295469	123		1847.84		127.44		
	289911	156		1429.54		98.46		

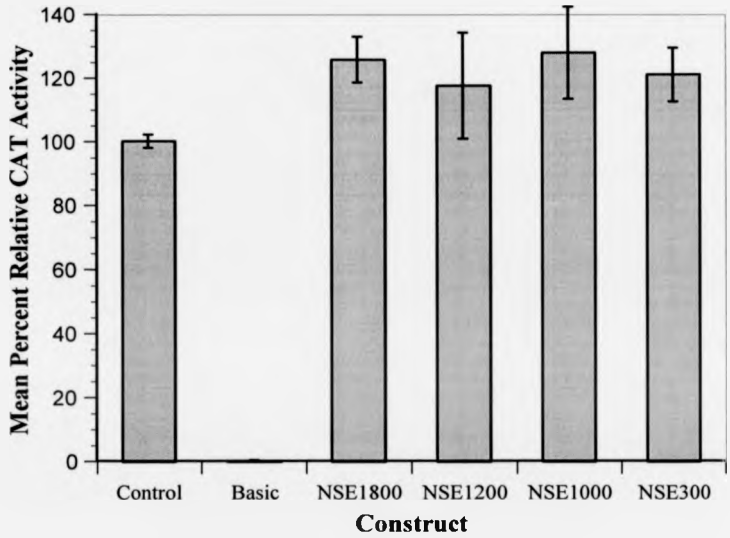

Figure 6.9: Table and histogram showing data from the third transfection of U-138 MG cells with the initial series of *NSE-cat* deletion constructs. Abbreviations used in table headings: CAT - CAT (chloramphenicol acetyltransferase) activity; GAL - β-galactosidase activity; MEC - Molar Equivalence Constant; ACA - Actual CAT Activity, xACA - mean Actual CAT Activity of control constructs; RCA - Relative CAT Activity; xRCA - mean Relative CAT Activity; semRCA - standard error of the mean Relative CAT Activity. A brief explanation of these terms can be found in Figure 6.1, a fuller explanation in section 5.5. The histogram shows mean Relative CAT Activities for each construct with error bars representing standard errors.

Construct	RCA1	RCA2	RCA3	xRCA123	semRCA123
Control	111.95	99.83	96.25	100.00	4.88
	92.97	72.96	100.26		
	95.08	127.21	103.49		
Basic	-0.57	0.06	0.38	0.00	0.14
	0.88	-0.05	-0.11		
	-0.31	-0.01	-0.27		
NSE1800	105.55	89.43	120.27	112.43	5.04
	102.76	116.21	116.69		
	98.19	122.89	139.91		
NSE1200	96.38	98.07	92.41	113.77	5.82
	119.17	121.92	148.92		
	112.54	123.57	110.96		
NSE1000	116.91	113.96	108.46	114.72	9.04
	97.68	153.66	156.09		
	96.99	70.09	118.67		
NSE300	130.90	81.43	116.54	104.63	8.37
	98.76	60.74	127.44		
	91.53	135.89	98.46		

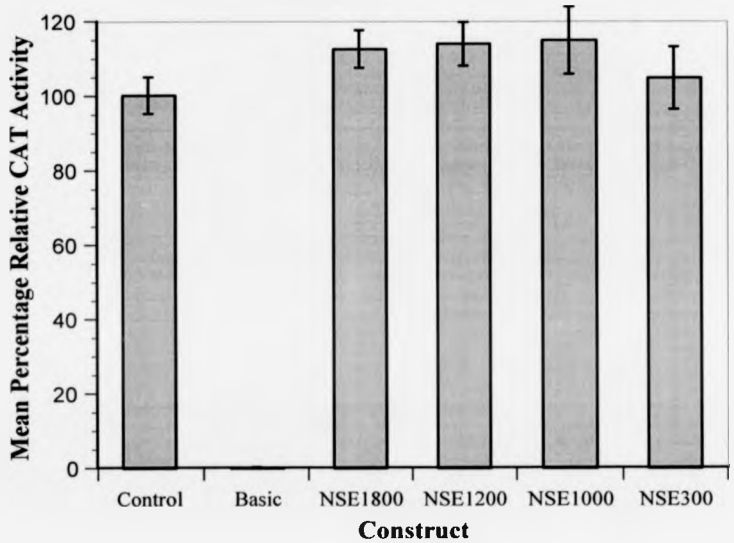

Figure 6.10: Table and histogram showing combined data from the transfection of U-138 MG cells with the initial series of *NSE-cat* deletion constructs. Abbreviations used in the table: RCA1, RCA2, RCA3 - Relative CAT Activities from the three individual experiments (as shown in Figures 6.7-6.9); xRCA123 - combined mean Relative CAT Activity for each construct over three experiments (nine transfections); semRCA123 - standard error of the combined mean Relative CAT Activities. A brief explanation of these terms can be found in Figure 6.1, a fuller explanation in section 5.5. The histogram shows combined mean relative CAT activity for each construct and illustrates the trend in reporter gene activity for reporter constructs containing stepwise deletions of the rat NSE 5' flanking region. Error bars represent standard errors of the combined mean Relative CAT Activities.

Construct	CAT	GAL	MEC	ACA	xACA	RCA	xRCA	semRCA
Control	497552	188	1.30	2035.81	1670.69	122.50	100.00	11.26
	369121	192		1478.85		88.18		
	391275	201		1497.42		89.32		
Basic	10023	187	1.41	38.01	48.30	-0.63	0.00	0.41
	14223	166		60.77		0.77		
	9561	147		46.13		-0.13		
NSE1800	25723	172	1.00	149.55		6.24	5.96	0.42
	28912	188		153.79		6.50		
	18923	144		131.41		5.12		
NSE1000	12840	122	1.13	93.14		2.76	3.23	0.80
	14377	101		125.97		4.79		
	10342	110		83.20		2.15		
NSE300	14883	124	1.30	92.33		2.71	4.46	1.09
	19832	131		116.45		4.20		
	20121	101		153.24		6.47		
NSE120	15932	131	1.34	90.76		2.62	2.64	0.53
	12900	126		76.40		1.73		
	16240	114		106.31		3.58		
NSE95	13021	122	1.35	79.06		1.90	1.35	0.28
	12783	141		67.16		1.16		
	14515	167		64.38		0.99		
NSE65	10231	132	1.35	57.41		0.56	0.74	0.16
	9462	121		57.92		0.59		
	9101	103		65.45		1.06		

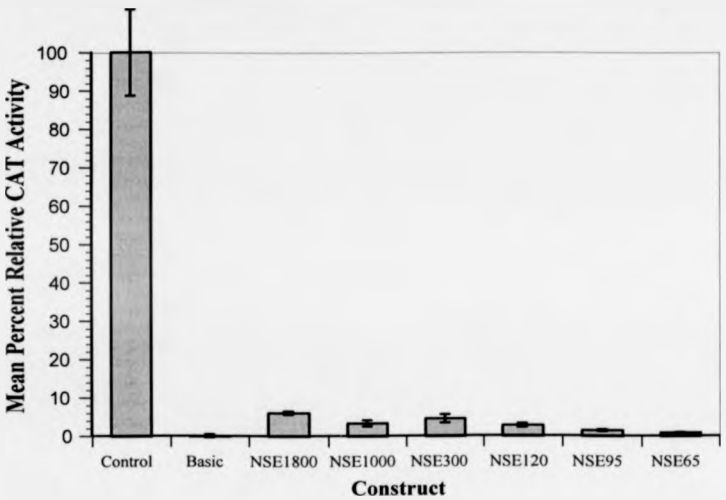

Figure 6.29: Table and histogram showing data from the first transfection of HeLa cells with the full series of *NSE-cat* deletion constructs. Abbreviations used in table headings: CAT - CAT (chloramphenicol acetyltransferase) activity; GAL - β-galactosidase activity; MEC - Molar Equivalence Constant; ACA - Actual CAT Activity, xACA - mean Actual CAT Activity of control constructs; RCA - Relative CAT Activity; xRCA - mean Relative CAT Activity; semRCA - standard error of the mean Relative CAT Activity. A brief explanation of these terms can be found in Figure 6.1, a fuller explanation in section 5.5. The histogram shows mean Relative CAT Activities for each construct with error bars representing standard errors.

6.4.4 Transfection of HeLa cells

HeLa cells were considered as a suitable nonpermissive cell line because of their use in previous studies of neuronal gene expression, including *NSE* (Sakimura *et al.*, 1995). Under the conditions described in section 5.4.6, HeLa cells were transfected with the full series of *NSE-cat* constructs and controls using calcium phosphate. Data from three individual experiments are presented in Figures 6.29-6.31, followed by combined results in Figure 6.32. A representative CAT assay is shown in Figure 6.33. The results showed that all *NSE-cat* constructs were expressed at minimal levels compared to pCAT-Control. The Relative CAT Activities for pNSE1800CAT ranged from 3% to 10%, although in one case a RCA of 18% was recorded. This was likely to be nonrepresentative of the construct and generated a standard error of >50% for this construct in the second transfection. The Relative CAT Activities of the first series of constructs were greater than those of pNSE120CAT and pNSE95 CAT, but only by two- to threefold. The Relative CAT Activities of pNSE65CAT were around 0% in each experiment.

6.3.3 Conclusions from first series of transfections

The first series of transfections showed that the reporter constructs driven by *NSE* regulatory sequence were more active in permissive U-138 MG cells than nonpermissive Ltk- cells. With all four constructs, the levels of reporter activity in the permissive cell line matched or exceeded the activity of the positive control construct, pCAT-Control, whilst in the nonpermissive cell line, the levels of reporter activity remained at 10-20% of the control level. The data from each transfection series are compared in Figure 6.12. The first major conclusion which could be drawn from this series of experiments was that the shortest of the constructs, pNSE300CAT, contained sufficient regulatory information to confer cell type-specificity upon the reporter gene. Secondly, the lack of significant modulation in the levels of reporter activity between this short construct and the more extensive ones in both permissive and nonpermissive cells indicated that, at least in these two cell lines, the regulatory information between 1800 and 300 bp upstream of the first intron was not critical for cell type-specificity. These two factors indicated that the logical next step was to generate constructs containing further stepwise deletions in the 5' regulatory region, as described in section 5.3.3. Endogenous *NSE* expression in Ltk- and U-138 MG cells was investigated by northern and western analysis as described in sections 5.2.3 and 5.2.4. These experiments showed that, whilst *NSE* mRNA and NSE protein could be easily detected in U-138 MG cells, the levels were undetectable in Ltk- cells. However, the transfections clearly showed that Ltk- cell RCA values for all four constructs were approximately 10% of those in U-138 MG cells. It is not clear why the level of reporter gene expression in nonpermissive Ltk- cells appears to be proportionately greater, compared to permissive U-138 MG cells, than the corresponding levels of endogenous gene expression. It is possible that sequences outside the 1800 bp region studied in this project are required for specific downregulation of the gene in nonneuronal cells, thus allowing some reporter expression in transfected Ltk- cells. The increased activity of *NSE-cat* constructs in Ltk- cells might also reflect the artificial nature of the transfection system: with

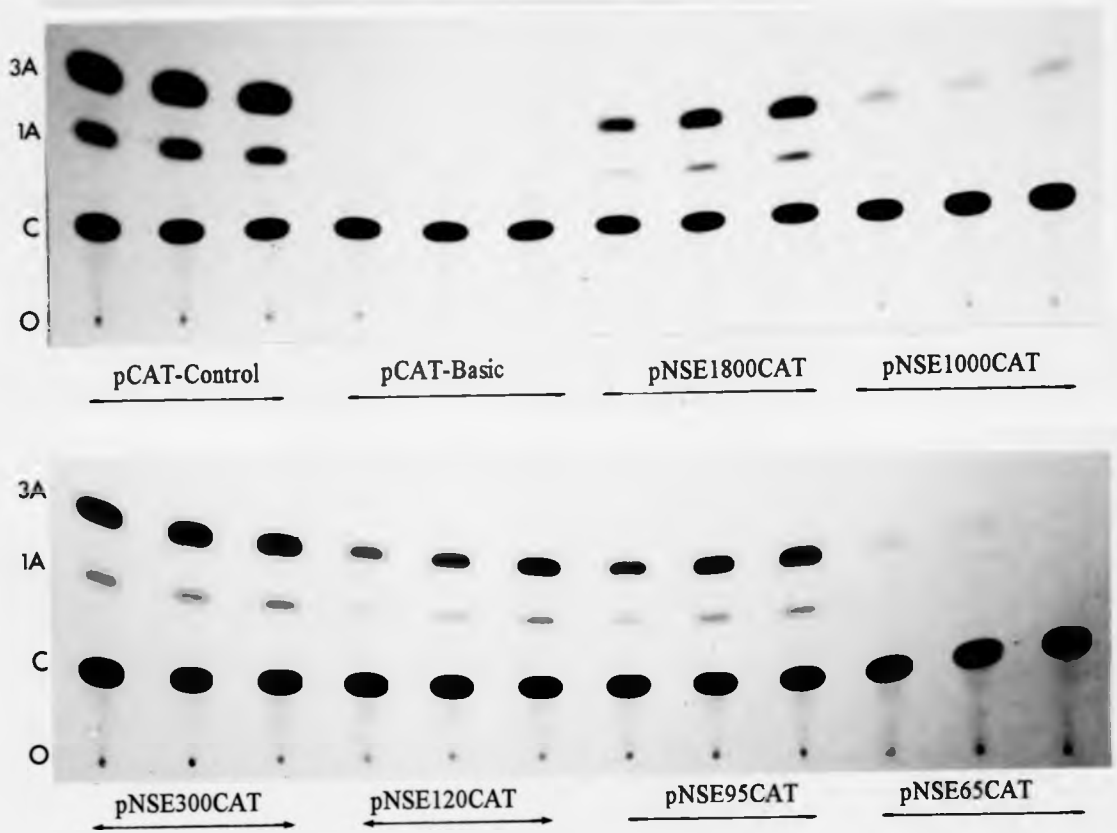

Figure 6.28: Representative CAT assay from the NB4-1A3 series of transfections with the full set of *NSE-cat* constructs. Each construct was transfected in triplicate and the lanes on the TLC plate were grouped accordingly. The assay above corresponds to the experiment described in Figure 6.25. Abbreviations: O = origin; C = chloramphenicol; 1A = 1-acetyl- chloramphenicol; 3A = 3-acetylchloramphenicol.

more regulatory DNA introduced into the cell than would ever normally exist *in vivo*, transcriptional repressors could be titrated out of the system and transcription could occur from the excess, unrepressed DNA; alternatively, low level transcription from the single copy gene *in vivo* could be amplified millions of times in transfected cells. A further possibility is that chromatin structure contributes to the silencing of *NSE* expression in nonneuronal tissue, and that because plasmids lack this epigenetic programming, some transcriptional leaking occurs. It has already been discussed in Chapter 5 that U-138 MG cells might represent a nonideal *ex vivo* model for the investigation of *NSE* gene expression because of their nonneuronal origin (see section 5.2.5). It was therefore desirable to investigate the expression of *NSE-cat* constructs in neuronal cell lines, as described in the following sections.

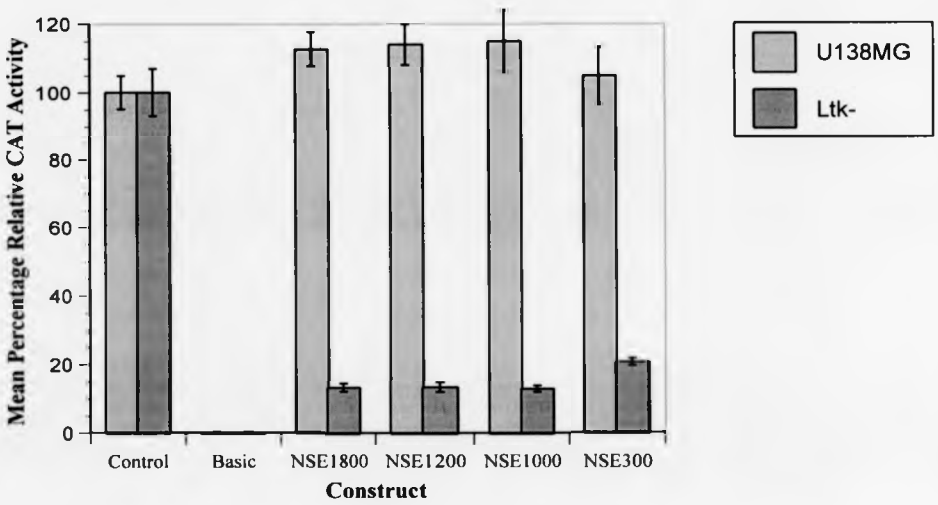

Figure 6.12: Comparison of transfection data from permissive U-138 MG cells and nonpermissive Ltk- cells. The values represented are combined mean Relative CAT Activities and standard errors from Figures 6.5 and 6.10.

6.4 Transfection with full series of *NSE-cat* constructs

The first series of *NSE-cat* constructs, as described in section 6.3, plus the second series, comprising the highly truncated pNSE120CAT, pNSE95CAT and pNSE65CAT, were transfected into two permissive cell lines of neuronal origin (Neuro-2A and NB4-1A3 neuroblastoma cells) and two nonpermissive cell lines of nonneuronal origin (Ltk- and HeLa cells). All except the HeLa cells were derived from murine sources, the HeLa cells being derived from a human carcinoma. As discussed above, studies involving the first series of constructs using one permissive and one nonpermissive cell line indicated that regulatory elements required for cell-type specific expression of *NSE* were probably located downstream of the *Xho* I site at position -255 (the upstream boundary of construct pNSE300CAT). For this reason, it was considered unnecessary to use all of the larger constructs for subsequent analysis and the intermediate-sized pNSE1200CAT was dropped from further transfection studies

6.4.1 Transfection of Ltk- cells

Experiments designed to optimise the transfection parameters of the two neuroblastoma cell lines showed that neither could be successfully transfected using DEAE-dextran (see sections 5.4.4 and 5.4.5). However, DNA could be introduced into Neuro-2A cells with great efficiency using calcium phosphate whilst NB4-1A3 cells could only take up DNA in the presence of liposomes. As experiments with the positive and negative cell lines were generally carried out in parallel, it was convenient to transfect Ltk- cells using both of these methods. As well as convenience, however, the Ltk- transfection experiments also served as a useful control for the effect of transfection method on the performance of the *NSE-cat* constructs. The results below reflect both calcium phosphate- and LipofectAMINE-mediated transfections as indicated in the figure legends. Under the conditions described in sections 5.4.1.2 and 5.4.1.3, Ltk- fibroblasts were transfected with the full series of *NSE-cat* constructs and controls. Data from three individual experiments are presented in Figures 6.13-6.15, followed by combined results in Figure 6.16. A representative CAT assay is shown in Figure 6.17. The results confirmed those obtained from DEAE-dextran-mediated transfection and indicated that the Relative CAT Activities of the first series of *NSE-cat* deletion constructs fell within the range 10-20%. The more truncated construct, pNSE120CAT, displayed mean Relative CAT Activities of 30-60%, generally a doubling over

corresponding values for pNSE300CAT which could be attributed to the removal of the 135 bp fragment separating the upstream boundaries of the two constructs. Transfection with pNSE95CAT generated mean Relative CAT Activities within the range 25-30%, reflecting a minor loss of reporter activity compared to the next largest construct. Finally, the most truncated construct pNSE65CAT demonstrated mean Relative CAT Activities of around 0%, indicating that very little transcription of the reporter gene had taken place.

Construct	CAT	GAL	MEC	ACA	xACA	RCA	xRCA	semRCA
Control	264532	159	1.30	1279.79	1142.34	112.42	100.00	13.44
	292837	173		1302.08		114.43		
	184581	168		845.15		73.14		
Basic	3440	100	1.41	24.40	35.73	-1.02	0.00	0.52
	6444	115		39.74		0.36		
	7224	119		43.05		0.66		
NSE1800	37763	185	1.00	204.12		15.22	14.09	1.60
	32775	153		214.22		16.13		
	29443	188		156.61		10.92		
NSE1000	28653	305	1.13	83.14		4.28	6.89	1.32
	36985	251		130.40		8.55		
	34408	249		122.29		7.82		
NSE300	59593	248	1.30	184.84		13.47	15.30	1.04
	52678	197		205.69		15.36		
	57506	197		224.55		17.06		
NSE120	157350	306	1.34	383.74		31.45	31.77	0.72
	137384	273		375.55		30.71		
	104087	193		402.47		33.14		
NSE95	74918	156	1.35	355.74		28.92	23.95	2.50
	69875	193		268.18		21.01		
	72560	193		278.49		21.94		
NSE65	15727	215	1.35	54.18		1.67	1.37	0.20
	13137	209		46.56		0.98		
	11616	166		51.83		1.46		

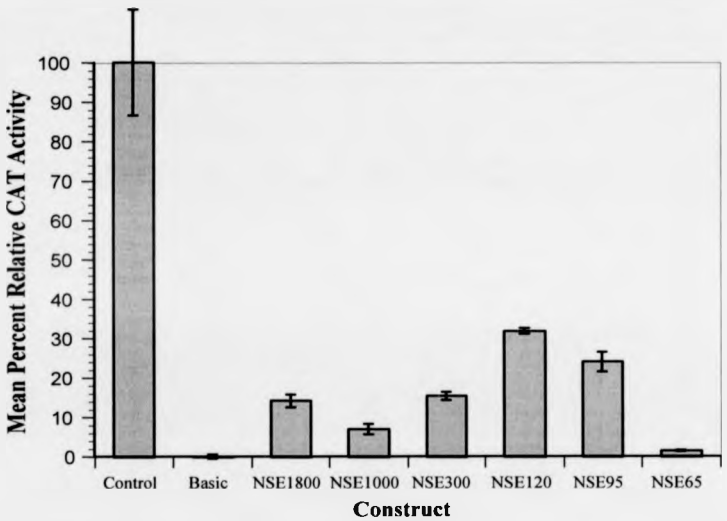

Figure 6.13: Table and histogram showing data from the first transfection of Ltk- cells with the full series of *NSE-cat* deletion constructs. Transfection was carried out using calcium phosphate. Abbreviations used in table headings: CAT - CAT (chloramphenicol acetyltransferase) activity; GAL - β-galactosidase activity; MEC - Molar Equivalence Constant; ACA - Actual CAT Activity, xACA - mean Actual CAT Activity of control constructs; RCA - Relative CAT Activity; xRCA - mean Relative CAT Activity; semRCA - standard error of the mean Relative CAT Activity. A brief explanation of these terms can be found in Figure 6.1, a fuller explanation in section 5.5. The histogram shows mean Relative CAT Activities for each construct with error bars representing standard errors.

Construct	CAT	GAL	MEC	ACA	xACA	RCA	xRCA	semRCA
Control	32950	188	1.30	134.82	123.72	109.27	100.00	6.53
	24573	174		108.63		87.39		
	28556	172		127.71		103.33		
Basic	1056	184	1.41	4.07	4.04	0.02	0.00	0.30
	877	134		4.64		0.50		
	683	142		3.41		-0.53		
NSE1800	2562	88	1.00	29.20		21.02	16.73	2.15
	2995	141		21.24		14.37		
	2870	132		21.74		14.79		
NSE1000	5956	199	1.13	26.49		18.75	21.56	1.80
	5661	148		33.85		24.91		
	6107	185		29.21		21.03		
NSE300	3569	100	1.30	27.45		19.56	15.92	4.71
	3929	101		29.92		21.63		
	1887	122		11.90		6.56		
NSE120	22746	232	1.34	73.17		57.76	56.97	5.54
	18745	232		60.30		47.00		
	27423	246		83.19		66.13		
NSE95	3563	60	1.35	44.05		33.43	33.37	3.29
	3118	62		37.12		27.64		
	2264	33		50.76		39.04		
NSE65	1004	188	1.35	3.96		-0.07	-0.41	0.57
	993	164		4.49		0.37		
	574	192		2.21		-1.53		

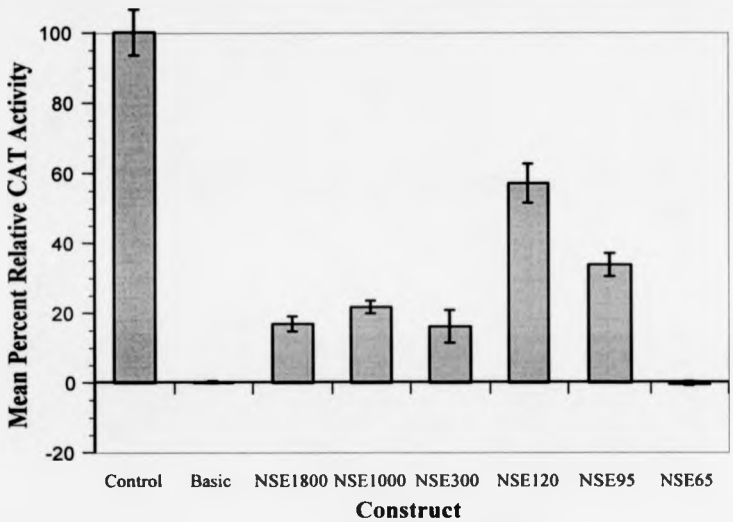

Figure 6.14: Table and histogram showing data from the second transfection of Ltk- cells with the full series of *NSE-cat* deletion constructs. Transfection was carried out using calcium phosphate. Abbreviations used in table headings: CAT - CAT (chloramphenicol acetyltransferase) activity; GAL - β-galactosidase activity; MEC - Molar Equivalence Constant; ACA - Actual CAT Activity, xACA - mean Actual CAT Activity of control constructs; RCA - Relative CAT Activity; xRCA - mean Relative CAT Activity; semRCA - standard error of the mean Relative CAT Activity. A brief explanation of these terms can be found in Figure 6.1, a fuller explanation in section 5.5. The histogram shows mean Relative CAT Activities for each construct with error bars representing standard errors.

Construct	CAT	GAL	MEC	ACA	xACA	RCA	xRCA	semRCA
Control	310946	177	1.30	1351.35	1427.01	94.56	100.00	6.93
	258788	123		1618.44		113.75		
	204555	120		1311.25		91.68		
Basic	1775	133	1.41	9.47	35.10	-1.84	0.00	1.04
	8440	165		36.28		0.08		
	12935	154		59.57		1.76		
NSE1800	44967	132	1.00	340.66		21.95	14.09	4.37
	39110	176		222.22		13.44		
	40634	311		130.66		6.86		
NSE1000	37346	211	1.13	156.63		8.73	9.94	1.08
	37921	165		203.38		12.09		
	36440	201		160.44		9.00		
NSE300	71399	225	1.30	244.10		15.01	20.26	8.27
	75469	107		542.55		36.46		
	75101	351		164.59		9.30		
NSE120	125105	111	1.34	841.10		57.90	45.29	6.45
	122745	168		545.24		36.65		
	101396	124		610.23		41.32		
NSE95	68336	156	1.35	324.48		20.79	25.09	7.15
	74531	221		249.81		15.43		
	81252	104		578.72		39.05		
NSE65	7758	175	1.35	32.84		-0.16	-1.00	0.42
	3523	184		14.18		-1.50		
	4955	222		16.53		-1.33		

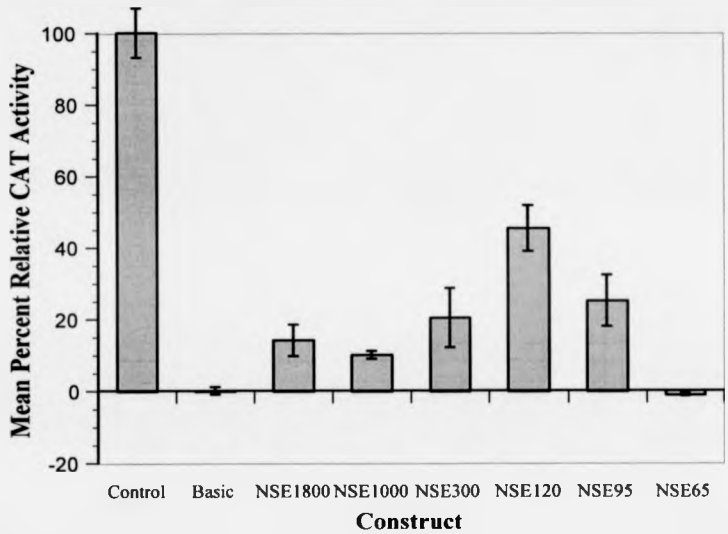

Figure 6.15: Table and histogram showing data from the third transfection of Ltk- cells with the full series of *NSE-cat* deletion constructs. Transfection was carried out using LipofectAMINE. Abbreviations used in table headings: CAT - CAT (chloramphenicol acetyltransferase) activity; GAL - β-galactosidase activity; MEC - Molar Equivalence Constant; ACA - Actual CAT Activity, xACA - mean Actual CAT Activity of control constructs; RCA - Relative CAT Activity; xRCA - mean Relative CAT Activity; semRCA - standard error of the mean Relative CAT Activity. A brief explanation of these terms can be found in Figure 6.1, a fuller explanation in section 5.5. The histogram shows mean Relative CAT Activities for each construct with error bars representing standard errors.

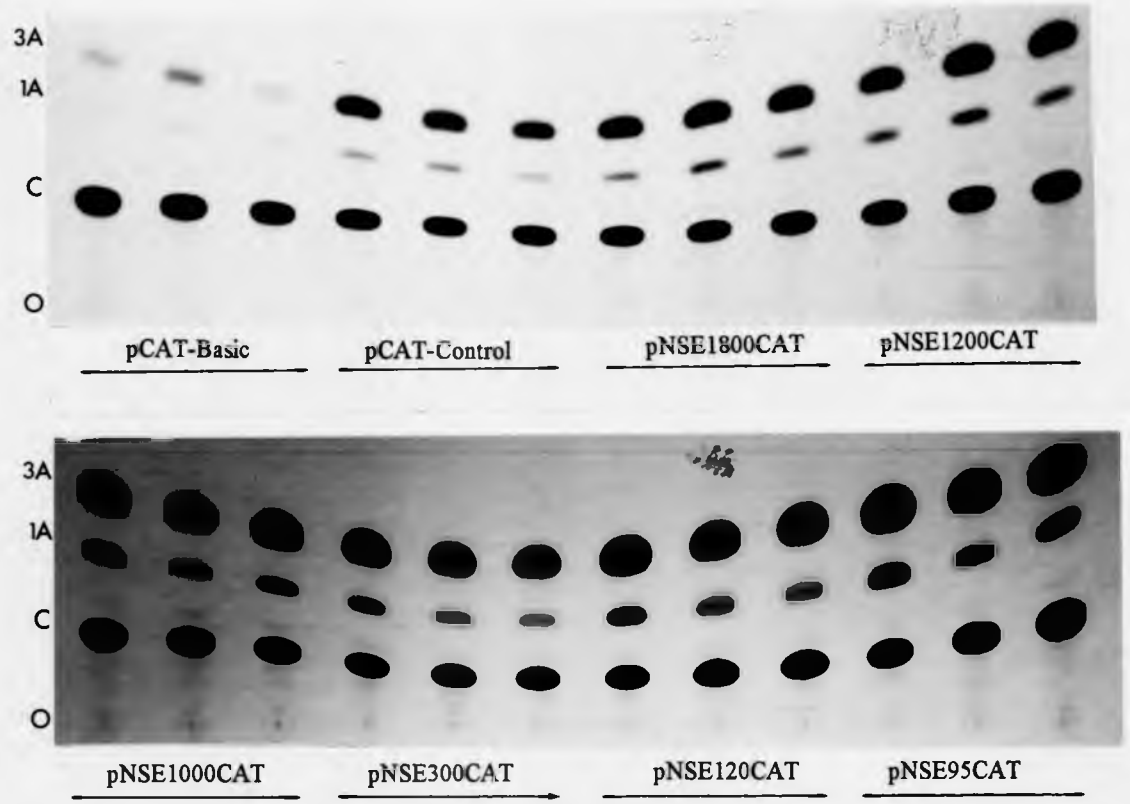

Figure 6.23: CAT assay from the initial Neuro-2A transfection experiment (Figure 6.18) using the full series of *NSE-cat* constructs excluding pNSE65CAT but including pNSE1200CAT, which was later dropped from transfection experiments. Each construct was transfected in triplicate and the lanes on the TLC plate were grouped accordingly. Abbreviations: O = origin; C = chloramphenicol; 1A = 1-acetylchloramphenicol; 3A = 3-acetylchloramphenicol.

Figure 6.22 (Opposite page): Table and histogram showing combined data from the transfection of Neuro-2A cells with the full series of *NSE-cat* deletion constructs. Abbreviations used in the table: RCA1, RCA2, RCA3, RCA4 - Relative CAT Activities from the four individual experiments (as shown in Figures 6.17-6.20); xRCA1234 - combined mean Relative CAT Activity for each construct over four experiments (maximum of twelve transfections); semRCA1234 - standard error of the combined mean Relative CAT Activities. Gaps in the table indicate where particular constructs were not used. A brief explanation of these terms can be found in Figure 6.1, a fuller explanation in section 5.5. The histogram shows combined mean relative CAT activity for each construct and illustrates the trend in reporter gene activity for reporter constructs containing stepwise deletions of the rat NSE 5' flanking region. Error bars represent standard errors of the combined mean Relative CAT Activities.

Construct	RCA1	RCA2	RCA3	RCA4	xRCA1234	semRCA1234
Control	141.01	94.29	90.85	117.67	100.00	5.37
	84.54	89.17	106.34	80.99		
	74.45	116.54	102.81	101.34		
Basic	-5.07	5.80	-1.99	-0.23	0.00	1.65
	13.25	-6.90	1.35	-0.04		
	-8.18	1.10	0.64	0.26		
NSE1800	160.73	117.67	129.55	121.11	132.59	12.02
	192.96	68.56	106.81	134.33		
	209.32	75.32	126.40	148.27		
NSE1200	105.58				124.96	25.36
	175.24					
	94.05					
NSE1000	167.09	97.54	101.04	106.42	133.01	14.86
	151.28	160.43	84.46	144.98		
	269.28	94.85	99.37	119.34		
NSE300	137.05	201.80	130.90	117.61	108.24	10.64
	80.76	102.00	67.31	100.93		
	100.03	103.38	81.36	75.84		
NSE120	591.70	243.04	286.99	191.46	291.07	30.98
	319.84	183.36	279.11	251.40		
	273.37	367.68	237.59	267.26		
NSE95	407.39	167.55	21.56	178.22	206.70	26.47
	231.89	262.65	192.85	160.19		
	278.45	241.28	163.10	175.28		
NSE65		-2.65	0.23	0.61	-1.49	0.79
		-7.29	-0.86	-0.54		
		-0.85	-0.92	-1.16		

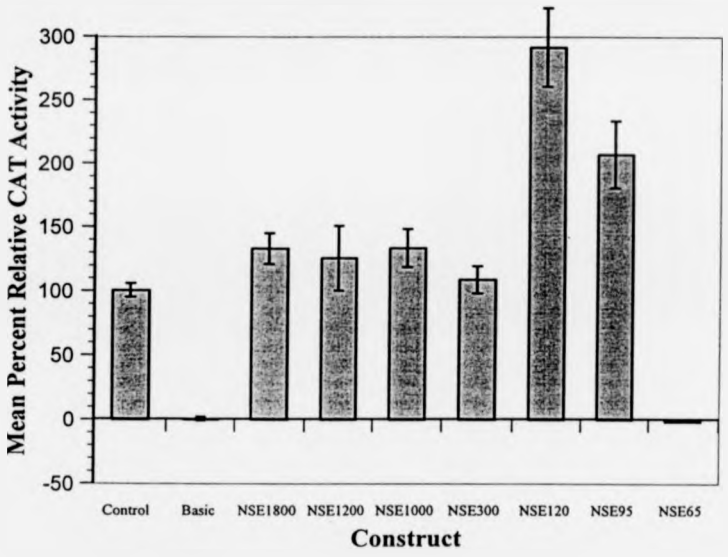

6.4.2 Transfection of Neuro-2A cells

Neuro-2A cells were made available just as the experiments involving U-138 MG glioma cells were coming to an end. The first transfection took place before any conclusions had been drawn from the U-138 MG experiments and before the most truncated construct used in this study, pNSE65CAT, had been produced. Therefore, Neuro-2A cells were, in the first instance, transfected with a mixed group of constructs comprising pNSE1800CAT, pNSE1200CAT, pNSE1000CAT, pNSE300CAT, pNSE120CAT and pNSE95CAT. The second and subsequent transfections followed a more orthodox pattern (in accordance with the routine introduction of DNA into other cell lines), with the following constructs used: pNSE1800CAT, pNSE1000CAT, pNSE300CAT, pNSE120CAT, pNSE95CAT and pNSE65CAT. Neuro-2A cells were transfected using calcium phosphate under the conditions described in section 5.4.4. Data from the first transfection and three subsequent transfections are presented in Figures 6.18-6.21, followed by combined results in Figure 6.22. Representative CAT assays are shown in Figures 6.23 and 6.24. The results, in common with other transfections mediated by calcium phosphate, showed a degree of variability between experiments. The initial series of *NSE-cat* constructs generally showed mean Relative CAT Activities in the range 90-140%, with standard error values to indicate that the differences between them were not significant. In the first transfection experiment, the mean Relative CAT Activities for these constructs were somewhat higher, falling within the range 100-200%, however, as found for the third U-138 MG transfection experiment (see section 6.3.2), the standard error value for the control vector, pCAT-Control, was greater than the arbitrary maximum of 15% of the mean, indicating that at least one of the data points in the control transfection was nonrepresentative. The consequence of one uncharacteristically low Actual CAT Activity for the control vector would be the reduction of the mean Actual CAT Activity and this would have a knock-on effect, generating unrealistically high Relative CAT Activities for each of the *NSE-cat* vectors. The scenario described above is most likely to be the case for this first experiment as the mean Relative CAT Activities for the whole series of constructs were higher than those for the same constructs in the subsequent three transfection experiments. Over the last three transfection experiments, the construct pNSE120CAT demonstrated mean Relative CAT Activities in the narrow range 235-270%, reflecting a two- to threefold increase upon the mean RCA values of pNSE300CAT. One again, the first transfection experiment generated a substantially higher mean Relative CAT Activity for this construct, approximately 400%, and the standard error was higher than 15%. The further truncated vector,

pNSE95CAT, demonstrated mean Relative CAT Activities in the range 125-225% over transfections 2, 3 and 4. The lower value was obtained in the third transfection experiment and the standard error for this construct was 42% of the mean. It is therefore very likely that one of the data points for this transfection was nonrepresentative, and from the sample of Relative CAT Activities shown for this construct in Figure 6.22, it can be seen that all values fall within the range 160-260% except one of 22% from the third experiment. It is clear that this aberrant result is responsible for the spread of Relative CAT Activities in the third transfection. Once again, the mean Relative CAT activity for pNSE95CAT was much higher in the first transfection (305%, with standard error in excess of 15%) for the reasons already discussed. The final construct, pNSE65CAT, showed mean Relative CAT Activities around 0% in all experiments, indicating that no transcription above the background value of the negative control vector, pCAT-Basic, had occurred.

Construct	CAT	GAL	MEC	ACA	xACA	RCA	xRCA	semRCA
Control	92090	264	1.30	268.33	200.11	141.01	100.00	20.71
	84789	374		174.39		84.54		
	57578	281		157.62		74.45		
Basic	13365	374	1.41	25.34	33.77	-5.07	0.00	6.68
	23684	301		55.80		13.25		
	10404	366		20.16		-8.18		
NSE1800	89135	296	1.00	301.13		160.73	187.67	14.27
	118841	335		354.75		192.96		
	98545	258		381.96		209.32		
NSE1200	74379	320	1.11	209.40		105.58	124.96	25.36
	119868	332		325.27		175.24		
	80658	382		190.22		94.05		
NSE1000	115530	328	1.13	311.70		167.09	195.88	36.98
	107399	333		285.42		151.28		
	154041	283		481.69		269.28		
NSE300	107527	316	1.30	261.75		137.05	105.95	16.52
	89385	409		168.11		80.76		
	82485	317		200.16		100.03		
NSE120	321939	236	1.34	1018.02		591.70	394.97	99.28
	206220	272		565.79		319.84		
	166266	254		488.50		273.37		
NSE95	308298	321	1.35	711.43		407.39	305.91	52.49
	189717	335		419.50		231.89		
	251584	375		496.96		278.45		

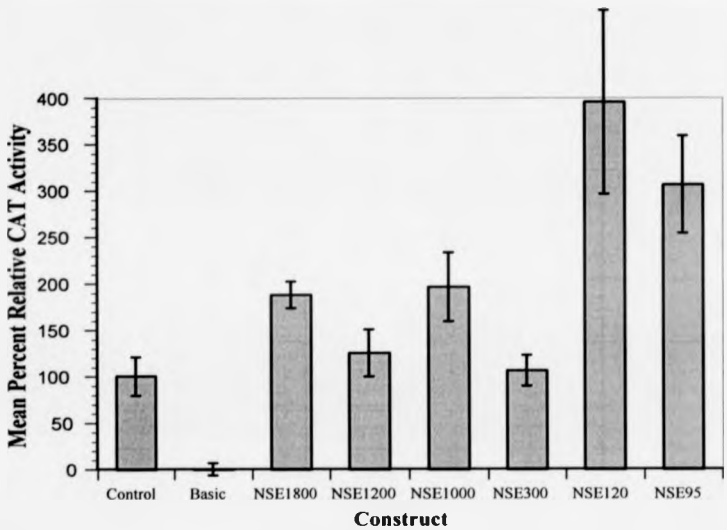

Figure 6.18: Table and histogram showing data from the first transfection of Neuro-2A cells. Abbreviations used in table headings: CAT - CAT (chloramphenicol acetyltransferase) activity; GAL - β-galactosidase activity; MEC - Molar Equivalence Constant; ACA - Actual CAT Activity, xACA - mean Actual CAT Activity of control constructs; RCA - Relative CAT Activity; xRCA - mean Relative CAT Activity; semRCA - standard error of the mean Relative CAT Activity. A brief explanation of these terms can be found in Figure 6.1, a fuller explanation in section 5.5. The histogram shows mean Relative CAT Activities for each construct with error bars representing standard errors.

Construct	CAT	GAL	MEC	ACA	xACA	RCA	xRCA	semRCA
Control	222424	466	1.30	367.16	387.38	94.29	100.00	8.40
	158823	350		349.06		89.17		
	193619	334		445.92		116.54		
Basic	2699	212	1.41	9.03	33.45	-6.90	0.00	3.71
	25123	330		53.99		5.80		
	17210	327		37.33		1.10		
NSE1800	329343	732	1.00	449.92		117.67	87.18	15.37
	300111	1087		276.09		68.56		
	325535	1085		300.03		75.32		
NSE1000	285814	680	1.11	378.66		97.54	117.61	21.43
	342368	513		601.25		160.43		
	245453	599		369.16		94.85		
NSE300	285570	293	1.30	747.68		201.80	135.73	33.04
	170275	332		394.47		102.00		
	166493	321		399.35		103.38		
NSE120	348465	291	1.34	893.64		243.04	264.69	54.30
	320634	351		682.40		183.36		
	365035	204		1334.77		367.68		
NSE95	270424	320	1.35	626.46		167.55	223.83	28.81
	308232	237		963.04		262.65		
	327058	273		887.42		241.28		
NSE65	13266	408	1.35	24.08		-2.65	-3.59	1.92
	3066	297		7.65		-7.29		
	13071	318		30.45		-0.85		

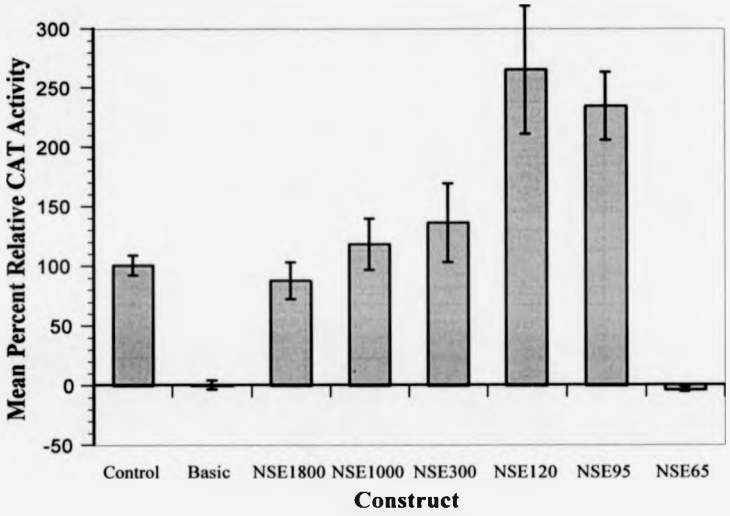

Figure 6.19: Table and histogram showing data from the first transfection of Neuro-2A cells with the full series of *NSE-cat* deletion constructs. Abbreviations used in table headings: CAT - CAT (chloramphenicol acetyltransferase) activity; GAL - β-galactosidase activity; MEC - Molar Equivalence Constant; ACA - Actual CAT Activity, xACA - mean Actual CAT Activity of control constructs; RCA - Relative CAT Activity; xRCA - mean Relative CAT Activity; semRCA - standard error of the mean Relative CAT Activity. A brief explanation of these terms can be found in Figure 6.1, a fuller explanation in section 5.5. The histogram shows mean Relative CAT Activities for each construct with error bars representing standard errors.

Construct	CAT	GAL	MEC	ACA	xACA	RCA	xRCA	semRCA
Control	452372	427	1.30	814.94	894.97	90.85	100.00	4.68
	429968	348		950.42		106.34		
	463822	388		919.55		102.81		
Basic	1044	297	1.41	2.49	19.87	-1.99	0.00	1.01
	16342	366		31.67		1.35		
	12994	362		25.46		0.64		
NSE1800	539853	468	1.00	1153.53		129.55	120.92	7.11
	603274	632		954.55		106.81		
	593387	527		1125.97		126.40		
NSE1000	668336	666	1.11	904.06		101.04	94.95	5.27
	588873	699		758.96		84.46		
	679232	688		889.42		99.37		
NSE300	666570	440	1.30	1165.33		130.90	93.19	19.29
	379943	480		608.88		67.31		
	396721	417		731.82		81.36		
NSE120	1339820	395	1.34	2531.31		286.99	267.90	15.32
	1164733	353		2462.33		279.11		
	1206660	429		2099.05		237.59		
NSE95	109816	390	1.35	208.58		21.56	125.84	52.84
	1081100	469		1707.49		192.85		
	1090112	558		1447.12		163.10		
NSE65	12887	437	1.35	21.84		0.23	-0.52	0.37
	9732	585		12.32		-0.86		
	9410	589		11.83		-0.92		

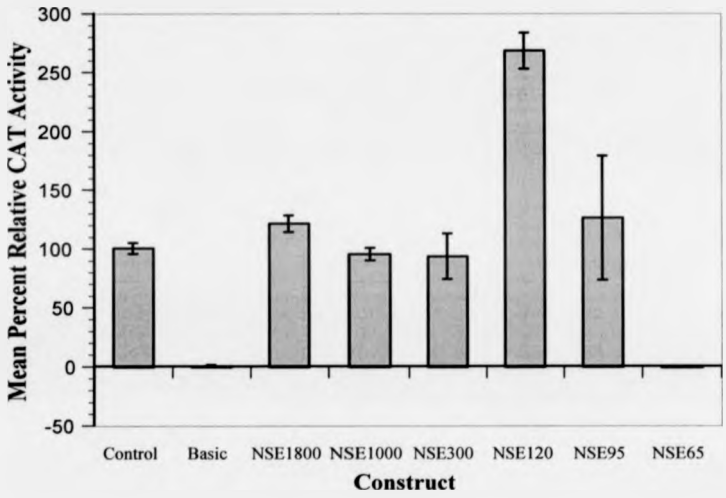

Figure 6.20: Table and histogram showing data from the second transfection of Neuro-2A cells with the full series of *NSE-cat* deletion constructs. Abbreviations used in table headings: CAT - CAT (chloramphenicol acetyltransferase) activity; GAL - β-galactosidase activity; MEC - Molar Equivalence Constant; ACA - Actual CAT Activity, xACA - mean Actual CAT Activity of control constructs; RCA - Relative CAT Activity; xRCA - mean Relative CAT Activity; semRCA - standard error of the mean Relative CAT Activity. A brief explanation of these terms can be found in Figure 6.1, a fuller explanation in section 5.5. The histogram shows mean Relative CAT Activities for each construct with error bars representing standard errors.

Construct	CAT	GAL	MEC	ACA	xACA	RCA	xRCA	semRCA
Control	1253529	427	1.30	2258.20	1923.05	117.67	100.00	10.61
	1017684	501		1562.54		80.99		
	972637	384		1948.39		101.34		
Basic	21748	686	1.41	22.48	26.82	-0.23	0.00	0.14
	25863	702		26.13		-0.04		
	22622	504		31.83		0.26		
NSE1800	1047835	451	1.00	2323.36		121.11	134.57	7.84
	1227849	477		2574.11		134.33		
	1339746	472		2838.44		148.27		
NSE1000	1783965	786	1.11	2044.75		106.42	123.58	11.33
	1861139	604		2776.00		144.98		
	1672366	658		2289.72		119.34		
NSE300	947685	323	1.30	2256.93		117.61	98.12	12.14
	885512	351		1940.64		100.93		
	759823	399		1464.86		75.84		
NSE120	1107577	226	1.34	3657.30		191.46	236.70	23.08
	1316899	205		4793.95		251.40		
	1331218	195		5094.60		267.26		
NSE95	1784253	388	1.35	3406.36		178.22	171.23	5.58
	1749946	423		3064.44		160.19		
	1800200	398		3350.46		175.28		
NSE65	30231	582	1.35	38.48		0.61	-0.36	0.52
	9462	421		16.65		-0.54		
	3167	488		4.81		-1.16		

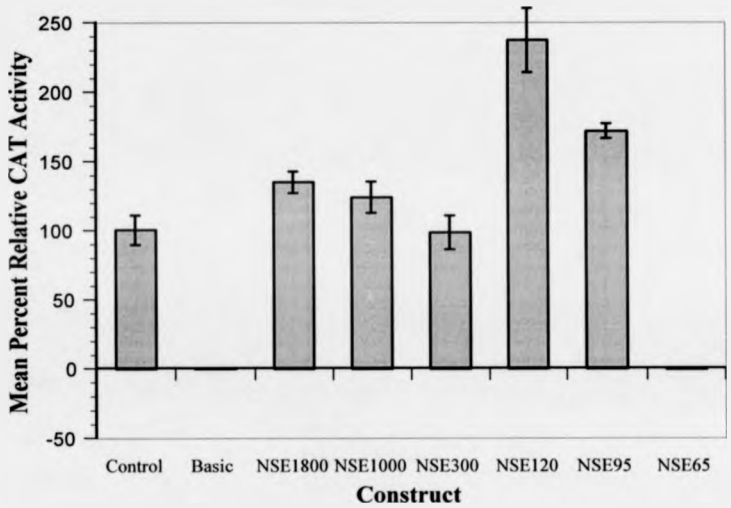

Figure 6.21: Table and histogram showing data from the third transfection of Neuro-2A cells with the full series of *NSE-cat* deletion constructs. Abbreviations used in table headings: CAT - CAT (chloramphenicol acetyltransferase) activity; GAL - β-galactosidase activity; MEC - Molar Equivalence Constant; ACA - Actual CAT Activity, xACA - mean Actual CAT Activity of control constructs; RCA - Relative CAT Activity; xRCA - mean Relative CAT Activity; semRCA - standard error of the mean Relative CAT Activity. A brief explanation of these terms can be found in Figure 6.1, a fuller explanation in section 5.5. The histogram shows mean Relative CAT Activities for each construct with error bars representing standard errors.

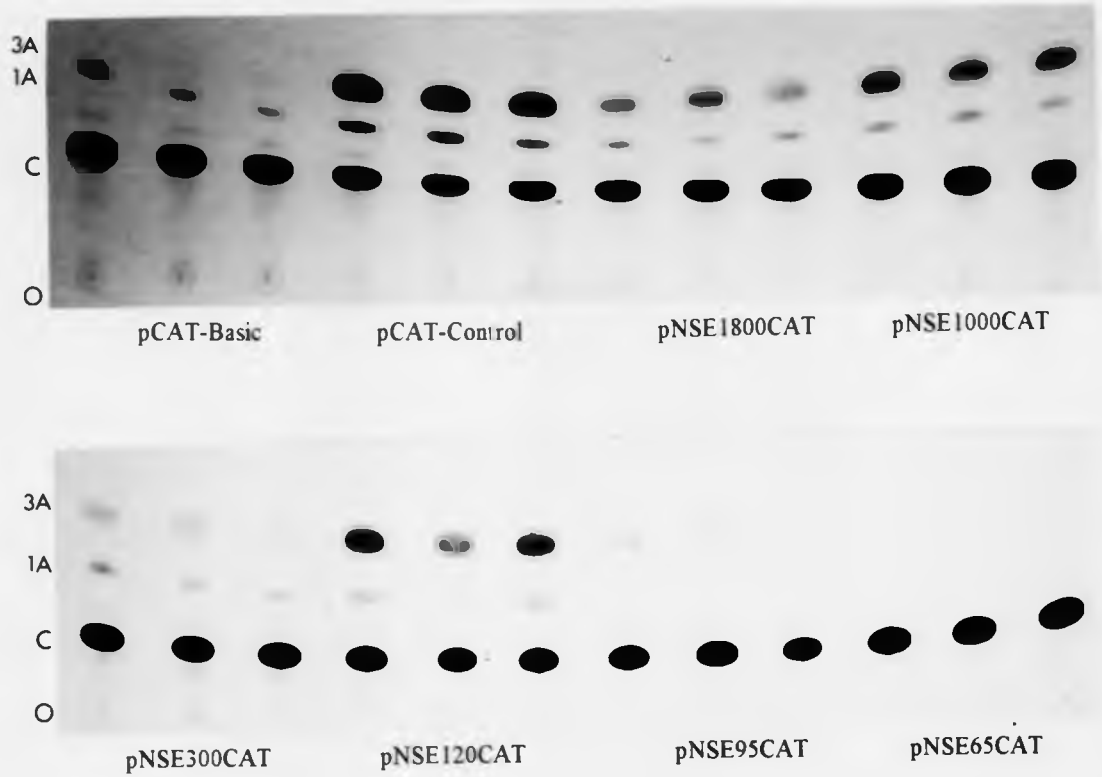

Figure 6.17: Representative CAT assay from the Ltk- series of transfections with the full set of *NSE-cat* constructs. Each construct was transfected in triplicate and the lanes on the TLC plate were grouped accordingly. The assay above corresponds to the experiment described in Figure 6.14 which was calcium phosphate-mediated. Abbreviations: O = origin; C = chloramphenicol; 1A = 1-acetyl-chloramphenicol; 3A = 3-acetylchloramphenicol.

Construct	RCA1	RCA2	RCA3	xRCA123	semRCA123
Control	112.42	109.27	94.56	100.00	4.75
	114.43	87.39	113.75		
	73.14	103.33	91.68		
Basic	-1.02	0.02	-1.84	0.00	0.35
	0.36	0.50	0.08		
	0.66	-0.53	1.76		
NSE1800	15.22	21.02	21.95	14.97	1.54
	16.13	14.37	13.44		
	10.92	14.79	6.86		
NSE1000	4.28	18.75	8.73	12.80	2.35
	8.55	24.91	12.09		
	7.82	21.03	9.00		
NSE300	13.47	19.56	15.01	17.16	2.87
	15.36	21.63	36.46		
	17.06	6.56	9.30		
NSE120	31.45	57.76	57.90	44.67	4.39
	30.71	47.00	36.65		
	33.14	66.13	41.32		
NSE95	28.92	33.43	20.79	27.47	2.81
	21.01	27.64	15.43		
	21.94	39.04	39.05		
NSE65	1.67	-0.07	-0.16	-0.01	0.42
	0.98	0.37	-1.50		
	1.46	-1.53	-1.33		

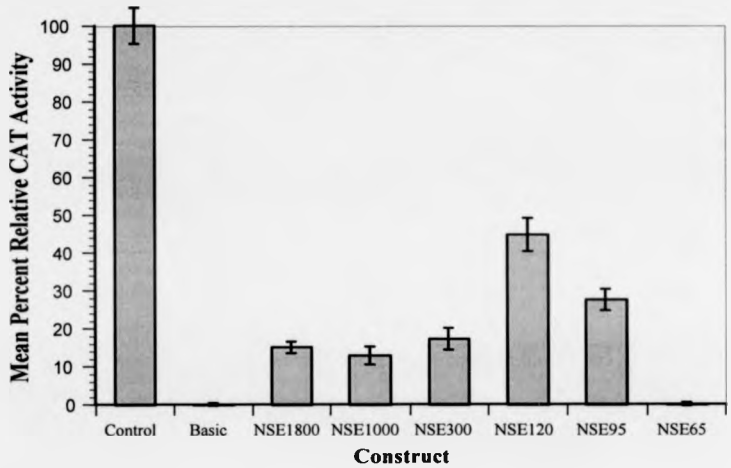

Figure 6.16: Table and histogram showing combined data from the transfection of Ltk- cells with the full series of *NSE-cat* deletion constructs. Abbreviations used in the table: RCA1, RCA2, RCA3 - Relative CAT Activities from the three individual experiments (as shown in Figures 6.13-6.15); xRCA123 - combined mean Relative CAT Activity for each construct over three experiments (nine transfections); semRCA123 - standard error of the combined mean Relative CAT Activities. A brief explanation of these terms can be found in Figure 6.1, a fuller explanation in section 5.5. The histogram shows combined mean relative CAT activity for each construct and illustrates the trend in reporter gene activity for reporter constructs containing stepwise deletions of the rat NSE 5' flanking region. Error bars represent standard errors of the combined mean Relative CAT Activities.

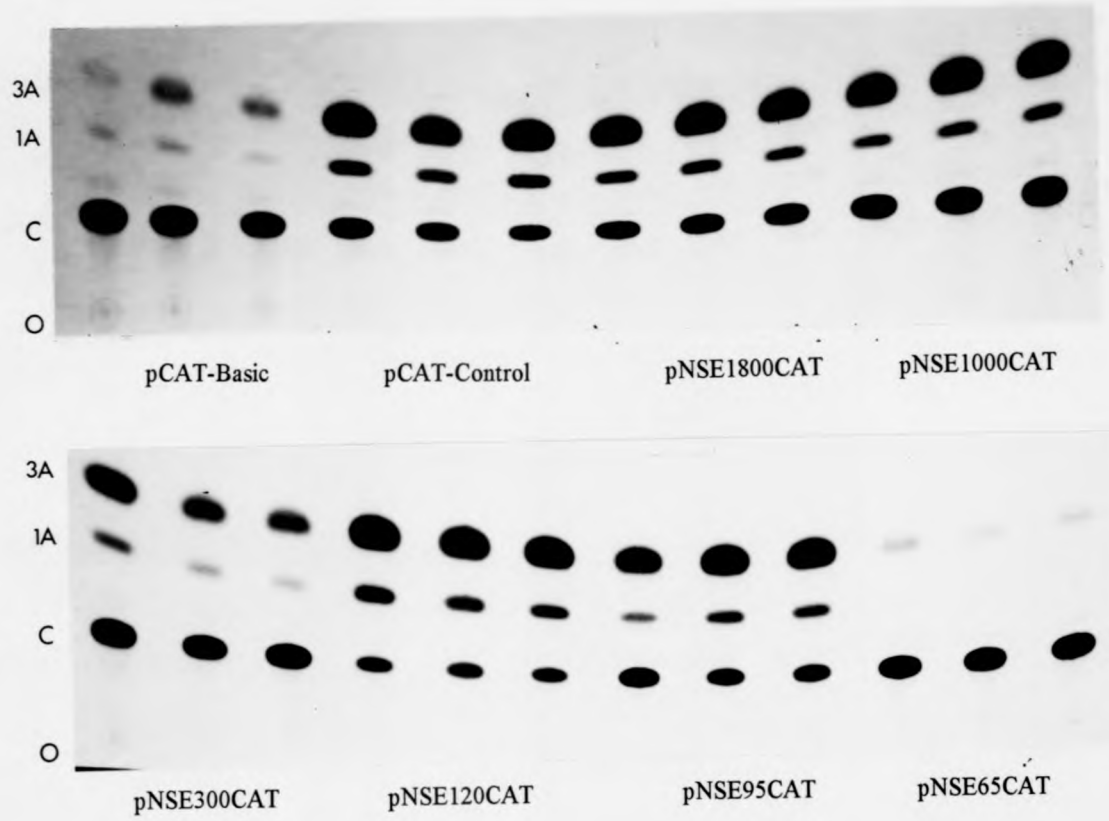

Figure 6.24: Representative CAT assay from the Neuro-2A series of transfections with the full series of *NSE-cat* constructs. Each construct was transfected in triplicate and the lanes on the TLC plate were grouped accordingly. The assay above corresponds to the experiment described in Figure 6.19. Abbreviations: O = origin; C = chloramphenicol; 1A = 1-acetylchloramphenicol; 3A = 3-acetylchloramphenicol.

6.4.3 Transfection of NB4-1A3 cells

Under the conditions described in section 5.4.5, NB4-1A3 neuroblastoma cells were transfected with the full series of *NSE-cat* constructs and controls using LipofectAMINE. Data from two individual experiments are presented in Figures 6.25 and 6.26, followed by combined results in Figure 6.27. A representative CAT assay is shown in Figure 6.28. The results for the longest construct, pNSE1800CAT, were consistent within each experiment but varied between them, with a mean Relative CAT Activities of 35% for the first transfection and 67% for the second. For the majority of the other constructs, the results appeared more repeatable. The shorter construct pNSE1000CAT demonstrated a low mean Relative CAT Activity of 5-6%, whereas pNSE300CAT demonstrated a mean Relative CAT Activity of 25-27%. The more truncated construct, pNSE120CAT, generally displayed Relative CAT Activities in the range 20-30%, however, in the second transfection, a one-off value of 81% increased the mean Relative CAT Activity to 43% and generated a standard error of 45%; it is therefore likely that this data point was nonrepresentative of this construct. Like pNSE1800CAT, the further truncated construct pNSE95CAT demonstrated a higher mean Relative CAT Activity in the second transfection compared to the first (32% compared to 17%), whilst in each individual transfection, the values were more consistent. Finally, the most truncated construct pNSE65CAT, displayed Relative CAT Activities of approximately 2% in each experiment.

Construct	CAT	GAL	MEC	ACA	xACA	RCA	xRCA	semRCA
Control	422623	188	1.30	1729.23	1839.06	94.01	100.00	8.19
	491762	229		1651.87		89.79		
	466520	168		2136.08		116.20		
Basic	2163	233	1.41	6.58	5.50	0.06	0.00	0.07
	871	216		2.86		-0.14		
	2109	212		7.06		0.08		
NSE1800	64046	142	1.00	452.14		24.36	35.23	5.52
	102304	142		719.94		38.96		
	139302	178		782.03		42.35		
NSE1000	23889	142	1.11	151.56		7.97	5.52	1.25
	14319	141		91.49		4.69		
	14521	170		76.95		3.90		
NSE300	164141	227	1.30	556.22		30.04	27.31	1.50
	181001	302		461.03		24.84		
	185875	285		501.69		27.06		
NSE120	62521	166	1.34	281.07		15.03	23.64	4.91
	82923	104		593.09		32.05		
	100208	169		442.58		23.84		
NSE95	78161	250	1.35	231.59		12.33	17.32	2.55
	105355	203		385.29		20.71		
	106044	223		352.32		18.92		
NSE65	14259	220	1.35	48.01		2.32	1.76	0.28
	11265	251		33.24		1.51		
	9312	215		32.08		1.45		

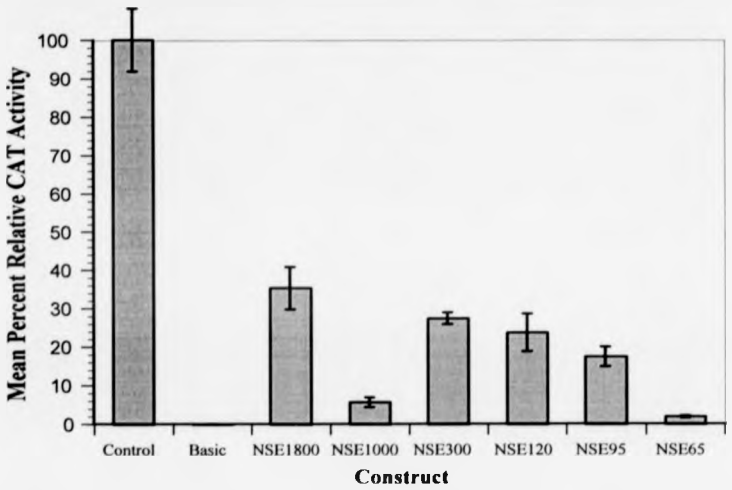

Figure 6.25: Table and histogram showing data from the first transfection of NB4-1A3 cells with the full series of *NSE-cat* deletion constructs. Abbreviations used in table headings: CAT - CAT (chloramphenicol acetyltransferase) activity; GAL - β-galactosidase activity; MEC - Molar Equivalence Constant; ACA - Actual CAT Activity, xACA - mean Actual CAT Activity of control constructs; RCA - Relative CAT Activity; xRCA - mean Relative CAT Activity; semRCA - standard error of the mean Relative CAT Activity. A brief explanation of these terms can be found in Figure 6.1, a fuller explanation in section 5.5. The histogram shows mean Relative CAT Activities for each construct with error bars representing standard errors.

Construct	CAT	GAL	MEC	ACA	xACA	RCA	xRCA	semRCA
Control	462333	112	1.30	3175.36	2770.62	114.68	100.00	7.82
	466198	147		2439.55		87.99		
	441758	126		2696.94		97.33		
Basic	2989	120	1.41	17.67	13.11	0.17	0.00	0.09
	1861	152		8.68		-0.16		
	2709	148		12.98		-0.00		
NSE1800	294600	149	1.00	1977.18		71.23	67.43	2.15
	290643	164		1772.21		63.79		
	177504	95		1868.46		67.28		
NSE1000	48553	178	1.11	245.74		8.44	6.43	2.16
	9605	121		71.51		2.12		
	30145	107		253.81		8.73		
NSE300	132572	104	1.30	980.56		35.08	25.06	8.24
	102743	90		878.15		31.37		
	25068	76		253.72		8.73		
NSE120	89516	118	1.34	566.13		20.05	42.72	19.23
	130703	128		762.03		27.16		
	382134	127		2245.47		80.96		
NSE95	248855	188	1.35	980.52		35.08	32.02	3.07
	201284	152		980.92		35.10		
	124592	127		726.70		25.88		
NSE65	10883	148	1.35	54.47		1.50	1.95	0.40
	12031	155		57.50		1.61		
	14409	120		88.94		2.75		

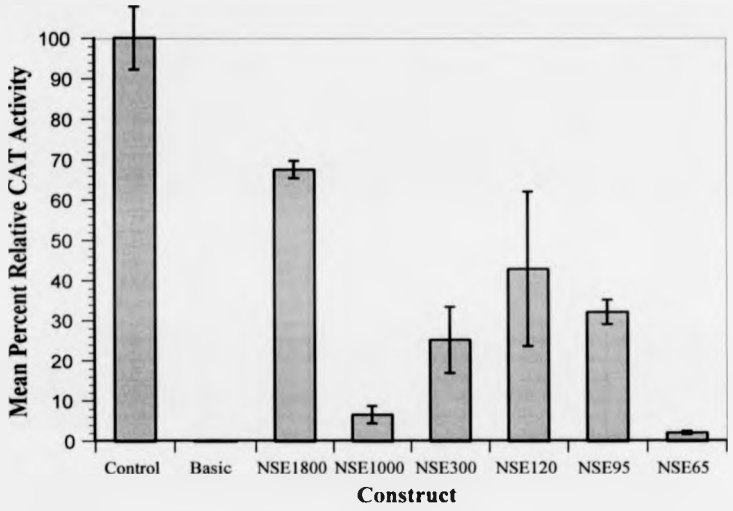

Figure 6.26: Table and histogram showing data from the second transfection of NB4-1A3 cells with the full series of *NSE-cat* deletion constructs. Abbreviations used in table headings: CAT - CAT (chloramphenicol acetyltransferase) activity; GAL - β-galactosidase activity; MEC - Molar Equivalence Constant; ACA - Actual CAT Activity, xACA - mean Actual CAT Activity of control constructs; RCA - Relative CAT Activity; xRCA - mean Relative CAT Activity; semRCA - standard error of the mean Relative CAT Activity. A brief explanation of these terms can be found in Figure 6.1, a fuller explanation in section 5.5. The histogram shows mean Relative CAT Activities for each construct with error bars representing standard errors.

Construct	RCA1	RCA2	xRCA12	semRCA12
Control	94.01	114.68	100.00	5.06
	89.79	87.99		
	116.20	97.33		
Basic	0.06	0.17	0.00	0.05
	-0.14	-0.16		
	0.08	0.00		
NSE1800	24.36	71.23	51.33	7.67
	38.96	63.79		
	42.35	67.28		
NSE1000	7.97	8.44	5.98	1.13
	4.69	2.12		
	3.90	8.73		
NSE300	30.04	35.08	26.19	3.78
	24.84	31.37		
	27.06	8.73		
NSE120	15.03	20.05	33.18	9.85
	32.05	27.16		
	23.84	80.96		
NSE95	12.33	35.08	24.67	3.74
	20.71	35.10		
	18.92	25.88		
NSE65	2.32	1.50	1.86	0.22
	1.51	1.61		
	1.45	2.75		

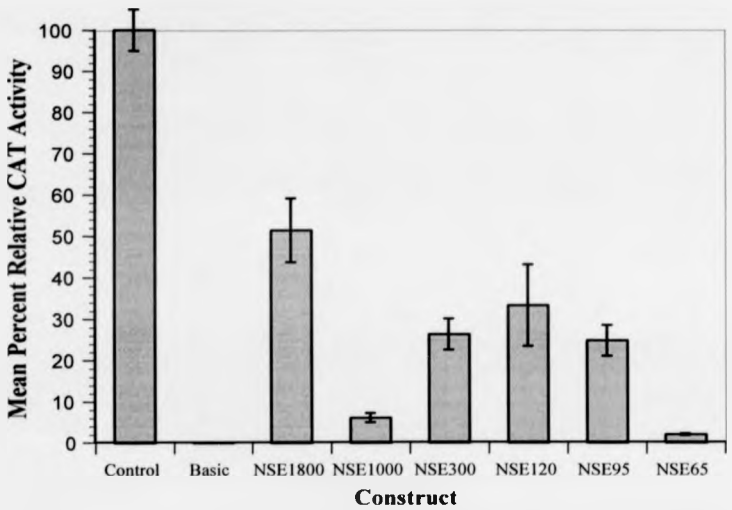

Figure 6.27: Table and histogram showing combined data from the transfection of NB4-1A3 cells with the full series of *NSE-cat* deletion constructs. Abbreviations used in the table: RCA1 and RCA2 - Relative CAT Activities from the two individual experiments (as shown in Figures 6.24 and 6.25); xRCA12 - combined mean Relative CAT Activity for each construct over two experiments (six transfections); semRCA12 - standard error of the combined mean Relative CAT Activities. A brief explanation of these terms can be found in Figure 6.1, a fuller explanation in section 5.5. The histogram shows combined mean relative CAT activity for each construct and illustrates the trend in reporter gene activity for reporter constructs containing stepwise deletions of the rat NSE 5' flanking region. Error bars represent standard errors of the combined mean Relative CAT Activities.

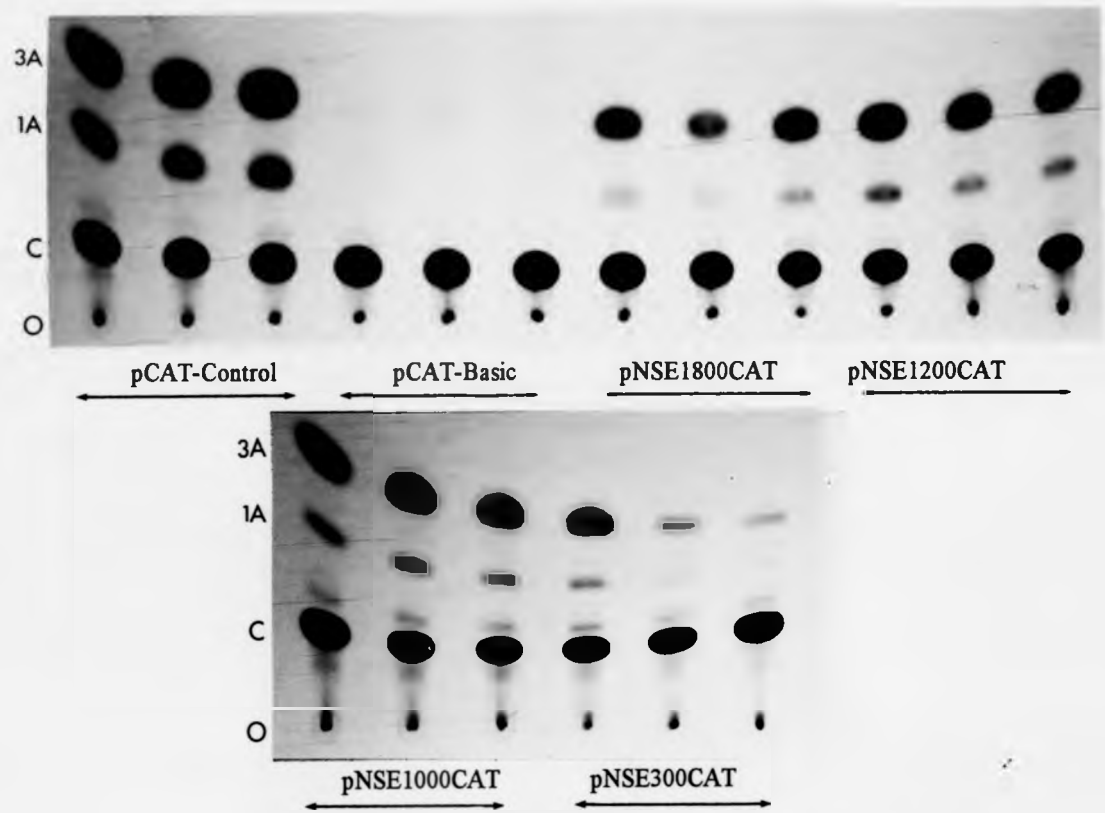

Figure 6.11: Representative CAT assay from the U-138 MG series of transfections with the initial set of *NSE-cat* constructs. Each construct was transfected in triplicate and the lanes on the TLC plate were grouped accordingly. The assay above corresponds to the experiment described in Figure 6.8. Abbreviations: O = origin; C = chloramphenicol; 1A = 1-acetylchloramphenicol; 3A = 3-acetyl-chloramphenicol

Construct	CAT	GAL	MEC	ACA	xACA	RCA	xRCA	semRCA
Control	561772	252	1.30	1714.81	2008.10	85.02	100.00	11.36
	333623	105		2444.12		122.28		
	293421	121		1865.36		92.71		
Basic	9034	187	1.41	34.26	50.70	-0.84	0.00	0.72
	12342	111		78.86		1.44		
	10992	200		38.98		-0.60		
NSE1800	41094	101	1.00	406.87		18.20	8.58	4.81
	25729	211		121.94		3.64		
	22453	177		126.85		3.89		
NSE1000	10111	99	1.13	90.38		2.03	2.08	0.71
	31788	243		115.77		3.32		
	11343	148		67.82		0.87		
NSE300	21999	100	1.30	169.22		6.06	3.25	1.54
	13783	162		65.45		0.75		
	18712	133		108.22		2.94		
NSE120	14982	132	1.34	84.70		1.74	1.38	0.36
	16231	143		84.70		1.74		
	21866	256		63.74		0.67		
NSE95	9632	98	1.35	72.80		1.13	1.52	0.26
	15101	124		90.21		2.02		
	15243	144		78.41		1.42		
NSE65	9220	142	1.35	48.10		-0.13	-0.05	0.12
	10501	143		54.40		0.19		
	14101	223		46.84		-0.20		

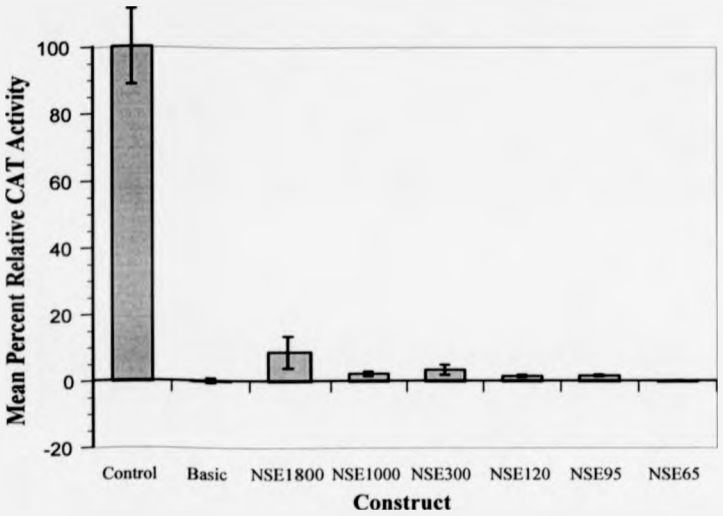

Figure 6.30: Table and histogram showing data from the second transfection of HeLa cells with the full series of *NSE-cat* deletion constructs. Abbreviations used in table headings: CAT - CAT (chloramphenicol acetyltransferase) activity; GAL - β-galactosidase activity; MEC - Molar Equivalence Constant; ACA - Actual CAT Activity, xACA - mean Actual CAT Activity of control constructs; RCA - Relative CAT Activity; xRCA - mean Relative CAT Activity; semRCA - standard error of the mean Relative CAT Activity. A brief explanation of these terms can be found in Figure 6.1, a fuller explanation in section 5.5. The histogram shows mean Relative CAT Activities for each construct with error bars representing standard errors.

Construct	CAT	GAL	MEC	ACA	xACA	RCA	xRCA	semRCA
Control	1125395	299	1.30	2895.28	2867.25	100.99	100.00	8.63
	1332592	313		3274.99		114.43		
	948277	300		2431.48		84.58		
Basic	17184	266	1.41	45.82	42.06	0.13	0.00	0.26
	20834	281		52.58		0.37		
	11237	287		27.77		-0.51		
NSE1800	94721	325	1.00	291.45		8.83	9.34	0.78
	82278	297		277.03		8.32		
	47121	135		349.04		10.87		
NSE1000	37128	131	1.13	250.81		7.39	7.84	0.40
	46555	144		286.10		8.64		
	42194	147		254.01		7.50		
NSE300	52568	167	1.30	242.14		7.08	6.77	0.81
	49144	141		268.11		8.00		
	25199	102		190.04		5.24		
NSE120	23771	150	1.34	118.26		2.70	2.97	0.16
	20067	112		133.71		3.24		
	25671	152		126.04		2.97		
NSE95	10503	105	1.35	74.10		1.13	1.75	0.32
	16005	113		104.92		2.22		
	13571	105		95.74		1.90		
NSE65	8031	165	1.35	36.05		-0.21	0.92	0.73
	12455	149		61.92		0.70		
	13923	97		106.32		2.27		

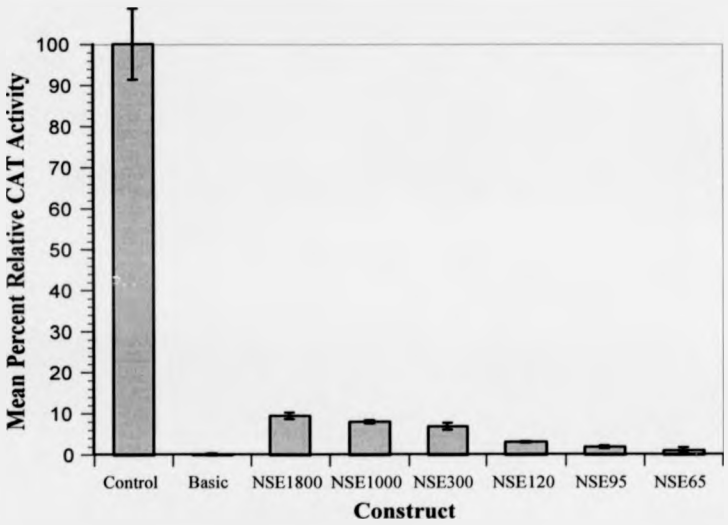

Figure 6.31: Table and histogram showing data from the third transfection of HeLa cells with the full series of *NSE-cat* deletion constructs. Abbreviations used in table headings: CAT - CAT (chloramphenicol acetyltransferase) activity; GAL - β-galactosidase activity; MEC - Molar Equivalence Constant; ACA - Actual CAT Activity, xACA - mean Actual CAT Activity of control constructs; RCA - Relative CAT Activity; xRCA - mean Relative CAT Activity; semRCA - standard error of the mean Relative CAT Activity. A brief explanation of these terms can be found in Figure 6.1, a fuller explanation in section 5.5. The histogram shows mean Relative CAT Activities for each construct with error bars representing standard errors.

Construct	RCA1	RCA2	RCA3	xRCA123	semRCA123
Control	122.50	92.71	100.99	100.00	5.25
	88.18	85.02	114.43		
	89.32	122.28	84.58		
Basic	-0.63	-0.84	0.13	0.00	0.25
	0.77	1.44	0.37		
	-0.13	-0.60	-0.51		
NSE1800	6.24	18.20	8.83	7.96	1.50
	6.50	3.64	8.32		
	5.12	3.89	10.87		
NSE1000	2.76	2.03	7.39	4.38	0.94
	4.79	3.32	8.64		
	2.15	0.87	7.50		
NSE300	2.71	6.06	7.08	4.83	0.79
	4.20	0.75	8.00		
	6.47	2.94	5.24		
NSE120	2.62	1.74	2.70	2.33	0.31
	1.73	1.74	3.24		
	3.58	0.67	2.97		
NSE95	1.90	1.13	1.13	1.54	0.16
	1.16	2.02	2.22		
	0.99	1.42	1.90		
NSE65	0.56	-0.13	-0.21	0.54	0.26
	0.59	0.19	0.70		
	1.06	-0.20	2.27		

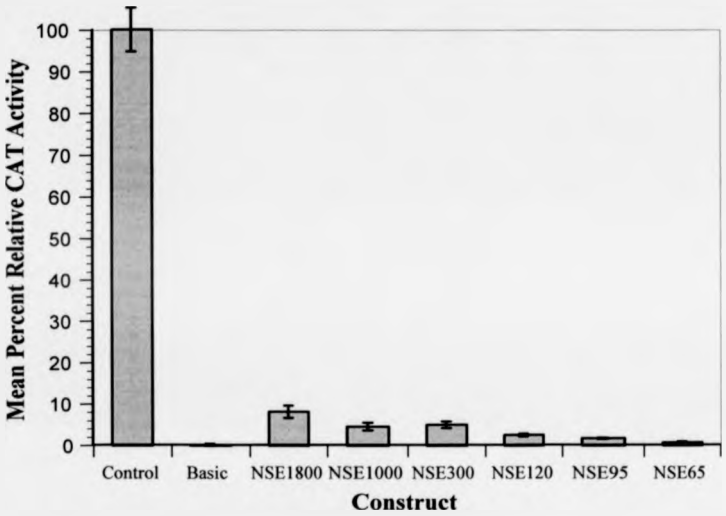

Figure 6.32: Table and histogram showing combined data from the transfection of HeLa cells with the full series of *NSE-cat* deletion constructs. Abbreviations used in the table: RCA1, RCA2, RCA3 - Relative CAT Activities from the three individual experiments (as shown in Figures 6.28-6.30); xRCA123 - combined mean Relative CAT Activity for each construct over three experiments (nine transfections); semRCA123 - standard error of the combined mean Relative CAT Activities. A brief explanation of these terms can be found in Figure 6.1, a fuller explanation in section 5.5. The histogram shows combined mean relative CAT activity for each construct and illustrates the trend in reporter gene activity for reporter constructs containing stepwise deletions of the rat NSE 5' flanking region. Error bars represent standard errors of the combined mean Relative CAT Activities.

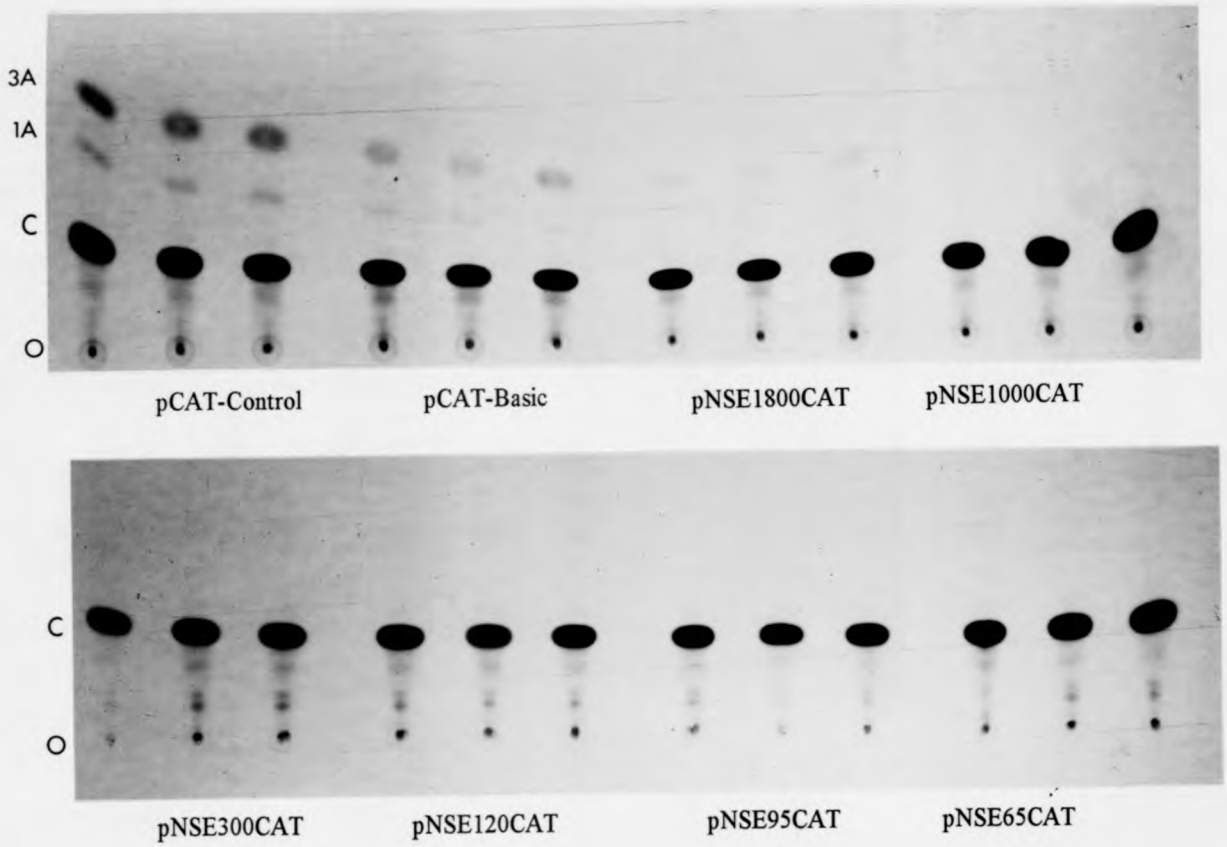

Figure 6.33: Representative CAT assay from the HeLa series of transfections with the full set of *NSE-cat* constructs. Each construct was transfected in triplicate and the lanes on the TLC plate were grouped accordingly. The assay above corresponds to the experiment described in Figure 6.30. Abbreviations: O = origin; C = chloramphenicol; 1A = 1-acetyl- chloramphenicol; 3A = 3-acetylchloramphenicol.

6.4.5 Conclusions from the full series of transfections

Transfection studies using the full series of *NSE-cat* constructs have provided a wealth of information concerning the cell type-specific regulation of *NSE*. In the first instance, the Ltk- cell line transfections have shown that the method used to introduce DNA into the cells has little effect upon the performance of the constructs. Initially, this conclusion might appear insignificant, as one would expect that a given construct would behave in the same manner once inside a cell regardless of its strategy for gaining access. However, due to the preferences of different cells, a number of alternative transfection strategies were utilised in this study, and it would be naïve to directly compare the results from two cell lines transfected by different methods without controlling for the effect of transfection technique. The most suitable control would be to find a cell line which could be transfected by all the available procedures and compare the results obtained by each method. The Ltk- cell line has fulfilled this role in the present study.

Analysis of the highly truncated constructs in Ltk- cells showed that deletion from position -255 (the upstream boundary of pNSE300CAT) to position -120 (the upstream boundary of pNSE120CAT) resulted in a two-to-threefold increase in reporter activity. This suggested the presence of a negative regulatory element between -255 and -120 bp upstream of the first intron. Further deletion to position -95 resulted in a drop in reporter activity to a level approximately 1.5-fold that of the longer constructs. Finally, deletion to position -65 resulted in a sharp fall in reporter activity to a level comparable with the negative control construct, pCAT-Basic. These results suggested that 95 bp of regulatory information upstream of the transcriptional start site was sufficient for basal expression of *NSE* whilst removal of a further 30 bp resulted in a complete loss of expression. It is interesting to note that the upstream boundary of pNSE65CAT lies one nucleotide *down*stream of the putative TATA-like box of the *NSE* gene, indicating that this element is essential for gene expression. It is unclear whether the observed increase in reporter activity, when comparing pNSE120CAT to pNSE300CAT is significant: it has already been discussed that the level of *NSE-cat* construct expression in Ltk- cells is greater than would be expected from analysis of endogenous gene expression. It is therefore not inconceivable that the observed upregulation, clear as it is from the transfection studies, could play only a minor role, if at all, in nonneuronal cells *in vivo*. Whether significant or not, studies in neuronal cells were required to show whether this upregulation was cell type-specific or constitutive in nature. In Neuro-2A cells, the long constructs showed a pattern of activity similar

to that shown by the U-138 MG cells. Analysis of the shorter constructs identified a similar increase in reporter activity upon reduction from 255 bp to 120 bp of 5' flanking sequence, although in this cell line, the original level of activity was much higher relative to pCAT-Control. Once again, further deletion to position -95 resulted in a fall in reporter activity, but not quite to the level demonstrated by the longer constructs, and deletion to position -65 resulted in reduction of reporter gene activity to background levels. These results suggested that a negative control element was indeed located between positions -255 and -120 relative to the transcriptional start, and that it was active in both neuronal and nonneuronal cells. Although the difference in the levels of reporter activity between pNSE300CAT and pNSE120CAT was approximately twofold in Neuro-2A cells, it ranged from threefold to fivefold in the Ltk- cells, suggesting a preference for the nonneuronal cell line. It is possible that a negative regulatory factor could be present in both neuronal and nonneuronal cells, but more abundantly or preferentially active in the latter. Also, the fact that neuroblastoma cells are derived from an early stage in the pathway of neuronal differentiation suggests that they might contain such a factor in greater quantities compared to mature neuronal cells.

Further analysis in other permissive and nonpermissive cells, however, failed to identify a similar phenomenon. In both NB4-1A3 neuroblastoma cells and HeLa cells, reduction of the *NSE* regulatory region from position -255 to position -120 had no significant stimulatory effect upon reporter gene expression. In NB4-1A3 cells, the levels of reporter gene expression were generally much lower than those in Neuro-2A cells. This might have reflected differences in the state of neuronal maturation each cell line was able to attain in culture as discussed in Chapter 9. In agreement with this, the levels of reporter activity in NB4-1A3 cells transfected with the full length construct pNSE1800CAT reached only 50% of the levels found in Neuro-2A cells. One surprising finding from the NB4-1A3 cell transfections was the sharp drop in reporter activity (to 10% of the pNSE1800 value) when the *NSE* promoter was reduced to 1 kbp in length. This was followed by a rise (to approximately 50% of the pNSE1800 value) when the promoter was truncated further to 255 bp. These data suggest that a strong, positive-acting element, located between 1800 and 1000 bp upstream of the transcriptional start, was removed to generate the levels of reporter activity observed in NB4-1A3 cells transfected with pNSE1000CAT. Further truncation sponsored a levelling of reporter expression, perhaps indicating that negative elements, located between 1000 and 255 bp upstream of the transcriptional start, were removed. It is unclear why this effect should be restricted to NB4-1A3 cells. Similarly, the upregulation observed in Ltk-

Construct	RCA1	RCA2	RCA3	xRCA123	semRCA123
Control	82.81	95.00	139.68	100.00	6.93
	98.12	100.41	94.12		
	119.07	104.59	66.20		
Basic	0.32	1.70	0.56	0.00	0.31
	0.27	-1.07	0.58		
	-0.59	-0.63	-1.14		
NSE1800	13.79	13.46	11.54	13.13	1.19
	12.18	19.20	7.85		
	18.15	10.97	11.07		
NSE1200	11.57	16.67	9.33	13.28	1.43
	10.46	17.68	20.79		
	11.86	13.43	7.75		
NSE1000	12.47	16.13	16.42	12.74	0.95
	13.93	12.09	9.35		
	10.65	14.99	8.59		
NSE300	16.49	25.51	20.50	20.47	1.09
	23.67	20.65	17.25		
	23.68	19.41	17.03		

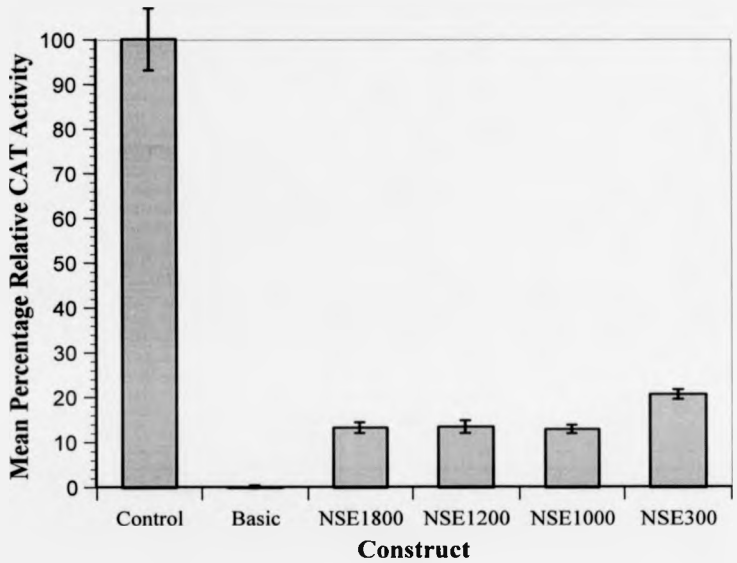

Figure 6.5: Table and histogram showing combined data from the transfection of Ltk- cells with the initial series of *NSE-cat* deletion constructs. Abbreviations used in the table: RCA1, RCA2, RCA3 - Relative CAT Activities from the three individual experiments (as shown in Figures 6.2-6.4); xRCA123 - combined mean Relative CAT Activity for each construct over three experiments (nine transfections); semRCA123 - standard error of the combined mean Relative CAT Activities. A brief explanation of these terms can be found in Figure 6.1, a fuller explanation in section 5.5. The histogram shows combined mean relative CAT activity for each construct and illustrates the trend in reporter gene activity for reporter constructs containing stepwise deletions of the rat NSE 5' flanking region. Error bars represent standard errors of the combined mean Relative CAT Activities.

cells, when the fragment of regulatory information lying between positions -255 and -120 relative to the transcriptional srart site was removed, was not observed in HeLa cells. Generally, the observed level of reporter expression in HeLa cells was lower, construct for construct, than that in Ltk- cells. If anything, the trend in HeLa cells is reduced expression as the 5' flanking region is progressively deleted.

It is clear from this series of transfections that information concerning the regulation of *NSE* is located throughout the 5' flanking sequence, although that located downstream from position -65 is insufficient alone to promote transcription. The varying behaviour of the reporter constructs in different cell lines with similar properties may reflect different mechanisms of neuronal gene expression *in vivo*. As discussed in Chapter 1, neurons isolated from different parts of the nervous system and from different developmental stages vary considerably in the amount of *NSE* gene products they express. Although no clear-cut mechanism of neuron-specific gene expression has emerged from this study, several regions of the 5' flanking sequence have been observed to influence the expression of a reporter gene. Experiments designed to investigate the nature of such fragments further are described in Chapter 8.

6.5 *NSE* gene regulation during *ex vivo* neuronal differentiation

As discussed above, the dissection of regulatory elements in cell lines maintained under constant and normal growth conditions can reveal the position of constitutive and cell type-specific *cis*-acting motifs. A more challenging application of the deletion-transfection approach, however, is to investigate the molecular basis of inductive responses. Where an endogenous gene responds to a given agent, and the mechanism of that response lies in the flanking regions of the gene, transfection of cells with reporter constructs containing various deletions in the flanking region can identify elements responsible for the inductive effect as variants with deletions covering the region involved will not respond to the inducing agent in the appropriate manner. If specific inductive responses can be tested, e.g. by introducing novel *trans*-acting factors into the system, the binding sites of such factors might be revealed. For example, such an approach was used by Dawson *et al.* (1994) to identify the site at which Oct-2 bound to the tyrosine hydroxylase promoter. Otherwise, more general responses can be studied, such as neuronal differentiation induced by retinoic acid or NGF. Such processes are known to involve complex signalling pathways and the switching of batteries of genes encoding transcriptional regulators and other neuronal proteins (see Barde, 1991), however, at the level of the *NSE* gene, there is likely to be a point where this hierarchy of unfolding events stops, and a region of the promoter which mediates the observed upregulation may be found. The molecular basis of neuronal differentiation is still poorly understood in mammals, although the recent identification of mammalian homologues of *Drosophila* proneural and neurogenic genes (e.g. *Mash1*, *Prox1*), other genes known to influence the determination of neuronal phenotype (e.g. *NeuroD*), and still other genes encoding transcription factors which are expressed at the right time and place (e.g. *Sox2*, *Sox11*) has allowed some advance in our knowledge of neuronal differentiation *in vivo* (see Chapter 2). Retinoic acid-mediated neuronal differentiation was investigated in P19 EC cells as these cells provide a unique opportunity for studying the process of differentiation from nonneuronal, *NSE*-nonpermissive stem cells through to *NSE*-permissive, differentiated neurons in an *ex vivo* environment. Although both NGF-treated and untreated PC12 cells were found to express similar levels of *NSE* mRNA and NSE protein, there was a slight induction following NGF treatment accompanying neurite outgrowth and exit from the cell cycle. The regulation of *NSE* gene expression was also investigated in these cells.

Construct	CAT	GAL	MEC	ACA	xACA	RCA	xRCA	semRCA
Control	227426	157	1.3	1114.29	1171.49	95.00	100.00	2.77
	220177	144		1176.16		100.41		
	241870	152		1224.04		104.59		
Basic	6547	101	1.41	45.97	26.48	1.70	0.00	0.86
	2090	104		14.25		-1.07		
	4661	172		19.22		-0.63		
NSE1800	24198	134	1.00	180.58		13.46	14.54	2.44
	30056	122		246.36		19.20		
	24636	162		152.07		10.97		
NSE1200	34988	145	1.11	217.38		16.67	15.93	1.28
	45226	178		228.90		17.68		
	38620	193		180.27		13.43		
NSE1000	27441	115	1.13	211.17		16.13	14.41	1.20
	31129	167		164.96		12.09		
	36725	164		198.17		14.99		
NSE300	51768	125	1.30	318.57		25.51	20.38	1.86
	35199	103		262.88		20.65		
	47211	146		248.74		19.41		

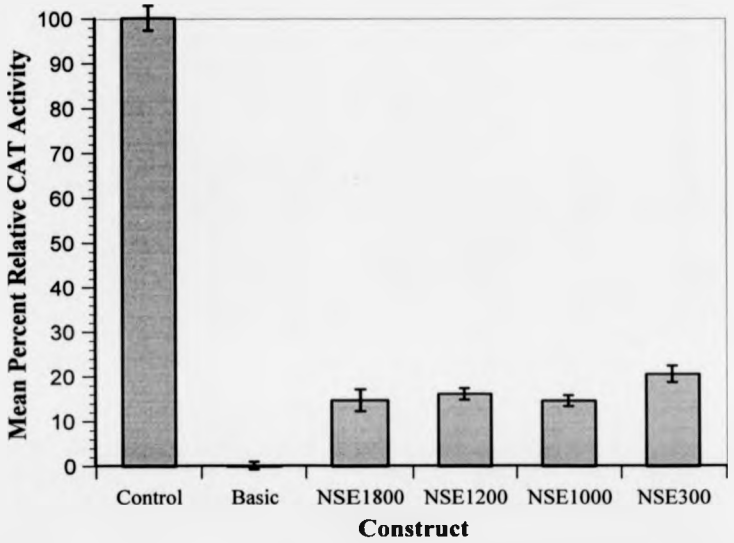

Figure 6.3: Table and histogram showing data from the second transfection of Ltk- cells with the initial series of *NSE-cat* deletion constructs. Abbreviations used in table headings: CAT - CAT (chlor-amphenicol acetyltransferase) activity; GAL - β-galactosidase activity; MEC - Molar Equivalence Constant; ACA - Actual CAT Activity, xACA - mean Actual CAT Activity of control constructs; RCA - Relative CAT Activity; xRCA - mean Relative CAT Activity; semRCA - standard error of the mean Relative CAT Activity. A brief explanation of these terms can be found in Figure 6.1, a fuller explanation in section 5.5. The histogram shows mean Relative CAT Activities for each construct with error bars representing standard errors.

6.5.1 Transfection of PC12 cells

As discussed in section 1.5.3, the rat PC12 cell line represents an excellent *ex vivo* model of neuronal differentiation. Upon exposure to low doses of NGF, PC12 cells undergo a dramatic change of morphology, spreading out, developing neurites and eventually forming synaptic associations (Green and Tischler, 1976). Concomitant with this shift towards a neuronal phenotype, is the reported induction of *NSE* gene expression (Vinores *et al.*, 1981) although in the present study, only a moderate elevation of gene expression was observed following treatment (see section 5.2.8). To investigate the molecular basis of NGF-mediated induction of *NSE*, undifferentiated and differentiated PC12 cells were transfected with the full series of *NSE-cat* constructs and the results were compared.

6.5.1.1 Transfection of undifferentiated PC12 cells

Under the conditions described in section 5.4.2.2, PC12 cells were transfected with the full series of *NSE-cat* constructs and control vectors using LipofectAMINE. Data from individual experiments are presented in Figures 6.34 and 6.35 followed by combined results in Figure 6.36. A representative CAT assay is shown in Figure 6.37. The results showed that, like other neuronal cell types, PC12 cells transfected with pNSE1800CAT demonstrated high levels of reporter activity, approximately equal to the activity of the positive control construct pCAT-Control. In the first transfection experiment (Figures 6.34 and 6.37), one dish of cells transfected with this construct gave an unusually low level of CAT activity, generating a Relative CAT activity of 32%. Compared to the other five values, which lie in the range 90-120%, this individual result can be regarded as aberrant and probably nonrepresentative. The mean Relative CAT activity of 85% is therefore probably underestimated. Reduction of the *NSE* 5' flanking region to 1 kbp and further to 255 bp appeared to cause an approximate 50% drop in reporter activity. The error range in transfections involving these two constructs suggested that there was no significant difference between them. Further reduction of the regulatory sequence to 120 bp resulted in a five- to sixfold reduction in CAT activity, suggesting that one or more *cis*-acting elements located in the 130 bp region between the upstream boundaries of pNSE300CAT and pNSE120CAT were responsible for elevated transcriptional activity of the gene in PC12 cells. It was interesting to note that experiments with Ltk- cells, described earlier in the chapter, also indicated the importance of this region of the promoter. As observed in

Construct	CAT	GAL	MEC	ACA	xACA	RCA	xRCA	semRCA
Control	234271	149	1.30	1209.45	1447.55	82.81	100.00	10.51
	253171	137		1421.51		98.12		
	284824	128		1711.68		119.07		
Basic	11864	126	1.41	66.78	62.41	0.32	0.00	0.29
	9699	104		66.14		0.27		
	10030	131		54.30		-0.59		
NSE1800	23827	94	1.00	253.48		13.79	14.71	1.78
	25416	110		231.05		12.18		
	31698	101		313.84		18.15		
NSE1200	42504	172	1.11	222.63		11.57	11.29	0.43
	39340	171		207.26		10.46		
	36480	145		226.65		11.86		
NSE1000	38307	144	1.13	235.16		12.47	12.35	0.95
	27120	94		255.32		13.93		
	27984	118		209.87		10.65		
NSE300	44617	118	1.30	290.85		16.49	21.28	2.39
	40077	79		390.23		23.67		
	41106	81		390.37		23.68		

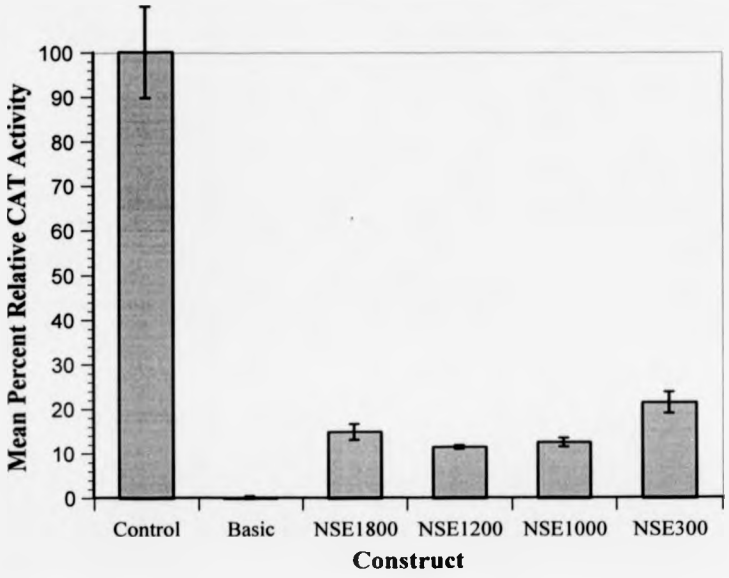

Figure 6.2: Table and histogram showing data from the first transfection of Ltk- cells with the initial series of *NSE-cat* deletion constructs. Abbreviations used in table headings: CAT - CAT (chloramphenicol acetyltransferase) activity; GAL - β-galactosidase activity; MEC - Molar Equivalence Constant; ACA - Actual CAT Activity, xACA - mean Actual CAT Activity of control constructs; RCA - Relative CAT Activity; xRCA - mean Relative CAT Activity; semRCA - standard error of the mean Relative CAT Activity. A brief explanation of these terms can be found in Figure 6.1, a fuller explanation in section 5.5. The histogram shows mean Relative CAT Activities for each construct with error bars representing standard errors.

Construct	RCA1	RCA2	xRCA12	semRCA12
Control	110.49	97.05	100.00	14.34
	148.50	90.98		
	41.01	111.97		
Basic	-0.07	-0.12	0.00	0.08
	-0.05	-0.22		
	0.12	0.33		
NSE1800	121.44	94.19	91.14	12.46
	101.93	103.58		
	32.33	93.36		
NSE1000	49.73	70.55	53.40	7.29
	24.23	55.23		
	73.34	47.34		
NSE300	29.10	54.33	55.59	12.49
	113.87	56.26		
	33.18	46.81		
NSE120	5.12	7.00	9.05	1.30
	11.24	14.08		
	8.20	8.63		
NSE95	3.25	5.78	5.76	0.68
	5.59	8.42		
	5.32	6.18		
NSE65	-0.57	-0.05	-0.31	0.11
	-0.56	-0.13		
	-0.52	0.00		

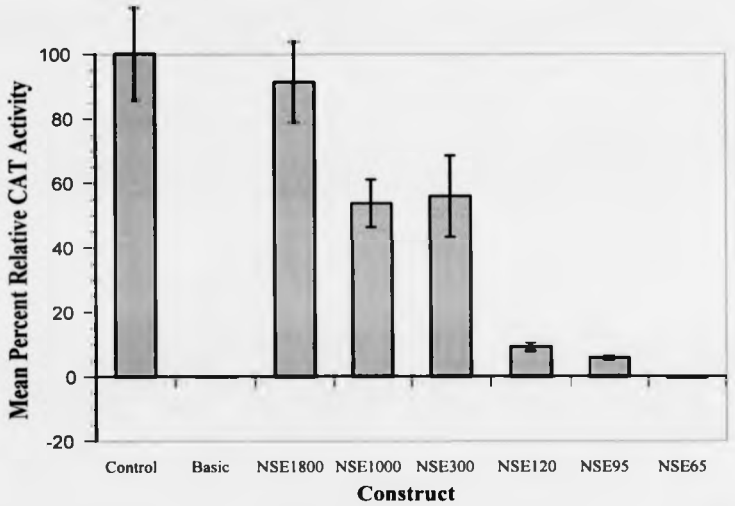

Figure 6.36: Table and histogram showing combined data from the transfection of undifferentiated PC12 cells with the full series of *NSE-cat* deletion constructs. Abbreviations used in the table: RCA1 and RCA2 - Relative CAT Activities from the two individual experiments (as shown in Figures 6.34 and 6.35); xRCA12 - combined mean Relative CAT Activity for each construct over two experiments (six transfections); semRCA12 - standard error of the combined mean Relative CAT Activities. A brief explanation of these terms can be found in Figure 6.1, a fuller explanation in section 5.5. The histogram shows combined mean relative CAT activity for each construct and illustrates the trend in reporter gene activity for reporter constructs containing stepwise deletions of the rat *NSE* 5' flanking region. Error bars represent standard errors of the combined mean Relative CAT Activities.

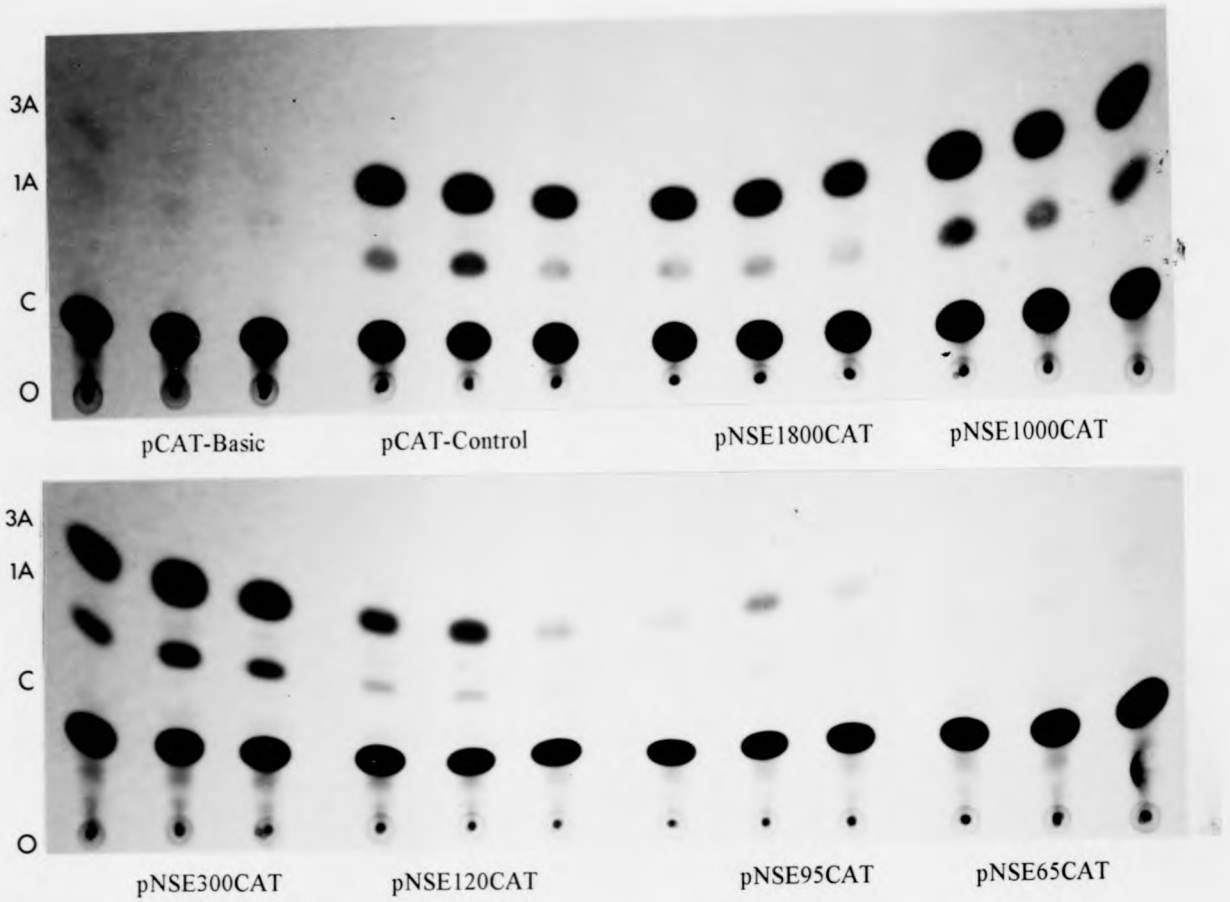

Figure 6.37: Representative CAT assay from the undifferentiated PC12 cells series of transfections with the full set of *NSE-cat* constructs. Each construct was transfected in triplicate and the lanes of the TLC plate were grouped accordingly. The assay shown above corresponds to the experiment shown in Figure 6.34. Abbreviations: O = origin; C = chloramphenicol; 1A = 1-acetyl-chloramphenicol; 3A = 3-acetylchloramphenicol.

6.5.1.2 Transfection of NGF-treated PC12 cells

Following differentiation under the influence of NGF as described in section 4.2.3, PC12 cells were transfected with the full series of *NSE-cat* constructs to determine the effects of NGF-induction. Data from individual experiments are presented in Figures 6.38 and 6.39, followed by combined results in Figure 6.40. A representative CAT assay is shown in Figure 6.41. It was immediately noticeable that neuronal differentiation caused a dramatic reduction in the efficiency of transfection. Whereas, in the case of the untreated cells, β-galactosidase activity was measured after two hours, a minimum assay time of six hours was required for the NGF-treated cells. It was thought that several factors contributed to this reduction in transfection efficiency. Firstly, the number of cells growing in each dish at the time of transfection was approximately half that observed for undifferentiated cells; secondly, whereas the untreated cells became confluent prior to harvesting, the treated cells did not proliferate; and thirdly, the PC12 neurons were probably more resistant to DNA uptake than the stem cells, as has been observed by other investigators (Kingston *et al.*, 1990) . The results obtained from NGF treated cells were similar to those obtained with untreated cells in that reduction of the regulatory sequence to 120 bp caused a dramatic reduction in reporter gene expression. All constructs containing more than 255 bp of regulatory information were expressed at levels similar to or above those of the positive control vector pCAT-Control. The major difference between untreated and treated PC12 cells therefore appeared to be the maintenance of high level reporter expression in cells transfected with pNSE1000CAT and pNSE300CAT. In the untreated cells, these constructs were expressed at approximately one half the level of the longest construct, pNSE1800CAT, whereas in the treated cells, all three of these constructs were expressed within a range 95-140% of the positive control vector pCAT-Control. Truncation to 120 bp of regulatory information reduced reporter expression to less than 5% of the positive control value, underscoring the evidence from untreated cells suggesting the presence of a critical enhancer element in the region between 255 and 120 bp upstream of the *NSE* gene transcriptional start site. In common with the undifferentiated cells and other cell lines, the most truncated construct was expressed at only background levels.

Construct	CAT	GAL	MEC	ACA	xACA	RCA	xRCA	semRCA
Control	18466	163	1.30	87.14	98.53	88.03	100.00	9.64
	26845	177		116.67		119.07		
	18134	152		91.77		92.90		
Basic	477	123	1.41	2.75	3.41	-0.69	0.00	0.75
	N/A	77		N/A		N/A		
	883	154		4.07		0.69		
NSE1800	18344	153	1.00	119.90		122.46	119.45	7.05
	18278	144		126.93		129.86		
	16992	163		104.25		106.01		
NSE1000	12574	122	1.13	91.21		92.31	95.17	13.22
	13744	104		116.95		119.37		
	11815	142		73.63		73.83		
NSE300	19231	101	1.30	146.47		150.40	138.01	6.40
	20673	121		131.42		134.58		
	16237	99		126.16		129.05		
NSE120	1099	155	1.34	5.29		1.98	4.30	1.48
	1254	132		7.09		3.87		
	1776	131		10.12		7.05		
NSE95	833	152	1.35	4.06		0.68	1.51	0.99
	916	105		6.46		3.21		
	827	183		3.35		-0.06		
NSE65	371	155	1.35	1.77		-1.72	-1.63	0.06
	427	172		1.84		-1.65		
	511	193		1.96		-1.52		

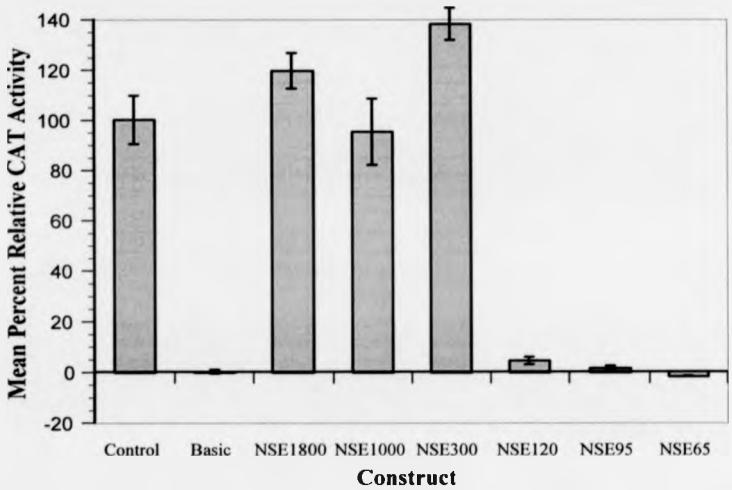

Figure 6.38: Table and histogram showing data from the first transfection of NGF-treated PC12 (Sheffield) cells with the full series of *NSE-cat* deletion constructs. Transfection was carried out using LipofectAMINE. Abbreviations used in table headings: CAT - CAT (chloramphenicol acetyltransferase) activity; GAL - β-galactosidase activity; MEC - Molar Equivalence Constant; ACA - Actual CAT Activity, xACA - mean Actual CAT Activity of control constructs; RCA - Relative CAT Activity; xRCA - mean Relative CAT Activity; semRCA - standard error of the mean Relative CAT Activity. A brief explanation of these terms can be found in Figure 6.1, a fuller explanation in section 5.5. The histogram shows mean Relative CAT Activities for each construct with error bars representing standard errors.

5.5 Processing data from cotransfection experiments

The general strategy for cotransfection experiments was described in section 4.2.5. The validity of conclusions drawn from such experiments, *vis-a-vis* the relative activity of various stepwise deletion mutants of the rat *NSE* 5' flanking region, relied very much on the manner in which the raw data were analysed, as discussed below.

5.5.1 Correcting and normalising the primary data

There were two sources of primary data arising from each transfection, *viz* the CAT activity, determined by phosphorimaging the acetylated chloramphenicol bands from the TLC plates, and the β-galactosidase activity, determined by a colourimetric assay. As discussed in section 4.2.5, all cells, including those transfected with the CAT control plasmids, were cotransfected with the same amount of pSV-β-Galactosidase in order to normalise CAT activities for transfection efficiency. It was also necessary to consider the molar amounts of each CAT plasmid introduced into the cells. This was because transfections were optimised according to the total *mass* of DNA in the transfection mix, with the consequence that less transcriptional start sites were available for cells transfected with the larger constructs compared to those transfected with smaller constructs. To take this factor into account, a dimensionless constant was calculated for each construct, which was termed the molar equivalence constant (MEC). MECs were determined by dividing the size (in nucleotides) of the largest construct (pNSE1800CAT) by the sizes of each of the other constructs as shown in Table 5.1.

Construct	CAT	GAL	MEC	ACA	xACA	RCA	xRCA	semRCA
Control	22533	112	1.30	154.76	176.52	87.25	100.00	6.82
	35912	142		194.54		110.55		
	42183	180		180.27		102.19		
Basic	823	147	1.41	3.97	5.82	-1.08	0.00	1.18
	226	151		1.06		0.00		
	1103	102		7.67		1.08		
NSE1800	48956	178		275.03		157.71	114.02	22.66
	23884	132		180.94		102.59		
	14101	97		145.37		81.75		
NSE1000	44231	146	1.13	268.10		153.65	99.34	27.16
	16394	114		127.26		71.14		
	17298	117		130.84		73.24		
NSE300	1546	87	1.30	13.67		4.60	20.74	15.48
	1677	81		15.93		5.92		
	12105	99		94.06		51.69		
NSE120	6193	177	1.34	26.11		11.89	16.70	3.88
	7222	183		29.45		13.84		
	11947	188		47.42		24.37		
NSE95	9231	172	1.35	39.75		19.88	18.99	1.13
	10074	184		40.56		20.35		
	8453	182		34.40		16.74		
NSE65	1104	172	1.35	4.75		-0.62	-0.75	0.18
	822	154		3.95		-1.09		
	746	112		4.93		-0.52		

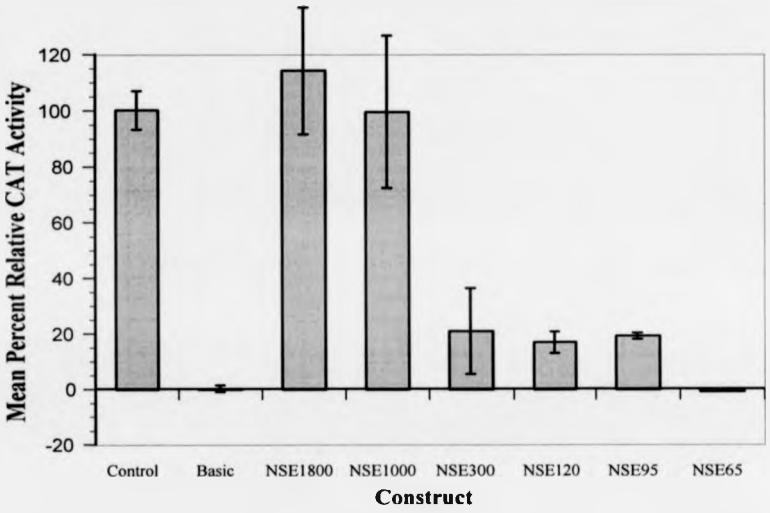

Figure 6.39: Table and histogram showing data from the second transfection of NGF-treated PC12 (Sheffield) cells with the full series of *NSE-cat* deletion constructs. Transfection was carried out using LipofectAMINE. Abbreviations used in table headings: CAT - CAT (chloramphenicol acetyltransferase) activity; GAL - β-galactosidase activity; MEC - Molar Equivalence Constant; ACA - Actual CAT Activity, xACA - mean Actual CAT Activity of control constructs; RCA - Relative CAT Activity; xRCA - mean Relative CAT Activity; semRCA - standard error of the mean Relative CAT Activity. A brief explanation of these terms can be found in Figure 6.1, a fuller explanation in section 5.5. The histogram shows mean Relative CAT Activities for each construct with error bars representing standard errors.

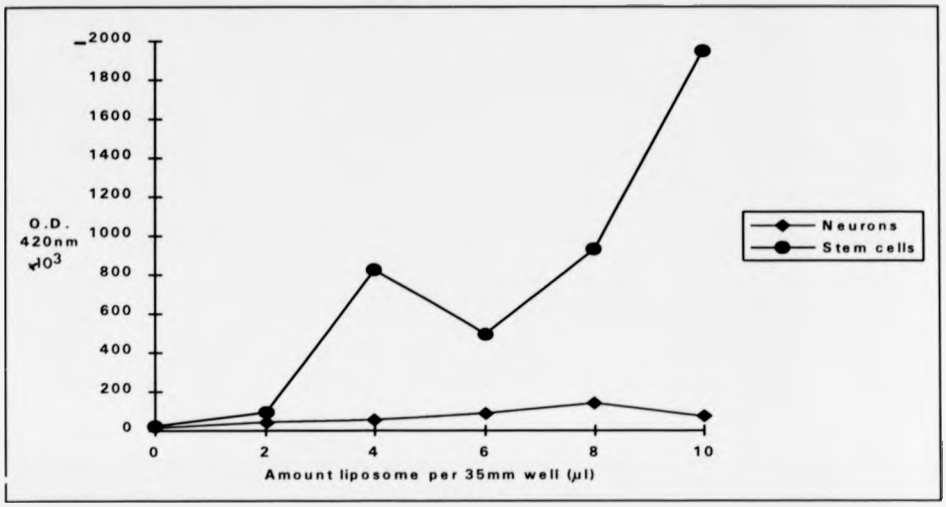

Figure 5.33: Optimisation of LipofectAMINE-mediated transfection of P19 stem cells and neurons by varying the amount of liposome. Other parameters: cells transfected at confluence of 80% (stem cells) or 60-70% (neurons), duration of transfection 5 hour, 2µg DNA per 35mm dish. Negative controls were transfected without LipofectAMINE, other conditions remaining constant (shown at position 0 on x-axis). Note that because both experiments were carried out in parallel, the highest OD readings for stem cells are outside the linear range of the assay, reflecting the relatively long assay time (6 hours) required to detect β-galactosidase activity in the transfected neurons.

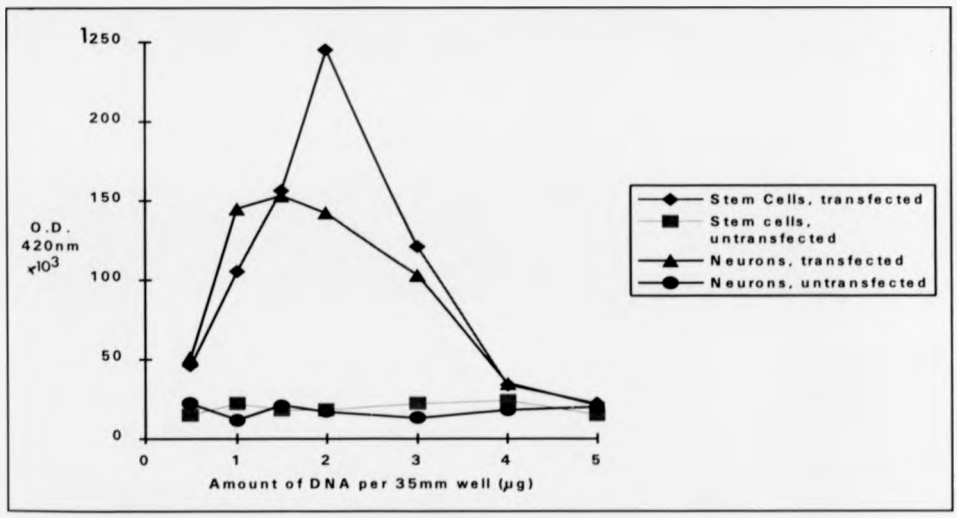

Figure 5.34: Optimisation of LipofectAMINE-mediated transfection of P19 stem cells and neurons by varying the amount of DNA. Other parameters: cells transfected at confluence of 80% (stem cells) or 60-70% (neurons), duration of transfection 5 hours, amount of LipofectAMINE per 35mm dish 10µl (stem cells) or 8µl (neurons). Untransfected cells were exposed to the same experimental conditions as the transfected cells with no LipofectAMINE in the transfection mixture. Assay time for stem cells was 2 hours, for neurons was 6 hours.

5.4.6 Transfection of HeLa cells using calcium phosphate

HeLa cells were transfected using the BBS calcium phosphate protocol optimised for the U-138 MG and U-373 MG lines as described in section 5.4.3. The transfection efficiency, using identical parameters, was found to be high and no attempt at further optimisation was made.

5.4.7 Optimisation of liposome-mediated transfection of P19 EC cells

It has been reported that P19 EC cells transfect with only minimal efficiency using calcium phosphate (Rudnicki and McBurney, 1987). The calcium phosphate approach was therefore forsaken and LipofectAMINE was used. Transfections were optimised according to manufacturers' recommendations starting with the following parameters: transfections were carried out at 80% confluence (stem cells) or 60-70% confluence (neurons). A lower density of neurons was used because high density plating has been reported to reduce neurite outgrowth (Green *et al.*, 1987), which might have unpredictable effects on the expression of *NSE*. In each case, the duration of transfection was 5 hours, and 2μg of DNA was used per 35mm well. The amount of LipofectAMINE was varied from 0 to 10μl per 35mm well. Cells were collected 48hrs posttransfection and higher transfection efficiency was evident in the stem cells compared to the neurons, probably reflecting cell proliferation (P19 stem cells proliferate voraciously) rather than ability to take up DNA. It was found that 10μl LipofectAMINE per 35mm well was optimal for the stem cells whilst 8μl was optimal for the neurons. These results are shown in Figure 5.33. The amount of DNA used per transfection was then optimised, using the LipofectAMINE reagent at its optimal dose. Keeping the other parameters unchanged, the amount of DNA was varied between 0.5 and 3 μg per 35mm well and it was found that 2μg per well was the optimal dose for P19 cells whereas P19 neurons demonstrated very similar transfection efficiencies over a broader range of DNA concentrations, with an optimal dose of 1.5μg per transfection. These results are shown in Figure 5.34.

6.5.2 Transfection of P19 EC cells

As discussed in section 5.2.7, the murine P19 EC cell line is a prime candidate for the study of *ex vivo* neuronal differentiation (Rudnicki and McBurney, 1987). Upon exposure to low doses of retinoic acid under conditions where attachment to a substrate is not possible, P19 stem cells form dense cell aggregates. When these are dispersed into medium without retinoic acid , the cells differentiate into large numbers of neurons and other neural cell types, the latter of which can be selectively destroyed by inhibitors of the cell cycle (Rudnicki and McBurney, 1987). Concomitant with this shift towards a neuronal phenotype is the induction of *NSE* gene expression (see section 5.2.7), making this cell line a good candidate for the study of *NSE* gene regulation during neuronal differentiation. To investigate the molecular basis of this process, undifferentiated and differentiated P19 EC cells were transfected with the full series of *NSE-cat* constructs and the results were compared.

6.5.2.1 Transfection of P19 stem cells

P19 stem cells were transfected under the conditions described in section 5.4.7 with the full series of *NSE-cat* constructs and controls. Data from individual experiments are shown in Figures 6.42 and 6.43, followed by combined results in Figure 6.44. A representative CAT assay is shown in Figure 6.45. P19 EC cells are proliferative cells which were found to take up pSV-β-galactosidase plasmid DNA with ease (see Figure 5.34). It was therefore surprising and disappointing to find that, unlike the pilot experiments described in section 5.4.7, the cotransfection experiments were marred by poor transfection efficiency. Moreover, construct pNSE95CAT appeared to be unaffected by the problems which dogged the transfections with other constructs, and transfection efficiencies up to fivefold greater that those found with other constructs were observed. It was thought at first that the origin of this problem was contamination of the plasmid DNA stocks. However, inoculation of sterile medium with each plasmid DNA failed to demonstrate bacterial or fungal contamination and the same plasmid stocks were used for the subsequent transfection of other cell lines without similar problems. Local contamination of the cell cultures was also discounted as an explanation: the morphology of all the parallel cultures was similar both pretransfection and posttransfection, and all the cultures appeared to proliferate in a similar fashion, becoming confluent approximately 36 hours posttransfection; subculturing posttransfection cells into fresh medium also failed to reveal contamination by

5.4.4 Optimisation of transfection of Neuro-2A cells

Neuro-2A cells were found to be refractory to DEAE-dextran mediated transfection although the same optimisation protocol was followed as for Ltk- cells and the other cell types. Calcium phosphate-mediated transfection was therefore attempted, using the same parameters optimised for the U-138 MG and U-373 MG cells and it was found that these conditions yielded very high transfection efficiencies. The cells were tested with a range of DNA concentrations, but the initial parameters were found to be ideal (Figure 5.30).

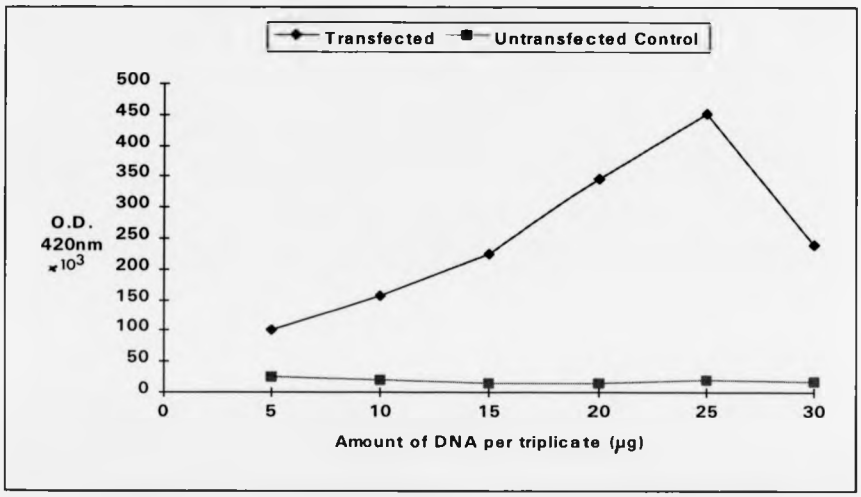

Figure 5.30: Optimisation of calcium phosphate-mediated transfection of Neuro-2A cells by varying the amount of DNA: Other parameters: cells transfected at 70% confluence, duration of transfection 18 hours, BBS at pH 6.95. Untransfected cells were exposed to the same experimental conditions as the transfected cells with the exception that no $CaCl_2$ was included in the transfection mixture.

Construct	CAT	GAL	MEC	ACA	xACA	RCA	xRCA	semRCA
Control	21468	79	1.30	209.04	179.07	117.04	100.00	11.03
	17113	71		185.41		103.60		
	25612	138		142.76		79.35		
Basic	1005	161	1.41	4.43	3.25	0.67	0.00	0.45
	994	198		3.56		0.18		
	492	199		1.75		-0.85		
NSE1800	1492	161	1.00	9.27		3.42	6.02	1.77
	1505	121		12.44		5.23		
	1799	91		19.77		9.40		
NSE1000	1376	134	1.13	9.09		3.32	2.87	0.77
	1522	133		10.13		3.91		
	1154	181		5.64		1.36		
NSE300	1338	186	1.30	5.53		1.30	1.21	0.66
	1277	298		3.30		0.03		
	1592	168		7.29		2.30		
NSE120	2315	215	1.34	8.04		2.72	3.58	0.95
	2519	146		12.88		5.48		
	1972	191		7.70		2.54		
NSE95	8616	245	1.35	26.05		12.97	7.89	2.56
	7219	460		11.62		4.76		
	7732	419		13.67		5.93		
NSE65	843	261	1.35	2.39		-0.49	0.02	0.26
	1065	223		3.54		0.17		
	909	171		3.94		0.39		

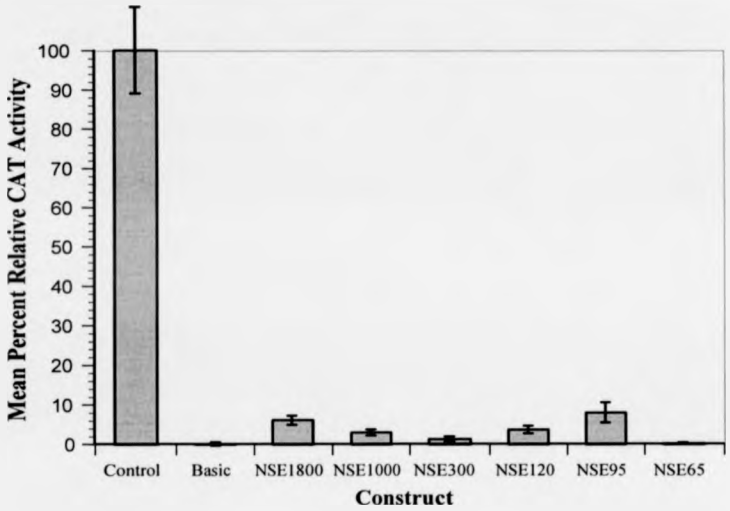

Figure 6.42: Table and histogram showing data from the first transfection of undifferentiated P19 EC cells with the full series of *NSE-cat* deletion constructs. Transfection was carried out using LipofectAMINE. Abbreviations used in table headings: CAT - CAT (chloramphenicol acetyltransferase) activity; GAL - β-galactosidase activity; MEC - Molar Equivalence Constant; ACA - Actual CAT Activity, xACA - mean Actual CAT Activity of control constructs; RCA - Relative CAT Activity; xRCA - mean Relative CAT Activity; semRCA - standard error of the mean Relative CAT Activity. A brief explanation of these terms can be found in Figure 6.1, a fuller explanation in section 5.5. The histogram shows mean Relative CAT Activities for each construct with error bars representing standard errors.

Construct	CAT	GAL	MEC	ACA	xACA	RCA	xRCA	semRCA
Control	18254	106	1.30	132.47	127.63	103.90	100.00	3.86
	19101	111		132.37		103.82		
	15192	99		118.04		92.28		
Basic	476	106	1.41	3.18	3.55	-0.30	0.00	0.47
	722	109		4.70		0.92		
	512	131		2.77		-0.63		
NSE1800	1011	124	1.00	8.15		3.71	4.63	0.79
	1182	105		11.26		6.21		
	993	117		8.49		3.98		
NSE1000	1182	98	1.13	10.67		5.74	3.38	1.18
	883	126		6.20		2.14		
	994	138		6.37		2.28		
NSE300	956	115	1.30	6.39		2.29	3.39	0.57
	1073	94		8.78		4.21		
	1042	99		8.10		3.66		
NSE120	991	106	1.34	6.98		2.76	2.22	0.36
	958	131		5.46		1.54		
	893	103		6.47		2.35		
NSE95	1091	225	1.35	3.59		0.03	-0.54	0.29
	986	301		2.43		-0.91		
	846	237		2.64		-0.73		
NSE65	891	107	1.35	6.17		2.11	2.60	0.33
	1052	103		7.57		3.24		
	1130	127		6.59		2.45		

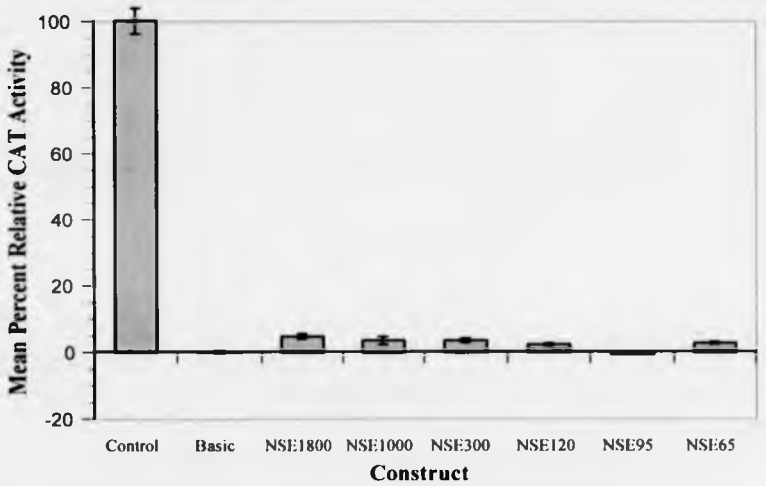

Figure 6.43: Table and histogram showing data from the second transfection of undifferentiated P19 EC cells with the full series of *NSE-cat* deletion constructs. Transfection was carried out using LipofectAMINE. Abbreviations used in table headings: CAT - CAT (chloramphenicol acetyltransferase) activity; GAL - β-galactosidase activity; MEC - Molar Equivalence Constant; ACA - Actual CAT Activity, xACA - mean Actual CAT Activity of control constructs; RCA - Relative CAT Activity; xRCA - mean Relative CAT Activity; semRCA - standard error of the mean Relative CAT Activity. A brief explanation of these terms can be found in Figure 6.1, a fuller explanation in section 5.5. The histogram shows mean Relative CAT Activities for each construct with error bars representing standard errors.

Construct	RCA1	RCA2	xRCA12	semRCA12
Control	117.04	103.90	100.00	5.22
	103.60	103.82		
	79.35	92.28		
Basic	0.67	-0.30	0.00	0.29
	0.18	0.92		
	-0.85	-0.63		
NSE1800	3.42	3.71	5.33	0.92
	5.23	6.21		
	9.40	3.98		
NSE1000	3.32	5.74	3.13	0.64
	3.91	2.14		
	1.36	2.28		
NSE300	1.30	2.29	2.30	0.62
	0.03	4.21		
	2.30	3.66		
NSE120	2.72	2.76	2.90	0.55
	5.48	1.54		
	2.54	2.35		
NSE95	12.97	0.03	3.68	2.21
	4.76	-0.91		
	5.93	-0.73		
NSE65	-0.49	2.11	1.31	0.61
	0.17	3.24		
	0.39	2.45		

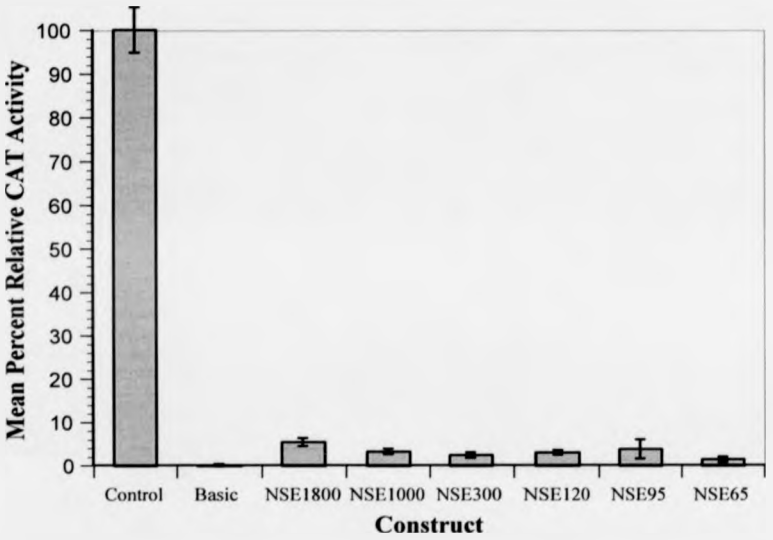

Figure 6.44: Table and histogram showing combined data from the transfection of undifferentiated P19 EC cells with the full series of *NSE-cat* deletion constructs. Abbreviations used in the table: RCA1 and RCA2 - Relative CAT Activities from the two individual experiments (as shown in Figures 6.42 and 6.43); xRCA12 - combined mean Relative CAT Activity for each construct over two experiments (six transfections); semRCA12 - standard error of the combined mean Relative CAT Activities. A brief explanation of these terms can be found in Figure 6.1, a fuller explanation in section 5.5. The histogram shows combined mean relative CAT activity for each construct and illustrates the trend in reporter gene activity for reporter constructs containing stepwise deletions of the rat *NSE* 5' flanking region. Error bars represent standard errors of the combined mean Relative CAT Activities.

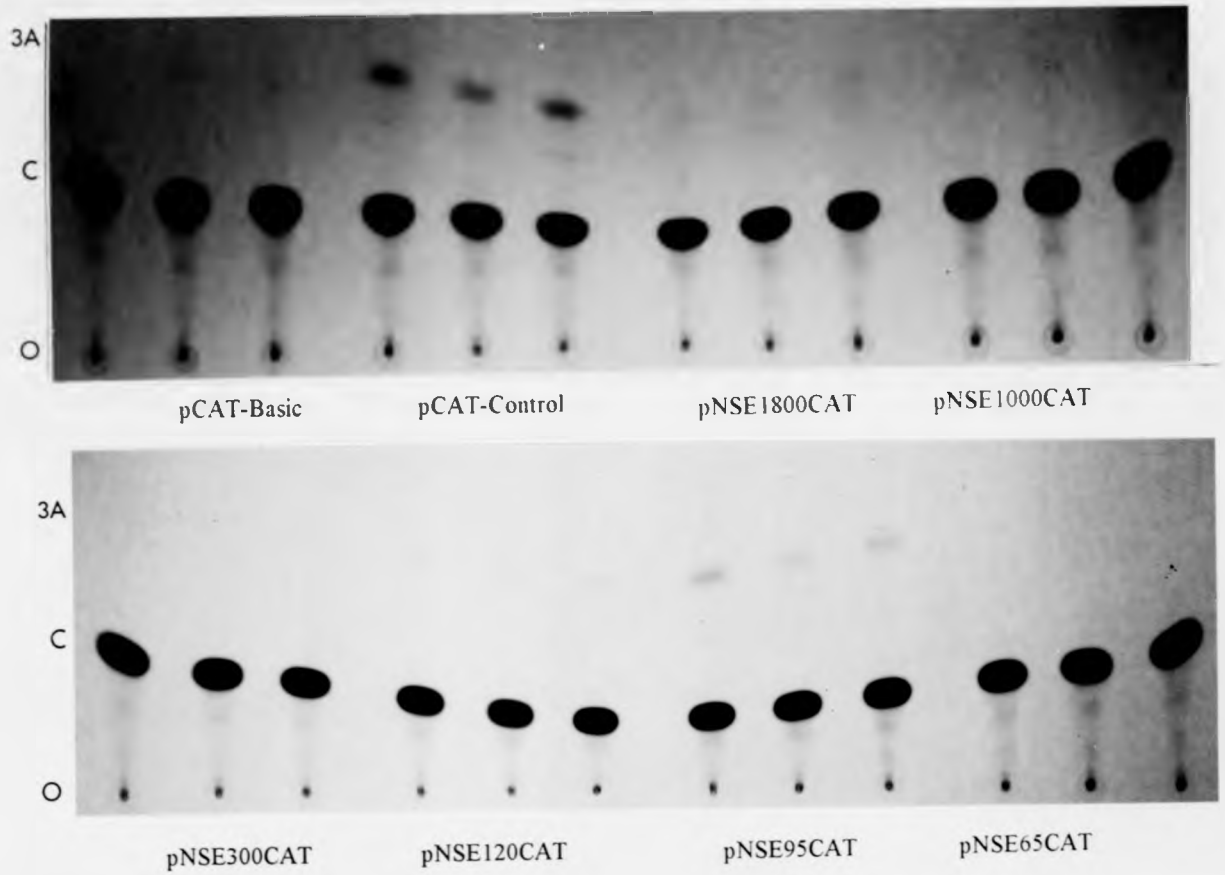

Figure 6.45: Representative CAT assay from the undifferentiated P19 EC cells series of transfections with the full set of *NSE-cat* constructs. Each construct was transfected in triplicate and the lanes of the TLC plate were grouped accordingly. The assay shown above corresponds to the experiment shown in Figure 6.42. Abbreviations: O = origin; C = chloramphenicol; 1A = 1-acetylchloramphenicol; 3A = 3-acetylchloramphenicol.

6.5.2.2 Transfection of P19 neurons

P19 neurons were transfected under the conditions described in section 5.4.7 with the full series of *NSE-cat* constructs and controls. Individual experiments are shown in Figures 6.46 and 6.47, followed by combined results in Figure 6.48. A representative CAT assay is shown in Figure 6.49. The transfection efficiency of neurons was variable, and this probably reflected differences in the number and distribution of transfection-competent cells per dish. Cells were seeded as small aggregates because monodispersed cells grew and attached poorly whilst large aggregates tended to yield densely crowded cells which produced few neurites and transfected poorly. The small aggregates were prepared by disruption of large aggregates (after four days in retinoic acid-supplemented medium) by gentle repeated passage through a 10ml pipette. The number of transfection-competent neurons per dish depended upon how these aggregates were dispersed. If too many aggregates were seeded, or where several aggregates attached close together, the neurons became crowded together and were difficult to transfect. If too few aggregates were seeded, the neurons were widely spaced and produced long processes which formed synaptic associations within a few days, but the number of cells was too low to yield results within the linear range of the soluble β-galactosidase assay. The trick was to seed enough aggregates for adequate numbers of cells but not too many to produce overcrowding, usually 10-20 per 3.5cm well, however, regional variations in the separation of aggregates resulted in variable transfection efficiency between parallel cultures. Normalised transfection results showed that neurons transfected with most of the *NSE-cat* constructs expressed relatively high levels of CAT. In the first experiment, all constructs from pNSE1800CAT through to pNSE95CAT showed mean Relative CAT Activities of approximately 100%; a lower level of activity was observed for pNSE1800CAT-transfected cells, but the transfection efficiencies for this triplicate were outside the linear range of the soluble β-galactosidase assay and the normalised CAT activities were likely to be underestimated. In the second experiment, the longer constructs demonstrated approximately twice the relative CAT activities of the corresponding constructs in the first experiment, although the *trend* in reporter activity was similar, indicating perhaps that the control transfections were not comparable. Accordingly, the standard error of the mean for pCAT-Control transfections in the first experiment was above the maximum permitted 15% of the mean value. For transfections with pNSE95CAT, there appeared to be a twofold reduction in reporter activity (compared to the longer construct pNSE120CAT) only in the second experiment, whilst no significant reduction in reporter expression was

observed in the first experiment. One of the pNSE95CAT Relative CAT Activities in the second experiment was 111% whilst the other two were approximately 50%. It is possible that these values were nonrepresentative and the standard error with respect to this transfection was approximately 25% of the mean, indicating that a nonrepresentative datum was found in this field. The levels of reporter activity from pNSE65CAT, which were at background levels in most cell lines, were uncharacteristically high in the first transfection of neuronal cells (approximately 5% of the control value) but not in the second transfection (approximately 0.2% of the control value).

Construct	CAT	GAL	MEC	ACA	xACA	RCA	xRCA	semRCA
Control	145231	775	1.30	144.15	211.64	67.18	100.00	17.72
	210655	602		269.17		127.97		
	192732	669		221.61		104.84		
Basic	3991	363	1.41	7.80	5.98	0.88	0.00	0.63
	2011	411		3.47		-1.22		
	2814	299		6.67		0.34		
NSE1800	15652	89	1.00	175.87		82.60	70.96	7.19
	8994	72		124.92		57.83		
	14101	91		154.96		72.44		
NSE1000	35741	117	1.13	270.34		128.54	113.97	7.34
	26372	105		222.27		105.17		
	30991	120		228.55		108.22		
NSE300	28873	106	1.30	209.53		98.97	93.80	3.57
	29461	112		202.34		95.48		
	30032	125		184.81		86.95		
NSE120	57823	205	1.34	210.50		99.44	111.37	8.80
	54992	183		224.26		106.13		
	46729	129		270.33		128.53		
NSE95	33250	104	1.35	236.82		112.24	103.17	5.91
	35712	119		222.30		105.18		
	34811	132		195.35		92.08		
NSE65	5285	193	1.35	20.28		6.95	5.48	1.43
	4769	176		20.07		6.85		
	4316	281		11.38		2.62		

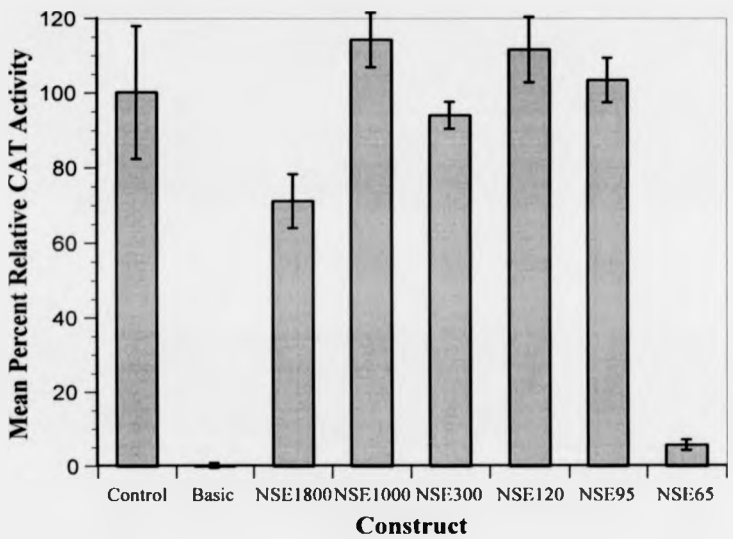

Figure 6.46: Table and histogram showing data from the first transfection of P19 neurons with the full series of *NSE-cat* deletion constructs. Transfection was carried out using LipofectAMINE. Abbreviations used in table headings: CAT - CAT (chloramphenicol acetyltransferase) activity; GAL - β-galactosidase activity; MEC - Molar Equivalence Constant; ACA - Actual CAT Activity, xACA - mean Actual CAT Activity of control constructs; RCA - Relative CAT Activity; xRCA - mean Relative CAT Activity; semRCA - standard error of the mean Relative CAT Activity. A brief explanation of these terms can be found in Figure 6.1, a fuller explanation in section 5.5. The histogram shows mean Relative CAT Activities for each construct with error bars representing standard errors.

Construct	CAT	GAL	MEC	ACA	xACA	RCA	xRCA	semRCA
Control	71699	299	1.30	184.46	202.16	90.61	100.00	5.07
	73456	276		204.73		101.36		
	62144	220		217.29		108.02		
Basic	4176	187	1.41	15.84	13.58	1.20	0.00	0.63
	4279	233		13.02		-0.29		
	5036	301		11.87		-0.91		
NSE1800	83169	136	1.00	611.54		317.08	239.01	39.32
	64194	171		375.40		191.87		
	60082	148		405.96		208.07		
NSE1000	91224	157	1.13	514.20		265.47	218.43	37.86
	86437	160		478.08		246.32		
	62950	196		284.22		143.52		
NSE300	71456	113	1.30	486.43		250.74	212.72	28.48
	51922	129		309.61		156.98		
	60007	103		448.15		230.44		
NSE120	55974	121	1.34	345.22		175.86	148.35	33.36
	51097	104		366.65		187.23		
	22306	99		168.14		81.96		
NSE95	38913	129	1.35	223.45		111.29	75.71	17.91
	16452	105		116.06		54.35		
	27111	155		129.56		61.50		
NSE65	5077	202	1.35	18.62		2.67	0.19	1.24
	2065	132		11.59		-1.05		
	2259	144		11.62		-1.04		

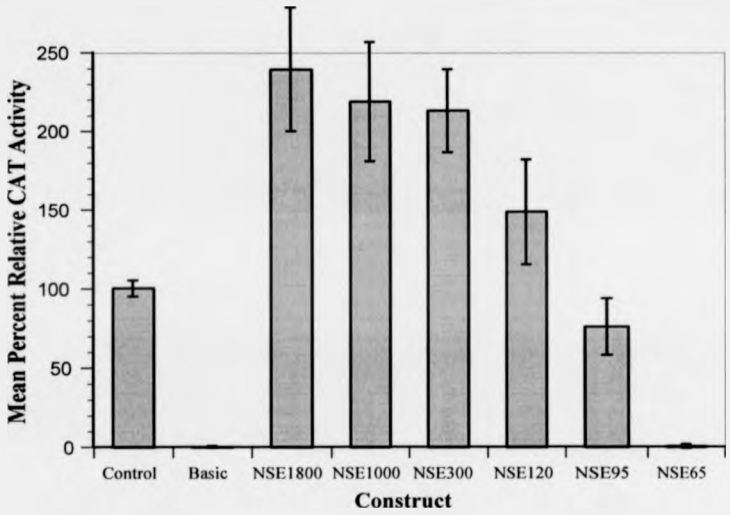

Figure 6.47: Table and histogram showing data from the second transfection of P19 neurons with the full series of *NSE-cat* deletion constructs. Transfection was carried out using LipofectAMINE. Abbreviations used in table headings: CAT - CAT (chloramphenicol acetyltransferase) activity; GAL - β-galactosidase activity; MEC - Molar Equivalence Constant; ACA - Actual CAT Activity, xACA - mean Actual CAT Activity of control constructs; RCA - Relative CAT Activity; xRCA - mean Relative CAT Activity; semRCA - standard error of the mean Relative CAT Activity. A brief explanation of these terms can be found in Figure 6.1, a fuller explanation in section 5.5. The histogram shows mean Relative CAT Activities for each construct with error bars representing standard errors.

Construct	RCA1	RCA2	xRCA12	semRCA12
Control	67.18	90.61	100.00	8.24
	127.97	101.36		
	104.84	108.02		
Basic	0.88	1.20	0.00	0.40
	-1.22	-0.29		
	0.34	-0.91		
NSE1800	82.60	317.08	154.98	41.60
	57.83	191.87		
	72.44	208.07		
NSE1000	128.54	265.47	166.21	29.03
	105.17	246.32		
	108.22	143.52		
NSE300	98.97	250.74	153.26	29.52
	95.48	156.98		
	86.95	230.44		
NSE120	99.44	175.86	129.86	17.50
	106.13	187.23		
	128.53	81.96		
NSE95	112.24	111.29	89.44	10.43
	105.18	54.35		
	92.08	61.50		
NSE65	6.95	2.67	2.83	1.45
	6.85	-1.05		
	2.62	-1.04		

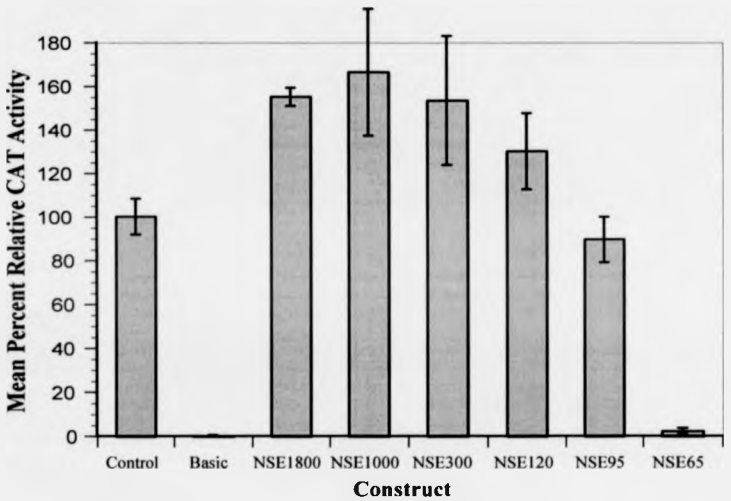

Figure 6.48: Table and histogram showing combined data from the transfection of P19 neurons with the full series of *NSE-cat* deletion constructs. Abbreviations used in the table: RCA1 and RCA2 - Relative CAT Activities from the two individual experiments (as shown in Figures 6.46 and 6.47); xRCA12 - combined mean Relative CAT Activity for each construct over two experiments (six transfections); semRCA12 - standard error of the combined mean Relative CAT Activities. A brief explanation of these terms can be found in Figure 6.1, a fuller explanation in section 5.5. The histogram shows combined mean relative CAT activity for each construct and illustrates the trend in reporter gene activity for reporter constructs containing stepwise deletions of the rat *NSE* 5' flanking region. Error bars represent standard errors of the combined mean Relative CAT Activities.

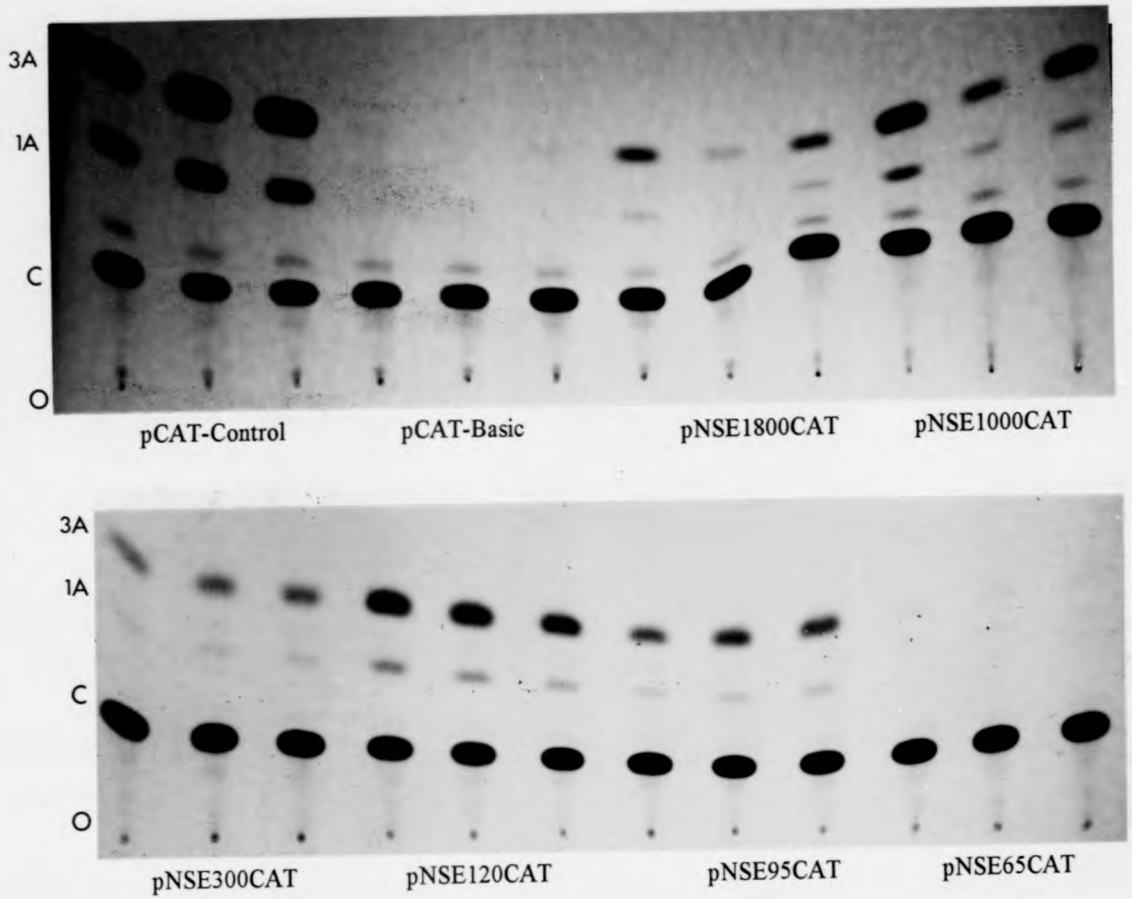

Figure 6.49: Representative CAT assay from the differentiated P19 neurons series of transfections with the full set of *NSE-cat* constructs. Each construct was transfected in triplicate and the lanes of the TLC plate were grouped accordingly. The assay shown above corresponds to the experiment shown in Figure 6.46. Abbreviations: O = origin; C = chloramphenicol; 1A = 1-acetyl-chloramphenicol; 3A = 3-acetylchloramphenicol.

5.4 Optimisation of transfection parameters

5.4.1 Optimisation of transfection of Ltk- cells

5.4.1.1 Optimisation of transfection of Ltk- cells using DEAE-dextran

DEAE-dextran-mediated transfection of Ltk- cells was attempted before any other method because a detailed protocol optimised for this cell line had been published (Selden, 1987). The published method recommended the use of 4μg DNA per 100mm dish with 200μg ml^{-1} DEAE-dextran in 12ml OptiMEM serum-reduced medium. To adjust this method for 35mm dishes, the concentrations were kept constant but the total volumes were reduced eightfold to account for the difference in area (and thus cell number) between the two types of dish. For the first experiment, therefore, 0.5μg DNA was used in a total volume of 1.5ml OptiMEM with 200μg ml^{-1} DEAE-dextran. As recommended, proliferating cells were transfected at 50% confluence and the duration of the transfection was 4 hours, followed by a 2 minute DMSO shock. It was found, however, that this treatment was extremely toxic and that the morphology of the cells changed from flat and fibroblastoid to thin and spindly by 12 hours posttransfection. Extensive cell death occurred in the next 24 hours and by 48 hours posttransfection, there were no attached cells remaining to be harvested.

The toxicity of DEAE-dextran mediated transfection is known to be both dose- and time-dependant. Experience has shown that transfections carried out using this method should be either of short duration with high doses of the reagent or of long duration with lower doses (Sambrooke *et al.*, 1989). Attempts were made to optimise transfection parameters by trying a range of very short transfection times, but keeping the other conditions constant. The results of this experiment are shown in Figure 5.20.

pNSE95CAT was generated by digestion with *Sma* I (which cleaves within the insert) and *Hin*d III (which cleaves in the polylinker). The *Hin*d III site was then blunted by end-filling and the vector reclosed. Finally, pNSE65CAT was generated by complete digestion with *Hin*d III followed by partial digestion with *Nar* I. The latter enzyme cuts once within the *NSE* 5' flanking region, but also between the SV40 large T region and the Amp^r gene of pCAT-Basic. The partial digestion was followed by gel isolation of the correct sized fragment (4.4 kbp), blunting by end-filling and reclosing of the vector. The *Nar* I site lies just downstream of the TATA box, just 1bp upstream of the most 5' transcriptional start site - this fragment thus probably lacks the basal promoter of the *NSE* gene.

5.3.4 Verification of constructs

The first generation of constructs, pNSE1800CAT, pNSE1200CAT, pNSE1000CAT, pNSE300CAT were verified by restriction mapping (data not shown). The more truncated constructs, pNSE120CAT, pNSE95CAT and pNSE65CAT were verified by restriction mapping and sequencing (data not shown).

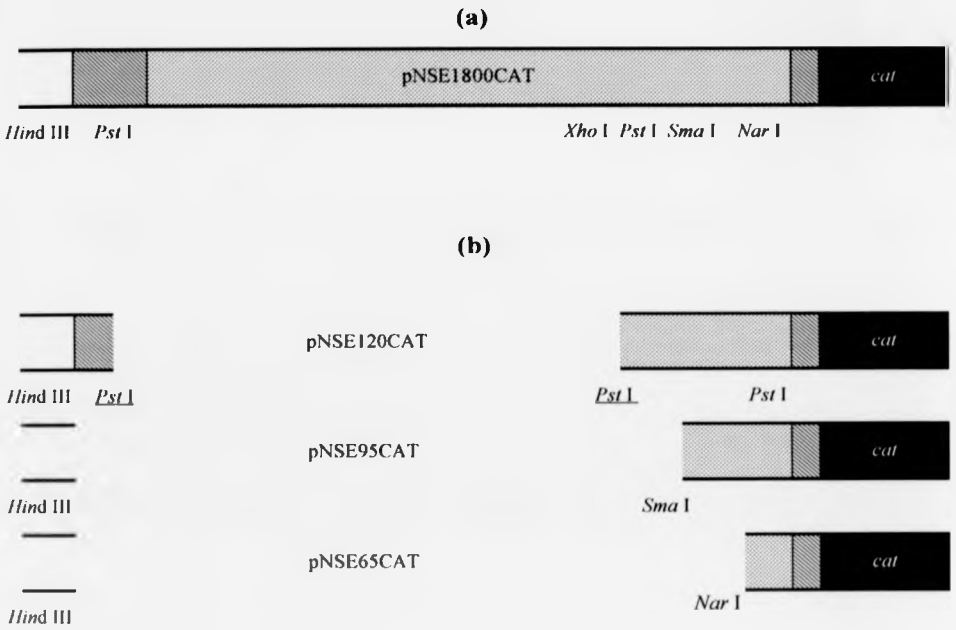

Figure 5.19. Cloning strategy and structure of the highly truncated second series of *NSE-cat* constructs. The starting material was vector pNSE1800CAT as shown in (a). The *NSE* regulatory sequence is lightly shaded, the *cat* gene is shown in black, the pCAT-Basic multiple cloning site is shown as a hatched box and vector sequence is unshaded. Restriction endonuclease sites used in this subcloning strategy are shown. b) Generation of the constructs: pNSE120CAT was made by partial digestion using the underlined *Pst* I sites and religation of the vector without the insert. pNSE95CAT and pNSE65CAT were made by digestion with *Sma* I and *Nar* I respectively, in combination with *Hind* III. Note that the *Hind* III site originally used to subclone the complete *NSE* regulatory sequence into pCAT-Basic (see Figure 5.18) was destroyed in this procedure and did not interfere with the subsequent cloning events described here.

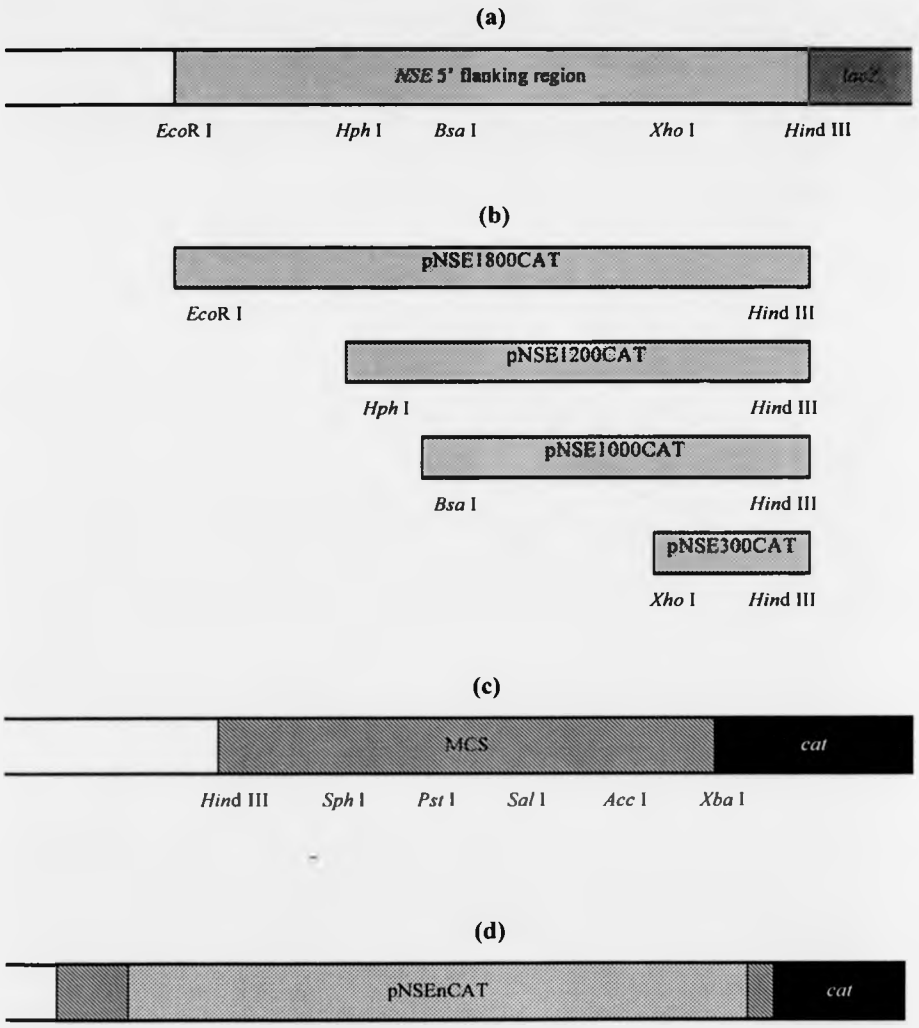

Figure 5.18. Cloning strategy and structure of the initial *NSE-cat* series of deletion constructs. a) The complete *NSE* regulatory sequence (light shading) was situated upstream of the *lacZ* gene (dark shading) in plasmid pNSElacZ (vector sequence unshaded). Restriction endonuclease sites used for subcloning are shown. b) The complete 1.8 kbp *NSE* regulatory sequence and other deletion derivatives of this sequence were removed using the restriction endonucleases shown in combination with *Hin*d III, and blunted using bacteriophage T4 DNA polymerase. c) The multiple cloning sequence (hatched) in pCAT-Basic (vector sequence unshaded) lies upstream of the *cat* gene (black). d) Each of the *NSE* fragments shown in (b) was ligated into the *Xba* I site in the pCAT-Basic multiple cloning sequence to generate the first series of constructs. Diagrams not to scale.

than pCAT-Control, with a mean Relative CAT Activity of 120-140%. In the presence of Sox2 and Sox3 expression vectors, transfection efficiency was reduced approximately twofold. As the same mass of pSV-β-galactosidase DNA was transfected in each case, the transfection efficiencies for the Sox cotransfections should have been similar to those for the control experiment. The different efficiencies observed therefore suggested that there was either an effect brought about by the Sox-cDNA-containing plasmids, or that the Sox factors were influencing the control plasmid promoters. Normalised CAT activities unexpectedly showed that both Sox2 and Sox3 caused a *rise* in *NSE*-driven reporter activity, and in the case of Sox3, a two- to threefold upregulation was observed. It was apparent, however, that the actual source levels of CAT activity from the control vector pCAT-Control were modulated by cotransfection, suggesting that the control vectors were indeed influenced by Sox expression. This point is expanded in the conclusion (section 6.7) and discussed in Chapter 9.

Construct	CAT	GAL	MEC	ACA	xACA	RCA	xRCA	semRCA
Control	45734	232	1.30	151.64	147.95	102.63	100.00	2.99
	48221	243		152.65		103.34		
	46266	255		139.57		94.03		
Basic	2465	212	1.41	8.25	7.53	0.51	0.00	0.66
	2771	346		5.68		-1.32		
	3263	267		8.67		0.81		
NSE1800	57235	291	1.00	196.68		134.71	123.03	9.63
	44195	288		153.45		103.92		
	58176	305		190.74		130.47		
Control + Sox2	79345	111	1.30	549.86	577.74	95.10	100.00	2.45
	81433	106		590.95		102.32		
	76243	99		592.41		102.58		
Basic + Sox2	1556	113	1.41	9.77	8.51	0.22	0.00	0.22
	1723	125		9.78		0.22		
	1139	135		5.98		-0.44		
NSE1800 + Sox2	99453	117	1.00	850.03		147.83	143.12	3.29
	102325	130		787.12		136.78		
	97391	117		832.40		144.74		
Control + Sox3	29364	102	1.30	221.45	205.55	108.85	100.00	9.26
	30015	134		172.30		81.49		
	36220	125		222.89		109.66		
Basic + Sox3	5119	120	1.41	30.25	25.90	2.42	0.00	1.21
	3923	116		23.99		-1.07		
	3673	111		23.47		-1.36		
NSE1800 + Sox3	88342	133	1.00	664.23		355.32	384.63	15.42
	91760	126		728.25		390.97		
	91732	121		758.12		407.59		

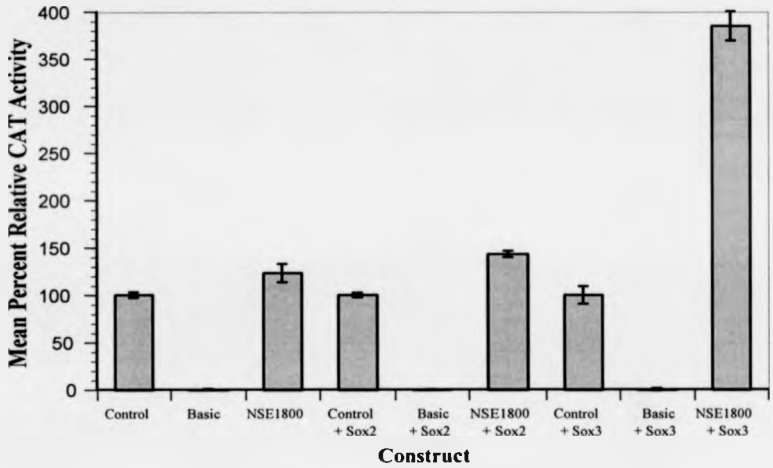

Figure 6.50: Table and histogram showing data from the first transfection of NB4-1A3 cells with pNSE1800CAT, CAT control vectors and Sox expression vectors.. Transfection was carried out using LipofectAMINE. Abbreviations used in table headings: CAT - CAT (chloramphenicol acetyltransferase) activity; GAL - β-galactosidase activity; MEC - Molar Equivalence Constant; ACA - Actual CAT Activity, xACA - mean Actual CAT Activity of control constructs; RCA - Relative CAT Activity; xRCA - mean Relative CAT Activity; semRCA - standard error of the mean Relative CAT Activity. A brief explanation of these terms can be found in Figure 6.1, a fuller explanation in section 5.5. The histogram shows mean Relative CAT Activities for each construct with error bars representing standard errors.

Construct	CAT	GAL	MEC	ACA	xACA	RCA	xRCA	semRCA
Control	60722	277	1.30	168.63	175.60	95.84	100.00	2.84
	65182	289		173.49		98.74		
	64823	270		184.68		105.42		
Basic	5912	312	1.41	13.44	8.03	3.23	0.00	1.64
	3006	344		6.20		-1.09		
	1884	301		4.44		-2.14		
NSE1800	87643	332	1.00	263.98	246.73	152.74	142.44	8.22
	84199	328		256.70		148.40		
	79237	361		219.49		126.19		
Control + Sox2	45193	151	1.30	230.22	246.67	92.98	100.00	8.77
	38720	134		222.27		89.59		
	50832	136		287.51		117.42		
Basic + Sox2	1678	144	1.41	8.26	12.27	-1.71	0.00	1.48
	1402	106		9.38		-1.23		
	3921	145		19.18		2.95		
NSE1800 + Sox2	72671	167	1.00	435.16	434.73	180.41	180.23	0.18
	77892	179		435.15		180.41		
	78100	180		433.89		179.87		
Control + Sox3	21166	155	1.30	105.04	105.82	99.23	100.00	8.51
	25812	164		121.07		115.11		
	20425	172		91.35		85.66		
Basic + Sox3	1053	151	1.41	4.95	4.88	0.06	0.00	0.09
	944	134		5.00		0.12		
	1007	152		4.70		-0.18		
NSE1800 + Sox3	26149	104	1.00	251.43	247.61	244.26	240.48	17.52
	32035	116		276.16		268.76		
	23462	109		215.25		208.41		

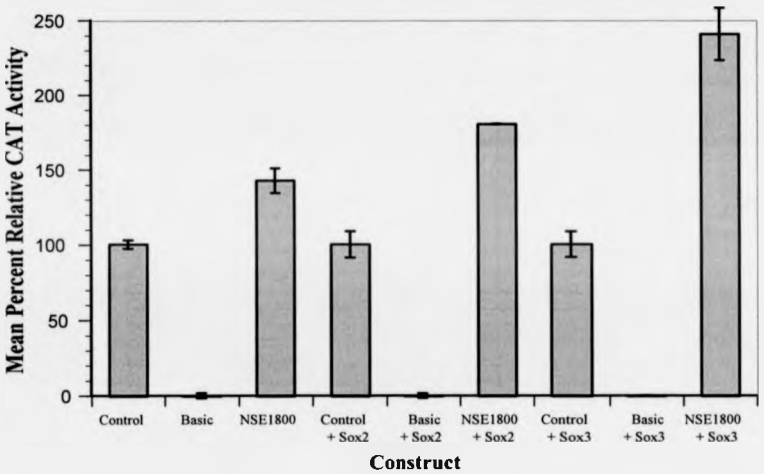

Figure 6.51: Table and histogram showing data from the second transfection of NB4-1A3 cells with pNSE1800CAT, CAT control vectors and Sox expression vectors. Transfection was carried out using LipofectAMINE. Abbreviations used in table headings: CAT - CAT (chloramphenicol acetyltransferase) activity; GAL - β-galactosidase activity; MEC - Molar Equivalence Constant; ACA - Actual CAT Activity, xACA - mean Actual CAT Activity of control constructs; RCA - Relative CAT Activity; xRCA - mean Relative CAT Activity; semRCA - standard error of the mean Relative CAT Activity. A brief explanation of these terms can be found in Figure 6.1, a fuller explanation in section 5.5. The histogram shows mean Relative CAT Activities for each construct with error bars representing standard errors.

Construct	RCA1	RCA2	xRCA12	semRCA12
Control	102.63	95.84	100.00	1.84
	103.34	98.74		
	94.03	105.42		
Basic	0.51	3.23	0.00	0.79
	-1.32	-1.09		
	0.81	-2.14		
NSE1800	134.71	152.74	132.74	7.13
	103.92	148.40		
	130.47	126.19		
Control + Sox2	95.10	92.98	100.00	4.07
	102.32	89.59		
	102.58	117.42		
Basic + Sox2	0.22	-1.71	0.00	0.67
	0.22	-1.23		
	-0.44	2.95		
NSE1800 + Sox2	147.83	180.41	161.67	8.43
	136.78	180.41		
	144.74	179.87		
Control + Sox3	108.85	99.23	100.00	5.62
	81.49	115.11		
	109.66	85.66		
Basic + Sox3	2.42	0.06	0.00	0.54
	-1.07	0.12		
	-1.36	-0.18		
NSE1800 + Sox3	355.32	244.26	312.55	33.87
	390.97	268.76		
	407.59	208.41		

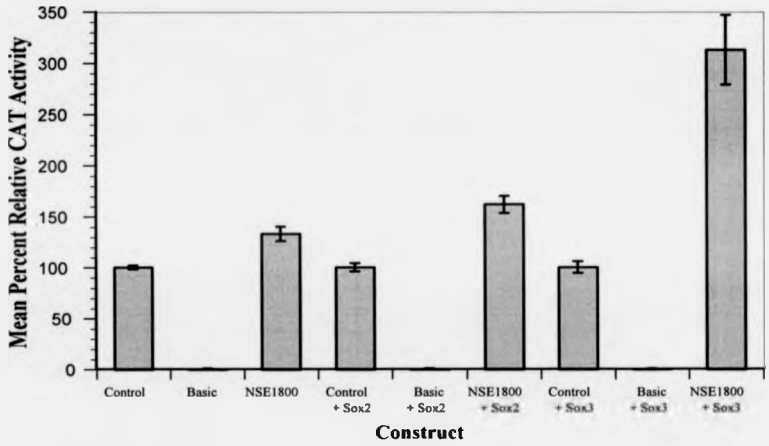

Figure 6.52: Table and histogram showing combined data from the transfection of NB4-1A3 cells with pNSE1800CAT, CAT control vectors and Sox expression vectors. Abbreviations used in the table: RCA1 and RCA2 - Relative CAT Activities from the two individual experiments (as shown in Figures 6.49 and 6.50); xRCA12 - combined mean Relative CAT Activity for each construct over two experiments (six transfections); semRCA12 - standard error of the combined mean Relative CAT Activities. A brief explanation of these terms can be found in Figure 6.1, a fuller explanation in section 5.5. The histogram shows combined mean relative CAT activity for each construct and illustrates the trend in reporter gene activity for reporter constructs in the presence of Sox transcription factors. Error bars represent standard errors of the combined mean Relative CAT Activities.

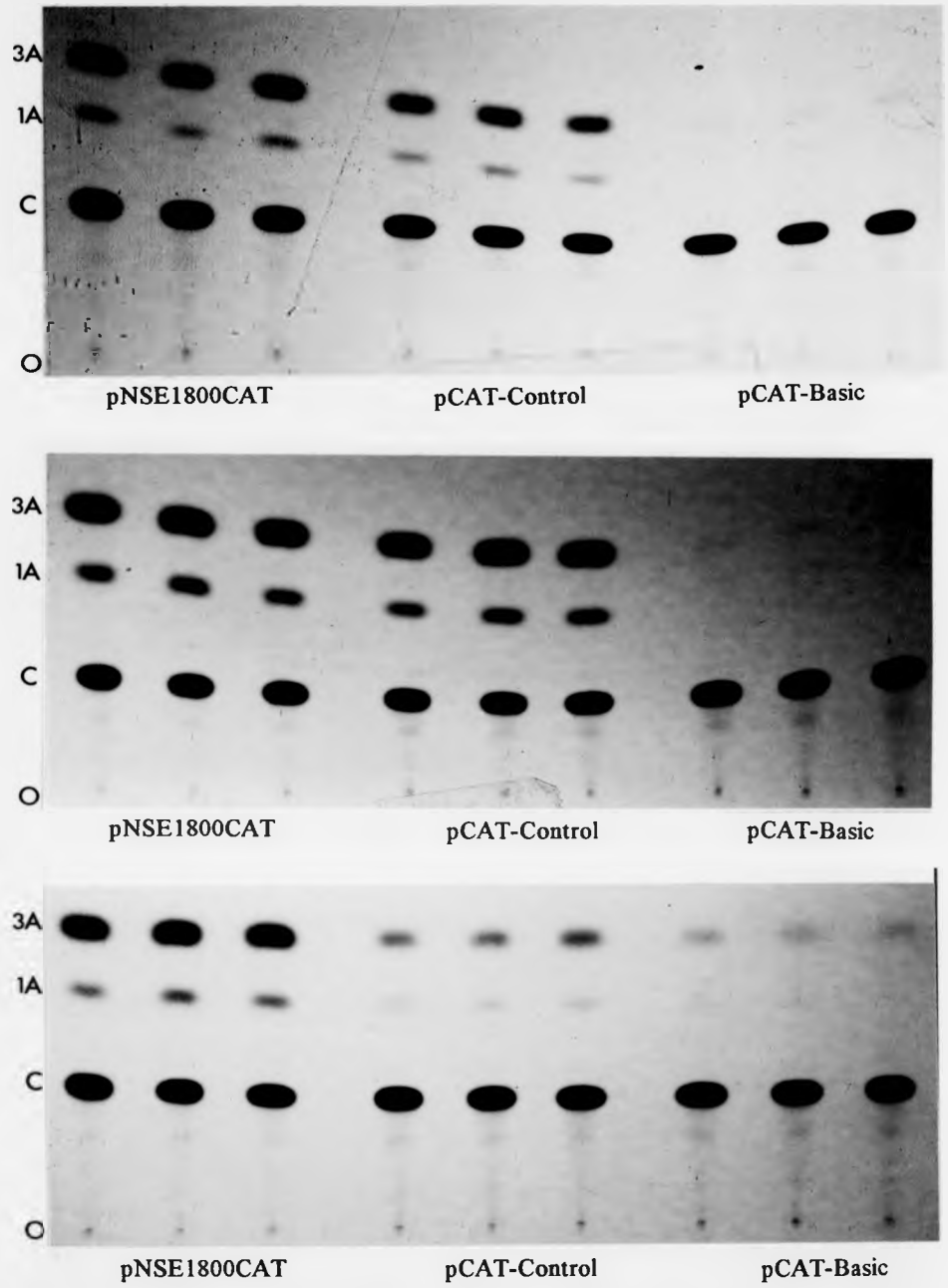

Figure 6.53: Representative CAT assay from the transfection of NB4-1A3 cells with pNSE1800CAT, pCAT-Control, pCAT-Basic and expression vectors for Sox2 and Sox3 transcription factors. Each construct was transfected in triplicate and the lanes of the TLC plate were grouped accordingly. The assay shown above corresponds to the experiment shown in Figure 6.50. Abbreviations: O = origin; C = chloramphenicol; 1A = 1-acetylchloramphenicol; 3A = 3-acetylchloramphenicol.

previous studies of rat *NSE* ontogeny (Forss-Petter *et al.*, 1986; Di Liergo *et al.*, 1991).

7.2.2 *In situ* detection of endogenous *NSE* gene products during mouse development

The expression of *NSE* mRNA and NSE protein was investigated by *in situ* hybridisation and *in situ* immunohistochemical analysis respectively. *In situ* immunohistochemical analysis was also used extensively by Forss-Petter and colleagues when the first *NSE-lacZ* transgenic mice were generated (Forss-Petter *et al.*, 1990). This was so because NSE protein and β-galactosidase could be detected on the same or serial sections, making comparative analysis relatively simple. The procedure was therefore granted similar predominance in the present investigation. Forss-Petter and her coworkers avoided an exhaustive immunohistological survey of *NSE* ontogeny, but published an account which was sufficient for detailed comparison with their transgene expression pattern. NSE protein and β-galactosidase were first detected *in situ* at E10.5. In the present study, therefore, NSE protein expression was investigated between E9.5 (early neurogenesis, when the neural tube has closed along most of its length) and E14.5 (later neurogenesis, when all the major events of nervous system development, such as regionalisation of the brain and spinal cord and definitive specialisation of neuronal cell populations, have been completed). *NSE* mRNA expression was investigated in embryos at E8.5 and E9.5, during the first stages of neurogenesis.

7.2.3 Expression of endogenous *NSE* mRNA - *in situ* hybridisation analysis

Although NSE expression in neuroglial precursor cells of the hypothalamus has been reported in early mouse embryos lacking mature neurons (De Vitry *et al.*, 1980), the onset of NSE protein synthesis is commonly accepted as a marker of overt neuronal differentiation. It was important to establish the nature of *NSE*

mRNA expression in neurogenic mouse embryos because several investigators have provided evidence for the accumulation of *NSE* mRNA prior to expression of the protein (Forss-Petter *et al.*, 1986; Di Liergo *et al.*, 1991). *NSE* mRNA (but not protein) has also been detected in murine embryonic stem cells, blastocysts and morulae (Alouani *et al.*, 1993). As E10.5 is the earliest stage at which NSE protein expression has been reported (Forss-Petter *et al.*, 1990), *NSE* mRNA expression was investigated in embryos at E9.5 and E8.5. The expression of *NSE* mRNA has been studied *in situ* in the brains of foetal and adult rats (Watanabe *et al.*, 1990; 1993; Katagiri *et al.*, 1993; Keller *et al.*, 1994) and humans (Schmechel *et al.*, 1987) but not previously in mouse embryos. *In situ* hybridisation studies of *MSE* mRNA in early myogenic structures such as the E7.25 cardiac tube demonstrated the onset of *MSE* gene expression much earlier than had originally been shown (Keller *et al.*, 1992a).

7.2.3.1 Construction of the transcription vector

In situ hybridisation, using *in vitro* transcribed antisense RNA probes incorporating digoxigenin-labelled UTP, is an established method for the analysis of patterns of mRNA expression in wholemount specimens (Höltke and Kessler, 1990). Before *in situ* hybridisation analysis was possible, however, it was necessary to construct a vector which would allow such a probe to be generated. A suitable basis for this transcription construct was pBluescriptIIKS+, a plasmid containing a multiple cloning site flanked by promoters specific for the RNA polymerase enzymes encoded by bacteriophages T7 and T3 respectively (Figure 7.2). To generate the recombinant transcription vector, a 1.3 kbp *Hin*d III - *Sma* I restriction fragment was isolated from the rat *NSE* cDNA sequence, carried in plasmid pcD169 (Forss-Petter *et al.*, 1986). This fragment contained the distal 1 kbp of the *NSE* coding sequence and the proximal 300 bp of 3' untranslated region. As discussed in section 5.2.1, all enolase coding regions are highly conserved, and cross-hybridisation to *MSE* and *NNE* transcripts would be likely to occur - especially across species boundaries - if the *NSE* coding region was used as a probe. For the

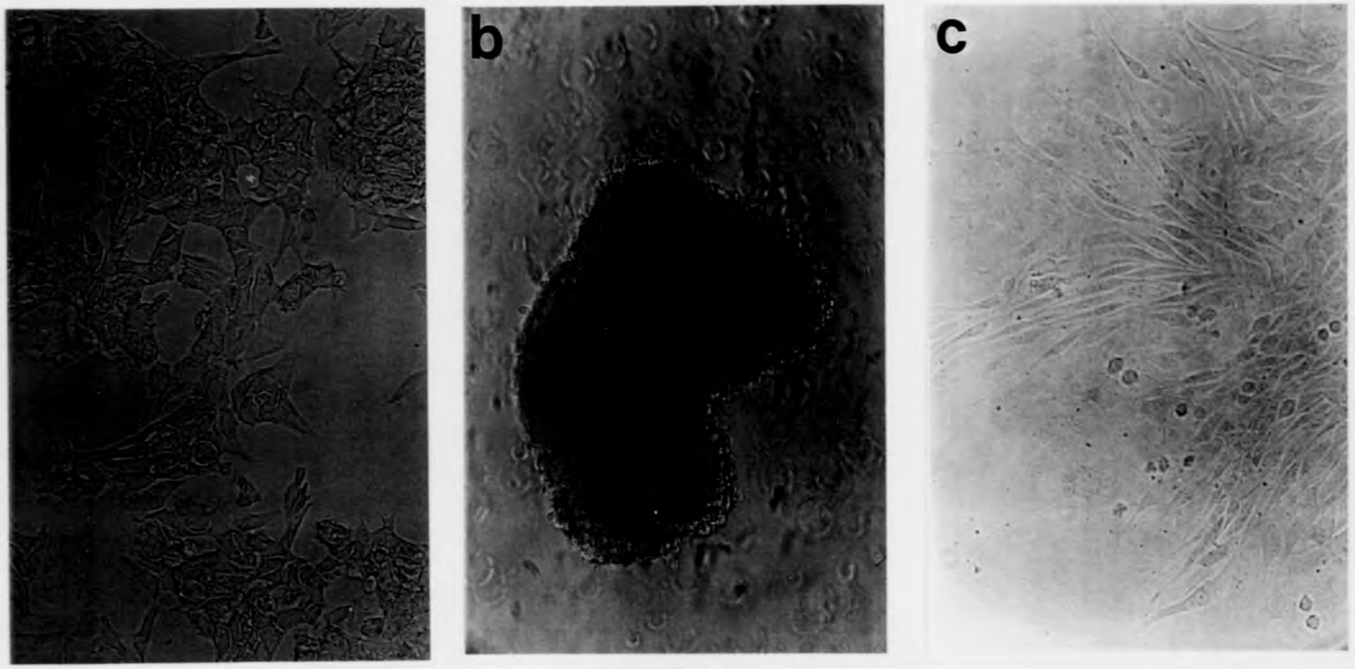

Figure 5.10 Differentiation of P19 EC into neuronal cells using retinoic acid. Photographs show a) proliferating stem cells; b) cell aggregate after four days exposure to 0.3μM retinoic acid and c) P19 neurons originating from a small aggregate after a total of eight days in culture. Neurites can be seen emerging from the differentiating cells. At this stage, mitogenic inhibitors were added to the culture to selectively destroy proliferating (nonneuronal cells). Cells were transfected after fourteen days in culture.

nonambigous detection of *NSE* transcripts, the probe had therefore to be derived from the isogene-specific 3' untranslated region of the cDNA. The template fragment was subcloned into pBluescriptIIKS+ using the *Hind* III and *Sma* I sites within the polylinker, and the recombinant was called pNSEprobe1. The template was linearised using a unique *Nco* I site within the *NSE* 3' untranslated region. Antisense RNA probes 330 b in length, complementary to the *NSE* 3' untranslated region, were generated using T7 RNA polymerase. As a negative control, sense RNA probes of 1100 b in length, corresponding to the *NSE* coding region, were generated using T3 RNA polymerase. Both probes contained approximately 70 b of vector sequence representing the polylinker region between the appropriate promoter and the position of insertion. The cloning strategy is shown in Figure 7.3.

determination step, which involves the switching off of *NSE*. Otherwise, the level of *NSE* mRNA in the P19 cells may simply be too low to be detected by the methods used in this study. Notwithstanding these contradictory reports, the results obtained in this study suggested that the P19 EC line represented and excellent model for the study of *NSE* gene regulation during *ex vivo* neuronal differentiation.

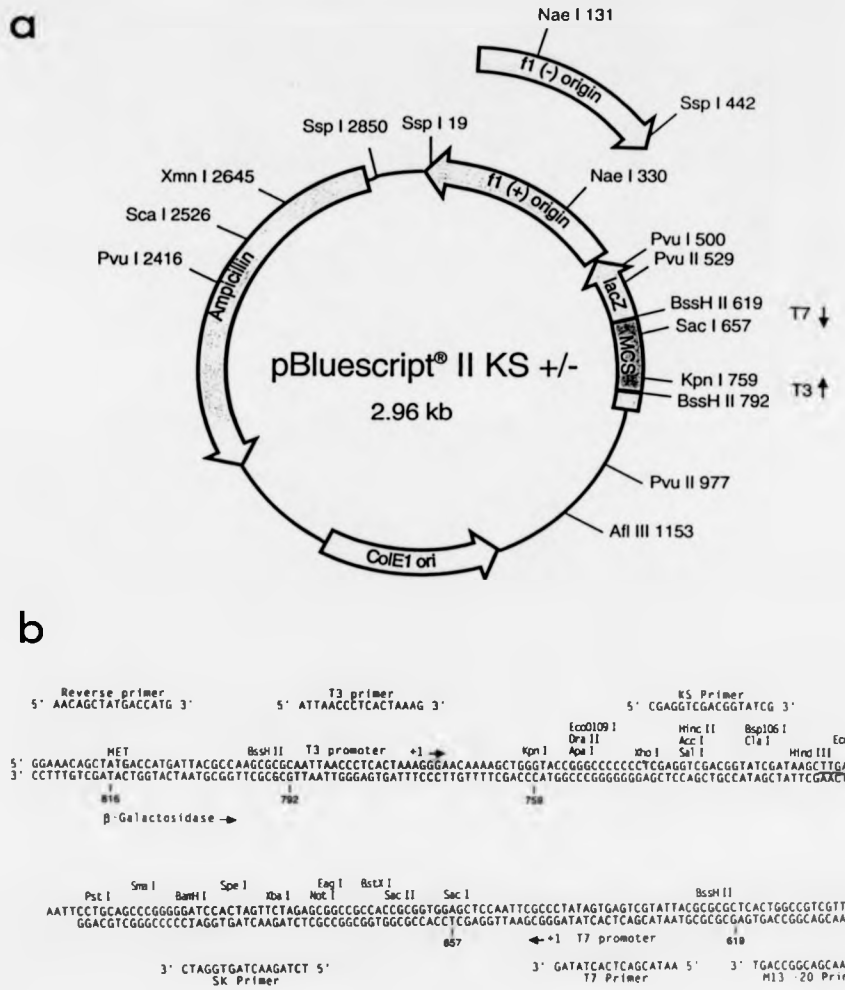

Figure 7.2: pBluescriptIIKS+, the source plasmid used to construct transcription plasmid pNSEprobe1. a) Plasmid map, showing the position of the ampicillin resistance gene (Ampicillin), the origin of replication (ColE1 ori), the *lacZ* gene (lacZ) the bacteriophage f1 (+) origin of replication (f1 (+) origin) and the multiple cloning site (MCS), indicating the direction of transcription from the bacteriophage promoters (T7, T3). A number of restriction endonuclease sites are also shown. b) Sequence of the pBluescriptIIKS+ multiple cloning site. The *Hin*d III and *Sma* I restriction endonuclease sites, used to insert the *NSE* cDNA fragment, are underlined. The position of the bacteriophage T7 and T3 promoters are indicated, and the direction and start of transcription from each promoter are indicated by → and +1 respectively. Both diagrams taken from Stratagene Product Catalogue, 1993.

5.2.7 *NSE* gene expression in P19 EC cells and their neuronal derivatives

P19 embryonal carcinoma (EC) cells may be persuaded to differentiate into neurons *in vitro* when treated with low doses (0.3μ*M*) of retinoic acid (Rudnicki and McBurney, 1987). This cell line therefore represented an excellent system for the analysis of *NSE* induction as part of neuronal differentiation. Although one would expect undifferentiated stem cells to lack neuronal gene products, Alouani and colleagues have recently reported the presence of endogenous *NSE* mRNA (but not protein) in embryonic stem cells and preimplantation murine embryos, suggesting that the factors responsible for cell type-specific transcription of the *NSE* gene were already present in these pluripotent cells (Alouani *et al.*, 1993). It was therefore very important to characterise the endogenous expression of *NSE* in the P19 cells because comparison between undifferentiated and differentiated cells transfected with *NSE-cat* reporter constructs would depend upon the potential of each construct for *transcription* of the reporter gene. Proliferating P19 cells were stimulated to differentiate into neurons as described in section 4.2.4 and both stem cells and neurons were studied by northern and western analysis as described in section 5.2.3. Figures 5.10a-c show the process of retinoic acid-mediated differentiation. Figures 5.11a and 5.11b show the results of northern and western analysis. As expected, western analysis demonstrated that NSE protein was undetectable in stem cells but abundant in neurons, more so than in adult brain (Figure 5.11b). Northern analysis showed a similar pattern, suggesting that *NSE* mRNA was not present in stem cells but was present in neurons, again at levels in excess of those observed in the brain. It is unknown why the results of the northern analysis described above disagreed with the data published by Alouani and colleagues. The cell lines used in the two studies were not the same (Alouani *et al.* used ES-12957 embryonic stem cells whilst P19 embryonic carcinoma cells were used in the present study) and perhaps the discrepancy reflects this difference. It is more likely, however, that different sensitivities of the detection methods were responsible, as discussed in Chapter 9. Alounai *et al.* also noted that levels of endogenous *NSE* mRNA fell before rising during neuronal differentiation, and it is possible that the P19 cell line reflects a molecular environment which has proceeded further towards this

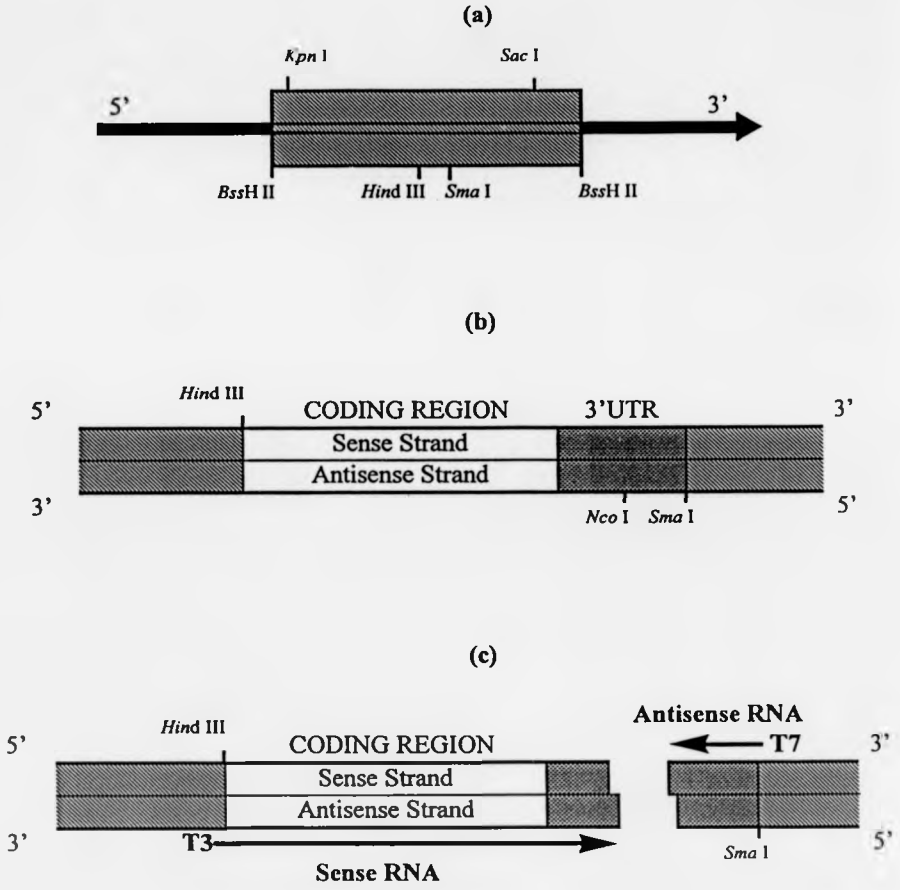

Figure 7.3: Strategy for the generation of antisense RNA probes for the *in situ* detection of *NSE* mRNA and sense RNA probes for negative control hybridisations. a) The multiple cloning site of pBluescriptIIKS+ (hatched) lies within the *lacZ* gene (dark bar, with arrow indicating orientation) and is flanked by *Bss*H II sites. The restriction endonuclease sites above (*Kpn* I, *Sac* I) indicate orientation of the polylinker whilst those below (*Hind* III, *Sma* I) indicate the site of insertion of the *NSE* sequence. b) A *Hind* III - *Sma* I restriction fragment containing both coding (unshaded) and untranslated (shaded) regions of the rat *NSE* cDNA was subcloned into the multiple cloning site of pBluescriptIIKS+ (hatched). c) The recombinant vector was linearised at a unique *Nco* I site within the insert and antisense RNA complementary to the untranslated region was generated by run-off transcription from the bacteriophage T7 promoter. Sense RNA corresponding to the coding region was generated by run-off transcription from the bacteriophage T3 promoter.

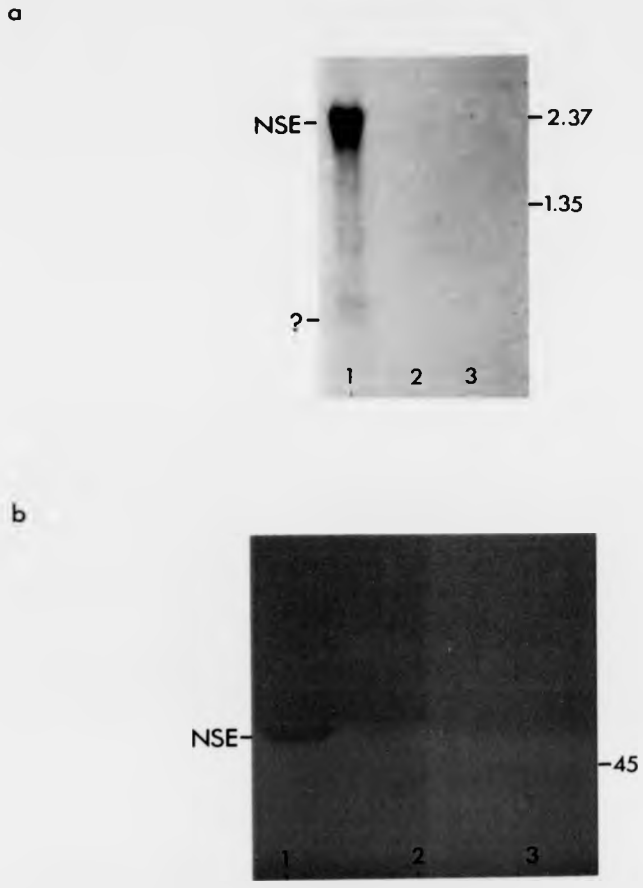

Figure 5.9: Northern and western analysis of HeLa cells. a) Northern analysis using the *Sma* I - *Nco* I fragment of the rat *NSE* 3' UTR as a probe - lanes loaded equally for total RNA, 10μg per lane: 1 - mouse brain, 2 - mouse liver, 3 - HeLa cells. Markers are Gibco BRL RNA ladder. b) Western analysis using anti-human NSE, detected with horseradish peroxidase-conjugated goat anti-rabbit IgG and revealed by staining with diaminobenzidine tetrahydrochloride without metal ion enhancement - lanes loaded equally for total protein, 5μg per lane: 1 - mouse brain, 2 - mouse liver, 3 - HeLa cells. 45kDa marker is ovalbumin. Immunocytochemical analysis of HeLa cells was also carried out and no staining for NSE protein was evident (results not shown).

7.2.3.2 *In vitro* transcription of antisense and sense RNA probes

Following verification of pNSEprobe1 by restriction mapping (data not shown), caesium chloride equilibrium centrifugation was carried out to prepare a large quantity of the vector, essentially free of randomly nicked and linearised material. Homogenous linearised template was prepared from 10μg plasmid DNA by digestion with *Nco* I as described in section 4.1.2.1 and purification of the DNA was carried out as described in section 4.1.4. 1μg of linearised template was used for each *in vitro* transcription reaction, as described in section 4.1.6.3. The results of one set of such synthesis reactions are shown in Figure 7.4.

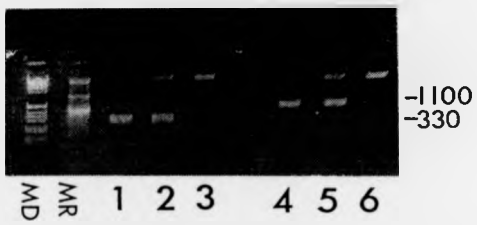

Figure 7.4: Confirmation of digoxigenin-UTP-labelled RNA probe synthesis. Polaroid photographs show 2% w/v agarose gels after 10 minutes electrophoresis at 200V in 1x TBE buffer. Lanes were loaded with 1μl aliquots from 20μl probe synthesis reactions or 0.1μg aliquots of linearised template: 1 - antisense probe (T7) transcription, post DNase treatment; 2 - antisense probe (T7) transcription, pre DNase treatment; 3 - 0.1μg linearised template; 4 - sense probe (T3) transcription, post DNase treatment; 5 - sense probe (T3) transcription, pre DNase treatment, 6 - 0.1μg linearised template. Markers are Gibco BRL RNA ladder (MR) and 1 kb DNA ladder (MD).

5.2.6 Endogenous NSE expression in HeLa cells

HeLa cells are nonneuronal cells which have been used as the nonpermissive cell line in the study of numerous neuronal genes, including *NSE* (Sakimura *et al.*, 1995; *see* Chapter 2). HeLa cells were used as a second nonpermissive cell line in the present study for this reason, even though their human origin was at odds with most of the other sources of biological material. To confirm that HeLa cells were nonpermissive for *NSE* gene expression, protein and mRNA were analysed as described in section 5.2.3. It is acknowledged by the author that no attempt was made to test the rat *NSE* 3' UTR probe on neuronal material of human origin to confirm that it would detect human *NSE* mRNA. However, the level of sequence identity between the human and rat *NSE* 3' UTRs is approximately 70% over the entire comparable region, with pockets of higher identity particularly surrounding the AT-rich repetitive motif encompassed by the probe (Oliva *et al.*, 1989). It is therefore likely that, under the moderate stringency conditions used in the posthybridisation washes (55°C, equivalent to 0.4x SSC), some of the human *NSE* message would be detected should it be present. Notwithstanding this conjecture, it is certain that human NSE protein would be detected by the antiserum used in this study, as it was originally raised against the human protein. The results, which are shown in Figures 5.9a and 5.9b, confirm that HeLa cells express NSE protein, and probably *NSE* mRNA also, at undetectable levels and are good candidates for nonpermissive cells.

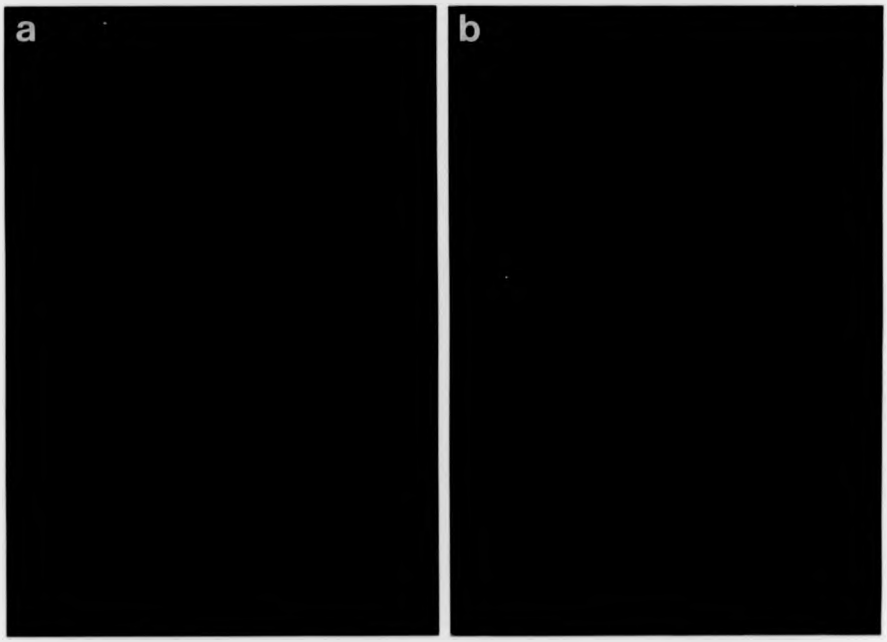

Figure 7.6: Mouse rostral neural tube at E14.5 stained for NSE protein. a) Normal experimental conditions, i.e. section incubated with primary antiserum. b) Negative control serial section incubated without primary antiserum. NSE was detected with primary antiserum raised against human NSE and a secondary FITC-conjugated antiserum specific for rabbit IgG. Photographs were taken under epifluorescent micoscopy using a 20x DIC objective.

7.2.4.1 Expression of endogenous NSE protein at E9.5

Transverse 10μm sections were taken through the head and anterior trunk of E9.5 mouse embryos and attempts were made to detect NSE protein as described above. In agreement with previous investigations (Forss-Petter *et al.*, 1990), NSE protein could not be detected in these embryos. As an example, Figure 7.7 shows a transverse section across the anterior neural tube of such an embryo, showing that no fluorescence was evident.

5.2.4 Endogenous *NSE* gene expression in U-138 MG and U-373 MG cells

Initial transfection experiments using the PC12 (Geneva) line were totally unsuccessful (see section 5.4.2.1). In the interests of continuing the investigation without delay, further permissive cell lines were sought within the department. Although no neuronal cell lines were available, two transformed cell lines of glial origin (U-138 MG glioblastoma and U-373 MG astrocytoma) were analysed. It is well known that although glial cells *in vivo* do not express *NSE*, transformed cell lines of glial origin often express relatively high levels of the gene product (Zomzely-Neurath, 1983). This property may reflect the common neurectodermal origin of neurons and glia, showing that relatively few genetic changes (i.e. those associated with growth transformation) are required to confer some aspects of neuronal phenotype upon glial cells. It has also been reported that neuroglial precursors express NSE protein in the early mouse embryo (De Vitry *et al.*, 1980; Schubert *et al.*, 1983). Northern, western and immunocytochemical analysis was carried out upon these cell lines as described in section 5.2.3 and the results of these experiments are shown in Figures 5.6a-c. Both glial lines appeared to express *NSE* mRNA and NSE protein at significant levels, albeit lower than those observed in mouse brain. Northern and immunocytochemical analysis indicated that U-138 MG cells expressed more of the gene product than U-373 MG cells, whilst the western analysis showed approximately equivalent levels of NSE protein in each cell line. The results of these experiments confirmed that either glial line could be used as a permissive system for the analysis of *NSE* gene expression. The U-138 MG cell line was eventually chosen, based upon its higher level of *NSE* transcription and its ease of transfection (see section 5.4.3).

Figure 7.7: Following two pages

Figure 7.7: Expression of NSE protein in mouse embryos at E9.5. a) Size and appearance of mouse embryo at E9.5 showing the position of the section to which the drawing and photograph in this figure refers. b) Schematic representation (with anatomical landmarks identified) and c) photomicrograph of a transverse section, magnification x85, showing the absence of NSE protein in the E9.5 mouse embryo. Attempts to detect NSE were made using a polyclonal antiserum raised against human NSE and a secondary FITC-conjugated antiserum specific for rabbit IgG. The photograph was enlarged from an original slide taken under epifluorescent microscopy using a x20 DIC objective lens.

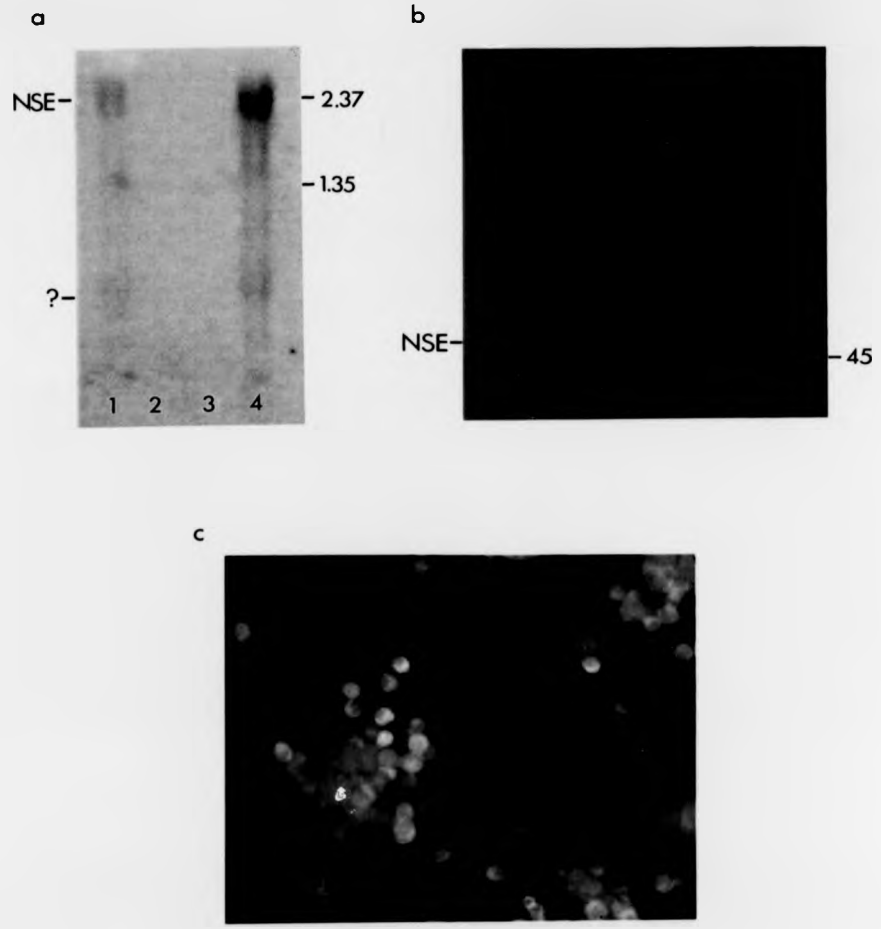

Figure 5.5: Northern, western and immunocytochemical analysis of Ltk- and PC12 (Geneva) cells. a) Northern analysis using the *Sma* I - *Nco* I fragment of the rat *NSE* 3' UTR as a probe - lanes loaded equally for total RNA, 10μg per lane: 1 - PC12, 2 - Ltk-, 3 - mouse liver, 4 - mouse brain. Markers are Gibco BRL RNA ladder. b) Western analysis using anti-human NSE, detected with horseradish peroxidase-conjugated goat anti-rabbit IgG and revealed by staining with diaminobenzidine tetrahydrochloride without metal ion enhancement - lanes loaded equally for total protein, 5μg per lane: 1 - PC12, 2 - Ltk-, 3 - mouse liver, 4 - mouse brain. 45kDa marker is ovalbumin. c) Immunocytochemical analysis of PC12 (Geneva) cells using anti-human NSE, detected with FITC-conjugated goat anti-rabbit IgG, x20 under epifluorescence microscopy. Intense staining was observed throughout the cell body of PC12 cells whilst none was seen in Ltk- cells treated in parallel (data not shown).

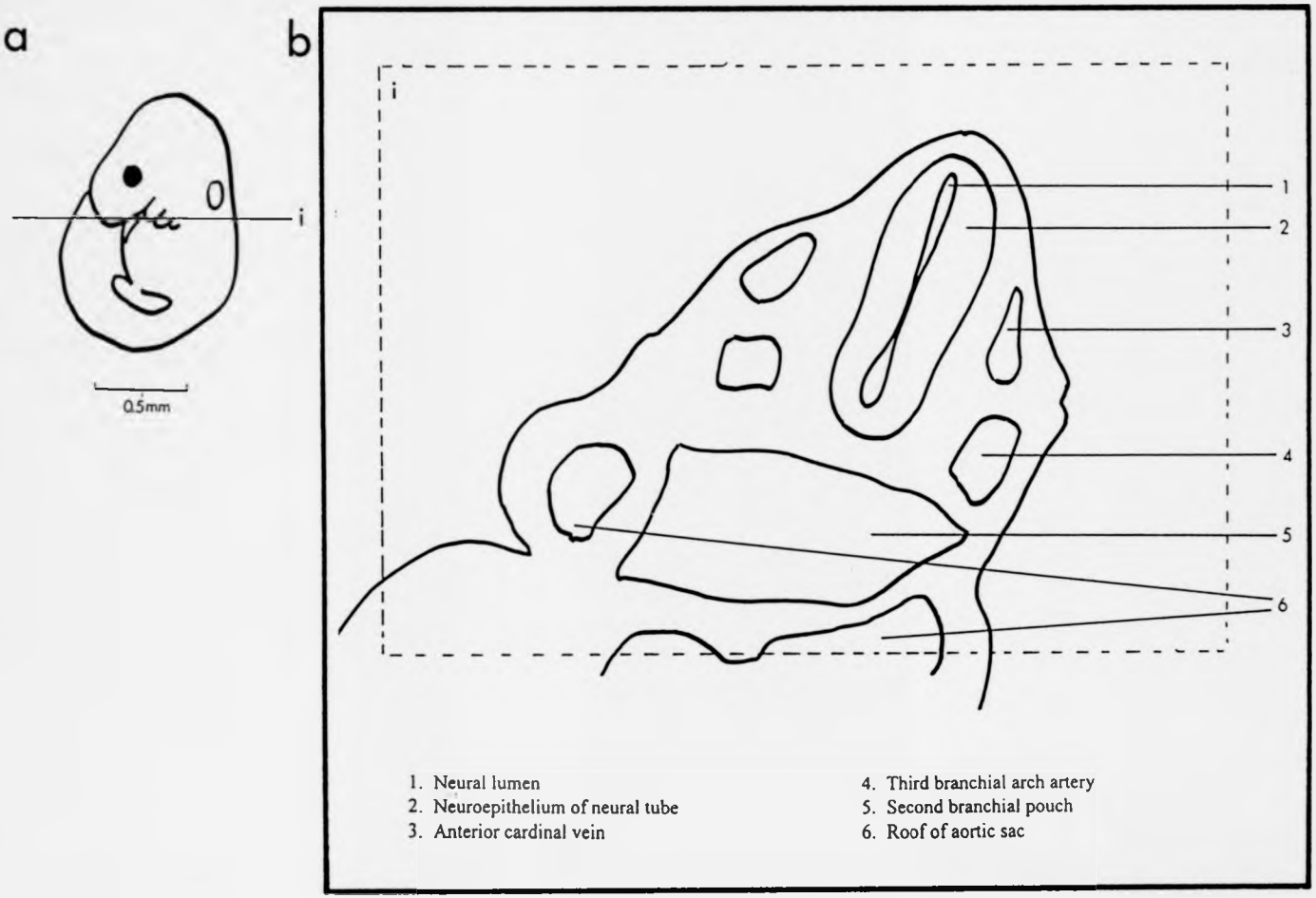
a
b
i
0
i
0.5mm
1
2
3
4
5
6
1. Neural lumen
2. Neuroepithelium of neural tube
3. Anterior cardinal vein
4. Third branchial arch artery
5. Second branchial pouch
6. Roof of aortic sac

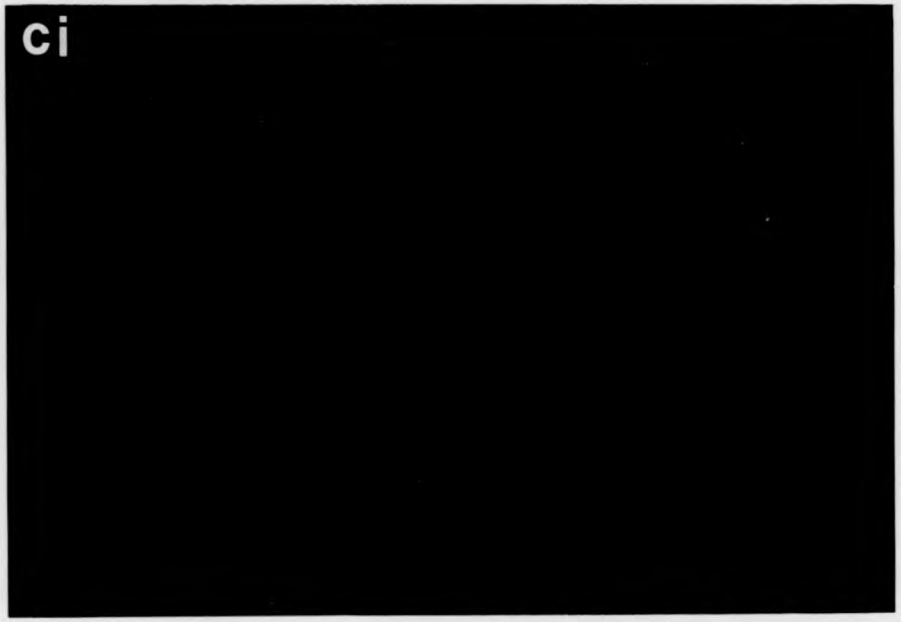

Figure 7.7: Expression of NSE protein in mouse embryos at E9.5. a) Size and appearance of mouse embryo at E9.5 showing the position of the section to which the drawing and photograph in this figure refers. b) Schematic representation (with anatomical landmarks identified) and c) photomicrograph of a tranverse section, magnification x85, showing the absence of NSE protein in the E9.5 mouse embryo. Attempts to detect NSE were made using a polyclonal antiserum raised against human NSE and a secondary FITC-conjugated antiserum specific for rabbit IgG. The photograph was enlarged from an original slide taken under epifluorescent microscopy using a x20 DIC objective lens.

a
i
ii
iii, iv
1mm
b
i
1
2
3
ii
iii
iv
1. Neural lumen
2. Neuroepithelium of neural tube
3. NSE-positive neurons of ventral horn

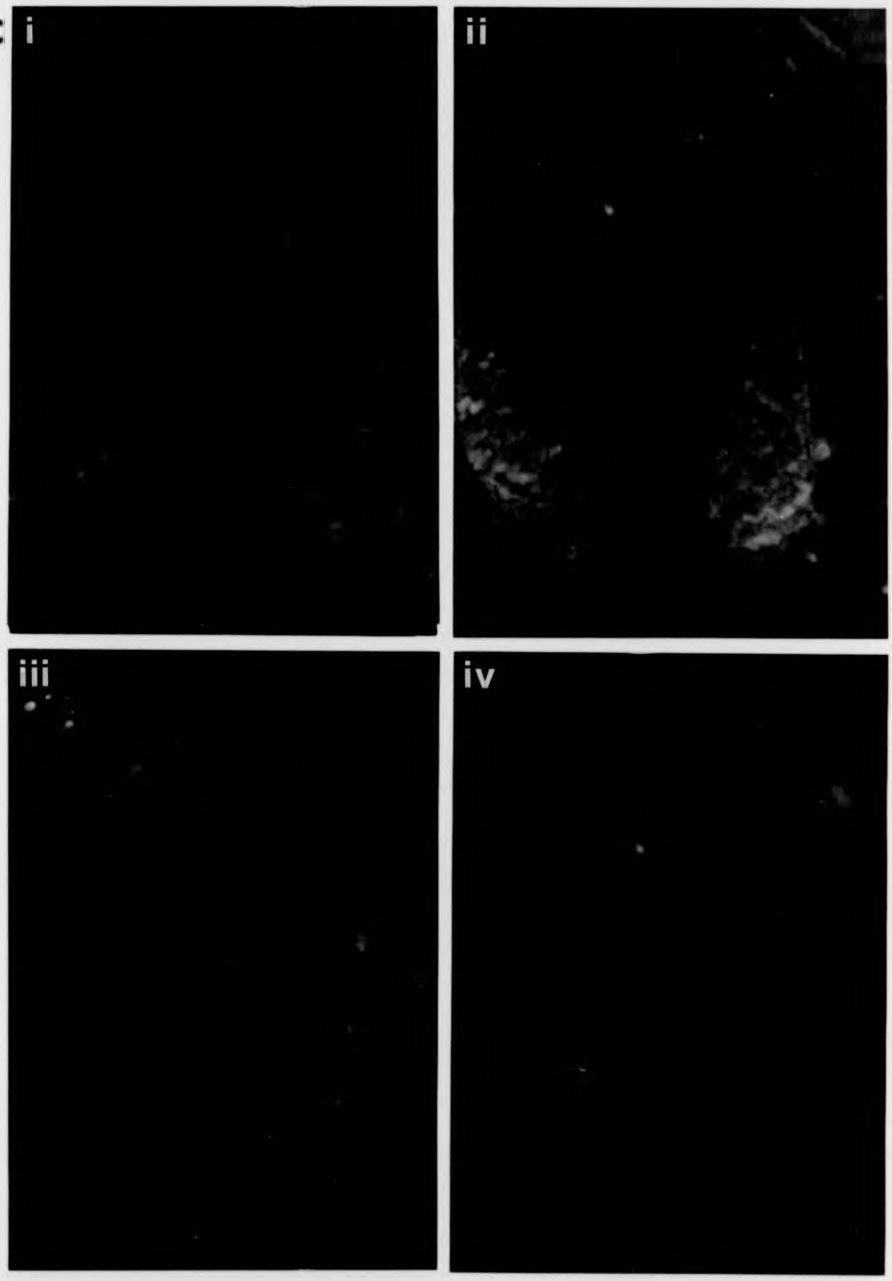
c
i
ii
iii
iv

7.2.4.3 Expression of endogenous NSE protein at E11.5

Transverse 10μm sections were taken throughout E11.5 mouse embryos and NSE protein was detected as described in section 7.2.4. The protein could be detected in sections of brain at all levels and in the rostral part of the neural tube. The domain of NSE expression in the neural tube had spread both rostrally and caudally compared to E10.5, although no expression was evident throughout the tail neural tube (data not shown). In the brain, NSE expression was restricted to small numbers of cells in the thin mantle layer, whilst no expression was evident in the inner ependymal layer. Representative transverse sections showing such staining in the wall of the midbrain and hindbrain are shown in Figures 7.9(i) and 7.9(ii). It was also apparent from this early stage of development that NSE was expressed in a rostrocaudal gradient of increasing intensity in the brain. Figure 7.9(iii) shows the midbrain-hindbrain boundary at a level corresponding to the rostral extremity of the otic vesicle. Intense staining could be seen in the mantle layer of the posterior wall of the fourth ventricle whilst staining of the anterior wall of the mesencephalic ventricle was much fainter. In the neural tube, ventrolateral staining of motor neurons had increased in intensity from E10.5, concomitant with the accumulation of postmitotic neuronal cell bodies in the mantle layer (Figure 7.9(iv)). There was also evidence of NSE-positive neurons in the dorsal root ganglia and of NSE-positive axons comprising the mixed spinal nerves. The accumulation of NSE-positive axons was also reflected in the intense staining observed in the marginal layer at the ventral extremity of the neural tube (Figure 7.9(iv)). This layer underlies both the central, NSE-negative, ependymal layer and the lateral, NSE-positive, mantle layer. Weak staining for NSE was also observed in the lateral marginal layer of the neural tube, extending dorsally. This staining became particularly intense at the level of the dorsal root, where efferent nerve fibres emanating from the ganglion could also be observed.

Figure 7.9: Following two pages

Figure 7.9. Expression of NSE protein in mouse embryos at E11.5. a) Size and appearance of mouse embryo at E11.5 showing the positions of sections to which the drawings and photographs in this figure refer. b) Schematic representations of the E11.5 mouse embryo in transverse section (the position of each section is shown in (a)), with anatomical landmarks identified, and the photographic field of each photomicrograph (as shown in (c)) marked with a dashed line. c) Photomicrographs of representative transverse sections, magnification x85, showing the expression of NSE protein in the E11.5 mouse embryo. NSE was detected using a polyclonal antiserum specific for human NSE and a secondary FITC-conjugated antiserum specific for rabbit IgG. Photographs were enlarged from slides taken under epifluorescent microscopy using a x20 DIC objective lens.

a
i
ii
iii
iv
1mm
b
i
ii
iii
iv
1. Neuroepithelium of roof of hindbrain
2. Otic vesicle
3. Fourth ventricle
4. Mesencephalic ventricle
5. Neural lumen
6. Marginal layer at position of dorsal root
7. Dorsal root nerve
8. Ependymal layer
9. Mantle layer
10. Marginal layer
11. Dorsal root ganglion
12. Mixed spinal nerve

7.2.4.4 Expression of endogenous NSE protein at E12.5

Transverse 10μm sections were taken throughout E12.5 mouse embryos and NSE protein was detected as described in section 7.4.2. The protein could be detected in sections of brain at all levels and throughout the neural tube, excluding the very caudal extremity of the tail (data not shown). In the brain, NSE expression was observed as a broad band of fluorescent cells corresponding to the thickening mantle layer. Sections corresponding the lateral wall of the hindbrain at the coronal apex and the anterior wall of the metencephalon (future pons and cerebellum) are shown in Figures 7.10(i) and 7.10(ii). In the more rostral segments of the neural tube, the domain of NSE expression had spread dorsally through the mantle layer whilst axonal accumulation was evident from intense staining in the marginal layer, forming an incomplete ring (Figure 7.10(iii)A). The dynamic impression of NSE ontogeny in the neural tube was thus like a closing pincer, with the jaws coming together towards the dorsal midline. Marginal staining was again particularly intense at the dorsal root (Figure 7.10(iii)B), with staining also present in the afferent nerve fibres originating from the dorsal root ganglion. NSE positive neuronal cell bodies were obvious in the dorsal root ganglion itself, and both efferent and afferent nerve fibres were visible in the mixed spinal nerves (Figure 7.10(iii)A). Caudal segments of the neural tube showed a progressively less extensive domain of NSE expression (data not shown) so that the rostrocaudal axis mirrored the temporal sequence of NSE ontogeny in reverse. Thus, NSE expression in the tail of E12.5 embryos was reminiscent of NSE expression in the rostral extremity of the neural tube in E10.5 embryos. The observed spatiotemporal sequence was coincident with the accumulation of mature, postmitotic neurons in the developing spinal cord.

Figure 7.10: Following two pages

Figure 7.10: Expression of NSE protein in mouse embryos at E12.5. a) Size and appearance of mouse embryo at E12.5 showing the positions of sections to which the drawings and photographs in this figure refer. b) Schematic representations of the E12.5 mouse embryo in transverse section (the position of each section is shown in (a)), with anatomical landmarks identified and the photographic field of each photomicrograph (as shown in (c)) marked with a dashed line. c) Photomicrographs of representative transverse sections, magnification x85 (i, ii, iiiB) or x40 (iiiA), showing the expression of NSE protein in the E12.5 mouse embryo. NSE was detected using a polyclonal antiserum specific for human NSE and a secondary FITC-conjugated antiserum specific for rabbit IgG. Photographs were enlarged from slides taken under epifluorescent microscopy using a x10 or x20 DIC objective lens.

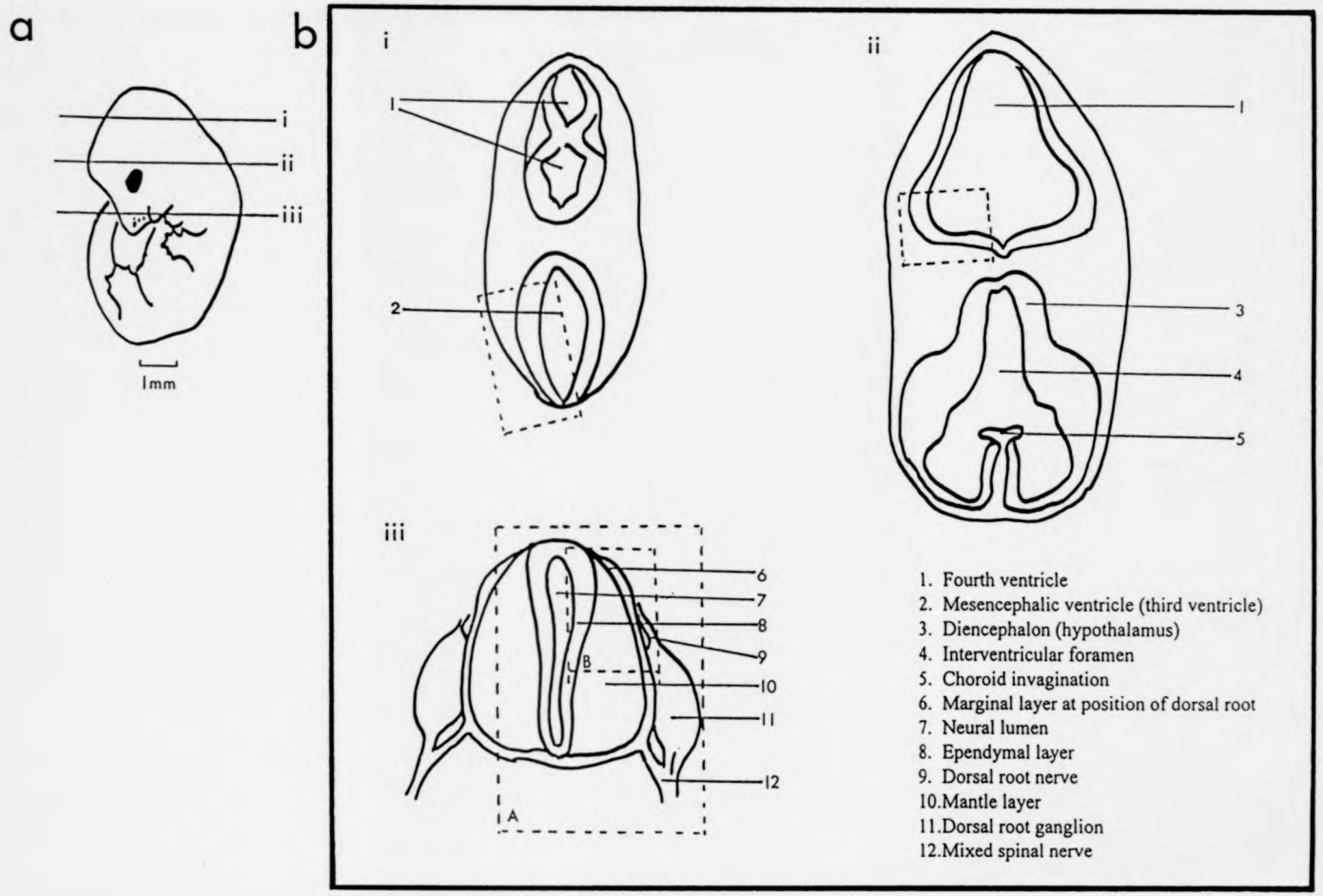
a
i
ii
iii
1mm
b
i
1
2
ii
1
3
4
5
iii
6
7
8
9
10
11
12
A
B
1. Fourth ventricle
2. Mesencephalic ventricle (third ventricle)
3. Diencephalon (hypothalamus)
4. Interventricular foramen
5. Choroid invagination
6. Marginal layer at position of dorsal root
7. Neural lumen
8. Ependymal layer
9. Dorsal root nerve
10. Mantle layer
11. Dorsal root ganglion
12. Mixed spinal nerve

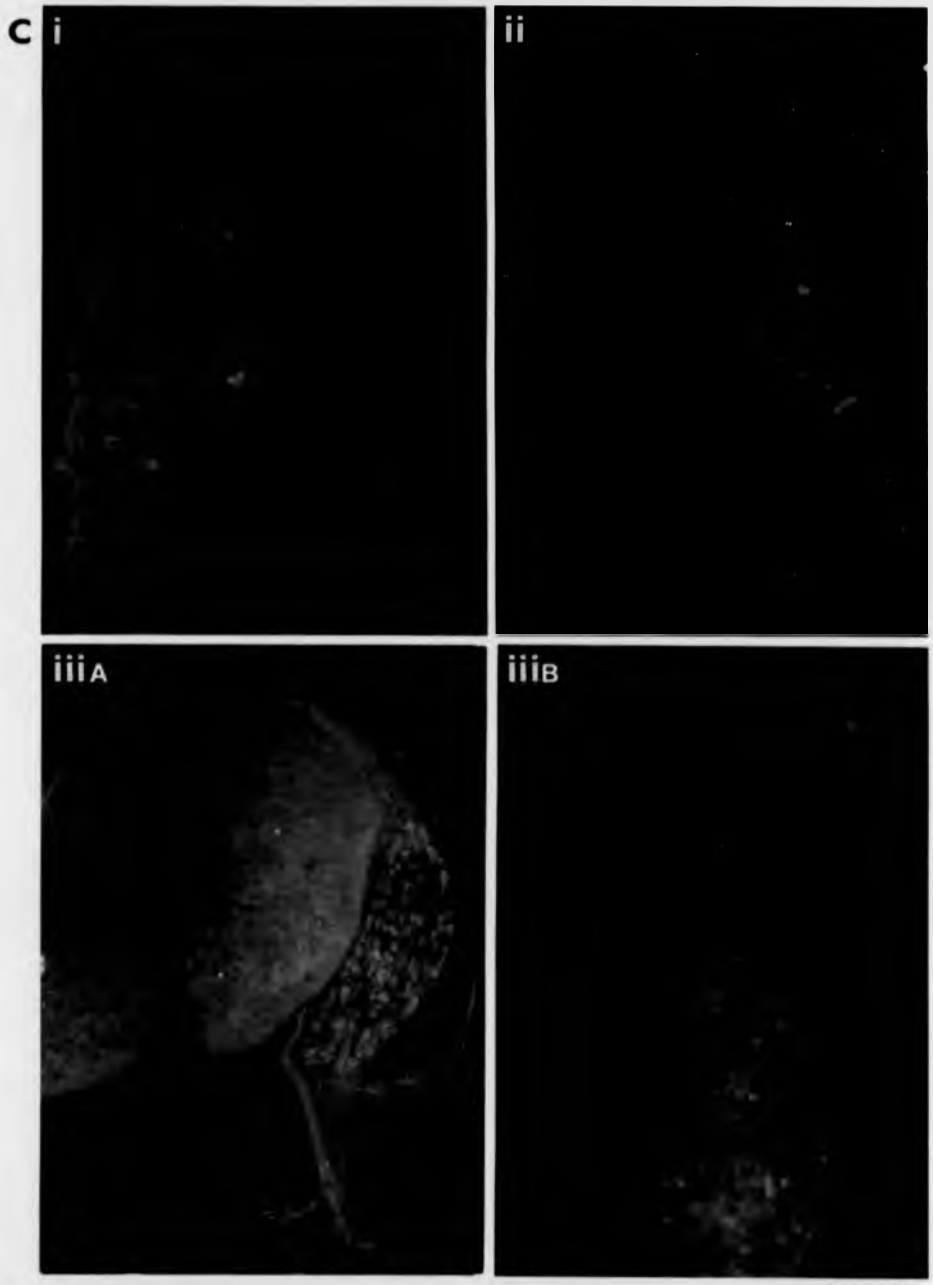
C
i
ii
iiiA
iiiB

7.2.4.5 Expression of endogenous NSE protein at E13.5

NSE protein expression was studied in greater detail in E13.5 embryos because this was the stage at which transgenic embryos were first isolated and examined. Transverse 10μm sections were taken throughout E13.5 mouse embryos and NSE protein was detected as described in section 7.2.4. The protein could be detected in sections of brain at all levels and throughout the neural tube. Examination of brain sections showed that NSE protein was abundant in the midbrain-hindbrain region but restricted to a narrow external bands of cells in the neopallial cortex (future cerebral cortex). Figure 7.11 shows NSE expression in cranial sections of the E13.5 brain. The extent of NSE protein in the midbrain is clear from Figure 7.11(i)A, as only a narrow band of NSE-negative cells can be observed in the ependymal layer surrounding the cerebral aqueduct. Conversely, Figure 7.11(i)C shows only a narrow band of NSE-positive cells on the lateral curve of the cortex. The lamina terminalis (roof of the midbrain) shows a curious pattern of NSE protein expression, with dense crowds of NSE-positive cells following the perimeter of the ependymal layer, as shown in Figure 7.11(i)B. Figure 7.11(ii)A shows the midbrain-hypothalamic boundary, with a greater intensity of NSE protein obvious in the midbrain. NSE protein was present in the hypothalamus, but the domain of expression narrowed towards its ventral extremity (Figure 7.11(ii)B) until, at the lamina terminalis, the protein was restricted to bilateral horns, tapering towards the ventral surface (Figure 7.11(ii)C). More caudal structures of the E13.5 mouse embryo are shown in Figure 7.12. In the brain, NSE protein was observed in the mantle layer (Figures 7.12(i)B and 7.12(i)C) and more abundantly in the marginal layer (Figure 7.12(i)B) but not in the ependymal layer (Figure 7.12(i)C) of the medulla oblongata. Once again, NSE expression in the cerebral cortex was reduced to a thin band of cells (data not shown). The rostral extremity of the spinal cord expressed NSE in a similar pattern to that observed in the medulla (Figure 7.12(i)A). More caudal sections showed a distinctive expression pattern in the spinal cord, characterised by abundant staining throughout the mantle layer, but superabundant staining in the peripheral marginal layer (Figures 7.12(ii)A-C).

Particularly noticeable at this stage of development was the appearance of bilaterally symmetrical spurs of NSE-positive cells in the marginal layer at the dorsal midline (Figures 7.12(ii)A and 7.12(ii)B), further reinforcing the 'pincerlike' image of NSE ontogeny during the development of the spinal cord.

Figure 7.11: Following three pages

Figure 7.11: Expression of NSE protein in mouse embryos at E13.5. a) Size and appearance of mouse embryo at E13.5 showing the positions of sections to which the drawings and photographs in this figure refer. b) Schematic representations of the E13.5 mouse embryo in transverse section (the position of each section is shown in (a)), with anatomical landmarks identified and the photographic field of each photomicrograph (as shown in (c)) marked with a dashed line. c) Photomicrographs of representative transverse sections, magnification x85, showing the expression of NSE protein in the E13.5 mouse embryo. NSE was detected using a polyclonal antiserum specific for human NSE and a secondary FITC-conjugated antiserum specific for rabbit IgG. Photographs were enlarged from slides taken under epifluorescent microscopy using a x20 DIC objective lens.

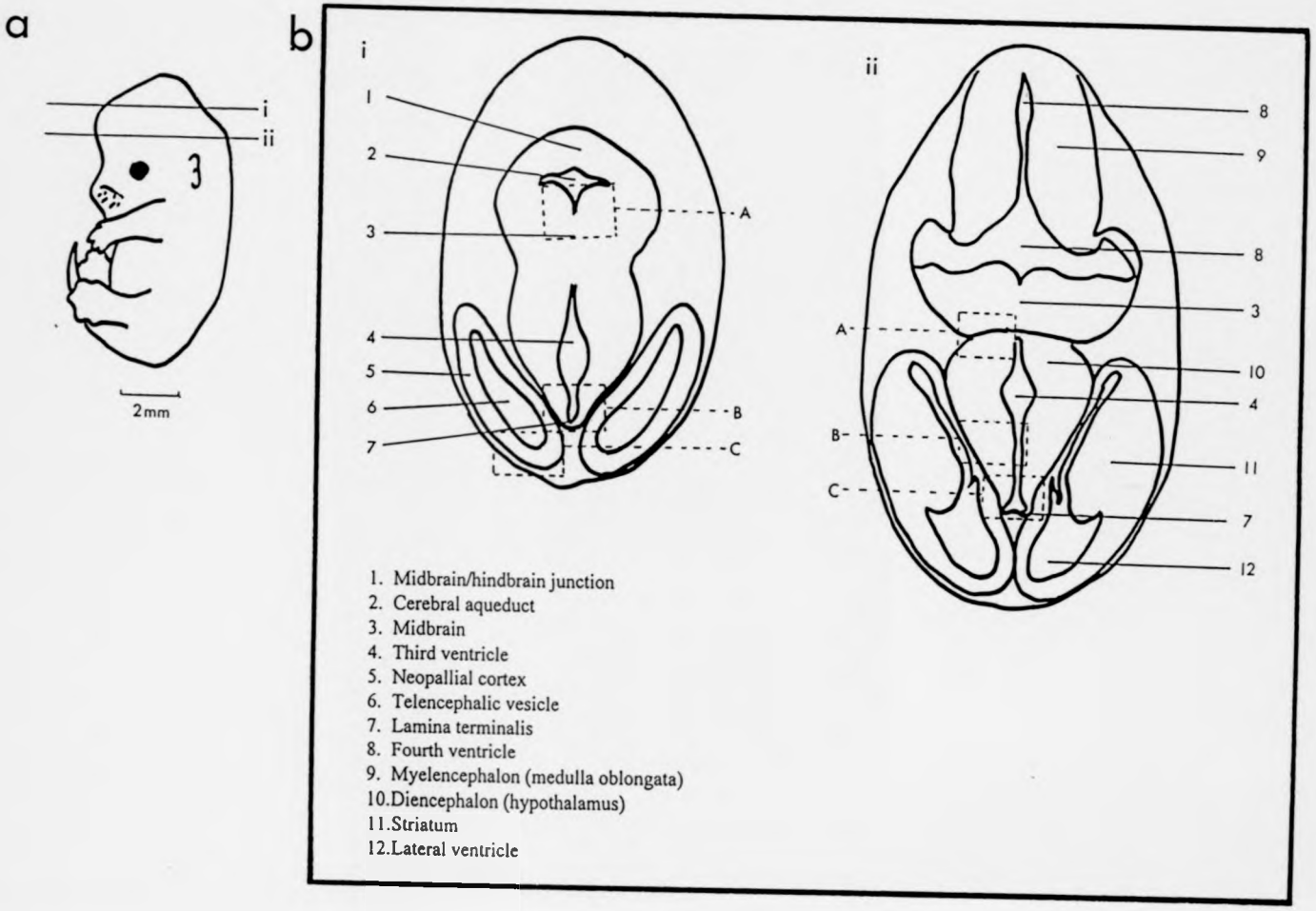

1. Midbrain/hindbrain junction
2. Cerebral aqueduct
3. Midbrain
4. Third ventricle
5. Neopallial cortex
6. Telencephalic vesicle
7. Lamina terminalis
8. Fourth ventricle
9. Myelencephalon (medulla oblongata)
10. Diencephalon (hypothalamus)
11. Striatum
12. Lateral ventricle

ci

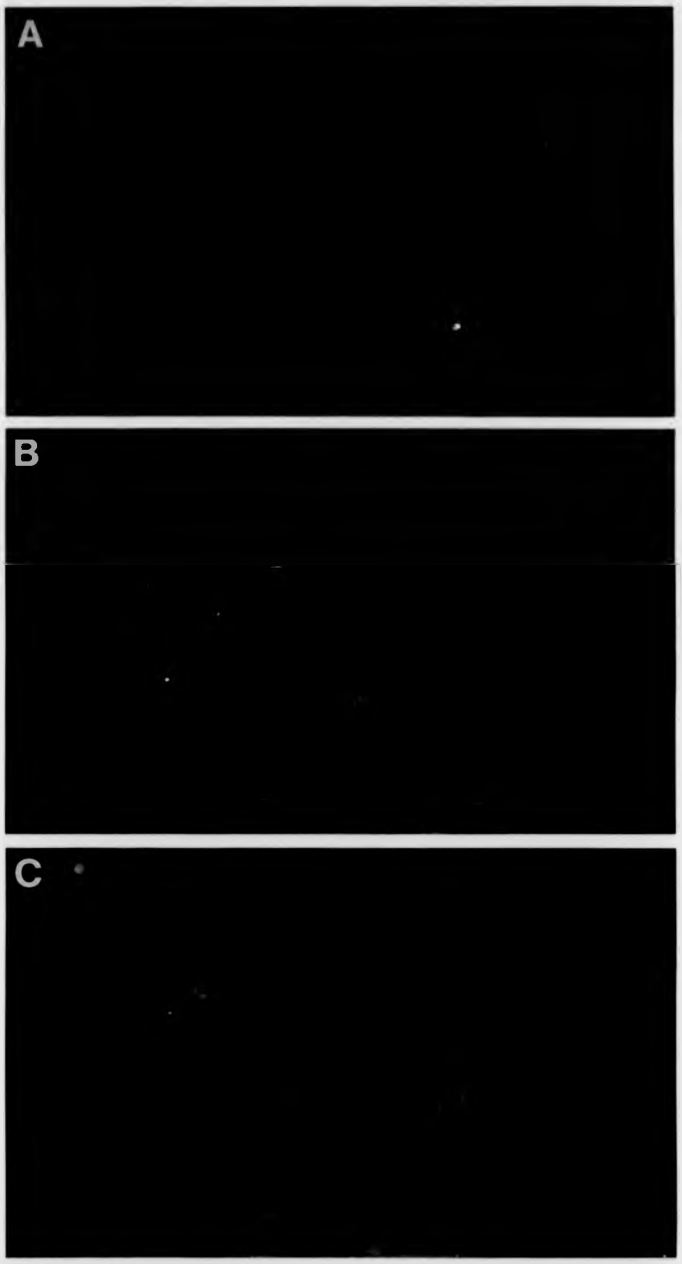

Figure 7.12: Following three pages

Figure 7.12: Expression of NSE protein in mouse embryos at E13.5. a) Size and appearance of mouse embryo at E13.5 showing the positions of sections to which the drawings and photographs in this figure refer. b) Schematic representations of the E13.5 mouse embryo in transverse section (the position of each section is shown in (a)), with anatomical landmarks identified and the photographic field of each photomicrograph (as shown in (c)) marked with a dashed line. c) Photomicrographs of representative transverse sections, magnification x85 (x40 for c(ii)A), showing the expression of NSE protein in the E13.5 mouse embryo. NSE was detected using a polyclonal antiserum specific for human NSE and a secondary FITC-conjugated antiserum specific for rabbit IgG. Photographs were enlarged from slides taken under epifluorescent microscopy using a x10 or x20 DIC objective lens.

a
i
ii
2mm
b
i
ii
A
B
C
1
2
3
4
5
6
7
8
9
10
11
12
13
14
15
1. Spinal cord
2. Central canal
3. Myelencephalon (medulla oblongata)
4. Fourth ventricle
5. Diencephalon (hypothalamus)
6. Third ventricle
7. Cerebellar cortex
8. Lateral ventricle
9. White matter (marginal layer)
10. Grey matter (mantle layer)
11. Ependymal layer
12. Dorsal root nerve
13. Neural lumen (central canal)
14. Dorsal root ganglion
15. Mixed spinal nerve

ci

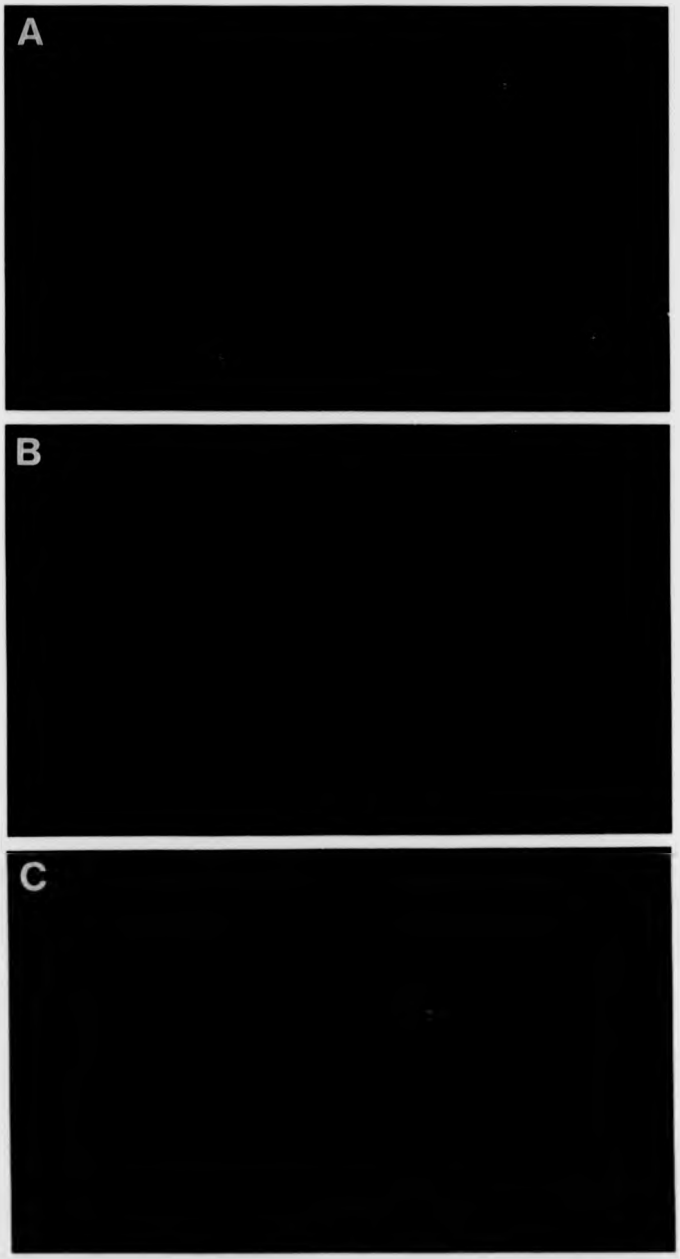

cii

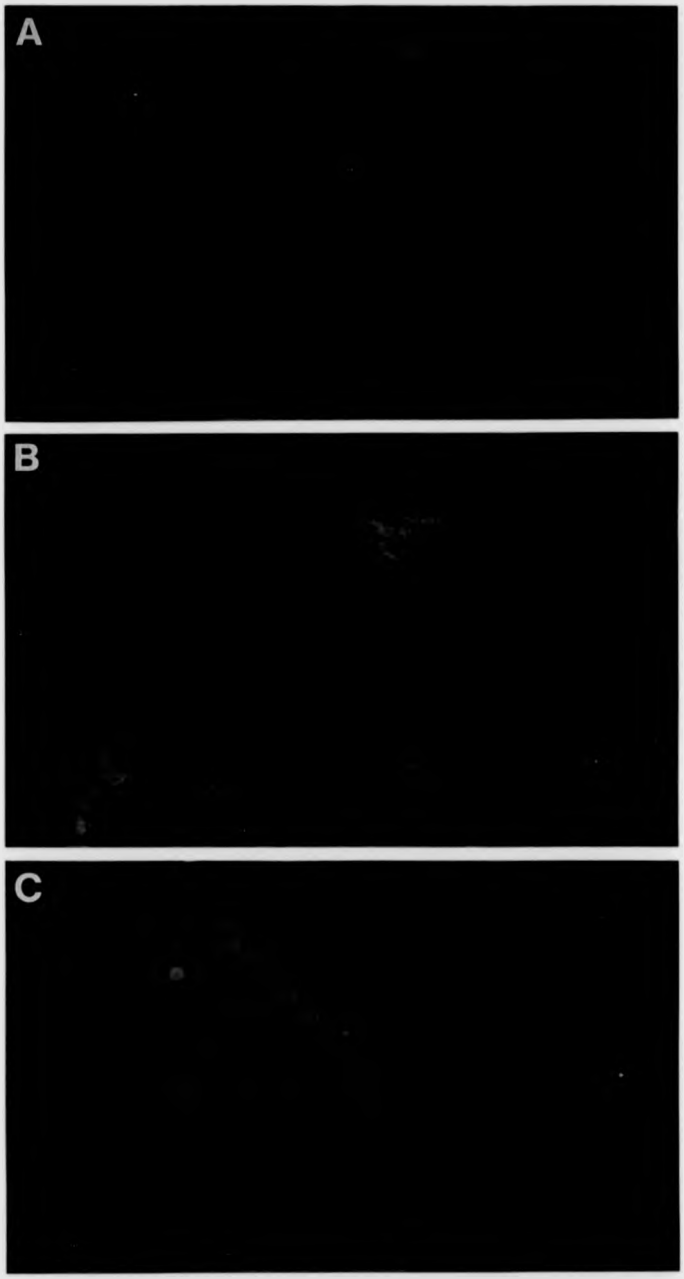

7.2.4.6 Expression of endogenous NSE protein at E14.5

E14.5 was the final stage at which NSE protein expression was investigated. Transverse 10μm sections were taken throughout E14.5 mouse embryos and NSE protein was detected as described in section 7.2.4. NSE protein could be detected in sections of brain at all levels and throughout the neural tube. Examination of brain sections showed that the rostrocaudal gradient of NSE expression was similar at E13.5 and E14.5. Cranial sections showed that most of the midbrain was NSE-positive (Figures 7.13(i)A and 7.13(i)B) whilst in the cerebral cortex, NSE protein was restricted to a peripheral band of cells. It was apparent that, unlike the E13.5 cerebral cortex where NSE-positive cells were restricted to the lateral curve, the E14.5 cortex displayed a complete ring of NSE-positive cell bodies (Figure 7.13(i)C shows the central region of the telencephalon). The epiphysis was NSE-negative (data not shown). The hindbrain structures (medulla oblongata and pons, Figure 7.13(ii)A) once again displayed a more intense level of NSE expression than the hypothalamus (Figures 7.13(ii)A-C). The regression of the NSE expression domain towards the anterior extremity of the hypothalamus was similar in pattern to that observed at E13.5 (Figure 7.13(ii)C). The difference in NSE expression levels between the medulla and hypothalamus could also be observed in more caudal sections (Figure 7.14(i)A). There was extensive staining throughout the medulla, with particularly intense staining in bilateral lanes flanking the narrow ependymal layer (Figure 7.14(i)B). NSE expression was again most intense in the marginal layer, continuous with the rostral extremity of the spinal cord (Figure 7.14(i)A). The expression of NSE in other neural structures was also investigated. In the E14.5 eye, NSE could be detected in the neural retina, but also in the pigmented layer which is not a neuronal structure (Figure 7.14(ii)B). Single NSE-positive cell bodies were also observed in the olfactory neuroepithelium (Figure 7.14(ii)C). Rostral sections of the spinal cord indicated a ventrodorsal gradient of NSE protein (Figure 7.15(i)A). NSE protein was abundant in the ventral marginal layer and ventral mantle layer (ventral grey horn), but the intensity of expression decreased towards the dorsal surface (dorsal grey horn, Figures 7.14(ii)A and 7.15(i)A). NSE

protein was also abundant in the dorsal marginal layer (Figures 7.15(i)A and 7.15(i)B) and the spurs of NSE-positive cells observed at E13.5 (Figure 7.12(ii)A) had fused at the median fissure and ingressed towards the central canal (Figure 7.15(i)A). NSE-positive cell bodies were particularly evident in the dorsal root ganglia (Figures 7.15(i)C and 7.15(i)D) and mixed spinal nerves also stained very intensely (Figure 7.15(i)D).

Figure 7.13: Following three pages

Figure 7.13: Expression of NSE protein in mouse embryos at E14.5. a) Size and appearance of mouse embryo at E14.5 showing the positions of sections to which the drawings and photographs in this figure refer. b) Schematic representations of the E14.5 mouse embryo in transverse section (the position of each section is shown in (a)), with anatomical landmarks identified and the photographic field of each photomicrograph (as shown in (c)) marked with a dashed line. c) Photomicrographs of representative transverse sections, magnification x85, showing the expression of NSE protein in the E14.5 mouse embryo. NSE was detected using a polyclonal antiserum specific for human NSE and a secondary FITC-conjugated antiserum specific for rabbit IgG. Photographs were enlarged from slides taken under epifluorescent microscopy using a x20 DIC objective lens.

a
i
ii
2mm
b
i
ii
1
2
3
4
5
6
A
B
C
7
8
9
10
11
3
6
12
1. Mesencephalic vesicle
2. Midbrain
3. Third ventricle
4. Telencephalic ventricle
5. Epiphysis
6. Cerebral cortex
7. Fourth ventricle
8. Myelencephalon (medulla oblongata)
9. Choroid plexus
10.Pons
11.Diencephalon (hypothalamus)
12.Lateral ventricle

ci

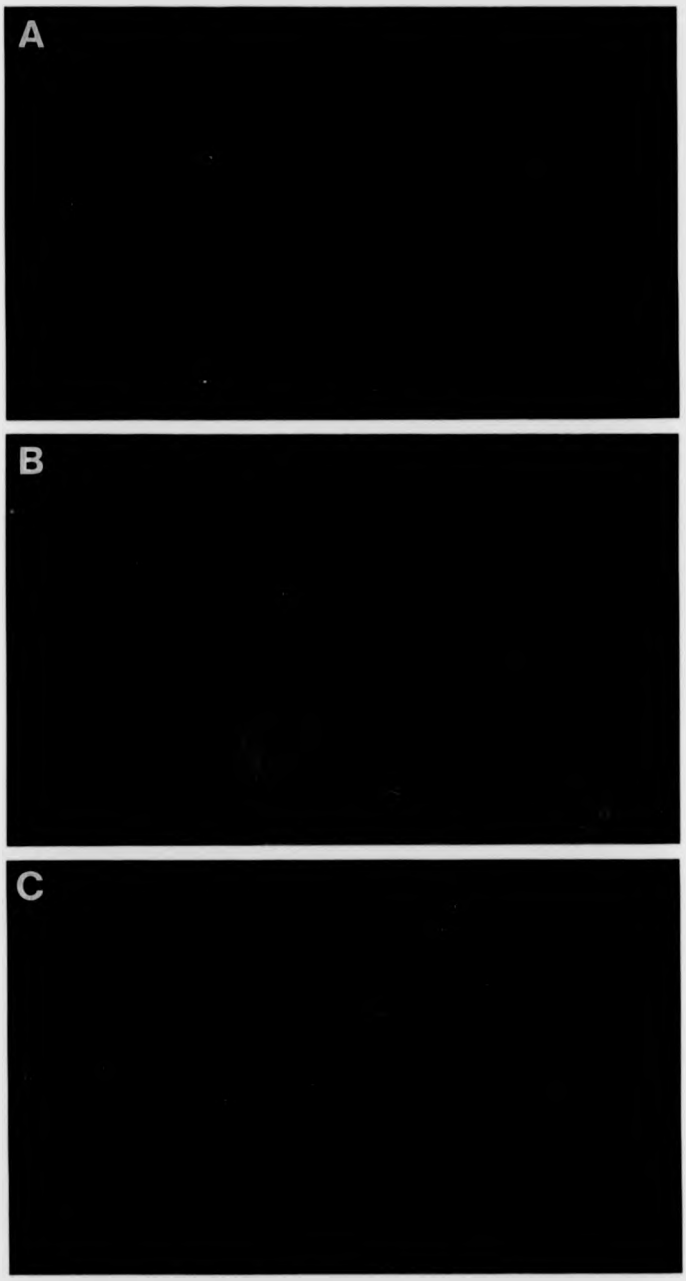

cii

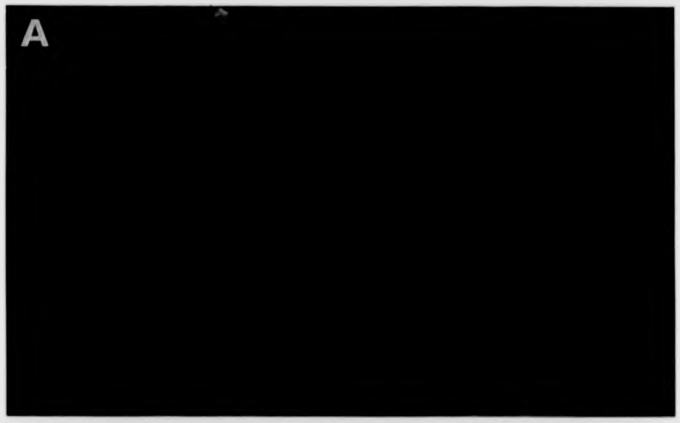

Figure 7.14: Following three pages

Figure 7.14: Expression of NSE protein in mouse embryos at E14.5. a) Size and appearance of mouse embryo at E14.5 showing the positions of sections to which the drawings and photographs in this figure refer. b) Schematic representations of the E14.5 mouse embryo in transverse section (the position of each section is shown in (a)), with anatomical landmarks identified and the photographic field of each photomicrograph (as shown in (c)) marked with a dashed line. c) Photomicrographs of representative transverse sections, magnification x85, showing the expression of NSE protein in the E14.5 mouse embryo. NSE was detected using a polyclonal antiserum specific for human NSE and a secondary FITC-conjugated antiserum specific for rabbit IgG. Photographs were enlarged from slides taken under epifluorescent microscopy using a x20 DIC objective lens.

a
i
ii
2mm
b
i
ii
A
B
C
1
2
3
4
5
6
7
8
9
10
11
12
13
14
1. Spinal cord
2. Central canal
3. Myelencephalon (medulla oblongata)
4. Lateral semicircular canal
5. Diencephalon (hypothalamus)
6. Third ventricle
7. Cerebral cortex
8. Cartilage primordium of vertebra
9. Cochlea
10. Cartilage primordium of splenoid bone
11. Pigmented layer of retina
12. Neural layer of retina
13. Lens
14. Olfactory epithelium

ci

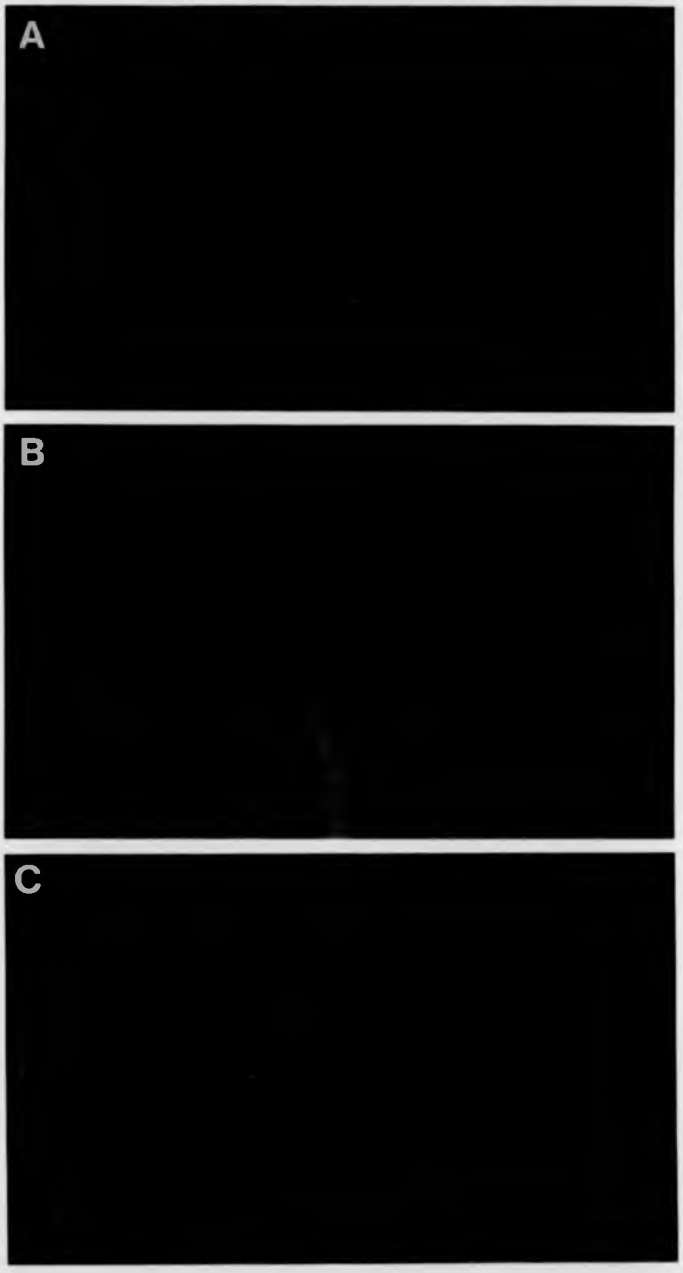

cii

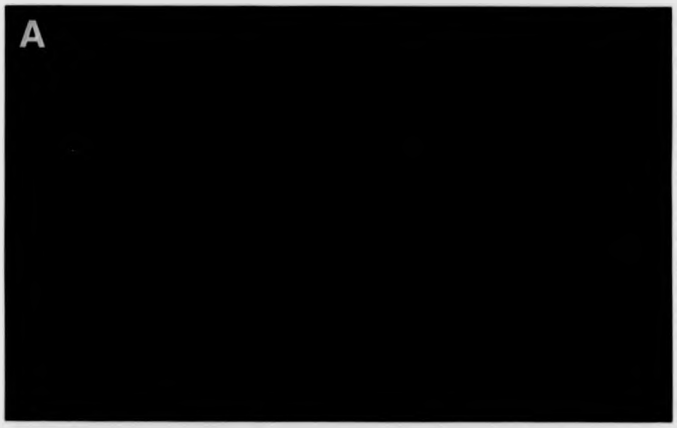

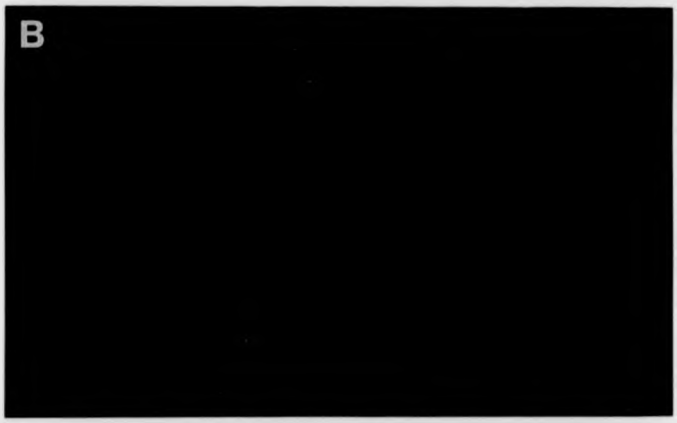

Figure 7.15: Following two pages

Figure 7.15: Expression of NSE protein in mouse embryos at E14.5. a) Size and appearance of mouse embryo at E14.5 showing the positions of sections to which the drawings and photographs in this figure refer. b) Schematic representations of the E14.5 mouse embryo in transverse section (the position of each section is shown in (a)), with anatomical landmarks identified and the photographic field of each photomicrograph (as shown in (c)) marked with a dashed line. c) Photomicrographs of representative transverse sections, magnification x85 (x40 for 15c(i)A), showing the expression of NSE protein in the E14.5 mouse embryo. NSE was detected using a polyclonal antiserum specific for human NSE and a secondary FITC-conjugated antiserum specific for rabbit IgG. Photographs were enlarged from slides taken under epifluorescent microscopy using a x10 or x20 DIC objective lens.

7.3 Generation of *NSE-lacZ* transgenic embryos

7.3.1 Construction of transgenes

Material for the generation of transgenes was derived directly and exclusively from plasmid pNSElacZ, the source of transgenes in the original study of *NSE-lacZ* transgenic mice (Forss-Petter *et al.*, 1990). As a preliminary experiment, pNSElacZ was transfected into permissive NB4-1A3 cells and nonpermissive Ltk- cells to ensure that the construct was capable of expression. The cells were fixed and assayed *in situ* for β-galactosidase activity by staining with X-gal as described in section 4.5.4. NB4-1A3 cells expressed β-galactosidase as expected whilst no such activity was observed in the Ltk- cells (data not shown).

Having demonstrated that the construct was capable of neuron-specific expression in an *ex vivo* context, two transgenes were generated to investigate *NSE* gene regulation *in vivo*. The first transgene contained the 1.8 kbp complete *NSE* regulatory sequence and this was prepared by linearisation of pNSElacZ with *Bam*H I followed by partial digestion with *Eco*R I as shown in Figure 7.16a. This transgene was equivalent in information content to transfection construct pNSE1800CAT. The second transgene contained 255 bp of 5' flanking sequence and was prepared by digestion of the longer transgene with *Xho* I as shown in Figure 7.16b. This construct contained the same amount of regulatory information as the transfection construct pNSE300CAT, which had been shown previously to be capable of full cell type-specific reporter expression *ex vivo*. The purpose of this shorter construct was therefore to determine if the same truncated regulatory information was capable of directing neuron-specific gene expression *in vivo*.

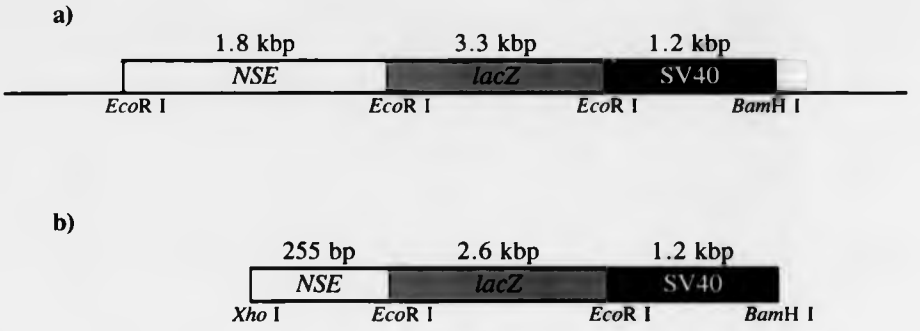

Figure 7.16: Generation of *NSE-lacZ* transgenes. White boxes represent *NSE* gene regulatory sequence, grey boxes represent the *E.coli lacZ* gene, black boxes represent the SV40 polyadenylation site and the line represents pNSElacZ vector sequence. a) TGNSE1800, 6.3 kbp in length, contained the complete *NSE* regulatory sequence and was generated by linearisation of pNSElacZ with *Bam*H I followed by partial digestion with *Eco*R I. b) TGNSE300, 4.75 kbp in length, contained the proximal 255 bp of the *NSE* 5' flanking region and was generated by digestion of TGNSE1800 with *Xho* I.

7.3.2 Generation of transgenic embryos

Transgenic mice were generated by pronuclear microinjection as described in section 4.5.2. No attempts were made to generate transgenic lines, as this type of experiment was not feasible within the time allowed for the project. All microinjections and embryo transfer procedures were carried out by Dr D Stott whose help in this area is gratefully acknowledged.

7.3.3 Identification of transgenic embryos

Transgenic mice were identified by testing genomic DNA for the presence of the *E. coli lacZ* coding region using a PCR-based assay as described in section 4.5.3.2. The detection of a 204 bp PCR product was taken as positive evidence for the successful integration of the transgene as genomic DNA from known nontransgenic mice did not yield such a band. In each experiment, genomic DNA from a known

lacZ-transgenic mouse was used as a positive control and genomic DNA from a wild type mouse was used as a negative control. A second negative control lacking DNA altogether was used to confirm the integrity of the reagents. Figure 7.17 shows a schematic diagram representing the PCR assay and a Polaroid photograph of such an experiment.

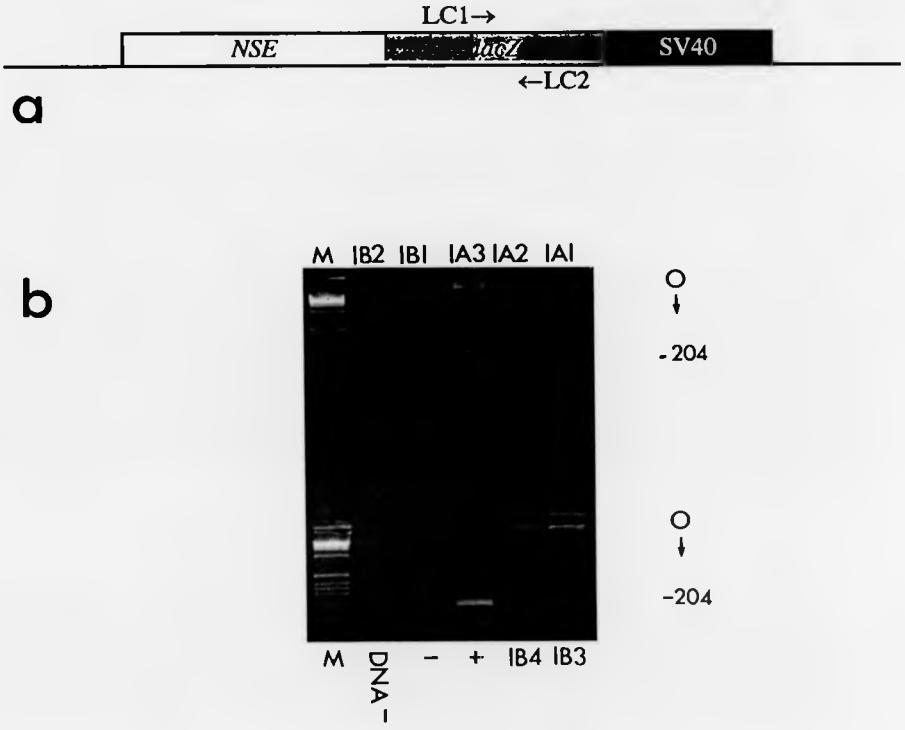

Figure 7.17: PCR test to identify transgenic embryos. a) Diagram showing transgene (white block represents *NSE* regulatory sequence, grey block represents *E. coli lacZ* coding region, black block represents SV40 polyadenylation site) integrated into genomic DNA (line). Primers (LC1 and LC2) anneal to the positions shown and DNA synthesis occurs in the direction of the arrows to yield an expected PCR product of 204 bp in length. b) Polaroid photograph of 1.5% w/v agarose gel showing the results of such an assay. Lanes labelled 1A1, 1A2, 1A3.....1B1, 1B2... etc. refer to individual embryos. The numbering system reflects the experiment number, the mother and the embryo, thus 1B2 refers to the second embryo isolated from the second mother in the first experiment. + indicates positive control, - refers to wild type mouse control and DNA- indicates negative control without DNA. Markers are Gibco BRL 1 kb ladder (M). O = origin.

7.3.4 Analysis of *NSE*-driven reporter expression in transgenic embryos

Embryos were isolated at E13.5 and prepared for X-gal staining as described in section 4.5.4. Transgenic embryos identified by the PCR assay described above were stained for 36-72 hours as wholemount specimens, as described in section 4.5.4, and then cleared in Murray's reagent for observation. The embryos were then washed in methanol to remove the clearing agent, equilibrated through a decreasing methanol/PBS series and finally incubated in PBS with 0.1% v/v Tween 20 for one hour. The embryos were then embedded and cryostat sectioned, as described in sections 4.3.2 and 4.3.3. β-galactosidase was detected using a polyclonal antiserum and cells expressing the protein were revealed using a horseradish peroxidase-conjugated secondary antiserum and diaminobenzidine tetrahydrochloride without metal ion enhancement.

7.3.5 Expression of transgene TGNSE1800

Of nineteen embryos isolated from implanted females, seven were identified as transgenic based on the results of PCR analysis. Of those seven, five were found to express no detectable β-galactosidase, even following prolonged (72hr) staining with X-gal. These embryos were removed from the staining solution, equilibrated by several hour-long washes with PBST, and incubated as wholemount specimens with rabbit anti-β-galactosidase antiserum, followed by detection with horseradish peroxidase-conjugated goat anti-rabbit IgG and diaminobenzidine tetrahydrochloride without metal ion enhancement. Staining was observed, but it was diffuse and nonspecific and similar staining was observed in nontransgenic littermates subjected to the same procedure (data not shown). It was concluded that these mice had failed to express the transgene, either because the transgene itself had been modified upon integration or because of unfavourable position effects, and they were not investigated further.

The remaining two embryos demonstrated weak β-galactosidase activity as shown in Figures 7.18a and 7.18b. Embryo 1A3 demonstrated β-galactosidase activity in the head and thoracic region. In the head, weak blue staining was observed in the dorsal extremity of the midbrain and hindbrain, continuous with the dorsal midline of the neural tube. This staining can be seen clearly from a ventral perspective (Figure 7.18a(i)) as a central blue line running along the rostrocaudal axis. From a lateral perspective (Figure 7.18a(ii)), it can be seen that this line follows the curvature of the hindbrain and stops at the rostral extremity of the neural tube (these structures are shown by a dotted line in Figure 7.18a). No β-galactosidase activity was observed in the neural tube of either embryo. Staining was also observed in other regions of the head: Greater magnification from a lateral perspective showed bilateral blue-stained structures in the basal region of the brain behind each eye (Figures 7.18a(iii) and 7.18a(iv), indicated by thin arrows). It was thought at first that these were the optic nerves. However, unlike endogenous NSE protein, β-galactosidase is not axonally transported and remains restricted to the cell body when expressed in neurons (see Forss-Petter *et al.*, 1990). Thus the optic nerves, which comprise bundles of sensory axons, would be unlikely to display β-galactosidase activity. It was more likely that these structures represented the primordial vestibular apparatuses or cochlea, both of which are found in the otic region of the skull (and, in birds, have been shown to express NSE at an equivalent stage of development (Whitehead *et al.*, 1982)). Weaker staining was observed in the nasopharyngeal region of the head which, from a lateral perspective, appeared nonspecific (Figures 7.18a(ii) and 7.18a(iii)). However, from a ventral perspective, the diffuse staining coalesced into several nodal regions which might well correspond to the facial and cervical ganglia (Figure 7.18a(i), indicated by thin arrows). In the body, staining was observed above the liver, probably representing the dorsal primordium of the pancreas which contains many NSE-expressing endocrine cells (Figure 7.18a(iii), indicated by thick arrow). Embryo 2B1 showed a similar, but weaker and less extensive pattern of β-galactosidase activity (Figure 7.18b). The ventral perspective (Figure 7.18b(i)) shows that the brain lacked β-galactosidase activity completely, except for a small dorsicentral region in the hindbrain at the rostral extremity of the neural tube (indicated by thick arrow). The

bilateral structures in at the base of the brain, appearing to extend towards the otic regions of the head were also stained (Figures 7.18b(i), 7.18b(ii) and 7.18b(iii), indicated by thin arrows) and there was a further, weakly stained region in the roof of the thoracic cavity (Figure 7.18b(ii), indicated by broken arrow).

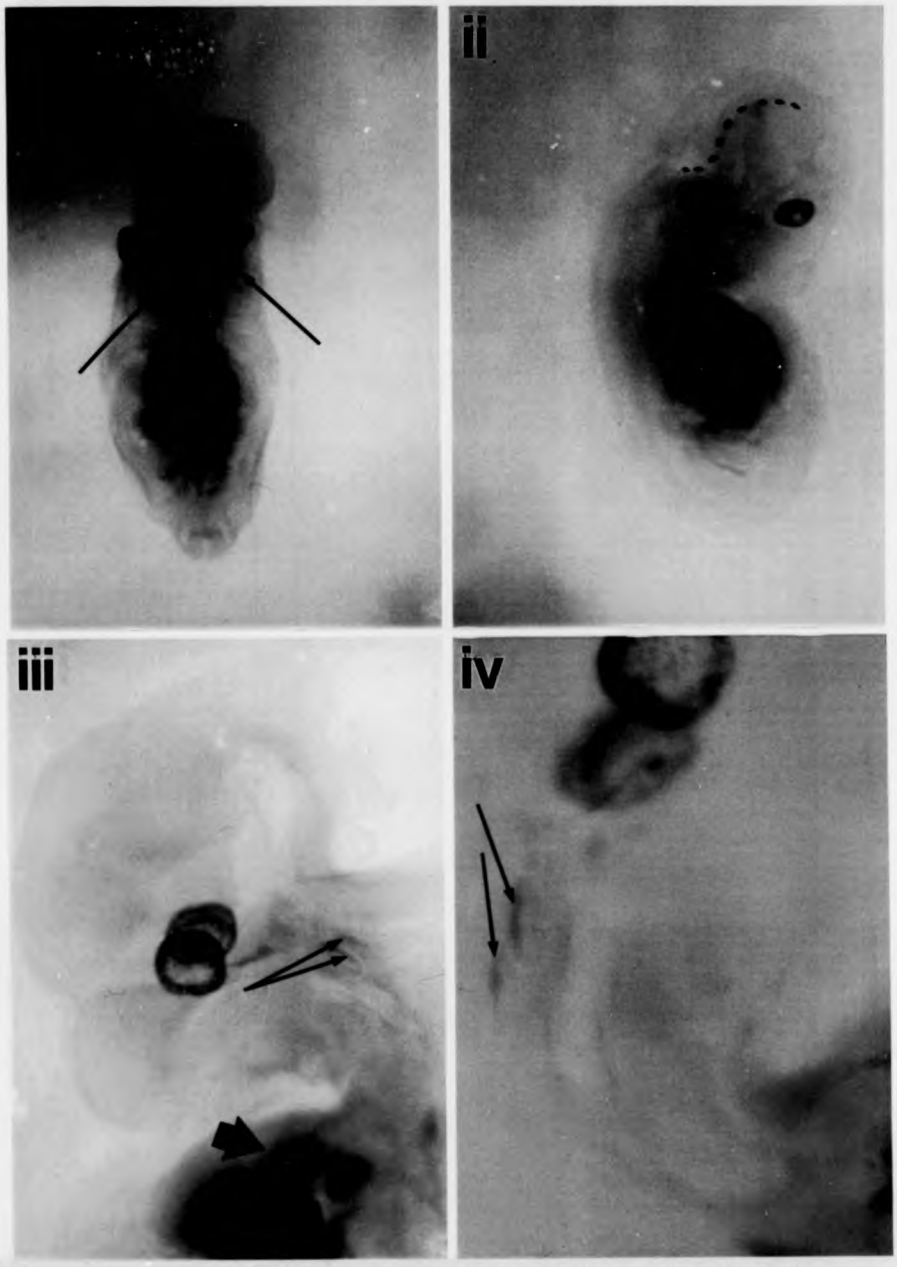

Figure 7.18a: Spatial expression of TGNSE1800 in embryo 1A3 (i) ventral perspective, (ii) lateral perspective, x5; (iii) lateral perspective of head, x10; (iv) lateral perspective of otic region, x15. Arrows indicate specific regions of the embryo staining positive for β-galactosidase (these regions are discussed in the text). Dotted line traces *lacZ* expression in dorsal midline of midbrain and hindbrain. Embryo is shown poststaining, cleared with Murray's reagent.

Figure 7.18b: Spatial expression of TGNSE1800 in embryo 2B1 (i) ventral perspective, (ii) lateral perspective, x5; (iii) lateral perspective, x7. Arrows indicate specific regions of the embryo staining positive for β-galactosidase (these regions are discussed in the text). Embryo is shown poststaining, cleared with Murray's reagent.

7.3.6 Comparison of transgene and endogenous gene expression

The TGNSE1800 transgene was expressed in only two out of seven transgenic embryos and in these two, the level of β-galactosidase activity was weak. Comparison of transgene and endogenous gene expression was carried out by taking cryostat sections of the stained transgenic embryos. No β-galactosidase activity was detected in sectioned embryos (data not shown), probably indicating that the level of enzyme activity was too low to be detected in thin tissue segments. The sections were subjected to immunohistochemical staining using a polyclonal antiserum raised against recombinant *E. coli* β-galactosidase and positive cells were revealed using a secondary horseradish peroxidase-conjugated goat anti-rabbit IgG followed by staining with diaminobenzidine tetrahydrochloride. As expected, few β-galactosidase-positive cells were revealed by this procedure and those that were corresponded to the regions displaying β-galactosidase activity in the wholemount specimens. In embryo 1A3, β-galactosidase-positive cells were observed in the midbrain and hindbrain at the dorsal midline (Figure 7.19a). Other regions of the brain contained no detectable staining cells, and as an example, a lateral segment of the medulla oblongata, which displays high levels of endogenous NSE protein (see Figure 7.12(ii)) is shown to be completely devoid of β-galactosidase-expressing cells in Figure 7.19b. Analysis of sections also ailowed expression of the *NSE-lacZ* transgene to be investigated in the eye: in wholemount specimens, the dark pigmentation of the retina prevented observation of blue stained cells. However, the eye also displayed a lack of β-galactosidase expression (Figure 7.20a). The paired β-galactosidase-positive structures in the basal region of the brain were of particular interest. Transverse sections taken throuh this region of the head revealed a bilateral and distinct line of positive cells at the ventral wall of the neural componenet of the pituitary gland, whilst the bilobar anterior pituitary contained no positive cells. The hypothalamus, lying dorsally to the pituitary gland, also contained no positive staining cells. These data are presented in Figure 20b.

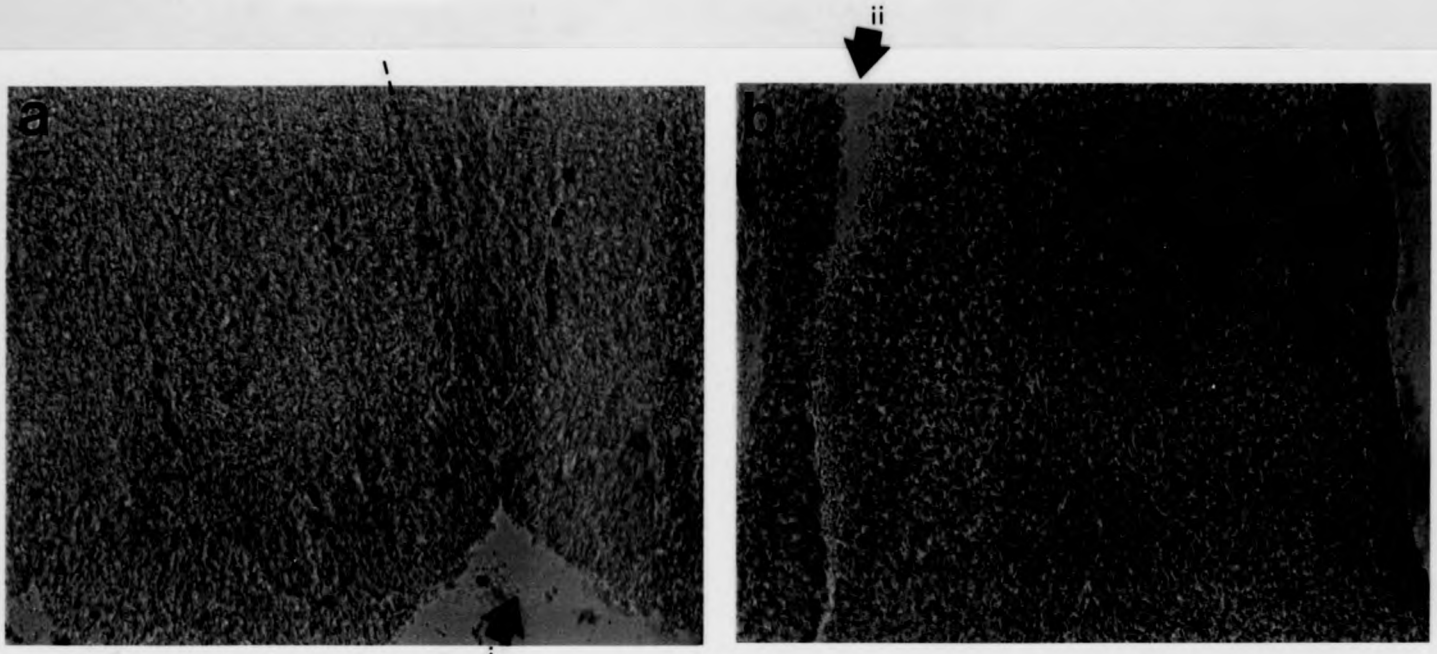

Figure 7.19: Transverse cryostat sections of a) midbrain and b) medulla oblongata (x85) taken from embryo 1A3 and stained immunologically for β-galactosidase protein using a polyclonal antiserum. Signal was detected using a horseradish peroxidase-conjugated secondary antiserum and staining was carried out using diaminobenzidine tetrahydrochloride. On the upper sheet, dashed line represents dorsal midline of the midbrain and arrows indicate (i) cerebellar aqueduct, (ii) fourth ventricle and (iii) alar plate of the medulla oblongata. Photographs were taken under phase contrast microscopy using a x20 objective.

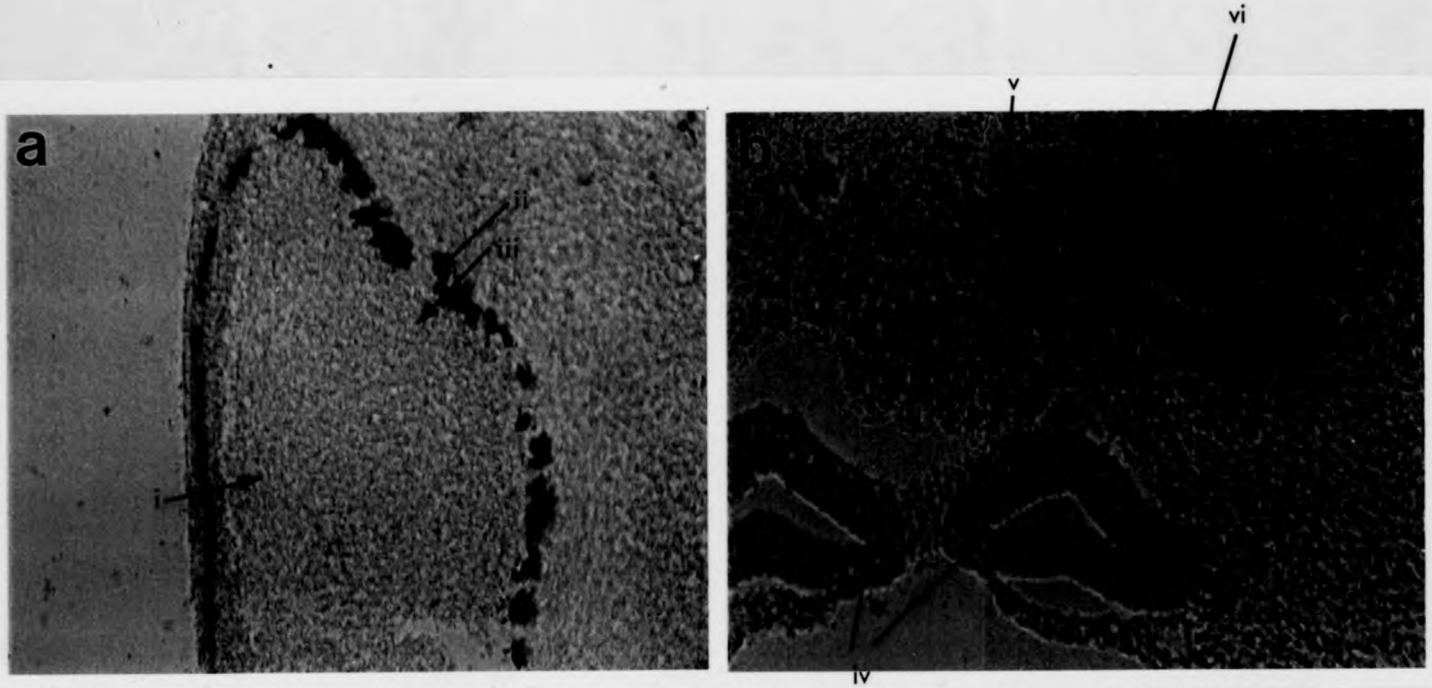

Figure 7.20: Transverse cryostat sections of a) the eye and b) basal region of brain (x85) taken from embryo 1A3 stained immunologically for β-galactosidase protein using a polyclonal antiserum. Signal was detected using a horseradish peroxidase-conjugated secondary antiserum and staining was carried out using diaminobenzidine tetrahydrochloride. On the upper sheet, arrows indicate (i) lens, (ii) pigmented layer of retina, (iii) neural layer of retina, (iv) bilobar structure of the anterior pituitary, (v) ventral wall of the neural component of the pituitary and (vi) the hypothalamus. Photographs were taken under phase contrast microscopy using a x20 objective.

7.3.7 Conclusions from the transgenic studies

The transgenic studies were disappointing because high levels of β-galactosidase staining were not observed, and this inability to repeat the results of previous studies using the same material prevented shorter constructs from being used. It is clear that in both previous studies of *NSE* transgenic mice, lines were used instead of single embryos in order to generate a large amount of material for analysis. The success rate was far from high, however, and it is possible that the generation of transgenic lines is the only way to push forward this investigation. Forss-Petter and coworkers generated eighty lines, of which eight successfully integrated a transgene (Forss-Petter *et al.*, 1990). Of those eight, one contained a partial insertion and was discarded whilst the remianing seven demonstrated variable levels of reporter expression. Only two demonstrated panneuronal expression and these were chosen for further analysis. Although strong, panneuronal transgene expression was not observed in this project, the construct driven by the complete *NSE* regulatory sequence appeared to be expressed in certain neuronal structures such as the pituitary gland, dorsal midline of the brain, and ganglia. It would be interesting to compare the expression of *lacZ* in transgenic animals containing shorter regions of the *NSE* 5' flanking region, however the variability observed in the patterns of transgene expression in single embryos may indicate that the 1.8 kbp *NSE* flanking sequence is malleable and very subject to position effects. Possible solutions to this problem and ways to further the investigation are discussed in Chapter 9.

Chapter 8 - Preliminary studies of protein-DNA interaction in the NSE *5' flanking region*

8.1 Chapter summary

The original aims of the project were to investigate *NSE* gene regulation using both *ex vivo* and *in vivo* analysis. From these opposite but complementary approaches, it was hoped that regions in the 5' flanking sequence could be identified which were responsible for cell type-specific and inducible gene expression, and that these could be subject to further analysis *in vitro*.

As discussed in the previous chapter, limited transgene expression ordained that the *in vivo* analysis was not pursued very far. However, the *ex vivo* analysis yielded a substantial amount of data concerning the regulation of *NSE* in various permissive and nonpermissive cell lines. The pattern of gene regulation emerging from these studies was complex, and different cell lines of the same type did not produce consistent trends of expression. This phenomenon probably reflected the lack of suitable cell lines, a problem discussed at some length in Chapter 9.

Notwithstanding these complications, the results of transient transfection studies revealed a number of regions within the 5' flanking sequence which, based upon their effects upon reporter gene expression in transfected cells, could contribute to the regulation of *NSE*. The regions demonstrating the most profound effects were chosen for preliminary analysis *in vitro*.

8.2 Summary of transfection data and choice of regions for *in vitro* analysis

The results of preliminary experiments described in the first part of Chapter 6 suggested that the proximal 255 bp of the *NSE* 5' flanking sequence plus the entire first (noncoding) exon was sufficient for cell type-specific gene expression. Although later experiments identified more upstream regions with putative regulatory roles in individual cell lines, it was this proximal element which drew initial attention, suggesting it should be truncated further.

Figure 8.1 summarises the results of transfection experiments involving the extremely truncated constructs pNSE300CAT, pNSE120CAT, pNSE95CAT and pNSE65CAT. These experiments showed that the proximal fragment of the *NSE* regulatory sequence

could be divided into four regions. Region A extended between the *Xho* I site at position -255 and the *Pst* I site at position -120. Region B extended from this *Pst* I site to the *Sma* I site at position -95. Region C extended from this *Sma* I site to the *Nar* I site at position -65 and included the TATA-like box thought to be required for basal transcriptional initiation of the *NSE* gene. Finally, region D extended from the *Nar* I site at position -65 to the beginning of the first intron. When region A was removed, there was a proportionally similar upregulation of reporter gene expression in Ltk- and Neuro-2A cells, slightly greater in the case of Ltk- cells, whilst in PC12 cells, deletion of region A caused a dramatic reduction in the levels of CAT activity. There appeared to be no significant effect when this element was deleted in transfected HeLa or P19 cells, although the very low levels of reporter activity observed in the former and the stem cells of the latter might have precluded such effects from being noticed. On aggregate, a moderate rise in reporter activity was observed in NB4-1A3 cells upon removal of region A, although the error range in this series of transfections suggested that further experiments were necessary to clarify the exact role of this element. These results indicated that region A could be important in Ltk-, Neuro 2A and PC12 cells and that these lines should be selected for further *in vitro* analysis. Region A was an ideal size for analysis by gel retardation assay and this approach was duly chosen (Dent and Latchman, 1993). The proximal 120 bp of the *NSE* promoter was able to confer high level reporter gene expression in P19 neurons and Neuro-2A cells but not in PC12 or NB4-1A3 cells. A higher level of reporter activity was also observed in Ltk- cells but not in HeLa cells nor P19 stem cells. Removal of region B had no significant effect in P19 neurons nor in PC12 cells (although the former demonstrated high levels of gene expression whilst the latter did not), nor was any significant effect observed in NB4-1A3 cells, HeLa cells or P19 stem cells. There was, however, an approximate 25% drop in reporter activity in both Ltk- and Neuro-2A cells. Removal of region C reduced reporter expression to background levels in all cell lines indicating the presence of a sequence critical for transcriptional initiation in this 30 bp segment. Although not rigorously tested, this sequence was probably the TATA-like box, which is known to be the centre at which the transcriptional complex forms in many, if not most, eukaryotic protein-encoding genes (Alberts *et al.*, 1994). The moderate to high levels of reporter expression observed in some of the cells lines when only 30 bp of 5' flanking sequence remained upstream of the TATA-like box suggested one of two possibilities. Either the elements responsible for cell type specific expression overlapped the TATA box, as they were found to do in the peripherin gene (Desmaris *et al.*, 1994) or such elements lay downstream of the TATA-box and removal of region C, whilst leaving these elements intact, switched off gene expression simply by preventing facilitation of the

basal transcriptional initiation process. Whatever the explanation, these results suggested that any analysis of the very proximal 5' flanking region and exon sequences would have to be undertaken at the nucleotide level. Such experiments would involve transfection of constructs altered by *in vitro* mutagenesis to generate single base substitutions and linker scanning mutations, and the investigation of protein-DNA interactions by *in vitro* footprinting and, if necessary, by *in vivo* footprinting and methylation interference assays.

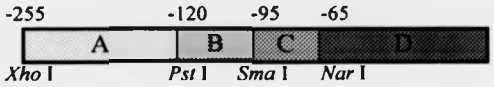

Properties: High level reporter gene expression in all permissive lines, minimal expression in nonpermissive lines.

Properties: High level reporter gene expression in P19 neurons, Neuro-2A and Ltk- cells, minimal expression in PC12 cells, P19 stem cells, HeLa cells, NB4-1A3 cells.

Effects of deletion: Upregulation in Ltk- cells and Neuro-2A cells, Dramatic downregulation in PC12 cells, no significant effect in P19 stem cells and neurons, HeLa cells, NB4-1A3 cells.

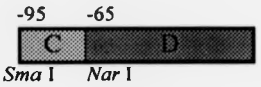

Properties: High level reporter gene expression in neurons, moderate levels in Ltk- cells and Neuro-2A cells, minimal levels in other cell types.

Effect of deletion: Approximate 25% drop in reporter gene activity in Ltk- cells and Neuro-2A cells. No significant effect in other cell types.

Properties: Shutdown of gene expression in all cell lines.

Effect of deletion: Presumed to remove element critical for basal transcriptional initiation.

Figure 8.1: Summary of the results of transfection experiments involving the most truncated *NSE-cat* constructs. Regions are defined as A, B, C and D with the flanking restriction endonuclease sites and position with respect to the transcriptional start site shown. The properties of each segment are described and the effects of each deletion discussed.

8.3 Preliminary analysis of region A by gel retardation assay

To determine whether region A could bind to proteins in extracts of cell lines wherein it had been shown to be of functional importance, a 135 bp *Xho* I - *Pst* I restriction fragment corresponding to this region was isolated from construct pNSE1800CAT and labelled at the *Xho* I cohesive end by end filling. This fragment was incubated with extracts of proliferating Ltk-, undifferentiated PC12 and NGF-treated PC12 cells as described in section 4.6.3 and the reaction products were resolved by nondenaturing polyacrylamide gel electrophoresis as described in section 4.6.4.

For preliminary analysis, incubations were carried out with increasing concentrations of nonspecific competitor DNA to titrate out the ubiquitous and abundant proteins which bind to DNA either without sequence specificity or to free ends (Dent and Latchman, 1993). Figure 8.2 shows the results of such analysis and indicates the presence of at least three binding complexes in Ltk- cells but no specific binding complexes in PC12 cells. This was surprising because the effect of removing region A in the PC12 transfection experiments was very clear, indicating the presence of a strong neuronal enhancer. The binding conditions were modified in an attempt to optimise binding in extracts of PC12 cells. Firstly, alternative nonspecific competitor DNAs were used with no improvement. Figures 8.3 and 8.4 show the results of using calf thymus DNA and poly[dI.dC] (polydeoxyinosinic-deoxycytidylic acid) respectively. In further experiments (results not shown), the binding reaction was carried out at room temperature instead of the usual 30°C and probe was added to the reaction immediately rather than following an initial 10 minute incubation. These steps were reported to affect the binding specificity of protein-DNA complexes and allow optimisation of binding conditions (H. Taylor, pers. comm.), however, neither of these modifications improved the binding conditions although the temperature change did cause the autoradiograph to appear fuzzy and ill-defined (results not shown).

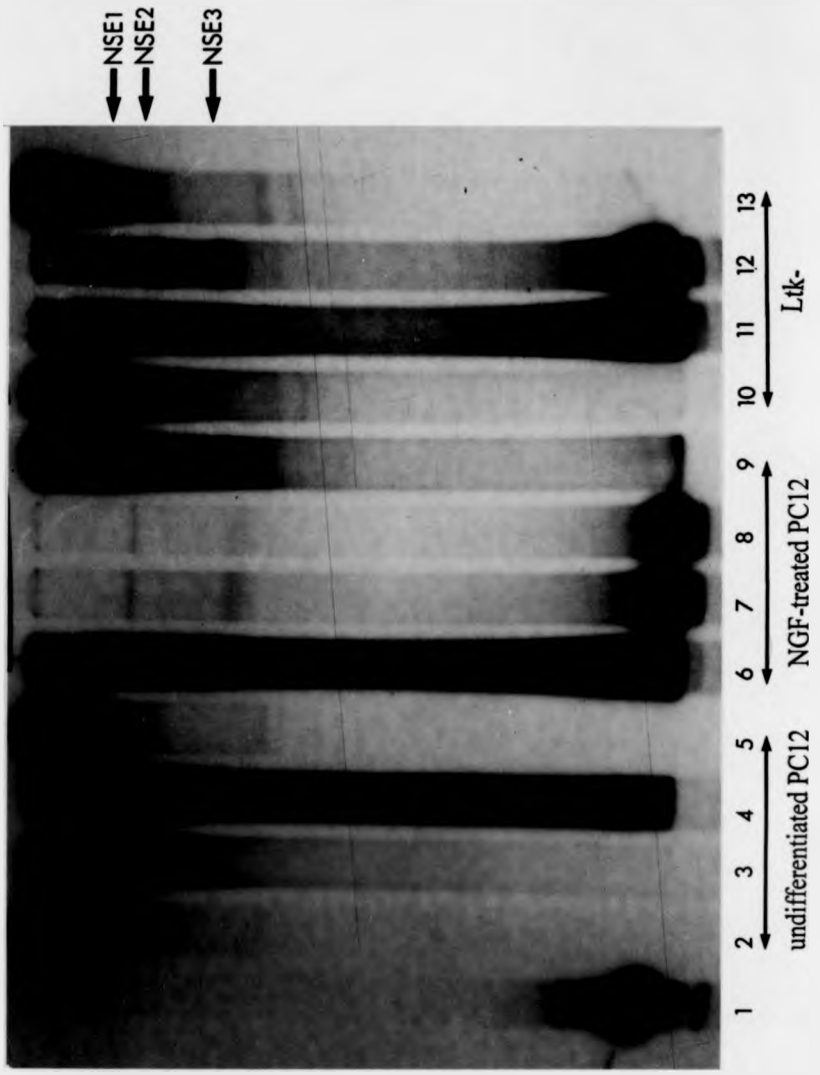

Figure 8.2: Preliminary analysis of DNA-protein interaction in region A of the *NSE* 5' flanking region using extracts of Ltk- and PC12 cells. Lanes were loaded equally for total protein (4 µg) and contained 1 ng probe. Lane 1 - probe in isolation. Lanes 2-5 contained extract of undifferentiated PC12 cells, lane 2 including 1µg sonicated salmon sperm DNA, lane 3 including 2.5µg sonicated salmon sperm DNA, lane 4 including 5µg sonicated salmon sperm DNA and lane 5 lacking nonspecific competitor. Lanes 6-9 contained extract of PC12 cells differentiated with NGF, lane 6 including 1µg sonicated salmon sperm DNA, lane 7 including 2.5µg sonicated salmon sperm DNA, lane 8 including 5µg sonicated salmon sperm DNA and lane 9 lacking nonspecific competitor. Lanes 10-13 contained extract of Ltk- cells, lane 10 including 1µg sonicated salmon sperm DNA, lane 11 including 2.5µg sonicated salmon sperm DNA, lane 12 including 5µg sonicated salmon sperm DNA and lane 13 lacking nonspecific competitor. The positions of binding complexes, labelled NSE1, NSE2 and NSE3, are indicated by arrows.

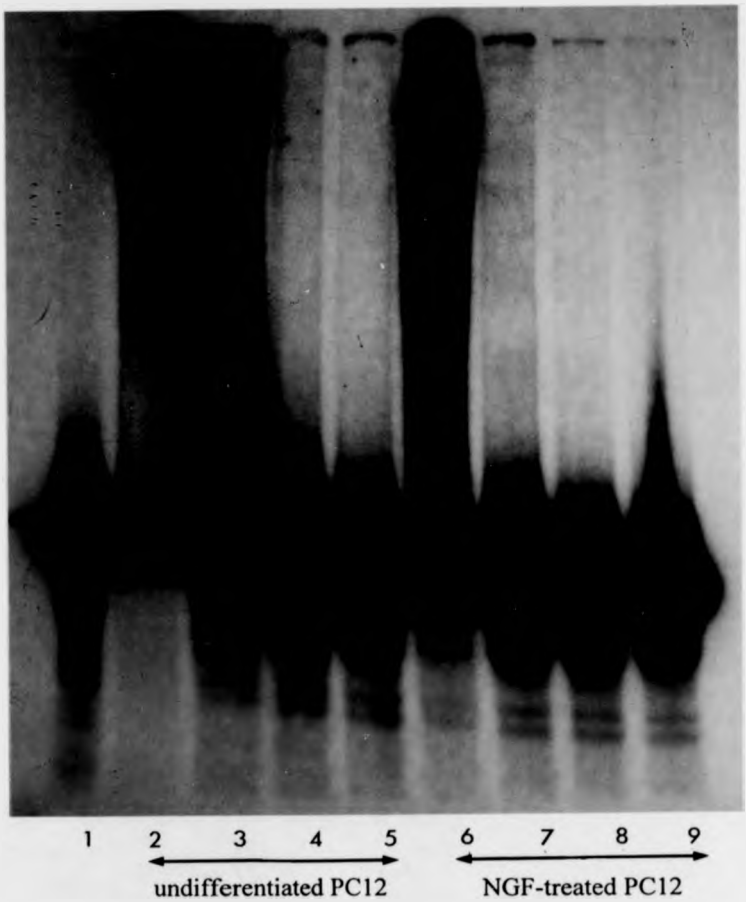

Figure 8.3: Attempts to identify protein-DNA binding activity with region A of the *NSE* 5' flanking region in PC12 cells. Lanes were loaded equally for total protein (4 μg) and contained 1 ng probe. Lane 1 - probe in isolation. Lanes 2-5 contained extract of undifferentiated PC12 cells, lane 2 lacking nonspecific competitor and lanes 3-5 including 1μg, 2.5μg and 5μg respectively of calf thymus DNA. Lanes 6-9 contained extract of PC12 cells differentiated with NGF, lane 6 lacking nonspecific competitor and lanes 7-9 including 1μg, 2.5μg and 5μg respectively of calf thymus DNA. No binding complexes were observed.

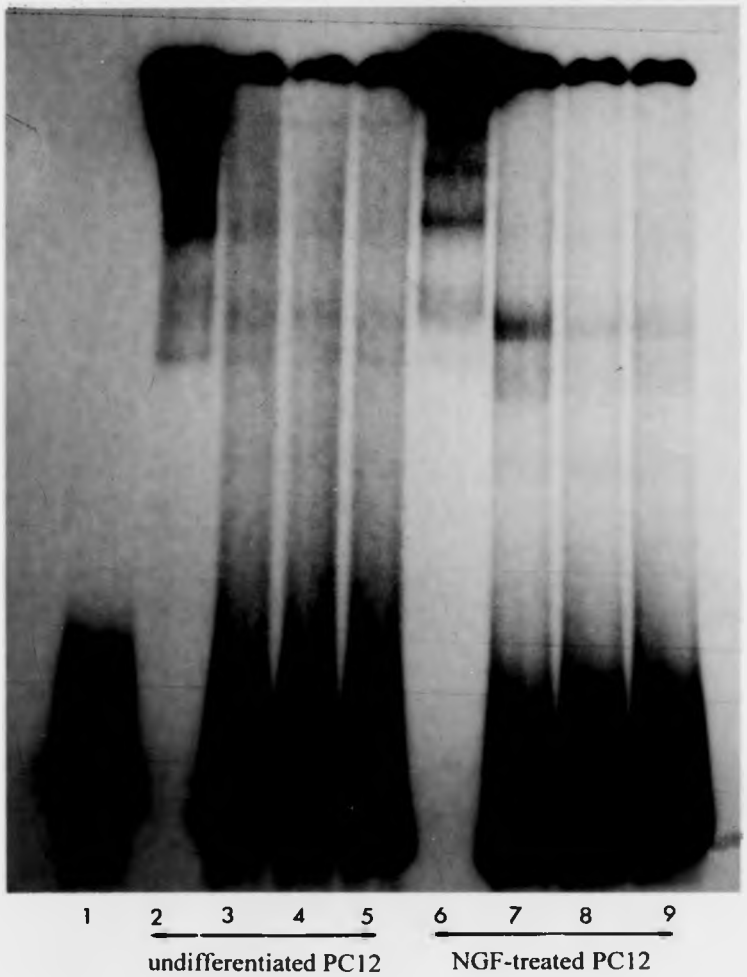

Figure 8.4: Further attempts to identify protein-DNA binding activity with region A of the *NSE* 5' flanking region in PC12 cells. Lanes were loaded equally for total protein (4 μg) and contained 1 ng probe. Lane 1 - probe in isolation. Lanes 2-5 contained extract of undifferentiated PC12 cells, lane 2 lacking nonspecific competitor and lanes 3-5 including 1μg, 2.5μg and 5μg respectively of poly[dI.dC] DNA. Lanes 6-9 contained extract of PC12 cells differentiated with NGF, lane 6 lacking nonspecific competitor and lanes 7-9 including 1μg, 2.5μg and 5μg respectively of poly[dI.dC] DNA. No binding complexes were observed.

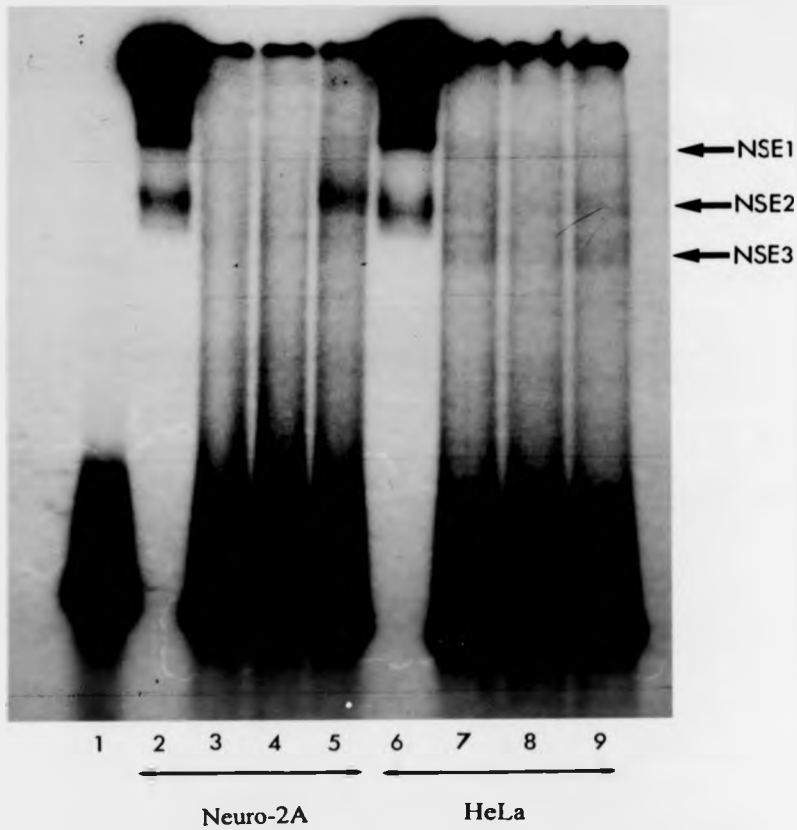

Figure 8.5: Preliminary analysis of DNA-protein interaction in region A of the *NSE* 5' flanking region using extracts of Neuro-2A and HeLa cells. Lanes were loaded equally for total protein (4 µg) and contained 1 ng probe. Lane 1 - probe in isolation. Lanes 2-5 contained extract of Neuro-2A cells, lane 2 lacking nonspecific competitor, lane 3 including 1µg sonicated salmon sperm DNA, lane 4 including 2.5µg sonicated salmon sperm DNA and lane 5 including 5µg sonicated salmon sperm DNA. Lanes 6-9 contained extract of HeLa cells, lane 6 lacking nonspecific competitor, lane 7 including 1µg sonicated salmon sperm DNA, lane 8 including 2.5µg sonicated salmon sperm DNA and lane 9 including 5µg sonicated salmon sperm DNA. The positions of binding complexes, labelled NSE1, NSE2 and NSE3, are indicated by arrows.

Region A was also shown to be active in Neuro-2A cells but not in HeLa cells. these two cell lines were subjected to gel retardation analysis as described above, with the latter acting as a negative control. The surprising result from this analysis (as shown in Figure 8.5) was that whilst no binding activity could be detected with Neuro-2A cell extracts, three binding complexes were observed in the HeLa cell extracts at a similar position to those observed in the Ltk- cell extracts.

8.4 Further analysis of binding complexes on region A in nonneuronal cells

Three similar binding complexes were observed in the same region of the *NSE* promoter in two nonneuronal cell lines. This suggested a common regulatory mechanism was operating in nonneuronal cells. To confirm that the complexes bound specifically to region A, competition experiments were carried out in which specific fragments, one corresponding to region A and one bearing no resemblance to region A were added to the binding reaction. This is the standard procedure used to determine the specificity of binding to a given fragment of DNA . The results, shown in Figures 8.6a and 8.6b, indicated that in both cell lines, the binding complexes observed were specific to region A. In the presence of 1x unlabelled region A, there was little specific reduction in the abundance of the three binding complexes. Similar results were obtained with the irrelevant specific competitor M.OCT, an unrelated fragment of similar length to the probe, which contained a nonfunctional octamer site. In the presence of 10x unlabelled region A, a marked decrease in the abundance of all three binding complexes was noted, but this effect was not observed in the presence of 10x M.OCT (Figures 8.6a and 8.6b, lanes 7 and 10). Of the three complexes, NSE2 was present in the lowest amounts and was almost totally outcompeted by 10x unlabelled region A. Complexes NSE1 and NSE3 were more abundant and were still visible, albeit at a much lower level, in the presence of 100x unlabelled region A. However, the abundance of the three complexes was unaffected by 100x M.OCT (Figures 8.6a and 8.6b, lanes 8 and 11).

To confirm that specific competition could completely remove the binding complexes, the experiment was repeated using 200x competition in addition to the original conditions. This experiment was carried out using a fresh batch of Ltk- and HeLa protein extracts. The results, shown in Figures 8.7a and 8.7b indicated that in the presence of 200x unlabelled region A, all three binding complexes were absent whilst in the presence of 200x M.OCT the abundance of the complexes were unchanged. This experiment did show, however, that NSE1 was far more prevalent than the other

two complexes in freshly prepared protein extracts compared to those prepared and stored at -70°C for several months. This perhaps indicated that the multiple complexes observed were more likely to represent protein degradation products rather than individual binding activities. It is also possible that multiple proteins bind to this region and that the three complexes observed might reflect different stages of assembly of the multicomponent structure.

a

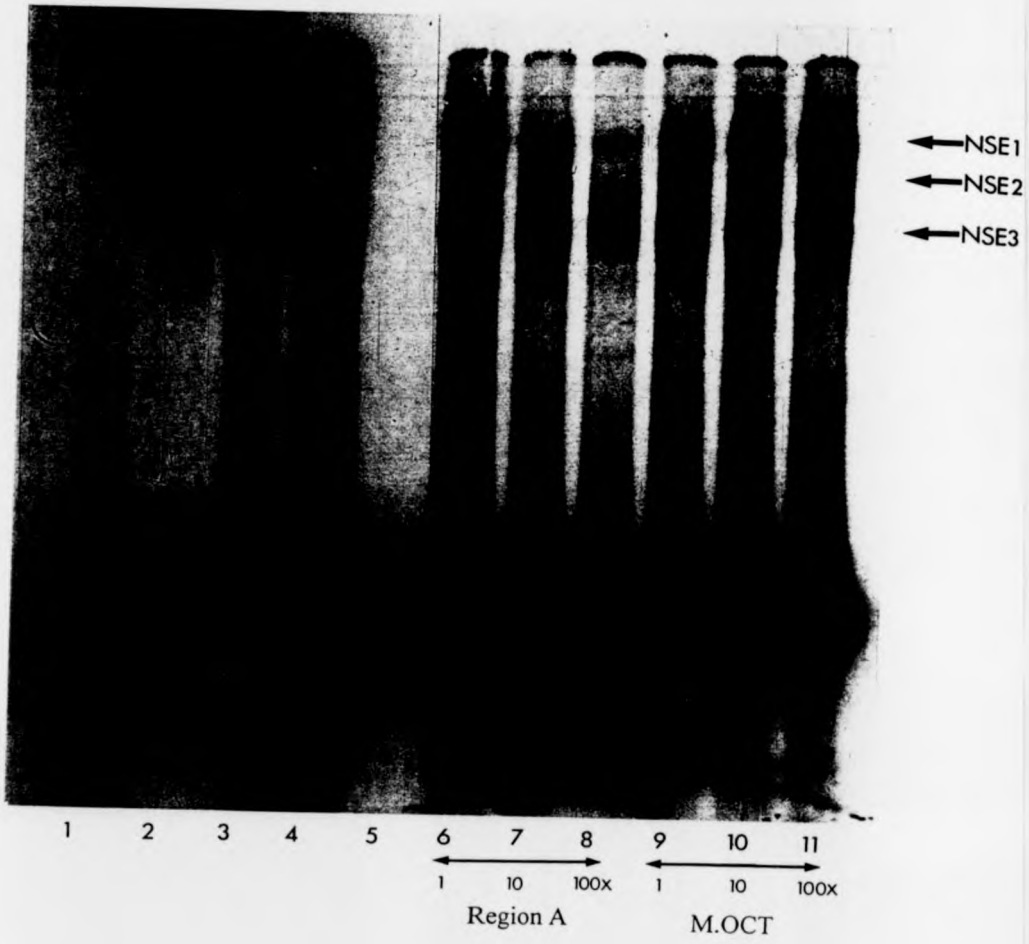
NSE1
NSE2
NSE3
1 2 3 4 5 6 7 8 9 10 11
1 10 100x
1 10 100x
Region A
M.OCT

b

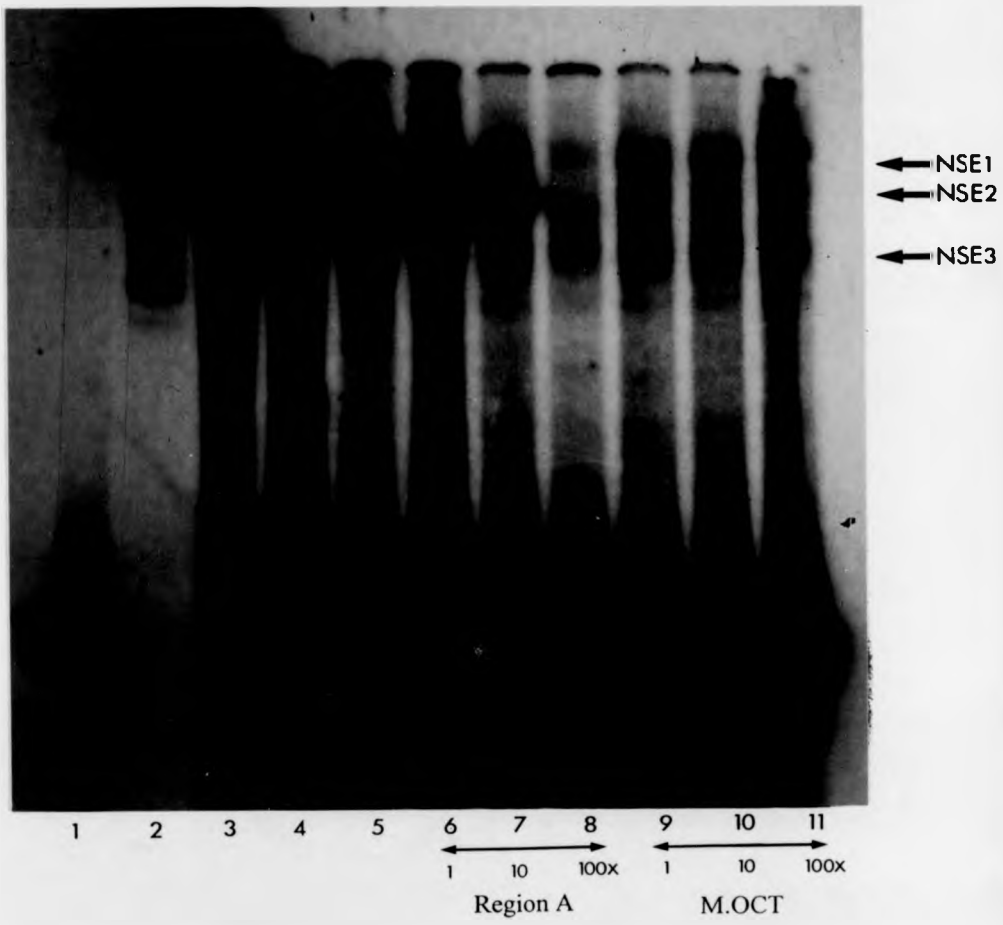

Figure 8.6: Competition assays to determine the specificity of three binding complexes on region A in extracts of (a) Ltk- cells and (b) HeLa cells. Lanes were loaded equally for total protein (4μg) and contained 1 ng probe. Lane 1 probe in isolation. Lanes 2-5 contained extract of (a) Ltk- or (b) HeLa cells, lane 2 lacking nonspecific competitor and lanes 3-5 including 1μg, 2.5μg and 5μg respectively of sonicated salmon sperm DNA. Lanes 6-11 contained extract of (a) Ltk- or (b) HeLa cells and 5μg sonicated salmon sperm DNA plus the indicated amount of specific unlabelled competitor, lanes 6-8 containing unlabelled region A, lanes 9-11 containing unlabelled M.OCT. The positions of binding complexes, labelled NSE1, NSE2 and NSE3, are indicated by arrows.

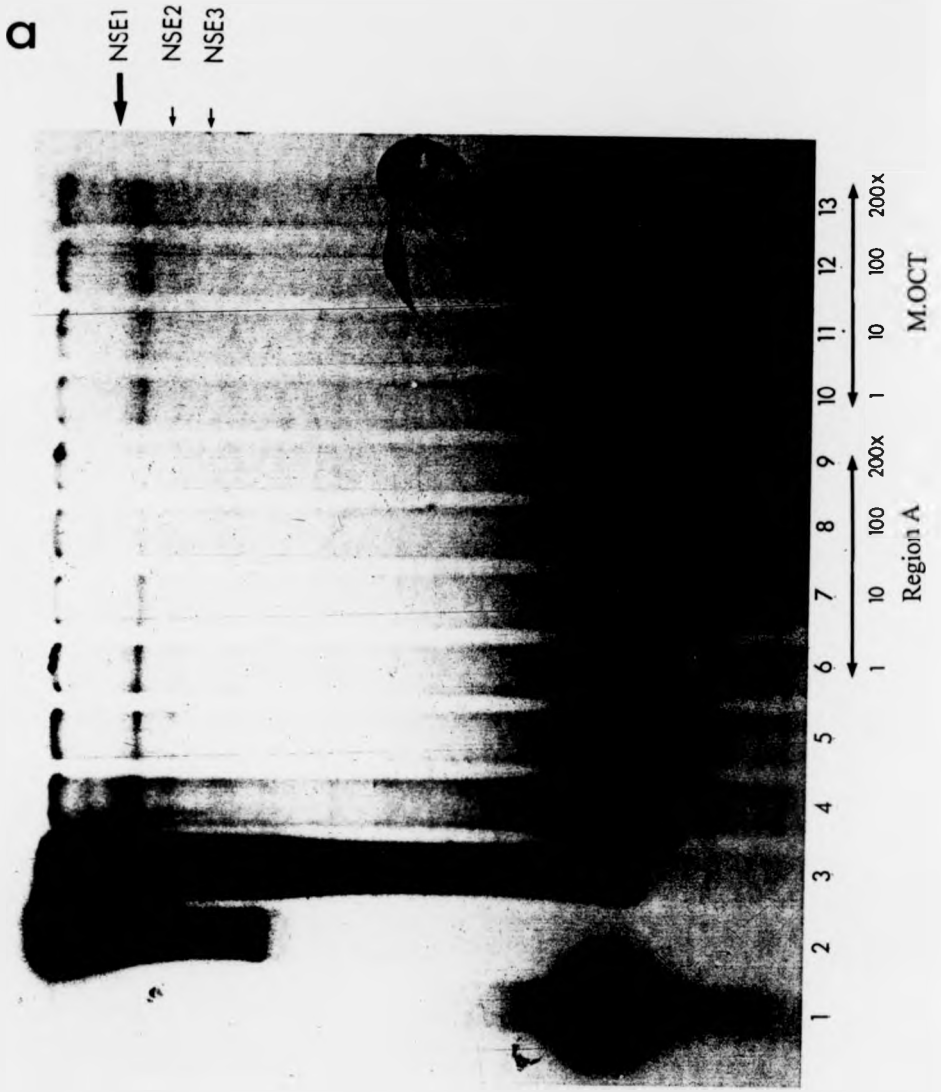
a
NSE1
NSE2
NSE3
1 2 3 4 5 6 7 8 9 10 11 12 13
1 10 100 200x
1 10 100 200x
Region A
M.OCT

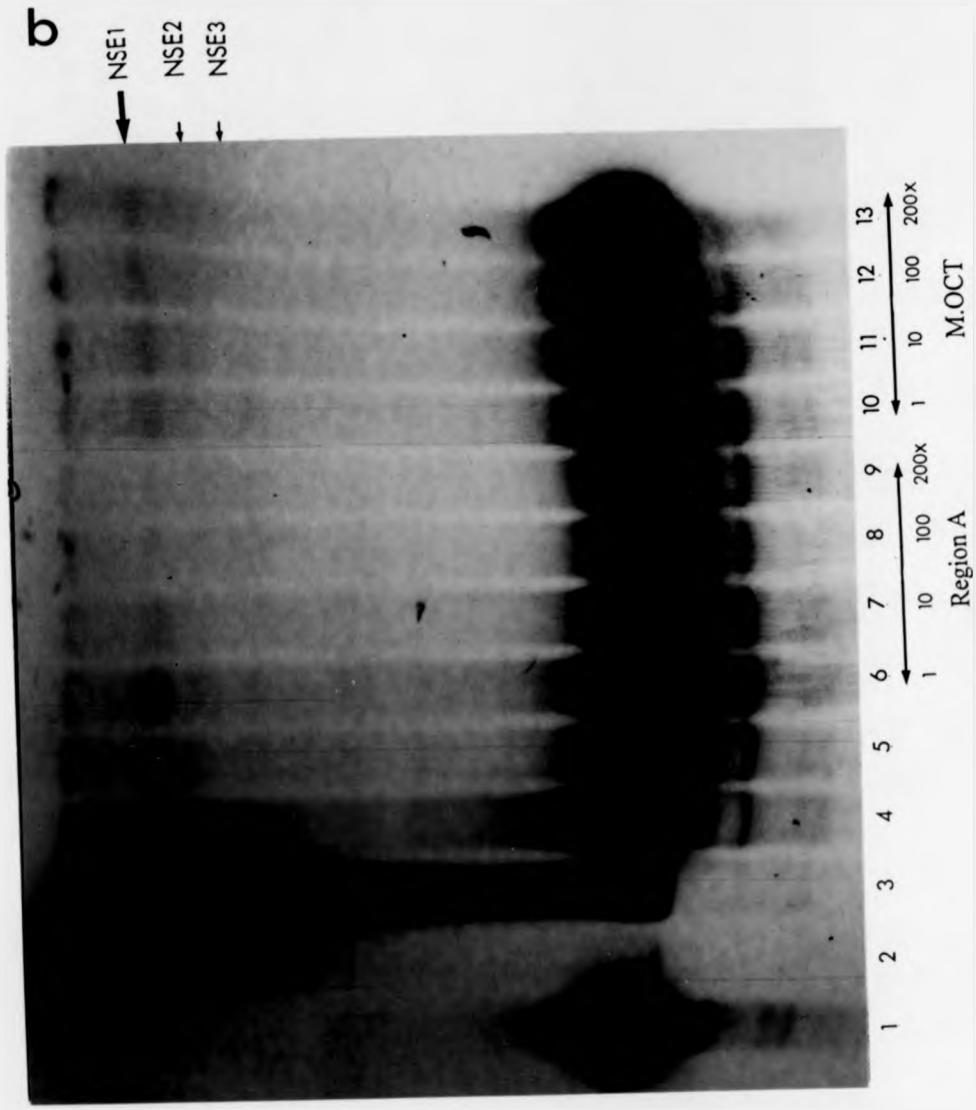

Figure 8.7: Further competition assays to determine the specificity of three binding complexes on region A in extracts of (a) Ltk- cells and (b) HeLa cells. Lanes were loaded equally for total protein (4 μg) and contained 1 ng probe. Lane 1 probe in isolation. Lanes 2-5 contained extract of (a) Ltk- or (b) HeLa cells, lane 2 lacking nonspecific competitor and lanes 3-5 including 1μg, 2.5μg and 5μg respectively of sonicated salmon sperm DNA. Lanes 6-13 contained extract of (a) Ltk- or (b) HeLa cells and 5μg sonicated salmon sperm DNA plus the indicated amount of specific unlabelled competitor, lanes 6-9 containing unlabelled region A, lanes 10-13 containing unlabelled M.OCT. The positions of binding complexes, labelled NSE1, NSE2 and NSE3, are indicated by arrows.

8.5 Preparation for analysis of the proximal 120 bp of the *NSE* 5' flanking region

The proximal region of the *NSE* regulatory sequence, extending from the *Pst* I site at position -120 to the beginning of the first intron, could not be excised and labeled in the manner of the more distal region A because it could only be isolated with endonucleases generating 3' overhanging. To facilitate the labelling of this fragment for future analysis of regions B, C and D, it was subcloned into the *Pst* I site of pBluescriptIIKS+. Two recombinant vectors were obtained with the insert cloned in opposite orientations. These vectors were named pNSE120>BS and pNSE120<BS. The insert can be excised using flanking sites which may or may not possess a 5' overhang and this facilitates labelling of either end of the fragment either individually or in combination. *In vitro* analysis of the proximal 120 bp of *NSE* 5' flanking sequence was not carried out due to time constraints. However, this cloning strategy should facilitate future studies.

8.6 Conclusions from *in vitro* studies of the *NSE* gene

Although time constraints prevented full exploitation of techniques which can be used to investigate protein-DNA interactions, the limited analysis carried out has identified one or more binding activities on region A of the *NSE* 5' flanking region which appear to be specific to nonneuronal cells. Furthermore, region A has been shown to modulate reporter gene expression in Ltk- cells by silencing. This fits in with a model whereby a protein binding to region A would downregulate transcription from the remainder of the promoter in nonneuronal cells but not in neuronal cells. Unfortunately, silencing activity was not revealed during transient transfection analysis of this region in HeLa cells. Furthermore, silencing activity was observed in (neuronal) Neuro-2A cells, but no binding activity was found in extracts of these cells. Nor was binding activity detected in PC12 cells even though region A was shown to be of great importance in this cell line. These results are discussed at some length in the following chapter with respect to the value of neuronal cell lines in the analysis of neuronal gene expression. It is also possible that further attempts to optimise binding activities or the use of alternative protocols (Dent and Latchman, 1993) might identify binding complexes which have not been observed in this study.

Obviously, firm conclusions cannot be drawn from this data without support from transgenic studies followed by the analysis of regions of the *NSE* promoter *in vitro*

using extracts of endogenous tissue. It would also be advantageous to investigate the abundance of any specific binding complexes observed in these experiments in extracts of mouse embryos to see whether the complexes arise at the time of *in vivo* neuronal differentiation. It is likely that the complexity of *NSE* gene expression reported *in vivo* would also be reflected in the protein -DNA interactions in the 5' flanking region of the gene. As brain extracts would contain proteins isolated from many different classes of neuronal cells plus a great excess of glial protein, which might squelch any neuron-specific effects, the conclusions from such studies would have to be made very carefully. It is likely that extracts of primary cultured neurons and nonneuronal cells would be extremely valuable in such studies to prevent the mixing of effects from various cell types. The observation of proteins binding to the first intron of the *NSE* gene in isolates of primary cultured neurons has already been reported (Sakimura *et al.*, 1995).

Chapter 9 - Discussion, conclusions and future work

9.1 Chapter summary

In this final Chapter, the experimental strategy used during the project, and the results of the experimental work set out in Chapters 5 through 8, are discussed in the light of the published literature. The results section was divided into four chapters reflecting the following major subject areas: (a) development of suitable systems for studying *NSE* gene regulation in cell lines; (b) analysis of *NSE* gene regulation in neuronal and nonneuronal cells and in the context of neuronal differentiation using transient transfection; (c) analysis of the *NSE* gene *in vivo* using transgenic mice; and (d) *In vitro* analysis of the *NSE* 5' flanking region defined as important in the previous chapters. The discussion is subdivided in a similar manner, with particular attention directed towards the limitations of the presented work and further experiments which could help to clarify issues not made clear in the project.

9.2 *Ex vivo* analysis of gene regulation - suitability of the approach and criticism of the way systems were chosen, tested and applied.

9.2.1 Suitability of transient transfection analysis for the study of gene regulation

As discussed in Chapter 2, the *ex vivo* transient transfection approach to the analysis of gene regulation has a number of advantages and disadvantages compared to *in vivo* analysis using transgenic animals. To recap, the major advantages of this approach are that (a) it can be repeated many times with relative ease to generate large amounts of data for statistical analysis and (b) DNA introduced into cells is maintained in an extrachromosomal state and is not subject to the position effects of integrated transgenes (which can modify their pattern of expression in unpredictable ways). The *ex vivo* approach also allows specific inductive responses to be

investigated simply by adding appropriate factors to the growth medium. The disadvantages of the *ex vivo* approach reflect its artificial nature. Established cell lines and the endogenous cells they represent often express different groups of genes and one example of this is the expression of *NSE* in glioma lines (Zomzely-Neurath, 1983). Also, under certain circumstances, it may be difficult to obtain cell lines with appropriate properties, e.g. it is sometimes difficult to find cells which express transiently expressed developmental genes (there is no shortage of cell lines which express *NSE*, however). Finally, from a mechanistic perspective, a false impression of gene regulation may be obtained from transiently transfected cells if the endogenous gene responds to distant *cis*-acting elements in the genome, or epigenetic factors such as DNA methylation or chromosome packaging as such factors are not represented in the extrachromosomal construct. Additionally, low abundance transcriptional regulators may be completely titrated out by the large molar amount of DNA introduced during transfection, resulting in abnormal expression from the excess free DNA. Some or all of these problems may influence the behaviour of transfected reporter genes in cultured cells. For some cell types, e.g. liver cells, cell lines appear to be almost perfectly representative of their endogenous counterparts. Neuronal cell lines are unusual, however, in that their very existence depends upon them differing fundamentally from endogenous neurons. This can make the interpretation of transfection experiments more difficult, a problem discussed in section 9.3.6.

9.2.2 Establishment of endogenous *NSE* gene expression in cell lines

The regulation of *NSE* was considered in both neuronal and nonneuronal cells, the former being shown to be permissive for *NSE* gene expression, the latter nonpermissive. This strategy was chosen on the basis that both positive and negative aspects of gene regulation could be studied. The expression of genes in neurons is known to be controlled by both positive and negative factors, and to illustrate this point, several well-characterised systems have been described in Chapter 2. The expression of *NSE* in the nervous system overlaps with that of

several putative positive regulators of neuronal gene expression, such as Brn-1 and other octamer-binding proteins (He *et al.*, 1989; Ninkina *et al.*, 1993; Lillycrop *et al.*, 1992), NeuN (Mullen *et al.*, 1992), BSF1 (Motejlek *et al.*, 1994), and mKr2 (Chowdhury *et al.*, 1988). The expression pattern is complementary to those of potential and known negative regulators of neuronal gene expression such as the NRSF (Schoenherr and Anderson, 1995) and Sox2 and Sox3 (Uwanogho *et al.*, 1995). Accordingly, previous studies of neuronal gene expression have often involved both permissive and nonpermissive cell lines (see section 2.5 and references therein) and this is also true of the most recent study of *NSE* gene regulation (Sakimura *et al.*, 1995).

9.2.3 Justification of combined northern and western analysis of gene expression

As evidence for the suitability of various cell lines for their proposed purposes in transient transfection assays, most authors have cited the results of RNA expression experiments. Whether by northern blot, *in vitro* translation, RNase protection or quantitative RT-PCR, this approach reflects the fact that upstream regions of the gene under investigation, subject to control by *transcriptional* regulators, are usually chosen to drive the reporter. In such cases, reporter expression is controlled almost fully at the level of transcription and it is therefore necessary to analyse expression of the endogenous gene at the equivalent level in order to determine whether or not the chosen cell line is a useful system. Such analysis also allows endogenous gene expression to be used as a reference, so that 'mutant' constructs containing deleted derivatives of the endogenous flanking sequence can be compared to the 'wild type' endogenous gene.

In a growing number of cases, however, posttranscriptional regulation has been shown to play an important role in the regulation of gene expression, and several well-characterised examples of gene regulation at the levels of RNA processing, nuclear export, RNA degradation and protein synthesis have been described (Alberts *et al.*, 1994). In this project, the reporter constructs contained not only upstream

regulatory information, but also the part of the 5' untranslated sequence delineated by exon 1 of the *NSE* gene. As there is some evidence for posttranscriptional regulation of *NSE* (Forss-Petter *et al.*, 1986 and references therein) and because posttranscriptional regulation is often controlled by noncoding regions of the transcript (Kozak, 1989), it was considered wise to investigate endogenous expression at both the RNA and protein levels. It was possible that reporter expression could be influenced by posttranscriptionally active *cis*-acting elements in the 5' untranslated region as well as by transcriptionally active *cis*-acting elements in the upstream region of the gene.

9.2.4 Comparison to previous investigations of *NSE* gene expression in cell lines

Endogenous gene expression in cell lines was analysed by northern and western analysis, and distribution of the protein was investigated by *in situ* immunocytochemistry. The suitability of the methods used to detect *NSE* mRNA and NSE protein was discussed at length in section 5.2.1 and will not be reiterated here except to say that each proved adequate for its purpose, underscoring the results of previous studies which have emphasised the cross-species conservation of these molecules (Clark-Rosenberg and Marangos, 1980; Jackson *et al.*, 1985; see Table 1.3). The results of northern and western analysis in different cell lines were set out in sections 5.2.2-5.2.8 and generally agreed well with previously published observations, as discussed below.

The expression of *NSE* mRNA and NSE protein in PC12 cells has been described previously in the context of neuronal differentiation following treatment with NGF (Vinores *et al.*, 1981; Sakimura *et al.*, 1995). Although, in the more recent study, no quantifiable data were presented, northern analysis appeared to suggest that levels of the *NSE* transcript were similar in untreated and treated cells (Sakimura *et al.*, 1995). This was very different from the picture presented in the earlier study (Vinores *et al.*, 1981) in which NSE protein was shown to be extremely sensitive to the NGF-induction in PC12 cells, with even low doses (1 ng ml^{-1}) producing the

maximal increase, a response not stimulated by EGF, growth hormone, insulin, cytochrome *c* or sodium butyrate. In the present study, only moderate stimulation of *NSE* gene expression was observed following NGF treatment of PC12 cells - this was shown at both the mRNA and protein levels. It is not clear why these three attempts at the same experiment provided such contradictory results. The author acknowledges that no other NGF-induced neuronal markers were used as positive controls for NGF activity, although the dramatic change in PC12 cell morphology accompanying exposure to NGF was thought adequate to verify the activity of the inducing agent. It is possible that differences in culture conditions, perhaps brought about by the distinct requirements of different PC12 subclones, contributed to the limited response. Unfortunately, details of NGF treatment and cell culture conditions were not provided in the report by Sakimura and colleagues (Sakimura *et al.*, 1995) so it was neither possible to comment on their approach, nor to compare their methodology to those used herein and those of Vinores *et al.* It should be noted, however, that PC12 cells also demonstrate density-dependent expression of *NSE* and that the response to NGF induction becomes less marked the longer the cells are cultured (Vinores *et al.*, 1981). After three days in culture, Vinores *et al.* observed only a minimal induction of NSE protein compared to the twentyfold upregulation observed in proliferating cells. Both PC12 clones used in the present project were also harvested after three days in culture, suggesting that the observed insensitivity to NGF reflected this density-dependent induction in undifferentiated cells. The two PC12 cell lines used in this project also demonstrated entirely different morphologies, growth conditions, and responses to transfection when compared to each other and to PC12 cells studied by others (Hawley-Nelson *et al.*, 1994). These factors may also have contributed to the different results obtained by Vinores *et al.*, Sakimura *et al.*, and myself.

NSE gene expression has not been previously investigated in the other permissive cell lines used in this project (U-138 MG, Neuro-2A and NB4-1A3), although further glioma and neuroblastoma lines have been studied in some detail (Zomzely-Neurath, 1983). Generally, both cell types have been shown to express lower levels of the *NSE* gene products than brain, and whilst significant levels can be detected in

many glioma lines, such as C6 (Sakimura *et al.*, 1995), the levels found in proliferating neuroblastoma cells are generally very much lower. At the protein level, NSE in different neuroblastoma lines has been shown to contribute 0.1-7% of total enolase activity (Zomzely-Neurath, 1983). Furthermore, where *NSE* mRNA generates a strong hybridisation signal in northern blots of brain RNA, the transcript is barely detectable in equivalent amounts of RNA from neuroblastoma lines (Sakimura *et al.*, 1995). The results presented in this project indicated that Neuro-2A and NB4-1A3 cells also expressed barely detectable levels of *NSE* mRNA and NSE protein, whilst *NSE* gene expression in the glioma line U-138 MG was more significant, but approximately tenfold less than that observed in adult brain.

As transfected cells were allowed to become confluent prior to harvesting, it was particularly interesting to note the observations of Matranga *et al.* with respect to *NSE* gene expression in confluent cultures of mouse N-115 neuroblastoma cells (Matranga *et al.*, 1992). These investigators showed that the levels of *NSE* mRNA increased as the cells became more confluent, a phenomenon which had previously been observed at the protein level for another neuroblastoma line (Legault-Demare *et al.*, 1980). Matranga and colleagues further suggested that the observed variation in the proportion of the brain enolase isoenzymes between different neuroblastoma cell lines (Zomzely-Neurath, 1983) might in part reflect unreported differences in cell density. The expression of *NSE* mRNA and NSE protein was investigated in cultures of Neuro-2A cells and it was found that a ten to twentyfold induction of gene expression occurred in confluent cells compared to proliferating cells. It was therefore apparent that although the proliferating cells could be regarded as nonpermissive or at least, not fully permissive for *NSE* gene expression, the posttransfection cells were suitable for use as a permissive system due to the high levels of *NSE* gene products resulting from this artefact of cell culture and transfection. It is possible that a second such artefact, serum withdrawal during transfection in serum-reduced medium, also resulted in a mild induction of *NSE* in some cell lines. However, exposure to serum-reduced medium was rarely longer than six hours, when fresh medium containing serum was added to the cells. It is therefore unlikely that serum withdrawal produced a significant effect, and any

response would probably have been reversed by the refreshment provided following transfection.

Analysis of the murine embryonic carcinoma cell line P19 showed that both *NSE* mRNA and NSE protein were undetectable in stem cells but abundant in neurons after 14 days in culture. Previously, it had been reported that *NSE* mRNA was expressed in murine ES-12957 embryonic stem cells, although NSE protein was not detected (Alouani *et al.*, 1993). The apparent discrepancy between these results could reflect properties of the different cell lines used. However, it is much more likely that differences in the sensitivity of the detection systems were responsible. Alouani and coworkers used the extremely sensitive RT-PCR assay to detect the *NSE* message in their experiments, whilst northern analysis was used in the present project. As an indication of the sensitivity of their approach, it should be noted that Alouani and coworkers used Neuro-2A cells as a control for *NSE* expression and these cells generated a signal more than 100-fold greater than that of the ES cells. As discussed above, *NSE* mRNA was barely detectable in proliferating Neuro-2A cells, even after a long (96 hour) exposure of northern filters. Expression of *NSE* mRNA in ES cells at levels two orders of magnitude less than those observed in Neuro-2A cells would therefore obviously lie well below the minimum threshold for detection by northern analysis. In this project, *NSE* mRNA and NSE protein were detected in differentiated P19 neurons after two weeks in culture, concomitant with the overt differentiation of neuronal cell types as judged by the formation of long neurites and synaptic associations. The levels of gene products were found to be at least as high as those found in adult brain, which was somewhat higher than those found by Alouani and coworkers in their differentiated cultures. This second discrepancy probably reflects the manner in which the differentiated cultures were treated. Alouani and coworkers allowed their cultures to differentiate freely, which, after several days, results in a large excess of proliferative nonneuronal cells (Rudnicki and McBurney, 1987). Conversely, the differentiated cultures generated in the present project were treated with mitotic inhibitors after four days to prevent the growth of such cells. In consequence, relatively pure neuronal cultures were obtained and the levels of *NSE* gene products were much higher. Neurons in the

brain itself are grossly outnumbered by glial cells, thus one would expect pure neuronal cultures to express *NSE* gene products at approximately tenfold the levels found in brain (Di Liergo *et al.*, 1992), and this is exactly what was found in primary cultures of rat neurons after five days in culture (Sakimura *et al.*, 1995). As the P19 neurons and brain expressed *NSE* at more or less the same level, this would indicate that the P19 neurons express *NSE* at levels tenfold *less* than those found for mature neurons *in vivo*. This suggests that P19 neurons (after 14 days in culture) are still relatively young and undifferentiated. Levels of endogenous *NSE* gene expression in neuronal derivatives of ES cells have been shown to rise further in long-term cultured cells concomitant with their maturing neuronal morphology (Alouani *et al.*, 1993). These data supports earlier investigations where the levels of *NSE* gene products in neuronal cultures were shown to increase with time, correlating to the degree of morphological differentiation (Secchi *et al.*, 1980; Bock *et al.*, 1980; Schmechel *et al.*, 1980; Ledig *et al.*, 1982; Jirikowski *et al.*, 1983; Weyhenmeyer and Bright, 1983; Di Liergo *et al.*, 1991).

NSE gene expression has not been investigated in Ltk- cells, which were used as a nonpermissive cell line in this project and this cell line has not been used in previous studies of neuronal gene expression. The second nonpermissive cell line, HeLa, has been used for several such studies, including the recent investigation of *NSE* gene regulation (Sakimura *et al.*, 1995). Other nonneuronal cell lines, such as BHK-1, which have been used for studies of *NSE* gene expression in the context of recombinant herpesvirus-mediated transductions (Roemer *et al.*, 1995), were not considered for use in this project. Both Ltk- and HeLa cell lines were shown to express *NSE* mRNA and NSE protein at levels undetectable by northern and western analysis and from these results, they were considered suitable as nonpermissive systems. As mentioned in Chapter 5, the HeLa cell line is of human origin and no control experiments were performed to establish whether the rat *NSE* 3' UTR probe could detect human *NSE* sequences. However, *NSE* mRNA was detected in U-138 MG and U-373 MG cells, which were also of human origin, and Matranga *et al.* used the human *NSE* sequence to detect mouse *NSE* mRNA in neuroblastoma cell lines indicating that cross-hybridisation was successful (Matranga *et al.*, 1992). The

use of HeLa cells as a noexpressing line by Sakimura *et al.* (1995) also supports the role chosen for this cell line in this project.

9.2.5 Strategy for the generation of deletion constructs

The deletion constructs used in the project were simple stepwise truncations of the 5' flanking sequence, spanning the 1.8 kbp element which was used successfully to drive neuron-specific reporter gene expression in transgenic mice (Forss-Petter *et al.*, 1990). In other studies, more extensive and complex strategies have been used for deletion analysis. For example, a recent study of peripherin gene regulation was facilitated by the generation of twenty stepwise deletion constructs spanning 3.5 kbp of flanking sequence (Desmaris *et al.*, 1992), whilst the rat *NSE* gene itself has been studied with the help of thirty constructs including stepwise and internal deletions and rearrangements of the flanking region (Sakimura *et al.*, 1995). The former study shows how such a maximalist approach can sometimes be inappropriate. Elements responsible for cell type-specific regulation of the peripherin gene were eventually located overlapping the TATA box, thus most of the constructs containing large tracts of upstream sequence were redundant. Pilot experiments could have been performed with two or three long constructs and the proximal elements could have been localised without all the effort involved in subcloning. The first approach does have the advantage that, if functional elements are located, their position can be narrowed down immediately to a small region of the sequence under investigation. However, in the second approach, preliminary studies would provide a basis for the generation of further constructs, and the same information could be found without constructing so many vectors. This strategy was pursued in the current project, thus a small number of constructs were generated and tested initially, providing the evidence that further deletion constructs were required. These constructs were then used to narrow down the regions of the *NSE* promoter required for cell type-specific activity, which, like those found in the peripherin gene promoter, were located close to the transcriptional start site of the gene.

9.2.4 Transfection strategy and data handling

Transfection methodology was considered at some length in Chapters 4 and 5. An exhaustive discussion of the transfection optimisation experiments is unnecessary in the present chapter, as their purpose was obvious and their contribution to the study of *NSE* gene regulation only peripheral. Such experiments were carried out according to established protocols (Selden and Rose, 1991) and for cationic liposome reagents, according to manufacturers' recommendations. It is necessary, however, to consider two aspects of the transfection methodology in detail as these often provoke the most criticism. These are the validity of cotransfection as an internal control and the handling of transfection data.

Cotransfection of a standard control vector, such as pSV-β-galactosidase, is one of several methods used to normalise comparative transfection data for cell number and transfection efficiency. Other methods include measurement of total protein concentration and quantitative hybridisation analysis, using a probe specific for the transfected DNA. The former can sometimes generate misleading results because the protein content of different cells varies (e.g. differentiated PC12 cells contain more protein than their undifferentiated precursors, Vinores *et al.*, 1981). The latter is labour intensive and time-consuming if many transfections are carried out. Cotransfection is advantageous in that reporter gene expression can be measured using a simple assay (in this project, by a soluble β-galactosidase assay) and that it does not depend upon any the property of the cell line used. The major disadvantage of cotransfection is that it is not easy to show, in a mixture of plasmid DNAs of known proportion, whether a representative proportion of each plasmid is taken up by the cells. Obviously, where numerous constructs are used, and one expects the level of reporter gene activity to differ between constructs, it is critical to normalise the primary transfection data without the control itself varying between parallel cultures. It has been reported that calcium phosphate-mediated transfection shows reliable cotransfection ratios (Kingston *et al.*, 1990) and there are many examples in the literature where cotransfection has been used to normalise

transfection data obtained by calcium phosphate-mediated and liposome-mediated protocols, including the recent study of *NSE* gene regulation (Sakimura *et al.*, 1995). Generally, β-galactosidase is accepted as a good internal control reporter because of its sensitivity and broad linear range (Kain and Ganguly, 1995).

When presented with primary transfection data, it is not only the normalisation for transfection efficiency which has to be carried out, but also the relative molar amounts of plasmid DNA introduced into the cells has to be taken into account. Because transfections were optimised according to the mass of DNA in the transfection mix, smaller vectors were introduced into cells in relatively greater molar amounts than larger vectors. In published articles dealing with transfection analysis, this aspect of data handling is seldom mentioned. However, just as gene dosage can be critical for the correct functioning of a cell, reporter gene dosage is likely to influence the mechanism of gene regulation. For example: if a given transcriptional regulator is present at a low abundance, it may be titrated out by a large number of short constructs but not by a smaller number of large constructs, given that it binds once to the transcriptional start site of the gene. This scenario would result in a differential effect from two constructs, resulting not from structural differences between the constructs but from an artefact of transfection. To take this into account, primary transfection data were adjusted by a dimensionless constant termed the MEC (molar equivalence constant) as shown in section 5.5. Elsewhere, this problem has been solved by adding nonspecific carrier DNA, such as sonicated salmon sperm DNA, to transfection mixes in order to bring a known molar quantity of plasmid DNA up to the optimal mass for transfection (D. Stott, pers. comm.). This approach, whilst equally valid, does add another unknown factor to the transfection process, and for this reason, the former approach was favoured.

The interpretation of transfection data also relied on valid comparison of parallel cultures within and between experiments using the same and different cell lines. Within an experiment, it was permissible to directly compare the absolute CAT activities when corrected for transfection efficiency and molar ratio, as all other

parameters would be expected to be identical. When comparing transfection data across experiments using the same cell line, the absolute CAT activities were unreliable, as even relatively minor modifications to technique or assay times could result in wide differences between absolute values, rendering such comparisons meaningless. This can be clearly seen if one compares absolute CAT activities across the experiments presented in Chapter 6. However, by expressing the absolute CAT activities, referred to as Actual CAT Activities (ACAs), as a percentage of the positive control vector, pCAT-Control, comparison between experiments was made valid because variations occurring between experiments would affect not only the experimental constructs, but the control vectors also. The percentage of control value, referred to as Relative CAT Activity (RCA), allowed large amounts of data to be accumulated and subjected to statistical analysis. This approach is common in transfection studies, and the control vector is generally driven by a viral promoter which would be expected to behave in a similar manner in most environments. This presumption is rarely tested, however, and nor were control-testing experiments carried out in this project. It is therefore not clear whether data should be legitimately compared across experiments using different cell lines, however, the precedent is for such comparisons to be made with impunity and certainly there are many examples of transfection studies in the literature where this aspect of data handling has not been addressed. This includes the recent study of *NSE* gene regulation by Sakimura *et al.* (1995).

Statistical analysis of the results was restricted to presenting means and standard errors from individual transfection experiments and the results of complete experimental series. One possible source of criticism is the use of mean control values to calculate the Relative CAT Activities of the experimental constructs: the control values themselves were subject to variation and this must have had a knock-on effect in the calculation of Relative CAT Activities for *NSE-cat* vectors. In an ideal world, the statistical reliability of the data would be unimpeachable. This however, would involve performing each experiment tens or hundreds of times and selecting data randomly for this population before carrying out the statistics. Of course, such an approach would be regarded as ridiculous by most researchers

outside the field of hardcore statistics, and the potential benefits would be far outweighed by the sheer cost and inconvenience of monotonous repetition. Each transfection was performed at least six times (each experiment twice in triplicate), or nine times (each experiment thrice in triplicate) for calcium phosphate and DEAE-dextran-mediated transfections. The confirmation of transfection data by at least one repetition is generally considered to be suitable proof of its reliability and this minimal prerequisite was certainly exceeded during this project.

9.3 Transfection experiments

Chapter 6 comprised the data from transfection experiments using the optimised and tested systems described in Chapter 5. Although the results were discussed at the end of each relevant section, it is necessary to place the data in the context of other investigations of neuronal gene expression, especially that of Sakimura and colleagues who have recently published an extensive analysis of *NSE* gene regulation using an identical strategy to the one used in this project (Sakimura *et al.*, 1995)

9.3.1 Preliminary attempts to isolate neuron-specific elements in the *NSE* 5' flanking region

In the first part of Chapter 6, the results of some preliminary experiments were presented, concerning the behaviour of *NSE-cat* constructs in one permissive and one nonpermissive cell line. These experiments showed quite conclusively that 255 bp of the 5' flanking region (i.e. the sequence up to and including the proximal *Xho* I site) were capable of conferring high level reporter gene expression in the permissive line but only minimal expression in the nonpermissive line. These results were backed up by studies in other cell lines: neuroblastoma cells, PC12 cells and P19 neurons transfected with construct pNSE300CAT demonstrated high levels of CAT activity whilst only minimal activity was observed in HeLa cells and P19

EC stem cells. The impression from these experiments taken as a whole was that elements required for cell type-specific expression were likely to reside downstream from position -255, in the very proximal region of the promoter. How did these firm conclusions stand up in the light of further transfection data from other researchers? Sakimura and colleagues showed that the most important regulator of neuronal gene expression did indeed lie downstream from position -255, although in an intergenic region not included in the constructs used during this project (Sakimura *et al.*, 1995); the importance of this intron-bound element is discussed in section 9.3.5. Even without the intron, however, the constructs used by Sakimura and colleagues were still neuron-specific although the difference between neuronal and nonneruonal cells was less extreme. Thus construct pX3CAT (identical to the pNSE300CAT construct generated during this project) was fortyfold and sevenfold more active, respectively, in neurons and PC12 cells, compared to HeLa cells. These data compare favourably with the results obtained in this project where pNSE300CAT was thrityfold and sixteenfold more active in P19 neurons and PC12 cells, respectively, when compared to HeLa cells.

The main reason for concluding that elements responsible for neuron-specific expression must lie downstream from position -255 was the similar activity of pNSE300CAT and constructs containing more extensive tracts of upstream sequence. Sakimura and colleagues did not carry out extensive analysis of long constructs lacking intron 1, but construct pA1CAT/Sac, which contained 1.8 kbp of 5' flanking sequence (equivalent to pNSE1800CAT) but also intron 1, was not significantly more active than a construct containing 255 bp of 5' flanking sequence and intron 1. A construct containing 2.7 kbp of 5' flanking sequence but no intron was slightly less active (in neurons) compared to pX3CAT. These data therefore support the conclusion made from the present study, which was that most of the onus for the control of gene regulation lay downstream from position -255.

9.3.2 Further analysis of *NSE* gene regulation in neuronal lines

Truncation of the *NSE* 5' flanking region beyond position -255 resulted in varying effects in different neuronal cell lines. In Neuro-2A cells, truncation from position -255 to position -120 caused a doubling of reporter activity suggesting that a silencer of some description had been removed. Conversely, in PC12 cells, the same deletion generated a five to sevenfold fall in CAT activity. And to box the compass, the same deletion in P19 neurons appeared to have no effect at all.

Generally, the analysis of neuronal cells failed to paint a clear picture of the mechanism used to regulate *NSE*. The neuroblastoma transfections alone demonstrated that neuronal cell lines vary considerably in the expression of transfected reporter constructs. There were really no common trends shared by both neuroblastoma lines except the shutdown of gene expression following truncation to position -65. NB4-1A3 cells generally demonstrated lower mean Relative CAT Activities than Neuro-2A cells, which was somewhat surprising considering that their morphology is rather more neuronal than the other cells. It is possible that this discrepancy reflected the ability of Neuro-2A cells to become confluent following transfection, whilst NB4-1A3 cells tended to become quiescent when 50-70% confluent. It is possible that such differences in growth properties could influence the regulation of *NSE*, although this has not been investigated. Studies of endogenous *NSE* gene expression in neuroblastoma lines have indicated considerable heterogeneity between lines (reviewed by Zomzely-Neurath, 1983) although this may reflect differing culture conditions when measurements were taken (Matranga *et al.*, 1992). To establish the nature of *NSE* gene regulation in neuroblastoma lines, an extensive study would be required using a large panel of different neuroblastoma lines grown and transfected under standardised conditions. Only limited data was presented by Sakimura and colleagues concerning neuroblastoma cells and generally, these behaved as nonneuronal cells (although the first intron did cause some stimulation of reporter activity over that observed in HeLa cells). Unfortunately, there was no discussion of neuroblastoma culture conditions and it is likely that the cells were harvested when still proliferating and thus expressing relatively low levels

of *NSE*. It would be useful to collect neuroblastoma cells at various confluences following transfection and assay for CAT activity. This would show the density dependent induction of *NSE* in more detail and might reveal the presence of *cis*-acting elements responsible for this effect.

PC12 cells can be regarded as better candidates for the study of *NSE* gene regulation because both the undifferentiated and differentiated cells have been shown to express *NSE* mRNA and NSE protein at high levels (Vinores *et al.*, 1981; Sakimura *et al.*, 1995; this project). As with the Neuro-2A and U-138 MG cells, PC12 cell cultures transfected with pNSE1800CAT demonstrated Relative CAT Activities of approximately 100%. Reduction of the 5' flanking region to 1000 bp and then to 255 bp produced a 50% drop in reporter expression in undifferentiated cells, although cells differentiated with NGF and transfected with these two constructs maintained Relative CAT Activities in the order of 100%. These data suggested that positive modulators active in the undifferentiated cells lay in the unsequenced region and/or the distal 200 bp of the sequenced region of the *NSE* promoter. Further reduction to 120 bp generated a 5-10-fold reduction in both differentiated and undifferentiated cells, indicating that strong positive modulators were positioned between -255 and -120 bp upstream of the transcriptional start site. Reduction of the 5' flanking region to 65 bp reduced reporter expression to background levels.

Sakimura and colleagues did not present any data for undifferentiated PC12 cells, however, NGF-treated PC12 cells transfected with pX3CAT (equivalent to pNSE300CAT) showed a mean Relative CAT Activity of 144% compared to 80% in this study. It should be noted, however, that poor transfection efficiency for pNSE300CAT in the second transfection, and the high standard error of the mean resulting from this, somewhat reduced the overall mean value (Figure 6.39). In the first experiment, where transfection efficiency was greater and the error range smaller, the Relative CAT Activity was 138%, much closer to the value obtained by Sakimura and colleagues. Their construct pX3CAT/Bc (equivalent to pNSE120CAT) yielded a mean Relative CAT Activity of 27%, which is somewhat higher than the 11% observed in this investigation, but indicative of a similar fall in

reporter expression when this short region of the promoter was removed. However, further reduction of the 5' flanking region to 95 bp maintained reporter expression at low levels in this project (approximately 10% Relative CAT Activity) whilst the equivalent construct generated by Sakimura *et al.* - pX3CAT/Ba, yielded a Relative CAT Activity of 151%. Other direct comparisons between the present study and that of Sakimura *et al.* are difficult to make because the longest constructs generated by Sakimura and colleagues contained the first intron of the *NSE* gene, which was absent from those used in this project. However, a construct lacking the intron, but containing 2.7 kbp of upstream sequence was only 1.23-fold more active than pX3CAT (equivalent to pNSE300CAT) whilst in this project, the mean Relative CAT Activity of pNSE1800CAT was 1.5-fold greater than the (underestimated) mean Relative CAT Activity for pNSE300CAT.

In P19 neurons, pNSE1800CAT, pNSE1000CAT, pNSE300CAT and pNSE120CAT constructs all showed similar Relative CAT Activities, in the range 130-160%. Truncation to 95 bp of 5' flanking sequence resulted in a drop to approximately 90% Relative CAT Activity and truncation to 65 bp again reduced CAT activity to background levels. These results were subject to a greater degree of variability than other transfections, and the reasons for this were discussed in section 6.5.2.2. Sakimura and colleagues obtained data from primary cultures of rat cortical neurons transfected with *NSE*-driven CAT constructs. Generally, the levels of CAT activity obtained by Sakimura *et al.* were much greater than those observed here. For instance, rat neurons transfected with pX3CAT (equivalent to pNSE300CAT) demonstrated a mean Relative CAT Activity of 766%, compared to a maximum of 240% and a mean value of 155% obtained from P19 neurons. Furthermore, rat neurons transfected with pX3CAT/Bc (equivalent to pNSE120CAT) showed a mean Relative CAT Activity of 82%, compared to 130% for the P19 neurons in the present study and rat neurons transfected with pX3CAT/Ba (equivalent to pNSE95CAT) generated a mean Relative CAT Activity of 612%, compared to 90% for the P19 neurons. There appears to be no correlation between these results, either in absolute levels of CAT activity or in trend as the 5' flanking region of the gene is progressively truncated. However, this is not really

surprising considering the differences in origin and relative differentiation of the two types of neuron. As discussed above, neurons studied *in vivo* vary considerably in their levels of endogenous *NSE* gene expression, depending upon their position in the central nervous system (Katagiri *et al.*, 1993; Frikke *et al.*, 1987). It is therefore likely that different populations of neurons regulate the gene in diverse ways, and it has been suggested that the multiple transcriptional start sites attributed to the gene may also reflect this heterogeneity, as the RNA used for such analysis is always obtained from whole brain rather than isolated neuronal populations (Forss-Petter *et al.*, 1986). Analysis of endogenous *NSE* gene expression in neurons isolated at different stages of development has also revealed extensive heterogeneity with respect to levels of expression and *ex vivo* ontogeny (Secchi *et al.*, 1980; Bock *et al.*, 1980; Schmechel *et al.*, 1980; Ledig *et al.*, 1982; Jirikowski *et al.*, 1983; Weyhenmeyer and Bright, 1983; Di Liergo *et al.*, 1991). This is thought to reflect different stages of maturation, starting with young postmitotic neurons equivalent to those deposited in the subventricular (inner mantle) layer of the neural tube at the beginning of neurogenesis and finishing with fully mature neurons such as those observed in the adult CNS. The neurons isolated by Sakimura and colleagues certainly differed from the P19 neurons in origin, and also probably in relative maturity, and this is another factor which could explain the differences in regulation. It is clear from the data presented in the report by Sakimura and colleagues that the neurons isolated from the rat neocortex expressed quantitatively greater amounts of *NSE* mRNA than did the P19 neurons considered here (Sakimura *et al.*, 1995). It should also be borne in mind that P19 neurons are generated by artificial mechanisms which may not apply *in vivo* and that the retinoic acid used in the differentiation process might also influence the expression of the reporter constructs. In the future, it would be advantageous to look at *NSE* gene regulation in different populations of cultured neurons and at neurons isolated from animals at different stages of development to determine the influence of such factors on the regulation of the gene. It would be necessary to correlate such studies carefully to investigations of endogenous gene expression in defined neuronal cell types to assess whether the observed differences were related to age and position of the cells.

9.3.3 Further analysis of *NSE* gene regulation in nonneuronal cells

Truncation of the *NSE* 5' flanking region beyond position -255 generally had no effect in nonneuronal cells. In HeLa and P19 EC stem cells transfected with pNSE300CAT, mean relative CAT Activities were less than 10% and remained so when the flanking region was truncated further. Unfortunately, Sakimura and colleagues did not carry out extensive analysis of HeLa cells using the highly truncated constructs so it is difficult to compare the transfection data obtained here with their investigation. However, both studies strongly suggested that *NSE* gene expression is regulated by positive modulators or enhancers rather than negative modulators or silencers. Notwithstanding this conclusion, truncation of the *NSE* 5' flanking region from 255 bp to 120 bp in Ltk- cells resulted in a two to fourfold increase in Relative CAT Activity. This was greater than the twofold stimulation observed in Neuro-2A cells suggesting that between positions -255 and -120 lay a negative modulator which was more active in a nonneruonal cell line. Incidentally, similar results were obtained using neuroblastoma cell line NB35, which showed 14% mean Relative CAT Activity when transfected with pX3CAT (equivalent to pNSE300CAT) compared to 29% when transfected with pX3CAT/Bc (equivalent to pNSE120CAT) (Sakimura *et al.*, 1995).

9.3.4 *NSE* gene regulation during neuronal differentiation and in the presence of Sox-2 and Sox-3 factors

As discussed in the final part of chapter 6, little conclusive data was obtained from experiments designed to investigate the mechanism of *NSE* gene regulation during neuronal differentiation. In the case of PC12 cells, this is perhaps not surprising because the preliminary experiments carried out and discussed in Chapter 5 suggested that only a mild induction of *NSE* followed treatment with NGF. As discussed above, this probably reflected density-dependent induction of *NSE* in undifferentiated PC12 cells, a phenomenon which would certainly occur following

transfection as the cells were allowed to become confluent prior to harvesting. The data from transfection experiments thus showed a similarly minor induction of reporter expression from construct pNSE1800CAT (90% mean Relative CAT Activity in untreated cells compared to 116% in NGF-treated cells). Truncation to 1000 bp resulted in a significant (50%) fall in reporter activity in untreated cells but no significant effect in differentiated cells. In both cultures, truncation from -255 to -120 resulted in a striking drop in mean RCA (to approximately 10%). These results suggested that during NGF-induced differentiation of PC12 cells, the control of neuron-specific gene expression was shifted from a system involving two positive modulators to one controlled by a single such modulator located between positions -255 and -120.

P19 stem cells expressed little CAT activity irrespective of which construct was introduced into them whilst high level reporter gene expression was demonstrated by all constructs transfected in P19 neurons, with the exception of the most truncated vector, pNSE65CAT. These results indicated that, once again, the activation of neuron-specific enhancers was central to the induction of *NSE* during neuronal differentiation, but suggested that such enhancers might lay downstream from position -95. As discussed above, Sakimura and colleagues also showed that a construct lacking the first intron and containing only 95 bp of 5' flanking material (termed pX3CAT/Ba) was capable of high level reporter expression in neurons. These results taken together suggest that sequences in the very proximal region of the 5' flanking sequence, perhaps overlapping the TATA-box or perhaps laying in the first exon, were activated during neuronal differentiation. The effects of these sequences, whilst appearing significant in the present study, are probably dwarfed by the gargantuan contribution of the first intron, as discussed below.

Coexpression of cSox2 or cSox3 appeared to upregulate *NSE*-reporter constructs in NB4-1A3 cells, although careful analysis of the data revealed that this was more likely to represent an artefact of transfection. This series of experiments was carried out due to the availability of expression vectors containing the cSox2 and cSox3 cDNAs and because of the exclusive and complementary expression domains of

Sox2/3 and NSE in the CNS. As discussed above, most of the evidence presented in Chapter 6 argues against negative regulation of *NSE*, and this, together with the absence of consensus Sox binding sites in the sequenced portion of the *NSE* 5' flanking region indicates that the Sox factors probably do not regulate neuron-specific enolase, at least not directly. There are several factors, however which may have prevented the identification of such an interaction. Firstly, the distal 800 bp of the *NSE* 5' flanking region has not been sequenced and may contain one or more Sox binding sites. Secondly, the mouse Sox clones were not available and the chicken ones, used in their place, might not function in the same manner across species as they would in a homologous environment. Thirdly, the Sox factors might influence *NSE* gene expression indirectly, or may act on a region outside that studied in this project. It is also acknowledged that no preliminary experiments were carried out to investigate the effects of Sox expression upon endogenous *NSE*. The seriousness of this omission is understood and should this avenue be pursued in the future, such an experiment would be vital. There are other proteins expressed in a similar pattern to Sox-2 and Sox-3, such as the NRSF (Schoenherr and Andersen, 1995) and these are not thought to regulate *NSE*. The expression of Sox2/3 must therefore be regarded as purely circumstantial evidence for a role in *NSE* gene expression.

9.3.5 The role of distal regulatory elements and intron 1

One of the basic axioms upon which this project was founded was the competence of the 1.8 kbp 5' flanking sequence of the rat *NSE* gene to confer upon a heterologous gene the spatial, temporal and inducible specificity of endogenous *NSE*. The ability of this sequence to control the onset of reporter expression in parallel with the endogenous gene and to match its expression in the embryo was clearly shown in transgenic mice (Forss-Petter *et al.*, 1990). Its competence to respond to several inducing agents, including retinoic acid and NGF, in the same manner as endogenous *NSE*, was shown in stably transfected ES cells (Alouani *et al.*, 1993). However, whilst embryonic expression and inducible specificity were faithfully

reproduced, the level of reporter gene expression in the adult brain failed to match that of endogenous *NSE*, indicating the absence of a strong, postnatally active enhancer element (Forss-Petter *et al.*, 1990). The recent transient transfection study carried out by Sakimura and colleagues identified roles for more distal flanking sequence and the proximal half of intron 1 in neurons and PC12 cells differentiated with NGF (Sakimura *et al.*, 1995). A construct termed pEXCAT, containing 4.5 kbp of 5' flanking sequence and the proximal half of intron 1 (up to and including the *Xba* I site) generated a mean Relative CAT Activity of 5600% in neurons. Reduction of the 5' flanking sequence all the way down to 255 bp (the proximal *Xho* I site used herein to generate construct pNSE300CAT) resulted in only a 30% fall in reporter activity, suggesting, in excellent agreement with the data presented in this thesis, that most of the potential for controlling neuron-specific gene expression lay downstream from this position. However, removal of the first intron fragment resulted in a striking twentyfold reduction in CAT activity in neurons, and this effect was not ameliorated by replacing the intron upstream from the start of transcription, indicating that both the presence and position of the intron were critical factors for high level expression in neurons. Removing the intron had a negligible effect in nonneuronal cells such as primary cultured glial cells and HeLa cells but an approximately twentyfold reduction was also observed in PC12 cells suggesting that the intron regulatory element was indeed a strong, neuron-specific enhancer. Unfortunately, Sakimura and colleagues did not present any intron data for neuroblastoma cells, however, because of the activity of this element in primary cultured neurons and differentiated PC12 cells, both *ex vivo* models of mature, postmitotic neurons, it is tempting to speculate that the intron represents the postnatally active enhancer missing from the *NSE-lacZ* transgenic mice (Forss-Petter *et al.*, 1990). The region in question contains a number of interesting motifs, including a cAMP response element, which is a potential regulator of several neuronal genes including the rat dopamine β-hydrogenase gene (Shaskus *et al.*, 1992), and a neuronal consensus element (see Table 2.6). It is possible that the 5' flanking region contains elements responsible for spatial, temporal and inducible control which are active from onset, but that the dramatic postnatal increase in *NSE* gene activity is governed by this strong positive modulator which may itself be

neuron-specific or may take its cue from its context within the gene. The 5' flanking sequence is obviously capable of neuronal gene regulation in the absence of the intron but to prove the reciprocal, one would require that the intron be placed downstream of a heterologous promoter, perhaps by replacing the first intron of an alternative, nonneuronal gene. Very recently, the first intron of the muscle-specific enolase gene has been shown to control its muscle-specific expression pattern and this gene is an excellent candidate for such an experiment. If the intron is neuron-specific in its own right, this would suggest two independent mechanisms of neuronal gene regulation, perhaps reflecting the postnatal activation or synthesis of an intron binding neuron-specific transcription factor. This scenario would predict the existence of two independent or semi-independent mechanisms of neuron-specific gene expression governing the neuron-specific enolase gene.

Intron 1 was not considered in the transfection experiments presented herein and given its demonstrated importance, does this omission reduce the relevance of the data? Of course, the 5' flanking region of the *NSE* gene is still competent for neuron-specific regulation in the absence of intron 1 and this has been demonstrated not only in transgenic mice (Forss-Petter *et al.*, 1990; Martinou *et al.*, 1994) but also by herpesvirus-mediated transduction and by the transfection data obtained by Sakimura and coworkers. Thus, although the effect of the 5' flanking region has less impact than that of the intron, it is still worthy of investigation in its own right and may help to identify further control elements responsible for the regulation of the gene.

9.3.6 How useful are neuronal cell lines?

As discussed in section 9.2.1, transient transfection is a generally useful method for the study of gene regulation. However, the system has a number of disadvantages compared to *in vivo* analysis, reflecting the episomal nature of the foreign DNA and the transformed nature of the cells themselves. It is this second point which may be particularly relevant in the case of neuronal cell lines because, unlike the postmitotic

cells from which they are derived, they have the ability to divide and proliferate in culture. It is therefore likely that the intracellular milieu of regulatory factors found in neurons *in vivo* is distinct from that found in neuronal cell lines and this may have unpredictable effects on the regulation of neuronal genes.

A second disadvantage of neuronal cell lines is that the vast majority are derived from the peripheral nervous system, e.g. PC12 cells (Green and Tischler, 1976) which are adrenal in origin. This means that most types of central neuron are not represented by cell lines and the value of peripheral lines in the study of panneuronal genes, such as *NSE*, is therefore questionable. Even if such lines were perfectly representative of the endogenous cells from which they were derived, studies involving them would still paint an incomplete picture of the mechanism of gene expression in the context of the whole nervous system. This is especially true of a gene such as *NSE* whose expression is characterised by different levels of mRNA and protein in different populations of neurons and neuroendocrine cells.

One of the most striking factors to emerge from the review of neuron-specific gene expression (see Chapter 2) was the level of conflict between transfection analyses using different cell lines and between *ex vivo* and *in vivo* studies. For example, the very proximal AP1 and overlapping E box-containing dyad were shown to be both required and sufficient for cell type-specific expression of the tyrosine hydroxylase gene in PC8b cells (Yoon and Chickaraishi, 1992) but irrelevant in the closely related line PC12 (Wong *et al.*, 1994). Further investigation in other cell lines highlighted the importance of a proximal octamer element (Dawson *et al.*, 1994). Conversely, short regions of the tyrosine hydroxylase gene promoter were shown to be nonfunctional in transgenic mice (Banerjee *et al.*, 1992) and more than 5 kbp of 5' flanking material were in fact required for correct cell type-specific expression *in vivo*. Such reports for this and other neuronal genes may reflect genuinely different mechanisms active in distinct cell types, but nevertheless, they certainly emphasise the value of combined *ex vivo* and *in vivo* analysis of neuronal gene expression.

9.4 Expression and regulation of *NSE in vivo*

9.4.1 Expression of endogenous *NSE*

An investigation of endogenous *NSE* expression *in vivo* was carried out so that patterns of transgene expression could be compared to that of endogenous *NSE*. This has been a standard approach to the investigation of roles of specific regions of regulatory information in transgenic mice (for example, see Hoyle *et al.*, 1994). Biochemical analysis was carried out first in order to confirm when the endogenous gene was expressed. However, northern and western analysis were insensitive to the low level expression of *NSE* occurring in young neurogenic structures, and neither mRNA not protein could be detected until E17.5. Similar studies carried out in the past a reached much the same conclusions. The earliest stage at which NSE protein could be detected was E15 (Fletcher *et al.*, 1976) using a sensitive radioimmunoassay. E15 embryos were not examined in this project but NSE protein could not be detected using western analysis at E14.5. *NSE* mRNA was also first detected at E15 by Zeitoun *et al.*, based upon its ability to programme *in vitro* protein synthesis (Zeitoun *et al.*, 1983) and Lucas *et al.*, using northern analysis (Lucas *et al.*, 1988).

In situ detection methods are more sensitive than northern and western blotting and have been used to detect gene products expressed at very low levels (Wilkinson, 1992). Such studies have also revealed the expression of enolase genes much earlier than biochemical analyses have suggested. NSE protein was first detected at E10.5 by *in situ* immunohistochemical analysis to cryostat sections (Forss-Petter *et al.*, 1990), and *MSE* mRNA was detected in cardiac tube at E7.25 by *in situ* hybridisation (Keller *et al.*, 1992a), both several days earlier than previously reported by northern and western analysis (Lucas *et al.*, 1988; Barbieri *et al.*, 1990). The expression of NSE protein was investigated by *in situ* immunohistochemical analysis between E9.5 and E14.5, *NSE* mRNA expression was investigated at E9.5 and E8.5 because of reports suggesting the accumulation of *NSE* transcripts prior to expression of the protein (Forss-Petter *et al.*, 1986; Di

Liergo *et al.*, 1990). The purpose of these experiments was dual: firstly, they were necessary to provide a reference to which transgene expression patterns could be compared and secondly, they were necessary to identify an appropriate stage of development at which transgenic embryos could be studied. This was an important strategy in the project because, due to time constraints, the transient transgenic approach was favoured over the generation of trangenic lines. In the latter case, once a line is generated it can yield a limitless supply of experimental material for analysis. Conversely, it is the founder mice themselves which are sacrificed and used for analysis in the transient transgenic approach so only single embryos representing a given insertion event can be studied. It was therefore essential to determine the optimal stage of development before the embryos were isolated and this could only be done by looking at the endogenous gene.

The *in situ* hybridisation data indicated that the gene was first activated at E9.5, just following closure of the neural tube and at the time when the first neurons exit the cell cycle. Expression of the protein was first observed in ventral neurons of the rostral portion of the neural tube at E10.5, agreeing with previous observations (Forss-Petter *et al.*, 1990), but judging by the dorsal extent of the expression domain in the transverse plane of the neural tube at this stage, it is likely that NSE protein expression begins at E10 or E10.25. This is because at a given level of the neural tube along the rostrocaudal axis, NSE protein expression was shown to begin in ventral (motor) neurons. As development proceeded, motor neurons in progressively more rostral and more caudal positions along this axis began to express NSE and, in a given transverse plane, expression spread progressively to interneurons in the lateral regions and eventually to sensory neurons in the dorsal neural tube. This spatiotemporal gradient along the rostrocaudal and dorsoventral axes gave the impression that more caudal segments were 'regressed' in comparison to more rostral segments. The expression of NSE in some lateral neurons at E10.5 (Figure 7.8c(i)) suggested that analysis at marginally earlier stages would have caught the onset of expression in the first motor neurons to differentiate. These data suggested that *NSE* transcripts accumulated just prior to the protein, a factor which has been demonstrated by biochemical analysis in rats (Forss-Petter *et* al., 1986) but

was not thought to occur in mice (Lucas *et al.*, 1988). Analysis of NSE protein expression from E11.5 to E1.5 revealed staining in neuronal structures as expected although both the neural and pigmented layers of the retina appeared NSE-positive (the pigmented retina is a nonneuronal structure, Browder *et al.*, 1988). Expression in the early brain was limited to the mantle layer (grey matter, mostly neurons) and peripheral marginal layer (rich in axon bundles) but absent from the ependymal layer (which contains proliferating cells). More intense staining was observed in midbrain and hindbrain structures (pons, medulla) compared to forebrain structures (hypothalamus, cerebral cortex) a phenomenon which has been observed previously and has been attributed to the relatively slow development of forebrain structures compared to other brain regions (Zomzely-Neurath and Walker, 1980). The amount of NSE positive material appeared to increase throughout development, consistent with the continued deposition of postmitotic neurons. From these studies it was decided that E13.5 would be a suitable stage at which to sacrifice transgenic embryos. This decision was taken on the basis that the pattern of NSE expression was characteristic and well-established at this stage throughout the brain and spinal cord, whilst the embryos were still a suitable and convenient size for wholemount staining.

9.4.2 Expression of β-galactosidase under control of the *NSE* promoter

From four embryo transfer procedures, nineteen embryos were isolated and seven were found to be transgenic based upon the results of PCR testing. Compared to previous such studies, this success rate (7/19 or 37%) was remarkably high. Forss-Petter and colleagues obtained eight founders from eighty transfers (10%) whilst Martinou and coworkers obtained six founders from the same number of transfers (7.5%) (Forss-Petter *et al.*, 1990; Martinou *et al.*, 1994). The proportion of transgenic embryos which expressed the transgene has also varied. In the present study, two embryos out of seven expressed detectable levels of β-galactosidase, although the staining was weak and limited to certain neuronal populations. One embryo was shown to express *lacZ* in individual cells at the dorsal midline of the

midbrain and hindbrain whilst both appeared to express *lacZ* in the neural component of the pituitary gland. However, most of the neuronal and nonneuronal cells in the embryo were β-galactosidase negative. In the study carried out by Forss-Petter *et al.*, one of the eight transgenic lines was shown to contain a partial transgene and was not investigated further. Of the remaining seven, only four expressed detectable levels of β-galactosidase, and only two of these showed the high level, neuron-specific and panneuronal embryonic expression which was the major subject of the published article (Forss-Petter *et al.*, 1990). Incidentally, the lines containing the lowest transgene copy number (3-5 copies, as determined by quantitative Southern analysis) were those that expressed the transgene most strongly. The two weakly-expressing lines had integrated approximately 10 copies of the transgene and the weak β-galactosidase activity could be detected only in a few discrete areas of the brain. *lacZ* mRNA and β-galactosidase activity could not be detected in a further line carrying more than 20 copies of the transgene. Of the six transgenic lines expressing human BCL-2 protein under the control of the *NSE* promoter (Martinou *et al*, 1994), five expressed high levels of the transgene product in neurons but in four lines this was restricted to the postnatal nervous system. The one line in which *NSE-BCL-2* expression was detected in embryos was found to contain two insertions which segregated independently, suggesting integration into two different chromosomes (termed 'a' and 'b'). Embryonic expression of the transgene was associated with females displaying an imperforate vagina, and this was thought to reflect the effects of ectopic *BCL-2* expression as the same effect was observed in transgenic mice in which *BCL-2* was expressed under the control of the phosphoglycerate kinase promoter. Early expression was associated with one specific insertion only as this and the imperforate vagina phenotype were found only in progeny of the double-insert founder which themselves carried both insertions (NSEab), or the first insert only (NSEa). Progeny carrying the other insertion (NSEb) expressed *BCL-2* in the postnatal nervous system, as did the other four lines, and did not display the vaginal phenotype. These results demonstrated that the expression of reporter genes under the control of the 1.8 kbp complete *NSE* regulatory sequence in transgenic mice was variable, probably reflecting the site of integration and probably also influenced by the transgene copy number. It is likely

that neuron-specific elements are found in the 1.8 kbp sequence but that these are very sensitive to position effects. Thus, whilst Martinou *et al.* found that the neuronal specificity of this element was normally restricted to postnatal animals, Forss-Petter *et al.* found that levels of transgene expression in embryos and adults were approximately the same. Evidence from comparisons between endogenous gene and transgene expression (Forss-Petter *et al.*, 1990) and from transfection experiments (Sakimura *et al*, 1995) have indicated that sequences outside the 1.8 kbp 5' flanking element are also important for *NSE* gene regulation, at least postnatally. It would be interesting to look at the effect of intron 1 sequences in transgenic mice, perhaps by comparing mice containing and not containing the intron. A dominant negative FGF receptor has recently been expressed in transgenic mice under the control of *NSE* 5' regulatory sequences plus the first intron and expression of the transgene was not detected until E18 (F. Walsh, unpublished data). However, analysis was carried out by western blot, not by the more sensitive immunohistochemical staining, therefore the onset may well be earlier (pers. comm.).

Two conclusions can be drawn from these studies which may suggest routes for further investigation of *NSE* expression in transgenic mice. Firstly, the expression of a reporter gene under the control of the *NSE* promoter is generally restricted to neuronal structures, although the extent of that expression may vary from limited regions of the nervous system and peripheral neuroendocrine tissue (as found herein) to full panneuronal expression (Forss-Petter *et al.*, 1990). The onset of expression is also variable and it is possible that analysis of the transgenic embryos obtained during this project at a later developmental stage would have been more rewarding. Secondly, and leading on from the first conclusion, it is probably nonproductive to conduct further experiments using the transient transgenic approach because of the limited analysis which can be carried out on single embryos. The variable expression of reporter genes driven by *NSE* flanking sequences is probably due to position effects but the competence of the 1.8 kbp regulatory sequence could be established in the absence of such effects, perhaps by flanking the transgene with boundary elements (Chada *et al.*, 1985; Eissenberg and Elgin, 1991; Mlynárová *et*

al., 1994). This competence should be firmly established before any conclusions can be drawn from the analysis of more truncated constructs.

9.4.3 How reliable are transgenic mice for the study of neuronal gene expression?

The advent of transgenic mouse technology has allowed reporter genes to be introduced directly into the nucleus of a mouse oocyte wherein they often integrate into the host DNA and become stably inherited and propagated in the mouse germline (Palmiter and Brinster, 1986). The expression of a transgene can then be observed in the context of the entire organism, which is a great advantage over cell line studies, and lines of transgenic animals yield a potentially limitless supply of experimental material (Twyman and Jones, 1995b). At present, the major disadvantage of transgenic analysis is that the site of transgene integration is random (unless specific allele replacement/gene knockout techniques are applied). The results of such random integration are position effects, whereby integrated genes come under the control of nearby endogenous regulatory elements, resulting in ectopic expression or inappropriate silencing which is not regulated by the integrated DNA. Position effects can lead to the misinterpretation of transgenic data and can generate contradictory results from independent studies using the same transgene. Many neuronal genes have been analysed in transgenic mice (Twyman and Jones, 1995b) and, at present, the only way around the problem of position effects is to generate a number of transgenic lines so that one-off misexpression phenomena can be identified as such. Other strategies for studying gene regulation *in vivo* have been developed recently and these may contribute to the study of neuronal gene expression in the future. Such tactics include the transfection of brain sections using a particle mediated or 'gene gun' approach (Lo *et al.*, 1994), the transduction of reporter genes into neurons using recombinant neurotrophic viruses (Crystal, 1995; for examples of *in vivo* transduction using *NSE* reporter sequences, see Andersen *et al.*, 1992 and 1993) and the transfection of living embryos *in utero* by injecting pregnant mice with DNA:liposome complexes (Tsukamoto *et al.*, 1995). These

approaches combine the convenience of transfection with the 'whole organism' context of transgenic analysis and may well feature strongly in future analysis of neuronal genes.

9.5 Protein-DNA interactions in the *NSE* 5' flanking region

The results from transfection experiments were summarised at the beginning of Chapter 8 and from this summary, a number of regions of the proximal 5' flanking sequence were identified as candidates for *in vitro* analysis. Region A, the fragment spanning between positions -255 and -120 which had been shown in this project to be active as a silencer in Ltk- and Neuro-2A cells, and similarly in NB35 neuroblastoma cells (Sakimura *et al.*, 1995), but as an enhancer in PC12 cells, was subjected to gel retardation analysis. This failed to identify consistent binding activity in extracts of PC12 cells or Neuro-2A cells, but a full range of experiments to optimise binding conditions was not attempted in the limited time remaining. A number of specific binding complexes was observed in extracts of Ltk- and HeLa cells but there was not time to pursue this discovery further. Future work could involve characterisation of the protein-DNA complexes by footprinting or methylation interference strategies. It might also be possible to identify the binding factor(s) by attempting to supershift the protein-DNA complexes with antibodies chosen on the basis of the consensus sites within this region. One putative target would be AP-2 (Imagawa *et al.*, 1987). There are also several interesting motifs which may well bind novel factors - these include two AC-rich sequence elements, CCCCCACCC at position -180 and CCCCACCACCACCC at position -160. It is noteworthy that these sequences are similar to the PER2 element (CCCCCCACCCCCC) which was found to be essential for the expression of another neuronal gene, peripherin (Desmaris *et al.*, 1992).

The most proximal 95 bp of 5' flanking region is still capable of neuron specific expression in P19 neurons and similar results were obtained using primary cultured neurons (Sakimura *et al.*, 1995). To facilitate future analysis of this region, the

most proximal 120 bp of 5' flanking material plus exon 1 was subcloned into pBluescriptIIKS+. This region contains consensus motifs for AP-1 (Lee *et al.*, 1987), AP-2 (Imagawa *et al.*, 1987), Sp-1 (Briggs *et al.*, 1986) and a putative TATA-like box. This region also contains several AC-rich elements similar to those described in the previous paragraph which may warrant further attention.

Sakimura an colleagues have reported the identification of brain-specific proteins binding to the intron and most proximal promoter region of the *NSE* gene, although further characterisation of these proteins has not been reported as yet (Katagiri *et al.*, unpublished observations). Confirmation of protein binding activity in the proximal promoter is very encouraging, and Sakimura *et al.* report that both gel retardation and DNA footprinting are being used to characterise these interactions. Hopefully, the further study of these regions will eventually provide a full understanding of the mechanisms used to control *NSE* gene expression and this may contribute to our understanding of neuron-specific gene expression and the molecular biology of the enolase gene family.

Section IV - Bibliography

Bibliography

Akazawa, C., Sasai, Y., Nakanishi, S., and Kageyama, R. (1992). Molecular characterisation of a rat negative regulator with a basic helix-loop-helix structure predominantly expressed in the developing nervous system. *J. Biol. Chem.* 267: 21879-21885.

Albert, V. R., Lee, M. R., Bolden, A, H,, Wurzburgerm R, J, and Aguanno, A. (1992). Distinct promoters direct neuronal and nonneuronal expression of rat aromatic L-amino acid decrboxylase. *Proc. Natl. Acad. Sci. USA* 89: 12053-12057.

Alberts, B., Bray, D., Lewis, J., Raff, M., Roberts, K., and Watson, J. (1994). *Molecular Biology of the Cell,* 3rd Edition (Robertson, M., Ed.; Garland Press, NY).

Alouani, S., Ketchum, S., Rambosson, C., and Eistetter, H. R. (1993). Transcriptional activity of the neuron-specific enolase (NSE) promoter in murine embryonic stem (ES) cells and preimplantation embryos. *Eur. J. Cell Biol.* 62: 324-332.

Altschuler, R. A., Reeks, K. A., Marangos, P. J., and Fex, J. (1985). Neuron-specific enolase-like immunoreactivity in inner hair cells but not outer hair cells in the guinnea pig organ of Corti. *Brain Res.* 327: 379-384.

Andersen, B., Schonemann, M. D., Pearse, R. V. II, Jenne, K., and Sugarman, J. (1994). Brn-5 is a divergent POU domain factor highly expressed in layer IV of the neocortex. *J. Biol. Chem.* 268: 23390-23398.

Andersen, J. K., Frim, D. M., Isacson, O., and Breakefield, X. O. (1993). Herpesvirus-mediated gene delivery into the rat brain: specificity and efficiency of the neuron-specific enolase promoter. *Cell. Mol. Neurobiol.* 13: 503-515.

Andersen, J. K., Garber, D. A., Meaney, C. A., and Breakefield, X. O. (1992). Gene transfer into mammalian central nervous system using Herpes Virus vectors: extended expression of bacterial *lacZ* using the neuron-specific enolase promoter. *Hum. Gene Therapy* 3: 487-499.

Anderson, D. J. (1989). The neural crest cell lineage problem: Neuropoiesis? *Neuron* 3: 1-12.

Anderson, D. J. (1993). *MASH* genes and the logic of neural crest cell lineage diversification. *Competes Rendus de l'Academie des Sciences Serie III Sciences de la Vie* 316: 1082-1096.

Andrews, P. W. (1984). Retinoic acid induces neuronal differentiation of a cloned human embryonal carcinoma cell line *in vitro*. *Dev. Biol.* 103: 285-293.

Ang, H. L., Carter, D. A., and Murphy, D. (1993). Neuron-specific expression and physiological regulation of bovine vasopressin transgenes in mice. *EMBO J.* 12: 2397-2409.

Angelova, P., Davidoff, M., Baleva, K., and Staykova, M. (1991). Substance P-like and neuron-specific enolase-like immunoreactivity of rodent leydig cells in tissue section and cell culture. *Acta Histochem.* 91: 131-139.

Archer, B. T. III, Özcelik, T., Jahn, R., Francke, U., and Südhof, T. C. (1990). Structures and chromosomal locations of two human genes encoding synaptobrevin I and synaptobrevin II. *J. Biol. Chem.* 265: 17267-17273.

Baetge, E. E., Behringer, R. R., Messing, A., Brinster, R. L., and Palmiter, R. D. (1988). Transgenic mice express the human phenylethanloamine *N*-methyltransferase gene in adrenal medulla and retina. *Proc. Natl. Acad. Sci. USA* 85: 3648-3652.

Banerjee, S. A., Hoppe, P., Brilliant, M., and Chikaraishi, D. M. (1992). 5' flanking sequences of the rat tyrosine hydroxylase gene target accurate tissue-specific, developmental and transsynaptyic expression in transgenic mice. *J. Neurosci.* 12: 4460-4467.

Banerjee, S. A., Roffler-Tarlov, S., Szabo, M., Frohman, L., and Chikaraishi, D. M. (1994). DNA regulatory sequences of the rat tyrosine hydroxylase gene direct correct catecholaminergic cell-type specificity of a human growth hormone reporter in the CNS of transgenic mice causing a dwarf phenotype. *Mol. Brain Res.* 24: 89-106.

Barbieri, G., De Angelis, L., Feo, S., Cossu, G., and Giallongo, A. (1990). Differential expression of muscle-specific enolase in embryonic and fetal myogenic cells during mouse development. *Differentiation* 45: 179-184.

Barde, Y. A. (1991). Trophic factors and neuronal survival. *Neuron* 2: 1525-1534.

Bargou, R. C. E. F., and Leube, R. E. (1991). The synaptophysin-encoding gene in rat and man is specifically transcribed in neuroendocrine cells. *Gene (Amst.)* 99: 197-204.

Bartels, H., and Vogel, I. (1971). Isoenzymes in human erythrocytes. *Z. Kinderheilk* 111: 247-251.

Bartholomä, A., and Nave, K-A. (1994). NEX-1: a novel brain-specific helix-loop-helix protein with autoregulation and sustained expression in mature cortical neurons. *MOD.* 48: 217-228.

Batke, J., Nazaryan, K. B., and Karapetian, N. H. (1988). Complex of brain D-phosphoglycerate mutase and γ-enolase and its reactivation by D-glycerate 2,3-bisphosphate. *Arch. Biochem. Biophys.* 264: 510-518.

Beaudet, L., Charron, G., Houle, D., Tretjakoff, I., Peterson, A., and Julien, P. (1992). Intragenic regulatory elements contribute to the transcriptional control of the neurofilament light gene. *Gene (Amst.)* 116: 205-214.

Benjamin, S., Habert, E., Berrard, S., Duman Milne Edwards, J. B., Loeffler, J-P., and Mallet, J. (1992). Promoter elements of the rat choline acetyltransferase gene allowing nerve growth factor inducibility in transfected primary cultured cells. *J. Neurochem.* 58: 1580-1583.

Bessis, A., Savatier, N., Devillers-Thiery, A., Benjanin, S., and Changeux, J. P. (1993). Negative regulatory elements upstream of a novel exon of the neuronal nicotinic acetylcholine receptor α2 subunit gene. *Nucleic Acids Res.* 21: 2185-2192.

Birnboim, H. C., and Doly, J. (1979). A rapid alkaline extraction procedure for screening recombinant plasmid DNA. *Nucleic Acids Res.* 7: 1513.

Bishop, A. E., Polak, J. M., Facer, P., Ferri, G. L., Marangos, P .J., and Pearse, A. G. E. (1982). Neuron-specific enolase - a common marker for the endocrine cells and innervation of the gut and pancreas. *Gastroenterology* 83: 902-915.

Bock, E., and Dissing, J. (1975). Demonstration of enolase activity connected to the brain specific protein 14-3-2. *Scand. J. Immunol. Suppl.* 2: 31-36.

Bock, E., Fletcher, L., Rider, C. C., and Taylor, C. B. (1978). The nature of the two proteins of brain-specific antigen 14-3-2. *J. Neurochem.* 30: 181-185.

Bock, E., Yavin, Z., Jørgenson, O. S., and Yavin, E. (1980). Nervous system-specific proteins in developing rat cerebral cells in culture. *J. Neurochem.* 35: 1297-1302.

Bodner, M., Castrillo, J. L., Theill, L. E., Dee Rinck, M., Ellisman, M., and Karin, M. (1988). The pituitary-specific transcription factor GHF-1 is a homeobox-containing protein. *Cell* 50: 267-275.

Bonnerot, C., and Nicholas, J-F. (1993). Application of *LacZ* gene fusions to postimplantation development. *Methods Enzymol.* 255: 461-465.

Boyd, R. T. (1994). Sequencing and promoter analysis of the genomic region between the rat neuronal nicotinic acetylcholine receptor β4 and α3 genes. *J. Neurobiol.* 25: 960-973.

Brady, S. T., and Lasek, R. J. (1981). Nerve-specific enolase and creatine-phosphokinase in axonal transport - soluble proteins and the axoplasmic matrix. *Cell* 23: 515-523.

Brand, A. H., Breeden, L., Abraham, J., Sternglanz, R., and Nasmyth, K. (1985). Characterization of a "silencer" in yeast: a DNA sequence with properties opposite to those of a transcriptional enhancer. *Cell* 41: 41-48.

Brewer, J. M. (1981). Yeast enolase: mechanism of activation by metal ions. *Crit. Rev. Biochem.* 11: 209-254.

Briggs, M. R., Kadonga, J. T., Bell, S. P., and Tjian, R. (1986). Purification and biochemical characterization of the promoter-specific transcription factor, SP-1. *Science* 234: 47-52.

Browder, L. W., Erickson, C. A., and Jeffery, W. R. (1991). *Developmental Biology,* 3rd Edition (Sanders College Publishing, Holt, Rinehart and Winston, Inc., Florida, USA)

Brown, L., and Baer, R. (1994). *HEN1* encodes a 20-kilodalton phosphoprotein that binds an extended E-box motif as a homodimer. *Mol. Cell. Biol.* 14: 1245-1255.

Brown, L., Espinosa, R. III, Le Beau, M. M., Sicilliano, M. J., and Baer, R. (1992). *HEN1* and *HEN2*: A subgroup of basic helix-loop-helix genes that are coexpressed in a human neuroblastoma. *Proc. Natl. Acad. Sci. USA* 89: 8492-8496.

Buchman, V. L., Ninkina, N. N., Bogdanov, Y. D., Bortvin, A. L., Akopian, H. N., Kiselev, S. L., Krylova, O. Y., Anokhin, K. V., and Georgiev, G. P. (1992). Differential splicing creates a diversity of transcripts from a neurospecific developmentally regulated gene encoding a protein with new zinc-finger motifs. *Nucleic Acids Res.* 20: 5579-5585.

Buckingham, M. E. (1994). Muscle: The regulation of myogenesis. *Curr. Op. Genet. & Dev.* 4: 745-751.

Budhram-Mahadeo, V., Theil, T., Morris, P. J., Lillycrop, K. A., and Latchman, D. S. (1994). The DNA target site for the Brn-3 POU family transcription factors can confer responsiveness to cyclic AMP and removal of serum from neuronal cells. *Nucleic Acids Res.* 22: 3092-3098.

Budhram-Mahadeo, V., Morris, P. J., Lakin, N. D., Theil, T., Ching, G. Y., Lillycrop, K. A., Mōröy, T., Liem, R. K. H., and Latchman, D. S. (1995). Activation of the α-internexin promoter by the Brn-3a transcription factor is dependent on the N-terminal region of the protein. *J. Biol. Chem.* 270: 2853-2858.

Bulleit, R. F., Cui, H., Wang, J., and Lin, X. (1994). NMDA receptor activation in differentiating cerebellar cell cultures regulates the expression of a new POU gene, *Cns-1*. *J. Neurosci.* 14: 1584-1595.

Buono, P., Deconciliis, L., Olivetta, E., Izzo, P., and Salvatore, F. (1993). *Cis*-acting elements in the promoter region of the human aldolase C gene. *FEBS Lett.* 328: 243-249.

Byrne, G. W., and Ruddle, F. H. (1989). Multiplex gene regulation - a two-tiered approach to transgene regulation in transgenic mice. *Proc. Natl. Acad. Sci. USA* 86: 5473-5477.

Cadd, G. G., Hoyle, C. W., Quaif, C. J., Marck, B., Matsumoto, A. M., Brinster, R. L., and Palmiter, R. D. (1992). Alteration of neurotransmitter phenotype in noradrenergic neurons of transgenic mice. *Mol. Endocrinol.* 11: 1951-1960.

Calì, L., Feo, S., Oliva, D., and Giallongo, A. (1990). Nucleotide sequence of a cDNA encoding human muscle-specific enolase (MSE). *Nucleic Acids Res.* 18: 1893.

Cambi, F., Fung, B., and Chikaraishi, D. (1989). 5' flanking DNA sequences direct cell-specific expression of rat tyrosine hydroxylase. *J. Neurochem.* 53: 1656-1659.

Campos-Ortega, J. A., and Knust, E. (1990). Molecular analysis of a cellular decision during embryonic development of *Drosophila melanogaster* - epidermogenesis or neurogenesis? *Eur. J. Biochem.* 190: 1-10.

Campos-Ortega, J. A., and Jan, Y. N. (1991). Genetic and molecular bases of neurogenesis in *Drosophila melanogaster*. *Annu. Rev. Neurosci.* 14: 399-420.

Cao, X., Koski, R. A., Gashler, A. K., McKiernan, M., Morris, C. F., Gaffney, R., Hay, R. U., and Sukhatme, V. P. (1990). Identification and characterization of the *Egr-1* gene product - a DNA-binding zinc finger protein induced by differentiation and growth signals. *Mol. Cell. Biol.* 10: 1931-1939.

Cardenas J. M., and Wold, F. (1971). Comparative studies on structural and catalytic properties of enolase. *Arch. Biochem. Biophys.* 144: 663-672.

Cervello, M., Giallongo, A., Damelio, L., Sciarrino, S., and Matranga, V. (1993). γ-enolase expression as early marker of neuronal differentiation of murine neuroblastoma cells N-115. *Cytotechnology* 11: 167-169.

Chada, K., Magram, J., Raphael, K., Radice, G., Lacy, E., and Costantini, F. (1985). Specific expression of a foreign β-globin gene in erythroid cells of transgenic mice. *Nature* 314: 377-380.

Chen, C., and Okayama, H. (1987). High efficiency transformation of mammalian cells by plasmid DNA. *Mol. Cell. Biol.* 7: 2745-2751.

Chen, C., and Okayama, H. (1988). Calcium phosphate-mediated gene transfer: A highly efficient transfection system for stably transforming cells with plasmid DNA. *BioTechniques* 6: 632.

Chen, S-H., and Giblett, E. R. (1976). Enolase: human tissue distribution and evidence for three different loci. *Ann. Hum. Genet.* 39: 277-280.

Chin, C. C. Q. (1990). The primary structure of rabbit muscle enolase. *J. Protein Chem.* 9: 427-432.

Chin, L-S., Li, L., and Greengard, P. (1994). Neuron-specific expression of the synapsin II gene is directed by a specific core promoter and upstream regulatory elements. *J. Biol. Chem.* 269: 18507-18513.

Ching, G. Y., and Liem, R. K. H. (1991). Structure of the gene for the neuronal intermediate filament protein α-internexin and functional analysis of its promoter. *J. Biol. Chem.* 266: 19459-19468.

Chirgwin, J. M., Ptzylyla, A. E., MacDonald, R. J., and Rutter, W. J. (1979). Isolation of biologically active ribonucleic acid from sources enriched in ribonuclease. *Biochemistry* 18: 294-299.

Chowdhury, K., Dressler, G., Breier, G., Deutsch, U., and Gruss, P. (1988). The primary structrure of the murine gene *mKr2* and its specific expression in developing and adult neurons. *EMBO J.* 7: 1345-1353.

Christy, B. A., Lau, L. F., and Nathans, D. (1988). A gene activated in mouse 3T3 cells by serum growth factors encodes a protein with "zinc finger" sequences. *Proc. Natl. Acad. Sci. USA* 85: 7857-7861.

Christy, B. A., and Nathans, D. (1989). DNA-binding site of the growth factor inducible protein zif268. *Proc. Natl. Acad. Sci. USA* 86: 8737-8741.

Chung, J. H., Whiteley, M., and Felsenfeld, G. (1993). A 5' element of the chicken β-globin domain acts as an insulator in human erythroid cells and protects against position effects in *Drosophila*. *Cell* 74: 505-514.

Church, G. M., and Gilbert, W. (1984). Genomic Sequencing. *Proc. Natl. Acad. Sci. USA* 81: 1991-1995.

Clark-Rosenberg, R. L., and Marangos, P. J. (1980). Phylogenetic distribution of neuron-specific enolase. *J. Neurochem.* 35: 756-759.

Clerc, R. G., Corcoran, L. M., Le Bowitz, J. H., Baltimore, D., and Sharp, P. A. (1988). The B-cell-specific Oct-2 protein contains POU box- and homeo-box-type domains. *Genes & Dev.* 2: 1570-1581.

Cohen, S. N., Chang, A. C. Y., and Hsu, L. (1972). Nonchromosomal antibiotic resistance in bacteria: Genetic transformation of *Escherichia coli* by R-factor DNA. *Proc. Natl. Acad. Sci. USA* 69: 2110.

Collum, R. G., Fisher, P. E., Datta, M., Mellis, S., Thiele, C., Huebner, K., Croce, C. M., Israel, M. A., Thiel, T., and Möröy, T. (1992). A novel POU homeodomain gene specifically expressed in cells of the developing mammalian nervous system. *Nucleic Acids Res.* 20: 4919-4925.

Cook, P. J. L., and Hammerton, J. L. (1979). Report on the committee on the genetics of chromosome 1. *Cytogenet. Cell Genet.* 25: 9-20.

Cooper, J. A., Reiss, N. A., Schwartz, R. J., and Hunter, T. (1983). Three glycolytic enzymes are phosphorylated at tyrosine in cells transformed by Rous sarcoma virus. *Nature* 302: 218-223.

Cooper, J. A., Esch, F. S., Taylor, S. S., and Hunter, T. (1984). Phosphorylation sites in enolase and lactate dehydrogenase utilised by tyrosine protein kinases *in vivo* and *in vitro*. *J. Biol. Chem.* 259: 7835-7841.

Coté, F., Collard, J. F., and Julien, J. P. (1993). Progressive neuronopathy in transgenic mice expressing the human neurofilament heavy gene: A mouse model of amyotrophic lateral sclerosis. *Cell* 73: 35-46.

Craig, S. P., Day, I. N. M., Thompson, R. J., and Craig, I. W. (1989). Localisation of human neuron-specific enolase to chromosome 12p13. *Cytogenet. Cell Genet.* 51: 980.

Criss, W. E. (1971). A review of isozymes in cancer. *Cancer Res.* 31: 1523-1542.

Crosby, S. D., Veile, R. A., Donis-Keller, H., Baraban, J. M., Bhat, R. V., Simburger, K. S., and Milbrandt, J. (1992). Neural-specific expression, genomic structure, and chromosomal localization of the gene encoding the zinc-finger transcription factor NGFI-C. *Proc. Natl. Acad. Sci. USA* 89: 4739-4743.

Crystal, R. G. (1995). Transfer of genes to humans: early lessons and obstacles to success. *Science* 270: 404-409.

Das, G. C., and Piatigorsky, J. (1986). The chicken δ1-crystallin gene promoter: binding of transcription factor(s) to the upstream G+C-rich region is necessary for promoter function *in vitro*. *Proc. Natl. Acad. Sci. USA* 83: 3131-3135.

Das, G. C., and Piatigorsky, J. (1988). Promoter activity of the two chicken δ-crystallin genes in HeLa cell extract. *Curr. Eye Res.* 7: 331-340.

Daubas, P., Salmon, A. M., Zoli, M., Geoffroy, B., Devillers-Thiery, A., Bessis, A., Medevielle, F., and Changeux, J. P. (1993). Chicken neuronal acetylcholine receptor α2 subunit gene exhibits neuron-specific expression in the brain and spinal cord of transgenic mice. *Proc. Natl. Acad. Sci. USA* 90: 2237-2241.

Dawson, S. J., Yoon, S. O., Chikaraishi, D. M., Lillycrop, K. A., and Latchman, D. S. (1994). The Oct-2 transcription factor represses tyrosine hydroxylase expression via a heptamer TAATGARAT-like motif in the gene promoter. *Nucelic Acids Res.* 22:1023-1028.

Day, I. N. M., Allsopp, M. T. E. P., Moore, D. C. McN., and Thompson, R. J. (1987). Sequence conservation in the 3'-untranslated regions of neuron-specifc enolase, lymphokine and protooncogene mRNAs. *FEBS Lett.* 222: 139-143.

Day, I. N. M., Peshavaria, M., and Quinn, G. B. (1993). A differential molecular clock in enolase isoprotein evolution. *J. Mol. Evolution* 36: 599-601.

De Vitry, F., Picart, R., Jacque, C., Legault, L., Dupouey, P., and Tixier-Vidal, A. (1980). Presumptive common precursor for neuronal and glial cell lineages in mouse hypothalamus. *Proc. Natl. Acad. Sci. USA* 77: 4165-4169.

Dent, C. L., and Latchman, D. S. (1993). The DNA mobility shift assay. In *Transcription Factors: A Practical Approach* (Latchman, D. S., Ed., IRL Press, Oxford, UK), pp 1-23.

Desmaris, D., Fillon, M., Lapointe, L., and Royal, A. (1992). Cell-specific transcription of the peripherin gene in neuronal cell lines involves a *cis*-acting element surrounding the TATA box. *EMBO J.* 11: 2971-2980.

Di Liergo, I., Cestelli, A., Barbieri, G., and Giallongo, A. (1991). Developmental changes of neuron-specific enolase mRNA in primary cultures of rat neurons. *Cell. Mol. Neurobiol.* 11:289-294.

Dong, J-M., Smith, P., Hall, C., and Lim, L. (1995). Promoter region of the transcriptional unit for the human α1-chimaerin, a neuron-specific GTPase-activating protein for p21rac. *Eur. J. Biochem.* 227: 636-648.

Duncan, M., Di Cicco-Bloom, E. M., Xiang, X., Benezra, R., and Chada, K. (1992). The gene for the helix-loop-helix protien Id is specifically expressed in neural precursors. *Dev. Biol.* 154: 1-10.

Dupin, E., Maus, M., and Fauquet, M. (1993). Regulation of quail tyrosine hydroxylase gene in neural crest cells by cAMP and β-adrenergic ligands. *Dev. Biol.* 159: 75-86.

Duvoisin, R. M., and Heinmann, S. F. (1993). Transcription control elements of the rat neuronal nicotinic acetylcholine receptor subunit α3. *Brazil. J. Med. Biol. Res.* 26: 137-150.

Edwards, Y. H., Tiler, T. P., Morgan-Hughes, J. A., Neerunjun, J. S., and Hopkinson, D. A. (1982). Isoenzyme patterns and protein profiles in neuromuscular disorders. *J. Med. Genet.* 19: 175-183.

Eggen, B. J. L., Nielander, H. B., Rensen de Leeuw, M. G. A., Schotman, P., Gispen, W. H., and Schrama, L. H. (1994). Identification of two promoter regions in the rat *B-50/GAP-43* gene. *Mol. Brain Res.* 23: 221-234.

Eigenbrodt, E., Fister, P., Rubsamen, H., and Friis, R. R. (1983). Influence of transformation by Rous sarcoma virus on the amount, phosphorylation and enzyme kinetic properties of enolase. *EMBO J.* 2: 1565-1570.

Eissenberg, J. C., and Elgin, S. C. R. (1991). Boundary functions in the control of gene expression. *Trends Genet.* 10: 335-340.

Elder, G. A., Liang, Z., Lee, N., Friedrich, V. L. Jr., and Lazzarini, R. A. (1992a). Novel DNA binding proteins participate in the regulation of human neurofilament H gene expression. *Mol. Brain Res.* 15: 85-98.

Elder, G. A., Liang, Z., Snyder, S. E., and Lazzarini, R. A. (1992b). Multiple nuclear factors interact with the promoter of the human neurofilament M gene. *Mol. Brain Res.* 15: 99-107.

Faraonio, R., Minopoli, G., Porcellini, A., Costanzo, F., Cimino, F., and Russo, T. (1994). The DNA sequence encompassing the transcription start site of a TATA-less promoter contains enough information to drive neuron-specific transcription. *Nucleic Acids Res.* 22: 4876-4883.

Farjo, Q., Jackson, A. U., Xu, J., Gryzenia, M., Skolnick, C., Agarwal, N., and Swaroop, A. (1993). Molecular characterization of the murine neural retina leucine zipper gene *Nrl*. *Genomics* 18: 216-222.

Feo, S., Oliva, D., Brabieri, G., Xu, W., Fried, M., and Giallongo, A. (1990a). The gene for the muscle-specific enolase is on the short arm of human chromosome 17. *Genomics* 10: 157-165.

Feo, S., Oliva, D., Arico, B., Braba, G., Calì, L., and Giallongo, A. (1990b). The human genome contains a single processed pseudogene for α-enolase located on chromosome 1. *DNA Sequence* 1: 79-83.

Finney, M., Ruvkin, G., and Horvitz, H. R. (1988). The *C. elegans* cell lineage and differentiation gene *unc-86* encodes a protein containing a homeodomain and extended sequence similarity to mammalian transcription factors. *Cell* 55: 757-769.

Fletcher, L., Rider, C. C., and Taylor, C. B. (1976). Enolase isoenzymes. III. Chromatographic and immunological characteristics of rat brain enolase. *Biochim. Biophys. Acta* 452: 245-252.

Fletcher, L., Rider, C. C., Taylor, C. B., Adamson, E. D., Luke, B. M., and Graham, B. M. (1978). Enolase isoenzymes as markers of differentiation in teratocarcinoma cells and normal tissues of mouse. *Dev. Biol.* 65: 462-475.

Forss-Petter, S., Danielson, P., and Sutcliffe, J. G. (1986). Neuron-specific enoalse: Complete structure of the rat mRNA, multiple transcriptional start sites, and evidence suggesting posttranscriptional control. *J. Neurosci. Res.* 16: 141-156.

Forss-Petter, S., Danielson, P. E., Catsicas, S., Battenberg, E., Price, J., Nerenberg, M., and Sutcliffe, J. G. (1990). Transgenic mice expressing β-galactosidase in mature neurons under neuron-specific enolase promoter control. *Neuron* 5: 187-197.

Frikke, M. J., Seshi, B., and Bell., C. E. (1987). Monoclonal antibodies to human neuron-specific enolase reveal heterogeneity of the enzyme in neurons of the central nervous system. *Brain Res.* 417: 283-292.

Frykberg, T., Esscher, T., Pahlman, S., and Olsson, Y. (1985). Neuron-specific enolase as a marker for intestinal neurons - an immunohistochemical study of the human intestinal tract. *Acta Neuropathalogica* 66: 184-187.

Fung, B., Yoon, S. O., and Chikaraishi, D. (1992). Sequences that direct rat tyrosine hydroxylase gene expression. *J. Neurochem.* 58: 2044-2052.

Gandelman, K-Y., Coker, G. T. III, Moffat, M. A., and O'Malley, K. L. (1990). Species and regional differences in the expression of cell type-specific elements in the human and rat tyrosine hydroxylase gene loci. *J. Neurochem.* 55: 2149-2152.

Gendon-Maguire, M., and Gridley, T. (1993). Identification of transgenic mice. *Methods Enzymol.* 255: 794-796.

Gerrero, M. R., McEvilly, R. J., Turner, E., Lin, C. R., O'Connell, S., Jenne, K. J., Hobbs, M. V., and Rosenfeld, M. G. (1993). Brn-3.0: A POU-domain protein expressed in the sensory, immune and endocrine systems that functions on elements distinct from known octamer motifs. *Proc. Natl. Acad. Sci. USA* 90: 10841-10845.

Ghandour, M. S., Langley, O. K., and Keller, A. (1981). A comparative immunohistological study of cerebellar enolases. *Exp. Cell. Res.* 41: 271-279.

Ghysen, A., and Dambly-Chaudiere, C. (1988). From DNA to form: the *achaete-scute* complex. *Genes & Dev.* 2: 495-501.

Giallongo, A., Feo, S., Moore, R., Croce, C. M., and Showe, L. C. (1986). Molecular cloning and nucleotide sequence of a full-length cDNA for human α enolase. *Proc. Natl. Acad. Sci. USA* 83: 6741-6745.

Giallongo, A., Oliva, D., Calì, L., Braba, G., Barbieri, G., and Feo, S. (1990). Structure of the human gene for α-enolase. *Eur. J. Biochem.* 190: 567-573.

Giallongo, A., Venturella, S., Oliva, D., Barbieri, G., Rubino, P., and Feo, S. (1993). Strucutral features of the human gene for muscle-specific enolase. Differential splicing in the 5'-untranslated sequence generates two forms of mRNA. *Eur. J. Biochem.* 214: 367-374.

Goc, A., and Stachowiak, M. K. (1994). Bovine tyrosine hydroxylase gene-promoter regions involved in basal and angiotensin II-stimulated expression in nontransformed adrenal medullary cells. *J. Neurochem.* 62: 834-843.

Gorman, C. M., Moffat, L. F., and Howard, B. H. (1982). Recombinant genomes which express chloramphenicol acetyltransferase in mammalian cells. *Mol. Cell. Biol.* 2: 1044-1051.

Green, G. A., Girardot, R., Baldacini, O., Ledig, M., and Monteil, H. (1993). Characterisation of enolase from *Clostridium difficile*. *Curr. Microbiol.* 26: 53-56.

Green, L. A., and Tishler, A. S. (1976). Establishment of a noradrenergic clonal line of rat adrenal pheochromocytoma cells which respond to nerve groowth factor. *Proc. Natl. Acad. Sci. USA* 73: 2424-2428.

Green, L. A., Aletta, J. M., Rukenstein, A., and Green, S. H. (1987). PC12 pheochromocytoma cells: culture, nerve growth factor treatment, and experimental exploitation. *Methods Enzymol.* 147: 207-216.

Gross, J., Zinsmeyer, J., Lessing, A., Wenzel, J., Prenzlau, P., Halle, H., and Grauel, E. L. (1990). Development of enolase isoenzymes in various regions of the human brain. *Biomed. Biochim. Acta* 49: 533-538.

Grzeschick, K. H. (1974). Assignment of human genes: β-glucuronidase to chromosome 7, adenylate kinase-1 to 9, a second enzyme with enolase activity to 12 and mitochondrial IDH to 15. *Cytogenet. Cell Genet.* 16: 142-148.

Gu, J., Polak, J. M., Tapia, F., Marangos, P. J., and Pearse, A. G. E. (1981). Neuron-specific enolase in *Merkell* cells - a new, simple and reliable histological marker. *J. Pathol.* 134: 315-316.

Guillemot, F., and Joyner, A. L. (1993). Dynamic expression of the murine *achaete-scute* homologue *Mash-1* in the developing nervous system. *MOD* 42:171-185.

Guillemot, F., Lo, L-C., Johnson, J. E., Auerbach, A., Anderson, D. J., and Joyner, A. L. (1993). Mammalian *achaete-scute* homolog 1 is required for the early development of olfactory and autonomic neurons. *Cell* 75: 463-476.

Gustafson, T. A., and Kedes, L. (1989). Identification of multiple proteins that interact with functional regions of the human cardiac α-actin promoter. *Mol. Cell. Biol.* 9: 3269-3283.

Haberner, J. F., Cwikel, B. J., Hermann, H., Hammer, R. E., Palmiter, R. D., and Brinster, R. L. (1989). Metallothionein-vasopressin fusion gene expression in transgenic mice. *J. Biol. Chem.* 264: 18844-18852.

Hachisuka, H., Sasai, Y., and Nakamura, Y. (1984). Immunohistochemical staining of neuron-specific enolase on muscles. *Acta Histochem. Cytochem.* 17: 733.

Hahn, M., Hahn, S. L., Stone, D. M., and Joh, T. H. (1992). Cloning of the rat gene encoding choline acetyltransferase, a cholinergic neuron-specific marker. *Proc. Natl. Acad. Sci. USA* 89: 4387-4391.

Haimoto, H., Takahashi, Y., Koshikawa, T., Nagura, H., and Kato, K. (1985). Immunohistochemical localisation of γ-enolase in normal human tissues other than nervous and neuroendocrine tissues. *Lab. Invest.* 52: 257-263.

Halprin, K. M., and Fukui, K. (1968). Isozymes of the human epidermis. *Arch. Derm.* 98: 299-309.

Hara, Y., Rovescalli, A. C., Kim, Y., and Nirenberg, M. (1992). Structure and evolution of four POU domain genes expressed in mouse brain. *Proc. Natl. Acad. Sci. USA* 89: 3280-3284.

Harlow, E., and Lane, D. (1988). *Antibodies: A Laboratory Manual* (Cold Spring Harbor Laboratory Press, New York, USA).

Hawley-Nelson, P., Ciccarone, V., Gebeyehu, G., Jessee, J., and Felgner, P. (1994). LipofectAMINE reagent: a new higher efficiency polycationic transfection reagent. *Gibco BRL Focus* 15: 3-6.

He, X., Treacy, M. N., Simmons, D. M., Ingraham, H. A., Swanson, L. W., and Rosenfeld, M. G. (1989). Expression of a large family of POU-domain regulatory genes in mammalian brain development. *Nature* 340: 35-42.

He, X., Gerrero, R., Simmons, D. M., Park, R. E., Lin, C. R., Swanson, L. W., and Rosenfeld, M. G. (1991). *Tst-1*, a member of the POU domain gene family, binds the promoter of the gene encoding the cell surface adhesion molecule P_0. *Mol. Cell. Biol.* 11: 1739-1744.

Herr, W., Strum, R. A., Clerc, R. G., Corcoran, L. M., Baltimore, D., Sharp, P. A., Ingraham, H. A., Rosenfeld, M. G., Finney, M., Ruvkin, G., and Horvitz, H. R. (1988). The POU domain: a large conserved region in the mammalian *pit-1, oct-1, oct-2* and *Caenorhabditis elegans unc-86* gene products. *Genes & Dev.* 2: 1513-1516.

Hersh, L. B., Kong, C. F., Sampson, C., Mues, G., Li, Y-P., Fisher, A., Hilt, D., and Baetge, E. E. (1993). Comparison of the promoter region of the human and porcine choline acetyltransferase genes: Localisation of an important enhancer region. *J. Neurochem.* 61: 306-314.

Hoesche, C., Saurwald, A., Veh, R. W., Krippl, B., and Kilimann, M. W. (1993). The 5' flanking region of the rat synapsin I gene directs neuron-specific and developmentally regulated reporter gene expression in transgenic mice. *J. Biol. Chem.* 268: 26494-26502.

Hoffman, P.W., and Chernak, J. M. (1994). The rat amyloid precursor protein promoter contains two DNA regulatory elements which influence high level gene expression. *Biochem. Biophys. Res. Commun.* 201: 610-617.

Hogan, B., Costantini, F., and Lacy, E. (1986). *Manipulating the Mouse Embryo: A Laboratory Manual*, 2nd Edition (Cold Spring Harbor Laboratory Press, New York, USA).

Holland, M. J., Holland, J. P., Thill, G. P., and Jackson, K. A. (1981). The primary structure of two yeast enolase genes. Homology between the 5' noncoding flanking regions of yeast enolase and gyceraldehyde-3-phosphate dehydrogenase genes. *J. Biol. Chem.* 256: 1385-1395.

Holmes, D. S., and Quigley, M. (1981). A rapid boiling method for the preparation of bacterial plasmids. *Anal. Biochem.* 114: 193.

Höltke, H. J., and Kessler, C. (1990). Non-radioactive labelling of RNA transcripts *in vitro* with the hapten digoxigenin (DIG); hybridisation and ELISA-based detection. *Nucleic Acids Res.* 18: 5843.

Howland, D. S., Hemmendinger, L. M., Carroll, P. D., Melloni, R. H. Jr., and Degennaro, L. J. (1991). Positive- and negative-acting promoter sequences regulate cell type-specific expression of the rat synapsin I gene. *Mol. Brain Res.* 11: 345-354.

Hoyle, G. W., Mercer, E. H., Palmiter, R. D., and Brinster, R. L. (1994). Cell-specific expression from the human dopamine β-hydroxylase promoter in transgenic mice is controlled via a combination of positive and negative regulatory elements. *J. Neurosci.* 14: 2455-2463.

Htun, H., and Dahlberg, J. E. (1989). Topology and formation of triple-stranded H-DNA. *Science* 243: 1571-1576.

Huang, Z., Thewke, D., Gong, Q., Schlichter, D., and Wicks, W. D. (1991). Functional recognition of the neuronal tyrosine hydroxylase cAMP regulatory element in different cell types. *Mol. Brain Res.* 11: 309-319.

Hullin, D. A., Brown, K., Kynoch, P. A. M., Smith, C., and Thompson, R. J. (1980). Purification, radioimmunoassay and distribution of human brain 14-3-2 protein (nervous system-specific enolase) in human tissues. *Biochim. Biophys. Acta* 628: 98-108.

Ibanez, C. F., and Persson, H. (1991). Localisation of sequences determining cell-type specificity and NGF responsiveness in the promoter region of the rat choline acetyltransferase gene. *Eur. J. Neurosci.* 3: 1309-1315.

Ibi, T., Sahashi, K., Kato, K., Takahashi, A., and Soube, I. (1983). Immunohistochemical demonstration of β-enolase in human skeletal muscle. *Muscle & Nerve* 6: 661-663.

Idia, H., and Yahara, I. (1985). Yeast heat shock protein of Mr 48,000 is an isoprotein of enolase. *Nature* 315: 688-690.

Imagawa, M., Chiu, R., and Karin, M. (1987). Transcription factor AP-2 mediates induction by two different signal transduction pathways: protein kinase C and cAMP. *Cell* 51: 251-260.

Iñiguez, M. A., Morte, B., Rodriguez-Peña, A., Muñoz, A., Gerendasy, D., Sutcliffe, J. G., and Bernal, J. (1994). Characterisation of the promoter region and flanking sequences of the neuron-specific gene *RC3* (neurogranin). *Mol. Brain Res.* 27: 205-214.

Ish-Horowicz, D., and Burke, J. F. (1981). Rapid and efficient cosmid cloning. *Nucleic Acids Res.* 9: 2989.

Ishiguro, H., Kim, K. T., Joh, T. H., and Kim, K. S. (1993). Neuron-specific expression of the human dopamine β-hydroxylase gene requires both the cAMP-response element and a silencer region. *J. Biol. Chem.* 268: 17987-17994.

Ivanov, T. R., and Brown, I. R. (1992). Interaction of multiple nuclear proteins with the promoter region of the mouse 68kDa neurofilament gene. *J. Neurosci. Res.* 32: 149-158.

Jackson, P., Thomson, V. M., and Thompson, R. J. (1985). A comparison of the evolutionary distribution of the two neuroendocrine markers, neuron-specific enolase and protein gene product 9.5. *J. Neurochem.* 45: 185-190.

Jirikowski, G., Reisert, I., and Pilgrim, C. (1983). Neuron-specific enolase - an indicator for the differentiation of nerve cells in dissociation cultures. *Acta Histochem.* 28: 283-284.

Johnson, J. E., Birren, S. J., and Anderson, D. J. (1990). Two rat homologues of *Drosophila achaete-scute* specifically expressed in neuronal precursors. *Nature* 346: 858-861.

Johnson, W. A., and Hirsh, J. (1990). Binding of a *Drosophila* POU-domain protein to a sequence element regulating gene expression in specific dopaminergic neurons. *Nature* 343: 467-470.

Jones, E. A., and Woodland, H. R. (1987). The development of animal cap cells in *Xenopus*: the effects of environment on the differentiation and the migration of grafted ectodermal cells. *Development* 101: 23-32.

Jones, E. A., and Woodland, H. R. (1989). Spatial aspects of neural induction in *Xenopus laevis*. *Development* 107: 785-791.

Jones, E. A., Abel, M. H., and Woodland, H. R. (1993). The possible role of mesodermal growth factors in the formation of endoderm in *Xenopus laevis*. *Roux's Arch. Dev. Biol.* 202: 233-239.

Jørgensen, O. S., and Centerval, G. (1982). αγ-enolasein the rat - ontogeny and tissue distribution. *J. Neurochem.* 39: 537-542.

Julien, J. P., Meijer, D., Flavel, D., Hurst, J., and Grosveld, F. (1986). Cloning and developmental expression of the murine neurofilament gene family. *Mol. Brain Res.* 1: 243-250.

Julien, J. P., Tretjakoff, I., Beaudet, L., and Peterson, A. (1987). Expression and assembly of a human neurofilament protein in transgenic mice provide a novel neuronal marking system. *Genes & Dev.* 1: 1085-1095.

Julien, J. P., Tretjakoff, I., Beaudet, L., and Peterson, A. (1988). Neurofilament human gene expression in transgenic murine nervous systems. *Canad. J. Neurol. Sci.* 15: 333.

Julien, J. P., Beaudet, L., Tretjakoff, I., and Peterson, A. (1990). Neurofilamant gene expression in transgenic mice. *J. Physiol. (Paris)* 84: 50-52.

Kaghad, M., Durmont, X., Chalon, P., Lelias, J-M., Lamandé, N., Lucas, M., Lazar, M., and Caput, D. (1990). Nucleotide sequences of cDNAs for α and γ enolase mRNAs from mouse brain. *Nucleic Acids Res.* 18: 3638.

Kain, S. R., and Ganguly, S. (1995). Uses of fusion genes in mammalian transfection. In *Current Protocols in Molecular Biology*, Volume 1 (Ausubel, F. M., Brent, R., Kingston, R. E., Moore, D. D., Seidman, J. G., and Struhl, K., Eds.) Greene Publishing Associates/J. Wiley & Sons Inc., Suuplement 29, pp 9.6.1-9.6.12.

Kamel, R., and Schwarzfischer, F. (1975). Multiple forms of enolase (EC 4.2.1.11) - their distribution in human tissues. *Humangenetik* 28: 259-261.

Kaneda, N., Sasaoka, T., Kobayashi, K., Kiuchi, K., Nagatsu, I., Kurosawa, Y., Fujita, K., Yokoyama, M., Nomura, Y., Katsuki, M., and Nagatsu, T. (1991). Tissue-specific and high level expression of the tyrosine hydroxylase gene in transgenic mice. *Neuron* 6: 583-594.

Kapur, K. P., Hoyle, G. W., Mercer, E. H., Brinster, R. L., and Palmiter, R. D. (1991). Some neuronal cell populations express human dopamine β-hydroxylase-*lacZ* transgenes transiently during embryonic development. *Neuron* 7: 717-727.

Karpov, V., Landon, F., Djabali, K., Gros, F., and Portier, M. M. (1992). Structure of the mouse gene encoding peripherin: A neuronal intermediate filament protein. *Biol. of the Cell* 76: 43-48.

Katagiri, T., Feng, X. L., Ichikawa, T., Usui, H., Takahashi, Y., and Kumanishi, T. (1993). Neuron-specific enolase (NSE) and nonneuronal enolase (NNE) mRNAs are coexpressed in neurons of the rat cerebellum - *in situ* hybridisation histochemistry. *Mol. Brain. Res.* 19: 1-8.

Kato, K., Suzuki, F., and Semba, R. (1981). Determination of brain enolase isozymes with an enzyme immunoassay at the level of single neurons. *J. Neurochem.* 37: 998-1005.

Kato, K., Ishiguro, Y., Suzuki, F., Ito, A., and Semba, R. (1982). Distribution of nervous system-specific forms of enolase in peripheral tissues. *Brain Res.* 237: 441-448.

Kato, K., Shumuzu, A., Semba, R., and Satoh, T. (1985). Tissue distribution, developmental profiles and effect of denervation of enolase isozymes in rat muscles. *Biochim. Biophys. Acta* 84: 50-58.

Keller, A., Ott, M. O., Lamandé, N., Gros, F., Buckingham, M., and Lazar, M. (1992a). Activation of the gene encoding the glycolytic enzyme β-enolase during early myogenesis preceeds an increased expression during fetal muscle development. *MOD* 38: 41-54.

Keller, A., Lucas, M., Lamandé, N., Brosset, S., Gros, F., and Lazar, M. (1992b). Multistep regulation of the murine β enolase gene. *J. Muscle Res. & Cell Motility* 14: 220.

Keller, A., Berod, A., Dussailant, M., Lamandé, M., Gros, F., and Lucas, M. (1994). Coexpression of alpha and gamma enolase genes in neurons of adult brain. *J. Neurosci. Res.* 38: 493-504.

Kemp, L. M., Debt, C. L., and Latchman, D. S. (1990). Octamer motif mediates transcriptional repression of HSV immediate early genes and octamer-containing cellular promoters in neuronal cells. *Neuron* 4: 215-222.

Khan, M. L., Doopert, B. A., Hagmmeijer, A., and Westerveld, A. (1974). The human loci for phosphopyruvate hydratase and guanylate kinase are syntenic with the PGD-PGM1 linkage group in man-Chinese hamster somatic cell hybrids. *Cytogenet. Cell Genet.* 13: 130-136.

Kim, K-S., Lee, M. K., Carroll, J., and Joh, T. H. (1993). Both the basal and inducible transcription of the tyrosine hydroxylase gene are dependent upon a cAMP response element. *J. Biol. Chem.* 268: 15689-15695.

Kim, R. Y., Lietman, T., Piatigorsky, J., and Wistow, G. J. (1991). Structure and expression of the duck α-enoalse/τ-crystallin-encoding gene. *Gene (Amst.)* 103: 193-200.

Kim, R. Y., and Wistow, G. J. (1993). Expression of the duck α-enolase/τ-crystallin gene in transgenic mice. *FASEB J.* 7: 464-469.

Kingston, R. E., Chen, C. A., and Okayama, H. (1990). Transfection of DNA into eukaryotic cells. Calcium phosphate transfection. In *Current Protocols in Molecular Biology*, Volume 1 (Ausubel, F. M., Brent, R., Kingston, R. E., Moore, D. D., Seidman, J. G., and Struhl, K., Eds.) Greene Publishing Associates/J. Wiley & Sons Inc., Suplement 17, pp 9.1.1-9.1.9.

Kobayashi, K., Sasoka, T., Morita, S., Nagatsu, I., Igushi, A., Kurosawa, Y., Fujita, K., Nomura, T., Kimura, M., Katsuki, M., and Nagatsu, T. (1992). Genetic alteration of catecholamine specificity in transgenic mice. *Proc. Natl. Acac. Sci. USA* 89: 1631-1635.

Korner, M., Rattner, A., Mauxion, F., Sen, R., and Citri, Y. (1989). A brain-specific transcription activator. *Neuron* 3: 563-572.

Kozak, M. (1989). The scanning model of translation: an update. *J. Cell Biol.* 108: 229-231.

Kraner, S. D., Chong, J. A., Tsay, H-J., and Mandel, G. (1992). Silencing the type II sodium channel gene: a model for neural-specific gene regulation. *Neuron* 9: 37-44.

Kudrycki, K., Stein-Izsak, C., Behn, C., Grillo, M., Akeson, R., and Margolis, F. L. (1993). Olf-1 binding site: Characterization of an olfactory neuron-specific promoter motif. *Mol. Cell. Biol.* 13: 3002-3014.

Lamandé, N., Mazo, A. M., Lucas, M., Montarras, D., Pinset, C., Gros, F., Legault-Demare, L., and Lazar, M. (1989). Murine muscle-specific enolase: cDNA cloning, sequence and developmental expression. *Proc. Natl. Acad. Sci. USA* 86: 4445-4449.

Lamandé, N., Brossett, S., Lucas, M., Keller, A., Rouzeau, J-D, Johnson, T. R., Gros, F., Ilan, J., and Lazar, M. (1995). Transcriptional upregulation of the mouse gene for the muscle-specific subunit of enolase during terminal differentiation of myogenic cells. *Mol. Reproduction & Dev.* 41: 306-313.

Lamouroux, A., Houhou, L., Biguet, N. F., Serk-Hannsen, G., Guibert, B., Icard-Liepkalns, C., and Mallet, J. (1993). Analysis of the human dopamine β-hydroxylase promoter: transcriptional induction by cyclic AMP. *J. Neurochem.* 60: 364-367.

Langley, O. K., Ghandour, M. S., Vincendon, G., and Gombos, G. (1980). An ultrastructural immunocytochemical study of nerve-specific protein in rat cerebellum. *J. Neurocytol.* 9: 783-798.

Langley, O. K., and Ghandour, M. S. (1981). An immunocytochemical investigation of nonneuronal enolase in cerebellum - a new astrocyte marker. *Histochem. J.* 13: 137-148.

Laudet, V., Stehelin, D., and Clevers, H. (1993). Ancestry and diversity of the HMG box superfamily. *Nucleic Acids Res.* 21: 2493-2501.

Law, M. L., and Kao, F. (1982). Regional mapping of the gene encoding enolase-2 on chromosome 12. *J. Cell Sci.* 53: 245-254.

Law., S. W., Conneely, O. M., Demayo, F. J., and Omalley, B. W. (1992). Identification of a new brain-specific transcription factor, Nurr1. *Mol. Endocrinol.* 6: 2129-2135.

Le Moine, C., and Young, W. S. III. (1992). *RHS2*, a POU domain-containing gene and its expression in developing and adult rat. *Proc. Natl. Acad. Sci. USA* 89: 3285-3289.

Le Van Thai, A., Coste, E., Allen, J. M., Palmiter, R. D., and Webber, M. J. (1993). Identification of a neuron-specific promoter of human aromatic L-amino acid decarboxylase gene. *Mol. Brain Res.* 17: 227-238.

Lebidoa, L., and Stec, B. (1988). Crystal structure of enolase reveals that enolase and pyruvate kinase evolved from a common ancestor. *Nature* 333: 683-686.

Lebidoa, L., Stec, B., and Brewer, J. M. (1989). The structure of yeast enolase at 2.25Å resolution. *J. Biol. Chem.* 264: 3685-3693.

Ledig, M., Tholey, G., and Mandel, P. (1982). Neuron-specific and nonneuronal enolase in developing chick brain and primary cultures of chick neurons. *Dev. Brain Res.* 4: 451-454.

Ledig, M., Tholey, G., and Mandel, P. (1985). Factors involved in expression of neuron-specific and nonneuronal enolase activity in developing chick brain and in primary cultures of chick neurons. *Dev. Brain Res.* 21: 107-113.

Ledoux, S., Nalbantoglu, J., and Cashman, N. R. (1994). Amyloid precursor protein gene expression in neural cell lines: influence of DNA cytosine methylation. *Mol. Brain Res.* 24: 144.

Lee, J. E., Hollenberg, S. M., Snider, L., Turner, D. L., Lipnick, N., and Weintraub, H. (1995). Conversion of *Xenopus* ectoderm into neurons by NeuroD, a basic helix-loop-helix protein. *Science* 268: 836-844.

Lee, V. M. Y., Elder, G. A., Chien, L. C., Liang, Z., Snyder, S. E., Friedrich, V. L. Jr., and Lazzarini, R. A. (1992). Expression of human mid-sized neurofillament subunit in transgenic mice. *Mol. Brain Res.* 15: 76-84.

Lee, W., Mitchell, P., Tjian, R. (1987). Purified transcription factor AP-1 interacts with TPA-inducible enhancer elements. *Cell* 49: 741-752.

Legault-Demare, L., Zeitoun, Y., Lando, D., Lamandé, N., Grasso, A., and Gros, F. (1980). Expression of a specific neuronal protein, 14-3-2, during *in vitro* differentiation of neuroblastoma cells. *Exp. Cell Res.* 125: 233-239.

Lemaire, P., Vesque, C., Schmitt, J., Stunnenberg, H., Frank, R., and Charnay, P. (1990). The serum-inducible mouse gene *Krox-24* encodes a sequence-specific transcriptional activator. *Mol. Cell. Biol.* 10: 3456-3467.

Lemke, G. (1993). Transcriptional regulation of the development of neurons and glia. *Curr. Op. Neurobiol.* 3:703-708.

Levi-Montaclini, R. (1987). The nerve growth factor 35 years later. *Science* 237: 1154-1162.

Lewis, S. A., and Cowan, N. J. (1986). Anomalous placement of introns in a member of the intermediate filament multigene family: an evolutionary conundrum. *Mol. Cell. Biol.* 6: 1529-1534.

Li, L., Suzuki, T., Mori, N., and Greengard, P. (1993). Identification of a functional silencer element involved in neuron-specific expression of the synapsin I gene. *Proc. Natl. Acad. Sci. USA* 90: 1460-1464.

Li, Y-P., Baskin, F., Davis, R., and Hersh, L. B. (1993). Cholinergic neuron-specific expression of the human choline acetyltransferase gene is controlled by silencer elements. *J. Neurochem.* 61: 748-751.

Li, Z., and Paulin, D. (1993). Desmin sequence elements regulating skeletal muscle-specific expression in transgenic mice. *Development* 117: 947-959.

Lillycrop, K. A., and Latchman, D. S. (1992). Alternative splicing of the Oct-2 transcription factor RNA is differentially regulated in neuronal cells and B cells and results in protein isoforms with opposite effects on the activity of octamer/TAATGARAT-containing promoters. *J. Biol. Chem.* 267: 24960-24965.

Lillycrop, K. A., Budhram, V. S., Lakin, N. D., Terrenghi, G., Wood, J. N., Polak, J. M., and Latchman, D. S. (1992). A novel POU family transcription factor is closely related to Brn-3 but has a distinct expression pattern in neuronal cells. *Nucleic Acids Res.* 20: 5093-5096.

Lim, L., Hall, C., Leung, T., Mahadevan, L., and Whatley, S. (1983). Neuron-specific enolase and creatine-phosphokinase are protein components of rat brain synaptic plasma membranes. *J. Neurochem.* 41: 1177-1182.

Lo, D. C., McAllister, K., and Katz, L. C. (1994). Neuronal transfection of brain slices using particle-mediated gene transfer. *Neuron* 13: 1263-1268.

Lo, L-C., Johnson, J. E., Wuenschell, C. W., Saito, T., and Anderson, D. J. (1991). Mammalian *achaete-scute* homolog 1 is transiently expressed by spatially restricted subsets of early neuroepithelial and neural crest cells. *Genes & Dev.* 5: 1524-1537.

Lok, S., Stevens, W., Breitman, M. L., and Tsui, L-C. (1989). Multiple regulatory elements of the murine γ2-crystallin promoter. *Nucleic Acids Res.* 17: 3563-3582.

Lu, X. P., Salbert, G., and Pfahl, M. (1994). An evolutionary conserved COUP-TF binding eleent in a neural-specific gene and COUP-TF expression patterns support a major role for COUP-TF in neural development. *Mol. Endocrinol.* 8: 1774-1788.

Lucas, M., Goblet, C., Keller, A., Lamandé, N., Gros, F., Whalen, R. G., and Lazar, M. (1992). Modulation of embryonic and muscle-specific enolase gene products in the developing mouse hindlimb. *Differentiation* 51: 1-7.

Lucas, M., Lamandé, N., Lazar, M., Gros, F., and Legault-Demare, L. (1988). Developmental expression of alpha- and gamma-enolase subunits and mRNA sequences in the mouse brain. *Dev. Neurosci.* 10: 91-98.

Luthman, H., and Magnusson, G. (1983). High efficiency polyoma DNA transfection of chloroquine treated cells. *Nucleic Acids Res.* 11: 1295.

Makeh, I., Thomas, M., Hardelin, J. P., Briand, P., Kahn, A., and Skala, H. (1994). Analysis of a brain-specific isozyme - expression and chromatin structure of the rat aldolase C gene and transgenes. *J. Biol. Chem.* 269: 4194-4200.

Mandel, G. (1992). Tissue-specific expression of the voltage sensitive sodium channel. *J. Membr. Biol.* 125: 193-206.

Mandel, G., and McKinnon, D. (1993). Molecular basis of neural-specific gene expression. *Annu. Rev. Neurosci.* 16: 323-345.

Mangalam, H. J., Albert, V. R., Ingraham, H. A., Kapiloff, M., Wilson, L., Nelson, C., Elsholtz, H., and Rosenfeld, M. G. (1989). A pituitary POU domain protein, Pit-1, activates both growth hormone and prolactin promoters transcriptionally. *Genes & Dev.* 3: 946-958.

Maniatis, T., Jeffrey, A., and Kleid, D. G. (1975). Nucleotide sequence of the ritghtward operator of phage λ. *Proc. Natl. Acad. Sci. USA* 72: 1184.

Maniatis, T., Goodbourn, S., and Fischer, J. A. (1987). Regulation of inducible and tissue-specific gene expression. *Science* 236: 1237-1245.

Mar, J. H., and Ordahl, C. P. (1990). M-CAT binding factor, a novel *trans*-acting factor governing muscle-specific transcription. *Mol. Cell. Biol.* 10: 4271-4283.

Marangos, P. J., Zomzely-Neurath, C., and York, C. (1975). Immunological studies of nerve-specific protein (NSP). *Arch. Biochem. Biophys.* 170: 289-293.

Marangos, P. J., Zomzely-Neurath, C., and York, C. (1976). Determination and characterisation of neuron-specific protein associated enolase activity. *Biochem. Biophys. Res. Commun.* 68: 1309-1316.

Marangos, P. J., Zomzely-Neurath, C., and Goodwin, F. K. (1977). Structural and functional properties of neuron-specific protein (NSP) from rat, cat and human brain. *J. Neurochem.* 28: 1097-1107.

Marangos, P. J., Schmechel, D. E., Parma, A., Clark, R. L., and Goodwin, F. K. (1979). Measurements of neuron-specific (NSE) and non-neuronal (NNE) isoenzymes of enolase in rat, monkey and human nervous tissue. *J. Neurochem.* 33: 319-329.

Marangos, P. J., Campbell, I. C., Schmechel, D. E., Murphy, D. L., and Goodwin, F. K. (1980). Blood platelets contain a neuron-specifc enolase subunit. *J. Neurochem.* 34: 1254-1258.

Marangos, P. J., Polak, J. M., and Pearse, A. G. E. (1982). Neuron-specific enolase - a probe for neurons and neuroendocrine cells. *Trends Neurosci.* 5: 193-196.

Marangos, P. J., and Schmechel, D. E. (1987). Neuron-specific enolase, a clinically useful marker for neurons and neuroendocrine cells. *Ann. Rev. Neurosci.* 10: 269-295.

Martinou, J-C., Dubois-Dauphin, M., Staple, J. K., Rodriguez, I., Frankowski, H., Missotten, M., Albertini, P., Talabot, D., Catsicas, S., Pietra, C., and Huarte, J. (1994). Overexpression of *BCL-2* in transgenic mice protects neurons from naturally occurring cell death and experimental ischemia. *Neuron* 13: 1017-1030.

Mathis, J. M., Simmons, D. M., He, X., Swanson, L. W., and Rosenfeld, M. G. (1992). Brain 4: a novel mammalian POU domain transcription factor exhibiting restricted brain-specific expression. *EMBO J.* 11: 2551-2561.

Matranga, V., Oliva, D., Sciarrino, S., D'Amelio, L., and Giallongo, A. (1993). Differential expression of neuron-specific enolase mRNA in mouse neuroblastoma cells in response to differentiation inducing agents. *Cell. Mol. Neurobiol.* 13: 137-145.

Matrisian, L. M., Rautmann, G., Magun, D. I., and Breathnach, R. (1985). Epidermal growth factor or serum stimulation of rat fibroblasts induces an elevation in messenger RNA levels for lactate dehydrogenase and other glycolytic enzymes. *Nucleic Acids Res.* 13: 711-726.

Matsuo, K., Ikeshima, H., Shimoda, K., Umezawa, A., Hata, J., Maejima, K., Nojima, H., and Takano, T. (1993). Expression of the rat calmodulin gene II in the central nervous system: a 294 base promoter and 68 base leader segment mediates neuron-specific gene expression in transgenic mice. *Mol. Brain Res.* 20: 9-20.

Matsushita, H., Yamada, S., Satoh, T., Kato, K., and Adachi, M. (1986). Muscle-specific β-enolase concentrations after cross- and random innervation of soleus and extensor digotorum longus in rats. *Exp. Neurol.* 93: 84-91.

Matsushita, H., Satoh, T., Kato, K., Yamada, S., and Adachi, M. (1991). Muscle proteins in rat fast and slow muscles after tenotomy and denervation. *Biomed. Res.* 12: 149-156.

Matter-Sadzinski, L., Hernandez, M-C., Roztocil, T., Ballivet, M., and Matter, J-M. (1992). Neuronal specificity of the α7 nicotinic acetylcholine receptor promoter develops during morphogenesis of the central nervous system. *EMBO J.* 11: 4529-4538.

Maue, R. A., Kraner, S. D., Goodman, R. H., and Mandel, G. (1990). Neuron-specific expression of the rat brain type II sodium channel gene is directed by upstream regulatory elements. *Neuron* 4: 223-231.

Maxwell, G. D., Whitehead, M. C., Conolly, S. M., and Marangos, P. J. (1982). Development of neuron-specific enolase immunoreactivity in avian nervous tissue *in vivo* and *in vitro*. *Dev. Brain Res.* 3: 401-418.

McAleese, S. M., Dunbar, B., Fothergill, J. E., Hinks, L. J. and Day, I. N. M. (1988). Complete amino acid sequence of the neurone-specific γ isozyme for enolase (NSE) from human brain and comparison with the non-neuronal α form (NNE). *Eur. J. Biochem.* 178: 413-417.

McDermott, J. C., Cardoso, M. C., Yu, Y-T., Andres, V., Leifer, D., Krainc, D., Lipton, S. A., and Nadal-Ginard, B. (1993). *hMEF2C* gene encodes skeletal muscle- and brain-specific transcription factors. *Mol. Cell. Biol.* 13: 2564-2577.

McKay, R. D. G. (1989). The origins of cellular diversity in the mammalain central nervous system. *Cell* 58: 815-21.

McKinnon, R. D., Shinnick, T. M., and Sutcliffe, J. G. (1986). The neuronal identifier element is a *cis*-acting positive regulator of gene expression. *Proc. Natl. Acad. Sci. USA* 83: 3751-3755.

Mercer, E. H., Hoyle, G. W., Kapur, R. P., Brinster, R. L., and Palmiter, R. D. (1991). The dopamine β-hydroxylase gene promoter directs expression of *E. coli lacZ* to sympathetic and other neurons in adult transgenic mice. *Neuron* 7: 703-716.

Miernyk, J. A., and Dennis, D. T. (1982). Isozymes of the glycolytic enzymes in endosprem from developing castor oil seeds. *Plant Physiol.* 69: 825-828.

Milbrandt, J. (1987). A nerve growth factor-induced gene encodes a possible transcriptional regulatory factor. *Science* 238: 797-799.

Milner, R. J., Bloom, F. E., Lai, C., Lerner, R. A., and Sutcliffe, J. G. (1984). Brain-specific genes have identifier sequences in their introns. *Proc. Natl. Acad. Sci. USA* 81: 713-717.

Milton, N. G. N., Bessis, A., Changeux, J-P., and Latchman, D. S. (1995). The neuronal nicotinic acetylcholine receptor α2 subunit gene promoter is activated by the Brn-3b POU family transcription factor and not by Brn-3a or Brn-3c. *J. Biol. Chem.* 270: 15143-15147.

Minowa, M. T., Minowa, T., Monsma, F. J., Sibley, D. R., and Mouradin, M. M. (1992). Characterization of the 5' flanking region of the human D_{1A} dopamine receptor gene. *Proc. Natl. Acad. Sci. USA* 89: 3045-3049.

Mitchell, C. J., Griffin, D. K., and Carritt, B. (1991). Assignment of the β-enolase locus, *ENO3*, to 17p13 by fluorescent *in situ* hybridisation. *Cytogenet. Cell Genet.* 58: 2008.

Mlynárová, L., Loonen, A., Heldens, J., Jansen, R. C., Keizer, P., Steikema, W. J., and Napp, J-P. (1994). Reduced position effect in mature transgenic plants conferred by the chicken lysozyme matrix-associated region. *The Plant Cell* 6: 417-426.

Monteiro, M. J., and Cleveland, D. W. (1989). Expression of *NF-L* and *NF-M* in fibroblasts reveals coassembly of neurofilament and vimentin subunits. *J. Cell Biol.* 108: 579-593.

Monteiro, M. J., Hoffman, P. N., Gearhart, J. D., and Cleveland, D. W. (1990). Expression of *NF-L* in both neuronal and nonneuronal cells of transgenic mice: Increased neurofilament density in axons without affecting caliber. *J. Cell Biol.* 111: 1543-1558.

Monuki, E. S., Kuhn, R., and Lemke, G. (1993). Repression of the myelin P_0 gene by the POU transcription factor SCIP. *MOD* 42: 15-32.

Moore, B. W. (1975). In *Advances in Neurochemistry*, Volume I (Agranoff, B. W., and Aprison, M. H., Eds., Plenum Press, NY), pp137-155.

Moore, B. W., and Perez, V. J. (1966). In *Physiological and Biochemical aspects of Nervous Integration.* (Carlson, F. D., Ed., Prentice Hall, Englewood Cliffs, New Jersey), pp 235-276.

Moore, B. W., and McGreggor, D. (1965). Chromatographic and electrophoretic fractionation of proteins of brain and liver. *J. Biol. Chem.* 240: 1647-1653.

Morgan, W. W., and Sharp, Z. D. (1991). *In vivo* tissue-specific expression of a chimaeric construct containing 3.5kb of the 5' flanking DNA for the mouse tyrosine hydroxylase gene. *Soc. Neurosci. Abstr.* 17: 358.

Mori, N., Stein, R., Sigmund, O., and Anderson, D. J. (1990). A cell-type preferred silencer element that controls the neuron-specific expression of the *SCG10* gene. *Neuron* 4: 583-594.

Mori, N., Schoenherr, C., Vandenbergh, D. J., and Anderson, D. J. (1992). A common silencer element in *SCG10* and the type II Na^+ channel genes binds a factor present in nonneuronal cells but not in neuronal cells. *Neuron* 9: 45-54.

Motejlek, K., Hauselmann, R., Leitgeb, S., and Luscher, B. (1994). BSF1, a novel brain-specific DNA-binding protein recognizing a tandemly repeated purine DNA element in the $GABA_A$ receptor δ subunit gene. *J. Biol. Chem.* 269: 15265-15273.

Mulderry, P. K., Chapman, K. E., Lyons, V., and Harmar, A. J. (1993). 5' flanking sequences from the rat preprotachykinin gene direct high level expression of a reporter gene in adult rat sensoty neurons transfected in culture by microinjection. *Mol. Cell. Neurosci.* 4: 164-172.

Mullen, R. J., Buck, C. k., and Smith, A. M. (1992). NeuN, a neuronal specific nuclear protein in vertebrates. *Development* 116: 201-211.

Murre, C., McCaw, P. S., and Baltimore, D. (1989). A new DNA binding and dimerization motif in immunoglobulin enhancer binding, *daughterless, MyoD* and *myc* proteins. *Cell* 56: 777-783.

Nagatsu, I., Yamada, K., Karasawa, N., Sakai, M., Takeuchi, T., Kaneda, N., Sasaoka, T., Kobayashi, K., Yokoyama, M., Nomura, T., Katsuki, M., Fujita, K., and Nagatsu, T. (1991). Expression in brain sensory neurons of the transgene in transgenic mice carrying human tyrosine hydroxylase gene. *Neurosci. Lett.* 127: 91-95.

Nagatsu, I., Karasawa, N., Yamada, K., Fuji, T., Takeuchi, T., Akai, R., Kobayashi, K., and Nagatsu, T. (1994). Expression of human tyrosine hydroxylase-chloramphenicol acetyltransferase (CAT) fusion gene in the brains of transgenic mice as examined by CAT immunohistochemistry. *J. Neural Trans.* 1: 85-104.

Nakahira, K., Ikenaka, K., Wada, K., Tamura, T. A., Furuichi, T., and Mikoshiba, K. (1990). Structure of the 68kDa neurofilament gene and regulation of its expression. *J. Biol. Chem.* 265: 19786-19791.

Nakamura, T., Donovan, D. M., Hamada, K., Sax, C. M., Norman, B., Flanagan, J. R., Ozato, K., Westphal, H., and Piatigorsky, J. (1990). Regulation the of mouse αA-crystallin gene: isolation of cDNA encoding a protein which binds to a *cis* sequence motif shared with the major histocompatibility complex class 1 gene and other genes. *Mol. Cell. Biol.* 10: 3700-3708.

Nakayama, M., Gahara, Y., Kitamura, T., and Ohara, O. (1994). Distinctive four promoters collectively direct expression of brain derived neurotrophic factor gene. *Mol. Brain Res.* 21: 206-219.

Nedivi, E., Basi, G. S., Akey, I. V., and Skene, J. H. P. (1992). A neural-specific *GAP-43* core promoter located between unusual DNA elements that interact to regulate its activity. *J. Neurosci.* 12: 691-704.

Nelson, C., Shen, L. P., Meister, A., Fodor, E., and Rutter, W. J. (1990). Pan: a transcriptional regulator that binds chymotrypsin, insulin and AP-4 enhancer motifs. *Genes & Dev.* 4: 1035-1043.

Neuman, T., Keen, A., Zuber, M. X., Kristjansson, G. I., Gruss, P., and Nornes, H. O. (1993a). Neuronal expression of regulatory helix-loop-helix factor Id2 gene in mouse. *Dev. Biol.* 160: 186-195.

Neuman, T., Metsis, M., Persson, H., and Gruss, P. (1993b). Cell type-specific negative regulatory element in low-affinity nerve growth factor receptor gene. *Mol. Brain Res.* 20: 199-208.

Ng , S-Y., Gunning, P., Liu, S-H., Leavitt, J., and Kedes, L. (1989). Regulation of the human β-actin promoter by upstream and intron domains. *Nucleic Acids Res.* 17: 601-605.

Ninkina, N. N., Stevens, G. E. M., Wood. J. N., and Richardson, W. D. (1993). A novel Brn3-like POU transcription factor expressed in subsets of rat sensory and spinal cord neurons. *Nucleic Acids Res.* 21: 3175-3182.

Oberdick, J., Smeyne, R. J., Mann, J. R., Zackson, S., and Morgan, J. I. (1990). A promoter that drives transgene expression in cerebellar *Purkinje* and retinal bipolar neurons. *Science* 248: 223-226.

Oh, S-K., and Brewer, J. M. (1973). Purification and properties of enolase from swine kidney. *Arch. Biochem. Biophys.* 157: 491-499.

Ohshima, Y., Mitsui, H., Takayama, Y., Kushiya, E., Sakimura, K., and Takahashi, Y. (1989). cDNA cloning and nucleotide sequence of rat muscle-specific enolase (ββ enolase). *FEBS Lett.* 242: 425-430.

Okamoto, K., Wakamiya, M., Noji, S., Koyama, E., Taniguchi, S., Takemura, R., Copeland, N. G., Gilbert, D. J., Jenkins, N. A., Murmatsu, M., and Hamada, H. (1993). A novel class of murine POU gene predominantly expressed in central nervous system. *J. Biol. Chem.* 268: 7449-7457.

Okazaki, T., Yoshida, B. N., Avraham, K. B., Wang, H., Wuenschell, C. W., Jenkins, N. A., Copeland, N. G., Anderson, D. J., and Mori, N. (1993). Molecular diversity of the SCG10/strathmin gene family in the mouse. *Genomics* 18: 360-373.

Oliva, D., Barba, G., Barbieri, G., Giallongo, A., and Feo, S. (1989). Cloning, expression and sequence homologies of cDNA for human γ-enolase. *Gene (Amst.)* 79: 355-360.

Oliva, D., Cali, L., Feo, S., and Giallongo, A. (1991). Complete structure of the human gene encoding neuron-specific enolase. *Genomics* 10: 157-165.

Oliver, G., Sosa-Pineda, B., Geisendorf, S., Spana, E. P., Doe, C. Q., and Gruss, P. (1993). *Prox-1,* a *Prospero*-related homeobox gene expressed during mouse development. *MOD.* 44: 3-16.

Özcelik, T., Lafreniere, R. G., Archer, B. T. III, Johnston, P. A., Willard, H. F., Francke, U., and Südhof, T. C. (1990). Synaptophysin: structure of the human gene and assignment to the X-chromosome in man and mouse. *Am. J. Hum. Genet.* 47: 551-561.

Palmiter, R. D., and Brinster, R. L. (1986). Germ line transformation of mice. *Ann. Rev. Biochem.* 63: 265-297.

Parsons, M. A., Royds, J. A., Taylor, C. B., and Timperley, W. R. (1981). Enolase isoenzymes as markers of cellular differentiation in the normal human foetus and adult. *J. Pathol.* 134: 314-315.

Pathak, B. G., Neurmann, J. C., Croyle, M. L., and Lingrei, J. B. (1994). The presence of both negative and positive elements in the 5' flanking sequence of the rat Na,K-ATPase α-3 subunit gene are required for brain expression in transgenic mice. *Nucleic Acids Res.* 22: 4748-4756.

Pearce, J. M., Edwards, Y. H., and Harris, H. (1976). Human enolase isoenzymes: electrophoretic and biochemical evidence for three loci. *Ann. Hum. Genet.* 39: 263-276.

Pecorino, L. T., Darrow, A. L., and Strickland, S. (1991). *In vitro* analysis of the tissue plasminogen activator promoter reveals a GC box-binding activity present in murine brain but undetectable in kidney and liver. *Mol. Cell. Biol.* 11: 3139-3147.

Penhoet, E., Rajkumar, T., and Rutter, W. J. (1966). Multiple forms of fructose diphosphate aldolase in mammalian tissue. *Proc. Natl. Acad. Sci. USA* 56: 1275-1282.

Peshavaria, M., and Day, I. N. M. (1991). Molecular structure of the human muscle-specific enolase gene (*ENO3*). *Biochem. J.* 275: 427-433.

Peshavaria, M., and Day, I. N. M. (1993). Methylation patterns in the human muscle-specific enolase gene (*ENO3*). *Biochem. J.* 292: 701-704.

Peshavaria, M., Hinks, L. J., and Day, I. N. M. (1989). Structure of human muscle (β) enolase mRNA and protein deduced from a genomic clone. *Nucleic Acids Res.* 17: 8862.

Peshavaria, M., Quinn, G. B., Reeves, I., Hinks, L. J., and Day, I. N. M. (1990). Molecular biology of the human enolase gene family: nerve (γ), muscle (β) and general (α) isoforms. *Biochem. Soc. Trans.* 18: 254-255.

Peterson, C. A., Cho, M., Rastinejad, F., and Blau, H. M. (1992). β-enolase is a marker of human myoblast heterogeneity prior to differentiation. *Dev. Biol.* 151: 626-639.

Pickel V. M., Reis, D. J., Marangos, P. J., and Zomzely-Neurath, C. (1976). Immunocytochemical localisation of nervous system specific protein (NSP-R) in rat brain. *Brain Res.* 105: 105-108.

Pleasure, S. J., Lee, V. M., and Nelson, D. L. (1990). Site-specific phosphorylation of the middle molecular weight human neurofilament protein in transfected non-neuronal cells. *J. Neurosci.* 10: 2428-2437.

Pospelov, V. A., Pospelova, T. V., and Julien, J. P. (1994). AP-1 and Krox-24 transcription factors activate the neurofilament light gene promoter in P19 embryonal carcinoma cells. *Cell Growth & Diff.* 5: 187-196.

Possenti, R., Di Rocco, G., Nasi, S., and Levi, A. (1992). Regulatory elements in the promoter region of *vgf*, a nerve growth factor-inducible gene. *Proc. Natl. Acad. Sci. USA* 89: 3815-3819.

Prewitt, M. A., and Salafsky, B. (1970). Enzymic and histochemical changes in fast and slow muscles after cross-innervation. *Am. J. Physiol.* 218: 69-74.

Quinn, J. P. (1992). Multiple protein binding sites within the rat preprotachykinin promoter: demonstration of a site with neuronal specificity that is 3' of the major transcriptional start. *Mol. Cell. Neurosci.* 3: 11-16.

Quinn, J. P., and McAllister, J. (1993). The preprotachykinin A promoter interacts with a sequence-specific single-stranded DNA binding protein. *Nucleic Acids Res.* 21: 1637-1641.

Reeben, M., Halmekyto, M., Alhonen, L., Sinervirta, M., and Jaenne, J. (1993). Tissue-specific expression of the rat light neurofilament promoter-driven reporter gene in transgenic mice. *Biochem. Biophys. Res. Commun.* 192: 465-470.

Reinhardt, E., Nedevi, E., Wegner, J., Skene, J. H. P., and Westerfield, M. (1994). Neural selective activation and temporal regulation of a mammalian *GAP-43* promoter in zebrafish. *Development* 120: 1767-1775.

Renner, K., Leger, H., and Wegner, M. (1993). The POU domain protein Tst-1 and papovaviral large tumour antigen function synergistically to stimulate glia-specific gene expression of JC virus. *Proc. Natl. Acad. Sci. USA* 91: 6433-6437.

Rich, A., Nordheim, A., and Wang, A. H. J. (1984). The chemistry and biology of left-handed Z-DNA. *Annu. Rev. Biochem.* 53: 791-846.

Rider, C. C., and Taylor, C. B. (1974). Enolase isoenzymes in rat tissues: Electrophoretic, chromatographic, immunological and kinetic properties. *Biochim. Biophys. Acta* 365: 285-300.

Rider, C. C., and Taylor, C. B. (1975a). Enolase isoenzymes. II. Hybridisation studies, developmental and phylogenetic aspects. *Biochim. Biophys. Acta* 405: 175-187.

Rider, C. C., and Taylor, C. B. (1975b). Evidence for a new form of enolase in rat brain. *Biochem. Biophys. Res. Commun.* 66: 814-820.

Rigby, P. W. J., Dieckmann, M., Rhodes, C., and Berg, P. (1977). Labelling deoxyribonucleic acid to high specific activity *in vitro* by nick translation with DNA polymerase I. *J. Mol. Biol.* 113: 237.

Ring, C. J. A., and Latchman, D. S. (1993). The human Brn-3b POU transcription factor shows only limited homology to the Brn3a/RDC-1 factor outside the conserved POU domain. *Nucleic Acids Res.* 21: 2946.

Robertson, M. (1988). Homoeo boxes, POU proteins and the limits to promiscuity. *Nature* 336: 522-524.

Roemer, K., Jophnson, P. A., and Friedmann, T. (1995). Transduction of foreign regulatory sequences by a replication-defective herpes simplex virus type 1: the rat neuron-specific enolase promoter. *Virus Res.* 35: 81-89.

Rosenfeld, M. G. (1991). POU-domain transcription factors: pou-er-ful developmental regulators. *Genes & Dev.* 5: 897-907.

Roth, H. J., Das, G. C., and Piatigorsky, P. (1991). Chicken βB1-crystallin gene expression: presence of conserved functional polyoma enhancer-like and octamer binding like promoter elements found in non-lens genes. *Mol. Cell. Biol.* 11: 1488-1499.

Rubin, H., and Fodge, D. (1974) in *Control of Proliferation in Animal Cells* (Clarkson, B. & Baserga, R. Eds., Cold Spring Harbour Laboratory, Cold Spring Harbour, NY), pp 801-816.

Rudner, G., Katar, M., Syner, F., and Maisel, H. (1988). Enolase in the chick lens. *Invest. Opthal. & Visual Sci.* 29(Suppl.): 72.

Rudnicki, M. A., and McBurney, M. W. (1987). Cell culture methods and induction of differentiation of embryonal carcinoma cell lines. In *Teratocarcinoma and Embryonic Stem Cells: A Practical Approach* (Robertson, E. J., Ed., IRL Press, Oxford, UK), pp 19-49.

Russel, G. A., Dunbar, B., and Fothergill-Gilmore, L. A. (1986). The complete amino acid sequence of chicken skeletal-muscle enolase. *Biochem. J.* 236: 115-126.

Ruth, R. C., Soja, D. M., and Wold, F. (1970). Purification and characterisation of enolases from coho (*Oncortynchus kisutch*) and chum (*Oncortynchus keta*) salmon. *Arch. Biochem. Biophys.* 140: 1-10.

Ruvkin, G., and Finney, M. (1991). Regulation of transcription and cell identity by POU domain proteins. *Cell* 64: 475-478.

Sakimura, K., Kushiya, E., Obinata, M., and Takahashi, Y. (1985a). Molecular cloning and the nucleotide sequence of cDNA to mRNA for non-neuronal enolase (αα enolase) of rat brain and liver. *Nucleic Acids Res.* 13: 4365-4376.

Sakimura, K., Kushiya, E., Obinata, M., Odani, S., and Takahashi, Y. (1985b). Molecular cloning and the nucleotide sequence of cDNA for neuron-specific enolase messenger RNA of rat brain. *Proc. Natl. Acad. Sci. USA* 82: 7453-7457.

Sakimura, K., Kushiya, E., Takahashi, Y., and Suzuki, Y. (1987). The structure and expression of the neuron-specific enolase gene. *Gene (Amst.)* 60: 103-113.

Sakimura, K., Kushiya, E., Ohshima-Ichimura, Y., Mitsui, H., and Takahashi, Y. (1990). Structure and expression of rat muscle-specific enolase gene. *FEBS Lett.* 277: 78-82.

Sakimura, K., Kushiya, E., Ogura, A., Kudo, Y., Katagiri, T., and Takahashi, Y. (1995). Upstream and intron regulatory regions for expression of the rat neuron-specific enolase gene. *Mol. Brain Res.* 28: 19-28.

Sambrook, J., Maniatis, T., and Fritsch, E. F. (1989). *Molecular Cloning: A Laboratory Manual* (Cold Spring Harbor Laboratory Press, New York, USA).

Sangameswaran, L. and Morgan, J. I. (1993). Structure and regulation of the gene encoding the neuron-specific protein PEP-19. *Mol. Brain Res.* 19: 62-68.

Sanger, F., Nicklen, S., and Coulson, A. R. (1977). DNA sequencing with chain terminating inhibitors. *Proc. Natl. Acad. Sci. USA* 74: 5463-5467.

Sato, K., Morris, H. P., and Weinhouse, S. (1972). Phosphorylase: a new isozyme in rat hepatic tumours and fetal liver. *Science* 178: 879-881.

Sato, T., Xiao, D-M., Li, H., Huang, F. L., and Huang K-P. (1995). Structure and regulation of the gene encoding the neuron-specific protein kinase C substrate neurogranin (RC3 protein). *J. Biol. Chem.* 270: 10314-10322.

Satoh, T., Matsushita, H., Kato, K., Yamada, S., and Adachi, M. (1991). Muscle β-enolase under tetrodotoxin-paralysis or chronic stimulation of the sciatic nerve. *Biomed. Res.* 12: 165-168.

Saurwald, A., Hoesche, C., Oschwald, R., and Kiliman, M. (1990). The 5' flanking region of the synapsin I gene. A G+C-rich TATA- and CAAT-less, phylogenetically conserved sequence with cell type-specific promoter activity. *J. Biol. Chem.* 265: 14932-14937.

Schmechel, D., Marangos, P. J., Brightman, M., and Goodwin F. K. (1978a). Brain enolases as specific markers of neuronal and glial cells. *Science* 199: 313-315.

Schmechel, D. E., Marangos, P. J., and Brightman, M. (1978b). Neuron-specific enolase is a molecular marker for peripheral and central neuroendocrine cells. *Nature* 276: 834-836.

Schmechel, D. E., Brightman, M., Marangos, P. J., and Kopin, I. J. (1980). Neurons switch from non-neuronal enolase to neuron-specific enolase during development. *Brain Res.* 190: 195-214.

Schmechel, D. E., Marangos, P. J., Martin, B. M., Winfield, S., Burkhart, D. S., Roses, A. D., and Ginns, E. I. (1987). Localisaton of neuron-specific enolase (NSE) mRNA in human brain. *Neurosci. Lett.* 76: 233-238.

Schoenherr, C. J., and Anderson, D. J. (1995). The neuron-restrictive silencer factor (NRSF): A coordinate repressor of multiple neuron-specific genes. *Science* 267: 1360-1363 .

Schöler, H. R. (1991). Octamania: The POU factors in murine development. *Trends Genet.* 7: 323-329.

Scholnick, S. B., Bray, S. J., Morgan, B. A., McCormick, C. A., and Hirsch, J. (1986). CNS and hypoderm regulatory elements of the *Drosophila melanogaster* dopa decarboxylase gene. *Science* 234: 998-1002.

Schreiber, E., Tobler, A., Malipiero, U., Schaffner, W., and Fontana, A. (1993). cDNA cloning of human N-Oct 3, a nervous system specific POU domian transcription factor binding to the octamer DNA motif. *Nucleic Acids Res.* 21: 253-258.

Schubert, D., Stallcup, W., La Corbière, M., Kidokoro, Y., and Orgel, L. (1985). Ontogeny of electrically excitable cells in cultured olfactory epithelium. *Proc. Natl. Acad. Sci. USA* 82: 7782-7786.

Schwartz, M. L., Katagi, C., Bruce, J., and Schlaepfer, W. W. (1994). Brain-specific enhancement of the mouse neurofilament heavy gene promoter *in vitro*. *J. Biol. Chem.* 269: 13444-13450.

Secchi, J., Le Caque, D., Cousin, M. A., Lando, D., Leagault-Demare, L., and Raynaud, J. P. (1980). Detection and localisation of 14-3-2 protein in primary cultures of embryonic rat brain. *Brain Res.* 184: 455-466.

Segil, N., Shrutkowski, A., Dworkin, M. B., and Dworkin-Rastl, E. (1984). Enolase isoenzymes in adult and developing *Xenopus laevis* and characterisation of a cloned enolase sequence. *Biochem. J.* 251: 31-39.

Sehgal, A., Patil, N., and Chao, M. (1988). A constitutive promoter directs expression of the nerve growth factor receptor gene. *Mol. Cell. Biol.* 8: 3160-3167.

Selden, R. F. (1987). Transfection of DNA into eukaryotic cells. Transfection using DEAE-dextran. In *Current Protocols in Molecular Biology*, Volume 1 (Ausubel, F. M., Brent, R., Kingston, R. E., Moore, D. D., Seidman, J. G., and Struhl, K., Eds.) Greene Publishing Associates/J. Wiley & Sons Inc., Suplement 30, pp 9.2.1-9.2.6.

Selden, R. F., and Rose, J. K. (1991). Transfection of DNA into eukaryotic cells. Optimisation of transfection. In *Current Protocols in Molecular Biology*, Volume 1 (Ausubel, F. M., Brent, R., Kingston, R. E., Moore, D. D., Seidman, J. G., and Struhl, K., Eds.) Greene Publishing Associates/J. Wiley & Sons Inc., Suplement 17, pp 9.9.1-9.9.3.

Semenza, G. L., Roth, P. H., Fang, H-M., and Wang, G. L. (1994). Transcriptional regulation of genes encoding glycolytic enzymes by Hypoxia-inducible Factor 1. *J. Biol. Chem.* 269: 23757-23763.

Sen, R., and Baltimore, D. (1986). Multiple nuclear factors interact with the immunoglobulin enhancer sequences. *Cell* 46: 705-716.

Shackelford, J. E., and Lebherz, H. G. (1981). Effect of denervation on the levels and rates of synthesis of specific enzymes in fast-twitch (breast) muscle fibres of the chicken. *J. Biol. Chem.* 256: 6423-649.

Shaskus, J., Greco, D., Asnani, L. P., and Lewis, E. J. (1992). A bifunctional genetic regulatory element of the rat dopamine β-hydroxylase gene influences cell type specificity and second messenger-mediated transcription. *J. Biol. Chem.* 267: 18821-18830.

Shaw, G., and Kamen, R. (1986). A conserved AU sequence from the 3' untranslated region of GM-CSF messenger RNA mediates selective messenger RNA degradation. *Cell* 46: 659-667.

Sheng, M., and Greenberg, M. E. (1990). The regulation and function of *c-fos* and other immediate early genes in the nervous system. *Neuron* 4: 477-485.

Sheppard, M.N., Wharton, J., Marangos, P. J., Bloom, S. R., and Polak, J. M. (1982). Neuron-specificenolase (NSE) distribution in the respiratory tract of man and other mammals. *J. Pathol.* 138: 90.

Shimizu, A., Suzuki, F., and Kato, K. (1983). Characterisation of αα, ββ γγ and αγ human enolase isoenzymes, and preparation of hybrid enolases αγ, βγ and αβ from homodimeric forms. *Biochim. Biophys. Acta* 748: 278-284.

Shinohara, H., Semba, R., Kato, K., Kashiwamata, S., and Tanaka, O. (1986). Immunohistochemical localisation of γ-enolase in early human embryos. *Brain Res.* 382: 33-38.

Shneidman, P. S., Bruce, J., Schwartz, M. L., and Schlaepfer, W. W. (1992). Negative regulatory regions are present upstream in the three mouse neurofilament genes. *Mol. Brain Res.* 13: 127-138.

Srivastava, D. K., and Bernard, S. A. (1986). Metabolic transfer via enzyme-enzyme complexes. *Science* 234: 1081-1086.

Stachowiak, M. K., Goc, A., Hong, J. S., Kaplan, B. B., and Stachowiak, E. K. (1990). Neural and hormonal regulation of the tyrosine hydroxylase gene in adrenal medullary cells: Participation of c-Fos and AP-1 factors. *Mol. Cell. Neurosci.* 1: 202-213.

Stapel, S. O., and de Jong, W. W. (1983). Lamprey 48-kDa lens protein represents a novel class of crystallin. *FEBS Lett.* 162: 305-309.

Starr, R. G., Lu, B., and Federoff, H. J. (1994). Functional characterisation of the rat *GAP-43* promoter. *Brain Res.* 638: 211-220.

Stec, B., and Lebidoa, L. (1990). Refined structure of yeast apo-enolase at 2.25Å resolution. *J. Mol. Biol.* 211: 235-248.

Stott, D., Kispert, A., and Herrmann, B. G. (1993). Rescue of the tail defect of *Brachyury* mice. *Genes & Dev.* 7: 197-203.

Südhof, T. C. (1990). The structure of the human synapsin I gene and protein. *J. Biol. Chem.* 265: 7849-7852.

Suri, C., and Chikaraishi, D. M. (1991). New catecholaminergic brain and adrenal cell lines from transgenic mice. *Soc. Neurosci. Abstr.* 17: 528.

Sutcliffe, J. G., Milner, R. G., Bloom, F. E., and Lemer, R. A. (1982). A common 82 nucleotide sequence unique to brain RNA. *Proc. Natl. Acad. Sci. USA* 79: 4942-4946.

Sutcliffe, J. G., Milner, R. J., Gottesfeld, J. M., and Lerner, R. A. (1984). Identifier sequences are transcribed specically in brain. *Nature* 308: 237-241.

Takei, N., Kondo, J., Nagaike, K., Ohsawa, K., Kato, K., and Kohsaka, S. (1991). Neuronal survival factor from bovine brain is identical to neuron-specific enolase. *J. Neurochem.* 57: 1178-1184.

Tamura, T. A., Sumita, K., Hirose, S., and Mikoshiba, K. (1990). Core promoter of the mouse myelin basic protein gene governs brain-specific transcription *in vitro*. *EMBO J.* 9: 3101-3108.

Tanaka, M., Sugisaki, K., and Nakashima, K. (1985a). Switching in levels of translatable mRNAs for enolase isozymes during development of chicken skeletal muscle. *Biochem. Biophys. Res. Commun.* 133: 868-872.

Tanaka, M., Sugisaki, K., and Nakashima, K. (1985b). Purification, characterisation, and distribution of enolase isoenzymes in chicken. *J. Biochem.* 98: 1527-1534.

Tanaka, M., Maeda, K., and Nakashima, K. (1995). Chicken α-enolase but not β-enolase has a Src-dependent tyrosine-phosphorylation site: cDNA cloning and nucleotide sequence analysis. *J. Biochem.* 117: 554-559.

Taylor, J. M., Davies, J. D., and Peterson, C. A. (1995). Regulation of the myoblast-specifc expression of the human β-enolase gene. *J. Biol. Chem.* 270: 2535-2540.

Thiel, G., Greengard, P., and Südhof, T. C. (1991). Characterization of tissue-specific transcription by the human synapsin I gene promoter. *Proc. Natl. Acad. Sci. USA* 88: 3431-3435.

Thiel, G., Schoch, S., and Petersohn, D. (1994). Regulation of synapsin I gene expression by the zinc finger transcription factor zif268/egr-1. *J. Biol. Chem.* 269: 15294-15301.

Thiel, T., McLean-Hunter, S., Zörnig, M., and Möröy, T. (1993). Mouse *BRN-3* family of POU transcription factors: a new aminoterminal domain is crucial for the oncogenic activity of *BRN-3A*. *Nucleic Acids Res.* 21: 5921-5929.

Thiell, L. E., Wilberg, O., and Vust, J. (1987). Cell-specific expression of the human gastrin gene. Evidence for a control element located downstream of the TATA box. *Mol. Cell. Biol.* 7: 4329-4336,

Thomas, M., Makeh, I., Briand, P., Khan, A., and Skala, H. (1993). Determinants of the brain-specific expression of the rat aldolase C gene - *ex vivo* and *in vivo* analysis. *Eur. J. Biochem.* 218: 143-151.

Thomas, P. S. (1980). Hybridisation of denatured RNA and small DNA fragments transferred to nitrocellulose. *Proc. Natl. Acad. Sci. USA* 77: 5201-5205.

Thompson, M. A., Lee, E., Lawe, D., Gizang-Ginsberg, E., and Ziff, E. B. (1992). Nerve growth factor-induced derepression of peripherin gene expression is associated with alterations in proteins binding to a negative regulatory element. *Mol. Cell. Biol.* 12: 2501-2513.

Timmusk, T., Palm, K., Metsis, M., Reintaman, T., Paalme, V., Saarma, M., and Persson, H. (1992). Multiple promoters direct tissue-specific expression of the rat *BDNF* gne. *Neuron* 10: 475-489.

Timmusk, T., Lendahl, U., Funakoshi, H., Arenas, E., Persson, H., and Metsis, M. (1995). Identification of brain-derived neurotrophic factor promoter regions mediating tissue-specific, axotomy- and neuronal activity-induced expression in transgenic mice. *J. Cell Biol.* 128: 185-199.

Toth, M., Ding, D. M., and Shenk, T. (1994). The 5' flanking region of the serotonin-2 receptor gene directs brain-specific expression in transgenic animals. *Mol. Brain Res.* 27: 315-319.

Treacy, M. N., He, X., and Rosenfeld, M. G. (1991). I-POU: a POU domain protein that inhibits neuron-specific gene activation. *Nature* 350: 577-584.

Tsokos, M., Scarpa, S., Ross, R. A., and Triche, T. J. (1987). Differentiation of human neuroblastoma recapitculates neural crest development. *Am. J. Pathol.* 128: 484-496.

Tsukamoto, M., Ochiya, T., Yoshida, S., Sugimura, T., and Terada, M. (1995). Gene transfer and expression in progeny after intravenous DNA injection into pregnant mice. *Nature Genetics* 9: 243-248.

Twyman, R. M., and Jones, E. A. (1995a). The molecular biology of enolase in mammals and birds. *Biochem. J.* Submitted for publication.

Twyman, R. M., and Jones, E. A. (1995b). The regulation of neuron-speicifc gene expression in the mammalian nervous system. *J. Neurogenetics* 10: 67-101.

Twyman, R. M., and Jones, E. A. (1995c). The functional diversity of enolase in eukaryotes. In preparation.

Twyman, R. M., and Jones, E. A. (1995d). Cell type-specific and inducible expression of the rat neuron-specific enolase (*NSE*) gene is controlled by *cis*-acting elements in the proximal 5' flanking region. In preparation.

Uwanogho, D., Rex, M., Cartwright, E. J., Pearl, G., Healy, C., Scotting, P. J., and Sharpe, P. T. (1995). Embryonic expression of the chicken *Sox2*, *Sox3* and *Sox11* genes suggests an interactive role in neuronal development. *MOD.* 49: 23-36.

Vaidya, T. B., Rhodes, S. J., Taparowsky, E. J., and Konieczny, S. F. (1989). Fibroblast growth factor and transforming growth factor β repress transcription of the myogenic regulatory gene *myoD1*. *Mol. Cell. Biol.* 9: 3576-3579.

Van Cong, N., Weil, D., Rebourcet, R., and Frézel, J. (1977). Localisation of enolase-1 and enolase-2 respectively on chromosome-1 and chromosome-12 using man-mouse hybrid analysis. *Ann. Genet.* 20: 153-157.

Van Obberghen, E., Kamholz, J., Bishop, J. G., Zomzely-Neurath, C., and Lazzarini, R. (1988). Human γ-enolase - isolation of a cDNA clone and expression in normal and tumour-tissues of human origin. *J. Neurosci. Res.* 19: 450-456.

Vandaele, S., Nordquist, D. T., Feddersen, R. M., Tretjakoff, I., Peterson, A. C., and Orr, H. T. (1991). *Purkinje cell protein-2* regulatory regions and transgene expression in cerebellar compartments. *Genes & Dev.* 5: 1136-1148.

Verhaagen, J., Koster, J. G., Schrama, L. H., Eggen, B. J. L., Van Der Neut, R., Gispen, W. H., and Destree, O. H. J. (1993). The rat *B-50* (*GAP-43*) promoter directs neural-preferred expression of a reporter gene in *Xenopus laevis* embryos. *Neurosci. Res. Commun.* 13: 83-90.

Verma, M., and Kurl, R. N. (1990). Human lung enolase: cloning and sequencing of cDNA and its inducibility with dexamethasone. *Biochem. Mol. Biol. Int.* 30: 293-303.

Vibert, M., Henry, J., Kahn, A., and Skala, H. (1989). The brain-specific gene for rat aldolase C possesses an unusual housekeeping-type promoter. *Eur. J. Biochem.* 181: 33-39.

Vidal-Sanz, M., Villegas-Perez, M. P., Carter, D. A., Julien, J. P., Peterson, A., and Aguayo, A. J. (1991). Expression of human neurofilament light transgene in mouse neurons transplanted into the brain of rats. *Eur. J. Neurosci.* 3: 758-763.

Vinores, S. A., Marangos, P. J., Parma, A. M., and Guroff, G. (1981). Increased levels of neuron-specific enolase in PC12 pheochromocytoma cells as a result of nerve growth factor treatment. *J. Neurochem.* 37: 597-600.

Vinores, S. A., Herman, M. M., Rubinstein, L. J., and Marangos, P. J. (1984). Electron microscopic localisation of neuron-specific enolase in rat and mouse brain. *J. Histochem. Cytochem.* 32: 1295-1302.

Wang, M. M., Tsai, R. Y. L., Schrader, K. A., and Reed, R. R. (1993). Genes encoding components of the olfactory signal transduction cascade contain a DNA-binding site that may direct neuronal expression. *Mol. Cell. Biol.* 13: 5805-5813.

Warwar, R. W., Kim, R. Y., Wistow, G. J., and Zelenka, P. S. (1992). The τ-crystallin/α-enolase gene: a candidate for regulation by *c-myc*. *Invest. Opthalmol. & Visual Sci.* 33: 794.

Watanabe, M., Nagamine, T., Sakimura, K., Takahashi, Y., and Kondo, H. (1993). Developmental study of the gene expression for α and γ subunits of enolase in the rat brain by *in situ* hybridisation histochemistry. *J. Comp. Neurol.* 327: 350-358.

Watanabe, M., Sakimura, K., Takahashi, Y., and Kondo, H. (1990). Ontogenic changes in expression of neuron-specific enolase (NSE) and its mRNA in the *Purkinje* cells of the rat cerebellum: immunohistochemical and *in situ* hybridisation study. *Dev. Brain Res.* 53: 89-96.

Wefald, F. C., Devilin, B. H., and Williams, R. S. (1990). Functional heterogeneity of mammalian TATA-box sequences revealed by interaction with cell-specific enhancer. *Nature* 344: 260-262.

Wegner, M., Drolet, D. W., and Rosenfeld, M. G. (1993). POU-domain proteins: structure and function of developmental regulators. *Curr. Op. Cell Biol.* 5: 488-498.

Weiss, B., Jacquemin-Sablon, A., Live, T. R., Fareed, G. C., and Richardson, C. C. (1968). Enzymatic breakage and joining of deoxyribonucleic acid. VI. Further purification and properties of polynucleotide ligase from *Escherichia coli* infected with bacteriophage T4. *J. Biol. Chem.* 243: 4543-4549.

Weyhenmeyer, J. A., and Bright, M. J. (1983). Expression of neuron-specific enolase in cultured neurons from the foetal rat. *Neurosci. Lett.* 43: 303-307.

Whilton, D. S., and Sobkowicz, H. M. (1988). Neuron-specific enolase during the development of the organ of Corti. *Int. J. Dev. Neurosci.* 6: 77.

Whitehead, M. C., Marangos, P. J., Connolly, S. M., and Morest, D. K. (1982). Synapse formation is related to the onset of neuron-specific enolase reactivity in the avian auditory and vestibular system. *Dev. Neurosci.* 5: 298-307.

Wilkinson, D. G. (1992). Wholemount *in situ* hybridisation using digoxigenin-labelled probes. In In Situ *Hybridisation: A Practical Approach* (Wilkinson, D. G., Ed., IRL Press, Oxford, UK), pp 1-24.

Williams, L. A., Ding, L., Horwitz, J., and Piatigorsky, J. (1985). τ-crystallin from the turtle lens: purification and partial characterisiation. *Exp. Eye Res.* 40: 741-749.

Wirak, D. O., Bayney, R., Kundel, C. A., Lee, A., and Scangos, G. A. (1991). Regulatory region of the human amyloid precursor protein (*APP*) gene promotes neuron-specific gene expression in the CNS of transgenic mice. *EMBO J.* 10: 289-96.

Wistow, G., and Piatigorsky, J. (1987). Recruitment of enzymes as lens strucural proteins. *Science* 236: 1554-1556.

Wistow, G., and Piatigorsky, J. (1988). Lens crystallins: evolution and expression of proteins for a highly specialised tissue. *Annu. Rev. Biochem.* 57: 479-504.

Wistow, G., Lietman, T., Williams, L. A., Stapel, S. O., de Jong, W. W., Horwitz, J., and Piatigorsky, J. (1988). τ-crystallin/α-enolase: one gene encodes both an enzyme and a lens structural protein. *J. Cell Biol.* 107: 2729-2736.

Wistow, G., Anderson, A., and Piatigorsky, J. (1990). Evidence for neutral and selective processes in the recruitment of enzyme-crystallins in avian lenses. *Proc. Natl. Acad. Sci. USA* 87: 6277-6280.

Witt, L., and Witz, D. (1970). Reinigung und Characterisierung von Phosphopyruvat-Hydratase (=Enolase EC 4.2.1.11) aus Neugeborenen - und Erwachsenen - Erythrozyten. [Purification and characterisation of phosphopyruvate hydratase (enolase, EC 4.2.1.11) from newborn - and adult - erythrocytes] *Z. Physiol. Chem.* 351: 1232-1240.

Wold, F. (1971). Enolase. In *The Enzymes*, Volume I (Boyer, P. D., Ed., Academic Press, New York), pp. 499-538.

Wong, S. C., Moffat, M. A., and O'Malley, K. L. (1994). Sequences distal to the AP1/E box motif are involved in the cell type-specific expression of the rat tyrosine hydroxylase gene. *J. Neurochem.* 62: 1691-1697.

Wood, T. (1964). The purification of enolase from cerebral tissue. *Biochem. J.* 91: 453-460.

Writh, T., Priess, A., Annweiler, A., Zwilling, S., and Oeler, B. (1990). Multiple Oct2 isoforms are generated by alternative splicing. *Nucleic Acids Res.* 19: 43-51.

Wuenschell, C. W., Mori, N., and Anderson, D. J. (1990). Analysis of *SCG10* gene expression in transgenic mice reveals that neural specificity is achieved through selective derepression. *Neuron* 4: 595-602.

Xu, Z., Cork, L. C., Griffin, J. W., and Cleveland, D. W. (1993). Increased expression of neurofilament subunit NF-L produces morphological alterations that resemble the pathology of human motor neuron disease. *Cell* 73: 23-33.

Yang, X., McDonough, J., Fyodorov, D., Morris, M., Wang, F., and Deneris, E. S. (1994). Characterization of an acetylcholine receptor α3 gene promoter and its activation by the POU domain factor SCIP/Tst-1. *J. Biol. Chem.* 269: 10252-10264.

Yazdanbakhsh, K., Fraser, P., Kioussis, D., Vidal, M., Grosveld, F., and Lindenbaum, M. (1993). Functional analysis of the human neurofilament light chain gene promoter. *Nucleic Acids Res.* 21: 455-461.

Yoon, S. O., and Chikaraishi, D. M. (1992). Tissue-specific transcription of the rat tyrosine hydroxylase gene requires synergy between an AP-1 motif and an overlapping E Box-containing dyad. *Neuron* 9: 55-67.

Yoshida, Y., Sakimura, K., Masuada, T., Kushiya, E., and Takahashi, Y. (1983). Changes in the levels of translatable mRNA for neuron-specific enolase and non-neuronal enolase during development of rat brain and liver. *J. Biochem.* 94: 1443-1450.

Young, W. S. III, Reynolds, K., Shepard, E. A., Gainer, H., and Castel, M. (1990). Cell-specific expression of the rat oxytocin gene in transgenic mice. *J. Neuroendocrinol.* 2: 917-925.

Zaiko, S. D., and Burbaeva, G. S. (1986). Content of neurospecific and non-neurospecific enolase isoenzymes in structures of the human brain. *Bull. Exp. Biol. & Medicine* 102: 892-894.

Zeitoun, Y., Lamandé, N., Gros, F., and Legault-Demare, L. (1983). Developmental changes in translatable mRNAs for the cerebral enolase isoenzymes αα and γγ. *EMBO J.* 2: 1445-1449.

Zeltzer, P. M., Sneider, S. L., Marangos, P. J., and Zweig, M. H. (1986). Differntial expression of neural isozymes by human medulloblastomas and gliomas and neuroectodermal cell lines. *J. Natl. Cancer. Inst.* 77: 625-631.

Zomzely-Neurath, C. E. (1983). Enolase. In *Handbook of Neurochemistry* Volume 4, 2nd Edition (Lajtha, A., Ed., Plenum Press, New York), pp 402-433.

Zomzely-Neurath, C., and Keller, A. (1977). Nervous system-specific proteins of vertebrates - a search for functions and physiological roles. *Neurochem. Res.* 2: 353-372.

Zomzely-Neurath, C., and Walker, W. A. (1980). Enolase. In *Proteins of the Nervous System,* 2nd Edition (Schneider, D. J., and Bradshaw, R. A. Eds., Raven Press, New York).

Zopf, D., Dineva, B., Betz, H., and Gundelfinger, E. D. (1990). Isolation of the chicken middle molecular weight neurofilament (*NF-M*) gene and characterization of its promoter. *Nucleic Acids Res.* 18: 521-530.

Zwaan, J. T., Wang, L., Garza, A., and Lam, K. W. (1994). Neuron-specific enolase expression during eye development in the chicken embryo. *Exp. Eye Res.* 58: 91-97.

4

DX

219086

Ci

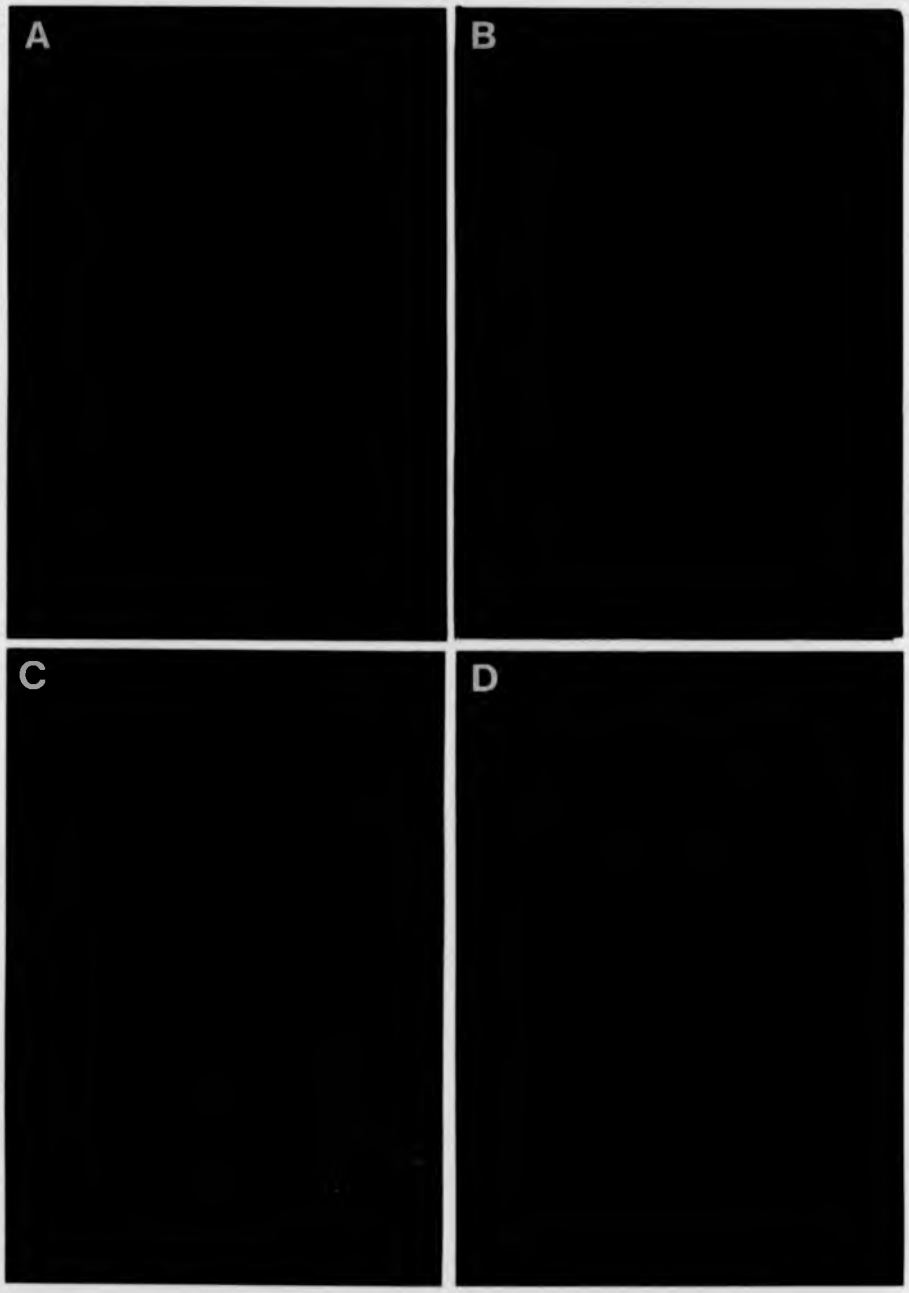

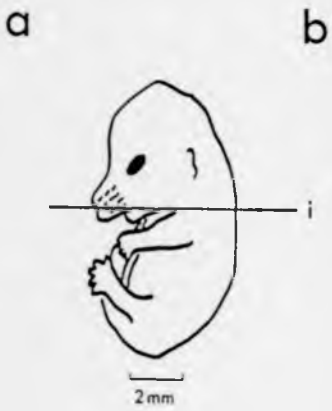

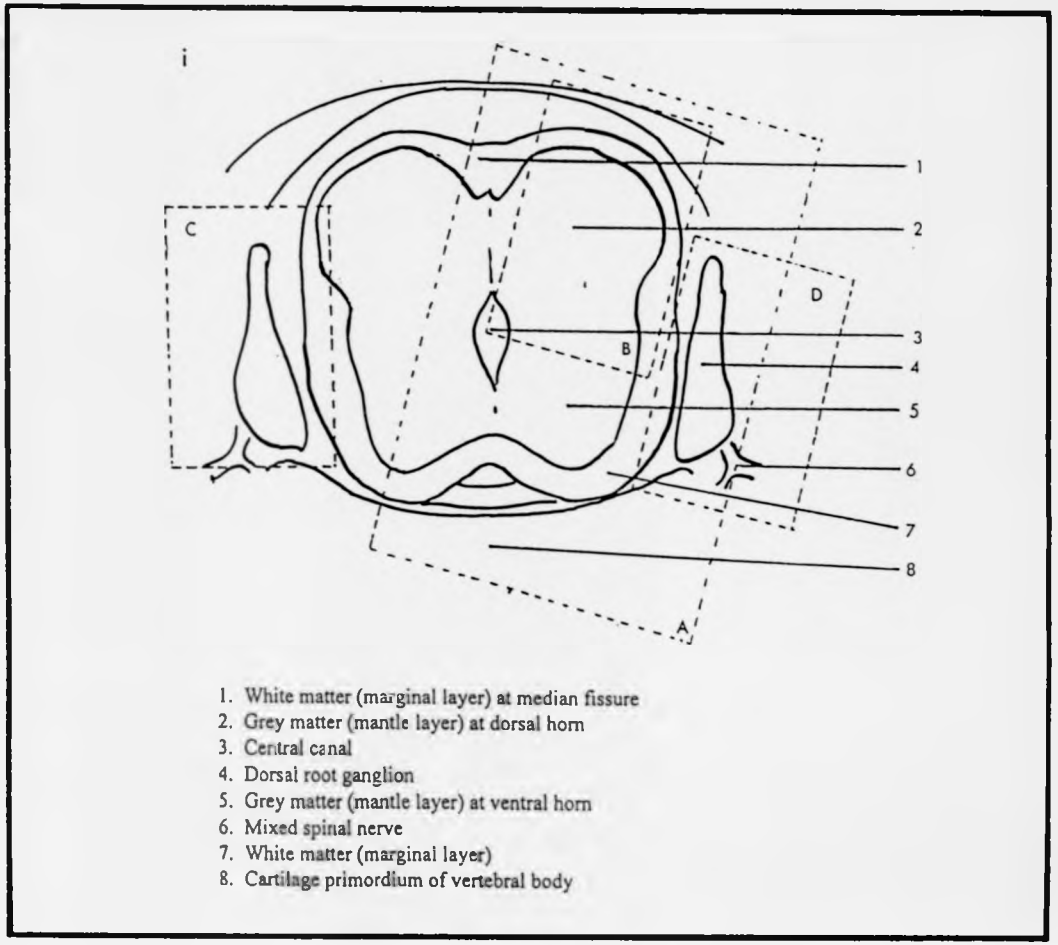

1. White matter (marginal layer) at median fissure
2. Grey matter (mantle layer) at dorsal horn
3. Central canal
4. Dorsal root ganglion
5. Grey matter (mantle layer) at ventral horn
6. Mixed spinal nerve
7. White matter (marginal layer)
8. Cartilage primordium of vertebral body

cii

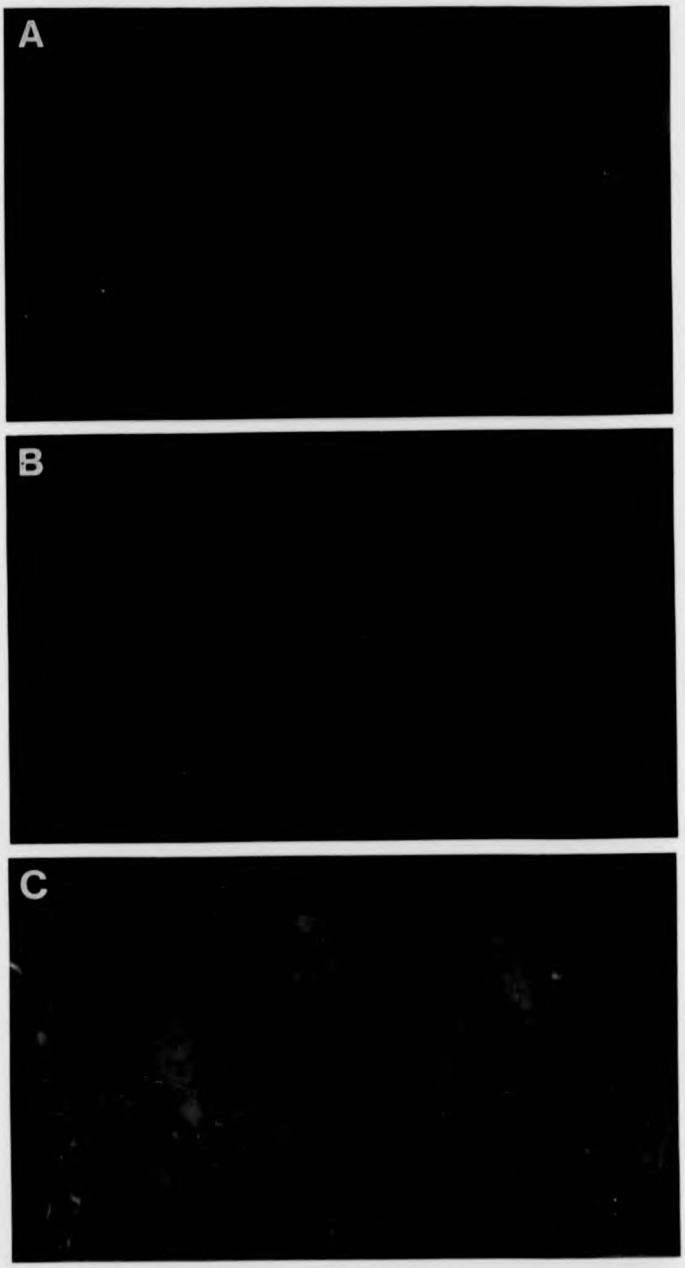

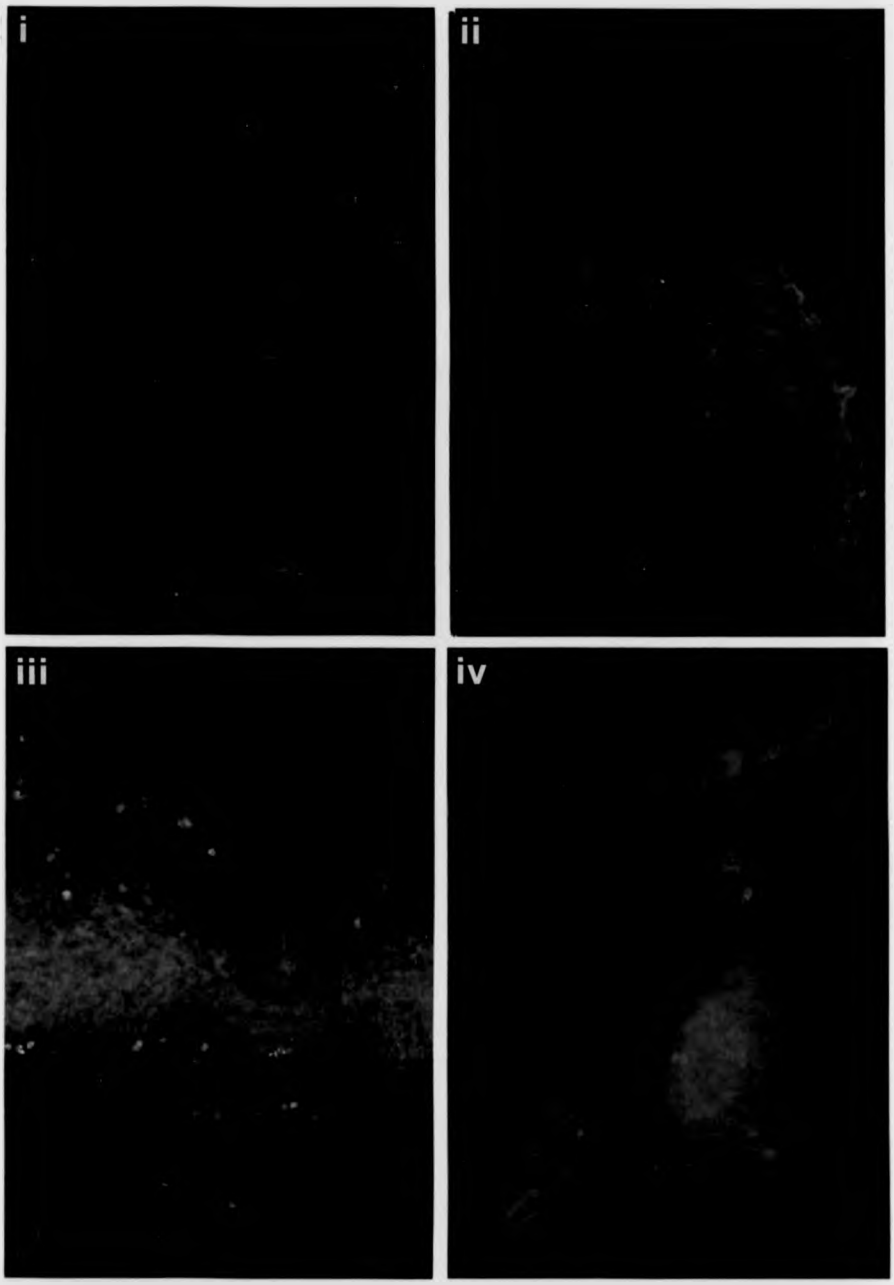
c
i
ii
iii
iv

Figure 7.8: Following two pages

Figure 7.8: Expression of NSE protein in mouse embryos at E10.5. a) Size and appearance of mouse embryo at E10.5 showing the positions of sections to which the drawings and photographs in this figure refer. b) Schematic representation of the E10.5 mouse neural tube in transverse section (the position of each section is shown in (a)), showing anatomical differences along the rostrocaudal axis. The expression domain of NSE protein is shaded in and the photographic field of each photomicrograph (as shown in (c)) is marked with a dashed line. c) Photomicrographs of representative transverse sections, magnification x85, showing the diminishing extent of NSE expression along the rostrocaudal axis of the E10.5 mouse neural tube. NSE was detected using a polyclonal antiserum raised against human NSE and a secondary FITC-conjugated antiserum specific for rabbit IgG. Photographs were enlarged from original slides taken under epifluorescent microscopy using a x20 DIC objective lens.

7.2.4.2 Expression of endogenous NSE protein at E10.5

Transverse 10μm sections were taken throughout E10.5 mouse embryos and NSE protein was detected as described in section 7.2.4. No NSE protein could be detected in the brain (data not shown) but expression was observed in the rostral part of the neural tube, specifically in cells believed to be motor neurons of the ventral horn (Figure 7.8). At the more rostral extremity of this domain of expression, NSE-positive neurons were visible in the mantle layer, which at this stage of development is restricted to bilateral crescents of tissue in the ventrolateral regions of the neural tube (Figure 7.8(i)). Sections taken progressively more caudally along the neural tube showed a regression of this domain, until at its caudal extremity, only a few individual NSE-positive cell bodies were detected (Figure 7.8(iv)).

was carried out with automatic exposure. This is also reflected in the relatively high background signals observed in photographs from early developmental stages, where the expression of NSE was weak and localised.

7.2.4 Expression of endogenous NSE protein - *in situ* immunohistochemical analysis

The expression of NSE protein was investigated by cutting cryostat sections of mouse embryos freshly prepared as described in section 4.3.2. Embryos were studied between E9.5 and E14.5 for the reasons discussed above. NSE protein was detected with a polyclonal primary antiserum raised against human NSE and an FITC-conjugated secondary antiserum specific for rabbit IgG as described in section 4.3.6. The suitability of the anti-human NSE antiserum for the detection of mouse antigen was established by immunoblot analysis (see Figure 5.2).

In this section, the expression of NSE protein is presented in the form of epifluorescent photomicrographs taken from cryostat sections subjected to treatment as described above and depicting various embryonic structures at various stages of development. Each set of photographs is accompanied by a drawing of an embryo, which shows the position of each cryostat section in relation to the whole organism, and a series of schematic sketches, showing the important anatomical landmarks within each cryostat section and the field of each photograph. Each figure is divided into three compartments, labelled (a), (b) and (c). Compartment (a) shows the size and appearance of the whole embryo, compartment (b) comprises the schematic sketches of the cryostat sections, and compartment (c) comprises the photographs. Consecutive sections are identified by numbering i, ii, iii....etc. In compartment (b), anatomical landmarks are labelled 1, 2, 3....etc., and are described in full under the sketches whilst dashed boxes, labelled A, B, C....etc., represent individual photographs and show the fields they cover.

For each cryostat section used to detect NSE, a serial section was used as a negative control. The negative controls were treated in the same manner as the experimental sections, but the primary antiserum was omitted from the first incubation. To conserve space, negative control photographs are not shown for each experiment described in this chapter, but an example is shown in Figure 7.6. It should be noted that the background signal is greater in the negative control because photography

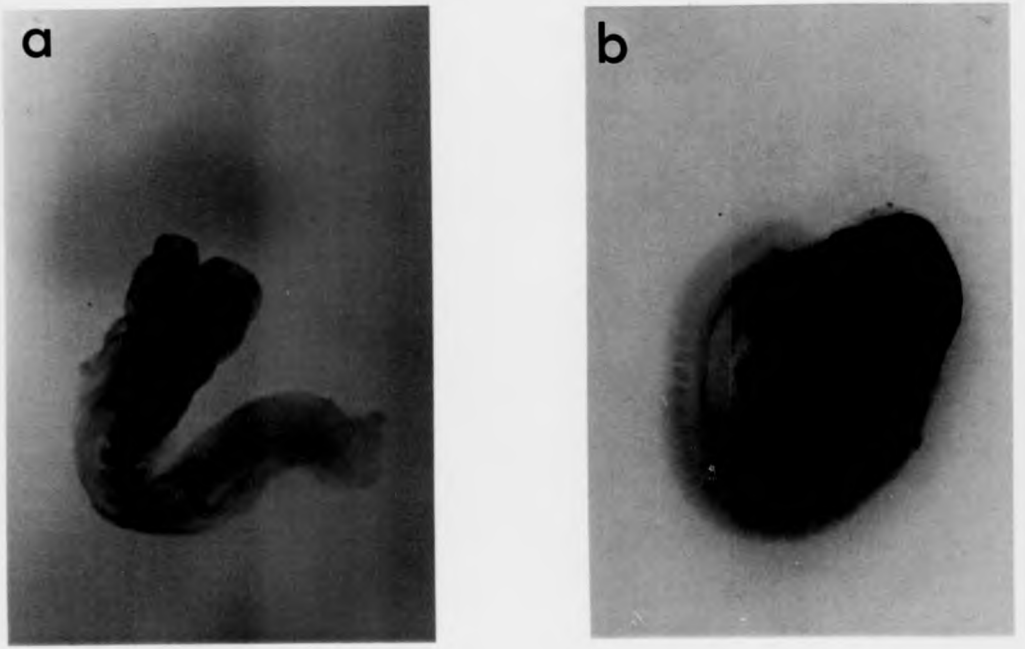

Figure 7.5: *In situ* hybridisation to (a) E8.5 and (b) E9.5 mouse embryos using a digoxigenin-UTP labelled antisense RNA probe complementary to the 3' untranslated region of the *NSE* message. Incorporated digoxigenin was detected using an alkaline phosphatase-conjugated antiserum and the signal was revealed using a colourimetric assay catalysed by alkaline phosphatase.

7.2.3.3 Wholemount *in situ* hybridisation to mouse embryos

In situ hybridisation to wholemount E8.5 and E9.5 mouse embryos was carried out as described in section 4.4. E8.5 mouse embryos treated with the antisense RNA probe showed no signal above the background observed in sense probe controls (Figure 7.5a). E9.5 mouse embryos demonstrated staining in the neuroepithelial lining of the forebrain, midbrain and hindbrain, but the signal was absent from the neural tube (Figure 7.5b). The brain-specific signal was not evident in control embryos treated with the sense probe.

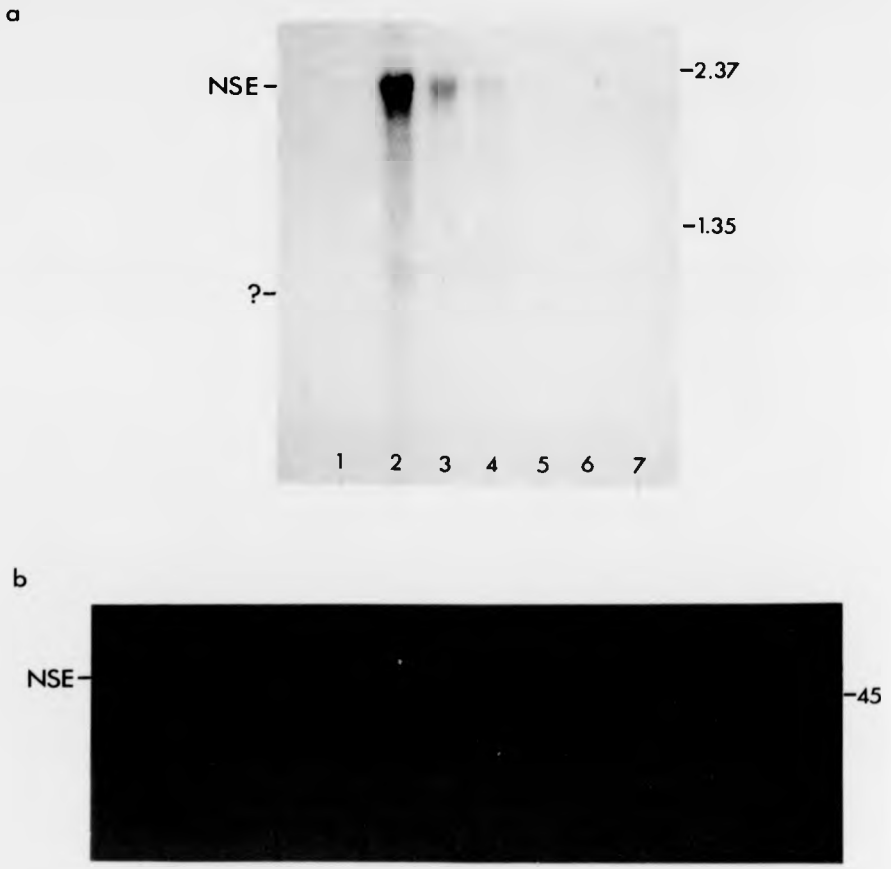

Figure 7.1. Biochemical analysis of *NSE* gene expression during mouse development. a) Northern analysis, lanes loaded equally for total RNA (10μg per lane) and probed with the *Sma* I - *Nco* I fragment of the rat *NSE* 3' UTR: 1 - adult liver (negative control); 2 - adult brain (positive control); 3 - P0 brain; 4 - E17.5; 5 - E14.5; 6 - E12.5; 7 - E10.5. Lanes 4 - 7 were extracts of whole embryos. Markers are Gibco BRL RNA ladder. b) Western analysis, lanes loaded equally for total protein (5μg per lane) and NSE detected with primary antiserum raised against human NSE and secondary, horseradish peroxidase-conugated secondary antiserum specific for rabbit IgG. Signal detected using diaminobenzidine tetrahydrochloride without metal ion enhancement: 1 - adult liver (negative control); 2 - adult brain (positive control); 3 - P0 brain; 4 - E17.5; 5 - E14.5; 6 - E12.5; 7 - E10.5. Lanes 4 - 7 were extracts of whole embryos. 45kDa marker is ovalbumin.

7.2.1 Biochemical analysis of endogenous *NSE* gene expression during mouse development

The expression of *NSE* mRNA and NSE protein was investigated by northern and western analysis as described in sections 4.1.7.3 and 4.1.8. Total RNA and protein was isolated from E10.5, E12.5, E14.5 and E17.5 embryos, from the brains of neonatal cubs and from adult brain and liver. The last two extracts represented positive and negative controls, respectively. Lanes were loaded equally for total RNA (10μg) or protein (5μg). *NSE* mRNA was detected using a probe corresponding to the rat *NSE* 3' untranslated region, as described in section 5.2.1, and NSE protein was detected using a primary antiserum raised against human NSE and a secondary, horseradish peroxidase-conjugated antiserum specific for rabbit IgG as described in section 5.2.1.

Similar studies in the past have shown that NSE protein can first be detected at E15 (Fletcher *et al.*, 1976). Although the expression of mouse *NSE* mRNA does not appear to have been investigated by northern analysis, its presence has been demonstrated as early as E14, based upon its ability to programme *in vitro* protein synthesis (Zeitoun *et al.*, 1983). In the present study, both mRNA and protein were first detected at E17.5. *NSE* mRNA was detected as a single hybridising band which comigrated with the 2.37 kb marker, corresponding to the expected size of the transcript (2233 b). NSE protein was detected as a single band which was slightly retarded with respect to the ovalbumin marker (45 kDa). Given that embryos from E15 and E16 were not considered, the first appearance of NSE protein broadly agreed with the previous studies of protein expression described above, however, the RNA analysis placed the onset of gene expression much later than previously reported. This discrepancy probably reflected differences in sensitivity between the two assays used. Both NSE protein and *NSE* mRNA were present at low levels in the embryo compared to adult brain. In each case, there was an approximate threefold increase in the level of gene product between E17.5 and P0, and a similar increase between P0 and adulthood. These results, shown in Figure 7.1, underscore the biphasic increase in gene expression observed in

Chapter 7 - Analysis of the NSE *promoter* in vivo *using transgenic mice*

7.1 Chapter summary

As discussed in the experimental overview, studies of neuronal gene regulation based purely upon *ex vivo* promoter analysis are often inadequate, primarily because the investigator has no idea of the spatial and temporal effects of his deletions in the context of an entire organism. Furthermore, the highly artificial nature of the transfection assay can override some of the normal constraints which apply *in vivo*; these factors are summarised in Table 2.1. If possible, therefore, such constructs that are made should be tested in both environments so that the advantages of each system can be maximised. Indeed, this strategy was attempted in the project discussed in this thesis. This chapter considers the *in vivo* analysis of *NSE* gene regulation, firstly discussing the endogenous expression of *NSE* and then the expression of reporter transgenes driven by parts of the rat *NSE* 5' flanking sequence.

7.2 Expression of endogenous *NSE* during mouse development

The importance of preliminary experiments to establish the endogenous expression of *NSE* in various cells lines was averred in Chapter 5. In a similar fashion, it was critical to characterise the endogenous expression of *NSE* during mouse development in order that patterns of reporter transgene expression could be compared and contrasted to those of the endogenous gene. In both cell lines and embryos, the expression of *NSE* mRNA and NSE protein was investigated using biochemical and *in situ* detection methods. In cell lines, the biochemical analysis was most important because the data from subsequent transfection experiments was largely quantitative. In embryos, however, the *in situ* analysis took on the more important role, as data concerning the spatial and temporal aspects of *NSE* gene regulation in mice were qualitative in nature.

6.7 Conclusions from the Sox factor cotransfection experiments

The Sox-cotransfection experiments unexpectedly showed that in NB4-1A3 cells transfected with pNSE1800CAT, higher mean Relative CAT Activities were observed following cotransfection with either cSox2 or cSox3 expression vectors. This was the opposite effect to that expected from factors expressed in the ventricular regions of the nervous system, where NSE is absent, and whose expression is strongly downregulated in areas of the nervous system characterised by the presence of postmitotic neurons. Whist the apparent induction of *NSE* by cSox2 was minimal, cSox3 cotransfection appeared to sponsor a two to threefold upregulation of reporter activity. However, careful inspection of the transfection data revealed that the Actual CAT Activities of pCAT-Control cotransfected with cSox3 were twofold less than those arising from cotransfection with cSox2 or the negative control vector pBluescriptIIKS+. As discussed in Chapter 5, it is permissible to compare absolute CAT activites within an experiment involving one cell line because all conditions are standardised. Such a significant difference between control activities within the bounds of the same experiment must indicate an exogenous cause, and cSox3 might well be the culprit. If the effect of cSox3 on the SV40 promoter is considered, and the Actual CAT Activites for cells cotransfected with pCAT-Control and pcDSox3 are normalised for this, the observed increase in Relative CAT Actvitiy becomes insignificant. One must also bear in mind that the control for transfection efficiency, pSV-β-galactosidase, is driven by the same promoter as pCAT-Control. The effect of Sox cotransfection is clearly revealed by inspection of the soluble β-galactosidase assay readings. There is an approximate twofold reduction in apparent transfection efficiency between the Sox contransfected cells and the controls. This phenomenon is observed for both cSox2 and cSox3, thus it is unclear why cSox2 appears not to influence pCAT-Control to the same extent as cSox3. These data suggest that the Sox factors do not influence the regulation of *NSE* and that careful controls must be carried out in future experiments to ensure that any observed effects of the Sox factors are true and not artefactual.

Activity of 120-140%. In the presence of cSox2 and cSox3 expression vectors, transfection efficiency was reduced approximately twofold. As the same mass of pSV-β-galactosidase DNA was transfected in each case, the transfection efficiencies for the Sox cotransfections should have been similar to those for the control experiment. The different efficiencies observed therefore suggested that there was either an effect brought about by the Sox-cDNA-containing plasmids, or that the Sox factors were influencing the control plasmid promoters. Normalised CAT activities unexpectedly showed that both cSox2 and cSox3 caused a *rise* in *NSE*-driven reporter activity, and in the case of cSox3, a two- to threefold upregulation was observed. It was apparent, however, that the actual source levels of CAT activity from the control vector pCAT-Control were modulated by cotransfection, suggesting that the control vectors were indeed influenced by Sox expression. This point is expanded in the conclusion (section 6.7) and discussed in Chapter 9.

6.6 Cotransfection of *NSE-cat* constructs with cSox2 and cSox3 expression vectors

The Sry-box containing transcription factors (Sox factors) were discussed in section 2.7.4 as potential regulators of neuronal gene expression and Sox-2 and Sox-3 were considered potential candidates for the regulation of *NSE* for several reasons. Expression of Sox-2 and Sox-3 factors in the developing chick and mouse nervous systems has been shown to be complementary to the expression of *NSE* (Uwanogho *et al.*, 1995; R. Lovell-Badge, unpublished data). Specifically, expression is observed in the proliferative zones, which are devoid of NSE protein (*see* Chapter 7). A similar pattern of expression has been shown for *NRSF* mRNA (Schoenherr and Anderson, 1995) and the NRSF protein is a candidate negative regulator of at least 18 neuronal genes, but not of *NSE*. It is possible, therefore, that the Sox factors could fulfil an equivalent role in the regulation of *NSE*. Although the sequenced portion of the *NSE* 5' flanking sequence appears to lack consensus binding sites for the Sox factors, there are several homologous elements and it should be borne in mind that the distal 800 bp of the complete *NSE* regulatory element has not been sequenced. In the first instance, therefore, transfections were carried out using pCAT-Control, pCAT-Basic and pNSE1800CAT in combination with expression vectors pcDSox2 and pcDSox3, which express the cSox2 and cSox3 factors, respectively. Control transfections were carried out with pBluescriptIIKS+ in place of the expression vectors. These experiments were designed to show whether the longest construct was modulated by the Sox factors. It was unfortunate that the mouse Sox-2 and Sox-3 expression vectors were unavailable, however, the chicken proteins display very similar patterns of expression and are 81% and 70% identical to the mouse proteins, respectively (Uwanogho *et al.*, 1995).
Transfections were carried out in NB4-1A3 neuroblastoma cells because they represent a stage between nonneuronal proliferative cells and neurons, which could be sensitive to modulation by transcriptional regulators such as the Sox-2 and Sox-3 factors. Furthermore, the slowing down of growth, which accompanies increasing cell confluence and the induction of *NSE* in neuroblastoma cells, might mimic the deposition of postmitotic neurons in the mantle layer, concomitant with the downregulation of cSox2 and cSox3, and the upregulation of cSox11 (Uwanogho *et al.*, 1995) and *NSE* (Zomzelly-Neurath, 1983). Thus, if these regulators were to be responsible for *NSE* gene regulation, one might expect to see repression of the *NSE*-driven construct compared to cells transfected with the control plasmid. The results showed that in the absence of Sox factors, the full length construct pNSE1800CAT was expressed at a greater level than pCAT-Control, with a mean Relative CAT

reduction following truncation from 120 bp to 95 bp, however, it is clear that the minimal 95 bp of 5' flanking sequence is quite capable, in the presence of the TATA-like box required for basal transcriptional initiation, of sponsoring high level neuronal gene expression. These data suggest that sequences downstream of the transcriptional start site may be required for specific enhancement of *NSE* gene expression whilst elements in the 5' flanking region control the temporal and spatial aspects of gene regulation. These factors are explored more thoroughly in Chapter 9 in the light of recent evidence from further analysis of the *NSE* gene.